DRAFT DISCLAIMER

This contractor document was prepared for the U.S. Department of Energy (DOE), but has not undergone programmatic, policy, or publication review, and is provided for information only. The document provides preliminary information that may change based on new information or analysis, and is not intended for publication or wide distribution; it is a lower level contractor document that may or may not directly contribute to a published DOE report. Although this document has undergone technical reviews at the contractor organization, it has not undergone a DOE policy review. Therefore, the views and opinions of authors expressed do not necessarily state or reflect those of the DOE. However, in the interest of the rapid transfer of information, we are providing this document for your information, per your request.

Civilian Radioactive Waste Management System
Management & Operating Contractor

Engineered Barrier System Degradation, Flow, and Transport
Process Model Report

TDR-EBS-MD-000006 REV 00

March 2000

Prepared for:

U.S. Department of Energy
Yucca Mountain Site Characterization Office
P.O. Box 30307
North Las Vegas, Nevada 89036-0307

Prepared by:

TRW Environmental Safety Systems Inc.
1211 Town Center Drive
Las Vegas, Nevada 89144

Under Contract Number
DE-AC08-91RW00134

Civilian Radioactive Waste Management System
Management & Operating Contractor

Engineered Barrier System Degradation, Flow, and Transport
Process Model Report

TDR-EBS-MD-000006 REV 00

March 2000

Prepared by:

(signature)

D.A. Chesnut

3/17/00
Date

Technical Checked by:

(signature)

D.J. Carpenter

03/17/2000
Date

Compliance Checked by:

(signature)

B.T. Stanley

3/17/2000
Date

Approved by:

(signature)

K.K. Bhattacharyya

03/17/00
Date

INTENTIONALLY LEFT BLANK

EXECUTIVE SUMMARY

The Engineered Barrier System Degradation, Flow, and Transport Process Model Report (EBS PMR) is one of nine PMRs supporting the Total System Performance Assessment (TSPA) being developed by the Yucca Mountain Project for the Site Recommendation Report (SRR). The EBS PMR summarizes the development and abstraction of models for processes that govern the evolution of conditions within the emplacement drifts of a potential high-level nuclear waste repository at Yucca Mountain, Nye County, Nevada. Details of these individual models are documented in 23 supporting Analysis/Model Reports (AMRs). Nineteen of these AMRs are for process models, and the remaining 4 describe the abstraction of results for application in TSPA. The process models themselves cluster around four major topics: *Water Distribution and Removal Model, Physical and Chemical Environment Model, Radionuclide Transport Model,* and *Multi-Scale Thermohydrologic Model.* One AMR (*Engineered Barrier System—Features, Events, and Processes/Degradation Modes Analysis*) summarizes the formal screening analysis used to select the Features, Events, and Processes (FEPs) included in TSPA and those excluded from further consideration.

Performance of a potential Yucca Mountain high-level radioactive waste repository depends on both the natural barrier system (NBS) and the engineered barrier system (EBS) and on their interactions. Although the waste packages are generally considered as components of the EBS, the EBS as defined in the EBS PMR includes all engineered components outside the waste packages. The principal function of the EBS is to complement the geologic system in limiting the amount of water contacting nuclear waste. A number of alternatives were considered by the Project for different EBS designs that could provide better performance than the design analyzed for the Viability Assessment. The design concept selected was Enhanced Design Alternative II (EDA II).

The design concepts in EDA II include the following:

- Waste packages incorporate a corrosion-resistant outer barrier

- Drip shields (DSs) and backfill are used to protect waste packages (WPs) from water contact and rockfall

- Ventilation is used to remove heat before closure

Major features of EDA II also include the waste form (WF), waste package supports, inverts constructed of steel and crushed tuff, and ground support.

Processes addressed in the EBS PMR include:

- Evolution of heat by radioactive decay, and its removal by preclosure ventilation

- Drift degradation by rockfall

- Seepage of water and its flow within the drift

- Evaporation and condensation

- Deposition of salts and precipitates within the drifts

- Gas exchange between the drifts and the surrounding rock

- Chemical reactions between water, rock, and introduced materials

- Accumulation of corrosion products within the drifts and their effect on chemistry and flow

- Colloids formed by corrosion products with high sorptive capacity for radionuclides

- Growth and activity of microbes in the EBS

- Transport of radionuclides through the invert by advection and diffusion

All model results summarized in the EBS PMR are based on AMRs developed prior to the end of calendar 1999 for the EDA II conceptual design (the Project Baseline design until late-January 2000). Since then, change requests were initiated to remove backfill from the reference design. The effects of this design change are currently being assessed. However, it is expected that detailed analyses of the impact of removing backfill, coupled with detailed design of the EBS, will produce a system with performance equal to or better than the EDA II conceptual design.

Regulatory issues, including Nuclear Regulatory Commission staff Key Technical Issues, subissues, and acceptance criteria, are addressed.

An abbreviated list from process models is presented here:

- No combination of model parameters led to a prediction of condensation beneath the drip shield. This is consistent with limited experimental data from ongoing quarter-scale experiments.

- Assuming complete degradation of the ground-support system at closure, time-dependent reduction in joint cohesion, thermal stresses, and seismic events combined will generate rockfall in less than 2.5 percent of the total length of emplacement drifts within 10,000 years after closure.

- A bounding analysis shows that more than 70% of the 100-year total decay heat can be removed by forced ventilation at 10 to 15 cubic meters per second.

- Water evaporating within the drifts can lead to the temporary accumulation of up to a few kilograms of soluble salts per meter of drift, depending upon the proximity to the repository center and the infiltration flux. An edge location with the same infiltration flux as a center location has less heat available for evaporating water, and is therefore less subject to salt accumulation. Salts will be deposited in the backfill, and the invert.

- Oxidation of carbon steel will be complete in hundreds to a few thousand years. The most important effects will be to consume oxygen in the environment, and produce iron

corrosion products. Some of the corrosion product material will be in the form of colloidal particles with the potential to increase the transport of actinides by one to two orders of magnitude over their solubility limits.

- Based on nutrient and energy availability, and estimated degradation rates for introduced materials, microbial growth is expected to produce only 10 g of biomass per meter of drift per year during the first 10,000 years. Effects on the bulk chemical environment are believed to be negligible, although localized microbial activity could accelerate corrosion of steel by a factor of 6 or more.

- Limiting the use of cement to grouting rockbolts will preclude a major impact of cement leachate on the pH of water within the drift. Around the peak temperatures, the pH within the drift may increase to about 11 due to evaporation and concentration of the constituents of seepage water. After salt deposits redissolve and the temperature returns to ambient, the pH is expected to remain between 8 and 9.

- A bounding analysis shows that little, if any, reduction in radionuclide transport rates can be expected for the invert.

- The Multi-Scale Thermohydrologic Model predicts that the DS/backfill combination can prolong the period of reduced relative humidity on the WP surface, because the WP remains hotter than the DS long after seepage returns to the drift. The peak WP temperature (60 years after closure) ranges from 305°C to 315°C, depending upon the infiltration flux. The difference in peak temperature between the hottest and coldest WPs is 42 C°. Between 56 and 76 percent of the host rock in the pillars is predicted to remain below boiling.

This report demonstrates that EBS performance is sufficiently well understood to support reasonable predictions of the environmental conditions at the drip shields and waste packages, and of conditions that will affect radionuclide transport in the emplacement drifts. Confidence has been increased through the use of available field and laboratory test data, and bounding models, to address predictive uncertainty. Model uncertainties are identified, alternative models are discussed, and model validation is addressed throughout. Process model uncertainties are appropriately represented in the approaches to abstraction of model results for TSPA.

INTENTIONALLY LEFT BLANK

CONTENTS

FIGURES

FIGURES (Continued)

TABLES

TABLES (Continued)

INTENTIONALLY LEFT BLANK

ABBREVIATIONS AND ACRONYMS

1-D	one-dimensional
2-D	two-dimensional
3-D	three-dimensional
AFC	active-fracture concept
AML	areal mass loading
AMR	analysis model report
ANL	Argonne National Laboratory
AP	Administrative Procedure
ASTM	American Society for Testing and Materials
BWR	boiling-water reactor
C-S-H	calcium-silicate-hydrate
CDF	cumulative distribution function
CLST	container life and source term
cms	cubic meters per second
CRM	corrosion-resistant material
CRWMS	Civilian Radioactive Waste Management System
CSNF	commercial spent nuclear fuel
DDT	discrete-heat-source, drift-scale thermal conduction
DE	disruptive event
DHLW	defense high-level waste
DI	document identifier
DIC	dissolved inorganic carbon
DIRS	Document Input Reference System
DKM	dual-permeability method
DLS	detailed line survey
DM	degradation mode
DOE	U.S. Department of Energy
DRKBA	Discrete Region Key-Block Analysis
DS	drip shield
DTN	data tracking number
EBS	engineered barrier system
EBSO	Engineered Barrier System Operations
EBST/RH	engineered barrier system temperature and humidity
ECM	equivalent-continuum method
ECRB	enhanced characterization of the repository block
EDA	enhanced design alternative
EIS	environmental impact statement
EMMA	Estimation of Maximum Microbiological Activity
EPA	U.S. Environmental Protection Agency

ABBREVIATIONS AND ACRONYMS (Continued)

ESF   Exploratory Studies Facility

FEP   feature, event, and/or process
FEPS&DM   features, events, processes, and degradation modes
FPGM   full-periphery geologic map

GFM   Geological Frame Model
GROA   geologic repository operations area

HLW   high-level waste
HRH   high relative humidity

IC   ion chromatography
ICP   inductively coupled plasma
ID   identification
IDGE   in-drift geochemical environment
IRSR   issue resolution status report

KTI   key technical issue

LA   License Application
LADS   License Application Design Selection
LDTH   line-averaged-heat-source, drift-scale thermohydrologic
LLNL   Lawrence Livermore National Laboratory
LRH   low relative humidity

M&O   management and operating
MIC   microbially induced corrosion
MSTH   multiscale thermohydrologic
MSTHAC   multiscale TH abstraction code
MSTHM   multiscale thermohydrologic model
MTU   metric tons uranium

NAT-J-13   natural well water from J-13 well
NBS   National Bureau of Standards
NBS   natural barrier system
NE   northeast
NF   near field
NFE   near-field environment
NMR   nuclear magnetic resonance
NQ   not qualified
NRC   U.S. Nuclear Regulatory Commission
NUFT   Nonisothermal Unsaturated-Saturated Flow and Transport
NW   northwest

P&CE   physical and chemical environment

ABBREVIATIONS AND ACRONYMS (Continued)

PA	performance assessment
PAO	Performance Assessment Operations
PDE	partial-differential equation
PF	principal factor
PHREEQC	pH-REdox EQuilibrium equation program in C language
PMR	process model report
PWR	pressurized-water reactor
Q	qualified
Q-List	quality assurance list
QA	quality assurance *or* quality-affecting
QAP	quality assurance procedure
QARD	Quality Assurance Requirements and Description
QL	quality level
RDTME	repository design and thermal-mechanical effects
REV	representative elementary volume
RH	relative humidity
RIP	Repository Integration Program
RN	radionuclide
RNT	radionuclide transport
RSS	repository safety strategy
SCC	stress corrosion cracking
SDT	smeared-heat-source, drift-scale thermal conduction
SI	saturation index
SMT	smeared-heat-source, mountain-scale thermal-conduction
SNF	spent nuclear fuel
SPW	synthetic porewater
SRR	site recommendation report
SYN-J-13	synthetic groundwater
SZ	saturated zone
TBV	to be verified
TCR	technical change report
TDMS	Technical Data Management System
TDS	total dissolved solids
TEF	thermal effects on flow
TH	thermal hydrology, thermal-hydrologic
THC	thermal-hydrologic-chemical
THM	thermal-hydrologic-mechanical
TM	thermomechanical
TSPA	Total System Performance Assessment
TSPA-SR	Total Site Performance Assessment–Site Recommendation
TSPA-VA	Total System Performance Assessment–Viability Assessment

ABBREVIATIONS AND ACRONYMS (Continued)

TSPA-95   Total System Performance Assessment–1995

USBR   U.S. Bureau of Reclamation
USGS   U.S. Geological Survey
UZ   unsaturated zone

VA   viability assessment

WAPDEG   WAste Package DEGradation
WD&R   water distribution and removal
WF   waste form
WP   waste package

XRD   x-ray diffraction

YM   Yucca Mountain
YMP   Yucca Mountain Site Characterization Project

1. INTRODUCTION

Performance of a potential Yucca Mountain high-level radioactive waste repository depends on both the natural barrier system (NBS) and the engineered barrier system (EBS) and on their interactions. Although the waste packages are generally considered as components of the EBS, the EBS as defined in the *Engineered Barrier System Degradation, Flow, and Transport Process Model Report* (PMR), herein referred to as the EBS PMR, includes all engineered components outside the waste packages. Waste packages and waste-form performance is described and modeled in other PMRs. Performance of the drip shield as a means of diverting water is included here, both as-built and following degradation because of various processes. The specific mechanisms and rates of drip shield failure from corrosion and seismic activity are described and modeled in the WP PMR.

To evaluate the postclosure performance of a potential repository at Yucca Mountain, a total system performance assessment (TSPA) will be conducted. A set of nine PMRs, of which this document is one, is being developed to summarize the technical basis for each of the process models supporting the TSPA model. These reports cover the following areas:

- Integrated Site Model
- Unsaturated Zone Flow and Transport
- Near Field Environment
- Engineered Barrier System Degradation, Flow, and Transport
- Waste Package Degradation
- Waste Form Degradation
- Saturated Zone Flow and Transport
- Biosphere
- Disruptive Events.

These PMRs are supported by analysis/model reports (AMRs) that contain the more detailed technical information to be input into each PMR and the TSPA. This technical information consists of data, analyses, models, software, and supporting documentation that will be used to defend the applicability of each process model for its intended purpose of evaluating the postclosure performance of the potential Yucca Mountain repository system. The PMR process will ensure the traceability of this information from its source through the AMRs, PMRs, and eventually to how that information is used in the TSPA.

This chapter summarizes the purpose for the EBS PMR, its basic organization, technical content, relationship to other PMRs, and other key Yucca Mountain Site Characterization Project (YMP) documents such as topical reports, the site recommendation report (SRR), and the license application (LA). It also provides a brief summary of the PMR technical content.

The purpose of the EBS PMR is to describe the EBS, to summarize its contribution to controlling the waste package and drip shield environment, and to document the thermal, mechanical, hydrologic, chemical, and radionuclide transport processes arising from the interaction of emplaced waste with the EBS and the surrounding host rock. EBS technical information, supporting data, analyses, models, abstractions, and software for evaluating postclosure performance of the EBS are documented in 23 AMRs. Finally, the EBS PMR supports the

Yucca Mountain SRR, by summarizing the AMR results used in the Total System Performance Assessment (TSPA) and the degree of confidence in the validity of conclusions based on those results.

1.1 OBJECTIVE

The objectives of the EBS PMR are to:

- Summarize the technical and scientific bases providing confidence that results from the analyses and models are reasonable bounds on the actual future behavior of the EBS as it affects repository performance

- Describe and quantify how the following in-drift processes and/or environments change with time after emplacement of nuclear waste in a potential repository:

  - Effects or controls of the EBS design on liquid water entry into the drift from the surrounding host rock, its distribution within the drift, and its removal by evaporation or by drainage back into the host rock

  - The physical and chemical environment within the different components of the EBS, and near the waste packages and drip shields. Specific items include the coupling among thermal hydrology, gas and water chemistry, effects of microbes, cementitious and other introduced materials, precipitates and salts, and the potential for colloid formation

  - The transport of radionuclides released from breached waste packages through the EBS, particularly through the invert below the drip shield

  - Variability of thermal-hydrologic responses within the emplacement drifts at various locations spanning the potential repository footprint

  - The degradation of the EBS as a result of features, events, and processes (FEPs) that are determined to be applicable to the various barriers

- Provide a guide to the use of modeling and analysis results developed in the AMRs and submitted to the Technical Database Management System (TDMS) to support the TSPA and other PMRs such as those covering the unsaturated zone (UZ), the near field (NF), the waste packages (WPs), and the waste forms (WFs)

- Evaluate the performance of the various EBS barriers in support of the SRR and for consistency with the repository safety strategy (RSS)

- Address resolution of Nuclear Regulatory Commission (NRC) key technical issues (KTIs) and related issue-resolution status reports (IRSRs) such as the Repository Design and Thermal-Mechanical Effects IRSR, the Evolution of the Near Field Environment IRSR, the Thermal Effects on Flow IRSR, and the Container Lifetime and Source Term IRSR.

1.2 SCOPE

Details of input data, analyses, and output are given in individual AMRs and will not be repeated here. The scope of this report is to summarize and integrate the analyses, models, and results of the supporting EBS AMRs and their abstractions and to provide guidance on the use of developed data and information to support TSPA, SR, and regulatory evaluations. This report also describes predicted long-term performance of the EBS and the reasonable representation of its contribution to the RSS and the use of testing and other information to enhance the credibility of the long-term performance predictions.

Table 1-1 lists the titles, EBS PMR report sections, planning identification (ID) numbers, and document identifier (DI) numbers for the 23 AMRs contributing to the EBS PMR. The major process model AMRs (shown in bold type) provide bounding analyses of related processes that can be used to develop engineering design bases. The other AMRs provide more detailed analyses of specific processes.

Table 1-1. Analysis and Model Reports Supporting the Engineered Barrier System Degradation, Flow, and Transport Process Model Report

Process AMR Title	Report Section	ID Number	DI Number
Water Distribution and Removal Model (CRWMS M&O 2000q)	3.1.1	E0090	**ANL-EBS-MD-000032**
Ventilation Model (CRWMS M&O 1999j)	3.1.1	E0075	ANL-EBS-MD-000030
Drift Degradation Analysis (CRWMS M&O 2000ad)	3.1.1	E0080	ANL-EBS-MD-000027
Water Drainage Model (CRWMS M&O 2000af)	3.1.1	E0070	ANL-EBS-MD-000029
Water Diversion Model (CRWMS M&O 2000ae)	3.1.1	E0085	ANL-EBS-MD-000028
In-Drift Thermal-Hydrologic-Chemical Model (CRWMS M&O 2000y)	3.1.1	E0065	ANL-EBS-MD-000026
Engineered Barrier System: Physical & Chemical Environment Model (CRWMS M&O 2000t)	3.1.2	E0100	**ANL-EBS-MD-000033**
In-Drift Corrosion Products (CRWMS M&O 1999g)	3.1.2.3	E0020	ANL-EBS-MD-000041
Seepage/Backfill Interactions (CRWMS M&O 2000k)	3.1.2.3	E0030	ANL-EBS-MD-000039
In-Drift Gas Flux and Composition (CRWMS M&O 2000e)	3.1.2.2	E0035	ANL-EBS-MD-000040
In-Drift Microbial Communities (CRWMS M&O 2000f)	3.1.2.4	E0040	ANL-EBS-MD-000038
In-Drift Colloids and Concentrations (CRWMS M&O 2000d)	3.1.2.6	E0045	ANL-EBS-MD-000042
Seepage/Cement Interactions (CRWMS M&O 2000l)	3.1.2.3	E0055	ANL-EBS-MD-000043
Seepage/Invert Interactions (CRWMS M&O 2000m)	3.1.2.3	E0060	ANL-EBS-MD-000044
In-Drift Precipitates/Salts Analysis (CRWMS M&O 2000g)	3.1.2.5	E0105	ANL-EBS-MD-000045
Engineered Barrier System Radionuclide Transport Model (CRWMS M&O 2000b)	3.1.3	E0050	**ANL-EBS-MD-000034**
Invert Diffusion Properties Model (CRWMS M&O 2000h)	3.1.3	E0000	ANL-EBS-MD-000031
Multiscale Thermohydrologic Model (CRWMS M&O 2000i)	3.1.4	E0120	**ANL-EBS-MD-000049**
Engineered Barrier System—Features, Events, and Processes/Degradation Modes Analysis (CRWMS M&O 2000c)	2.4	E0015	ANL-EBS-MD-000035

Table 1-1. Analysis and Model Reports Supporting the Engineered Barrier System Degradation, Flow, and Transport Process Model Report (Continued)

Abstraction Process AMR Title	Report Section	ID Number	DI Number
Physical and Chemical Environment Abstraction Model (CRWMS M&O 2000j)	3.2.3.1	E0010	ANL-EBS-MD-000046
Engineered Barrier System Degradation Modes & Features, Events, and Processes Abstraction (CRWMS M&O 2000r)	2.4	E0110	ANL-WIS-PA-000002
Abstraction of Near-Field Environment, Drift Thermodynamic Environment, and Percolation Flux (CRWMS M&O 2000w)	3.2.3.3	E0130	ANL-EBS-HS-000003
EBS Radionuclide Transport Abstraction (CRWMS M&O 2000a)	3.2.3.2	E0095	ANL-WIS-PA-000001

1.3 QUALITY ASSURANCE

The activities documented in this technical report were evaluated in accordance with CRWMS M&O procedure QAP-2-0, *Conduct of Activities*, and determined to be subject to the requirements of the *Quality Assurance Requirements and Description* (QARD) document (DOE 2000). This evaluation is documented in the activity evaluation for *Engineered Barrier System Performance Modeling* (CRWMS M&O 1999a). The engineered barrier system (EBS) is also identified on the *Q-list* (YMP 1998) as QA-1, important to radiological safety, and as QA-2, important to waste isolation.

This document was prepared in accordance with AP-3.11Q, *Technical Reports*, and the *Development Plan for the Engineered Barrier System Degradation, Flow, and Transport Process Model Report* (CRWMS M&O 1999c), which was prepared in accordance with AP-2.13Q, *Technical Product Development Planning*. A *Technical Change Request* (T2000-0039) was processed in accordance with AP-3.4Q, *Level 3 Change Control*.

The qualification of data used in the AMRs supporting this report is addressed in the AMRs. The qualification and use of input data follows the requirements of AP-3.10Q, *Analyses and Models*, and AP-3.15Q, *Managing Technical Product Inputs*. The qualification status of software is also described in the AMRs supporting this report. Qualification of software (including routines and macros) is based on the requirements of AP-SI.1Q, *Software Management*.

1.4 RELATIONSHIP TO OTHER PROCESS MODEL REPORTS AND KEY PROJECT DOCUMENTS

The calculated in-drift environmental conditions provided by the EBS process model provide input to determine the degradation modes and rates for the drip shields, waste packages, and waste forms. These effects are abstracted by TSPA from the appropriate EBS AMRs and integrated with abstractions from AMRs supporting other PMRs to develop the radionuclide source term. There are no direct data feeds from the EBS PMR to other PMRs. The EBS is not a principal factor in the repository safety strategy. The EBS PMR provides input to the site-recommendation consideration report and the license application.

1.5 OVERVIEW

This section briefly describes the characteristics of Yucca Mountain relevant to EBS performance, the conceptual design and functions of the EBS, and the processes affecting or affected by the EBS.

One unique feature of the Yucca Mountain site is its 700-meter-thick vadose zone. Although this zone is partially water-saturated, it is generally called the unsaturated zone (UZ). The emplacement drifts for the potential repository will be located about halfway between the ground surface and the water table (Figure 1-1), where the ambient water saturation in the host rock is more than 90 percent. Figure 1-2 shows a schematic plan view of the potential repository layout, an enlargement of a section containing several emplacement drifts connecting the service drifts, and a drift cutaway showing the three most numerous types of waste packages.

The principal function of the engineered system, using a design to complement the geologic system and take advantage of its unique characteristics, is to help prevent water from contacting nuclear waste. Figure 1-3 presents a schematic cross-section of an emplacement drift, showing the EDA II conceptual design for the EBS, comprising the waste package (WP), waste form (WF), waste package support, drip shield (DS), backfill, invert, and ground support. The flow paths of liquid water seeping into the drift are also indicated, along with an indication that rockfall may occur after degradation of the ground support system.

All model results summarized in the EBS PMR are based upon AMRs developed by the end of calendar 1999 for the EDA II conceptual design, which was the Project Baseline design until late January 2000. Change requests have been initiated to remove backfill from the reference design and to change the emplacement drift orientation to minimize the effects of rockfall. The effects of this design change are currently being assessed, and will be documented by ICN or revision of selected AMRs. They will be incorporated in the next revision of this PMR. The following AMRs will be the most significantly affected:

- E0120 Multiscale Thermohydrologic AMR
- E0100 Physical & Chemical Environment AMR
- E0015 EBS FEPS/Degradation Analysis
- E0050 EBS Radionuclide Transport AMR
- E0080 Drift Degradation Analysis AMR
- E0090 Water Distribution & Removal AMR.

The removal of backfill will have major effects on temperature and relative humidity within the drift during the first few thousand years, on the importance of rockfall, on the flow pathways of water entering the drifts, and on the chemistry of water contacting the drip shields and waste packages. Detailed evaluations are underway as of this writing. It is expected that detailed analyses of the impact of removing backfill, coupled with detailed design of the EBS, will produce a system with the performance equal to or better than the EDA II conceptual design

The waste package is the principal engineered barrier, and it has been designed to last well beyond the 10,000-year design life for the potential Yucca Mountain repository. Degradation by corrosion is the expected WP failure mode, and materials have been selected to have very small

corrosion rates under anticipated environmental conditions. However, other degradation modes, including material or manufacturing defects, undetected damage in handling, and other factors may lead to early failure of a small number of waste packages.

Other components of the EBS, such as drip shields and backfill, are collectively referred to as the EBS in this PMR. The WP lifetime will depend to some degree on EBS system performance and other operational controls on the waste package environment. Key environmental variables controlling waste package corrosion rate include the presence and chemical composition of liquid water on the waste package surface. The flux of liquid water at the waste package surface has little effect on the corrosion rate, and is not a factor in the waste package degradation model. However, it is the most important determinant of the rate of waste-form degradation and, ultimately, the rate of radionuclide mobilization and release, after the WPs are breached.

The major functions of the EBS—combined with suitable preclosure thermal management operations—are to control the amount of water contacting the containers, to control the time at which water contact occurs, and to provide predictable near-field environmental conditions. In this report, "near-field" is used to describe the region within the drift and the host rock within a few meters of the drift. Successful implementation of these functions will provide defense in depth and reduce uncertainty in performance analyses.

Figure 1-4 is a schematic cross-section of an emplacement drift for the EDA II conceptual design, showing major components and processes that are addressed in the EBS PMR. These processes include the evolution of heat by radioactive decay, seepage into and flow within the drift, evaporation and condensation, deposition of salts and precipitates, gas exchange with the surrounding rock, chemical reactions between water, rock, and introduced materials, corrosion, formation of colloids, growth of microbes, and transport of radionuclides through the invert by advection and diffusion.

Both design and pre-closure operations affect these processes and their impact on repository performance. For example, the drip shield and backfill work together to divert water from contact with the waste package and direct it to the invert, from which it must drain into the host-rock fracture system. The backfill also performs the following functions:

- Protects the drip shield from damage by rockfall

- Provides a capillary barrier reducing water seepage through a degraded drip shield

- Limits salt deposition directly on the drip shield

- Helps moderate the water chemistry inside the drift, providing some buffering of pH and silica concentration

Ventilation is an example of a preclosure operation affecting postclosure processes that determine the evolution of the in-drift environment. Ventilation removes heat from the drifts and moisture from the surrounding rock, resulting in a cooler and drier initial condition at closure than would be the case without ventilation. Evolution of the in-drift physical and chemical

environment also depends upon the choice of materials for engineered components, such as ground support, invert, backfill, and others.

After closure, evolution of the in-drift physical and chemical environment for the EDA II design must take into account the following processes and phenomena:

- Exchange of liquid water and its dissolved species between the drift and the surrounding rock

- Exchange of water vapor, CO_2, and O_2 between the drift and its surroundings, including the host rock, access drifts, and other underground openings

- Formation of corrosion products

- Chemical reaction of water with introduced materials (e.g., rockbolts, grout, rails, copper bus bars, backfill, and invert ballast)

- Growth of microbes

- Changes in water chemistry resulting from reactions with rock, gases, and introduced materials

- Deposition and dissolution of salts and precipitates

- Formation of colloids that sorb radionuclides.

Corrosion may be accelerated if conditions favor microbial growth, and radionuclide solubility may be affected by the concentration of major ions in water within the drift. Colloids produced by corrosion of carbon steel strongly sorb some radionuclides, potentially increasing their total concentration in contaminated water above the amount in solution.

After release from the waste packages, radionuclides dissolved, or suspended as colloids, will be transported through the invert, either by advection or diffusion. If the advective flux is small enough, and the water content of the invert is low, diffusion will be the dominant radionuclide-transport mechanism through the invert, and the diffusion coefficient will be small. Under these conditions, the mass-release rate at steady state could be reduced by the presence of the invert. Otherwise, the invert will not contribute significantly to overall performance of a potential repository because it will provide, at most, a small transient delay between the time of release from the waste package and the time of entry into the host rock.

Process-model results addressing topics introduced in the preceding paragraphs were developed for selected locations within the potential repository footprint. To assess the effects of laterally variable boundary conditions (e.g., infiltration and thermal edge effects), a multiscale thermohydrologic (MSTH) process model provides both the spatial variation and the temporal evolution of thermohydrologic environmental conditions, accounting for the interactions among emplacement drifts. Output data from that model include temperature, relative humidity, liquid saturation and flux, gas flux and air-mass fraction, capillary pressure, and evaporation rates as

functions of time. These data are calculated for selected locations within and near the emplacement drifts.

Features, events, and processes (FEPs) potentially affecting system performance are addressed in a formal screening process. They are also used to develop an analysis of possible failure modes for the EBS as a whole.

Finally, results of the major process models are abstracted for input to the Total System Performance Assessment for Site Recommendation (TSPA-SR).

1.5.1 Features, Events, and Processes for the Engineered Barrier System

The purpose of the EBS is to ensure that any release of radioactive materials from the waste material in the repository into the environment results in doses to potentially impacted populations that are below allowable levels as set by the NRC and EPA. While the primary barrier to such release is the waste package within which the high level nuclear waste is placed prior to emplacement in the repository, there are many aspects of the remainder of the engineered portion of the repository that have a significant influence on repository performance. Key features of the EBS (drip shield, invert, etc.), EBS-impacting events that may occur over the life of the repository (seismic activity, igneous activity, etc.), and processes that go on within the EBS (mechanical and/or corrosive damage to the drip shield, transport of released radionuclides through the EBS, etc.) must be considered when evaluating repository performance. This section summarizes the rationale for determining which FEPs should be "included" in, or "excluded" from the TSPA, and identifies the associated key issues for the EBS. A more complete discussion of how these FEPs were identified, and a description of the included FEPS can be found in Section 2.4.

Based on the experience obtained from other geologic repository programs, prior TSPAs done for the Yucca Mountain project, and a general scientific understanding of the processes that may go on within the entire repository, it is possible to develop a comprehensive list of FEPs that may be important to repository performance. In determining importance relative to the EBS at Yucca Mountain, there are three important issues that must be considered; (a) how the EBS impacts the failure (corrosion or mechanical) of the waste package, (b) how the EBS impacts mobilization of contaminants subsequent to waste package failure, and (c) how the EBS impacts the transport of contaminants from the drift.

a) Corrosion and/or mechanical failure of the waste packages is an EBS issue with respect to how the EBS impacts these processes. Specifically one must be concerned with such issues as the amount of water (liquid or vapor) transported to the waste package, the chemistry of such water, and the degree to which the EBS may limit mechanical damage due to rockfall. Key aspects of the EBS that are important for water transport include the drip shield and backfill (if used). For the water chemistry, corrosion of metallic components within the EBS (ground supports, pedestal, rails, etc.) and interaction with cementitious materials (grout around rock bolts) is important. For mechanical failure assessment, the drip shield, backfill (if used), and the pedestal are potentially important.

b) Mobilization of contaminants is an EBS issue with respect to how the EBS impacts such mobilization. Of specific importance are 1) the volumetric rate of liquid water directed to the container/container carcass (focusing of drip/flow by the drip shield or ground support), and 2) the chemistry of the liquid water redirected to the container/container carcass (as altered by engineered materials and mineral dissolution).

c) Transport from the EBS is specifically an EBS problem with respect to EBS control of 1) physical alteration of drainage (fines, TM fracture closure, colloid filtration, etc), and 2) chemical alteration of drainage (THC mineral alteration in fractures and pores in the floor, colloid agglomeration, etc).

Relative to these three issues, a FEP must generally be considered in the Yucca Mountain TSPA unless one of the following criteria can be demonstrated to be met:

- Exclude on the basis of "Low Probability", if a FEP has less than one chance in 10,000 of occurring over 10,000 years.

- Exclude on the basis of "Low Consequence", if omission of the FEP does not significantly change the expected annual dose.

Based on the three EBS-important issues discussed above and the two exclusion criteria, comprehensive screening and assessment of potential EBS FEPs have been performed (AMR E0015, AMR E0110). A summary of the results of this assessment is found below in Table 1-3. The string of numbers following each FEP refers to the identification of the primary FEP within the comprehensive Yucca Mountain FEPs database (CRWMS M&O 2000c). FEPs identified as "Exclude" have been determined to be unimportant by virtue of having met one of the four criteria above. FEPs that did not meet one of these criteria are by default designated "Include" and are to be considered in the TSPA. FEPs that are relevant to the important EBS issues (designated a, b, or c above) are identified. Some of the "included" FEPs are applicable to process model reports other than the EBS PMR. These FEPs are identified as "N/A" for the EBS PMR, and the applicable PMR is referenced parenthetically. Some FEPs are addressed in the repository design process, and are identified as "Design FEPs." They are "included," but are not part of TSPA. Several FEPs are excluded because they go beyond what the regulations require of TSPA. An example of such FEPs are operational accidents. These exclusions are explained as "regulatory". In these cases the applicable design regulations and requirements are relied upon to minimize the FEP detrimental effects.

Table 1-3. Summary of EBS FEP Screening

FEP Name and Reference YMP FEP Database Number	Screen-ing Result	Exclusion Rationale or Exclusion Basis	Important EBS Issues
Excavation/Construction - YMP 1.1.02.00.00	Exclude	Low Consequences	
Site Flooding (During Construction and Operation) – YMP 1.1.02.01.00	Exclude	Regulatory	
Effects of Preclosure Ventilation – YMP 1.1.02.02.00	Include		(a)
Undesirable Materials Left – YMP 1.1.02.03.00	Exclude	Low Consequences	
Error in Waste or Backfill Emplacement – YMP 1.1.03.01.00	Exclude	Regulatory	
Repository Design – YMP 1.1.07.00.00	Include	Design FEP	(a), (b), (c)
Quality Control – YMP 1.1.08.00.00	Include	Design FEP	(a), (b), (c)
Accidents and Unplanned Events During Operation – YMP 1.1.12.01.00	Exclude	Regulatory	
Retrievability – YMP 1.1.13.00.00	Include	Design FEP	(a), (b), (c)
Igneous Intrusion into Repository – YMP 1.2.04.03.00	Include	N/A (see DE PMR)	(a), (b), (c)
Corrosion of Waste Containers – YMP 2.1.03.01.00	Include	N/A (see WP PMR)	(a)
Container Healing – YMP 2.1.03.10.00	Include	N/A (see WP PMR)	(b)
Container Failure (Long-term) – YMP 2.1.03.12.00	Include	N/A (see WP PMR)	(a), (b), (c)
Preferential Pathways in the Backfill – YMP 2.1.04.01.00	Include		(a)
Physical and Chemical Properties of Backfill – YMP 2.1.04.02.00	Include		(a), (b), (c)
Erosion or Dissolution of Backfill – YMP 2.1.04.03.00	Exclude	Low Consequences	
Mechanical Effects of Backfill – YMP 2.1.04.04.00	Include		(a)
Backfill Evolution - YMP 2.1.04.05.00	Include		
Properties of Bentonite – YMP 2.1.04.06.00	Exclude	Not in Baseline	
Buffer Characteristics – YMP 2.1.04.07.00	Exclude	Not in Baseline	
Diffusion in Backfill – YMP 2.1.04.08.00	Exclude	Low Consequences	
Radionuclide Transport Through Backfill – YMP 2.1.04.09.00	Exclude	Low Consequences	
Degradation of Cementitious Materials in Drift – YMP 2.1.06.01.00	Include		(a), (b), (c)
Effects of Rock Reinforcement Materials – YMP 2.1.06.02.00	Include		(a), (b), (c)
Degradation of the Liner – YMP 2.1.06.03.00	Exclude	Not in Baseline	
Flow Through the Liner – YMP 2.1.06.04.00	Exclude	Not in Baseline	
Degradation of Invert and Pedestal – YMP 2.1.06.05.00	Include		(a), (b), (c)
Effects and Degradation of Drip Shield – YMP 2.1.06.06.00	Include		(a), (b), (c)

Table 1-3. Summary of EBS FEP Screening (Continued)

FEP Name and Reference YMP FEP Database Number	Screen-ing Result	Exclusion Rationale or Exclusion Basis	Important EBS Issues
Effects at Material Interfaces – YMP 2.1.06.07.00	Exclude	Low Consequences	
Rockfall (Large Block) – YMP 2.1.07.01.00	Exclude	Low Consequences	
Mechanical Degradation or Collapse of Drift – YMP 2.1.07.02.00	Exclude	Low Consequences	
Movement of Containers – YMP 2.1.07.03.00	Include	N/A (see WP PMR)	(a)
Hydrostatic Pressure on Container – YMP 2.1.07.04.00	Exclude	Low Probability	
Creeping of Metallic Materials in the EBS – YMP 2.1.07.05.00	Exclude	Low Consequences	
Floor Buckling – YMP 2.1.07.06.00	Exclude	Low Consequences	
Increased Unsaturated Water Flux at the Repository – YMP 2.1.08.01.00	Include		(a)
Enhanced Influx (Philip's Drip) – YMP 2.1.08.02.00	Exclude	Low Consequences	
Condensation Forms on Backs of Drifts – YMP 2.1.08.04.00	Include		(a), (b), (c)
Flow Through Invert – YMP 2.1.08.05.00	Include		(c)
Wicking in Waste and EBS – YMP 2.1.08.06.00	Include		(c)
Pathways for Unsaturated Flow and Transport in the Waste and EBS – YMP 2.1.08.07.00	Include		(a), (b), (c)
Induced Hydrological Changes in the Waste and EBS – YMP 2.1.08.08.00	Include		(a), (b), (c)
Saturated Groundwater Flow in Waste and EBS – YMP 2.1.08.09.00	Exclude	Low Consequences	
Resaturation of Repository – YMP 2.1.08.11.00	Include		(c)
Properties of the Potential Carrier Plume in the Waste and EBS – YMP 2.1.09.01.00	Include		(a), (b), (c)
Interaction with Corrosion Products – YMP 2.1.09.02.00	Include		(b), (c)
In-drift Sorption – YMP 2.1.09.05.00	Exclude	Low Consequences	
Reduction-oxidation Potential in Waste and EBS – YMP 2.1.09.06.00	Include		(b), (c)
Reaction Kinetics in Waste and EBS – YMP 2.1.09.07.00	Exclude	Low Consequences	
Chemical Gradients/Enhanced Diffusion in Waste and EBS – YMP 2.1.09.08.00	Exclude	Low Consequences	
Waste-Rock Contact – YMP 2.1.09.11.00	Exclude	Low Consequences	
Rind (Altered Zone) Formation in Waste, EBS, and Adjacent Rock – YMP 2.1.09.12.00	Include		
Complexation by Organics in Waste and EBS – YMP 2.1.09.13.00	Exclude	Low Consequences	
Colloid Formation in Waste and EBS – YMP 2.1.09.14.00	Include		(b), (c)
Formation of True Colloids in Waste and EBS – YMP 2.1.09.15.00	Exclude	Low Consequences	
Formation of Pseudo-colloids (Natural) in Waste and EBS – YMP 2.1.09.16.00	Include		(b), (c)
Formation of Pseudo-colloids (Corrosion Products) in Waste and EBS – YMP 2.1.09.17.00	Include		(b), (c)

Table 1-3. Summary of EBS FEP Screening (Continued)

FEP Name and Reference YMP FEP Database Number	Screening Result	Exclusion Rationale or Exclusion Basis	Important EBS Issues
Microbial Colloid Transport in the Waste and EBS – YMP 2.1.09.18.00	Exclude	Low Consequences	
Colloid Transport and Sorption in the Waste and EBS – YMP 2.1.09.19.00	Exclude	Low Consequences	
Colloid Filtration in the Waste and EBS – YMP 2.1.09.20.00	Exclude	Low Consequences	
Suspensions of Particles Larger than Colloids – YMP 2.1.09.21.00	Exclude	Low Consequences	
Biological Activity in Waste and EBS – YMP 2.1.10.01.00	Include		(a), (b), (c)
Heat Output / Temperature in Waste and EBS – YMP 2.1.11.01.00	Include		(a), (b), (c)
Exothermic Reactions in Waste and EBS – YMP 2.1.11.03.00	Exclude	Low Consequences	
Temperature Effects / Coupled Processes in Waste and EBS – YMP 2.1.11.04.00	Include		(a), (b), (c)
Differing Thermal Expansion of Repository Components – YMP 2.1.11.05.00	Exclude	Low Consequences	
Thermally-induced Stress Changes in Waste and EBS – YMP 2.1.11.07.00	Include		(a)
Thermal Effects: Chemical and Microbiological Changes in the Waste and EBS – YMP 2.1.11.08.00	Include		(b), (c)
Thermal Effects on Liquid or Two-phase Fluid Flow in the Waste and EBS – YMP 2.1.11.09.00	Include		(c)
Thermal Effects on Diffusion (Soret effect) in Waste and EBS – YMP 2.1.11.10.00	Exclude	Low Consequences	
Gas Generation – YMP 2.1.12.01.00	Exclude	Low Consequences	
Gas Generation (He) from Fuel Decay – YMP 2.1.12.02.00	Exclude	Low Consequences	
Gas Generation (H_2) from Metal Corrosion – YMP 2.1.12.03.00	Exclude	Low Consequences	
Gas Generation (CO_2, CH_4, H_2S) from Microbial Degradation – YMP 2.1.12.04.00	Exclude	Low Consequences	
Gas Generation from Concrete – YMP 2.1.12.05.00	Exclude	Low Consequences	
Gas Transport in Waste and EBS – YMP 2.1.12.06.00	Exclude	Low Consequences	
Radioactive Gases in Waste and EBS – YMP 2.1.12.07.00	Include	N/A (see WF PMR)	(c)
Gas Explosions – YMP 2.1.12.08.00	Exclude	Low Consequences	
Radiolysis – YMP 2.1.13.01.00	Include	N/A (see WF PMR)	
Radiation Damage in Waste and EBS – YMP 2.1.13.02.00	Exclude	Low Consequences	
Mutation – YMP 2.1.13.03.00	Exclude	Low Consequences	
Episodic / Pulse Release from Repository – YMP 2.2.07.06.00	Include	N/A (see NFE PMR)	(a), (b), (c)
Redissolution of Precipitates Directs More Corrosive Fluids to Containers – YMP 2.2.08.04.00	Include		(a), (b), (c)
Gas Pressure Effects – YMP 2.2.11.02.00	Exclude	Low Consequences	

The degradation of some repository elements may be initiated simultaneously by events or processes that are referred to as "common mode" degradation events or processes. These include: increased seepage, thermal-hydrologic-mechanical (THMC) coupled processes, THMC rock alteration, thermal-hydrologic-chemical (THC) coupled processes, THC salt production, Faulting, and seismicity. Common mode degradation events and processes are discussed in more detail in Section 2.4.

1.5.2 Water Distribution and Removal

The water distribution and removal (WD&R) process model bounds the fraction of liquid water entering the drift that will be prevented from contacting waste by the combined effects of engineered controls on water distribution and on water removal. The approach is flexible, yet detailed enough to analyze different design solutions for water diversion (e.g., drip shields alone, drip shields with backfill, capillary barriers with or without drip shields). Water can be removed during preclosure operation by evaporation from ventilation and after closure by drainage into the fractured host rock. Engineered drains may be required to ensure that adequate drainage capacity survives the thermal pulse.

1.5.3 Description of Physical and Chemical Environment Process Model

This section provides an overview of the *Engineered Barrier System: Physical & Chemical Environment Model* (CRWMS M&O 2000t), hereafter referred to as the P&CE AMR, its supporting models, and the eight in-drift geochemical environment process models listed below the P&CE AMR in Table 1-1. The P&CE model provides bounding predictions for changes in aqueous chemistry and gas-phase composition within the emplacement drifts as a result of interaction of engineered materials and components with heat and water. It accounts for some variability in seepage and drainage fluxes, the effects of temperature changes on chemical equilibria and reaction kinetics, the physical processes of evaporation and condensation, and the effects of rockfall debris. The P&CE AMR defines and provides documentation for seven models:

1. P&CE Thermal Hydrology Model
2. P&CE Gas Flux and Fugacity Model
3. P&CE Cementitious Materials Model
4. P&CE Microbial Effects Model
5. P&CE Precipitates and Salts Model
6. P&CE Colloid Model
7. P&CE Chemical System Model

As previously noted in Table 1-1, these models are discussed in Sections 3.1.2 and 3.2.2, along with the related process AMRs feeding directly to the abstraction AMRs.

1.5.4 Engineered Barrier System Radionuclide-Transport Model

The radionuclide transport model quantifies and evaluates radionuclide transport within the emplacement drift invert, as a result of releases from one or more breached waste packages. Advective-dispersive-diffusive contaminant transport and the sorption of radionuclides are described in the radionuclide transport model. Results generated by the *Water Distribution and*

the Removal Model (CRWMS M&O 2000q) provide the input to the one-dimensional contaminant transport equation used in this analysis.

1.5.5 Multiscale Thermohydrologic Model

The heat decay emitted from nuclear waste emplaced in the potential geologic repository will change the original condition of the host rock. One of the most obvious disturbances is the change in thermal-hydrology (TH) conditions in both the near field and far field. The multiscale thermohydrologic model (MSTH) (CRWMS M&O 2000i) simulates the thermally-driven physical changes to the underground water (evaporation and condensation) and host rock (heating and cooling) surrounding the potential repository. In this model, THM, THC, and THMC coupled effects are not included explicitly – i.e., flow properties such as fracture and matrix porosity and permeability are unaltered by thermal processes. This approach is consistent with previous sensitivity studies (CRWMS M&O, 1998g; Sections 3.6.8.1.3 and 3.6.8.2) which showed that TH effects from order-of-magnitude decreases in fracture permeability, are small because the initial permeability greatly exceeds that required to sustain TH flow processes. Also, recent modeling work (CRWMS M&O 2000x) indicates that absolute changes in fracture porosity from mineral dissolution and precipitation are on the order of 10^{-4}, which is much smaller than the values for fracture porosity (approximately 10^{-2}) used for the host rock in these models.

The need for a multiscale modeling approach stems from the fact that the performance measures depend on TH behavior within a few meters of the emplacement drifts and also on thermal and TH behavior on a potential repository (or mountain) scale. A single numerical model (e.g., embedding a 3-D drift-scale model with a relatively fine mesh into a 3-D mountain-scale model with a coarse mesh) would require an unfeasible number (millions) of grid blocks. The MSTH model has been developed for estimating the results that would be obtained if such a single model were feasible. In addition to coupling the drift scale and mountain scale, the MSTH also allows for consideration of the effect of different waste packages types (e.g., different CSNF waste packages, co-disposal of defense HLW) on the various performance measures.

The MSTH consists of four major models and includes multiple scales (mountain and drift), multiple dimensions (1-D, 2-D and 3-D) and varying assumptions regarding the coupling of heat transfer to fluid flow (conduction-only and fully coupled thermohydrologic). These four models (described in Section 3.1.4.3) are:

- LDTH (Line-averaged-heat-source, Drift-scale, Thermohydrologic) Submodel
- SMT (Smeared-heat-source, Mountain-scale, Thermal-conduction) Submodel
- SDT (Smeared-heat-source, Drift-scale Thermal-Conduction) Submodel
- DDT (Discrete-heat-source, Drift-scale Thermal-conduction) Submodel

The MSTH Model estimates the temporal evolution of the key TH response variables, including liquid-phase flux, temperature, relative humidity, gas-phase air-mass fraction, and evaporation rate, at selected locations within and near the drift. The model accounts for the following effects:

- Site-scale variability of percolation flux
- Temporal variability of percolation flux

- Uncertainty in percolation flux
- Site-scale variability in hydrologic properties
- Edge-cooling effects
- Dimensions and properties of the EBS components
- WP heat variability
- Site-scale variability in thermal conductivity and overburden thickness.

Key output variables (as functions of time) include host-rock, WP-surface, and drift-wall temperatures; relative humidity values at the DS and WP surfaces; and fluxes of water vapor and liquid within and near the drifts.

1.5.6 EBS Model Abstractions

For the P&CE Abstraction, aqueous flow and transport paths in the emplacement drifts define representative locations where important chemical and physical processes occur, such as changes in water composition, corrosion of drip shields and waste packages, and dissolution of waste forms. These locations, and associated processes, are given below:

- Air Gap and Backfill - Seepage and capillary fluxes of water

- Drip Shield Surface - Water diversion, and possible leakage to the WP

- WP Surface - Water diversion, and possible leakage to the WF

- Waste Form - Advective transport and molecular diffusion of radionuclides from the WF to the invert

- Invert - Mixing of water from different flow paths, and radionuclide transport to the host rock by advection and molecular diffusion

- Except for the waste form location, inputs for the P&CE abstraction are obtained from AMRs supporting the EBS PMR. These include the AMRs listed under the P&CE heading in Table 1-1.

The P&CE abstraction model includes processes affecting gas composition in the drift, and the flux of gas-phase components to the drift from the host rock. The major processes that can affect composition include:

- Ambient and thermally perturbed gas-phase mass flux through the drifts

- Liquid-phase seepage flux

- Boiling, evaporative concentration, and evaporative precipitation in the emplacement drifts

- Possible sources and sinks involving water in the host rock

- Chemical reactions in the emplacement drifts, including those which involve introduced materials.

The effects of introduced materials on the P&CE are abstracted from AMRs for Seepage-Cement Interaction, Seepage/Backfill Interactions, Seepage/Invert Interactions, and Corrosion Products. These address the following processes:

- Evaporation of influent seepage water

- Precipitation of dissolved solids

- Dissolution of quartz and redissolution of precipitates

- Porosity reduction from precipitates

- Corrosion and consumption of oxygen

- Formation of colloids that sorb radionuclides.

The *In-Drift Microbial Communities Model* (CRWMS M&O 2000f) is used to bound the mass of microbes and biomass that could be present, per meter of drift, as a function of time. Outputs from this model are used to describe microbially induced corrosion (MIC) of the WP, and the potential generation of microbial colloids.

The *In-Drift Precipitates/Salts Analysis* (CRWMS M&O 2000g) is abstracted to determine the effects of evaporative processes on water composition in the EBS. Important parameters include relative humidity, temperature, CO_2 fugacity, influent seepage composition, and rates of liquid influx and evaporation. Calculated results include pH, chloride concentration, and ionic strength, which are used to estimate DS and WP corrosion rates, and for estimating dissolved and colloidal radionuclide concentrations.

The *In-Drift Colloids and Concentrations* AMR (CRWMS M&O 2000d) is abstracted to estimate the role of colloids in radionuclide transport through the EBS to the host rock.

The Multi-scale TH Model abstraction provides a modified description of the MSTH process model output, which directly supports TSPA-SR. The abstracted information includes appropriately averaged temperature, liquid saturation, relative humidity, evaporation rate, and percolation flux as functions of time and location in the potential repository. The abstracted quantities used by TSPA are based on assignment of waste packages to "bins" based on the local infiltration rate. Additionally, the hottest and coolest waste packages are identified.

Abstraction includes characterization of the spatial and temporal variability, and uncertainty in model results represented by sets of calculations run with different input parameter sets.

The EBS Radionuclide Transport Abstraction model accounts for water contact with the waste packages by condensing under the DS, by flow through a failed DS, or by leakage through an intact DS. Proper design and placement of the DS may eliminate the latter contact pathway. Pathways into the breached waste package include stress corrosion cracks and corroded patches

through the sides of the WP. Pitting of the WP is not anticipated to occur because of the chemical environment around the WP.

The radionuclide-transport abstraction model is based on 1-D advective and diffusive transport. The transport pathway from the WF downward to the drift wall is defined using model cells in the following order:

- A WF/WP cell that represents the release of radionuclides from the WF and the transport of radionuclides in the WP through breaches in the WP

- A cell that represents transport through the granular invert.

These cells require definitions of volume, material properties, and radionuclide solubility limits. Both advective- and diffusive-transport mechanisms are included in the transport connections between cells.

The two primary inputs are: 1) the release rate of radionuclides from the WF, and 2) the flux and chemistry of water moving through the WP and invert. These two inputs are boundary conditions for the transport abstraction. Dissolved radionuclide concentrations mobilized from the WF are constrained by the solubility limit of each radionuclide. The solubility constraints are described as functions of the water composition along the transport pathway. Similarly, the flux and chemistry of water moving through the EBS is based on abstractions from NUFT calculations and other chemistry calculations.

1.5.7 Validity of the Abstractions

Abstraction analyses and reports are categorized according to those that support quantitative models that are used directly in TSPA-SR, and those that are conceptual in nature and provide more qualitative input. Discussion of validity is limited to the quantitative models:

- *In-Drift Precipitates/Salts Analysis* (CRWMS M&O 2000g)
- *In-Drift Microbial Communities Model* (CRWMS M&O 2000f)
- *EBS Radionuclide Transport Abstraction* (CRWMS M&O 2000a).

Given accurate inputs, the In-Drift Precipitates/Salts Analysis is expected to provide results that are within an order of magnitude for chloride concentrations and ionic strength, and within a pH unit for pH predictions. These accuracy criteria can provide useful reduction of uncertainty on the listed parameters. To test the High Relative Humidity (HRH) Salts Model, results were compared to measured data from three laboratory evaporation tests. Each test involved evaporation of representative waters under particular test conditions. Two used synthetic J-13 water and one used synthetic Topopah Spring tuff porewater. For each test, the HRH Salts Model calculated the pH within one unit, and the chloride concentration within 20 percent. The ionic strength calculation was within a factor of two.

Empirical data are not available to test the accuracy of the Low Relative Humidity (LRH) Salts Model. However, the model produces plausible results for chloride concentration and ionic strength in the relative humidity range 50 percent to 85 percent, while adequately negotiating the

transition to the HRH Salts Model at relative humidity of 85 percent. Although simplifying assumptions are used in these models, they tend to contribute conservatism.

Three general validation tests were conducted for the *In-Drift Microbial Communities Model* (CRWMS M&O 2000f). The first test replicated a predictive model that was developed for the Swiss low-level waste repository program. The second test demonstrated that the model can simulate certain observed features of the host rock in the Exploratory Studies Facility (ESF), and observations from an analog site in another tuff unit. The calculated results agree with observations, to within an order of magnitude. The results are also consistent with laboratory-based findings that availability of water and phosphorous are limiting factors to microbial growth. A third comparison showed that the numbers of organisms calculated by the model are within an order of magnitude of measured values. Together these tests provide confidence that the model satisfactorily represents the factors controlling microbial growth, and that microbial growth and activity in the host rock are in fact nutrient-limited.

The EBS Radionuclide Transport abstraction model is a conservative, bounding model, which helps to ensure that it is valid for use in TSPA-SR. Bounding approximations used in the model include:

- After stress corrosion cracks form in the lid of the WP, the WF is assumed to be covered with a thin liquid film that supports radionuclide diffusion. This is a conservative approach for two reasons. First, thin films may not be able to flow through the stress corrosion cracks in the lid of the WP. And second, the heat from the WP may evaporate all liquid from the inside of the waste package, leading to a dry environment that does not support diffusive or advective transport.

- Release of radionuclides by advective transport is proportional to the total axial length of all patches divided by the total axial length of the barrier (DS or WP). This assumption is conservative because it assumes that all the flux on the barrier will flow into an open patch if it flux is located at the same axial location as the patch. It is also conservative because it ignores the factor of 2 inherent in flux splitting to the right-hand or left-hand side of the crown.

- Diffusive transport through the invert uses a conservative calculation for the value of the diffusion coefficient. First, the free water diffusion coefficient is based on the self-diffusivity of water, a bounding value for all radionuclides of interest for the TSPA-SR. Second, the correction to the diffusion coefficient for porosity and saturation in the invert is based on a conservative version of Archie's law.
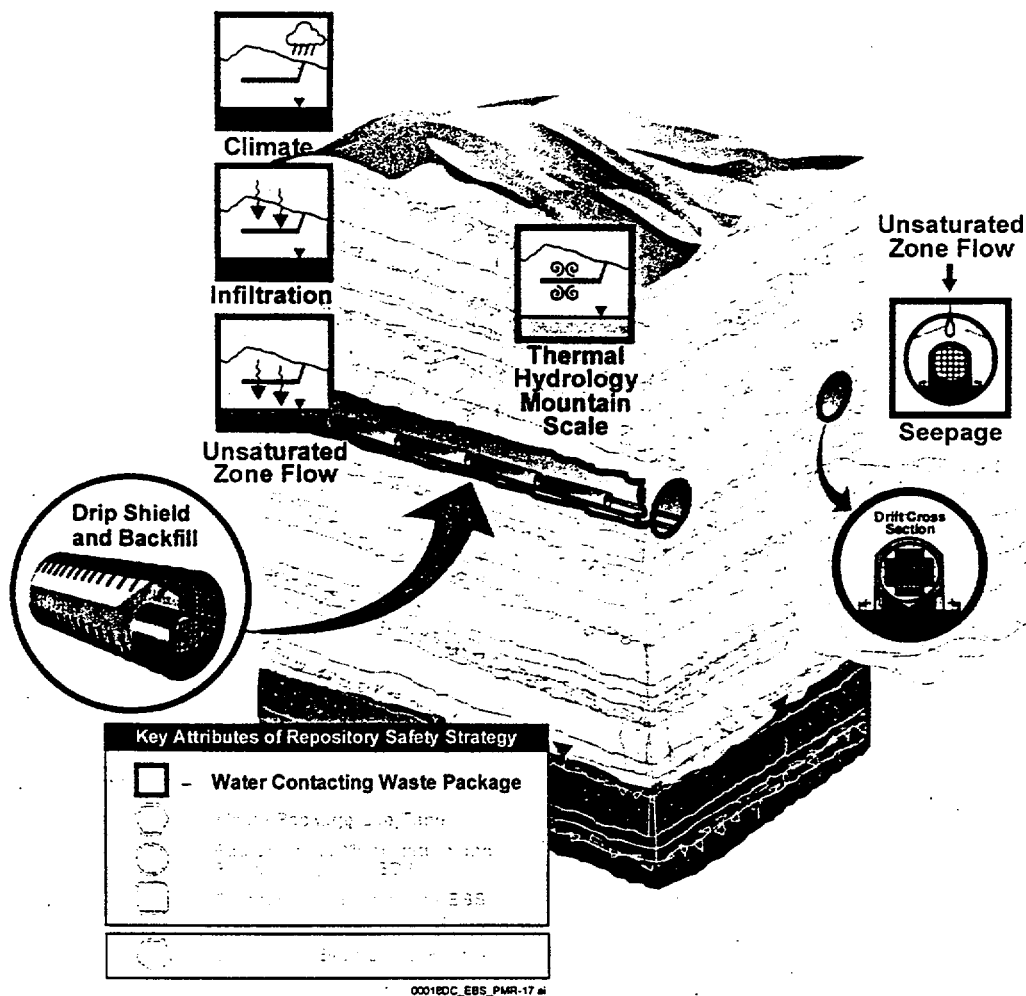
Figure 1-1. Schematic Cutaway View of the Yucca Mountain Unsaturated Zone, Showing Emplacement Drifts and Processes That Determine Water Entry In the Drifts

Plan View
Repository Layout
~1125 acres

North
Ramp

Emplacement Drifts

South
Ramp

Expansion Area

Service Drift

Emplacement Drift

Enlargement of
a Section of Drifts

Service Drift

Cutaway of a Drift with
Three Representative
Waste Package Types

Drip
Shield

Boiling Water
Reactor (BWR)
Waste Package

Co-disposal Five Waste
Package Containing
High-Level Waste (HLW)
Canisters with One DOE
Spent Nuclear Fuel (SNF)
Assembly

Steel Sets
for Ground
Control

Gantry
Crane Rail

Pressurized Water
Reactor (PWR)
Waste Package

00018DC_EBS_PMR-08.ai

Figure 1-2. Schematic View of the Potential Repository Layout, Drift Connections and
Representative Waste Package Types Within an Emplacement Drift
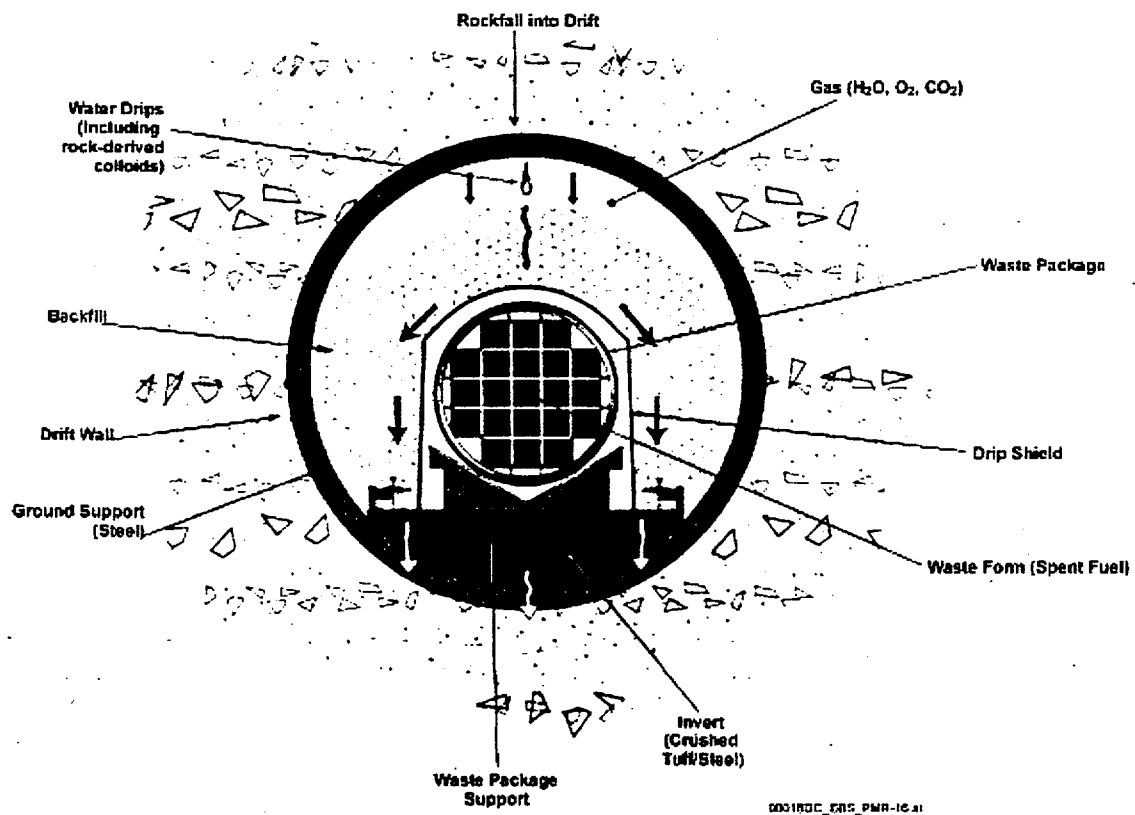
Figure 1-3. Schematic Cross-section of an Emplacement Drift Containing a 21-PWR Waste Package, Showing Major Elements of the EDA II Design for the EBS

Processes Controlling the In-Drift Chemical Environment

Gas Flux and Fugacity in the Host Rock
- pCO_2, pO_2
- Flux CO_2
- Flux O_2
- Flux H_2O
- Relative Humidity

Water-Solids Chemistry
- pH, Na^+, K^+, Ca^{2+}, Mg^{2+}
- Fe^{3+}, Al^{3+}, $SiO_2(aq)$,
- Cl^-, F^-, SO_4^{2-}, ΣCO_3^{2-}

Colloids
- Natural Colloid Abundances

In-Drift

Gas Flux and Fugacity
- pO_2, Flux O_2
- pCO_2, Flux CO_2
- Relative Humidity, Flux H_2O

Water-Solids Chemistry
- pH, Na^+, K, Ca^{2+}, Mg^{2+}
- Fe^{3+}, Al^{3+}, $SiO_2(aq)$,
- Cl^-, F^-, SO_4^{2-}, ΣCO_3^{2-}
- Ionic Strength (I)
- ΔpO_2, ΔpCO_2

Microbial Communities
- Microbial Mass
- Potential Bulk Chemical Effects Threshold Conditions for Microbial Activity

Colloids
- Clay Colloid Concentrations
- Iron-Oxide Colloid Concentrations

00018DC-_EBS_PMR-01.ai

Figure 1-4. EDA II Emplacement Drift Cross-section Showing the Processes Considered in the Evolution of the Physical and Chemical Environment Within the Emplacement Drifts

2. EVOLUTION OF THE ENGINEERED BARRIER SYSTEM PROCESS MODELS

In early calendar year 1999, the Yucca Mountain Site Characterization Project (YMP) Management and Operating Contractor (M&O) personnel began developing process model reports (PMRs) to provide the primary documentation in support of the safety argument and, ultimately, the license application for a potential Yucca Mountain high-level radioactive waste repository.

Initial analyses and models for EBS components were developed for the License Application Design Selection (LADS) process. A number of alternative conceptual designs were evaluated for possible improvements in the projected total system performance beyond that presented in the Total System Performance Assessment–Viability Assessment (TSPA-VA). Although the site characteristics alone are expected to prevent the release of most radionuclides to the accessible environment, additional engineering measures were proposed to reduce uncertainty and to provide defense in depth. The LADS effort resulted in the adoption, in June 1999, of Enhanced Design Alternative II (EDA II) (Wilkins and Heath 1999). The design concepts in EDA II include the following:

- Improved Waste Packages incorporating a corrosion resistant outer barrier

- The use of drip shields (DSs) and backfill to protect waste packages (WPs) from water contact and rockfall

- The use of ventilation to remove heat before closure

The EBS PMR summarizes and integrates 23 analysis/model reports (AMRs) developed to address the performance assessment of EDA II. A brief description of the component AMRs is given in Section 1.

2.1 DEVELOPMENT PHILOSOPHY FOR THE ENGINEERED BARRIER SYSTEM PROCESS MODEL REPORT

Where possible, EBS performance models are based on measured data for engineered material properties and on experiments designed to test the validity of approximations used in the models. Coping with the timing of design-selection decisions, and the continued evolution of design details requires a very flexible approach to both modeling and testing in support of the EBS PMR. Defensible bounds are presented where data are not available to support more rigorous process models.

2.2 PAST ENGINEERED BARRIER SYSTEM MODELING, ANALYSIS, AND ABSTRACTION

2.2.1 Process Models and Abstractions Prior to Total System Performance Assessment of 1995 (TSPA-95)

In analyses completed prior to the Total System Performance Assessment of 1995 (TSPA-95) (Barnard et al. 1992; Wilson et al. 1994; CRWMS M&O 1994) the EBS was incorporated as a number of compositional variables within subsystem models or implicitly within some of the

ranges used for performance parameters (e.g., solubility-limited radionuclide concentrations) where the interior conditions of failed (or perforated) WPs were immediately the same as the drift conditions. The radionuclide release from the EBS was then available to the unsaturated zone (UZ) for transport in the geosphere.

At this time, much of the EBS process modeling was simplistic and generally only dealt with WF and WP modeling under ambient conditions.

2.2.2 TSPA-95 Process Models and Abstractions

Likewise, at the time TSPA-95 was developed, much of the EBS chemical modeling was simplistic and generally only dealt with WF and WP modeling under ambient conditions. All conceptual models that were available were used to constrain EBS processes. The following paragraphs describe some of the highlights of the TSPA-95 models for in-drift chemistry, flow, and transport.

The EBS chemistry and transport models for TSPA-95 incorporated the ambient water composition from Well J-13 and atmospheric oxygen and carbon dioxide fugacities. The impacts of pH variation and temperature variation were explicitly entered into models of WP degradation, WF dissolution, and the solubility-limited concentrations of neptunium (Np), plutonium (Pu), and americium (Am) (CRWMS M&O 1995). A variable pH condition covering values of 6 to 9 (with 7 taken as the base case) was incorporated implicitly into the distributions of solubility-limited concentrations to define the mobile radionuclide concentration. This range of pH reflected the range of measurements for fluids from Well J-13. Gas-phase composition was assumed to be buffered to atmospheric values because of ready gas flow through the mountain.

For TSPA-95, EBS transport modeling of the drift was handled within the Repository Integration Program (RIP) software code using the following conceptual models for radionuclide release (CRWMS M&O 1995).

Drips-On-Waste Form–This conceptual model assumed that after one pit penetrated a WP, conditions inside of the WP became the same as those of the drift environment. Advective flux through the WP and onto the WF was also permitted as soon as a single pit penetrated the WP. Diffusive releases depended on the surface area of the WP, which was degraded or pitted through, and on the water-film thickness on the WF.

Drips-On-Waste Package–This conceptual model assumed only diffusive releases out of the WP. Advective flow remained on the surface of the WP and did not flow into the WP. The corrosion products in the pits were assumed to prevent the advective or dripping water from entering the WP.

No Advective Transport through the Drift–This conceptual model assumed no advective flow into the drift, leading to only diffusive release from the EBS. This model could be operational if the engineered system provided for diversion of all advective flow away from the drift by means of mechanisms such as a capillary barrier or a drip shield.

2.2.3 Total System Performance Assessment–Viability Assessment Process Models and Abstractions

After finalization of TSPA-95 and prior to development of the Total System Performance Assessment–Viability Assessment (TSPA-VA), the development of performance assessment models was integrated with the development of process models. Workshops were held to solicit inputs, discuss important processes, and provide input about those process models that could be used directly and those that should be developed (e.g., CRWMS M&O 1997).

In some areas, such as the TH modeling, where the process models were sufficiently developed, the process models provided input that could be used directly. In other areas, the models were not at a sufficient state of development to be used. Therefore, simplified process models were developed using process conceptual models provided by external organizations (Hardin 1998; Triay et al. 1996) that could be used directly or be abstracted for TSPA-VA.

The following subsections summarize the improvements to the TSPA-95 model that were incorporated into TSPA-VA:

2.2.3.1 In-Drift Geochemical Environment

A more detailed representation of the chemical processes within the potential emplacement drifts was included for TSPA-VA. This in-drift geochemical environment (IDGE) component included changing the composition of gas, water, colloids, and solids within the emplacement drifts under the perturbed conditions of the potential repository environment (CRWMS M&O 1998d). A set of five models was developed for TSPA-VA to represent the IDGE:

- Incoming gas, water, and colloids model (compositions of those phases as they entered the drift): this model represented the boundary conditions that were imposed on the in-drift environment

- In-drift gas phase model (composition of the gas phase relative to major gas sinks in the drift)

- In-drift water–solid chemistry model (evolution of water composition reacting with major materials and the in-drift gas phase)

- In-drift colloids model (stability and quantity of clay and iron-oxide colloids in the drift)

- In-Drift Microbial Communities

Some of the five models listed previously contained process-level calculations to represent the evolution of water, solid, and gas reactions in the system. Other models consisted of bounding arguments for applying observed values. In all five of these models, efforts were made to remain consistent to the results of the thermal-hydrologic process models and other boundary-condition process models that governed the temperature and hydrology of the EBS environment. These models were abstracted or used to develop parameters for the TSPA model.

2.2.3.2   EBS Transport

In the TSPA-VA model, the release of radionuclides into the natural environment was controlled by the transport of the radionuclides out of the WPs and through the concrete invert (included in the VA conceptual design, but replaced in EDA II by crushed tuff). Key factors affecting the transport of radionuclides through the EBS were the following (CRWMS M&O 1998e):·

- Performance of the WP
- Protection provided by cladding
- Matrix dissolution rate
- Entry and movement of water through WPs
- Colloidal transport of radionuclides
- Sorption affinity of radionuclides to the concrete below the WPs.

These key factors to EBS transport were abstracted and modeled using the RIP code.

2.3   PROCESS-MODEL DEVELOPMENT FOR THE ENGINEERED BARRIER SYSTEM

A complete list of reports documenting the analyses and models developed for the EBS PMR is given in Table 1-1. Section 1.2 summarizes the scope of the different reports and their relationship to each other. Of necessity, many of these reports, including the performance assessment (PA) abstractions, have been developed in parallel, and the EBS PMR has been developed concurrently with other, closely related PMRs [those covering unsaturated-zone (UZ)] flow and transport, waste package, and waste form). The EBS process model was developed for a baseline EBS design implementation consistent with EDA II (Wilkins and Heath 1999), with details documented in Table 2 of the *Water Distribution and Removal Model* report (CRWMS M&O 2000q, p. 20).

The potential repository design has continued to evolve, resulting in some changes in details, but the overall preclosure thermal-management goals, EBS system elements, and their intended functions remain consistent with EDA II. Forced ventilation will continue throughout the preclosure period to remove heat and moisture, WP spacing will be selected to optimize thermal performance, and the choice of drift orientation will minimize rockfall. Just prior to closure, a titanium DS will be placed over the packages. In EDA II, the DS will be covered with engineered backfill. The backfill protects the DS from rockfall; provides a more predictable in-drift thermal, hydrologic, and chemical environment than would be provided by rockfall; and works with the DS and the invert ballast to control the distribution of water within the drift.

To accommodate integration among concurrently developed AMRs contributing to the EBS PMR, and to maintain the flexibility needed to analyze changes in design details, many of the calculations documented in the AMRs were performed as sensitivity analyses. This strategy also assists in integration with other PMRs being developed in parallel. For example, ranges of parameters (e.g., seepage flux) were used instead of direct feeds from other process models. The intent is to provide the basis for assigning performance benefits to the EBS to compensate for uncertainty in the long-term predictions of natural system behavior. Model parameters for the UZ can only be loosely constrained by the application of accepted scientific principles in

analyzing available data. They cannot be measured directly. As the EBS process models mature, the confidence limits for their parameter values may be narrowed for the EBS PMR.

2.4 ENGINEERED BARRIER SYSTEM FEATURES, EVENTS, AND PROCESSES

This section summarizes the process of identifying features, events, and processes (FEPs) that are applicable to the EBS (CRWMS M&O 2000c, 2000r). The screening of candidate FEPs identified in a preliminary draft of the Yucca Mountain Site Characterization Project (YMP) FEP Database is discussed. The results are presented as a list of FEPs that are addressed in EBS process models. The FEPs are provided as input to the YMP FEP Database for consideration in the Total System Performance Assessment (TSPA). Common-mode degradation events and processes that affect the repository are identified for system-wide impact analysis.

2.4.1 Engineered Barrier System Feature, Event, or Process Identification Process

This section summarizes the analysis documented in *EBS FEPs and Degradation Modes Analysis* (CRWMS M&O 2000c). The baseline design (enhanced design alternative EDA II; (Wilkins and Heath 1999)) of the potential repository was used as the reference design to determine basic EBS design features and events. A basis for EBS FEPs was then developed by identifying a number of process categories (based on issues, concerns, and advice from various principal investigators) relevant to degradation of the EBS. Table 2-1 lists these process categories, and significant potential processes in each category. Conceptual figures to assist in visualizing these performance factors were developed. A context of event and process occurrence and water availability conditions was defined to permit the organization of the EBS FEPs, and to provide a perspective of their importance. A logic diagram was then developed to systematically identify the EBS FEPs.

The FEPs that were identified in the process described above are listed and described in Table 2-2, using ebsx numbers. Table 2-2 also lists EBS FEPs that are identified (following a screening process described in Section 2.4.2) as "primary" FEPs in the YMP FEP Database, and are applicable to each process category. Database primary FEPs are identified using a string of numbers "w.x.y.z.00". While the listing of Database FEPs is redundant, it is added to ensure completeness. The FEPs listed in Table 2-2 are EBS FEPs that are addressed in the analyses and models supporting this report and in TSPA.

Table 2-1. Basis for Engineered Barrier System Features, Events, and Processes Identification

	Process Categories	Significant Potential Processes	Remarks
1.	Flow Types	Weeps	Locally-saturated flow, presumed to be fracture flow
		Drip	Dropping of water from the drift crown or fracture openings
		Matrix flow	Classic two-phase flow through the matrix
2.	Water Sources	Infiltrate	Fracture and matrix flow of water entering from the surface

	Process Categories	Significant Potential Processes	Remarks
		Condensate	Condensate formed in rock and in drift, accumulated because of thermal-hydrologic processes
		Condensate under the drip shield (DS)	Condensation of water vapor beneath the DS from water in the invert
3.	Chemistry	Rock–water interactions for condensate	Alters solutes for corrosion processes
		Rock–water interactions for infiltrate	Alters solutes for corrosion processes
		Rock–water interactions for WP effluent	Interaction of dissolved and colloidal contaminants with invert and drift floor for transport
		Rock–water interactions of fines and minerals in fractures along flow pathways	Interactions potentially plugging fractures
		Colloids	Stability in the invert; filtration and alteration in the exit transport
4.	Heat	Thermomechanical interaction, stress-evolution	Rotation of least principal stress; fracture closure; thermal expansion of rock; residual drift size
		Thermochemical interaction, transport, and sorption	Temperature rate and phase dependencies
		Thermochemical interaction, corrosion of ground support, pedestals, rails, etc.	Temperature rate dependencies
5.	Drift Alteration	Floor heave (buckling)	Buckling due to mechanical stress relief and to thermomechanical coupling
		Ground-support failure	Failure due to mechanical stress relief and thermomechanical coupling
		Rockfall	.
		Stopping up fracture zones	Localized rockfall affecting water intrusion
		Invert movement	Associated with floor and wall movement
6.	Pathways	Infiltrate entering the EBS	Fracture and matrix flow of surface water
		Condensate entering the EBS	Condensate in the rock and in the drift providing a local water source
		Movement around the DS	DS functions as designed
		Movement through the DS	DS failure in some locations
		Movement under the DS in the invert	Condensate flows along DS inner wall and then drips
		Movement through the invert	Water chemistry changes, affects consequences of ponding
		Flow–transport exiting in open fractures	Fracture exits in the drift floor
		Flow–transport exiting in plugged fractures	Fines, clays, mineral alterations, etc plug fracture exits.
		Flow–transport exiting as matrix flow	Idealized transport in porous media

Table 2-1 Basis for Engineered Barrier System Features, Events, and Processes Identification
(Continued)

7.	Corrosion	Chemical properties of infiltrate and condensate	Rock–water interactions expected to provide different water constituents for these different sources
		Corrosion of DS	Direct corrosion (water contact) and contact corrosion (with WPs or rails).
		Corrosion of pedestals	Pedestal failure putting WP on or in invert
		Corrosion of ground support	Failure of rockbolts, wire mesh, and steel sets affecting drift stability
8.	Mobilization of Contaminants	Fuel–WF effects on mobilization	Effects on solubility, speciation, colloid formation, stability
		Interaction with invert	Alteration of solute phases; sorption
		Interaction with drift floor	Alteration of solute phases; sorption
		Interaction with fractures and fracture-plugging	Mineral alterations (e.g., reaction with fines); possible ponding
9.	Transport	Through invert	Alteration of solute phases; sorption
		Along drift floor	Alteration of solute phases; sorption
		Through drift floor	Fracture and matrix flow–transport, including plugging
		Ponding and localization of flow	Ponding, episodic release, solubility limited transport
10.	Ventilation	Mine: water removal or dryout	Establishes initial conditions
		Mine: heat removal	Establishes initial conditions
		Mountain: background	Heat driven: postclosure affects temperature, moisture, exchange with atmosphere
		Mountain: chimney effects	Chimney behavior of fault zones
11.	Seals	Ramps	Not in the waste-emplacement drifts
		Shafts	Undefined in the EBS
		Drifts	Undefined purpose
12.	Drains	Location	Floor, lower ribs
		Design	Rock-filled; intercepts likely locations of stress-relief fractures
		Functional lifetime	Probably not needed during the thermal period (no liquid water)
		Plugging and other failure modes	Thermomechanical compression; fines; mineralogical changes

Table 2-2. Engineered Barrier System Features, Events, and Processes

FEP Category		FEP Number	FEP Name	FEP Description
Features				
F1	Drip Shield	ebs 2	Drip shield	Liquid water contact with the waste package is believed to affect the rate of corrosion of the metals, thus exposing the waste. The drip shield is intended to reduce direct liquid contact with the containers.
		ebs 3	Drip-shield supports	Failure of the drip-shield supports allows the drip shield to make contact with the waste package or with the rails. Because the drip shields are made of Ti, the rails of steel, and the waste packages of a high-nickel alloy, contact results in contact corrosion, possibly affecting the integrity of the waste package.
F2	Ground Support	ebs 21	Ground support – wire mesh and rockbolts	The expected life of ground support after the operational phase of the potential repository is unknown. Failure of ground support allows rockfall and development of a chimney or enlarged drift and filling of fracture or fault zones.
		ebs 22	Ground support – rockbolts and grout	Ground support introduces materials (Fe, grout, etc.) into the facility, which affects water chemistry. All ground support eventually fails, allowing rockfall, altering drift size and properties, and affecting flow pathways.
		2.1.06.01.00	Degradation of cementitious materials in drift	Degradation may occur through physical, chemical, and microbial processes. Degradation of cementitious material used for any purposes in the disposal region may affect long-term performance.
		2.1.06.02.00	Effects of rock-reinforcement materials	Degradation of rock bolts, wire mesh, and other materials used in ground control may affect the long-term performance of the potential repository.
F3	Backfill	ebs4	Backfill	Crushed rock is placed as protection for the waste package, or the drip shield and waste package, from rockfall and failure of ground support and possibly as a Richard's barrier for flow. Location of backfill and the size and material type all affect water chemistry (as well as the corrosion rates for drip shield and waste packages and dissolution rates for waste) and thermal properties (as well as waste temperatures and cladding failure). Suggestions for material type currently include sand, crushed limestone, marble, and crushed tuff. The last is the subject of investigation.
		2.1.04.02.00	Physical and chemical properties of backfill	The physical and chemical properties of the backfill may affect groundwater flow, waste package and drip shield durability, and radionuclide transport in the waste-disposal region.

Table 2-2. Engineered Barrier System Features, Events, and Processes (Continued)

FEP Category		FEP Number	FEP Name	FEP Description
		2.1.04.05.00	Backfill evolution	Properties of the backfill change through time because of processes such as silica cementation, alteration of minerals, thermal effects, and physical compaction. These changes then affect the movement of water and radionuclides in the backfill.
F4	Invert	ebs5	Invert	The invert materials, currently expected to be crushed rock, form the bed for the rails and will be the resting place for the waste package after the support pedestals fail. The invert is part of the flow pathway from the waste to the drift bottom and exit from the drift. The invert is also part of the flow pathway for water deflected by the drip shield from the waste packages. Water can accumulate in the invert, acting as a water-vapor source for corrosion or possibly ponding. Accordingly, invert materials can affect water chemistry for transport.
F5	Drains (if used)	ebs23	Drains (if used)	Water accumulation in the drift would wet the invert materials, possibly pond, and provide a continuing source of water vapor beneath the drip shield and backfill for interaction with waste packages and their supports.
F6	Operational Equipment	ebs7	Rails	Rails represent a material, steel, added to the potential repository, which is not necessary to long-term isolation, but which may have an impact on corrosion of the drip shield and on water chemistry for transport. If the Ti drip shield and the steel rails are in contact, contact corrosion is expected, which could affect the long-term ability of the drip shield to divert water from the waste package. Such contact would be expected locally as a result of a seismic disturbance, rockfall, or ground-support failure.
		ebs8	Pedestal	The pedestal may be distorted or racked because of floor heave (thermomechanical stress adjustment) and ground motion (seismic event) or may fail because of corrosion. Failure by any mode will drop the waste package onto or into the invert.
Events				
E1	Rockfall	ebs6	Rockfall-loading distortion of drip shield	Contact corrosion, compromising the drip shield or the waste package, develops as a result of displacement or distortion of the drip shield.
		2.1.04.04.00	Mechanical effects of backfill	Backfill may alter the mechanical evolution of the drift environment by providing resistance to rock creep and rockfall, by changing the thermal properties of the drift, or by other means. Impacts of the evolution of the properties of the backfill itself should be considered.

Table 2-2. Engineered Barrier System Features, Events, and Processes (Continued)

FEP Category		FEP Number	FEP Name	FEP Description
E2	Seismic Event	ebs9	Ground motion	Ground motion, generated by seismic events, provides accelerations to components of the potential repository, including the waste packages, drip shield, backfill, surrounding rock, and ground support. These accelerations cause relative motion of the components and could generate ground-support failure, rockfall, and damage to waste packages and drip shields.
		ebs11	Relative seismic motion	Ground motion in the potential repository could generate waste package displacement; relative displacement between waste package, drip shield, and rails; ground-support failure; and rockfall.
E3	Ground Support Failure	ebs12	Ground-support failure	Failure of ground support, for whatever reason, would allow rockfall, displacement of backfill and waste packages, and development of new flow pathways. Possible cases include ground motion, thermomechanical stress adjustment, and corrosion.
		2.1.11.07.00	Thermally induced stress changes in waste and EBS	Thermally induced stress changes in the waste and EBS may affect performance of the potential repository. Relevant processes include rockfall.
Processes				
P2	Dryout of Rock	2.1.08.11.00	Resaturation of potential repository	Water content in the potential repository increases following the peak thermal period.
P4	Thermo-mechanical Evolution of Potential repository Rock	ebs13	Thermomechanical evolution of a potential repository block	Thermomechanical coupling, which alters the stress state of the rock surrounding the potential repository, affects floor buckling, fracture sealing and openings to the EBS, and loading and unloading of ground support.
		2.1.04.04.00 [a]	Mechanical effects of backfill	
		2.1.08.08.00	Induced hydrologic changes in the waste and EBS	Thermal, chemical, and mechanical processes related to the construction of the potential repository and the emplacement of waste may induce changes in the hydrologic behavior of the system.

Table 2-2. Engineered Barrier System Features, Events, and Processes (Continued)

FEP Category		FEP Number	FEP Name	FEP Description
		2.1.11.07.00 [a]	Thermally induced stress changes in waste and EBS	
		2.1.11.09.00	Thermal effects on liquid or two-phase fluid flow in the waste and EBS	Temperature differentials may result in convective flow in the waste and EBS.
P5	Shear Fracture/Fault Movement and Relaxation	ebs14	Shear fracture and fault movement and relaxation	Fractures that might otherwise be closed during the thermal period, because of compression from thermal expansion, are maintained as open pathways because of shear movement. Movement also allows distortion of the drift and the relative location of drip shield, rails, and waste packages, with possible contact being established.
P6	Condensation	ebs15	Condensation beneath drip shield	Condensation on the inner surface of the drip shield circumvents its performance and provides water to drip onto the waste package and its supporting pedestal. Enhanced corrosion of waste package and pedestal becomes possible.
		2.1.06.06.00	Effects and degradation of drip shield	The drip shield will affect the amount of water reaching the waste package. Behavior of the drip shield in response to rockfall, ground motion, and physical and chemical degradation processes should be considered. Effects of the drip shield on the disposal region environment (for example, changes in relative humidity and temperature below the shield) should be considered for both intact and degraded conditions. Degradation processes specific to the chosen material should be identified and considered (for example, oxygen embrittlement should be considered for titanium drip shields).
		2.1.08.04.00	Condensation forming on backs of drifts	Emplacement of waste in drifts creates a large thermal gradient across the drifts. Moisture condenses on the roof and flows downward through the backfill.
P8	Reflux	ebs16	Reflux drainage of condensate zone	Condensate zones could contain a substantial amount of mobile water able to flow back into the drifts, perhaps as a single extended episode.
P9	Flow Along Drip Shield Wall	ebs17	Flow along drip shield (inside) wall	Water vapor is available from water otherwise diverted from the waste packages, which flows down the drip shield and enters the invert, where it may accumulate.

Table 2-2. Engineered Barrier System Features, Events, and Processes (Continued)

FEP Category		FEP Number	FEP Name	FEP Description
		ebs24	Flow along drip shield (outside) wall	Because the segmented drip shield will see liquid water, the concerns are the effectiveness of the diversion (i.e., will liquid flow pass through the overlaps) and the corrosion resistance of the drip shield material to the water chemistry in the impinging water.
		2.1.04.01.00	Preferential pathways in the backfill	Preferential pathways for flow and diffusion may exist within the backfill and may affect long-term performance of the waste packages. Backfill may not preclude hydrologic, chemical, and thermal interactions between waste packages within a drift.
		2.1.08.01.00	Increased unsaturated water flux at the potential repository	An increase in the unsaturated water flux at the potential repository affects thermal, hydrologic, chemical, and mechanical behavior of the system. Extremely rapid influx could reduce temperatures to below the boiling point during part or all of the thermal period. Increases in flux could result from climate change, but the cause of the increase is not an essential part of the FEP.
P10	Flow Through Backfill	ebs18	Flow through backfill	Flow through the backfill reacts chemically with the backfill. This chemically altered water then interacts with the drip shield and rails to eventually reach the invert.
		2.1.04.01.00 [a]	Preferential pathways in the backfill	
		2.1.08.01.00 [a]	Increased unsaturated water flux at the potential repository	
P11	Movement of Backfill Through Gaps and Separations in Drip Shield	ebs19	Movement of backfill through gaps and separations in drip shield	The continuity of the drip shield and its ability to deflect liquid water could be compromised as a result of movement produced by thermomechanical or seismic processes.
		2.1.04.04.00 [a]	Mechanical effects of backfill	
P12	Fluid Flow Into Gaps and Separations in Drip Shield	ebs20	Fluid flow into gaps and separations in drip shield	The ability of the drip shield to deflect liquid water could be compromised as a result of the movement of liquid water through gaps or spaces that develop between drip-shield segments.
		2.1.06.06.00 [a]	Effects and degradation of drip shield	
P13	Microbial Activity	ebs25	Microbial activity	The concern is microbially accelerated corrosion and mobilization occurring in the warm, moist environment of the EBS.

Table 2-2. Engineered Barrier System Features, Events, and Processes (Continued)

FEP Category		FEP Number	FEP Name	FEP Description
		2.1.10.01.00	Biological activity in waste and EBS	Biological activity in the waste and EBS may affect disposal-system performance by altering degradation processes such as corrosion of the waste packages and waste form (including cladding), by affecting radionuclide transport through the formation of colloids and biofilms, and by generating gases.
		2.1.11.08.00	Thermal effects: chemical and microbiological changes in the waste and EBS	Temperature changes may affect chemical and microbial processes in the waste and EBS.
P14	Alteration of Infiltrate Chemistry (abiotic)	2.1.04.02.00 [a]	Physical and chemical properties of backfill	
		2.1.09.01.00	Properties of the potential carrier plume in the waste and EBS	When unsaturated flow in the drifts is reestablished following the peak thermal period, water will have chemical and physical characteristics influenced by the near-field host rock and EBS. Water chemistry may be strongly affected by interactions with cementitious materials.
P15	Rockbolt & Grout Corrosion	ebs26	Rockbolt and grout corrosion	Corrosion and alteration changes the flow path for water entrance and alters the chemistry of the water following those flow paths.
		2.1.06.01.00 [a]	Degradation of cementitious materials in drift	
		2.1.06.02.00 [a]	Effects of rock reinforcement materials	
		2.1.09.02.00	Interaction with corrosion products	Corrosion products produced during degradation of the metallic portions of the EBS and waste package may affect the mobility of radionuclides. Sorption/desorption and coprecipitation/dissolution processes may occur.
P16	Wire Mesh Corrosion	2.1.09.02.00 [a]	Interaction with corrosion products	

Table 2-2. Engineered Barrier System Features, Events, and Processes (Continued)

FEP Category		FEP Number	FEP Name	FEP Description
P17	Drainage With Transport	ebs27	Drainage with transport – sealing and plugging	Normal functioning of drainage in the drifts is not established, so how drainage will change if fractures are plugged is unclear. Suggestions include ponding until fractures in the wall are reached by the water level or until there is sufficient head to clear the fractures.
		ebs28	Drainage with transport – through constructed drains	Water accumulation would be possible in a drift, particularly in a region of floor buckling, if normal drainage is blocked. Such blockage could occur if fines and debris were deposited in fractures or as sediment along the drift floor. Excess water could allow more rapid corrosion and contaminant mobilization. The conundrum here is that rapid draining of water sooner might also mean rapid draining of contaminated water later.
		ebs29	Drainage with transport – ponding	Water could accumulate in the invert in sufficient amounts to flood the waste package, enhancing corrosion and eventual mobilization. Criticality could be a possible consequence.
		2.1.08.05.00	Flow through invert	Flow through invert results in transport of contaminants to the unsaturated zone
		2.1.08.06.00	Wicking in waste and EBS	Capillary rise, or wicking, is a potential mechanism for water to move through the waste and engineered barrier system.
		2.1.08.07.00	Pathways for unsaturated flow and transport in the waste and EBS	Unsaturated flow and radionuclide transport may occur along preferential pathways in the waste and EBS. Physical and chemical properties of the EBS and waste form, in both intact and degraded states, should be considered in evaluating pathways.
P18	Drip Shield Corrosion	ebs25 [a]	Microbial activity	
		ebs30	Drip-shield corrosion – flow of backfill through corroded elements	The continuity of the drip shield and its ability to deflect liquid water could be compromised because of holes produced by corrosion.
		ebs31	Drip shield corrosion – fluid flow through corroded elements to waste packages	Deflection of liquid water away from the waste packages depends on continuity of the drip shield and the absence of penetrations.
		ebs32	Corrosion of waste packages	Corrosion may contribute to waste-package failure. Corrosion is most likely to occur at locations where water drips on the waste packages, but other mechanisms should be considered.
		2.1.06.06.00 [a]	Effects and degradation of drip shield	

Table 2-2. Engineered Barrier System Features, Events, and Processes (Continued)

FEP Category		FEP Number	FEP Name	FEP Description
P19	Drip Shield Movement Relative to Waste Package/ Rails	ebs1	Pedestal collapse	As a result of pedestal collapse, the waste package lies on or in the invert and could be in contact with the drip shield and the rails and thus be exposed to contact corrosion. While bedded in the invert, the waste package is more likely to see local ponding and the enhanced corrosion and mobilization that might accompany it.
		ebs6 [a]	Rockfall-loading distortion of drip shield	
		ebs10	Drip-shield movement relative to waste packages and rails	Contact of the Ti drip shield with the waste package or with the steel rails will cause contact corrosion. In the former case, corrosion of the waste package will be enhanced; in the latter case, corrosion of the drip shield will be accelerated. Presumably, the fate of the rails is inconsequential.
		ebs11 [a]	Relative seismic motion	
		2.1.06.05.00	Degradation of invert and pedestal	Degradation of the materials used in the invert and the pedestal supporting the waste package may occur by physical, chemical, or microbial processes and may affect the long-term performance of the potential repository.
P20	Alteration of Temperature-Dependent Chemical Activity	2.1.04.02.00 [a]	Physical and chemical properties of backfill	
		2.1.09.06.00	Reduction-oxidation potential in waste and EBS	The redox potential in the waste and EBS influences the oxidation of barrier and waste-form materials and the solubility of radionuclide species. Local variations in the redox potential can occur.
	_	2.1.09.12.00	Rind (altered zone) formation in waste, EBS, and adjacent rock	Thermochemical processes involving precipitation, condensation, and redissolution alter the properties of the waste, EBS, and adjacent rock These alterations form a rind, or altered zone, with hydrologic, thermal, and mineralogical properties that are different from the current conditions.
		2.1.09.14.00	Colloid formation in waste and EBS	Colloids in the waste and EBS may affect radionuclide transport. Different types of colloids may exist initially or may form during the evolution of the system by a variety of mechanisms. This FEP aggregates all types of colloids into a single category.

Table 2-2. Engineered Barrier System Features, Events, and Processes (Continued)

FEP Category		FEP Number	FEP Name	FEP Description
		2.1.09.16.00	Formation of pseudo-colloids (natural) in waste and EBS	Pseudo-colloids are colloidal-sized assemblages (between approximately 1 nanometer and 1 micrometer in diameter) of nonradioactive material that have radionuclides bound to them. Pseudo-colloids include microbial colloids, mineral fragments, and humic and fulvic acids. This FEP addresses radionuclide-bearing colloids formed from host-rock materials and all interactions, except corrosion, of the waste and EBS with the host rock environment. Pseudo-colloids formed from corrosion of the waste form and EBS are discussed in FEP 2.1.09.17.00.
		2.1.09.17.00	Formation of pseudo-colloids (corrosion products) in waste and EBS	Pseudo-colloids are colloidal-sized assemblages (between approximately 1 nanometer and 1 micrometer in diameter) of nonradioactive material that have radionuclides bound to them. Pseudo-colloids include microbial colloids, mineral fragments, and humic and fulvic acids. This FEP addresses pseudo-colloids such as iron oxyhydroxides formed from corrosion and degradation of the metals in the waste form and EBS. Radionuclide-bearing colloids formed from host-rock materials and all interactions, except corrosion, of the waste and EBS with the host rock environment are discussed in FEP 2.1.09.16.00.
		2.1.11.04.00	Temperature effects / coupled processes in waste and EBS	This FEP broadly encompasses all coupled-process effects of temperature changes within the waste and EBS.
		2.1.11.09.00 [a]	Thermal effects on liquid or two-phase fluid flow in the waste and EBS	
		2.2.08.04.00	Redissolution of precipitates directs more corrosive fluids to waste packages	Redissolution of precipitates, will have plugged pores as a result of evaporation of ground water in the hot zone, produces a pulse of fluid reaching the waste packages when gravity-driven flow resumes; this pulse of fluid is more corrosive than the original fluid in the rock.
P21	Ventilation	1.1.02.02.00	Effects of preclosure ventilation	The duration of preclosure ventilation acts together with waste-package spacing (as per design) to control the extent of the boiling front.

NOTE: [a] a repeated FEP

2.4.2 Screening of Candidate Features, Events, and Processes

This section summarizes the screening process (CRWMS M&O 2000c, 2000r) that was applied to EBS FEPs listed in the YMP FEP Database. To initiate the development of the YMP FEP Database, a preliminary set of FEPs was defined and subjected to screening. The screening confirmed the applicability of the candidate FEPs to the EBS. FEPs were "excluded" from, or

"included" in TSPA considerations based on two principal criteria:

- Exclude on the basis of "Low Probability", if a FEP has less than one chance in 10,000 of occurring over 10,000 years.

- Exclude on the basis of "Low Consequence", if omission of the FEP does not significantly change the expected annual dose.

In addition, two other types of FEPs were excluded: FEPs that are not applicable to repository design baseline, and FEPs that are not applicable to the EBS, and are covered in other PMRs, e.g., the Waste Package, Waste Form, and Disruptive Events PMRs. The EBS FEPs abstraction (CRWMS M&O 2000r) includes a rationale for including or excluding each FEPs.

The results of the Database FEPs screening process are summarized in Table 1-3 of this report. Table 2-2 lists only FEPs that are "included". The FEPs are organized in categories, and include the FEPs that were systematically and independently identified, as well as the applicable primary Database FEPs (numbered ebsx, and w.x.y.z.00, see Section 2.4.1).

2.4.3 Common Mode Degradation

The potential repository is designed so that there is defense-in-depth, that is, individual barriers can degrade or fail to perform without compromising repository performance. It is conceivable that certain events or processes affect the degradation of multiple components simultaneously, and thus produce "common-mode" degradation. Typically, "common mode" describes the degradation of multiple, redundant components due to a single event that simultaneously affects all critical components. A more complete definition distinguishes between repository components, and processes that cause radionuclide release and transport. The definition used in conjunction with the repository includes degradation of multiple, critical repository components by: 1) a single event such as faulting through the repository; 2) a single process such as increased water flow; and 3) multiple processes initiated by a single event, such as increased water inflow and creation of new transport pathways, caused by faulting.

To cause common-mode degradation, an event or process must have the potential to affect release of radionuclides from the repository. The degradation can be local (affecting only a few waste packages), or non-local (affecting a large part of the potential repository). The consequences of an initiating event or process may be delayed by varying degrees, but these situations are not distinguished in this description.

A simplified fault tree for common-mode degradation is shown in Figure 2-1, to help identify initiating processes and events. If common degradation modes exist, the initiating event or process appears beneath multiple branches. The fault tree starts at the top with increased radionuclide release from the potential repository, and the branches identify changes that must occur to reach initiating processes or events. Three principal branches are identified: 1) increased water contacting waste packages; 2) decreased waste package lifetime; and 3) increased rate of radionuclide release from the waste form. Increased seepage into emplacement drifts, for example, is a common-mode initiating process for many branches of the fault tree. Table 2-3 summarizes the common modes for the repository based on Figure 2-1.

fault tree. Table 2-3 summarizes the common modes for the repository based on Figure 2-1. Further details and references are provided in the detailed EBS FEPs analysis (CRWMS M&O 2000c), and process model reports pertinent to the specific event or process. It is noted that the common-mode events and processes are covered in the screening summary of Table 1-3 and in Table 2-2. They are identified here as a subject for system-wide analysis.

Table 2-3. Summary of Common Modes Identified in Figure 2-1

Common Mode	Description	Remarks
Increased seepage	Increased water flow into drifts from long-term or episodic increases in infiltration, or locally from modification of flow pathways.	Infiltration changes associated with possible future climate changes, are incorporated in predictive models.
Seismicity	Disruptive ground motion produced by an earthquake occurring outside the potential repository	Likelihood estimated in the Probabilistic Seismic Hazard
Faulting	Rupture of a new or existing fault within the potential repository causes disruptive ground motion, displacement of engineered components, and changes to flow pathways through the host rock.	Likelihood estimated in the Probabilistic Seismic Hazard Assessment
Thermal-hydrologic-chemical-mechanical (THCM) alteration of host rock characteristics	Stress changes cause rockfall and ground support failure	Uncertain importance; thought to be limited by gradual and local failure of ground support
Thermal-hydrologic-chemical (THC) salt production	Thermally driven processes involving water and chemical constituents, concentrate salts and precipitates originating from the host rock, and deposit them in the EBS. Aqueous corrosion can begin at lower values of relative humidity, and the chemical environment can be more corrosive.	Likely only during the thermal period, and related directly to seepage
Microbially influenced corrosion (MIC)	The corrosion rate of Alloy 22 is enhanced by microbial activity on the waste package surface	Moderate rates of MIC are observed in lab experiments, and may occur in the potential repository if sufficient nutrients are present
Igneous intrusion	A basaltic intrusion intersects potential repository drifts, or transport pathways for radionuclides, and may reach the surface.	Likelihood estimated in Probabilistic Volcanic Hazards Assessment (CRWMS M&O 1996)

2.5 REFERENCE CASE FOR THE ENGINEERED BARRIER SYSTEM

The reference case used in the development of the engineered barrier system (EBS) analysis/model reports (AMRs) and process model report (PMR) is based on the technical requirements baseline of the Civilian Radioactive Waste Management System program (Wilkins and Heath 1999). In this reference case, the capacity of the potential repository is designed for the emplacement of 70,000 metric tons of uranium (MTU) (63,000 MTU commercial spent nuclear fuel (CSNF) + 7,000 MTU U.S. Department of Energy (DOE) spent nuclear fuel (SNF) and high-level waste (HLW)).

An areal mass loading of approximately 60 MTU/acre, combined with preclosure ventilation for 50 years, will prevent the boiling zones from coalescing in the pillars between emplacement

drifts. Waste packages are placed in the emplacement drifts in a line load configuration with a WP to WP spacing of approximately 10 cm. The diameter of a waste emplacement drift is 5.5 m. Emplacement drifts are arranged with a uniform spacing of 81 m between their centerlines. The total emplacement drift length is calculated from adding the WP inventory (including DOE WPs) and the WP-to-WP gaps. The emplacement area encompasses 1050 acres in the upper emplacement level of the characterized area.

The WP design for this case consists of two layers. The inner layer is stainless steel (Alloy 316L), approximately 5 –cm –thick, and the outer layer is Alloy 22, approximately 2 cm thick. Waste packages heat output at emplacement is not to exceed 11.8 kW. This specification requires blending fuel assemblies to no more than 20 percent above the average pressurized-water reactor (PWR) thermal heat output (9.8 kW per package). The average age of the CSNF is assumed to be 26 years, with no additional aging beyond that imposed by reactor and potential repository operation schedules.

The potential repository is designed to allow closure at 50 years after the start of emplacement and to accommodate up to 125 years of operation if necessary. Each emplacement drift segment will be ventilated during the entire preclosure period (50 years for the reference case), at a ventilation rate selected to remove at least 70 percent of the WP heat output before closure.

Quartz sand and crushed tuff were selected as reference materials for the EBS backfill and invert, respectively. The reference drip shield is made of titanium Grade 7 with a minimum thickness of 2 cm.

INTENTIONALLY LEFT BLANK

Increased Radionuclide Releases
from Engineered Barriers

Increased Water Contacting WPs
- Ponding in Drifts
  - Seepage; THCM Fracture Plugging
- Penetration of Drip Shield
  - Drip Shield Displacement; Rockfall; Salt/Ppt Contact
- Condensation
  - Invert Saturation

Decreased WP Lifetime
- Mechanical Penetration
  - Rockfall & Ground Support Failure
- Corrosion Penetration
  - Microbial Activity; Salt/Ppt Contact

Increased Waste Form Release
- Increased Dissolution
- Colloidal Release
  - Intrinsic Colloid & Pseudo-Colloid Formation

Initiating Common-mode Processes/ Events

- Increased seepage
- THCM rock alteration

- Increased seepage
- THCM rock alteration
- Faulting
- Seismicity
- THC salt production

- Increased seepage

- THCM rock alteration
- Faulting
- Seismicity

- Increased seepage
- THC salt production

- Increased seepage

- Increased seepage

THCM – Thermal-hydrologic-chemical-mechanical coupled processes
THC – Thermal-hydrologic-chemical coupled processes

Notes:
Igneous intrusion into the potential repository, or along transport pathways, could initiate increased releases along many branches of the tree. However, igneous intrusion is not shown for simplicity.

The initiating processes and events shown here are limited to common modes; those limited to a single branch of the tree are not shown.

Figure 2-1. Common-mode Degradation Events and Processes

3. MODELS AND ABSTRACTIONS

The EBS PMR includes four major process models, and the associated abstractions whereby the processes are incorporated in TSPA. The process models are organized as follows:

- Water Distribution and Removal (WD&R) Model
- Physical & Chemical Environment (P&CE) Model
- EBS Radionuclide Transport (EBS RNT) Model
- Multi-Scale Thermal-Hydrologic (MSTH) Model

Section 3.1 describes these models and summarizes their results. Section 3.2 describes the abstraction process, including model integration and representing uncertainties.

3.1 MODEL DESCRIPTIONS

Sections 3.1.1 through 3.1.4 describe the four major EBS process models and their constituent submodels. For each submodel ("model" and "submodel" are used interchangeably in this context) there is discussion of model inputs, assumptions, uncertainties, and validation, in addition to model development and results relevant to the potential repository. The discussion is generally taken directly from the cited AMRs, but other sources are used where appropriate. The source documents can be consulted for additional details, particularly regarding software, data sources (e.g., Data Tracking Numbers), and additional discussion of the open literature.

This section describes a range of models and submodels, which are organized within the major EBS process models, and have three general objectives:

- Increase understanding of processes

- Support the design basis, including bounding of EBS environmental conditions

- Provide direct feeds to TSPA in the form of computational results or modeling approaches

In the following sections, the particular objectives satisfied by each model are described in the introductory paragraphs. The model relationships are summarized in Figure 3-13. Those models that provide direct feeds to TSPA are discussed further in Section 3.2.

3.1.1 Water Distribution and Removal Model

The *Water Distribution and Removal Model* (CRWMS M&O 2000q) quantifies and evaluates the distribution of liquid water within emplacement drifts and its removal by drainage. The model comprises a set of (2-D) numerical simulations using the NUFT computer code, plus ancillary calculations. Most of the simulations describe liquid water distribution in the EBS, and drainage from the drifts, for ambient temperature (post-thermal), steady-state conditions. Thermal-hydrology simulations are also described, because the model includes evaluation of changes in water distribution and drainage that could result from heating of the potential repository.

The Water Distribution and Removal Model combines results from:

- Water Diversion Model (CRWMS M&O 2000ae)
- Water Drainage Model (CRWMS M&O 2000af)
- Ventilation Model (CRWMS M&O 1999j)
- In-Drift Thermal-Hydrologic-Chemical Model (CRWMS M&O 2000y)

The objectives satisfied by these models include improved understanding of EBS processes, and development of the design basis. Direct feed of water distribution information to TSPA is provided by the Multi-Scale TH Model (Section 3.1.4). The Water Diversion Model provides a bounding analysis of potential leakage flow through cracks in the drip shields, or gaps between drip shield segments. The Water Drainage Model evaluates the conditions that could produced by water ponding in the invert, and the potential effectiveness of engineered measures to prevent ponding. The Ventilation Model is only briefly discussed because the focus of these process models is on post-closure performance. Also, the Ventilation Model is used to estimate the proportion of waste-generated heat that will be removed by pre-closure ventilation, whereas for the TH calculations described here, ventilation is assumed to remove 100 percent of waste-generated heat. Results from the Ventilation Model are the basis for pre-closure heating conditions used in Section 3.1.2 and 3.1.4. The In-Drift Thermal-Hydrologic-Chemical Model, in the version cited here, is briefly discussed and used as the basis for reporting that moisture conditions in the invert can control moisture condensation underneath the drip shield.

The Water Distribution and Removal Model provides support for:

- *Engineered Barrier System Radionuclide Transport Model* (CRWMS M&O 2000b)

- *Engineered Barrier System—Features, Events, and Processes Degradation Modes Analysis* (CRWMS M&O 2000c)

Invert moisture conditions are used in developing the EBS Radionuclide Transport Model (Section 3.1.3). Water distribution is the focus of several FEPs, for which process descriptions are provided by this model.

3.1.1.1 Water Distribution and Removal Model Input Data

For developing the model geometry of the NBS, the Water Distribution and Removal Model receives stratigraphic information from the Unsaturated-Zone (UZ) Site-Scale Model and develops a lithostratigraphic column (L4C4) column corresponding to a location near the geographic center of the potential repository. The UZ Site-Scale Model is a three-dimensional (3-D) model used to simulate the unsaturated hydrology of Yucca Mountain for ambient (unheated) conditions. The rock units present at this geographic location represent much of the potential repository layout area.

The EBS model geometry is developed from the License Application Design Selection (LADS) Enhanced Design Alternative II (EDA-II) (CRWMS M&O 2000q, Table 2). A 2-D model is justified for simulating water flow and drainage in the potential repository drifts, because the strategy for controlling flow and drainage, in its simplest form, does not require axial flow in the

drifts. Because of symmetry, a 2-D model of NUFT is constructed to include only half of the WP, half of the drift, and half of the adjacent pillar. The width of the NUFT model grid is 40.5 m, which is half of the drift spacing in the conceptual design. The two vertical edges of the model grid are treated as no-flow boundaries. The model extends from the ground surface to the water table about 340 m below the potential repository. A model grid for the entire domain is shown in Figure 3-1, with the grid spacing varying from 0.02 to 45.0 m. A schematic of the emplacement drift with the drip shield and WP, is shown in Figure 1-3. Figure 3-2 shows the model grid in more detail, where it represents the EBS.

The following hydrologic and thermal properties for the host rock and other stratigraphic units at the site, are used in this model (CRWMS M&O 2000q, Tables 3–6):

- Fracture porosity
- Matrix porosity
- Tortuosity factor
- Fracture bulk permeability
- Matrix bulk permeability
- Maximum and residual saturation in fractures,
- Maximum and residual saturation in matrix
- van Genuchten parameters α and m (or λ) for fractures
- van Genuchten parameters α and m (or λ) for matrix

Hydrologic and thermal properties for the backfill, the invert, and a material representing both (where they are in contact) are also defined (CRWMS M&O 2000q, Tables 7 and 8). The source of data for temperature and pressure boundary conditions at the ground surface and water table, and infiltration at the ground surface for present-day and glacial conditions, is the UZ Site-Scale Model (CRWMS M&O 2000q, pp. 20, 21 and 41).

Several NUFT models include the effects of potential repository heating, whereby the geometry and heat generation characteristics of the WPs are also input. These characteristics include the WP dimensions and thermal properties, and time-dependent heat-generation (CRWMS M&O 2000q, p. 27).

3.1.1.2 Water Distribution and Removal Model Assumptions

Use of the NUFT code requires a number of assumptions (CRWMS M&O 2000q, p. 30) which are summarized below. Also, ancillary calculations are used to analyze flow through breaches in the drip shield, and several additional assumptions are used for this purpose.

To facilitate NUFT simulations, the top of the drip shield is represented by a stepped contour (Figure 3-2). The drip shield is assumed to be impermeable and to have the same effective physical properties as the WP (CRWMS M&O 2000q, p. 30). The dimensions of the drift, invert material, and drip shield correspond to the EDA II design. For ancillary calculations of flow through breached drip shields, the modeled thickness is 2 cm.

Crushed tuff (CRWMS M&O 2000q, p. 30) is used as the invert ballast material. The invert will contain steel structural members, but the flow characteristics will be controlled mainly by the

ballast. Crushed tuff also provides radionuclide retardation performance for certain conditions (Section 3.1.3).

Overton Sand (CRWMS M&O 2000q, p. 30) is used for the backfill material. In these NUFT models, the backfill completely fills the outer annulus between the drip shield and the drift wall, rather than leaving an air gap above the backfill. This has the effect that the total water flux through the drift is approximately equal to the ambient percolation flux that impinges on the drift opening, in these models. In this way, seepage inflow, including extreme seepage conditions, can be readily simulated with little sensitivity to model gridding and other uncertainties that attend to seepage modeling.

It is important to note that this approach is different from model used to describe diversion of seepage around drift openings. This approach allows unsaturated flow of percolation flux in the host rock, directly into drift openings. By contrast, seepage models address the fact that for dripping to occur into an air gap, the water must achieve locally saturated conditions at the drift wall. With the presence of saturation gradients in the surrounding host rock, there is the potential for diversion of unsaturated flow around the drift openings. The approach described here is conservative, and represents seepage conditions that might occur in a small portion of the potential repository.

A tortuosity factor value of zero is assigned to the WPs and drip shields in the NUFT models, because these barriers are impermeable (except where breached, but such failures are not considered in the NUFT models). A factor of 0.7 is assigned to the invert ballast material because it is a granular, with behavior similar to the host rock. This coefficient was estimated for soils, over a range of liquid saturation, and found to be approximately 0.7 (CRWMS M&O 2000q, p. 30).

The NUFT models are used to evaluate the distribution of flow, the effects of flow focusing in the host rock, and the effects of fracture plugging below the drifts (CRWMS M&O 2000q, p. 34). For flow-focusing, the infiltration rate is increased so that 90 percent of the infiltration in the entire model domain occurs over the top of the drift, and the remainder is distributed.

To evaluate fracture plugging in NUFT models, the potential thermal-hydrologic-chemical (THC) and thermal-hydrologic-mechanical (THM) effects are simulated by decreasing the permeability of the fractured rock directly below the invert to that of the rock matrix. The conservative basis for this assumption is that THC processes would likely impact the flow properties of existing fractures, and that permeability would not be increased by THM processes (CRWMS M&O 2000q, p. 38). For these runs the fracture permeability is zero to a distance of 3 m from the invert, representing penetration of fracture plugging into the host rock. Such penetration could be associated with the extent of boiling conditions and a dryout zone around the drift.

To assess the function of a engineered drainage features, as a measure to mitigate the possible expected effects of fracture plugging, NUFT runs are presented which include a drainage feature extending 6 m below the invert and filled with the same Overton Sand material used as backfill (Case 9). These NUFT models are 2-D, so the modeled drain feature represents a slot or a linear array of closely spaced borings.

As discussed above, several assumptions are used in ancillary analyses of flow through the drip shield. The overlapping joint between drip shield segments is described as a parallel plate aperture (CRWMS M&O 2000q, p. 33). Flow through the overlap aperture is assumed to be limited by the local moisture potential. As a bounding calculation, the flow-aperture is assumed to be the maximum aperture that could retain pendular water at a specified value of the moisture potential.

3.1.1.3   Water Distribution and Removal Model Uncertainties

Models for water flow in the EBS describe the response of engineered materials with known hydrologic properties, in the designed configuration, to specified rates of seepage inflow. An alternative view is that thermal effects on flow, and coupled-process effects on hydrologic properties, could change water distribution and movement in the EBS so as to degrade the performance of the potential repository. Analyses presented in this report show that two of the most plausible mechanisms for changes in EBS or near-field properties, i.e. fracture plugging and backfill porosity reduction, are negligible or can be controlled using design measures.

Another effect that is not emphasized in this model is reflux of liquid water in the backfill during the thermal period. This effect is limited to the thermal period, localized to the drift, and will not contribute to advective release of water-borne radionuclides. It is addressed in the TH calculations performed in Section 3.1.2.1, in which fluxes between the backfill and the drip shield surface (Zones 3 and 4) are calculated.

3.1.1.4   Water Distribution and Removal Model Development

The EBS domain for modeling water distribution and removal consists of backfill, the drip shield, the invert, and the surrounding fractured host rock. Water enters the drift and flows through the backfill, where it is partitioned into: 1) water flow through potential breaches in the drip shield; 2) water flow through the backfill directly to the invert; and 3) water flow that contacts the drip shield but is diverted through the backfill to the invert. Water diversion by the backfill and drip shield, and accumulation in the invert, is addressed using NUFT modeling (CRWMS M&O 2000q, Section 6.2). The NUFT runs performed for this model are described in Table 3-1.

The host rock contains a freely draining system of fractures which has sufficient capacity to drain water that enters the drifts as seepage, unless fracture permeability is insufficient or occluded by thermally driven processes. The potential effects of fracture plugging are addressed by several NUFT runs that are described in Table 3-1 (cases indicated as "Plugged"). The *Water Drainage Model* (CRWMS M&O 2000af) is based on NUFT simulations using a 2-D, steady-state, ambient temperature model with the seepage flux equivalent to the infiltration flux.

Coupled processes during the thermal period may significantly alter hydrologic properties that influence reflux activity and seepage. Changes in host rock permeability are discussed below. Scoping calculations of potential changes in backfill permeability are discussed in Section 3.1.2.3.3.

The *In-Drift Thermal-Hydrologic-Chemical Model* (CRWMS M&O 2000y) simulates the open-air void space inside the drip shield to evaluate the potential for moisture condensation.

The model evaluates the tendency for liquid water to evaporate from the invert and condense elsewhere in the annular space between the waste package and the drip shield. The model is implemented using NUFT, with properties and boundary conditions similar to those discussed above.

The *Water Diversion Model* (CRWMS M&O 2000ae, p. 36) provides an analysis of drip shield performance in conjunction with the Overton Sand backfill, based on analytical solutions for unsaturated flow around a cylindrical inclusion, and for flow through capillary bundles representing breaches in the drip shield. When seepage into the drift occurs, saturation increases above the drip shield, with increased potential for flow through a breached drip shield. The presence of sand backfill ensures that moisture tension (i.e. negative moisture potential) exists on the drip shield surface for a wide range of seepage conditions. For water to flow through a breach in the drip shield, requires that the hydrologic characteristics of the breach are sufficient to imbibe water from the unsaturated sand. Such conditions are associated with decreased transmissivity of the breach to water, which implies limited flow and a threshold-type response. Breaches through the drip shield are modeled as fully-wetted capillary bundles, and parallel plate apertures, which have negligible transmissivity until fully saturated at a threshold moisture potential (i.e., relative humidity).

The *Drift Degradation Analysis* (CRWMS M&O 2000ad) provides information on the potential changes in drift geometry during the postclosure period. The change in drift profile resulting from progressive deterioration of the emplacement drifts is assessed with and without backfill. Drift profiles are determined for four time increments, including static (i.e., at excavation), and at 200, 2000, and 10,000 yr. The effect of seismic events on rockfall is analyzed. Block-size distributions and drift profiles are determined for three seismic events, including a 1,000-yr event, a 5,000-yr event, and a 10,000-yr event. It is shown that the seismic effect on rockfall is relatively minor. Time-dependent and thermal effects also have a minor impact on rockfall.

The expected drift geometry is a nearly circular, 5.5-m diameter opening. The circular configuration is used for all NUFT models discussed in the following sections.

The *Ventilation Model* (CRWMS M&O 1999j) analyzes the effects of preclosure continuous ventilation in the emplacement drifts. The principal purpose is to provide heat-removal data for EBS design. The model provides a general description of heat-transfer by preclosure ventilation, and estimates the in-drift temperatures and the fraction of heat removed. The model is implemented using the ANSYS code, which models ventilation air convection and radiation within the drifts, but does not model water movement as liquid or vapor. The results are probably conservative, and actual heat removal could be somewhat greater for a given volumetric ventilation rate. For the *Water Distribution and Removal Model* (CRWMS M&O 2000q), the NUFT thermal-hydrology models assume 100 percent heat removal for a preclosure period of 100 years. This approximation minimizes the time until return of water, and resultant water inflow to the EBS, and is therefore conservative. Results from the *Ventilation Model* are not used directly, but support this bounding approximation. For the ambient NUFT models no heating is imposed.

Case Number	Infiltration Rate			Focusing		Heating		Plugging		Design	
	Glacial	Monsoon	Current	Uniform	Focused	Ambient	Elevated	None	Plugged	No Sand Drains	Sand Drains
1	X				X	X		X		X	
2	X			X		X		X		X	
3	X				X		X	X		X	
4	X			X			X	X		X	
5	X				X	X			X	X	
6	X			X		X			X	X	
7	X				X		X		X	X	
8	X				X		X		X	X	
9	X			X		X			X		X
10	X				X	X		X			X
11			X		X	X		X			X
12			X	X		X			X	X	
13			X		X	X			X	X	

Table 3-1. Summary of Parametric Cases for the Water Distribution Model

3.1.1.5   Water Distribution and Removal Model Validation

NUFT Calculations

Calculations for the Water Distribution and Removal Model are performed using the same numerical simulator (NUFT), and some of the same modeling concepts described in Sections 3.1.2 and 3.1.4. The TH calculations in this section are mostly ambient temperature, steady-state simulations of water movement through the EBS. Model validity is established by comparison to pilot-scale test results, and through selection of valid model inputs:

- Hydrologic properties of the natural and engineered materials in the model
- Temperature, total pressure, and infiltration flux boundary conditions
- Numerical gridding, convergence criteria, and other model settings

Model validity is based primarily on appropriate selection of model inputs. Pilot-scale tests for backfilled openings, and data comparisons with model predictions, are underway.

The properties used for the host rock are taken directly from the drift-scale results of the *Unsaturated Zone (UZ) Flow and Transport Model* (CRWMS M&O 2000aa). The properties are defined in a way that describes the unsaturated hydrology of the host rock (e.g., using the AFC) according to current understanding. Property values are estimated using a procedure by which they are constrained using appropriate observations and measured data from Yucca Mountain.

The temperature boundary conditions used for these models are based on average temperatures for the ground surface and water table, which are related by the lapse rate, and constrained by measured data. Similarly, the average total pressure boundary conditions are consistent with known variation of atmospheric pressure. Values for average infiltration flux are also taken directly from the UZ Model, for a central location with infiltration characteristics typical of the average over the layout area of the potential repository. These calculations demonstrate the hydrologic response of the EBS to extreme seepage conditions. To do this, the infiltration flux boundary condition is selected from the "upper" infiltration distribution developed for the UZ Model, and for certain calculations this value is further increased to represent extreme focusing of flow into the emplacement drifts.

From this discussion it is concluded that the TH models used for the Water Distribution and Removal Model are valid for their intended use. The models are based on appropriate inputs, including properties and boundary conditions. Gridding, convergence, and other model settings used for these models are consistent with past practice.

A small subset of calculations presented in this section includes transient response to repository heating, as a check on results obtained for ambient temperature. Validity for thermal-hydrology models of this type is addressed in Section 3.1.4.

Analytical Models for Water Diversion and Leakage

Bounding approaches are used to develop upper bounds on water movement through breaches in the drip shield (e.g., fully wetted surfaces, water potential gradient, parallel plates). In addition, a bounding approach is taken that all leakage through the drip shield is available at the waste

package surface. Film flow effects are not taken into account but their effects are relatively small, compared with the bounds developed using parallel-plate flow. Accordingly, the analytical solution is a valid, bounding approximation for flow through cracks in the drip shield, or parallel-plate partings between adjacent segments.

3.1.1.6 Water Distribution and Removal Model Results

Table 3-1 summarizes the parametric studies performed using NUFT for the *Water Distribution and Removal Model* (CRWMS M&O 2000q). The glacial infiltration rate is used as a conservative, bounding representation of the rate of percolation in the host rock. Results are presented for the glacial climate, with uniform and focused infiltration at the ground surface, with ambient temperature and heated conditions, and without fracture plugging (Cases 1 through 4). Results are also presented for the same hydrologic conditions, but with fracture-plugging, and also for the combination of plugging and an engineered drainage feature. In addition, another run (Case 10) is presented with a drainage feature, but without fracture plugging, to evaluate the effect of such a feature on nominal performance of the EBS.

Base Case and Flow Focusing

The results of the NUFT analyses for the water distribution and removal model for the base case (Case 1) of focused flow at ambient temperature are presented in Figure 3-3 through Figure 3-6. The following aspects of the calculated hydrologic results are discussed below: capillary water potential, liquid water flux in fractures, and the fracture and matrix saturation.

For the base case, the capillary pressure (i.e. moisture tension) ranges from approximately 370 cm in the rock matrix above the drift, to 220 cm in the drift backfill above the drip shield (Figure 3-3). Saturation levels are somewhat elevated immediately above the drip shield. These changes are similar to the moisture potential values predicted at the drip shield surface, by the analytical solution used in the *Water Diversion Model* (CRWMS M&O 2000ae, p. 36).

Below the drip shield, the capillary pressure in the host rock ranges from approximately 370 cm, to 510 cm in drier regions. A relatively dry, shadow region is predicted to occur in the host rock below the drift, consistent with the analytical solution used in the *Water Diversion Model* (CRWMS M&O 2000ae, p. 36).

Figure 3-6 illustrates that the liquid flux is increased adjacent to, and somewhat below the drip shield, to a value of approximately 145 mm per year (4.6×10^{-6} kg/m^2-sec in the figure). This is caused by the flow-focusing geometry of the drip shield and backfill (with seepage flux into the drift that is comparable in magnitude to percolation flux in the host rock). These values are in qualitative agreement with predictions from the *Water Diversion Model* (CRWMS M&O 2000ae, Figure 16) and the *Water Distribution and Removal Model* (CRWMS M&O 2000q, p. 52).

The NUFT model results for the infiltration conditions and hydrologic properties used, show that matrix saturation in the host rock is approximately 0.90, while fracture saturation is at or near the residual saturation (i.e., a few percent; Figure 3-4). Flow in the host rock is dominated by unsaturated flow in fractures.

Comparison of NUFT results for the base case (Case 1) with 90 percent focusing of infiltration directly above the drift at the ground surface, with the case of uniformly distributed infiltration at the ground surface (Case 1), shows that the flow regime is nearly identical and that focusing of infiltration at the surface has no significant effect on flow at the potential repository horizon. This is equivalent to a statement that hydrologic features responsible for focusing flow into potential repository drifts, where such features exist, must be situated (very approximately) within a few tens or hundreds meters from the drifts, in the vertical direction. Effects from more distant features tend to be smoothed by dispersive behavior in the UZ.

Effects of Heating in the Potential Repository on Water Distribution and Removal

Results from NUFT modeling of focused flow with potential repository heating, are presented in the *Water Distribution and Removal Model* (CRWMS M&O 2000q, p. 54) for conditions at up to 1,000 years after waste emplacement. Peak temperatures in the backfill are predicted to occur during the period 100 to 1,000 years. The predicted effects of potential repository heating on water distribution in the EBS generally include less seepage into the drift opening, lower saturation in the backfill, and increased capillary pressure (i.e., drier conditions; increased moisture tension).

After approximately 1,000 years liquid water returns to the EBS. (Note that the 2-D NUFT models of the L4C4 location represent potential repository center conditions, and that return of water will occur sooner at the potential repository edges.) The capillary pressure in the backfill decreases during cooldown, as saturation increases. Examination of the liquid flux within the drift during cooldown shows that as water returns to the EBS, thermally-driven reflux activity subsides, and the flux distribution in the backfill resembles ambient conditions (Figure 3-7) (CRWMS M&O 2000q, p. 55).

Fracture Plugging

Results from NUFT simulation with fracture plugging, and focused flow at ambient temperature, are presented in the *Water Distribution and Removal Model* (CRWMS M&O 2000q, p. 55). The results show that seepage flux into the drift, and liquid flux through the backfill, are decreased slightly compared with the base case. This probably results from flow diversion due to decreased permeability in the floor plugged zone. Compared to the base case, the capillary pressure in the backfill is decreased slightly (i.e., less moisture tension), and saturation is increased.

The most important effect from fracture plugging below the drift is increased saturation in the invert and adjacent rock (CRWMS M&O 2000q, p. 62). Saturation in the invert increased to nearly full saturation, and the capillary pressure decreased to near zero (i.e., nearly free water conditions). Saturation in the invert increased to approximately 0.98, or nearly full saturation.

Potential Engineered Drainage Features

The results of NUFT analysis for cases that include an idealized, 2-D engineered drainage feature at ambient temperature, are presented in Figure 3-8 through Figure 3-11. The current design does not include any engineered drainage features. However, the results show that a drainage feature filled with Overton Sand strongly influences the flow regime in the invert and in

the host rock below the potential repository horizon. The distribution of capillary pressure in and around the drainage feature (Figure 3-8) shows that capillary pressures are greater (i.e., drier conditions) in the invert and the adjacent host rock. Saturation within the drainage feature increases with distance below the drift, and there is nearly full saturation at the base. The drainage feature strongly influences the liquid flux in the invert, as shown in Figure 3-11.

Liquid flux in the drainage feature is much greater than in the invert of backfill, within the drift opening. The drainage feature causes increased capillary pressure (drier conditions) and decreased saturation in the invert above the region of plugged fractures. The capillary pressure is approximately 200 cm for this case; without the drainage feature the capillary pressure in the invert was nearly zero (i.e. nearly complete liquid saturation).

Flow Through the Drip Shield to the Waste Packages

For the models for which results are described above, the drip shield is impermeable. In this section an analytical model is developed to describe the flow rate through breaches in the drip shield (CRWMS M&O 2000ae, p. 37). The boundary condition for the state of moisture in the backfill contacting the drip shield, is obtained from the base case NUFT model discussed previously. This model shows that for ambient temperature conditions, capillary pressure in the backfill is relatively uniform around the drip shield and the invert. This is consistent with steady-state percolation at a rate equal to the unsaturated hydraulic conductivity, flowing under the impetus of the gravitational potential gradient.

An aperture in the region of overlap between drip shields is characterized by a moisture potential (ψ). A water retention expression relates the largest aperture that can retain capillary water at potential ψ (CRWMS M&O 2000ae, p. 31):

$$B = \frac{2\sigma}{\rho_w g} \cdot \frac{1}{\psi}$$

(Eq. 3-1)

where σ is the surface tension of water, ρ_w is water density, and g is the acceleration of gravity. For a uniform, parallel-plate gap, the aperture extent is the perimeter of the overlapping joint. Substituting Equation 3-1 into the cubic law (CRWMS M&O 2000ae, p. 31) and applying a unit head gradient (P), gives an expression for the maximum flow rate as a function of the potential:

$$Q = \frac{\rho_w \cdot g}{12 \cdot v} \cdot \left(\frac{2 \cdot \sigma}{\rho_w \cdot g \cdot \psi} \right)^3 \cdot P$$

(Eq. 3-2)

where v is the dynamic viscosity. Figure 3-12 presents the relationships for flow rate through the backfill around a drip shield, and through the gap between adjacent drip shields, plotted against the backfill percolation rate determined from the moisture potential and the unsaturated hydraulic conductivity at that potential (CRWMS M&O 2000ae, p. 22). The backfill flow rate is determined from the unsaturated hydraulic conductivity for the backfill, and the drift diameter. The drip shield flow rate is calculated form Equation 3-2. The analysis shows that over the range

of moisture potential expected within the backfill for ambient conditions, the bounding flow rate through the drip shield is a fraction of the backfill flow rate. Importantly, this is a bounding expression that does not take into account features of the drip shield joint that could inhibit leakage, and also assumes a unit head gradient (i.e. the flow path through the joint is assumed vertical).

The foregoing discussion has analyzed a breach in the drip shield, as a parallel-plate opening. This type of breach could arise from relative displacement of adjacent drip shield segments, due to rockfall, faulting, or seismic ground motion. For such a breach to form, the joint between segments would have to fail. The probability of such a breach depends for each cause, on the probability of the initiating event and the probability of failure. Further discussion of the EBS abstractions is provided in Section 3.2.1.

Moisture Condensation Under the Drip Shield

The *In-Drift Thermal-Hydrologic-Chemical Model* (CRWMS M&O 2000y) results show that evaporation in the invert is regulated by the relative efficiency of conductive heat transfer in the invert, and of heat transfer directly from the waste package to the drip shield, compared to latent heat transfer by evaporation in the invert. If the volumetric moisture content in the invert ballast material is relatively high, the evaporation rate may be significant so that condensation underneath the drip shield is possible, whereas if the moisture content is low, the unsaturated permeability of the invert ballast material limits the moisture flux available for evaporation.

Moisture-retention relations for the invert ballast material, based on unsaturated flow measurements by centrifugation, have been developed for moisture potential values of 100 cm and greater (i.e. more moisture tension) (CRWMS M&O 2000ad, p. 37). Interpretation of these measured data with respect to the evaporation rate model discussed above, shows that for moisture potential of 100 cm or greater (i.e., drier), the volumetric moisture content in the crushed tuff invert will be low, such that the evaporative flux from the invert below the drip shield will be limited by unsaturated permeability. With less heat transferred from the waste package to the invert and converted to latent heat by evaporation, there is relatively more heat transferred to the drip shield. The temperature of the drip shield is thereby greater, which inhibits condensation.

These studies indicate the benefits from keeping the invert relatively dry. If the natural variability of host rock properties and hydrologic conditions can produce moist invert conditions during the thermal period, then engineered drainage features can serve to prevent condensation under the drip shield. Other measures could probably be taken to control condensation under the drip shield, if needed, such as inhibiting heat transfer to the invert, or ensuring higher temperature at the drip shield than the invert.

3.1.1.7 Summary of Results from the Water Distribution and Removal Model

Models for water distribution in the EBS use properties and boundary conditions that are consistent with the UZ Site-Scale Model. Hydrologic conditions in the EBS are evaluated for the conditions of greatest infiltration, that are used with the UZ Model (glacial, "upper" infiltration distribution). The EBS models are configured to show how the engineered diversion barriers

perform, even if the seepage flux into potential repository drifts approaches the ambient percolation flux in the host rock, which may occur with increasing percolation rates.

The geometry of the drip shield and the drift opening causes flow focusing in the backfill, such that liquid flux magnitudes of approximately three times the ambient percolation flux, may occur locally in the drifts. Potential repository heating causes lower saturation, lower liquid flux, and greater capillary pressure (i.e. greater moisture tension) during the thermal period. Thermally driven reflux cells in the backfill may increase the calculated liquid flux magnitude, locally in the drifts, during the thermal period. Liquid water flow from the host rock returns to the EBS at approximately 1,000 years, for potential repository center locations.

Fracture plugging below the invert can cause high saturation (or full saturation) in the invert, for all infiltration conditions evaluated. Engineered drainage features such as vertical boreholes filled with sand, can control saturation conditions in the invert even with the conditions of greatest infiltration, and fracture plugging.

Liquid flux through possible gaps between drip shields can be bounded using simple models, and further decreases in the bounding flux may be possible if refinements to the design and to the model assumptions, are incorporated.

Condensation under the drip shield is not predicted for the model conditions considered.

3.1.2 Physical and Chemical Environment Model

The overall objective of the EBS Physical and Chemical Environment (P&CE) Model is to assess changes in the bulk environment that can affect drip-shield and waste-package degradation, and radionuclide migration. This includes changes in aqueous chemistry resulting from interaction of introduced materials with heat, and water seeping into the drift, taking into account thermal effects on chemical equilibria and rate processes, and physical processes such as evaporation and condensation.

The specific objectives of the EBS P&CE Model are to improve understanding of EBS processes, support the EBS design basis, and provide direct support to TSPA. The EBS P&CE Model described in this section primarily supports specification of environmental conditions for corrosion and mechanical performance of the drip shield, and corrosion performance of the waste package. Aspects of this model are bounding, for example, selection of a reference TH model for chemical modeling. The results of this bounding approach are summarized in Section 3.1.2.7.

Some submodels described in this section directly support TSPA, which includes assessment of EBS environmental conditions and their consequences. Importantly, the TSPA incorporates models and data which are outside the scope of this PMR (e.g., UZ flow and drift seepage) for a more complete overall assessment of potential repository performance, including performance of the EBS. The EBS P&CE Model provides scoping and bounding analyses, and conceptual support, in addition to the submodels that feed TSPA directly. Description (i.e., abstraction) of EBS processes in the TSPA is described in Section 3.2.

The EBS P&CE model is developed as several models, integrated in a Chemical Reference Model, from which conclusions are drawn concerning the bulk chemical environment.

General Approach to Modeling the Physical and Chemical Environment

The model domain extends from the ground surface to the water table for modeling thermal-hydrology and gas-phase transport, but is limited to the emplacement drifts and nearby host rock for chemical modeling. For chemical modeling, the host rock and the emplacement drifts are represented by a set of reaction cells, or zones. These are defined explicitly in the TH model (using NUFT), and the TH model output describes conditions within each zone and the fluxes between zones.

Geochemical modeling concepts are used to describe the chemical evolution of each zone through time, incorporating the effects of temperature, evaporative concentration, and interaction with solid mineral phases present. For the EBS P&CE Model, chemical reactions are described by equilibrium models using the B-dot activity expression (CRWMS M&O 2000t). Another approach using an extended Pitzer formulation is also developed in this section, for use in TSPA.

The P&CE model includes chemical modeling of the host rock as well as the EBS, because the host-rock temperature is high enough during the thermal period to change the composition of naturally percolating waters. The modeling approach for the host rock is similar to that used for in-drift processes and is based on temperature and water flux information from the same TH models.

Processes including cement leaching, colloid formation, and microbial activity are evaluated using related, but separate models to assess whether there are important effects on the bulk P&CE.

Relationships Among Models

The following sections present a set of process models that are combined to assess EBS P&CE conditions. Some models are used directly and quantitatively in the Chemical Reference Model, while others are used to address the importance of microbial activity, coupled processes, and cement leaching (Figure 3-13). The following are used directly in the Chemical Reference Model:

- Thermal-Hydrology Model
- Gas Flux and Fugacity Model
- Precipitates and Salts Normative Model

while the following generate additional information that is used to evaluate sensitivity of the bulk chemical environment to different processes:

- Introduced Materials Models (including the Kinetic Model for Water-Quartz Interaction, Model for Seepage-Backfill Interaction at High Ionic Strength, Analytical Model for Porosity Reduction in Quartz Sand Backfill, Model for Corrosion of Carbon Steel in the EBS, and the Cementitious Materials Model)

- Microbial Effects Models (including the Model of Threshold Conditions for Microbially Influenced Corrosion, and the Microbial Communities Model)

- Other precipitates and salts models (including the LRH Salts Model, Condensed Water Model, and the HRH Salts Model)

- EBS Colloids Model.

Together, these elements represent current process-level understanding of the bulk EBS P&CE. As a next step, aspects of the process models are transferred to the EBS P&CE Abstraction Model (Section 3.2.3), where they are incorporated in the TSPA.

3.1.2.1   Thermal Hydrology

This section describes application of the NUFT code to simulation of thermal-hydrologic (TH) conditions in discrete zones representing the host rock and the emplacement drifts. The calculated temperatures, fluxes between zones, and other results are used in the Gas Flux and Fugacity Model, the Cementitious Materials Model, and the Chemical Reference model. These results represent the effects of heating and hydrologic flow that can affect chemical processes in the EBS.

3.1.2.1.1   Conceptual Model Development and Alternative Models

The TH simulations reported here implement energy balance and mass balance in multiphase gas and liquid flow systems that are described by Darcy's Law for partially saturated media. These models describe heat and mass transfer the host rock and the EBS, during and after the thermal period. They predict development of a dryout zone around the drifts (Figure 3-14), which collapses over time in response to ambient percolation, as thermal output decays. Heat is transferred by thermal conduction, liquid- and gas-phase convection, and latent heat effects (i.e., evaporation and condensation).

An important conceptual aspect of TH modeling is representation of fractured rock, which exhibits strongly bimodal and spatially heterogeneous flow characteristics. The fracture system is represented as a porous continuum, to save computational effort, while the rock matrix is represented by a separate continuum having different properties. This approach has been demonstrated in modeling of results from field testing (discussed later in this section). Fractures can also be represented effectively as discrete discontinuities, but the computational effort is prohibitive for meaningful applications.

The TH models described in this report represent fractured rock using a dual-permeability continuum approach based on the active-fracture concept (AFC) of Liu et al. (1998). The AFC conceptual model is also used in the *Unsaturated Zone Flow and Transport Model* (CRWMS M&O 2000aa; referred to as the UZ Model in this discussion) and the extraction of input data from the UZ Model is discussed in the *Multi-Scale Thermohydrologic Model* report (CRWMS M&O 2000i). Previous TH models for fractured rock have included dual-permeability (DKM) models with constant or saturation-weighted fracture-matrix interaction, and the equivalent (single) continuum (ECM) model (Hardin et al., 1998; Chapter 3). The AFC model incorporates

much of the conceptual basis for previous DKM models, while allowing for reduction in fracture-matrix interaction to represent sparseness of flow paths through the fracture system.

Thermal-hydrology models have been used extensively to design field thermal tests at Yucca Mountain and elsewhere, and to interpret the data obtained from such tests (Hardin et al. 1998, Chapter 3; Wilder 1996, Section 1; also see Sections 3.1.4.4.1 and 3.1.4.4.2). As discussed in Section 3.1.4 below, field testing has resulted in improved understanding of thermally-driven flow processes, and revised property sets. The TH calculations described here are based on this foregoing body of work, and are relatively simple models specifically intended to support reaction-cell modeling of the bulk chemical environment.

3.1.2.1.2   Thermal and Hydrologic Input Data, Assumptions, and Uncertainties

Drift-scale, two-dimensional (2-D) TH simulations using the NUFT code are reported here for the L4C1 and L4C4 locations. Preclosure ventilation is represented by diminished heat output, closure is at 50 years after emplacement, and backfill is included at closure.

The L4C1 and L4C4 locations are developed in the *Multi-Scale Thermohydrologic Model* (CRWMS M&O 2000i). That model represents, by an array of discrete locations, variation of TH conditions throughout the potential repository. These two locations are used because:

- L4C4 is typical for locations internal to the potential repository layout. It is near the geographic center of the potential repository layout, where temperatures and evaporation rates will be relatively high. Thermal loading for the L4C4 model is equivalent to the average for the potential repository layout (60 MTU/acre), and the infiltration flux is close to the average.

- L4C1 is located at the potential repository edge where the rate of cooling will be relatively high because of conductive heat loss to external regions. Drift spacing for the L4C1 model is increased so that the thermal loading is equivalent to 36 MTU/acre with the same thermal output, which is appropriate for edge locations (CRWMS M&O 2000i).

For each of these locations, the TH conditions are simulated with both the "lower" and "upper" infiltration distributions from the UZ Model (CRWMS M&O 2000t), for a total of four NUFT cases. Different hydrologic property sets are associated with the different infiltration conditions.

In-Drift Properties and Processes

The NUFT cases developed in this report are 2-D symmetry models. The model domain is a vertical plane perpendicular to the axis of a single emplacement drift, and is reflected symmetrically about the drift centerline and the pillar centerline. The vertical boundaries of the model domain (passing through the center of the drift and through the center of the pillar) are adiabatic, no-flow boundaries.

For the calculations described here, the backfill extends to the drift crown so there is no head space in the drift opening. This has the effect that percolation flux in the backfill is approximately equal to the percolation flux in the host rock, for ambient (post-thermal)

conditions. By eliminating head space in the drift opening, the model can more readily simulate locations in the potential repository where seepage occurs. The result is conservative in that EBS performance is analyzed for conditions in which diversion of percolation flux in the rock around the drift openings, is minimized.

Greater evaporation rates are achieved with greater seepage flux because of the proximity of percolating waters to the hottest parts of the EBS. Production of water vapor causes displacement of air, thus decreasing CO_2 fugacity (other factors can cause CO_2 fugacity to increase). Decreased CO_2 promotes high pH and is conservative with respect to corrosion of EBS components. Thus the choice of "upper" infiltration, a potential repository-center location, and conditions for which seepage occurs, support a conservative design basis for the EBS.

Geometry of the Drift, Drip Shield, and Waste Package

The drift diameter is 5.5 m. For these NUFT cases the waste package (WP), drip shield (DS), and the WP support are combined into a single composite body with outside dimensions representing those of the DS, and thermal properties scaled to represent the composite body. This is based on a simplifying assumption that heat and mass transport between the WP and DS are not critical to the bulk physical and chemical environment, and that if water penetrates the DS for any reason then the WP is exposed to the same chemical environment as the DS. The NUFT grid is designed so that the regions of grid blocks representing the drift, invert, backfill, and the DS have cross-sectional areas that are approximately the same as those specified in the design.

Thermal Loading and Aging of Waste Inventory

The NUFT simulations described here are 2-D calculations in which the WPs are represented as a line-heat source. The line-source strength decays with time, to represent the radioactive decay of a composite of (SNF) spent nuclear fuel and defense high-level waste (DHLW) (CRWMS M&O 2000t). The line-source strength is modified for heat-removal by ventilation in the preclosure period; the source strength is decreased by 70 percent.

Hydrostratigraphic Unit Thicknesses, Contact Elevations, and Properties

The UZ Model unit thicknesses, contact elevations, and lateral extents are honored in these calculations. The hydrologic properties used in the TH portion of this report are fully consistent with the one-dimensional (1-D), drift-scale property sets from the UZ Model (CRWMS M&O 2000t). Each property set contains descriptions for the rock matrix and for the fracture network for each hydrostratigraphic unit. The continuum properties assigned to the fracture network, are homogeneous within each hydrostratigraphic unit (CRWMS M&O 2000t). The UZ Model derives the unit properties that are used in this model, so the same assumptions apply here.

The property sets also include parameters that describe nonequilibrium fracture–matrix interaction using the AFC, which are used directly in NUFT. The effective tortuosity for gas-phase diffusive mass-transfer in both the matrix and fracture continua is assumed to have a value of 0.7, which is the scale-invariant path tortuosity that would be encountered in a medium

composed of impervious, cubical blocks (CRWMS M&O 2000t). The tortuosity value for liquid-phase mass-transfer is negligible by comparison and is assumed to be zero.

Net Infiltration Boundary Conditions

Grid files describing the variation of infiltration over the site area were obtained from the U.S. Geological Survey (USGS) (CRWMS M&O 2000t). These data were reformatted and interpolated for use as boundary conditions in NUFT models (CRWMS M&O 2000t). For the climate model represented by these files, the climate state changes from present-day conditions to a monsoonal climate beginning at 600 years after waste emplacement, and to a glacial climate at 2,000 years. To represent uncertainty in present and future infiltration values, both the "lower" and "upper" infiltration distributions from the USGS grid files are used in this model.

Temperature, Total Pressure, and Air Mass-Fraction Boundary Conditions

For the TH models described here, the model domain extends from the ground surface to the water table, and temperature and total pressure conditions are specified at each boundary. Values for the L4C1 and L4C4 locations are interpolated from the UZ Model results (CRWMS M&O 2000t). The air mass-fraction at the ground surface is calculated from the temperature and total pressure such that the relative humidity is 100 percent. This prevents water from diffusing upward through the ground surface in the NUFT simulations, a mode of mass transfer that is already taken into account in the prescribed infiltration boundary condition. At the water table, the air mass-fraction is assigned a small value (comparable to the solubility of air-constituent gases in water).

Thermal Properties for Natural Barrier Materials

The thermal properties used by NUFT are: dry thermal conductivity (zero liquid saturation), wet thermal conductivity (at 100 percent water saturation), specific heat, and grain density for each hydrostratigraphic unit. The values used for these properties are based on best-available, unqualified information and are subject to change. For partially saturated conditions, the NUFT code linearly interpolates between dry and wet values, based on liquid saturation.

Thermal and Hydrologic Properties for EBS Materials

The EBS backfill and invert materials are Overton Sand (quartz sand) and crushed tuff, respectively. These materials are unfractured but are represented in the DKM model by splitting the total property value between the fracture and matrix continua, with strong interaction between the continua (CRWMS M&O 2000t). The AFC is not used for EBS material properties because these are better represented as porous media. There are no open cavities; therefore, there is no radiative heat transfer in the NUFT models described in this report.

Component Properties

Vapor-pressure lowering is active for these calculations. This feature of the NUFT code simulates the interaction between capillary water potential and the vapor pressure governing water mass-transfer between the liquid and gas phases. The vapor pressure is lowered by an

amount determined from the capillary pressure, which increases the boiling temperature for water in partially saturated capillary media (CRWMS M&O 2000t).

Zero values are assumed for dispersion coefficients, thus the hydrodynamic dispersion of water moving as liquid or vapor is assumed to be negligible. This is justified because thermal and hydrologic changes occur slowly (over many years) in these simulations.

Environmental Conditions That Promote Corrosion of Drip Shield and Waste Package

Environmental conditions that accelerate corrosion rates and the accumulation of damage from general, localized, and stress-cracking mechanisms, include:

- Duration of exposure to adverse conditions

- Temperature at which adverse chemical conditions occur

- Precipitation of salts that provide ions needed for some corrosion processes and that promote aqueous conditions at higher temperatures by osmolality

- Alkaline (high-pH) conditions in the bulk chemical environment, which are associated with low CO_2 fugacity caused by evaporation that decreases the air mass-fraction.

It is anticipated that ongoing testing and modeling will verify these aspects of corrosion performance.

Thermal-Hydrologic Model Uncertainties

The Thermal-Hydrology Model presented in this section has associated uncertainties which derive from consideration of alternative models and other views (discussed in Section 3.1.2.1.8), and from model validation issues (Section 3.1.2.1.4). In addition, the discussion of model uncertainties related to the TH modeling approach using NUFT, in Section 3.1.4.1, also apply.

3.1.2.1.3   Modeling Approach and Numerical Simulation

Separate but linked NUFT runs are used for initialization and to represent preclosure and postclosure conditions. The initialization model calculates ambient saturation and temperature conditions without a drift opening. The preclosure model uses the initialization results as initial data, adds the drift opening without backfill, and adds preclosure heating. The postclosure model uses the final preclosure saturation and temperature fields as initial data, adds backfill, and increases heating to account for the cessation of ventilation. A total of 12 NUFT runs are needed for the four TH cases (CRWMS M&O 2000t).

Specific TH performance measures calculated for the continuum representing the rock matrix are temperature, saturation, relative humidity, and the rate of evaporation. For the continuum representing the fracture network, these same measures and the air mass-fraction are calculated. In addition, the gas-phase total mass flux (air plus water vapor) in the matrix and fractures combined is reported, as a vector field.

Postprocessing NUFT Output

Postprocessing is used to prepare and simplify NUFT output for further analysis. Zone processing is used to describe the spatial subdomains and the temporal intervals for chemical reaction cell modeling. Vertical profiles of key variables are used for modeling gas fluxes. The conservative solute analysis is used to support selection of a reference TH model for chemical modeling.

Zone Fluxes

To represent TH changes taking place in key parts of the NUFT model domain, six zones are defined a priori for the NUFT models (Figure 3-15 and Figure 3-16). These zones are as follows:

- **Zone 0**: The "far-field" host rock. Within Zone 0, the temperature rises after closure and then falls as the WP heat output decays with time, but there is little evaporation or condensation, hence no significant change from ambient water chemistry. Zone 0 above the emplacement drift is the source of water entering Zone 1, and provides the boundary condition for chemical composition.

- **Zone 1**: Host rock above the drift–Extends outward from the drift wall approximately 10 m, or beyond the extent of dryout. Boiling and evaporative concentration can occur in Zone 1, and vapor generated in the drift is likely to condense. Zone 1 is above the drift midplane (the horizontal plane passing through the drift springlines).

- **Zone 2**: Host rock at the drift wall–Includes the grid blocks that represent host rock at the drift wall, along the upper half of the drift opening above the spring line.

- **Zone 3**: Backfill above the spring line

- **Zone 4**: Backfill at the drip shield surface–Includes the grid blocks that represent backfill at the drip-shield surface, along the upper part of the drip shield above the midplane

- **Zone 5**: Lower backfill–Includes the grid blocks that represent backfill outside the DS, below the mid-plane, and above the invert

- **Zone 6**: Invert below the backfill, DS, and WP

Using NUFT output files, a software routine collects the output for each zone and produces a summary table of gas and liquid fluxes between zones, combining fracture and matrix fluxes as a function of time. Figure 3-17 is an example plot showing the liquid fluxes between zones for the L4C4 location and "upper" infiltration distribution. The zone fluxes are transferred to a spreadsheet routine for further analysis prior to use in chemical modeling.

Zone-Averaged Temperature, Saturation, and Air Mass-Fraction

Zone-averaged scalar variables describe the state of each zone as a function of time. To compute zone averages, the value for each grid block is weighted by its volume (CRWMS M&O 2000t). The zone-averaging procedure is implemented in a software routine that produces a table of zone-averaged values for each time step listed previously. For each NUFT model, the zone-averaged output for the matrix and the fractures are transferred to a spreadsheet routine for further analysis.

Vertical Mass-Flux Profiles

Another software routine is used to sort NUFT output and produce a table containing the vertical component of the gas-phase total mass flux (air and water components) in the fracture continuum along a vertical profile passing through the drift centerline. A plot of the vertical component of the gas-phase total mass flux for the L4C4 location, "upper" infiltration, and simulation time of 1,000 years is shown in Figure 3-18. For each NUFT model the vertical mass-flux profile is transferred to a spreadsheet routine for further analysis.

3.1.2.1.4   Thermal-Hydrology Model Validation

Thermal-hydrology calculations for the EBS Physical and Chemical Environment Model are made using the same numerical simulator, and the same model concepts as the models described in Sections 3.1.1 and 3.1.4. The results include evolution of key performance measures (e.g., temperature, saturation, fluxes, air mass-fraction) through the 10,000-yr performance period.

Validity of model results is established by comparison of similar models, using the same properties, boundary conditions, and other inputs, to field-scale test results (Large-Block Test, Drift-Scale Test; see Sections 3.1.4.4.1 and 3.1.4.4.2). Such comparisons for thermal-hydrology models are discussed in Section 3.1.4.

Validation also requires appropriate selection of model inputs:

- Hydrologic properties for natural and engineered materials
- Thermal properties for natural and engineered materials
- Thermal output of emplaced waste
- Temperature, total pressure, and infiltration flux boundary conditions
- Numerical gridding, convergence criteria, and other model settings

which are also discussed in Section 3.1.4. The hydrologic properties used for these models are taken directly from the Unsaturated Zone (UZ) Flow and Transport Model (CRWMS M&O 2000aa). Thermal properties are based on laboratory-measured data. It is noted that values for "wet" thermal conductivity are currently under review. Thermal output of the emplaced waste is based on best-available information for the characteristics of spent fuel and defense high-level waste.

The temperature and pressure boundary conditions used for these models are based on averages for the ground surface and water table, constrained by measured data. Values for average

infiltration flux are also taken directly from the UZ Model, for representative center and edge locations. Alternative infiltration flux boundary conditions are selected from both the "lower" and "upper" infiltration distributions developed for the UZ Model, to represent the range of uncertainty. These alternative values are used comparatively in several cases discussed in this section.

From this discussion (and Section 3.1.4.4) it is concluded that the TH models used for the EBS P&CE Model are valid for their intended use. The models are based on appropriate inputs, including properties, boundary conditions, and thermal output. Gridding, convergence, and other model settings used for these models are consistent with past practice.

3.1.2.1.5 Model Results Representing a Range of Potential Repository Conditions

Plots of temperature, saturation, and gas-phase air mass-fraction for Zone 4 at the DS surface are shown in Figure 3-19 through Figure 3-21. These figures were generated in the spreadsheet routines used to analysis zone-averaged data (CRWMS M&O 2000t). The plots compare results from the four NUFT cases, which are summarized in the following sections.

Temperature

- Cooldown occurs sooner at the potential repository edge.

- Low-flux conditions produce greater peak temperatures and slower cooldown because less liquid water is available to evaporate and transfer heat.

Saturation

- The spatial extent of dryout (zero or low liquid saturation) is greater for low-flux conditions.

- Water returns to the EBS environment sooner for high-flux conditions, and near the potential repository edge.

After cooldown, the liquid water saturation in the upper part of the backfill is approximately 10 percent to 20 percent, depending on the infiltration magnitude.

Air Mass-Fraction

The air mass-fraction represents the displacement of air by water vapor from evaporation. At high relative humidity, when the temperature is near the boiling point, the air mass-fraction approaches zero. This is importance because the partial pressures of CO_2 and O_2 may also approach zero. Evaluation of the calculated air mass-fraction has shown:

- Matrix air mass-fraction is smaller, and relative humidity is greater, than in the fractures. This is due to vapor pressure lowering, which retains water in the matrix.

- The minimum air mass-fraction is approximately 10^{-3} when thermal output and infiltration (seepage) are maximized, i.e. for the L4C4 location and "upper" infiltration.

Evaporation Rate

Evaporation rate is calculated by NUFT using a mass balance on liquid and gas-phase water fluxes, for the entire model domain, and for both the matrix and the fractures. A plot of the evaporation rate in the fracture continuum at the L4C4 location with "upper" infiltration, at a simulation time of 1000 years, is shown in Figure 3-22. The total evaporation rate (all zones, fractures plus matrix) versus time is plotted in Figure 3-23 for all four NUFT cases, and compared with the potential repository thermal output vs. time (CRWMS M&O 2000t). Examination of evaporation rate plots shows the following:

- The rate of evaporation in the fracture continuum is greater than that in the matrix at the same locations, during the thermal period, because of vapor pressure lowering.

- Evaporation tends to be localized to a narrow zone above the drift, where condensate water and ambient percolation meet the dryout zone. The evaporation zone recedes toward the DS surface as the heat source strength decays with time.

- For the "upper" infiltration distribution, there is more sustained evaporation that occurs sooner for the L4C1 location (repository edge) than for the L4C4 location (center).

- For all cases, the rate of evaporation for all zones is much smaller than the total thermal output of the WPs for the first few hundred years. At later time (after 4,000 years) the proportion of thermal output that causes evaporation decreases for all cases.

Gas-Phase Mass Flux

Calculations show that the vertical component of the gas-phase total mass flux (air + water vapor), along a vertical profile passing through the drift center, is generally upward during the thermal period (CRWMS M&O 2000t). This is caused by a combination of buoyant convection and the upward egress of water vapor produced in the host rock. Excess pressure from evaporation, causes gas to be expelled at the ground surface. The maximum value of upward vertical flux does not necessarily occur at the drift wall but may occur in the host rock.

A horizontal profile of the vertical component of the gas-phase total mass flux for the L4C4 location and "upper" infiltration is shown in Figure 3-24 for a simulation time of 1,000 years. This figure shows that there is buoyant convection in the host rock because of downward flux near the center of the pillar, but that gas-phase circulation is dominated by egress of water vapor from evaporation. The maximum upward mass flux occurs directly above the drift.

3.1.2.1.6   Representing Thermal-Hydrologic Evolution by Uniform Time Intervals

To support chemical-reaction cell modeling, the potential repository thermal evolution is simplified to a series of intervals during which zone temperatures and fluxes are held constant, as shown in Table 3-2.

Table 3-2. Intervals during Which Zone Temperatures and Fluxes Are Held Constant

Nominal Time (yr)	Time Interval (yr)	
	From	To
100	50	300
500	300	700
1000	700	1,500
2000	1500	2,500
5000	2500	10,000

Source: CRWMS M&O 2000t

The assigned time intervals correspond approximately to the assumed transitions in climate at 600 and 2000 years, so the effects of those transitions are incorporated at 700 and 2500 years. The stepwise representation of temperatures, and fluxes between zones, plots reasonably close to the NUFT output (e.g. zone-to-zone fluxes represented in Figure 3-17).

Preclosure (≤50 years) TH conditions in the EBS are not evaluated because they will be dominated by ventilation. Whereas the heat-removal effects of ventilation are explicitly simulated, the drying effects on the host rock are not. (The effects of preclosure processes on the composition of mobile waters and the accumulation of precipitates in the host-rock fractures and matrix are assumed to be negligible.)

3.1.2.1.7   Selection of a Reference Model for Bounding Chemical Calculations

Conservative Solute Analysis Using Zone-to-Zone Fluxes

The zone-averaged saturations and fluxes between zones are analyzed to gain insight into requirements for chemical modeling. The four calculated TH cases are analyzed and compared, and one is chosen for additional chemical system modeling (CRWMS M&O 2000t).

An ideal conservative solute tracer (a substance that can be present in any concentration) is assumed to be present at a constant concentration ($C_0 = 1$) in water entering the host rock (Zone 1) from above (Zone 0). The solute is then transported between zones at rates that are determined by the solute concentration in each zone and by the liquid flow rates between zones. The approach is used with the zone-averaged, stepwise constant descriptions of liquid mass and fluxes between zones. The result describes the potential accumulation of a conservative solute with unlimited solubility (an approximation for soluble salts such as NaCl) in a system described by stepwise variation of liquid and vapor fluxes.

Derivation of Conservative Solute Analysis

In the conservative solute analysis for a given zone, when the influent concentration is greater than the outfluent concentrations, the concentration tends to increase; when the outfluent concentration is greater than the influent concentrations, the concentration tends to decrease. In each cell, the concentration tends to be increased by evaporation and decreased by condensation. For a single zone, the rate of change of the concentration is

$$\frac{\partial C_i}{\partial t} = \frac{1}{V_i}\sum_j q_{ji}C_j - \frac{C_i}{V_i}\sum_j q_{ik}$$
(Eq. 3-3)

where

C_i = concentration in the ith zone (normalized mass/kg solvent)

q_{ji} = inflow rate from the jth zone into the ith zone (kg/sec)

C_j = concentration in the jth zone (normalized mass/kg solvent)

V_i = volume of the ith zone (volume of solvent; expressed as mass assuming 1 kg/liter)

q_{ik} = outflow rate from the ith zone to the kth zone (kg/sec)

This formulation represents the change in concentration during a time interval during which the hydrologic conditions are constant but the solute concentration can vary. The fluxes (q_{ji}, q_{ik}) and volumes (V_i) are provided from NUFT calculations. The volume, or alternatively the mass of solvent present in each cell, is invariant during each time interval. The mass of solute in each cell is determined from the product of the volume and the concentration. Expanding Equation 3-3 to represent all possible connections between zones, a system of simultaneous differential equations is developed and solved for each time interval (CRWMS M&O 2000t).

Results from Conservative Solute Analysis

The procedure described in the foregoing subsection is repeated for each of the four TH cases. The results are plotted as normalized solute mass vs. time for each zone (Figure 3-25 through 3-28). Solute mass is normalized to that present in 1 kg of solvent at the reference concentration ($C_0 = 1$).

The maxima on these plots represent conditions for which there is liquid inflow to a zone, but no liquid outflow, so all the transported solute is accumulated. When liquid through-flow conditions return to such a zone, the solute rapidly disperses (infinite solubility of an ideal conservative tracer). Accordingly, these calculations underestimate the time for which the accumulated solute remains in each zone. For solutes with finite solubility and prograde solubility variation with temperature (e.g., silica), an accumulation of solute could actually remain for hundreds or thousands of years. The minima on these plots represent conditions for which there is either condensation, or no inflow.

The results of the conservative solute calculations are summarized as follows:

- When zones have significant transitory or continuous inflow, but no liquid outflow, a substantial mass of soluble salts accumulates (the zones need not be dry for this to occur).

- Solute mass on the order of 10^5 times that present in 1 kg of the reference water composition may accumulate near the DS surface (Zone 4; see Figure 3-27). If chloride is present in the reference water at 7 mg/l (J-13 water), the accumulated chloride mass could exceed 1 kg per meter of drift.

- There is the potential for solute to accumulate in the backfill and at the DS surface (Zones 3 and 4) before these zones have cooled through boiling. Thus, there is the potential for brines to form at temperatures greater than 96°C.

- For locations at the edge of the potential repository (L4C1) the potential accumulation of soluble salts is less than at center locations (L4C4) because there is less heat available for evaporation.

- Comparing the "upper" and "lower" infiltration distributions (e.g., Figure 3-27 and Figure 3-28) less solute accumulates at the DS surface (Zone 4) for "lower" infiltration conditions because there is less evaporation there, even though temperatures may be greater.

- For certain conditions, there is potential for solute accumulation in the backfill, to migrate to the invert (Zones 5 and 6). This may occur because, for an interval of time, salts in the backfill are redissolving, while the invert is the hottest part of the drift that is accessible to liquid flow.

The principal factors that limit solute accumulation on the DS are rapid cooling (to less than 96°C) and less seepage. These factors are not correlated because greater flux causes faster cooling, but also increases drift seepage.

It should be noted that NUFT, as used for this report, does not modify liquid boiling temperatures to account for solute concentration. Thus, there is the potential to underpredict solution migration toward heat sources, and solute accumulation. However, the effect is probably small because the fluids in question are evaporated by at least 100- to 1000-fold; thus, their volume is small.

Selection of a Thermal-Hydrologic Model for Chemical Modeling

The L4C4 location with the "upper" infiltration distribution is selected as a reasonable-bound case for chemical modeling of the in-drift environment. This is based on assessment of the TH calculation results with respect to the environmental conditions that promote corrosion (identified previously): duration of adverse conditions, temperature at which adverse conditions occur, precipitated salts, and alkaline (high-pH) conditions.

From discussion of the TH calculations described in this section, the following criteria are found to represent the environmental conditions that promote corrosion:

- Potential for accumulation of salts in Zone 4 (Figure 3-25 through Figure 3-28)

- Temperature at which aqueous conditions occur in Zone 4 (Figure 3-19)

- Duration for which adverse conditions occur at elevated temperature in Zone 4 (Figure 3-19 and Figure 3-21)

- Proportion of thermal output that produces evaporation, especially during sustained periods when aqueous conditions occur in Zone 4 (Figure 3-23)

The L4C4 location with "upper" infiltration produces reasonable-bound conditions according to these criteria. For chemical modeling, these data are further consolidated to expedite chemical calculations:

- Zone 1-2 represents the host rock above the drift
- Zone 3-4 represents backfill between the DS and the drift crown
- Zone 5-6 represents backfill and invert materials in the lower part of the drift

The calculation details are described in the source analysis/model report (CRWMS M&O 2000t). These results are used as the basis for the Chemical Reference Model calculations in this report.

3.1.2.1.8   Comparison with Alternative Models and Approaches

Fully coupled reactive-transport simulations, combining chemical reactions with TH processes, could obviate the need for the zones and uniform time intervals described here. Such simulation methods can be applied as they become available and as the required input data, including the numerical settings used to operate the simulation codes, are qualified. The approach used here is readily applied to address conceptual issues and to evaluate bounding conditions for performance of the engineered barriers.

Changes in the TH models are possible to make representation of the WP, DS, backfill, invert, and host rock more detailed and realistic. Possible changes include finer gridding, explicit simulation of the WP and DS (instead of a single body with lumped properties), an air-filled space above the backfill, and spatial heterogeneity in the host rock. For this report, these potential enhancements would probably not lead to more reliable bounds nor to less favorable bounds on environmental conditions.

3.1.2.2   Gas Flux and Fugacity

This section develops an analytical model for fugacities of CO_2 and O_2 in the potential repository during the thermal period. The model provides lower-bound estimates of gas fugacities, using input from TH calculations (Section 3.1.2.1). It is calibrated by means of a unique application of ^{14}C abundance measurements from boreholes at Yucca Mountain. It describes an inverse relationship between fugacity and flux, which can be used to calculate the respective increase or decrease in fugacity that would be associated with a source or sink of CO_2 or O_2 in the EBS.

In the Chemical Reference Model (Section 3.1.2.7) the analytical model is used to constrain CO_2 and O_2 fugacities. The results are bounding for CO_2 in the sense that low CO_2 concentration contributes to higher pH, which can promote degradation of engineered materials such as steel or titanium. The approach allows comparison of the calculated rate of CO_2 consumption in the EBS, with the flux-fugacity relationship from the model, to evaluate whether in-drift processes are likely to strongly perturb the CO_2 fugacity in the host rock and EBS. A similar comparison is made for consumption of O_2 by corrosion of structural steel in the EBS.

The model development and discussion in this section includes the following elements:

- Identify the processes that control the flux and fugacity for CO_2 and O_2.

- Estimate the magnitude of gas-phase mass transfer, applicable to both CO_2 and O_2 gases, based on mass balance of $^{14}CO_2$ for ambient conditions. Develop a mass-transfer function that can represent gases other than CO_2, and modify the function to represent thermal effects.

- Develop reasonable lower-bound estimates for CO_2 and O_2 fugacities in the gas phase and the relationships between flux and fugacity for the thermal period extending to 10,000 years.

In addition to the analytical mass-transfer model, two alternative models are discussed: (a) the air mass-fraction approach and (b) reactive transport simulation. Each is shown to produce CO_2 fugacity values for the thermal period, which are comparable to results from the analytical mass-transfer model.

3.1.2.2.1 Gas Flux Conceptual Model Development and Alternative Models

Carbon dioxide can strongly affect pH for solutions present in the emplacement drifts during the thermal and post-thermal periods. The gas-phase CO_2 concentration can range over several orders of magnitude, and the associated solution compositions can range from sub-alkaline to pH 11 or greater. Within this range, there are important differences in mineral solubility conditions and corrosion rates for engineered materials.

Conceptual Discussion of Transport Processes for Gas Species

Carbon dioxide is present in the host rock under ambient conditions in three forms: CO_2 gas, dissolved inorganic carbon species in fracture and matrix waters, and mineral carbonate solids. Gaseous and dissolved inorganic carbon are readily available for chemical reactions. Carbonate solids may dissolve and contribute to the available labile carbon, and they are common secondary minerals at Yucca Mountain.

Gas-phase CO_2 at Yucca Mountain can be transported by three processes:

- **Molecular diffusion**–Fickian diffusion along a concentration gradient.

- **Advective-dispersive transport**–The gas column in the UZ undergoes volume reduction and expansion in response to changes in barometric pressure at the ground surface. Gas molecules move back and forth and disperse in a manner that is mathematically analogous to diffusion (CRWMS M&O 2000t).

- **Convective circulation**–Gas-phase convection in the UZ could be driven by seasonal changes in gas density at the ground surface, and associated effects from variable topography. Convective circulation has been shown to readily displace air in the Tiva Canyon caprock, but the effect apparently does not extend deeper (CRWMS M&O 2000t). Ambient, large-scale convective circulation could contribute to mass transport of CO_2 and other gases, but is neglected in this bounding model.

Liquid-phase, dissolved inorganic carbon at Yucca Mountain can be transported by two processes:

- **Advective transport**–Percolation occurs in the fractures and the rock matrix. Flow velocity is small in the matrix, such that tens of thousands of years could be needed for penetration of porewater to the potential repository depth. This is not consistent with borehole ^{14}C activity data. Accordingly, aqueous transport of dissolved inorganic carbon, if it occurs, must do so primarily in fractures.

- **Molecular diffusion**–Aqueous diffusion is approximately four orders of magnitude slower in liquids than in gases, and is restricted by path tortuosity. For the Gas Flux and Fugacity Model, diffusive transport is limited to isotopic equilibration of matrix porewater with nearby fractures. This is justified because ^{14}C activity for gas-phase and matrix porewater samples from the same or nearby locations are isotopically similar (CRWMS M&O 2000t).

From the above discussion, the two most important processes for ambient transport of CO_2 to the host rock are gas-phase diffusion-dispersion and liquid-phase advective transport. Episodic recharge occurs, so transport of CO_2 through the host rock is evidently a nonequilibrium process in which rapid recharge in fractures penetrates the host rock, with limited isotopic interaction and therefore limited mass exchange. This is verified by inspection of measured ^{14}C activity versus depth for borehole SD-12 (Figure 3-29). Radiocarbon exists as $^{14}CO_2$, for which transport behavior is similar to CO_2 (interpreted differences in relative abundance of ^{14}C must be small compared to isotopic fractionation). The distribution of $^{14}CO_2$ can be interpreted as that which would be observed for average CO_2, with a sink analogous to radioactive decay. The increase of ^{14}C activity near the bottom of the Topopah Spring welded tuff occurs at a transition from mostly fracture flow in the host rock, to mostly matrix flow in the underlying vitrophyre and nonwelded Calico Hills unit.

The Gas Flux and Fugacity Model distinguishes the $^{14}CO_2$ flux transported in rapid aqueous recharge, from the $^{14}CO_2$ flux required to replenish radioactive decay in the host rock. The $^{14}CO_2$ flux to the host rock may be due entirely to gas-phase processes. This approach is used to develop lower bounds on gas-phase transport. It is bounding because it maximizes the contribution of recharge waters for replacing ^{14}C decay deep in the UZ, thus minimizing the need for gas-phase transport to penetrate there, and thus minimizing the efficacy of gas-phase transport *through* the host rock.

Interpretation of ^{14}C data from the site shows that barometrically driven advective processes increase the transport of CO_2 to the UZ. This is represented in the Gas Flux and Fugacity Model as a process whereby barometric pressure fluctuation at the surface causes 1-D oscillatory gas movement in UZ, resulting in diffusive-dispersive gas-phase mass transport.

Gas Transport Processes During the Thermal Period

Processes that can affect gas-phase composition in the EBS during the thermal period are summarized in Figure 3-30. Nitrogen gas (N_2) is included in the discussion because it is a component in the Microbial Communities Model (Section 3.1.2.4) and O_2 is included because it

is a reactant in the EBS (Section 3.1.2.7). The source of these gases is the atmosphere, or soil gas where a soil zone covers the surface. Soil zone processes cause the CO_2 concentration to exceed that of the atmosphere. In response to heating, CO_2 is produced by degassing of pore water, and by reaction of calcite with other minerals in the presence of water. During heating, large volumes of water vapor are also produced which tend to dilute the concentrations of CO_2, O_2, and N_2 gases. Where this water condenses, the gases tend to redissolve in the condensate.

Convective circulation in the gas phase can occur because of buoyancy caused by density changes from thermal expansion and increased humidity. Through the combined effects of flow-field geometry, flow resistance from lower-permeability units above and below the host rock, and displacement of air by water vapor, convective activity will be maximal at the potential repository edges and may be nil near the potential repository center. Large-scale convective circulation is neglected as a CO_2 transport process for this bounding model. The conceptual model for ambient processes, and the associated 1-D model, are applied to the thermal period with modification to account for thermally driven transport processes.

Conceptual Discussion of O_2 Transport

Oxygen is more abundant than CO_2 in air. Measured values for gas-phase O_2 concentration in the UZ are in the range 20 percent to 22 percent and are generally indistinguishable from atmospheric values (CRWMS M&O 2000t). Oxygen is much less soluble than CO_2 in water, so the gas phase is the most important reservoir and transport pathway for O_2. Both gases exhibit decreased (retrograde) solubility with increasing temperature, but this effect is insignificant for O_2 transport.

Tuff mineralogy is mostly oxidized, and minerals containing reduced species tend to be armored by oxides and are not accessible. Thus, oxidation of the tuff is slow, and the ambient O_2 concentration in the gas phase is closely similar to atmospheric composition. Oxygen can react with materials such as steel in the potential repository environment.

Alternative Models: Air Mass-Fraction Approach

Previous mountain-scale TH modeling showed that gas-phase convective circulation during the thermal period may be limited (CRWMS M&O 1998d, Chapter 4). Calculation of the air mass-fraction at the potential repository horizon, which decreases because of the displacement of air by water vapor, showed that the CO_2 fugacity (as a proportion of the air mass-fraction) could decrease by many orders of magnitude from prerepository levels (Figure 3-31). However, temporal integration of the gas-phase convective circulation showed that the flow of gas moving through the host rock could deliver significant amounts of CO_2 and O_2 gases to the emplacement drifts over time.

Two example figures from the Total System Performance Assessment–Viability Assessment (TSPA-VA) Technical Basis Document are reproduced here as Figure 3-31 and Figure 3-32, (CRWMS M&O 1998d, Figure 4-16 and Figure 4-18). These plots summarize results from simulation using a 2-D, mountain-scale NUFT model, to represent gas-phase circulation for the VA potential repository design. The conceptual basis for these plots is discussed further in the *In-Drift Gas Flux and Composition Analysis/Model Report* (CRWMS M&O 2000e). They are

presented here for comparison purposes and are not used directly in the gas flux and fugacity model. It should be recognized that the viability assessment (VA) design was intended to produce higher peak temperatures and a longer-lasting thermal period than is the current conceptual design.

Several interesting points emerge from the comparison. For the potential repository center location, the air mass-fraction decreased by as many as nine orders of magnitude during the time period from approximately 300 to 1,000 years. At the same time, the flux of air through the potential repository horizon decreased to effectively zero. In contrast, at the potential repository edge location, the air mass-fraction was much greater, and the air mass flux was always greater than zero.

With the current potential repository design concept, the thermal loading is less, and the drift spacing is greater than for the VA design. The 2-D drift-scale TH models described in the previous section predict more mixing of the gas phase and a small downward circulation in the pillar (Section 3.1.2). The calculated air mass-fraction at the drip shield, for the potential repository center (L4C4 location; Figure 3-21) is similar to, or greater than the air mass-fraction calculated for the VA design (Figure 3-31). The 2-D drift-scale model does not include mountain-scale circulation, so the air mass-fraction calculations in Section 3.1.2.1 are probably lower bounds.

The mass-transfer approach used in this report is a departure from the air mass-fraction approach based on TH modeling, primarily for the following reasons:

- Mountain-scale TH processes are not taken into account in the mass-transfer approach. The advantage of not including large-scale TH processes is that the results do not depend on large-scale hydrologic properties of the mountain, which vary and for which data are sparse.

- Natural advective-dispersive mass-transfer processes that operate in the UZ were not included in the air mass-fraction approach. An advantage of including data on the ambient distribution of radiocarbon in the UZ is integration of models and their supporting data.

For both the air mass-fraction and the mass-transfer approaches, there is a time period during which evaporation is active and the CO_2 and O_2 fugacities are small (e.g., 1 percent of ambient values). Therefore, with either approach there is the potential for the development of alkaline solution conditions in the drift, and the potential for changes in corrosion processes due to decreased O_2 fugacity.

Alternative Models: Multicomponent Reactive Transport Simulation

Coupled reactive transport simulations couple TH with transport of chemical components, mass balance of components, chemical speciation and heterogeneous reactions, and rate-dependent reactions. Modeling of this type for the potential repository host rock, including the emplacement drifts, is presented in the *Drift-Scale Coupled Processes Analysis/Model Report (Drift-Scale Test and Seepage)* (CRWMS M&O 2000x). Gas-phase chemistry is an appropriate

measure for comparison of chemical models because the pH and mineral precipitation depend strongly on the CO_2 fugacity.

Host-rock water composition and CO_2 fugacity values were calculated, for several different assumptions on the infiltration flux magnitude, in this series of drift-scale reactive transport simulations. Results for the "upper" infiltration distribution (CRWMS M&O 2000t) are shown in Figure 3-33. Two cases are discussed here: Case 1 includes representative clay and zeolite minerals in addition to silica and calcite, and Case 2 includes only silica and calcite.

The CO_2 fugacity at the drift wall as a function of time, calculated from reactive transport, the air mass-fraction approach, and the 1-D mass-transfer approach, is shown in Figure 3-33. The air mass-fraction and mass-transfer approaches are discussed in more detail in later sections of this report. The CO_2 fugacity from reactive transport simulations is reported at the drift crown, which is the highest point on the drift wall directly above the DS. For all three modeling approaches considered, the values are generally within a factor of approximately 30 during the thermal period. At late time, the reactive transport simulations show increased CO_2 fugacity as the air mass-fraction increases and as the gaseous CO_2 liberated during heating returns to the drift environment. The other approaches effectively require that the CO_2 released by heating, is dissipated before cooldown.

The reactive transport simulations are subject to ionic strength limitations that also exist for other approaches to chemical modeling. The chemical activity models (e.g., B-dot model; (CRWMS M&O 2000t) can be used for ionic strength values up to approximately 1 molal. When evaporative concentration causes solution ionic strength to exceed this limit, approximations are used to represent chemical conditions. In the reactive transport simulations, chemical speciation and dissolution/precipitation reactions are suspended when the ionic strength limit is reached and until dilution by water returning during cooldown. The extreme values for CO_2 fugacity occur during this period of approximation.

An advantage of the reactive transport approach is the integration of chemical processes, with spatial and temporal resolution limited only by the model design. Disadvantages include computational effort, the representation of the host rock and simulation of engineered barriers using only a few chemical species and precipitates, and restricted flexibility in handling ionic-strength limitations. Simulations of this type will be incorporated in this model as applicable calculations become available.

3.1.2.2.2   Input Data, Assumptions, and Uncertainties

CO_2 and ^{14}C Data from SD-12 and Other Surface-Based Boreholes

Total gas-phase CO_2 concentration data from several surface-based boreholes are used to support the average value of 1000 ppm for the concentration of CO_2 in the UZ gas phase, used in this report. This is an average value consistent with surface-based borehole data (CRWMS M&O 2000t). Gas composition measurements obtained from the Exploratory Studies Facility (ESF), or from boreholes drilled from the ESF, are not used for this purpose because of the potential for contamination by ventilation air.

Measured data for the dissolved inorganic carbon content of porewater samples extracted from samples of SD-12 drill core, are used to quantify the transport of dissolved CO_2 in recharge water (Figure 3-34). As a suitable approximation, the total dissolved inorganic carbon in recharge waters is represented by bicarbonate concentration, because the waters are at near-neutral pH (CRWMS M&O 2000t).

Additional Input Data and Assumptions Used to Analyze CO_2 Transport at Borehole SD-12

In addition to the data discussed previously, additional input includes hydrostratigraphic unit definitions and properties, including fracture and matrix porosities and stratigraphic contact elevations in borehole SD-12 (CRWMS M&O 2000t). Correlation between stratigraphic units and hydrostratigraphic units is based on TSPA-VA stratigraphy (CRWMS M&O 2000t) interpreted for newly defined hydrostratigraphic units at the location of borehole SD-12. Ambient matrix saturation for hydrostratigraphic units intercepted by borehole SD-12 is estimated from published data (CRWMS M&O 2000t).

Three values of the present-day average infiltration flux at Yucca Mountain are used to represent the range of conditions. The average flux over all multi-scale TH model locations (CRWMS M&O 2000i) for the lower, middle, and upper flux distributions are 0.56, 5.98, and 14.56 mm/yr, respectively.

The mass transfer model described in this section is a tool for estimating reasonable-bound values for gas fluxes and fugacities. Several assumptions are made in developing this model:

- **Steady-State, 1-D Conditions**—A dynamic steady state is assumed for interpretation of present-day isotopic conditions and mass transfer. The assumption of vertical, 1-D transport supports lower-bound estimates for gas flux and fugacity because multidimensional effects are associated with mixing.

- **Dissolved Inorganic Carbon**—The composition of water from Well J-13 is used as an analogue for the dissolved inorganic carbon content of percolating waters in the UZ. The nominal reported bicarbonate alkalinity is 128.9 mg/L (CRWMS M&O 2000t).

- **Limited Interaction of CO_2 with Solid-Phases**—CO_2 interaction with solid-phase carbonates is limited. For ambient conditions, this is consistent with a dynamic steady-state whereby near-equilibrium of waters with calcite is maintained throughout the UZ. During the thermal period, exsolution of CO_2 by warming and evaporation, and dissolution of carbonate by condensate, are compensating processes.

- **Representative Formation Properties**—For interpreting ambient ^{14}C data, depth-averaged fracture porosity, volumetric water content, temperature, total pressure, and other properties are assumed.

- **Other Assumptions**—Ambient temperature values for gas diffusion coefficients and gas solubility, are used in the bounding mass transfer model for thermal response. Isotopic fractionation associated with dissolution or exsolution of [14]CO_2 is assumed to be a small effect compared with variations in ^{14}C activity caused by radioactive decay. The

average ambient ^{14}C signature for CO_2 in recharge water or gas is assumed to be 100 pmc (percent modern carbon).

Additional detail on input data and assumptions is provided in the source documentation (CRWMS M&O 2000t). Uncertainty is addressed in the Gas Flux and Fugacity Model primarily through the use of a bounding approach and also by comparison to other approaches.

Gas Flux and Fugacity Model Uncertainties

The foregoing discussion has shown that this model has associated uncertainties which derive from consideration of alternative models, and from assumptions related to input data and from selections made in model development. Uncertainty is addressed by making this a bounding model. The greatest uncertainty is probably associated with the assumption of limited CO_2 interaction with solid phases, in application of the model to gas transport during the thermal period. This uncertainty can be addressed through additional modeling using alternative methods, calibrated to ambient CO_2 data and gas-phase composition observations from field thermal testing.

3.1.2.2.3   Analytical Models for Gas Flux and Fugacity

Oxygen fugacity is an important chemical boundary condition for corrosion of metals. Flux and fugacity for O_2 gas are more strongly dominated by gas-phase processes than they are for CO_2 because the solubility of O_2 in water is smaller and because the gas phase contains more O_2. Oxygen has limited solubility in water, and when it is consumed by aqueous reactions, the local fugacity can be strongly depleted relative to the bulk environment.

3.1.2.2.3.1   Mass Balance Model for Ambient, Steady-State $^{14}CO_2$ Transport in the UZ

Using a steady-state radiocarbon mass balance, the $^{14}CO_2$ flux delivered to the host rock by ambient natural processes is estimated from the ^{14}C activity of the carbon found there:

$$\frac{d\,^{14}M_{mat}}{dt} = 0 = \frac{^{14}C_{aq,in}\,q_{aq}\left(^{14}a_{in} - {}^{14}a_{out}\right)}{^{14}a_{in}} + {}^{14}m_{gas,in} - \lambda_{14}\,^{14}M_{mat} \qquad \text{(Eq. 3-4)}$$

where

$^{14}M_{mat}$ = mass of $^{14}CO_2$ per unit area, principally in the matrix porewater (kg/m^2)

$^{14}C_{aq,in}$ = concentration of $^{14}CO_2$ in recharge water (kg/m^3)

q_{aq} = flux of recharge water (m/sec)

$^{14}m_{gas,in}$ = mass flux of $^{14}CO_2$ transported in the gas phase (kg/m^2-sec)

λ_{14} = ^{14}C decay constant (3.84×10^{-12} sec^{-1})

$^{14}a_{in}$ = ^{14}C activity for influent water, e.g. recharge (pmc)

$^{14}a_{out}$ = ^{14}C activity for effluent water, e.g. to the saturated zone (pmc)

A steady-state mass balance approach based on Equation 3-4 can be applied to the entire UZ or to intervals, such as above and below a hydrologic confining unit that acts as a barrier to gas flux

but not to liquid flux. Below a confining unit, aqueous flux must be the predominant mechanism for transport and storage of $^{14}CO_2$. Such confinement is inferred in borehole SD-12 immediately below a depth of 397 m (Figure 3-29) where a hydrologic confining unit has been inferred from barometric efficiency observations (CRWMS M&O 2000t).

The following discussion analyzes the $^{14}CO_2$ data from borehole SD-12, using a mass-balance approach (CRWMS M&O 2000t). The stratigraphic column is divided into a set of discrete intervals, and the water content, dissolved inorganic carbon, and ^{14}C activity are determined for each interval from site data. The steady-state influx of modern CO_2 needed to replace the ^{14}C lost to radioactive decay is calculated for each interval. The results for borehole SD-12 are plotted as both the incremental and cumulative CO_2 flux (Figure 3-35). The mass balance results are summarized as follows:

- **CO_2 demand in the UZ**–The ^{14}C mass balance for the entire UZ thickness at borehole SD-12 shows that approximately 586 mg/m^2-yr of modern carbon (100 pmc) are required to replace ^{14}C decay and maintain the inventory at steady state (CRWMS M&O 2000t). This is a minimum flux that is not adjusted for through-flux of $^{14}CO_2$ to the saturated zone.

- **Below the confining zone**–For the interval below 397 m depth in borehole SD-12, the flux of modern CO_2 required to replace ^{14}C decay is approximately 287 mg/m^2-yr. This flux is aqueous because of confining conditions present in the rock. It is also a minimum flux that is not adjusted for through-flux of $^{14}CO_2$ to the saturated zone.

- **Host rock and other units above the confining zone**–For the interval above 397 m depth in borehole SD-12, the flux of modern CO_2 required to replace ^{14}C decay is approximately 299 mg CO_2/m^2-yr. Because the aqueous infiltration flux at this location is not enough to transfer this much aqueous CO_2 (in addition to that transferred to the lower interval) except under extreme infiltration conditions, gas-phase transfer is evident.

3.1.2.2.3.2   Model for 1-D Transport of $^{14}CO_2$ for Ambient Conditions

Murphy (1995) derived an analytical expression for ambient CO_2 fugacity and fluxes that is based on the idea that transport occurs in both the liquid and gas phases. The 1-D, steady-state model assumed that the UZ has uniform properties and that the surface boundary composition is constant. Transport behavior was assumed to include both molecular diffusion and advective-dispersive effects. The following discussion modifies this analytical model by addition of an advective term; it then evaluates gas-phase CO_2 transport in borehole SD-12. The resulting mass transfer relation is used to represent transport of gases into the potential repository.

In the discussion that follows, diffusive and analogous dispersive processes are assigned to the gas phase, while advection occurs in the liquid phase as percolation. A mass-balance equation taking into account transport and decay of ^{14}C is

$$\frac{\partial\,^{14}C_{bulk}}{\partial t} = \phi_{gas}D_{gas}\frac{\partial^2\,^{14}C_{gas}}{\partial z^2} - u\frac{\partial\,^{14}C_{aq}}{\partial z} - \lambda_{14}\,^{14}C = 0$$

$$^{14}C_{bulk} = \phi_{gas}\,^{14}C_{gas} + \phi_{aq}\,^{14}C_{aq}$$

$$^{14}C_{aq} = K_d\,^{14}C_{gas}$$

(Eq. 3-5)

where

$^{14}C_{bulk}$ = bulk concentration of $^{14}CO_2$ in the UZ (kg/m^3)

$^{14}C_{gas}$ = $^{14}CO_2$ concentration in the gas phase (kg/m^3)

$^{14}C_{aq}$ = $^{14}CO_2$ concentration in the aqueous phase (kg/m^3)

D_{gas} = diffusion-dispersion coefficient for gas-phase $^{14}CO_2$ transport (m^2/sec)

ϕ_{aq} = volume fraction liquid, predominantly in matrix porewater

ϕ_{gas} = volume fraction gas in which diffusive-dispersive transport occurs, predominantly fracture porosity

u = liquid flux that is isotopic equilibrium with gas (m/sec)

K_d = dimensionless distribution coefficient for CO_2 partitioning between gaseous and aqueous phases

Making the necessary substitutions, Equation 3-5 is linear with constant coefficients. Obtaining a solution and applying the boundary condition $^{14}C_{gas}$ (z→0) = $\gamma_{14}a_{in}C_{gas,in}$ yields (CRWMS M&O 2000t)

$$^{14}C_{gas} = g_{14}a_{in}C_{gas,in}\exp\left\{z\left[\frac{uK_d - \sqrt{u^2K_d + 4\lambda_{14}\phi_{gas}D_{gas}\left(\phi_{gas} + \phi_{liquid}K_d\right)}}{2\phi_{gas}D_{gas}}\right]\right\}$$

$$^{14}a = \,^{14}a_{in}\exp\left\{z\left[\frac{uK_d - \sqrt{u^2K_d + 4\lambda_{14}\phi_{gas}D_{gas}\left(\phi_{gas} + \phi_{liquid}K_d\right)}}{2\phi_{gas}D_{gas}}\right]\right\}$$

(Eq. 3-6)

where $C_{gas,in}$ is the concentration of total carbon (all isotopes) representing the influent or recharge composition. Equation 3-6 is fit to measured data for ^{14}C activity vs. depth in borehole SD-12 (Figure 3-36). The following additional details are needed to obtain solutions and are discussed more fully in the source documentation (CRWMS M&O 2000t):

- **Gas-liquid CO$_2$ distribution coefficient**–CO$_2$ partitioning is estimated using the 1000 ppmv CO$_2$ concentration for the gas phase and 94 mg CO$_2$/L for matrix porewater. Converting to common units (kg/m^3) and taking the ratio of aqueous to gaseous concentrations yields a distribution coefficient $K_d = 53.1$ (dimensionless).

- **Gas volume fraction in the UZ (ϕ_{gas})**–The gas volume fraction in which transport occurs is dominated by the fracture porosity, which is estimated for the host rock and overlying units at the SD-12 location using hydrostratigraphic properties.

- **Liquid volume fraction (ϕ_{aq})**—The aqueous liquid volume in which CO_2 is stored and retarded is dominated by the matrix porewater, which is estimated for the host rock and overlying units at the SD-12 location using hydrostratigraphic properties and saturation data.

- **Diffusion-dispersion coefficient (D_{gas})**—The diffusion-dispersion coefficient in Equation 3-5 and Equation 3-9 is calculated as a multiple of the molecular diffusion coefficient for CO_2 in air:

$$D_{gas} = D_{CO_2}\tau \qquad\qquad \text{(Eq. 3-7)}$$

where

D_{CO_2} = diffusion coefficient for gas in air (1.60×10^{-5} m^2/sec for CO_2 and 2.1×10^{-5} m^2/sec for O_2; at 298 K)

τ = tortuosity-dispersion coefficient (dimensionless)

In Equation 3-7, the effect of gas-phase advective-dispersion is represented by a coefficient (τ) rather than by an additive term. This is consistent with the conceptual model, in which molecular diffusion works in the same manner as path-dispersion to increase bulk dispersion.

Ambient $^{14}CO_2$ Transport in Borehole SD-12

Plots of ^{14}C activity versus depth, calculated using Equation 3-6, are compared with measured data in Figure 3-36 (CRWMS M&O 2000t). The measured data are represented by separately calculated curves for "lower," "mean," and "upper" average infiltration values. A value of $\tau = 5$ is used for fitting, indicating that gas-phase mobility of CO_2 is five times greater than with molecular diffusion alone. As discussed previously, gas-phase transport is required because the ambient percolation flux is insufficient to account for recharge of all of the ^{14}C present in the UZ.

Comparison with Data from Other Boreholes

Equation 3-6 has also been plotted with ^{14}C activity data from boreholes UZ-6/6S, UZ-1, NRG-5, and SD-7 (CRWMS M&O 2000t). The same input data are used, with a range of values for the tortuosity-dispersion coefficient (τ). Transport behavior is apparently stronger for the other boreholes, and a value of $\tau = 13$ is selected to calculate gas fugacity estimates for the Chemical Reference Model.

3.1.2.2.3.3   Model for Gas Transport During the Thermal Period

Gas-phase flux of CO_2 or O_2 is estimated using diffusion and advection terms, corresponding to the first two terms on the right-hand side of Equation 3-5. The approach calculates gas-phase mass flux in response to a sink at the potential repository horizon, such as would be caused by chemical reactivity, analogous to the effect of radioactive decay. Mass flux is calculated for constant concentration conditions at the ground surface and at the potential repository level as

$$m_{gas} = -\phi_{gas}D_{gas}\frac{\partial C_{gas}}{\partial z} - v\phi_{gas}C_{gas} \qquad \text{(Eq. 3-8)}$$

where

m_{gas} = flux (i.e. consumption from decay or reaction) of gas-phase reactant (kg/m²·sec)

D_{gas} = gas diffusion coefficient (m²/sec, different for O_2 and CO_2)

v = velocity of gas phase (positive upward, m/sec)

and the other notation is basically similar to that of Equation 3-5. The gradient $\partial C_{gas}/\partial z$ is calculated from the difference between the gas concentration at the surface and that in the potential repository. Use of a single value of D_{gas} in Equation 3-8 instead of multiple values corresponding to the layered stratigraphy, is analogous to the effective 1-D hydraulic conductivity for a stack of layers with different conductivity values (CRWMS M&O 2000t).

The binary gas-diffusion coefficients for CO_2 and O_2 increase with temperature, and the effect is bounded in this model by using tabular values at 298K. Coefficients of binary diffusion for CO_2 and O_2 gases in water vapor are assumed to be no less than the coefficients in air.

Calculations show that gas-phase velocity (v) above the drifts tends to be negative (directed upward) during the thermal period because water vapor is convected upward. Although 2-D drift-scale TH simulations (Section 3.1.2.1) show that the gas-phase may actually circulate in the pillars, which would tend to increase availability of CO_2 and O_2 gases, the upward velocity above the drift openings is used in this bounding model. The gas-phase velocity varies with depth and location in the host rock; however, for this bounding model the maximum upward velocity in the host rock directly above the drift is used (CRWMS M&O 2000t). Note that absolute concentration (C_{gas} times the air mass-fraction) is used to compute the gradient in Equation 3-8.

Equation 3-8 is rearranged to relate the gas flux and concentration (or fugacity), using ($C_{gas,in}-C_{gas}$)/z to represent $\partial C_{gas}/\partial z$. The maximum concentration at depth (C_{gas}) is found by setting the mass flux (m_{gas}) to zero, and the maximum mass flux is computed by setting the concentration at depth to zero. Both of these limits vary with time, as the air mass-fraction and the gas-phase velocity change with thermal evolution of the potential repository. This mass-flux relation is implemented for the L4C4 location and the "upper" infiltration flux (CRWMS M&O 2000t). The L4C4 location is near the geographic center of the potential repository, where large-scale thermally-driven gas-phase convection is likely to be smallest. Selection of the L4C4 location and "upper" infiltration distribution is discussed in Section 3.1.2.

3.1.2.2.4   Gas Flux and Fugacity Model Validation

Analytical solutions are developed to describe the variation of ^{14}C activity with depth in the gas phase. These models are extended, to describe the transport of CO_2 and O_2 gases in the UZ during the thermal period in response to chemical sources or sinks at depth. Bounding values are used for most parameters of these models, in the sense that the values tend to minimize the fugacity of CO_2 and O_2 gases during the thermal period, or any other time when these constituents are being consumed in the drift environment. One parameter, the diffusion-

dispersion parameter that controls gas-phase transport, is calibrated to field data from borehole SD-12. The results show that ^{14}C observations can be represented by an envelope of curves corresponding to uncertainty in the infiltration flux (Figure 3-29).

The model is also applied to four other boreholes in the same manner. The same bounding parameter values are used to approximate the other boreholes, and the diffusion-dispersion parameter is fitted for each borehole. The results show that the fitted parameter has a greater value (more transport) in the other boreholes. This indicates that the SD-12 value is a conservative representation for the overall site area, so this value is used in the gas flux and fugacity calculations.

The 1-D analytical solution includes multiple bounding approximations. It is a valid bounding model as shown by checking against ^{14}C data from four other boreholes in addition to SD-12. The bounding nature of the model for gas fugacity is also shown by comparison to the air mass-fraction method, and comparison to results from reactive transport simulations.

3.1.2.2.5 Results for Gas Flux and Fugacity in the EBS Environment

Calculated results for CO_2 and O_2 gas fugacity, as functions of time after emplacement, are shown in Figure 3-37 and Figure 3-38. In these plots, both the fugacity values and the mass flux values are normalized to their maximum values. The normalized results for CO_2 and O_2 differ only with respect to the values used for diffusion coefficients.

The mass-transfer model shows that for a maximum CO_2 fugacity of 1000 ppm, the minimum CO_2 fugacity during the thermal period is approximately 1 ppmv. Similarly, for a maximum O_2 fugacity of 0.2 atm, the lower bound values for O_2 fugacity are approximately 200 ppmv. Further decrease of either the CO_2 or O_2 fugacity by consumption in the EBS environment would not be substantial until the rate of consumption approached 90 percent of the maximum mass flux.

3.1.2.2.6 Comparison with Alternative Models and Approaches

Comparison of the mass-transfer model represented by Equation 3-8 with the air mass-fraction in Figure 3-37 and Figure 3-38 shows that the mass-transfer model predicts greater minimum fugacities, but is slower to recover during cooldown. The air mass-fraction estimation approach is most similar to the mass-transfer model with low flux (i.e., low consumption in the potential repository environment). This is appropriate because the air mass-fraction approach does not relate fugacity with flux.

Discussion of Conservatism in Calculated Results

The gas-phase CO_2 and O_2 fugacities and their variation with mass flux represent lower-bound availability of these constituents for chemical reaction in the drifts for the following reasons:

- Aqueous fluxes of CO_2, and O_2 to a lesser extent, are neglected in the model

- One-dimensional transport is assumed, but there are indications from the TH models that multidimensional gas-phase circulation may occur because of the wide drift spacing

- Release of CO_2 by exsolution and evaporation of pore water, is neglected in the model.

- Increase of molecular diffusion coefficients with temperature is neglected in the model.

The use of lower-bound estimates for CO_2 and O_2 availability, for conservative assessment of the EBS chemical environment, is based on the principle that alkaline conditions are adverse to corrosion resistance.

3.1.2.3 Introduced Materials Models

This section presents a set of models used primarily for analysis of the sensitivity of bulk chemical conditions in the EBS, to changes in the properties and composition of introduced materials. A typical inventory of EBS materials in addition to the quartz sand backfill and crushed tuff invert ballast, is presented as a starting point for discussion. For quartz sand backfill, the importance of kinetic dissolution/precipitation behavior is evaluated for inclusion in the Chemical Reference Model (Section 3.1.2.7). Potential dissolution of quartz backfill by evaporatively concentrated waters, and potential changes in backfill porosity from evaporative precipitation, are evaluated and found to be minor. Potential consumption of O_2 by corrosion of steel used in the EBS is estimated from laboratory corrosion rates, and found to be potentially important to the bulk chemical environment until degradation of the steel is complete. Consumption of O_2 by corrosion of the DS and WP is much less important. Leaching of the cement that will be used in grouted rockbolts, is evaluated and found to be a minor contributor to the bulk chemical environment.

3.1.2.3.1 Materials Present in the Emplacement Drifts

The EBS design calls for a backfill composition of quartz sand (>99% SiO_2). The non-quartz fraction has predominantly feldspar mineralogy, and limited concentrations of halides and organic material (CRWMS M&O 2000t). The invert ballast material will be composed of Topopah Spring welded tuff that has been crushed to gravel-sized particles ranging in size from 9.5 mm to 19 mm. The mineralogy of the ballast will be substantially the same as host rock from which the drifts are excavated.

The materials to be used for the WPs and their supports are inventoried in Table 3-3. Other materials to be used in the potential repository emplacement drifts, and committed for the postclosure period, are inventoried in Table 3-4 (CRWMS M&O 1999g).

Use of cementitious materials will be limited to fully grouted rockbolts, which will be used only in the nonlithophysal host rock (CRWMS M&O 2000t). An average of four rockbolts per meter of drift will be used. The grout will be a Type K expansive cement, with admixtures to promote workability and to decrease permeability.

Table 3-3. Quantities and Compositions of Materials Used per Each Meter of a 21 PWR Waste Package and Its Supports, Excluding the Waste Form Inside the Package

Material	Material	Quantity [a] (kg/m)	Composition [b] (percent)							
			Fe	Mn	Ni	Mo	Ti	Al	Cr	B
WP supports	Alloy 22	267	6.0	0.5	50.015	14.5	n/a	n/a	22.5	n/a
WP supports	stainless Steel	128	62.05	2.0	14.0	3.0	n/a	n/a	18.0	n/a
WP Outer Barrier	Alloy 22	1173	6.0	0.5	50.015	14.5	n/a	n/a	22.5	n/a
WP Inner Barrier	Stainless Steel	2106	62.06	2.0	14.0	3.0	n/a	n/a	18.0	n/a
Thermal Shunt	Aluminum	63	0.7	0.15	n/a	n/a	n/a	95.85	0.35	n/a
Absorber plates	Neutronit A 978	387	66.66	n/a	13.0	n/a	n/a	n/a	18.5	1.6 [c]
Basket Guides	Steel	1073	97.91	1.3	n/a	n/a	n/a	n/a	n/a	n/a
Drip Shield	Titanium Grade 7 [d]	563	0.3	n/a	n/a	n/a	98.665	n/a	n/a	n/a
Drip Shield	Alloy 22	16	6.0	0.5	50.015	14.5	n/a	n/a	22.5	n/a

NOTES: [a] Quantity refers to 1-m length of potential repository drift.
[b] This table presents only selected constituent elements, not the total composition of every material.
[c] See (CRWMS M&O 1999g) for source of this value
[d] Titanium composition also contains 0.25 percent palladium (CRWMS M&O 1999g)

Table 3-4. Quantity and Compositions of Materials to Be Used for Facilities and Ground Support in the Potential Repository Emplacement Drifts

Material	Material	Quantity [a] (kg/m)	Composition [b] (percent)							
			Fe	Mn	Ni	Mo	Co	W	Cr	Cu
Rockbolt Sets [c]	Steel	48	99.022	n/a	n/a	N/a	n/a	n/a	n/a	n/a
Welded Wire Fabric	Steel	70	98.8	n/a	n/a	N/a	n/a	n/a	n/a	n/a
Gantry Rail	Steel	133.9	97.59	1.0	n/a	N/a	n/a	n/a	n/a	n/a
Rail Fittings	Steel	13.4	74.44	n/a	n/a	N/a	n/a	n/a	n/a	25.0
Steel Sets	Steel	369	97.48	1.65	n/a	N/a	n/a	n/a	n/a	n/a
Conductor Bar Fittings	Steel	0.2	97.48	1.65	n/a	N/a	n/a	n/a	n/a	n/a
Communications Cable [d]	Copper	0.79	N/a	n/a	n/a	N/a	n/a	n/a	n/a	50.0
Conductor Bar [e]	Copper	5.32	N/a	n/a	n/a	N/a	n/a	n/a	n/a	100
Steel Invert	Steel	587	97.48	1.65	n/a	N/a	n/a	n/a	n/a	n/a

NOTES: [a] Quantity refers to 1-m length of potential repository drift.
[b] This table presents only selected constituent elements, not the total composition of every material.
[c] Rockbolts will be used only for the nonlithophysal portion of the potential repository drift design (CRWMS M&O 1999g).
[d] Wire conductor is not included because its relative abundance is small compared to other materials.
[e] Loading-docks, isolation doors, and related components which will be used only at the ends of the emplacement drifts and not in the waste emplacement area, are not considered here.

3.1.2.3.2   Conceptual Models for Degradation of Introduced Materials

Environmental Conditions

The abundances of O_2 and N_2 pore gases from the UZ are close to atmospheric values (CRWMS M&O 1999g). Measurements of gas composition from various UZ boreholes demonstrate that gas-phase CO_2 concentration averages approximately 1000 ppmv (Section 3.1.2.2). Water composition in the host rock is represented by J-13 well water. Use of this composition in

bounding models of the chemical environment is discussed in Section 3.1.2.5. J-13 water is compositionally similar to perched waters from the site and to waters recovered from fractures in similar tuffs at Rainier Mesa (CRWMS M&O 1999g). The composition of J-13 water is consistent with model predictions for water interaction with the host rock. Porewaters extracted from Yucca Mountain tuff generally contain more Ca, Mg, chloride, and sulfate and have proportionately less bicarbonate than J-13 water. However, based on the best available information, composition similar to J-13 water is reasonable for water in fractures of the Topopah Spring welded tuff at ambient and elevated temperature (CRWMS M&O 2000t).

Increased temperatures will evaporate much of the water in the potential repository drifts and produce a boiling zone in the host rock at or near the drift wall. As thermal output decays with time, all introduced materials will eventually have been subjected to boiling-zone conditions. In the boiling zone, mineral precipitates, including salts, will form and can contribute to degradation of introduced materials through formation of brines. Evaporatively concentrated water will be enriched in alkalis, chloride, and sulfate; with pH 9 or greater (CRWMS M&O 1999g). Mineral precipitation will occur, and chemical species that remain dissolved can become concentrated by 1,000-fold or more relative to J-13 water. The composition of evaporatively concentrated waters depends on the gas-phase composition and on the open-system assumptions that can be made in modeling.

Quartz-Sand Backfill

Interaction of quartz in the environment will result primarily from aqueous dissolution and precipitation rate processes. The solubility of quartz in the potential repository environment will be affected by pH, temperature, solution composition, and ionic strength. At pH 9 and above, the solubility of silica increases by as much as several orders of magnitude, as the species $H_3SiO_4^-$ and $H_2SiO_4^{2-}$ become increasingly abundant. The presence of quartz or other silica minerals in the potential repository environment can therefore serve to buffer the pH in these ranges.

The dissociation constants for silica species and the equilibrium solubility constant for quartz are affected by changes in temperature. A temperature increase from 25°C to 100°C increases the solubility of quartz and other forms of silica, including amorphous silica, by an order of magnitude. Solubility also increases when other ions modify the solution; thus, for brines, the solubility can increase 100-fold in the presence of alkali and alkaline earth cations.

The postulated dissolution rate for quartz, at conditions expected in the potential repository, is relatively slow compared to other minerals such as cristobalite (CRWMS M&O 2000k). Quartz dissolution and precipitation rates in the potential repository environment will be controlled by intrinsic factors, including temperature, solution composition, and pH (CRWMS M&O 2000k) as well as the specific surface area available for reaction. The rates generally increase with temperature; for example, the quartz dissolution rate increases 1000-fold at temperatures from 25°C to 100°C. The quartz dissolution rate also increases with greater concentrations of dissolved salts. For dilute aqueous solutions, equilibrium with quartz typically does not occur at temperatures less than 200°C, but other factors such as salt concentration may decrease this temperature to 190°C or less. The dissolution and precipitation rates for lower-order SiO_2 precipitates such as chalcedony are not as strongly inhibited over the temperature range of 25°C

to 100°C. Therefore, any lower-order precipitates present in the potential repository environment would tend to dissolve faster than quartz, and silica precipitation is more likely to occur as the lower-order forms unless the reactive surface area of quartz is large.

Three conceptual approaches are used for modeling of aqueous processes involving quartz-sand backfill:

- **Kinetic model for water–quartz interaction**–This involves modeling the effects of quartz dissolution and precipitation on pH, for conditions when water is flowing in the emplacement drifts. This approach is incorporated in the Chemical Reference Model (Section 3.1.2.7).

- **Effects of quartz backfill at high ionic strength**–This involves evaluation of quartz solubility at high ionic strength (CRWMS M&O 2000k). This approach considers the composition of fluids that have been evaporatively concentrated well beyond 100-fold and which are present in very small amounts in the potential repository environment. Quartz behavior is inferred from calculated saturation indices, which indicate whether precipitation or dissolution is thermodynamically favored.

- **Porosity reduction in quartz backfill**–This involves modeling of porosity changes produced by precipitates derived from influent seepage and dissolution of backfill (CRWMS M&O 2000t). This approach is used to evaluate the sensitivity of backfill flow properties to chemical precipitation.

Structural Steel and Waste Package Alloys

The alteration of steels and alloys, as discussed in *In-Drift Corrosion Products* (CRWMS M&O 1999g) will produce metal oxide and metal hydroxide corrosion products in the drift and may also form metal-silicate minerals. As the iron and other metals corrode, they represent a sink for oxygen. Oxidation reactions represent a source of metabolic energy for microbial activity, which can enhance the rate of metal corrosion. The corrosion products have potentially important sorptive properties and may form colloidal particles that can transport radionuclides.

Of the 12 elements addressed in Table 3-3 and Table 3-4, and discussed in the source documentation (CRWMS M&O 1999g), the following will each be present in amounts less than 1 percent of the total of introduced materials: Pd, Co, W, B, and Cu. Because such small quantities are present, a simplifying assumption is made to exclude these elements from assessment of the bulk chemical environment. Accordingly, the following elements are discussed further: Fe, Mn, Ni, Mo, Cr, Ti, and Al. Natural waters from the site contain low concentrations of these metals, so introduced materials represent a potentially significant perturbation on the chemical environment. Literature information on the behavior of these elements (CRWMS M&O 1999g) is summarized below:

- **Iron (Fe)**–Corrosion of the structural steel and corrosion-resistant alloys will cause precipitation of hematite or goethite, depending on pH, temperature, and Ti-concentration. The hematite or goethite can act as sorbents for Ni, Mn, or Mo, and Fe may coprecipitate to form solid solutions.

- **Manganese (Mn)**—Corrosion of the steel and alloys can lead to precipitation of a form of MnO_2 (e.g., pyrolusite). These oxides are active sorbents and act as oxidants for other metal species. In the presence of iron, Mn could be reduced to Mn(II) and may precipitate with hematite or goethite to form solid solutions.

- **Nickel (Ni)**—Corrosion of the corrosion-resistant alloys will cause precipitation of $Ni(OH)_2$. In the presence of Fe and Mn, Ni could also precipitate with hematite, goethite, or MnO_2 to form solid solutions. Aqueous nickel will compete with other metal species for sorption sites on metal oxides.

- **Chromium (Cr)**—Corrosion of the corrosion-resistant alloys will cause precipitation of Cr_2O_3. The oxide can dissolve very slowly, yielding aqueous Cr(III). In the presence of ferric iron or manganese oxides, Cr(III) will strongly sorb and can coprecipitate to form solid solutions. Chromium(III) will slowly oxidize, and the resulting chromate (CrO_4^{2-}) may be present as a trace species.

- **Molybdenum (Mo)**—Corrosion of the steel and corrosion-resistant alloys will cause precipitation of Mo_3O_8. Molybdenum may also be found in solution as the molybdate ion (MoO_4^{2-}) and can precipitate with hematite or goethite to form solid solutions or can compete with other aqueous metal species for available sorption sites on Fe and Mn oxides.

- **Titanium (Ti)**—Corrosion of Ti alloys will cause precipitation of TiO_2. Relatively small amounts of Ti may also precipitate with hematite or goethite to form solid solutions or may compete with other aqueous metal species for available sorption sites on Fe and Mn oxides.

- **Aluminum (Al)**—Corrosion of aluminum components inside the WP may cause the precipitation of $Al(OH)_3$ or $AlOOH$. Aluminum oxide solids can be sorbents for both anions and cations in solution. Aqueous aluminum will form clay minerals in the presence of silica. On exposure to alkaline fluids (e.g., pH 11) Al can react to form hydrogen gas, which is possible in association with evaporatively concentrated fluids inside the waste package.

The geochemical environment will eventually corrode the steels and alloys that contain these elements. The metals are thermodynamically unstable and will react with water and the available oxygen to produce corrosion products. Some introduced materials will be more resistant to corrosion (typically because of passivating metal-oxide films), while others may corrode more readily, especially in the presence of waters concentrated by evaporation and boiling.

Corrosion of introduced materials, particularly steel, can alter radionuclide transport in the EBS environment. The presence of metal oxidesys could retard radionuclide transport, and at the same time, contribute colloidal material that increases radionuclide mobility. The two elements with the greatest potential to contribute colloidal corrosion products are Fe and Al. Ferric colloids from introduced materials from corrosion processes will be more abundant in the EBS,

than natural ferric colloids contributed by groundwater inflow. Aluminum-hydroxide colloids may be formed by corrosion of materials inside the WPs.

Crushed Tuff Invert Ballast Material

This discussion provides justification for treatment of the invert in process models and performance assessment. It is taken from the analysis/model report on invert–seepage interaction (CRWMS M&O 2000m).

If water–rock interaction in the invert reproduces reactions that occur elsewhere in the host rock, the small size of the invert argues that invert–seepage interactions are not important. Chemical reactions in the host rock will replicate seepage–invert interactions because the invert ballast will consist of locally derived tuff. The invert will also contain appreciable amounts of steel, which will eventually form Fe-oxides similar to those in the host rock. The invert will contain copper, which may support reactions that do not occur in the host rock. No significant effect of copper on waste isolation performance has been recognized, but further analysis would be required to identify and evaluate reactions involving copper.

The importance of the invert in conditioning the chemistry of water depends on the flow rates. Low-flow conditions in the invert will effectively decrease the water–rock mass ratio for chemical interaction and can diminish the mobility of chemical species, including radionuclides, from hydrologic and chemical considerations. If the flow of water circulating through the drifts is large, the importance of the invert is minimized, and water-rock interactions will be dominated by the host rock because more surface area will be available for reactions in the host rock within a short travel time from the drift wall.

Flow of water from breached WPs is not considered for the thermal period, but only for ambient conditions (CRWMS M&O 2000s). Changes in composition of water returning to the invert will be caused primarily by leaching, dissolution, and alteration of the WFs. For an environment in which drift seepage flows through the backfill, and through breaches in the DS and the WP to reach the WF, much of the seepage will never encounter the WF. Thus, changes in water chemistry caused by flow through the WP, will be subject to dilution in the invert. Further discussion of radionuclide transport in the invert is presented in Section 3.1.3.

Cementitious Materials

The mineralogy of the cement grout proposed for use with rockbolts, will determine how it reacts with groundwater. Mineral phases present in young cement are represented by portlandite, ettringite, tobermorite, and brucite. Young cement also contains a major fraction of calcium-silicate-hydrate (C-S-H) gel, a noncrystalline phase with composition similar to tobermorite. The C-S-H gel converts to crystalline phases as the cement ages. With further aging, the initial mineral assemblage tends to alter as minerals convert to more thermodynamically stable crystalline phases. Finally, reaction with CO_2 causes carbonation of alkaline minerals such as portlandite, producing less soluble, less alkaline carbonate minerals such as calcite.

For bounding potentially deleterious effects from leaching of alkaline constituents from cement grout, the young cement assemblage is used because it is least thermodynamically stable, most

soluble, and potentially most alkaline. The conceptual model for interaction of percolating water with these mineral phases consists of gradual dissolution. The constituent phases dissolve incongruently in relation to their solubilities. The resulting leachate can have high pH and elevated concentrations of anions such as sulfate, which will vary with temperature because of temperature's effects on solubility.

As an alternative model, carbonation of the cement will cause the leachate pH to become more neutral with time, but the rate of carbonation depends on access of the gas-phase to unreacted grout minerals, which has not been established for the current models. While CO_2 fugacity in the potential repository environment has been investigated, access of CO_2 to rockbolts has not been established; thus, the carbonation process is not incorporated explicitly in present models of leachate composition. Carbonation will be at least partial, however, so calcite and similar carbonate mineral phases will be present. Calcite is included in chemical models of cement leaching, to represent the effects of partial carbonation.

Factors that lessen the potential impacts of cement leachate on the bulk chemical environment include:

- Partitioning of seepage flow such that most seepage is not affected by cement
- Carbonation of the cement minerals
- Buffering of leachate pH by interaction with CO_2 in the gas-phase
- Buffering of leachate pH by interaction with quartz backfill (or other siliceous minerals)
- Dilution of leachate by mixing with other waters

Only a portion of the potential seepage flow into potential repository drifts will be affected by cement, and the effects will be chemically moderated and diluted downstream from the rockbolts.

3.1.2.3.3 Models for Interactions Involving Backfill

3.1.2.3.3.1 Kinetic Model for Water-Quartz Interaction

As a backfill material, quartz reaction rates are kinetically limited to some extent, and quartz sand is comparatively free of impurities that could promote corrosion or microbial activity. The kinetic model for water-quartz interaction is used to determine whether quartz should be included as a kinetically hindered reactant, or an equilibrium solid, in the Chemical Reference Model.

Input Data, Assumptions and Uncertainties

Grain-size distribution for the Overton Sand backfill material (unsieved) is obtained from measured data (CRWMS M&O 2000t). A corresponding lower-bound specific surface area, calculated assuming spherical particles, is used in kinetic calculations. Using volumes for the zones defined in Section 3.1.2.1, the total surface area of quartz sand in each zone is calculated. The surface area could be as much as three times greater if irregular particle geometry is taken into account. The presence of a very fine fraction (< 0.053 mm particle size) with relatively

large surface area is also not accounted for. These estimates for surface area are therefore lower-bound values.

Although the backfill will be unsaturated and the flow field will probably be nonuniform, the entire surface area of particles constituting the backfill is used in kinetic calculations. This is consistent with the capillary nature of sand, which tends to disperse water on the surfaces of all particles, and the reaction cell approach to chemical modeling (used in Section 3.1.2.7). The calculated surface area and residence time values are averages for the backfill present in each zone.

The principal uncertainties associated with this model are the residence time of liquid water in the backfill, and the effective surface area for reaction. Channeling of flow in the backfill from heterogeneity of flow properties, or focusing of seepage sources, could limit the contact time for reaction. Reactive surface area could be much greater than the specific surface area used in this model, but this would support water-quartz equilibrium.

Development of Kinetic Model for Water-Quartz Interaction

The kinetics of quartz precipitation is potentially important with the use of quartz sand as backfill. In the host rock, quartz—and its less stable polymorph, cristobalite—coexist in a steady, chemical disequilibrium over geologic time because the growth (precipitation) rate of quartz is small. The concentration of dissolved silica in J-13 water and similar waters corresponds to near-equilibrium with cristobalite and to supersaturation with respect to quartz. This condition is maintained because of the slow growth kinetics of quartz. The relationship can be inferred directly from measured water compositions and the observation of quartz and cristobalite as constituent minerals.

Because of the increased reactive surface area for quartz and the lack of other silica phases in the backfill, the quartz-cristobalite disequilibrium will be modified as water enters the backfill. The dissolved silica concentration will decrease, all other factors such as temperature and evaporative concentration held constant. For pH values of 10 or greater (which will occur at low CO_2 fugacity during the thermal period), the decrease in silica concentration will decrease the associated buffering capacity (pH buffers such as $H_3SiO_4^-/SiO_2(aq)$, and $NaH_3SiO_4(aq)/cristobalite$ and $NaH_3SiO_4(aq)/quartz$) so that the pH will increase further. These relationships are included in the Chemical Reference Model calculations (Section 3.1.2.7).

A published rate law and data for quartz growth are used to examine the rate of quartz precipitation in the backfill via overgrowth (CRWMS M&O 2000t). The precipitation and dissolution of silicate minerals are generally considered to be surface area–mediated processes (i.e., the rates are proportional to the area of the water-mineral interface). In the backfill, the surface area of quartz exceeds that accessible by fracture waters in the surrounding rock (per unit mass of water). Contact of influent water with the sand backfill can cause development of quartz overgrowths and a significant decrease in the dissolved silica concentration. As the water flows back into the rock, the dissolved silica will increase again from dissolution of cristobalite.

Results from Kinetic Model for Water-Quartz Interaction

The following briefly describes a set of calculations performed for the Chemical Reference Model (Section 3.1.2.7). An EQ6 calculation is performed for composite Zone 3/4, in Time Period 3 after redissolution of evaporative precipitates deposited in previous time periods. The calculation starts with the composition of seepage water from the host rock, modified by temperature, CO_2 fugacity, and evaporative concentration. It uses the kinetic rate law and surface area data discussed previously.

The computation yields a decline in dissolved silica, to a concentration corresponding to quartz equilibrium, in less than 1 year. The actual reactive surface area is probably greater because of surface roughness, so less time could be required to produce the same result. Also, the silica concentration declines exponentially with time, so that most of the decline takes place early, and most of the effect could be achieved in less time. On the other hand, the water is assumed to access the entire surface area of the unsaturated sand, which could lead to overestimation of the extent of interaction if the flow field is highly nonuniform. These are compensating uncertainties, and it is likely that for residence time on the order of 1 year, water-quartz interaction approaches equilibrium. Accordingly, final calculations for the Chemical Reference Model that involve backfill, are made assuming equilibrium with quartz.

3.1.2.3.3.2   Model for Seepage-Backfill Interaction at High Ionic Strength

This section describes an approximate model used to evaluate whether precipitation or dissolution of quartz in the backfill is likely during the thermal period when waters in the EBS are evaporatively concentrated (relative to fracture waters in the host rock). The model is based on the Pitzer formulation for thermochemical modeling, with an extended data base developed to include silica at elevated temperature.

Input Data, Assumptions, and Uncertainties

The quartz solubility calculations require thermodynamic properties of backfill and key groundwater constituents, at high ionic strength and elevated temperature. The thermodynamic data set used in the model simulations is the Pitzer (PT4) database developed for the *In-Drift Precipitates/Salts Analysis* (CRWMS M&O 2000g). In addition to the Pitzer database, other input parameters for this model include:

- Composition and flow rate for influent seepage

- Temperature

- Fugacity of CO_2

- Relative evaporation rate (expressed relative to seepage; inversely related to evaporative concentration factor)

The composition of J-13 well water is adopted for the incoming seepage, which is conservative from the perspective of high pH produced by evaporative concentration, and the potential interaction of alkaline fluid with quartz.

Important uncertainties for this model include applicability of the extended Pitzer (PT4) database, particularly to carbon species and silica. In addition, the significance of under-saturation or super-saturation of concentrated waters with respect to quartz, does not indicate whether the implied dissolution/precipitation reactions would be kinetically hindered.

Development of Model for Seepage-Backfill Interaction at High Ionic Strength

The model is implemented using the EQ3/6 geochemical modeling code. The model development and results are described in detail, in the *In-Drift Precipitates/Salts Analysis* report (CRWMS M&O 2000g).

Results from Model for Seepage-Backfill Interaction at High Ionic Strength

Quartz saturation indices were obtained for each combination of the following:

- Temperatures of 95°, 75°, 45°, and 25°C
- CO_2 fugacity of 10^{-1}, 10^{-3}, and 10^{-6} atm
- Relative evaporation rates of 0, 0.1, 0.5, 0.9, 0.99, and 0.999

The results show that the interaction of quartz sand with seepage derived from partially evaporated J-13 well water, will likely be negligible. Dissolution of quartz, which makes up more than 99 percent of the backfill, is generally not favored except in the most unlikely scenarios (even for the high-pH conditions produced by selecting J-13 water as the influent composition). Saturation indices calculated for the cases described above are summarized in Figure 3-39.

The composition of evaporated seepage water predicted by the EQ3/6 Pitzer model is already at or near saturation with respect to quartz, when it contacts the backfill. The only cases for which quartz dissolution is predicted (saturation indices less than zero) are unlikely combinations involving high temperature (95°C), low CO_2 fugacity (10^{-6} atm), and low relative evaporation rates (seepage rate more than 10 times the evaporation rate). The high temperature makes low relative evaporation an unlikely condition, and the low evaporation rate makes the low CO_2 fugacity an unlikely condition. From these results, dissolution or precipitative overgrowth of the quartz backfill is not predicted.

3.1.2.3.3   Analytical Model for Porosity Reduction in Quartz Sand Backfill

Precipitation of stable precipitates such as silica, and the carbonates and sulfates of Ca and Mg, could affect the porosity and flow properties of the backfill. Sodium and potassium compounds are not as important because they are highly soluble. This section describes a mass balance

Input Data, Assumptions and Uncertainties

The porosity-reduction model is a calculation of the potential change in backfill porosity, as a function of the seepage rate, the dimensions of the backfill, a focusing factor, and the incoming concentrations of Si, Ca, and Mg. The input parameters include the following:

- Concentrations of Si, Ca, and Mg in the influent seepage
- Backfill composition
- Backfill porosity
- Backfill dimensions (cross-sectional area 12.92 m^2)

Porosity reduction is modeled as the result from precipitation of calcite ($CaCO_3$), magnesite ($MgCO_3$), and opal (hydrated SiO_2).

For complete evaporation of influent seepage in the backfill (a bounding approach) the principal uncertainty associated with this model is the relative importance of porosity reduction. Although the densities of the assumed precipitated minerals are known (and alternative minerals would have similar densities) the impact on permeability of quartz sand is may not be simply related to porosity reduction.

Development of Model for Backfill Porosity Reduction

Porosity-reduction is evaluated in a bounding calculation that determines the porosity occupied by precipitating all the dissolved silica, Ca, and Mg present in seepage. The seepage rate is treated parametrically, i.e., the potential porosity reduction is considered over a wide range of seepage rates.

Precipitation may occur in a small portion of the cross-sectional area, so a focus factor is used to represent the fraction of the total volume of backfill where precipitation occurs. For example, if precipitation occurs only in 1 percent of the backfill (such as the area immediately above the DS) a focus factor of 0.01 is used:

$$V_f = ALf \qquad \text{(Eq. 3-9)}$$

where:

A = cross-sectional area
L = length
f = focus factor

The model requires all the seepage to evaporate in the focus volume. This is conservative (i.e., maximizes porosity-reduction in the focus volume) but it is reasonable because flow in the backfill will be nonuniform, and there is the potential for development of thermally-driven reflux whereby evaporative precipitation could be localized to a narrow boiling zone. The model does not address the relation between porosity-reduction and permeability reduction.

Results from Model for Backfill Porosity Reduction

According to this calculation, porosity reduction in quartz-sand backfill will be minor unless a high seepage rate is sustained, and mineral precipitation is concentrated in a small portion of the backfill (less than 10 percent) for thousands of years. The results of this model are summarized in Figure 3-40.

For the highest seepage rate considered in this analysis (100 kg/yr per meter of drift), inflow of J-13 water for 10,000 years is estimated to deliver enough silica, Ca, and Mg to reduce the average porosity of the backfill from 0.41 to approximately 0.406. If this precipitation is concentrated in 1 percent of the backfill, the porosity would decrease from 0.41 to approximately 0.06. However, such a high seepage rate, with sustained and complete precipitation of solutes for thousands of years, is not realistic.

3.1.2.3.4 Model for Corrosion of Carbon Steel in the EBS

Steels and alloys introduced to the potential repository from ground-support materials, drip shields, and waste packages will corrode with time, and the aqueous metal concentrations will depend on precipitation, coprecipitation, and sorption processes. The important effects of metal corrosion on the bulk environment, and the approaches used to represent those effects in the EBS process models are summarized as follows:

- Oxygen in the drift environment will be consumed, decreasing the O_2 fugacity while corrosion is active. This effect is modeled by converting rates for metal corrosion to rates of O_2 consumption, and comparing with mass-flux values developed for the Gas Flux and Fugacity Model (Section 3.1.2.2).

- Corrosion products can increase in volume because they have greater molar volume than the original metals; this can change the geometry and flow characteristics adjacent to metal surfaces. Also, particles of corrosion products can move in the backfill and invert and can change flow characteristics in the EBS. These effects are neglected in this report because the liquid flux in the drifts will be orders of magnitude smaller than the flow capacity of the backfill or invert, so impact on the flow distribution will be minor. The potential impact of introduced materials and thermal effects on drainage capacity of the drifts is addressed elsewhere in this report (Section 3.1.1)

- Metal-oxide colloids with affinity for radionuclides can be produced. This can lead to increased mobility for certain radionuclides, and is considered in Section 3.1.2.6.

- Released radionuclides can be retarded by sorption or coprecipitation involving corrosion products. This effect has the potential to enhance waste-isolation performance, and is addressed in Section 3.1.2.3.

The following sections present a corrosion-rate model for structural steel, converted to oxygen-consumption rate, for comparison to estimates of oxygen availability. The potential consumption of oxygen from structural steel vs. other alloys is also compared.

Input Data, Assumptions and Uncertainties

Corrosion rates for A516 steel have been measured for vapor-phase (not immersion) conditions, elevated temperature, and proximity to synthetic groundwater with composition similar to evaporatively concentrated J-13 water. The tests were performed with alloy A516 because it had been selected as the corrosion-allowance material for the Viability Assessment (VA) WP design. Test data for conditions representing the potential repository environment when water returns during the thermal period are not available for A572 steel, so the A516 data are used to develop rough estimates for steel-corrosion effects.

A constant corrosion rate for structural steel is assumed for each time period in this model. The rate can vary with temperature, pH, and water composition. Modification of the corrosion rate from accumulation of corrosion products is assumed to be insignificant because of the tendency for spallation of corrosion products from steel surfaces.

Steel corrosion is assumed to be insignificant until the relative humidity exceeds 70 percent. This is consistent with the approach used to model the Viability Assessment waste-package corrosion allowance material (CRWMS M&O 1998c, Section 5.5.3.1, pp. 5-31). The threshold humidity could be greater, except that the presence of precipitates and salts on the steel can form brines at lower humidity.

Laboratory data (CRWMS M&O 2000t) suggest an approximate 6- to 7-fold increase in the corrosion rate for C1020 steel, once moisture returns to the emplacement drifts, due to microbial activity for environmental conditions representative of the potential repository. Carbon steel (A572) used for ground-support and invert material is assumed to have similar behavior.

The principal uncertainty associated with this model concerns the effect of steel corrosion on decreasing the in-drift oxygen fugacity, and any corresponding change in the steel corrosion rate. If measured corrosion rates at atmospheric O_2 fugacity are applied to repository conditions, then comparison with results from the Gas Flux and Fugacity Model indicates that the O_2 fugacity could greatly decrease. This could impact other chemical processes in the drift such as radionuclide speciation and waste package corrosion.

Surface Area of Exposed Structural Steel

The surface area of steel that will be used for ground support and the invert structural supports was obtained from design calculations, for which the results are shown in Table 3-5.

Table 3-5. Mass and Surface Area for Structural Steel Used in the Engineered Barrier System

Zone	Steel Mass (kg/m)	Surface Area (m^2/m)	Remark
3	260	6.95	Ground support above springline (full drift)—maximum value developed for 30 percent of drifts in which rockbolts will be installed
5	140	1.49	Ground support and other structures above invert and below springline (full drift)
6	785	2.50	Ground support and other structures within the invert (full drift)
Composite 1/2	0	0	
Composite 3/4	260	6.95	
Composite 5/6	925	3.99	

Source: CRWMS M&O 2000t

Model Uncertainties

Steel corrosion may proceed rapidly where humidity conditions permit, accelerated by the presence of evaporatively deposited precipitates and salts. Corrosion could proceed at a rate similar to that measured in laboratory tests under oxidizing conditions, possibly accelerated by microbial activity, decreasing the O_2 fugacity to sub-oxic or anoxic conditions. Anoxic conditions could change mechanisms for degradation of engineered materials, and alter the microbial ecology. The importance of this uncertainty depends on the corrosion rate of steel for potential repository conditions. The measured data used as the basis for the current model were acquired for oxidizing conditions. In the potential repository the corrosion rate will tend to slow as the O_2 fugacity decreases, and the manner in which this occurs will determine the fugacity. This can be evaluated, if necessary, through testing of abiotic and microbially influenced corrosion of structural steel under oxygen-deprived conditions.

Development of Model for the Corrosion Rate of Carbon Steel

Rate data for general corrosion of A516 steel are taken from laboratory test results (CRWMS M&O 2000t). The correlation function developed for these data is

$$r = \exp\left(b_0 + b_1 \frac{1000}{T+273} + b_2 \cdot pH + b_3 \cdot C_{NaCl} \right) \qquad \text{(Eq. 3-10)}$$

where

r	= Penetration rate (μm/yr)	
b_0	= -10.035	
b_1	= -0.4657	
b_2	= 1.5795	
b_3	= 1.8258	
T	= Temperature (°C)	
C_{NaCl}	= Concentration of NaCl in the aqueous phase, expressed as weight percentage	

This model is a curve fit to scattered data, so the uncertainty of the corrosion rate is as much as one order of magnitude. This function applies to corrosion in a system that is based on J-13 water composition; the parameter C_{NaCl} is a surrogate for evaporative concentration of the system up to 1,000-fold (chloride is conserved during such evaporation). Oxygen fugacity was not measured in the test series, but the operant air mass-fraction may be inferred from the temperature, assuming saturated humidity at ambient pressure. A small flow of air was circulated in the apparatus, so consumption of O_2 by corrosion did not significantly affect the O_2 fugacity in the bulk test environment.

Results from the Model for the Corrosion Rate of Carbon Steel

Equation 3-10 is applied to A572 steel in the potential repository environment. Values for temperature, pH, and NaCl concentration are obtained from the TH model for the L4C4 location, with the "upper" infiltration distribution (Section 3.1.2.1). Zone-averaged values are used for

conditions in the backfill (composite Zone 3/4) and the invert (composite Zone 5/6). The zone-averaged pH and NaCl concentrations are obtained from the Chemical Reference Model (Section 3.1.2.7). Steel-corrosion rates are calculated separately for the zones and summed. The results (CRWMS M&O 2000t) are summarized as follows:

- Steel present in the drifts will completely corrode in a few decades or at most a few hundred years, starting during the thermal period when humidity and water return to the potential repository drifts. Depending on the infiltration flux and the location within the repository, steel corrosion will begin when relative humidity exceeds 70 percent, which will occur at times from approximately 300 to 2,000 years.

- The calculated rate of steady-state oxygen consumption (forming Fe_2O_3) exceeds the maximum 1-D mass flux of O_2 calculated to intercept the 5.5-m diameter drift footprint (Section 3.1.2.2). This means either that O_2 will be scavenged from gas present in the pillars, or the rate of steel corrosion will be limited by O_2 depletion, or both.

- The steel corrosion rate is sensitive to pH, which is predicted to vary by approximately 2 pH units during the thermal period. Equation 3-10 shows that the rate sensitivity to pH is an order of magnitude greater than the sensitivity to temperature, and is greater than the sensitivity to salt concentration except for the extremes of solution composition calculated in Section 3.1.2.7.

Results indicate that O_2 fugacity in the EBS could be substantially decreased through a combination of steel corrosion and the air mass-fraction effect discussed in Section 3.1.2.1. Steel will start to corrode when the relative humidity exceeds approximately 70 percent. Corrosion will first occur when the EBS temperature is near boiling and the air mass-fraction is small, so steel corrosion could drive the O_2 fugacity even lower. How much lower will depend on the corrosion rate response to oxygen fugacity, and the composition of water contacting the steel.

Steel corrosion rates calculated using Equation 3-10 are upper bounds for the potential repository because the tests were ventilated, so O_2 availability was not limiting. Additional measured data and modeling can further constrain and bound the effects of steel on O_2 fugacity in the potential repository.

The important issue for predicting the EBS environment is the relation between the corrosion rate for steel and the O_2 fugacity in the bulk chemical environment. Improved prediction can be based on measurements of the corrosion rate versus O_2 fugacity for structural steel. Advancement in modeling of gas transport in the host rock could be useful for elucidating the O_2 fugacity in the drift, for a given rate of steel corrosion. However, in modeling of gas transport, values of O_2 fugacity less than approximately 10^{-3} atm may be indistinguishable from zero. Accordingly, sensitivity of the rate of steel corrosion to O_2 fugacity is the principal uncertainty in predicting the O_2 fugacity in the drifts.

Microbial activity has been shown to accelerate the corrosion rate for carbon steel by a factor of approximately six. Thus, microbial activity could further affect the O_2 fugacity in the bulk chemical environment. The steel corrosion rate, the O_2 fugacity in the bulk chemical environment, and the overall rate of microbial activity in the EBS are interrelated.

Comparison of Oxygen Consumption by Corrosion of Steel versus Other Alloys

The DS, WP, and pedestal are made of titanium, Alloy 22, and stainless steel. Compared with corrosion of carbon steel, corrosion of these materials is slow to consume oxygen and produce corrosion products. Slow consumption of oxygen by corrosion of Ti-7 or Alloy 22 could contribute slightly to depletion of oxygen in the EBS. However, the potential rate of consumption is a small fraction of the oxygen availability calculated from the Gas Flux and Fugacity Model (Section 3.1.2.2).

For example, a DS made of Ti having surface area of 10 m^2 per meter of drift, corroding to TiO_2 at a rate of 1 $\mu m/yr$, would require an oxygen flux of

$$O_2 \text{ Mass Flux} = Ar\rho_{Ti} \cdot \frac{MW_{O_2}}{MW_{Ti}} \qquad \text{(Eq. 3-11)}$$

where

A	=	area (e.g., 10 m^2/m)
r	=	general corrosion penetration rate (e.g., 10^{-6} m/yr = 3.17×10^{-14} m/sec)
ρ_{Ti}	=	Ti density (4.5×10^3 kg/m^3; (CRWMS M&O 2000t)
MW_{O_2}	=	molecular weight of O_2 (0.032 kg/mol; (CRWMS M&O 2000t)
MW_{Ti}	=	formula weight of Ti (0.0479 kg/mol; (CRWMS M&O 2000t)

Substituting these values gives a mass flux of 9.5×10^{-10} kg O_2/sec per meter of drift, for general corrosion of 1 $\mu m/yr$. This is less than the maximum flux calculated using the model presented in Section 3.1.2.2, when it is applied to the drift diameter of 5.5 m. Corrosion of the WP and its supports would consume oxygen at a similar rate because the surface area, corrosion rate, and stoichiometry are similar.

In summary, corrosion of the DS and the WP will consume oxygen at a rate that is substantially less than the maximum rate for corrosion of structural steel, and will be comparable to, or less than the maximum O_2 availability from Section 3.1.2.2. Corrosion of the steel will be complete long before corrosion of the other alloys; thus, O_2 consumption will continue at a lower level for the long-term (e.g., beyond 1,000 years).

3.1.2.3.4.1   Results from Scoping Calculations on the Effects of Steel Corrosion

Order-of-magnitude estimates for steel corrosion rate and O_2 consumption (CRWMS M&O 2000t) indicate the following:

- Steel present in the drifts can completely corrode in a few decades or a few hundreds of years. The corrosion rate for steel is especially sensitive to increased pH. Equation 3-10 shows that the pH effect is greater than the temperature effect and the salt concentration effect, except when C_{NaCl} exceeds 1 percent (which occurs only when evaporative precipitates are dissolved in Time Periods 3A and 4A).

- The rate of steady-state oxygen consumption can exceed the maximum 1-D flux calculated to intercept the 5.5-m diameter drift, by applying the mass flux rate calculated in Section 3.1.2.2 (CRWMS M&O 2000t).

3.1.2.3.5   Cementitious Materials Effects Model

This section describes a bounding model for the effects of cement grout used in rockbolts. The model is based on dissolution of cement mineral phases and subsequent interaction of cement leachate with CO_2 and silica in the drift environment. The potential contribution of chemical constituents to the bulk chemical environment is minor, compared with the overall chemistry of seepage modified by elevated temperature and gas-phase chemistry.

Input Data, Assumptions, and Uncertainties

The rockbolts evaluated for this model are nominally 2.15-m long, 1.125-in. diameter steel bolts grouted into 2.5-inch diameter holes (CRWMS M&O 2000t). They will be installed in the rock roof in radial arrays of six bolts installed every 1.5 m along drift. The rockbolts will be used in addition to steel sets in those areas of the potential repository constructed in the middle nonlithophysal unit of the Topopah Spring tuff.

A modified, Type-K (Portland-based) expansive cement will be used for rockbolt anchorage. The mix will contain silica fume (5 percent dry weight), an organic plasticizer to improve workability (1 percent of dry weight), and a water–cement ratio between 0.4 and 0.6 to promote strength and durability. To allow for loss to voids in the rock, the total grout used for each rockbolt will be limited to three times that needed to fill the annulus around the steel bolt. The mass of cement used in the grout will be 22.65 kg per rockbolt (including the three-fold excess). With six rockbolts every 1.5 m along the drift opening, the cement usage will be 91 kg/m.

Saturated permeability of the grout will initially be 0.1 µdarcy ($10^{-19}m^2$) This value can be readily achieved for the initially cured grout (CRWMS M&O 2000t). As aging and carbonation of the grout progress, permeability is assumed to remain at this value for purposes of calculating leaching rates. This is justified because: 1) aging and carbonation cause regrowth of mineral phases with reduction of porosity; and 2) additional water flow could occur through flaws that form in the grout, but such flow will tend to bypass unreacted cement.

For as long as the grout remains alkaline (e.g., pH > 10) at the surface of the steel, the rockbolt is assumed not to fail in a way that significantly changes the quantity or composition of leachate. Centering of the steel bolts in the holes would tend to increase the time until this type of failure occurs. Corrosion of the steel bolt accelerates when pH decreases because grout constituents are leached or carbonated.

Potentially important uncertainties associated with this model include the transient effects of rockfall, which could cause rapid rockbolt failure and comminution of the grout. Conversely, the model does not consider cement carbonation from diffusion of gas-phase CO_2, which could completely neutralize the alkaline constituents well within the 10,000-yr performance period.

Input Data and Assumptions for Chemical Modeling of Cement Grout Leaching

Chemical equilibrium calculations for young cement are performed using the PHREEQC code and thermodynamic database, with additional thermodynamic data for cement mineral phases taken from the "com" database associated with the EQ3/6 modeling code (CRWMS M&O 2000t).

The temperature and CO_2 fugacity conditions used for modeling cement grout correspond to the L4C4 model location with the "upper" infiltration distribution, from calculations described in Sections 3.1.2.1 and 3.1.2.2.

The cement mineral assemblage shown in Table 3-6 is assumed, based on the assemblage for "young" cement grout (CRWMS M&O 2000t). Mineral assemblages representing modification of Portland cement by aging and carbonation are available from the same sources, but they tend to produce less alkaline leachate; therefore; young cement minerals are used in this model.

Table 3-6. Grout Mineral Assemblage Used for the Cementitious Materials Model

Phase	Weight percent	Mass per Rockbolt [a] (kg)
Tobermorite (also representing C-S-H [1.7] gel and gehlenite hydrate)	57.5	13.0
Ettringite	18.0	4.08
Portlandite	21.5	4.87
Brucite	3.0	0.68

From (CRWMS M&O 2000t)

NOTE: [a] Mass of each mineral in the grout used for one rockbolt, including 3x excess grout use, totaling 22.65 kg per rockbolt

In developing this assemblage, the C-S-H gel and gehlenite hydrate phases in young cement are represented by tobermorite, which has better known characteristics and similar elemental composition. This assumption is justified because aging of the cement at elevated temperature during the preclosure period of 50 years or more will cause the C-S-H gel to crystallize, and tobermorite is a likely product. The gehlenite hydrate is a minor phase used to account for aluminum in the assemblage that is not incorporated in ettringite. Thermodynamic solubility data are not available for gehlenite hydrate, so it is represented by tobermorite (instead of ettringite, thereby preserving the ratio between ettringite and portlandite). In the chemical calculations, partial carbonation of the grout assemblage is represented by the presence of calcite.

When first installed, the grout will be fluid-saturated from make-up water that will be similar to J-13 water in composition. The potential contribution of make-up water to grout chemistry is minor because key species such as cations, chloride, and sulfate are much more abundant in the cement.

For significant leachate to form and flow into the drifts, the source of the water will mainly be fracture flow because the matrix permeability is low and the availability of water is limited. Accordingly, the initial composition of water that interacts with the cement is likely to be that of

fracture water, and the composition of groundwater from well J-13 is used to represent fracture water. The potential contribution of influent water to the composition of cement leachate is minor, particularly for the range of plausible water compositions, because leachate composition (before equilibration with CO_2 or backfill) will be dominated by changes in Ca and sulfate concentrations that are controlled by the cement. For the same reason, only the major chemical constituents of J-13 water are considered in models of leachate composition.

Conceptual Development for Water–Grout Chemical Interaction

The following information is documented in the *Engineered Barrier System: Physical & Chemical Environment Model* report (CRWMS M&O 2000t). Chemical equilibrium is assumed along the cement-water reaction path, so solubility equilibria control the leachate composition. This model is suitable for slowly changing, low-flux conditions that will occur in the grout. Reaction of groundwater with the grout is assumed to be closed with respect to gas-phase constituents, particularly CO_2. This is justified for the following reasons:

- The grout will be very fine-grained, and the pore structure will retain capillary water at in situ moisture potentials, so gas saturation will be small.

- The intrinsic permeability of the grout will be very low, which will provide resistance to diffusion.

- The grout column around each rockbolt will be surrounded by intact rock matrix over much of its length. Exposure of the grout to gas-phase CO_2 is thus limited by the surrounding host rock.

Flowing water and gas-phase CO_2 will most readily access the grout at fracture intersections. If the grout is near liquid saturation, access by gas-phase CO_2 to unreacted grout will be limited. If cracks form in the grout, water and gas will penetrate them, and more surface area could become available for diffusion of CO_2; however, the leachate composition would still be bounded by the closed-system calculations.

Biotic processes such as those that could be related to the presence of the plasticizer and the steel rockbolt, are assumed to have negligible effect on leachate composition and rockbolt lifetime. The organic content of the plasticizer admixture is probably biologically recalcitrant (CRWMS M&O 2000t).

Equilibrium with CO_2 and Quartz Sand in the Drift Environment

Once the leachate flows into the drift opening or the surrounding rock, it will be exposed to ambient CO_2 conditions. Because of the small amount of leachate compared to the total percolation through the host rock, open-system conditions are assumed for evaluating leachate reaction with CO_2 and quartz backfill.

After it emerges from the grout, leachate will interact chemically with the quartz-sand backfill. The interaction will produce silica-buffering activity whereby silica dissolves to form aqueous SiO_2, which then interacts with water and speciates to produce $H_3SiO_4^-$ and $H_2SiO_4^{2-}$ ions, with release of protons that increases acidity. In this model, the leachate is assumed to equilibrate

with quartz, although the dissolution of quartz is rate-limited at temperatures at or less than boiling. This is a reasonable approximation for the following reasons:

- The rate of quartz dissolution declines exponentially with time, so substantial silica-buffer activity will result even if dissolution does not proceed to equilibrium.

- The alkaline leachate will be greatly undersaturated with respect to quartz.

- The leachate will readily disperse in the unsaturated backfill because of unsaturated flow processes, thus maximizing the surface area available for reaction.

Model Uncertainties

Cementitious materials such as rockbolt grout may degrade structurally, possibly with rockfall, and become available for rapid leaching. A transient pulse of alkaline leachate could result from such failure. Models for the effects of cementitious materials that are presented in this report, do not explicitly address the breakup of rockbolt grout. However, they show that the chemical composition of leachate would be similar to evaporatively concentrated waters that can form in the drift, so the engineered barriers would not be exposed to chemical conditions that are not already included in the models. In addition, estimates show that small quantities of leachate are likely to be produced, allowing margin for greater quantities should the flow area increase due to structural degradation. Finally, other models would be used to describe the interaction of water with cement grout in a disturbed, particulate state. Diffusion of CO_2 into the unreacted cement, and equilibration of leachate with the drift environment, would be more important in such a model and would tend to moderate the leachate composition.

3.1.2.3.5.1 Development of the Cementitious Materials Model

The Cementitious Materials Model is used to evaluate the potential impact on the EBS bulk chemical environment from percolating water that contacts grouted rockbolts and subsequently interacts with quartz-sand backfill and gas-phase CO_2. Grouted rockbolts are planned for use in the portion of the potential repository that is constructed in the middle nonlithophysal tuff. The Cementitious Materials Model does not address mixing of cement-affected waters with seepage in the drift, nor does it address thermal effects on flow in the host rock. These are considered in the other parts of the *Engineered Barrier System: Physical & Chemical Environment Model* (CRWMS M&O 2000t).

The PHREEQC Code

The U.S. Geological Survey (USGS) solution equilibrium modeling code PHREEQC (pH-REdox EQuilibrium equation program in C language) was used for the Cementitious Materials Model to assess three types of geochemical effects:

- Changes in water and solid composition resulting from groundwater contacting grout

- Effects from grout-modified groundwater interacting with the CO_2 in the gas phase in the emplacement drift

- Effects of the grout- and gas-modified groundwater contacting backfill material

Two capabilities of PHREEQC were used for this model: 1) speciation and saturation-index (SI) calculations, and 2) reaction-path calculations involving specified irreversible reactions and mineral- or gas-phase equilibria. Different CO_2 conditions were used to represent formation of leachate within the grout column and reaction of the leachate with the environment outside:

- Grout system closed with respect to CO_2 (i.e., the CO_2 available within the grout column is that dissolved in the influent water)

- Leachate and quartz-sand system open with respect to CO_2 (i.e., fugacity is held constant so that no reaction extent is limited by the availability of CO_2)

Analysis of Flux Through a Water-Saturated Grout Cylinder

Flow through a saturated vertical grout cylinder is estimated using Darcy's Law (CRWMS M&O 2000t). Substituting the listed values for grout geometry, saturated permeability of 10^{-19} m^2, and a unit hydraulic gradient yields a flow rate through one vertical grout cylinder of less than 0.1 mL/yr. Allowing for flow through several grout faces (for example, if the rock containing a rockbolt is broken up and falls into the drift) each rockbolt will contribute less than 1 mL/yr leachate to the drift environment.

The time to completely dissolve a mineral phase for the stepwise, steady-flow conditions developed in Section 3.1.2.1 is given by

$$t = \frac{m}{SQ}$$
(Eq. 3-12)

where m is the mass present, S is the solubility, and Q is the flow rate of water. Using the ettringite solubility of 10.1 kg/m^3 at 90°C, and a mass of 4.08 kg ettringite per rockbolt, the time to dissolve the ettringite with a flow rate of less than 1 mL/yr is on the order of half a million years. This may be unrealistic, but the practical implication is that ettringite will be present for thousands of years, especially if the grout cylinder remains intact. The flux-scaling approach presented subsequently offers an alternative that addresses the possibility that the grout will be fractured and subject to the same flux as the surrounding rock.

Estimating the Leachate Flow Rate from Flux-Scaling

An alternative bounding approach is to consider the seepage flux intercepted by the grout at the drift wall. Taking the interception area for one rockbolt as the cross-sectional area of grout, the flow of water that could interact with the grout is

$$Q_{grout} = Aq_{seep}$$
(Eq. 3-13)

where

Q_{grout} = flow of water interacting with one rockbolt (m^3/sec)

A = exposed area of grout $(2.53 \times 10^{-3} \text{ m}^2)$

q_{seep} = seepage flux calculated from seepage inflow and drift geometry $(\text{m}^2/\text{m-sec})$

For the 300- to 700-yr time period, the seepage inflow is 2.51×10^{-6} kg/sec per meter of drift (Table 3-7). Dividing by the density of water (965.254 kg/m^3 at 90°C) and the drift diameter (5.5 m) and multiplying by 2 for full-drift inflow gives a seepage flux of q_{seep} = 29.8 mm/yr. Substituting in Equation 3-13 gives a flow rate of approximately 75 mL/yr per rockbolt. Implementation of this calculation for all time periods used in chemical modeling (except Time Period 1, for which there is no seepage flow) is shown in Table 3-7.

3.1.2.3.5.2   Results from the Cementitious Materials Model

Calculations show that leachate composition will differ strongly from the influent fracture-water composition for at least several thousand years. For the mineral assemblage and environmental conditions considered, the solubilities of portlandite and ettringite cause them to be completely leached before tobermorite, brucite, and calcite are leached. As temperature increases, portlandite solubility decreases, whereas ettringite solubility increases. The PHREEQC modeling results show that for temperatures greater than approximately 50°C, ettringite is the most soluble constituent phase and will strongly affect leachate composition until completely dissolved.

Leachate composition will be controlled by the dissolving phases until they are completely dissolved. Any changes in leachate composition during this period will be caused primarily by direct temperature and CO_2 effects on leachate composition rather than by mineralogical changes in the cement phases.

Table 3-7. Summary of Leaching Conditions for Rockbolt Cement Grout (L4C4 Location; "Upper" Infiltration)

	Time Period 2	Time Period 3	Time Period 4	Time Period 5
Time Period from (yr)	300	700	1500	2500
To (yr)	700	1500	2500	10000
Temperature (in Zone 1/2 representing the host rock; °C)	90.05	88.42	79.96	51.69
Water Density (kg/m^3)	965.254	966.390	971.799	987.259
Zones 3 and 4 Inflow Rate (kg/m-sec)	2.51E–06	1.11E–05	5.65E–06	8.67E–06
Seepage Flux (m/sec)	9.46E–10	4.16E–09	2.11E–09	3.19E–09
Seepage Flux (m/yr)	2.98E–02	1.31E–01	6.67E–02	1.01E–01
Scaled Flow per Rockbolt (m^3/yr)	7.53E–05	3.31E–04	1.68E–04	2.55E–04

Source: CRWMS M&O 2000t

NOTE: Time Periods are defined in Section 3.1.2.1

Sensitivity of Grout-Leachate Composition to Temperature, CO_2, and Quartz Sand

The calculations show that prior to contact with atmospheric CO_2 and quartz backfill, the grout leachate is highly alkaline (Table 3-8). The alkalinity is caused primarily by dissolved calcium derived from portlandite. The leachate pH decreases with increasing temperature because of portlandite retrograde solubility.

Table 3-8. Grout Leachate pH for Equilibrium with Cement (Closed System) and for Equilibrium with Quartz and CO_2 in the Drift Environment (Open System)

Grout Leachate pH	Temperature			
	30°C	50°C	70°C	90°C
Before Reaction with CO_2 or Quartz	12.3	11.6	11.1	10.5
After Reaction with Quartz and Gas-Phase CO_2 at 9.5 ppmv	9.2	8.8	8.6	8.7
After Reaction with Quartz and Gas-Phase CO_2 at 952 ppmv	8.0	7.8	7.6	7.7
After Reaction with Quartz and Gas-Phase CO_2 at 9520 ppmv	7.4	7.4	7.1	7.2

Source: CRWMS.M&O 2000t

At higher temperatures, the solution is calculated to contain more dissolved sulfate (as much as approximately 1200 mg/L) from dissolution of ettringite, with moderate increases in dissolved aluminum and calcium.

Evolution of Leachate Composition for the Reference Model

Modeling the evolution of leachate composition is based on the time steps used in the TH Model, with corresponding temperatures and fluxes (Section 3.1.2.1) and CO_2 fugacity values (Section 3.1.2.2). As discussed previously, the cement–water equilibration is assumed to be closed to gas-phase CO_2, while the leachate-quartz-CO_2 equilibrium is assumed to be open. The water compositions predicted to result from grout-leachate and leachate-sand equilibria are presented in Table 3-9. Note that for Time Period 1, the TH model predicts zero seepage.

Upon equilibration of the leachate with CO_2 and quartz-sand backfill, quartz dissolves, pH decreases, and calcite precipitates (Table 3-9). The magnitudes of calcite precipitation and quartz dissolution are sensitive to temperature, but are relatively insensitive to CO_2 fugacity.

Table 3-9. Evolution of Leachate Composition with Time, for Reference Model Conditions (L4C4 Location; "Upper" Infiltration)

	Time Period 2 300–700 yr T = 90.05°C P_{CO_2} = 10 ppmv		Time Period 3 700–1500 yr T = 88.42°C P_{CO_2} = 9 ppmv		Time Period 4 1500–2500 yr T = 79.96°C P_{CO_2} = 20 ppmv		Time Period 5 2500–5000 yr T = 51.69°C P_{CO_2} = 53 ppmv	
	Grout Equil.	Quartz Equil.	Grout Equil.	Quartz Equil.	Grout Equil.	Quartz Equil.	Grout Equil.	Quartz Equil.
Al (mg/L)	218.7	218.7	203.7	203.7	0.0	0.0	0.0	0.0
CO_2 (total) (mg/L)	0.4	0.9	0.4	0.9	0.4	2.5	0.3	21.4
Ca (mg/L)	894.2	674.9	859.3	633.3	353.9	33.5	521.4	5.1
Cl (mg/L)	7.1	7.1	7.1	7.1	7.1	7.1	7.1	7.1
F (mg/L)	2.2	2.2	2.2	2.2	2.2	2.2	2.2	2.2
K (mg/L)	5.0	5.0	5.0	5.0	5.0	5.0	5.0	5.0
Mg (mg/L)	0.0	0.0	0.0	0.0	0.0	0.0	0.0	0.0
NO_3 (mg/L)	8.78	2.0	8.78	2.0	8.78	2.0	8.78	2.0
Na (mg/L)	45.7	45.7	45.7	45.7	45.7	45.7	45.7	45.7
SO_4 (mg/L)	1186.3	1186.3	1106.6	1106.6	18.4	18.4	18.4	18.4
Si (mg/L)	0.0	209.8	0.0	210.4	0.0	203.3	0.0	110.7
PH	10.5	8.7	10.5	8.7	10.8	8.9	11.6	8.9
Portlandite dissolved (g/L)	0.05		0.1		0.85		1.2	
Ettringite dissolved (g/L)	10.1		9.4		Note [a]		Note [a]	
Quartz dissolved (g/L)		0.45		0.45		0.43		0.24
Calcite precipitated (g/L)		0.55		0.57		0.80		1.29

Source: CRWMS M&O 2000t

NOTE: [a] Ettringite is completely dissolved after 1500 years.

Cement Mineral Dissolution Times for the Reference Model

The grout-dissolution model is used in conjunction with flow rates from the reference model to calculate the time until complete dissolution of ettringite and portlandite. The dissolution rate of an individual mineral phase is estimated by multiplying the flow of water through the grout (from the flux-scaling model discussed previously) by the calculated solubility at the prescribed temperature.

The results show that the ettringite will be depleted in 1,500 years for the reference model (L4C4 location, "upper" infiltration distribution). Dissolution of the portlandite under the same conditions could require 10,000 years or more. These results do not consider the "excess" grout, which could increase the leaching times by as much as a factor of three. The time until complete dissolution is controlled by temperature, and to a lesser extent by CO_2.

Summary of Cementitious Materials Model Results

The grout permeability is small, which limits chemical interaction of the grout with the EBS environment while increasing the longevity of the grout to dissolution. Very small flow rates (a few mL/yr per rockbolt) are obtained using the saturated permeability of the grout. A more conservative bounding approach is presented, based on the ratio of the rockbolt grout

cross-sectional area to the drift diameter. This method produces flow rates on the order of 75 to 330 mL/yr per rockbolt, or a few percent of the total seepage inflow to the drifts. For as long as the grout remains substantially intact inside the rockbolt holes, the flow of water that interacts directly with grout is projected to be a small fraction of the seepage inflow into the drifts.

Reasonable-bound estimates are developed for the chemistry of grout leachate. Leachate pH values of 10.5 to 11.6 are predicted; these are readily buffered on contact with CO_2 and quartz-sand backfill in the drift environment. The leachate pH depends primarily on the solubility of portlandite, which increases at lower temperature, thus causing the leachate pH to be elevated at later stages of cooldown. Depending on the solubility of ettringite, sulfate concentrations as great as 1200 mg/L are predicted.

After the leachate reacts with CO_2 and quartz-sand backfill, pH of approximately 8.5 is predicted. Accordingly, elevated pH values for leachate will not apply at the DS or at the WP because of mixing with other water in the backfill and because of reaction with the quartz and gas-phase CO_2.

Neither ettringite nor portlandite completely dissolves until at least 1,500 years, depending on the water flow rate and the temperature. Other cement phases (e.g., tobermorite) are relatively stable to dissolution and tend to alter to even more thermodynamically stable minerals. These results are based on the reference TH Model (Section 3.1.2.1; L4C4 location, "upper" infiltration distribution) which provides reasonable-bound infiltration and seepage rates and therefore tends to maximize the contribution of leachate to the bulk chemical environment.

3.1.2.3.6 Introduced Material Model Validation

The introduced materials models consist of the kinetic model for water-quartz interaction, the model for seepage-backfill interaction at high ionic strength, the analytical model for backfill porosity reduction, an empirical model describing corrosion rates for carbon steel, and the cementitious materials model. Each of these is a conservative, bounding model in the sense that chemical interaction and its potential deleterious effect on the bulk chemical environment are maximized. The models are valid for their intended uses.

Kinetic Model for Water-Quartz Interaction

This model implements a widely used rate law for quartz precipitation, from published scientific literature. The purpose of the model is to establish whether quartz kinetics is an important influence on water composition in the EBS, and should be implemented in the EBS Chemical Reference Model (Section 3.1.2.7). Surface area information is provided from measured data for the Overton Sand, and is bounding because the smallest size fraction is neglected, and the sand particles are assumed to be spherical.

Kinetic rate laws tend to be uncertain, but the behavior of quartz is well understood compared to many other minerals. The model shows that water-quartz interaction approaches solubility equilibrium, for contact times of months to years in the backfill during the thermal period, as calculated by the Thermal-Hydrology Model (described in Section 3.1.2.1). Accordingly, water-quartz equilibrium is used in the EBS Chemical Reference Model. This approximation is bounding in the sense that precipitation of dissolved silica causes loss of silica buffering, with

resulting increase of pH, which is conservative with respect to potential corrosion of the drip shield (which may increase at higher pH). The validity of this approximation is also supported by the exponential form of the rate law, which ensures that much of the water-quartz interaction occurs relatively soon after contact.

Seepage-Backfill Interaction Model

The seepage-backfill model is based on the High Relative Humidity (HRH) Salts Model developed in Section 3.1.2.5. The tendency for quartz to precipitate in the sand backfill, during evaporative concentration of water in the drifts, is calculated along with the water composition. Chemical equilibrium is assumed, which is a bounding approximation because quartz precipitation is relatively slow. For ranges of evaporative concentration and temperature, the model calculates whether quartz tends to dissolve or precipitate.

This model depends on the assumptions which are associated with extension of the Pitzer database, for the HRH Salts Model (Section 3.1.2.5). Accordingly, the results are designated to-be-verified. This status is appropriate considering that silica (or Si) is the only component of quartz, and that Pitzer data for silica are estimated by extrapolation from CO_2 and other species.

Analytical Model for Backfill Porosity Reduction

This is a parametric model for solute accumulation, as precipitated calcite, silica, and other species. Accumulation of precipitates is considered for 10,000 yr which is a bounding approximation because it exceeds the duration of thermal effects that could cause significant evaporative concentration and precipitation. The results of this model show that 10,000-yr accumulation for typical conditions would be a small portion (less than one tenth) of the backfill porosity. This is a valid bounding model for the effect of waters that have equilibrated to the host rock (composition similar to J-13 water) when they are strongly concentrated by evaporation in the backfill.

Steel Corrosion Rate Model

The correlation model for the corrosion rate of carbon steel as a function of pH, NaCl concentration, and temperature, is based on laboratory measured data for unsaturated conditions. The range of test conditions closely approximates the environment to which steel ground support will be exposed in the emplacement drifts. The test conditions were oxidizing, with atmospheric composition in the air fraction. This constitutes a bounding approximation that tends to maximize the corrosion rate, because some depletion of O_2 fugacity can be expected to occur in the potential repository when oxygen is consumed by corrosion. The test data were acquired for a steel alloy that is slightly different from the steel proposed for ground support, and the correspondence of corrosion rates is to-be-verified.

Laboratory tests have shown that microbial activity increases the corrosion rate for carbon steel, by a factor of 6 to 7. This factor is applied directly to the abiotic rates discussed above. The initial microbial tests may have produced lower bound estimates on the microbial effect because they were closed reactors and probably developed anoxic conditions. The applicability of the results to repository conditions is to-be-verified.

This model calculates the composition and flow rate of leachate that has interacted with fully-grouted rockbolts. (Such bolts would be used only in the portion of the potential repository that is constructed in the Tptpmn unit, in the current design concept.)

A mineral assemblage is selected based on "young" cement (Hardin et al., 1998) with the exception that the gel phase is replaced by tobermorite, a compositionally similar crystalline phase. Use of a modified "young" is a bounding approximation because the labile, alkaline solids present in cement tend to produce less alkaline, carbonate minerals over tens or hundreds of years, on exposure to atmospheric CO_2. The result of the approximation is that alkaline leachate is produced for thousands of years from dissolution of portlandite. Other bounding approximations include equilibration of the leachate with cement minerals, and closed-system conditions whereby gas-phase CO_2 does not interact directly with leachate in the grout. Interaction of the leachate with gas-phase CO_2, and quartz sand backfill, is calculated for conditions outside the grout.

The flow rate of leachate associated with a rockbolt is calculated from seepage estimates, which are taken from the conservative TH models described in Section 3.1.2.1. Interaction of seepage with cement grout is calculated from the ratio of the grout annulus area of the rockbolt, to the plan area of the drift. This is a bounding approximation because the saturated hydraulic conductivity of the grout will be very small. If saturated permeability were used to limit the flow rate of leachate, the result would be orders of magnitude less than the area ratio result.

The cementitious materials model is a valid bounding model for leachate chemistry and flow rate. The model does not consider diffusive transport of alkaline species from the interior of the grout to the surface (nor transport of gas-phase CO_2 to the interior).

3.1.2.4 Microbial Effects Models

The greatest potential for microbial effects on potential repository performance is microbially influenced corrosion (MIC) of EBS and WP materials. Timing of the onset of MIC is addressed by the Threshold Conditions Model discussed below. The rate of MIC for the WP, along with other aspects of WP performance, is reported elsewhere.

Another potentially important effect is changes in the EBS bulk chemical environment from microbial activity, which are bounded by the Microbial Communities Model presented below. Other potential effects including microbially facilitated transport of radionuclides, are mentioned but not addressed in detail by this report.

3.1.2.4.1 Threshold Conditions Model for Microbially Influenced Corrosion

There are approximately 10^4 to 10^5 total bacteria per gram of Yucca Mountain tuff at the potential repository horizon, which is low compared to microbially rich environments (e.g., marine sediments, agricultural soils) that may contain as many as 10^9 bacteria per gram, but high compared to barren environments such as arid-desert sands, or recent volcanics. Over time, the microbiological community in the potential repository may accelerate degradation of introduced materials, including the drip shields and waste packages.

Conceptual Basis for Factors Limiting Microbial Activity

Bacteria are ubiquitous in nature, but they require the following for growth and metabolic activity: favorable environmental conditions, nutrients, and energy sources. All of these have been observed to limit microbial growth and metabolic activity in Yucca Mountain tuff or in analogous settings. Additional discussion of these limitations is provided below.

Water Availability

Experiments have determined that the primary environmental factor limiting microbial growth in the Yucca Mountain welded tuff host rock is lack of water (CRWMS M&O 2000t). The experiments duplicated ambient environmental conditions at Yucca Mountain except for 100 percent saturation with tuffaceous groundwater. (Saturated conditions are not expected in the potential repository, except for possible seepage caused by locally heavy flow in fractures.) Under these saturated conditions, microbial growth increased to 10^6 to 10^7 aerobic carbon-degrading cells per milliliter groundwater. Many types of microorganisms can survive long periods of desiccation because of specialized dormant structures such as spores, cysts, and resting stages. Free water, however, is required for resumption of active metabolism and growth.

Microbiologists commonly use the term "water activity" (a_w) to describe microbial water relationships in complex environments. Water activity has been defined as a ratio of vapor pressures, equivalent to relative humidity. Most bacteria require $a_w > 0.9$ for active metabolism; a specialized group of salt-tolerant bacteria (halophiles) can remain active at a_w values of 0.75 or less. Fungi are generally more tolerant of desiccation and remain active to a_w as low as 0.55 but have specific metabolic requirements (CRWMS M&O 2000t). These values define bounding values for the relative humidity at which microbial activity in the potential repository can resume during cooldown.

Elevated Temperature

Elevated temperature can also limit microbial activity and growth. Mesophiles that inhabit temperate environments such as the potential repository host rock (before or after potential repository heating) typically have growth optima in the range of 25 to 40°C (CRWMS M&O 2000t). Microorganisms found in extreme environments can exhibit higher optimal growth temperatures. The consensus among workers in this field is that the upper limit to any bacterial growth is approximately 120°C (CRWMS M&O 2000t). Where temperatures in the potential repository exceed 120°C, no bacterial activity will be possible (although sporulated bacteria could survive such conditions). At temperatures less than 120°C hyperthermophiles can become active if they are present and if water availability and other environmental conditions permit. Whether hyperthermophilic organisms are present at Yucca Mountain, or will be introduced into potential repository drifts by potential repository construction, is not determined.

Gamma Irradiation

Another factor that will limit bacterial growth in the potential repository is ionizing radiation generated by decaying radioactive waste. Because radiation must penetrate the waste package wall to affect the EBS environment, only gamma radiation is considered. Resistance of microbes to gamma irradiation varies depending on the species. Bacterial spores are relatively radiation-

resistant, and a dose of 0.3 to 0.4 Mrad is required to effect 90 percent kill. Most vegetative cells (active, nonsporulated) require only a tenth of this dose for the same rate of kill. Generally, a gamma dose of 2.5 to 3 Mrad is used to sterilize food and medical instruments. Gamma radiation doses will be on the order of 100 rad/hr immediately following emplacement of waste packages containing nuclear fuel assemblies. Thus, a dose of 1 Mrad could accumulate on the surface of waste packages within a period of just more than a year.

When considering the effects of irradiation on activity and growth, it is important to consider the shielding provided by backfill, ground support materials, and rock. Organisms located a few meters from the waste packages will receive a much smaller gamma dose than will those at the waste-package surface. These organisms could readily re-enter the EBS during cooldown when liquid flux resumes; therefore, even if much of the EBS is sterilized by high radiation, later recolonization will occur. It can occur rapidly (relative to the 10,000-yr performance period) when liquid flux conditions are conducive to transport and environmental conditions (water, heat, radiation) are within ranges that permit growth.

Nutrient Availability

Phosphate–Testing has shown that when sufficient water is available, and temperatures and radiation are within ranges conducive to growth, phosphate availability is the primary factor that limits bacterial growth in cultures containing Yucca Mountain tuff. Phosphate is a principal component of nucleic acids (DNA and RNA) and phospholipids, which are major constituents of biological membranes. Phosphate is therefore an essential nutrient for activity and growth of all biological organisms.

Phosphate is the predominant phosphorous species in groundwaters, and UZ waters contain low concentrations. J-13 water is an analogue to fracture waters in the host rock, and using standard methods of analysis, the phosphate concentration has been found to be approximately 120 μg/L (CRWMS M&O 2000t).

Experimental studies have shown that under saturated conditions, when Yucca Mountain tuff is used as a source of microbial inoculum and incubated in synthetic Yucca Mountain groundwater, microorganisms mobilize the phosphate contained in the tuff to support growth to densities of at least 10^6 bacteria per milliliter of water (CRWMS M&O 2000t). When such cultures are amended with added phosphate, bacterial densities increase well beyond 10^6 to 10^7 bacteria per milliliter. Thus, it is likely that any EBS material that contains biologically labile phosphate will stimulate microbial growth beyond bacterial densities that are achieved with tuff only (other environmental conditions permitting). Other "macronutrients" (those used at higher concentrations), including carbon, sulfur, and nitrogen, have been found not to be limiting for growth to abundances up to 10^9 cells per milliliter.

It is important to note that phosphate is cycled in microbial communities. This means that the same phosphate mass inventory can continue to sustain the activity of a microbial population even as the abundance of other nutrients fluctuates and despite the birth and death of individual organisms. For limiting microbial activity on the waste-package surface, this fact lowers the threshold for allowable phosphate transport to the waste package, relative to chemical species that are consumed such as energy sources.

Investigation of phosphate limitation has focused exclusively on those types of organisms that degrade organic carbon (as a carbon source) and utilize oxygen (as a terminal electron acceptor). Investigations in progress are examining the growth of Yucca Mountain anaerobes, which use alternative electron acceptors such as sulfate, and are capable of using CO_2 as a carbon source for growth. It is expected that these organisms will also be phosphate-limited.

Carbon Sources–Investigations using Yucca Mountain tuff have examined only the growth of aerobic carbon-degrading organisms. These include organisms capable of obtaining carbon from the CO_2 in air or equivalently from dissolved inorganic carbon. This selection is justified because there are no other significant natural sources of carbon in the host rock nor sources of organic carbon in the EBS, except the possibility of small concentrations of dissolved organic carbon in percolating groundwater.

Like phosphate, the carbon contained in the biomass is cycled in microbial communities; thus, organic carbon may become available for supporting increasingly diverse types of organisms once a microbial community becomes established. Because of the availability of CO_2 in the gas phase, it cannot be argued that a carbon source is limiting for any type of microbial activity for any location in the potential repository where conditions favor the growth of carbon-reducing bacteria.

Energy Sources–Bacteria generally extract energy from the environment by mediating thermodynamically favored oxidation-reduction reactions. As part of a subsistence strategy, the organisms may alter their environment, and the alteration often has the effect of promoting solubilization of reactants. This is one important basis for microbially influenced corrosion (MIC) in which bacteria on metal surfaces change the local environment.

Energy sources for bacteria exist in the host rock, as is evident from the existing population of viable organisms. The host rock contains reduced iron, manganese, and traces of other oxidation-reduction-sensitive metals (CRWMS M&O 2000t) that can act as electron donors. For potential electron acceptors, the environment has abundant oxygen in the gas phase, and UZ waters contain available sulfate and nitrate.

The potential repository environment will therefore be associated with some level of microbial activity after the return of moisture during cooldown. If the potential repository is constructed without adding electron donors or acceptors other than those already qualitatively present in the host rock, the types of energy sources will not change. The changes that will occur include the distribution of water, the effects of heat, the composition of the aqueous phase, and the relative amounts and spatial distribution of potential nutrients represented by introduced materials.

The microbial population in the host rock may be capable of alternative exploitation strategies if environmental and nutrient conditions are substantially modified. This is the reason why other classes of organisms that are present in the host rock, particularly sulfate-reducing forms, are under investigation. Also, the in situ population will be augmented by exogenous organisms during construction and operation. The combined types are currently considered capable of metabolizing any energy sources present in the potential repository.

Conceptual Basis for Microbially Influenced Corrosion of CRMs

MIC can be important to waste isolation without significantly altering the bulk chemical environment. The hallmark of MIC is the establishment of a biofilm or accretion of a consortium of bacteria on a metal surface. Concentrations of various chemical species are greater within the micro-environment than in the bulk environment. As energy sources, the CRMs are electron donors similar to steel, but are less available for biological use because of their greater resistance to attack. Some alloy components (e.g., Ti) are spontaneously and abiotically oxidized in aerobic environments, thus forming products with low solubility and minimal availability to microorganisms, which is the basis for MIC resistance.

Conceptual Basis for Interaction of Bacteria with EBS Materials

The following discussion is included as background information and shows that under certain environmental conditions, microbial activity can degrade all of the materials present in the EBS.

Carbon Steel–Historically, MIC of metals has been attributed to a single class of organisms: the sulfate-reducing bacteria. Currently, MIC is recognized as a group of interacting processes carried out by multiple classes of bacteria. Bacteria that secrete exopolysaccharides into the extracellular environment form slime capsules that obstruct the free diffusion of oxygen to the metal surface, thus creating a reducing environment. This condition is accentuated by aerobes within the slime layer that consume oxygen. The creation of anoxic regions within the slime layer facilitates the growth of anaerobic sulfate reducers. Differential oxygen gradients within the slime film contribute to creation of anodes, where metal dissolution occurs. In the aerobic regions of the film, iron and sulfur oxidizers may oxidize dissolved metal components and generate mineral acids. These conditions degrade the protective metal oxide film and produce pitting. These processes require the formation of biofilms and sufficient water availability to prevent desiccation.

Electrochemical batch studies have shown that, for the experimental conditions employed, Yucca Mountain bacteria can increase corrosion rates of carbon steel alloy C1020 by a factor of 6 to 7 (CRWMS M&O 2000t). This result may be a lower bound on the corrosion rate enhancement because the experimental batches were closed, and not replenished with reactants of any type. Continual-flow (i.e., replenished) experiments using synthetic J-13 groundwaters and nonsterile Yucca Mountain tuff are underway. Chemical analyses of the surfaces of corroded carbon steel alloy C1020 coupons showed accretion of calcite, greenalite (a reduced-iron silicate oxyhydroxide), rancieite (a calcium-manganese oxide), and an unidentified iron-silicate phase. A particulate phase detached from the coupons, and consisted of spalled corrosion products and tuff fines as well as precipitated minerals from the aqueous phase. In ongoing work, these results are being compared to identical systems containing sterilized tuff (i.e., not containing Yucca Mountain or other bacteria) to determine the contributions of microbial activity.

Host Rock Degradation–As discussed previously, tuff can serve as a source of phosphate for the growth of Yucca Mountain organisms. The potential Topopah Spring host rock contains approximately 0.007 weight percent phosphate (CRWMS M&O 2000t). Microbial processes that produce acidity could enhance the extraction rate for phosphate. Manganese has been

shown to solubilize from Yucca Mountain tuff in the presence of Yucca Mountain microorganisms, while iron contained in tuff is not mobilized to the same extent.

Cementitious Materials—Certain types of microorganisms, such as sulfur-oxidizing bacteria, are capable of degrading cementitious materials by producing acids. Sulfur-oxidizing bacteria have been found in every sample of Yucca Mountain tuff tested for their presence (CRWMS M&O 2000t). In environments where reduced sulfur compounds are limited (e.g., at the ground surface), nitric acid–producing bacteria have been found to play a role in cement degradation. Concrete can also be corroded by organic acids produced by fermentative bacteria under reducing conditions. Fungi have also been implicated in concrete degradation and are present in Yucca Mountain tuff as well (CRWMS M&O 2000af). Notwithstanding such observations, microbial degradation of cement in the potential repository will be limited, because the use of cement is limited to rockbolt grout in only part of the waste emplacement area, and because other conditions associated with concrete degradation (e.g., organic carbon, and anoxic-oxic interfaces) will be scarce.

Input Data, Assumptions, and Uncertainties for Threshold Model

The following assumptions and the attendant uncertainties, are incorporated in the threshold model:

Electrical Equipment and Removal of Organics—Haulage will be electrically driven (i.e., no hydrocarbon fuels will be used in the emplacement drifts). Hydrocarbon-based lubricants and other organic materials will be used in construction equipment, but will be recovered from the drift environment prior to waste emplacement.

Purity of Backfill and Invert Materials—Backfill and invert materials will be washed and contain only trace amounts of organic matter. In addition, backfill material will contain only trace amounts of phosphate and electron acceptors such as sulfate.

Organic Carbon Content of Host Rock—The organic carbon of the host welded-tuff rock units is zero, or insignificant as a carbon source to support microbial activity and growth.

Microbial Growth and Activity on Waste-Package Surface—Microbially influenced corrosion of the waste-package surface (Alloy 22) may be negligible for humidity conditions (not liquid-saturated or dripping), even for relative humidity greater than 90 percent, as long as liquid groundwater (with its endogenous complement of phosphate and other nutrients) has not penetrated the drip shield. Investigations using Yucca Mountain tuff and unsaturated humidity conditions are currently under way to determine whether MIC can occur for these conditions. The results are expected to better define the capability of Yucca Mountain organisms to colonize surfaces as a function of relative humidity.

Microbial Effect on Carbon Steel Corrosion Rate—Available test data show a six-fold increase in the corrosion rate for C1020 steel, relative to abiotic rates measured with sterile controls. Carbon steel used for ground support and invert material has a similar composition, and is assumed to exhibit similar corrosion behavior.

Threshold Conditions Model Development

Water-activity, temperature, and radiation-dose conditions can be combined to formulate limits for microbial activity. Published results based on extreme behaviors of known organisms are used as a guide where site-specific data are unavailable. More precise estimates based on characterization of organisms at Yucca Mountain are unwarranted because of uncertainty about which types of organisms will be present, and because of the potential for biological adaptation.

Threshold Conditions for Microbially Induced Corrosion of the Waste Package

- Growth and activity are nil until the waste-package surface temperature drops to less than 120°C

- Growth and activity on the waste-package surface are limited, and may be negligible, even after relative humidity increases above 90 percent, as long as water has not leaked through the drip shield onto the waste package, and the waste package has not directly contacted the backfill, invert, or corrosion products of the steel ground support (to be verified).

Threshold Conditions for Microbially Induced Corrosion of the Drip Shield

- Growth and activity are nil until the drip-shield surface temperature decreases to less than 120°C for all environmental conditions.

- For water contacting the drip shield during the thermal period, microbial growth and activity are negligible as long as the relative humidity is less than 75 percent to 90 percent, depending on whether halophiles are active.

Environmental Conditions for Aqueous Corrosion

When threshold conditions for aqueous corrosion occur on the waste package or drip shield, MIC can occur at rates observed in laboratory tests. At present, test data are available to support an empirical model for MIC of Alloy 22, and testing is also under way to develop a model for Ti Grade 7 (results may show that MIC is not important for Ti). The results are expected to provide upper bounds on rates of MIC for potential repository conditions, because: 1) the test cells are augmented with glucose, which has no analogue in the potential repository environment; 2) test cells contain crushed tuff, whereas the upper part of the drip shield will contact quartz sand backfill, which is not a phosphate source; and 3) the waste package will be supported by a structure made from CRM, and will not contact crushed tuff until the support structure or the drip shield fails.

Threshold Model Validation

The threshold model is based on information from the literature, describing the environmental conditions for which microbial growth and activity are observed. The model is bounding in the sense that extreme microbial observations (e.g. halophiles and hyperthermophiles) are included, but these types of organisms will not necessarily be important in the potential repository. The basic threshold conditions for growth and activity are relative humidity (> 90 percent, or lower if

halophiles are active) and temperature (< 120°C). No distinction is made between environmental conditions necessary for microbial activity, and for biofilm development, which is conservative. Use of these conditions constitutes a valid model that is based on accepted information.

3.1.2.4.2 Microbial Communities Model

Microbes can promote corrosion of waste packages and other potential repository materials, modify the bulk chemical environment, and potentially alter the rate of radionuclide transport from breached waste packages. In addition, microbes may contribute to degradation of cementitious materials, and produce gas. These effects are depicted in Figure 3-41, as two major classifications of effects: impacts to EBS performance, and effects on radionuclide transport. The Microbial Communities Model provides a means to quantify the abundance and metabolic activity of microorganisms in the EBS environment.

The Microbial Communities Model is based on models used in the Swiss and Canadian nuclear waste programs (CRWMS M&O 2000f). An idealized elemental composition for microbial biomass is used, consisting of carbon, nitrogen, sulfur, and phosphorous in fixed proportions, plus water. The rates of supply for these constituents are input as constant release rates for each introduced material in the EBS. The other major constraint is the energy available for microbes to grow, estimated from the free energy released by oxidation/reduction reactions.

Application of the Microbial Communities Model to the TSPA-VA design, showed that approximately 10 to 12 grams of biomass would be produced per lineal meter of emplacement drift per year during the first 10,000 years (Figure 3-42). Based on this small generation rate, effects on the bulk chemical environment were considered negligible for the TSPA-VA. Localized effects of microbial activity could nevertheless alter the longevity of materials and the transport of radionuclides.

The following description is taken from the *In-Drift Microbial Communities Model* (CRWMS M&O 2000f).

3.1.2.4.2.1 Conceptual Development

Ambient Environmental Conditions

The presence of water, nutrients, and energy sources are required for microbial growth and activity. Environmental conditions (temperature, radiation, water activity) are also required. These conditions are summarized in the foregoing discussion of the threshold model.

Introduced Materials

There are three main categories of introduced materials that could potentially affect microbial activity: steels/alloys, cementitious materials, and organic substances.

- **Steels and Alloys**–The Fe, Mn, and other metals in the steel/alloys can oxidize, and serve as energy sources. Additionally, the steel/alloys contain trace elements needed for microbial growth.

- **Cementitious Materials**–Cementitious materials are strongly alkaline and may contain organic compounds, sulfates, and nitrates. Alkaline pH does not preclude microbial activity, and some constituents of cement may be utilized by bacteria.

- **Organic Substances**–The organics used in potential repository construction can be minimized and removed prior to waste emplacement.

The effects of introduced materials on microbial growth and activity are incorporated by including these materials in the Microbial Communities Model.

Code Development Concepts

Three basic approaches to modeling microbial nutrient and energy balances are possible, and have been documented in previous reports (CRWMS M&O 2000f):

- **Nutrient Mass Balance**–Biomass is limited by the inventory and/or supply rate of some essential element (e.g., C, N, P, and S). If the biomass is small, it may be justified to neglect microbial processes when compared with competing abiotic reactions.

- **Thermodynamic Approach**–Microbial growth and activity are constrained by energy sources, in addition to nutrients.

- **Kinetic Approach**–Microbial processes are explicitly modeled using measured or derived kinetic data, and representing metabolic activity by rate reactions.

The MING modeling code (CRWMS M&O 2000f) combines the nutrient and thermodynamic approaches. Abiotic considerations are used to estimate the rates at which nutrients and energy sources become available to microorganisms. Introduced materials are decomposed into their basic elements, and their contributions to the microbial ecology are included with the constituents available from groundwater and gas fluxes through the potential repository. The model does not bound the potential phenomenology of individual microbial colonies or biofilms, but quantifies the overall effects on the bulk chemical environment. The kinetic approach is possible, but it is impractical to obtain the needed information describing all relevant microbial processes.

3.1.2.4.2.2 Input Data, Assumptions, and Uncertainties

The input data for the Microbial Communities Model includes quantities, compositions, and physical properties of introduced materials, and the degradation lifetimes for those materials in the potential repository environment. Similar information is required for each type of waste form, and for the materials that make up the waste package. Uncertainty with respect to degradation lifetime is addressed in the model interpretation and sensitivity analysis. Additional parameters required for modeling with MING consist of temperature cutoff values, humidity cutoff values, gas utilization parameters, and energy cutoff values that control the release of chemical constituents from potential repository materials. Descriptors for the potential repository environment include temperature, relative humidity, liquid seepage flux, and gas flux

through the host rock as functions of time. In addition, the composition of seepage water is also used.

Model Assumptions

Major assumptions made in conjunction with MING modeling include those listed below (CRWMS M&O 2000f):

- **Relative Humidity**–A representative value of relative humidity is used as a surrogate for water activity throughout the environment.

- **Degradation Lifetimes**–Supporting information is sparse for estimating degradation lifetimes, particularly for cement grout and it components, so values are selected to represent reasonable ranges.

- **Iron Release Rates from Host Rock**–Degradation lifetimes of 10 million years, and 1 million years, are assumed for release of iron from biotite and hematite, respectively.

Model Uncertainties

The principal uncertainty associated with the Microbial Communities Model results from the degradation rates assigned to EBS materials. This is the primary source of rate information incorporated in the model.

Uncertainties associated with application of the Microbial Communities Model include competition between biotic and abiotic processes, and interpretation of the estimates for microbial biomass production. The model assumes that all available nutrients and redox energy sources are used for microbial processes, and is therefore bounding. The other point is that the Microbial Communities Model is not intended to quantify localized microbial activity or its consequences, but bounds overall microbial growth and activity in the EBS.

3.1.2.4.2.3   Microbial Communities Model Development

MING is used to evaluate potential impacts of the potential repository on microbial populations, and the associated effects on radionuclide release and transport. The MING code takes into account the availability of nutrients, the energy necessary to convert nutrients to microbes, the oxygen fugacity, and the temperature and humidity.

The starting point for the MING model development was the software model entitled: Estimation of Maximum Microbiological Activity also known as EMMA (CRWMS M&O 2000f) and is based on documented results from the Swiss Low/Intermediate Level Waste program. The MING model incorporates the same basic modeling approach and structure for calculating nutrient and energy limitations. Two main components were brought forward into MING from the original approach: 1) the numerical solution for the energy available for microbial growth; and 2) the general method for calculating nutrient availability. Other aspects brought forward include the average empirical microbial formula ($C_{160}H_{280}O_{80}N_{30}P_2S$) with a dry weight of 3,994 g/mole. In addition, MING also uses an average microbial water content of 99 weight percent and an average microbial volume of 1.5×10^{-13} mL. MING uses the same basic approach to

thermodynamic modeling, whereby microbes use oxidation-reduction couples to supply the energy required to carry out basic metabolic functions. MING uses the same limits of usable energy from oxidation-reduction reactions, whereby 15 kJ are obtained per mole of electrons transferred, and 64 kJ are needed to maintain 1 g of biomass (CRWMS M&O 2000f). Some enhancements to the original code are as follows:

- Addition of temperature dependence for free energy calculations

- Incorporation of time-dependent gas flux among nutrient constraints

- Time-dependent water composition entering the drift

- pH dependence of the governing oxidation-reduction equations

- Capability to sequence degradation of one potential repository material before another (e.g. for a layered waste package)

- Incorporation of threshold conditions for microbial growth

Within MING, only the standard-state free energies are used and these are not corrected for either Eh or the activity of dissolved species to derive the actual nonstandard-state free energies. By not calculating the nonstandard-state free energies, the calculation is not precise, but produces a rough estimate. The method for incorporating temperature dependence of free energies of reaction is also approximate, based on regression analyses of standard-state free energy values at various temperatures (0°, 25°, 50°, 60°, 75°, 100°, 125°, and 150°C) for selected half-reactions.

3.1.2.4.2.4   Microbial Communities Model Validation

The microbial communities model is based on an inventory of materials present in the drift, and how degradation of those materials can support microbial nutrient and energy requirements. The model is implemented in the MING code. It is validated by comparison to laboratory and field data. In these applications, approximate agreement is obtained with observed microbial abundance. The model can correctly identify nutrient-limited vs. energy-limited conditions, in agreement with other information from microbial investigations. The Microbial Communities Model is valid for its intended use, as a bounding model for microbial activity in the bulk EBS environment.

Comparison With Laboratory and Field Data

Three sets of model validation tests for MING are documented (CRWMS M&O 2000f):

- Replication of model results originally calculated for the Swiss potential repository program

- Depiction of ambient conditions found in the ESF and at Rainier Mesa (a natural analog)

- Modeling of independent lab tests conducted at LLNL

Replication of the Swiss case demonstrates that MING functions correctly when compared to previous modeling activities, where natural barrier material components are combined with engineered material components to calculated microbial growth.

Modeling of ambient data from the ESF and Rainier Mesa demonstrates that the selection of oxidation-reduction equations and the handling of material degradation produce reasonable results. The calculated results replicate the ambient system data (cell counts) to within an order of magnitude. This exercise confirms that water and phosphorous availability are limiting factors to microbial growth. Calculated results also show that the natural system is energy limited, because when material degradation lifetimes are lowered there is a notable increase in energy produced.

Modeling of the LLNL lab tests provides perspective on the uncertainty associated with modeled results. Comparison with laboratory test data shows that the numbers of organisms calculated by MING can agree to within an order of magnitude with measured data from controlled tests. Both energy-limited and nutrient-limited tests are analyzed. The model confirms that the primary factor limiting microbial growth in the host rock is availability of water, and the primary limiting nutrient is phosphorous. An example showing how test data are modeled using MING, is described below.

The test series conducted by LLNL used several different growth media to grow microbes. Each medium was selected to investigate limiting nutrients in the potential repository environment. The reader is referred to CRWMS M&O (2000f) for references to more detailed descriptions of the tests. Each medium was placed in a flask with a known quantity of Topopah Spring tuff, and cultured for approximately seven days. Microbial abundance in the liquid media was determined by live plating. Two types of tests were conducted: (1) a set of microcosm tests in which the growth medium was continuously supplied, and (2) a set of batch tests in which the tuff was exposed to a single aliquot of growth medium. The batch tests are best suited for modeling using MING because the conditions are easily specified.

Comparison of the batch and microcosm results for the "Dilute Complete" medium, with the microbial abundance predicted by MING, shows reasonable agreement as shown in Figure 3-43. (The "Dilute Complete" medium was similar to J-13 water, and augmented with glucose.) The model also indicated that the system was energy-limited, i.e., the nutrients present could have produced more microbes.

3.1.2.4.3   Summary of the Effects of Microbial Activity in the EBS

Microorganisms are capable of degrading all EBS materials. The primary electron donors in the EBS will be metals (such as steel) or metal ions in reduced form. The primary electron acceptors will be sulfate, nitrate, and gas-phase oxygen. Microbial growth and activity in the host rock are limited by the availability of water and phosphate. Dryout of the EBS and high temperatures during the thermal period will arrest microbial growth and activity. Microbial activity will not occur at temperatures greater than 120°C in aqueous environments. Reported dependence on humidity shows that growth and activity do not generally occur at less than approximately 90 percent relative humidity. When salts are present, the threshold humidity may decrease depending on the deliquescent behavior of the salts and the presence of salt-tolerant organisms.

When the titanium drip shield is exposed to sufficient humidity or liquid water, MIC may occur (if it can be shown to occur in laboratory tests). EBS water-diversion features (including the drip shield) will protect the waste package during the thermal period and beyond. Salts, and nutrients such as phosphate, will not be deposited on the waste package while the drip shield is intact.

MIC will oxidize metallic barriers and likely consume oxygen as an energy source while obtaining carbon from an inorganic source such as CO_2. Sulfur reduction may also occur. The effects of CRM degradation on the bulk chemical environment will be these processes will be small or negligible, because of inherent resistance of CRMs to microbial attack and consequent slow rates of corrosion.

The corrosion rate for the carbon steel ground support and invert supports will increase because of MIC, and this is the major potential effect of microbial activity on the bulk chemical environment. Laboratory test data show that the corrosion rate can increase by a factor of at least 6 to 7. Steel corrosion will consume oxygen and lower the O_2 fugacity in the drift environment.

3.1.2.5   Precipitates and Salts

Several modeling approaches are presented in this section:

- **Normative Precipitates and Salts Models**–Based on empirical data, and used to predict which minerals and salts will form when waters are completely evaporated. Used in conjunction with the EBS Chemical Reference Model in Section 3.1.2.7.

- **Condensed Water Model**–Calculates the composition of condensate that can form on the waste package or the underside of the drip shield, affected only by gas-phase CO_2. Used in TSPA to predict water compositions that can affect drip shield and waste package corrosion when there is no seepage, only condensation.

- **Low- and High-Relative-Humidity Salts Models**–The Low-Relative-Humidity (LRH) Salts Model describes the behavior of salts at relative humidity less than 85 percent, while the High-Relative-Humidity (HRH) Salts Model calculates water composition and dissolution/precipitation reactions for solutions that can occur when relative humidity is greater than 85 percent. These models are used in TSPA to determine the timing of environmental conditions that permit aqueous corrosion, and to estimate the ionic strength of waters that can transport released radionuclides.

3.1.2.5.1   Conceptual Models for Precipitates and Salts Formation

Boiling and evaporation of water in the potential repository emplacement drifts will cause dissolved solids in the water to concentrate and precipitate. The precipitates that form will depend on water composition, temperature, gas fugacities, and rates of evaporation and seepage.

Boiling temperatures (>96°C) and low relative humidity are expected during the first few hundred years after closure. Seepage into the drifts during this period, if it occurs, may be transient, but the nonvolatile dissolved constituents can accumulate in the drifts as salts and minerals. These solids will include relatively insoluble minerals like silicates and carbonates,

and also soluble salts with the potential to form brines when sustained humidity returns during cooldown.

Dissolved salts in water decrease the saturation water vapor pressure because they reduce the chemical activity of water. The chemical activity of water is proportional to the mole fraction of water, and is equivalent to the equilibrium relative humidity of the solution (CRWMS M&O 2000g). As a result, brines reach liquid–vapor equilibrium at relative humidity values below 100 percent. There is a critical value of relative humidity, determined by the solubility of the salt, below which brine cannot exist at equilibrium with the gas phase, and will evaporate. Relative humidity above the critical value for a salt will cause moisture to condense and form a brine, even if there is no other liquid present. Impacts of brine formation on potential repository performance include earlier return of aqueous conditions, and potentially aggressive corrosion conditions.

Studies of saline lakes in the western United States show that alkaline sodium carbonate brines are common. Many of these waters occur in volcanic terrain and have high silica content. They also are typically enriched in chloride and sulfate. Highly soluble components precipitate in the late stages of evaporation. In carbonate-rich brines, these components include sodium, chloride, sulfate, carbonate, and silica. The predominant components in carbonate-poor brines, such as those resulting from evaporation of sea water, are sodium, calcium, magnesium, chloride, and sulfate. Other dissolved components that have been observed to become enriched in some brines include fluoride, bromide, strontium, phosphate, and boron. Nitrate is highly soluble, but is not mentioned in these studies, perhaps because it has greater biological activity.

During cooldown, dissolution of salts will occur rapidly when the relative humidity exceeds the critical value for each salt present. Rapid dissolution is consistent with the observation that puddles of dissolved salt (primarily NaCl) occur overnight on salt flats when the relative humidity exceeds the stability limit for NaCl but remains below the dew point (CRWMS M&O 2000g). These puddles can then dry up during the day when the relative humidity decreases.

The lowest critical relative humidity values important for the EBS environment, approximately 50 percent, correspond to the nitrate salts KNO_3 and $NaNO_3$. In the potential repository the corresponding temperature at 50 percent relative humidity will be less than 120°C, which is the approximate boiling point for a concentrated solution of $NaNO_3$. The next threshold will occur at approximately 80 percent relative humidity, when NaCl, NaF, Na_2CO_3, $NaHCO_3$, $Na_2Si_2O_5$, and Na_2SiO_3 will dissolve. Except for NaCl, there are few data available on the critical relative humidity values for these salts. The final threshold will be at approximately 90 percent relative humidity, when Na_2SO_4 dissolves. This will leave $CaCO_3$ as the principal remaining salt.

During cooldown, the rate at which liquid water enters the drift will eventually exceed the evaporation rate, so that liquid accumulates, brines are diluted, and the liquid-phase composition is no longer controlled by the behavior of salts. As the potential repository environment approaches ambient (prerepository) conditions, water chemistry in the drifts will not depend on evaporative processes.

3.1.2.5.2 Normative Precipitates and Salts Model

3.1.2.5.2.1 Model Input Data

Synthetic J-13 Water Evaporation Tests

Well J-13 is a producing water well that is screened in the Topopah Spring welded tuff. J-13 water is of the dilute $NaHCO_3$ type, and its composition is used as a chemical analogue for fracture waters in the potential repository host rock (CRWMS M&O 2000t). A synthetic J-13 well water was mixed for use in evaporation tests. Preparation was performed at room temperature, under ambient atmospheric gas conditions. The batch was decanted to remove undissolved reagents, and the resulting solution was analyzed for pH, metals (Ca, Mg, Na, K, and Si), and for anions (chloride, fluoride, nitrate, and sulfate).

Laboratory batch tests were conducted at Lawrence Livermore National Laboratory in 1998 and 1999. In the first two tests, 30 L of synthetic J-13 well water were evaporated down to 30 mL, resulting in an evaporative concentration factor of approximately 1000×. In all tests, the actual concentration factors were estimated by total mass measurements and are accurate to approximately 10 percent. Synthetic J-13 water was pumped into a 1-L Pyrex™ beaker at a constant rate using a peristaltic pump, while the sample evaporated at 85°C over a hot plate. The fluid-delivery rate and heat flux were balanced to maintain constant temperature in the fluid contained within the beaker.

Aqueous samples for cation and anion analyses were collected in plastic syringes, and filtered through a rinsed 0.45-μm filter. For analysis of total dissolved inorganic carbon, a small split of each unacidified sample was injected directly into an infrared CO_2 analyzer. Speciation of DIC as bicarbonate or carbonate was determined from the measured pH. The anions of fluoride, chloride, nitrate, and sulfate were determined using ion chromatography (IC). The analytical protocol supports detection of several other anion analytes, but these four were the only ones detected (other than carbonate species). Cations were determined using inductively-coupled plasma emission spectroscopy (ICP).

Solution pH was determined using a method recommended by the National Bureau of Standards; which is best suited for low ionic strength solutions, although useful measurements can be made up to ionic strength as great as that of seawater (0.7 molal). For J-13 water and similar compositions, accurate pH measurement is limited to less than 200× evaporative concentration. Accordingly, pH measurements for the rewet samples of the evap1 and evap2 runs are approximate. No attempt was made to measure the pH of the batches concentrated to 1000× or greater.

Solids samples (tests evap1 and evap2) were dried, weighed, and analyzed using x-ray diffraction (XRD). The purpose of the XRD analysis was to identify the phases produced, and quantification was not attempted.

The tests were performed at sub-boiling conditions to represent evaporation of slowly migrating waters in the EBS, such as could occur in the backfill. The 85°C temperature is similar to predicted conditions for inflow to the potential repository during the thermal period, should it occur, while maintaining sub-boiling conditions for the test. At these temperatures, the

assemblage of mineral phases resulting from the evaporation is controlled predominantly by precipitation kinetics, and it is thought that the assemblages observed are representative of potential repository conditions.

One potentially important aspect of the batch tests, is that the precipitates are still available for reaction after they form. Flowing water in the potential repository would tend to leave behind precipitates, and the precipitates would develop zones. While zonation is theoretically possible, it would require extensive evaporative concentration. The available flux of concentrated water is small and therefore slow in the unsaturated backfill, a porous medium.

In the first test (evap1), detailed chemical analysis was performed on the initial starting water composition and on a sample collected after approximately 1000x concentration. A small split of the solids that had precipitated at the 1000x stage (not yet dry) was collected for mineralogic analysis. The solution was then evaporated to complete dryness, and another small split of the solids was collected. The remaining solids were then rewet with 200 mL of deionized water and evaporatively concentrated to 100 mL at 75°C; the resulting solution was collected for detailed water-chemistry analysis. The rewetting step was incorporated to evaluate the reproducibility of precipitate formation at supersaturated conditions. Three water compositions (including the initial solution) and two solid samples were analyzed.

The second test (evap2) was the same except that the beaker contained 10 g of crushed Topopah Spring welded tuff (CRWMS M&O 2000af). The tuff was prepared by sieving the original material (<2 mm grain size) to >0.5 mm to remove the fine fraction. The sized material was washed three times in isopropanol. The grains were allowed to settle before decanting to remove adhering fine particles and were then air-dried. The test was taken to complete dryness, and a rewetting step was incorporated as described previously. Three water compositions (including the initial solution) and two solid samples were analyzed.

A short-term test (evap4) was conducted to further investigate the evolution of pH during evaporative concentration to approximately 100x. The initial and final solutions were sampled for chemical analysis. The results of these tests (evap1, evap2, and evap4) are summarized in Table 3-10 through Table 3-14.

Table 3-10. Evolution of Water Composition in Test with Synthetic J-13 Water (evap1)

Species (mg/kg)	Synthetic J-13 (mg/kg)	Species Conc. (mg/kg) w/ Evap. Factor: 956x [a]	Concentration Ratio	Rewet [b] (mg/kg)	Concentration Ratio
Ca	6.40	29.9	4.70	3.48	0.54
Cl⁻	6.90	4.84×10^3	701	1.77×10^3	257
F⁻	2.20	1.55×10^3	705	530	241
HCO₃⁻	108	2.49×10^4	231	9.54×10^3	88.3
K	5.30	4.79×10^3	904	1.36×10^3	257
Mg	2.20	0.14	0.06	0.09	0.04
Na	46	4.41×10^4	958	1.25×10^4	272
NO₃⁻	8.0	5.53×10^3	694	2.02×10^3	252
SO₄²⁻	18.1	1.29×10^4	714	4.63×10^3	256
SiO₂(aq)	11.3	1.80×10^4	1.59×10^3 [c]	3.61×10^3	319
pH	7.84	[d]		10.6	

Source: CRWMS M&O 2000t .

NOTES: [a] 30 L of synthetic J-13 well water were evaporated to 30 mL, resulting in a concentration factor of approximately 1000x.

[b] After evaporation to complete dryness, the solids were rewet with 200 mL of deionized water and evaporatively concentrated to 100 mL.

[c] The apparent concentration ratio for SiO₂ is greater than that estimated from total mass measurements and the concentration ratios for other ions, possibly because of analytical errors associated with the high ionic strength.

[d] Not analyzed

Results from Synthetic J-13 Water Evaporation Tests

The results summarized in Table 3-10 through Table 3-14 were obtained from an open system (free exchange with gas-phase CO_2) under ambient atmospheric composition conditions. Following are some major findings from these tests:

- Divalent cations (Ca^{2+}, Mg^{2+}) tend to precipitate early in evaporative evolution, both with and without tuff present (evap1 and evap2), from precipitation of carbonate (probably calcite and low-Mg calcite).

- Halite and niter apparently contain the chloride and nitrate from the starting solution. Niter is among the last solids to precipitate.

- Polymorphic phases (e.g., aragonite and calcite; anhydrite and gypsum) indicate that solubility constraints changed during the final stages of evaporation.

- Test results provided no indication of hydroxides (portlandite, NaOH) for evaporation under ambient atmospheric composition conditions.

Table 3-11. Evolution of Water Composition in Test with Synthetic J-13 Water and Tuff (evap2)

Species (mg/kg)	Synthetic J-13 (mg/kg)	Species Conc. (mg/kg) w/ Evap. Factor: 1114x [a]	Concentration Ratio	Rewet [b] (mg/kg)	Concentration Ratio
Ca	5.60	6.90	1.2	3.0	0.5
Cl$^-$	7.20	6.12×10^3	850	2.35×10^3	326
F$^-$	2.20	1.52×10^3	691	605	275
HCO$_3^-$	104	3.14×10^4	303	1.34×10^4	129
K	5.30	3.72×10^3	702	1.55×10^3	292
Mg	2.10	< 0.28	c	< 0.08	c
Na	44.3	3.77×10^4	851	1.45×10^4	327
NO$_3^-$	7.80	6.73×10^3	863	2.60×10^3	333
SO$_4^{2-}$	18.3	1.57×10^4	858	6.14×10^3	336
SiO$_2$(aq)	9.40	7.12×10^3	758	2.69×10^3	287
PH	8.03			9.99	

Source: CRWMS M&O 2000t

NOTES: [a] 30 L of synthetic J-13 water were evaporated to 30 ml, for a concentration factor of approx. 1000x.
[b] After evaporation to complete dryness, the solids were rewet with 200 mL of deionized water and evaporatively concentrated to 100 mL.
[c] Not analyzed

Table 3-12. Evolution of pH in Short-Term Test with Synthetic J-13 Water (evap4)

Concentration Factor	pH
1.00	8.46
1.00	8.65
1.05	9.04
1.29	9.43
1.60	9.58
2.41	9.67
6.08	9.67
6.37	9.77
7.59	9.79
11.6	9.95
12.6	10.00
15.3	10.03
20.9	10.08
25.2	10.09
34.4	10.12
52.1	10.18
104	10.18
157	10.18

Source: CRWMS M&O 2000t

Table 3-13. Mineralogical Results from Test with Synthetic J-13 Water (evap1)

evap1—956x	evap1—Complete Evaporation
SiO_2 (amorphous)	SiO_2 (amorphous)
aragonite ($CaCO_3$)	aragonite ($CaCO_3$)
calcite ($CaCO_3$)	calcite($CaCO_3$)
	halite (NaCl)
	niter (KNO_3)
	thermonatrite ($Na_2CO_3{:}H_2O$)
	gypsum ($CaSO_4{:}2H_2O$) [a]
	anhydrite ($CaSO_4$) [a]
	hectorite ($Na_{0.33}Mg_3Si_4O_{10}(F,OH)_2$) [a]

Source: CRWMS M&O 2000t

NOTE: [a] Species is a minor constituent, and identification is uncertain.

Table 3-14. Mineralogic Results from Test with Synthetic J-13 Water and Tuff (evap2)

evap2—1114x [a]	evap2—Complete Evaporation [a]
SiO_2 (amorphous)	SiO_2 (amorphous)
trona ($Na_3H(CO_3)_2{:}2H_2O$)	trona ($Na_3H(CO_3)_2{:}2H_2O$)
Thermonatrite ($Na_2CO_3{:}H_2O$)	thermonatrite ($Na_2CO_3{:}H_2O$)
halite (NaCl)	halite (NaCl)
calcite ($CaCO_3$)	calcite ($CaCO_3$)
Aragonite ($CaCO_3$)	aragonite ($CaCO_3$)
Anhydrite ($CaSO_4$)	anhydrite ($CaSO_4$)
smectite ($Na_{.3}(Al,Mg)_2Si_4O_{10}(OH)_2$)	smectite ($Na_{.3}(Al,Mg)_2Si_4O_{10}(OH)_2$)
niter (KNO_3)	niter (not detected by XRD)

Source: CRWMS M&O 2000t

NOTE: [a] Only the minerals produced by evaporation and not present in the starting tuff are reported. The major minerals constituting the tuff are probably crystobalite (α), K-feldspar, albite, anorthite, and quartz.

- The measured pH of the rewet solution with tuff present (evap2) was 9.99, compared to pH 10.59 without tuff (evap1), probably from buffering associated with the dissolution of SiO_2 and silicates.

- pH was approximately 10 to 11 for concentrated J-13 water up to approximately 150x, with and without tuff present, under ambient atmospheric conditions

- The Si concentration was lower in the concentrated evap2 solutions than in the evap1 solutions, which suggests that the presence of the silicate and aluminosilicate minerals in the tuff enhances precipitation.

- The presence of tuff appears to have little effect on relative concentrations of the anions, except for fluorides; this indicates that fluorite precipitation may be enhanced by increased Ca concentration derived from tuff.

Synthetic Porewater Evaporation Tests

Another set of tests was performed to investigate precipitates that could be produced by evaporation of matrix porewater, a reference water composition based qualitatively on reported analyses for porewater extracted from the Topopah Spring welded tuff (CRWMS M&O 2000t). Such waters have substantially less Na and K and more Ca and Mg than J-13 water, and the anionic species are dominated by sulfate and chloride instead of bicarbonate. A synthetic porewater was created for use in evaporation tests. The preparation and analysis were performed in the same manner as for the synthetic J-13 water.

The laboratory batch tests with synthetic porewater conducted at LLNL in 1998 and 1999 were completely analogous to those done with synthetic J-13 well water. An initial test investigated the evaporation of water to dryness (evap3) and a subsequent test added 10 g of Topopah Spring welded tuff (CRWMS M&O 2000af). Another test (evap5) investigated the evolution of pH during short-term evaporative concentration to approximately 100×. The results of these experiments are summarized in Table 3-15 through Table 3-19.

Table 3-15. Evolution of Water Composition in Test with Synthetic Porewater (evap3)

Species (mg/kg)	SPW (mg/kg)	Species Conc. (mg/kg) w/ Evap. Factor: 1243×	Concentration Ratio	Rewet (mg/kg)	Concentration Ratio
Ca	57.2	15,629	273	6,010	105
Cl$^-$	78.0	53,084	681	19,248	247
F$^-$	2.30	< 577	b	< 301	b
HCO$_3^-$	16.2	< 35	b	< 37	b
K	4.20	2,779	661	973	232
Mg	11.7	5,478	470	1,949	167
Na	8.20	5,961	727	2,077	253
NO$_3^-$	11.0	b	b	2,647	241
SO$_4^{2-}$	81.7	2,077	25	1,564	19
SiO$_2$(aq)	9.80	513	52	340	35
PH	7.68	6–6.5 [a]		5.56	

Source: CRWMS M&O 2000t

NOTES: [a] Semiquantitative measurement using pH paper
[b] Not analyzed or determined

Table 3-16. Evolution of Water Composition in Test with Synthetic Porewater and Tuff (evap6)

Species (mg/kg)	SPW (mg/kg)	Species Conc. with Evap. Factor: 564x	Concentration Ratio	Rewet	Concentration Ratio
Ca	59.2	12,553	212	10,249	173
Cl⁻	76.1	37,198	489	30,359	399
F⁻	2.10	< 248	a	< 284	a
HCO_3^-	20.2	< 60	a	< 36	a
K	4.10	2,006	488	1,622	395
Mg	12.0	3,615	300	2,889	240
Na	8.70	4,420	508	3,574	411
NO_3^-	10.5	5,267	501	4,344	413
SO_4^{2-}	85.2	1,316	15.4	1,516	17.8
$SiO_2(aq)$	11.5	696	60.6	355	30.9
pH	7.52	5.14		5.43	

Source: CRWMS M&O 2000t

NOTE: [a] Not analyzed

Table 3-17. pH and Carbonate Evolution from Short-Term Test with Synthetic Porewater (evap5)

Concentration Factor	pH	HCO_3^+ (mg/L)
1.00	7.45	24.7
1.06	8.69	a
1.38	9.01	a
1.76	8.99	a
2.31	8.86	a
4.19	8.57	a
6.09	a	20.1
6.36	8.55	a
8.16	8.51	a
8.19	a	19.5
12.0	8.45	19.4
29.9	8.29	14.0

Source: CRWMS M&O 2000t

NOTE: [a] Not analyzed

Table 3-18. Mineralogical Results from Test with Synthetic Porewater (evap3)

evap3—1243×	evap3—Complete Evaporation
gypsum ($CaSO_4 \cdot 2H_2O$)	gypsum ($CaSO_4 \cdot 2H_2O$)
	tachyhydrite ($CaMg_2Cl_6O_{10} \cdot 12H_2O$)

Source: CRWMS M&O 2000t

Table 3-19. Mineralogical Results from Test with Synthetic Porewater and Tuff (evap5)

evap6—564×	evap6—Complete Evaporation [a]
gypsum ($CaSO_4 \cdot 2H_2O$) halite (NaCl)	gypsum ($CaSO_4 \cdot 2H_2O$) halite (NaCl) Mg-smectite ($Na_{.3}(Al,Mg)_2Si_4O_{10}(OH)_2$) Kenyaite ($NaSi_{11}O_{20.5}(OH)_4 \cdot 3 H_2O$)[b]

Source: CRWMS M&O 2000t

NOTES: [a] Only the minerals produced by evaporation and not present in the starting tuff are reported here. The major minerals constituting the tuff are probably crystobalite (α), K-feldspar, albite, anorthite, and quartz.

[b] Species is a minor constituent and identification is uncertain.

Results for Synthetic Porewater Evaporation Tests

The results summarized in Table 3-15 through Table 3-19 were obtained from an open system (free exchange with gas-phase CO_2) under ambient atmospheric composition conditions. Following are some major findings from these tests:

- Sulfate is the predominant anion; therefore, the effects of carbonate species are substantially less important in the synthetic porewater tests.

- The pH decreases to approximately 5.5 to 6.0, with evaporative evolution of the Ca-sulfate porewater, instead of increasing to pH ~10 as was observed for the J-13 water.

Larger discrepancies between the concentration factors computed from measured species concentrations and the total mass concentration factor are noted for the porewater tests when compared to the J-13 water tests. For species such as chloride (e.g., Table 3-10 and Table 3-15) the apparent concentration factor for dissolved species is substantially less than the total mass concentration factor. This probably occurred because the greater dissolved-solids content of the porewater starting solution caused the system to exceed solubility conditions, so that precipitation occurred.

Comparison of results from analogous tests using synthetic J-13 and porewater (Table 3-10 and Table 3-15) shows that bicarbonate waters such as J-13 are more likely to produce high-pH conditions than are sulfate-type waters such as the synthetic porewater. Selection of J-13 water composition for investigating the EBS chemical environment is therefore bounding with respect to alkaline pH. The J-13 composition is used for modeling the EBS chemical system in Section 3.1.2.7.

3.1.2.5.2.2 Model Assumptions

Bounding Water Composition

With respect to the performance of corrosion-resistant materials, high-pH conditions and the presence of anions such as fluoride, chloride, and sulfate represent the most aggressive conditions for corrosion that are possible in the potential repository environment, and constitute a reasonable-bound composition for modeling the EBS chemical environment.

3.1.2.5.2.3 Model Uncertainties

The principal uncertainty associated with this model is caused by simplification of the reaction path that culminates in complete evaporation. Precipitates that form relatively early in the evolution of the mineral assemblage, are exposed to aqueous solution conditions, and are therefore available to redissolve and participate in further precipitation reactions. The implication is that salts can form other than those predicted. Agreement with test results is therefore important, and extension to other starting solution compositions should be verified by testing.

Another uncertainty for low-CO_2 conditions that may be encountered in the potential repository during the thermal period, it is that sufficient CO_2 will be present to produce thermonatrite ($Na_2CO_3 \cdot H_2O$) and calcite ($CaCO_3$). If this assumption is incorrect, portlandite or NaOH could precipitate in the EBS (e.g., on the drip-shield surface). This could have different implications for corrosion of metallic barriers. Thermodynamic equilibrium calculations show that sufficient CO_2 is likely to be available to prevent hydroxide formation (CRWMS M&O 2000t), but test data for low-CO_2 conditions are not available.

3.1.2.5.2.4 Normative Precipitates and Salts Model Development

For waters having compositions similar to the synthetic J-13 and synthetic porewater, a set of precipitates is identified that is consistent with the observations reported in Table 3-13 and Table 3-18. This model describes an assemblage of precipitates formed by complete evaporation. The order of formation of different salts during evaporation, is not a feature of this model.

Nitrate, Fluoride, and Chloride Salts

Nitrate precipitates as niter (KNO_3), which is the likely disposition for all nitrate (Table 3-20). The amount of KNO_3 that forms is determined by the molality of K or NO_3, whichever is smaller. If there is insufficient potassium to precipitate all the nitrate, sodium is used to form Na-niter ($NaNO_3$). Any excess potassium is precipitated as sylvite (KCl). Halite (NaCl) is precipitated, limited by the available sodium or chloride, whichever is smaller. Fluorite (CaF_2) is formed from Ca and fluoride, which is reasonable because of its relative insolubility. Any remaining fluoride is precipitated as villiaumite (NaF), which is reasonable because sodium is abundant and NaF is generally less soluble than KF. For J-13 water, these steps eliminate nitrate, chloride, fluoride, and potassium from the problem. For the synthetic porewater, some chloride may remain.

Clays

For waters similar to J-13, clays can form in relatively small amounts, limited by the available Al in solution. Mg-smectite, Ca-smectite and, ultimately, Na-smectite, compositions are used as needed to precipitate the Al. The approach does not include precipitates that could accommodate Mg in excess of the Al or instead of Mg-smectite. However, calcite is included in the model, and a low-Mg calcite would be plausible in this case. With an open-system, constant-fugacity condition placed on CO_2, the choice of clay or calcite as the endpoint for a minor amount of Mg is not critical to pH.

Table 3-20.   Normative Mineral Assemblage for Complete Evaporation of Waters Similar to J-13 under Near-Atmospheric CO_2 Conditions

Minerals in Assemblage	Remarks [a]
Niter (KNO_3)	Use all nitrate or all potassium
Na-niter ($NaNO_3$)	Use all remaining nitrate
Fluorite (CaF_2)	Use all fluoride
Villiaumite (NaF)	Use all remaining fluoride
Sylvite (KCl)	Use all remaining potassium
Halite ($NaCl$)	Use all sodium or chloride
Mg-smectite ($Mg_{0.165}Al_{2.33}Si_{3.67}O_{10}(OH)_2$)	Use all magnesium or aluminum
Ca-smectite ($Ca_{0.165}Al_{2.33}Si_{3.67}O_{10}(OH)_2$)	Use all calcium or aluminum
Na-smectite ($Na_{0.33}Al_{2.33}Si_{3.67}O_{10}(OH)_2$)	Use all remaining aluminum
Thenardite (Na_2SO_4)	Use all sodium or all sulfate
Anhydrite ($CaSO_4$)	Use all remaining sulfate
Calcite ($CaCO_3$)	Use all remaining calcium (CO_2 is from open-system)
Thermonatrite ($Na_2CO_3{:}H_2O$)	Use all remaining sodium (CO_2 is from open-system)
Amorphous silica (SiO_2)	Use all remaining silica

Source: CRWMS M&O 2000t

NOTES: [a] Minerals are presented in order of calculation, not in order of precipitation.

Sulfates and Carbonates

Thenardite is used to precipitate sulfate, although gypsum and anhydrite were suspected or detected in the laboratory tests (Table 3-13 and Table 3-14). This selection is based on thermodynamic arguments (CRWMS M&O 2000t) which show that:

- Anhydrite ($CaSO_4$) is thermodynamically favored over gypsum ($CaSO_4{:}2H_2O$) under the humidity conditions calculated for the EBS.

- Calcite ($CaCO_3$) is thermodynamically favored over portlandite ($Ca(OH)_2$) under the CO_2 fugacity conditions calculated for the EBS.

- Thenardite (Na_2SO_4) and calcite ($CaCO_3$) are a more stable assemblage than thermonatrite ($Na_2CO_3{:}H_2O$) and anhydrite ($CaSO_4$); therefore, thenardite is the more likely sulfate precipitate.

Accordingly, thenardite is used to precipitate all the sulfate. If there is insufficient Na to precipitate all of the sulfate (e.g., synthetic porewater), anhydrite could form at the expense of calcite. This could happen sequentially so that anhydrite and thenardite are not in equilibrium. Any remaining chloride is precipitated as tachyhydrite ($CaMg_2Cl_6O_{10} \cdot 12H_2O$), which was observed in the laboratory tests with synthetic porewater. Calcite is then used to precipitate the remaining Ca, and thermonatrite is used to precipitate the remaining Na. Any remaining magnesium is precipitated, possibly as Mg-calcite, which is represented in the model by precipitation of magnesite ($MgCO_3$).

Silica

The final species considered in the assemblage is amorphous silica (SiO_2), which was detected in all of the laboratory samples derived from the synthetic J-13 water (Table 3-13 and Table 3-14). Amorphous silica is used to precipitate of all the remaining silica, leaving only trace and minor species, which have limited influence, on redissolution, on bulk chemical conditions such as pH.

3.1.2.5.2.5   Discussion and Summary

The trends in solution chemistry for the evap1 and evap2 tests using synthetic J-13 water (Table 3-10 through Table 3-11) are consistent with the XRD results for the solid precipitates produced (Table 3-13 and Table 3-14). The presence of the tuff allows for more geochemical processes to occur, particularly mineral dissolution and precipitation and silicate buffering.

Test results for synthetic J-13 water are sensitive to the ambient atmospheric CO_2 fugacity, which limits pH to the range 10 to 11 for evaporative concentration values up to 150× and probably higher. Smaller values for the CO_2 fugacity will tend to cause higher pH. The empirical nature of these results is attributable to limitations on the state-of-the-art for measuring and modeling pH at high ionic strength.

Bicarbonate-type waters such as J-13 water are more sensitive to CO_2 fugacity, particularly during evaporative concentration, and are more likely to produce high-pH conditions than are sulfate-type waters such as the synthetic porewater investigated. The synthetic J-13 results are therefore bounding with respect to high-pH conditions at the surface of the drip shield or the waste package during the thermal period. Sulfate-type or chloride-type waters tend to produce lower pH values when concentrated evaporatively (a difference of 4 pH units was observed) and are therefore not bounding compositions. The J-13 water composition is used for modeling the EBS chemical system in Section 3.1.2.7.

Test results for synthetic J-13 water (with and without tuff) show that for pH >10, evaporative concentration factors greater than 150× are required. Thus, the potential volumes and flow rates of affected solutions will be small. Saturation of the backfill in affected locations will be small, and the relative permeability and consequent mobility of these solutions will be limited.

If a water composition that is similar to, but more dilute than, J-13 water (e.g., condensate) is used, the results will be similar to the synthetic J-13 results presented here; however, greater evaporative concentration factors would be required to achieve the same high pH values. Thus, the mass of solute involved, and the potential volume of high-pH liquid, would be smaller.

3.1.2.5.2.6   Normative Model Validation

In this section, the normative approach described previously and summarized in Table 3-20, is applied quantitatively to the complete evaporation of synthetic J-13 water and synthetic porewater used in laboratory tests (Table 3-21 and Table 3-22). In these tables, compositionally equivalent predicted species (e.g. calcite and aragonite) are grouped. Also, observed and predicted species are grouped for comparison, even where they have different composition (e.g. thenardite and gypsum or anhydrite).

The comparisons shown in Tables 3-21 and 3-22 show that the normative approach can produce qualitative agreement for the synthetic J-13 water and synthetic porewater. Silica, thermonatrite, halite, niter, and calcite (or aragonite) are identified as major products of J-13 evaporation in both the predictions and observed data. The normative model predicts thenardite to form where gypsum and anhydrite are observed, so there evidently is some sensitivity to the relative availability of Ca and Na, which is not accounted for in the model. Minor species such as sylvite (or an alternative potassium-bearing phase) identified by the normative model for synthetic J-13 water may not have been detected by XRD. Similarly, minor species such as the niters, fluorite, halite, and calcite, and amorphous silica, which are predicted by the normative model for synthetic porewater, were not detected by XRD.

Table 3-21.   Normative Model for Precipitates Formed from Evaporating 1 kg of Synthetic J-13 Water, Compared with Qualitative Laboratory Observations

Predicted Normative Species	Predicted Moles/kg	Observed Species
Species Constituting >90% of Total Molality		
silica (amorphous)	7.925E–04	SiO_2 (amorphous)
thermonatrite ($Na_2CO_3:H_2O$)	6.917E–04	thermonatrite ($Na_2CO_3:H_2O$)
halite (NaCl)	1.975E–04	halite (NaCl)
thenardite (Na_2SO_4)	1.926E–04	gypsum ($CaSO_4:2H_2O$) [a]
		anhydrite ($CaSO_4$) [a]
niter (KNO_3)	1.274E–04	niter (KNO_3)
calcite/Aragonite ($CaCO_3$)	8.208E–05	calcite ($CaCO_3$)
		aragonite ($CaCO_3$)
Remaining Species		
magnesite ($MgCO_3$) [b]	8.638E–05	hectorite ($Na_{0.33}Mg_3Si_4O_{10}(F,OH)_2$) [a]
fluorite (CaF_2)	6.263E–05	
sylvite (KCl)	5.594E–06	

Source: CRWMS M&O 2000t

NOTES: [a] A minor constituent; identification is uncertain.

[b] Magnesium may precipitate as Mg-calcite but is represented stoichiometrically as magnesite.

Table 3-22. Normative Model for Precipitates Formed from Evaporating 1 kg of Synthetic Porewater, Compared with Laboratory Qualitative Observations

Predicted Normative Species	Predicted Moles/kg	Observed Species
Species Constituting >90% of Total Molality		
Gypsum/anhydrite ($CaSO_4$)	8.734E–04	gypsum ($CaSO_4{:}2H_2O$)
Tachyhydrite ($CaMg_2Cl_6O_{10}{:}12H_2O$)	2.427E–04	tachyhydrite ($CaMg_2Cl_6O_{10}{:}12H_2O$)
Silica (amorphous)	7.925E–04	
Calcite ($CaCO_3$)	2.567E–04	
Halite (NaCl)	3.021E–04	
Remaining Species		
Niter (KNO_3)	1.023E–04	
Na-niter ($NaNO_3$)	7.025E–05	
Fluorite (CaF_2)	5.684E–05	

Source: CRWMS M&O 2000t

From the above discussion, the normative model is valid for its intended use. It provides a valid approximation to the major species formed on complete evaporation of waters with composition similar to J-13 water, and matrix porewater. It does not account for mineral replacement (e.g., gypsum vs. anhydrite) caused by commingling of precipitates with concentrated solutions. Accordingly, for species identification (e.g. salts that can form on the drip shield) this should be taken into account by inclusion of all possible minerals that can form.

3.1.2.5.3 LRH Salts Model, Condensed Water Model, and HRH Salts Model

3.1.2.5.3.1 Input Data

Equilibrium Relative Humidity Values

Handbook values are used for the equilibrium relative humidity associated with aqueous solutions that are saturated with respect to different sodium and potassium salts. These values represent the maximum relative humidity at which a salt is stable at the given temperature.

Composition of Influent Seepage

For the LRH and HRH Salt Models, the composition of water from well J-13 is used to represent influent seepage. Other compositions may also be used.

Test Data Used for Model Validation–Three sources of test data from Lawrence Livermore National Laboratory are used in the model validation discussion:

- Synthetic J-13 water evaporation tests
- Synthetic Topopah Spring matrix porewater evaporation tests
- Tuff leaching/Synthetic 100× J-13 evaporation tests

The first two of these test series were described previously, for the normative model. The third test (called "Batch 1") involved dripping of 100× synthetic J-13 water through a column of

heated tuff into a Teflon^{TM} beaker. The recipe used for synthetic 100× J-13 well water did not include Si, Al, or Fe. The beaker was open to the atmosphere and maintained at a constant temperature of 90°C and relative humidity of 85 percent. The starting and final solution compositions are shown in Table 3-23.

Table 3-23. Water Composition Data from Tuff Leaching/Synthetic 100 × J-13 Evaporation Tests (CRWMS M&O 2000g)

Constituent	Units	Synthetic 100× J-13 Well Water	Evaporated Synthetic 100× J-13 Well Water
Ca	mg/L	5.48	26
Mg	mg/L	2.04	0
Na	mg/L	4210	79700
K	mg/L	517	10020
NO$_3$	mg/L	732	14600
CO$_3$	mg/L as HCO$_3$	790 [a]	11370
Cl	mg/L	730	15200
F	mg/L	208	3500
SO$_4$	mg/L	1633	30400
pH	pH	nr [b]	nr [b]

NOTES: [a] Calculated from concentration factor of 14.4 (CRWMS M&O 2000g)
      [b] not reported

Ranges of Temperature, Relative Humidity, and CO$_2$ Fugacity

Model calculations are performed for the following conditions:

- Temperature is evaluated at 95°C, 75°C, 45°C, and 25°C to develop a response surface that is intended to cover a range of conditions in the potential repository for use in TSPA.

- Relative humidity as a function of temperature and time, was approximated using previous TSPA-VA calculations (CRWMS M&O 2000g) corresponding to a simulation for which no backfill was included in the drift.

- CO$_2$ fugacity values are 10^{-1}, 10^{-3}, and 10^{-6} atm

Relative Evaporation Rate

The relative evaporation rate, or flux (R$_{rel}$) refers to the steady-state evaporation flux (Q$_{evap}$) divided by the influent seepage rate flux (Q$_{seep}$):

$$R_{rel} = \frac{Q_{evap}}{Q_{seep}}$$

(Eq. 3-14)

The values for R_{rel} used in this analysis are: 0, 0.1, 0.5, 0.9, 0.99, and 0.999. These are used to generate a lookup table that is intended to cover the range of evaporative concentration anticipated in TSPA.

Equilibrium Conditions

The LRH and HRH models assume chemical equilibrium. Chemical reactions are assumed to occur rapidly compared to anticipated seepage and evaporation rates. Several slow-forming minerals are not allowed to precipitate (see below).

3.1.2.5.3.2   Assumptions

Assumptions for the LRH Salts Model

Several simplifying assumptions are used in development of the LRH Salts Model. The LRH Salts Model assigns a constant seepage rate (Q_{seep}) and a constant seepage composition to discrete time periods representing thermal evolution of the potential repository. The dissolved solids in the seepage composition are restricted to Na, K, NO_3, SO_4, Cl, and CO_3 because, in accordance with previous discussions, these components are the most soluble and will dominate the solution composition as evaporation proceeds.

The model begins by precipitating all dissolved components in the seepage flux, according to a normative distribution. As relative humidity increases, the salts are redissolved according to the tabulated threshold behavior discussed previously, to produce brine. This brine can then be transported out of the EBS at the liquid flow rate determined using the thermal-hydrologic models (Section 3.1.4) to estimate seepage. The amount and composition of brine produced are controlled by the solubilities of the salts and the assumed fraction of each salt that is allowed to dissolve as a function of time. For the nitrate salts the entire amount is allowed to dissolve when the relative humidity reaches 50 percent. For the remaining salts, the fraction dissolved is assumed to increase exponentially from zero to unity as time increases from relative humidity 50 percent to 85 percent. At 85 percent relative humidity, all of the accumulated salts are completely dissolved.

In addition to the foregoing discussion, the following other assumptions and uncertainties are identified:

Vapor Pressure Lowering–In porous media or on solid surfaces, there are other mechanisms that decrease the saturation water vapor pressure of the liquid, such as capillary binding of water by surface tension, osmotic binding of water in double layers, and direct adhesion of water molecules to solid surfaces by London van der Waals forces (CRWMS M&O 2000g). For the LRH Salts Model it is assumed that these effects are negligible.

Limiting Solubilities–As a simplifying assumption in the LRH model, the limiting solubilities are assumed to be 24.4 molal for nitrate salts (based on the pure-phase solubility of KNO_3) and approximately 3 to 4 molal for non-nitrate salts. The latter range for the non-nitrate salts is chosen to provide a fit between the LRH Salts Model and the HRH EQ3/6 Pitzer model at 85 percent relative humidity. This range of solubility is within the ranges for pure chloride, carbonate, and sulfate salts.

Behavior of Carbonate–The carbonate concentration used in the LRH Salts Model is assumed to be "soluble" carbonate, which is determined from the Pitzer model of J-13 water evaporated to an ionic strength of approximately 10 molal (corresponding to approximately 85 percent relative humidity). According to the EQ3/6 results, a considerable amount of carbonate precipitates with Ca and Mg, but carbonate continues to concentrate. At 10 molal ionic strength, the carbonate that remains in solution is considered "soluble" because it can only combine with K or Na.

The LRH Salts Model assumes that dissolved inorganic carbon does not exchange with the atmosphere. To facilitate a smooth transition from the LRH Salts Model to the HRH Salts Model (at 10 molal ionic strength and 85% relative humidity) the carbonate concentration in the LRH brine composition is adjusted to achieve, for all values of relative humidity from 50 percent to 85 percent, a Na:CO$_3$ ratio equivalent to the value of this ratio in the EQ3/6 model results for J-13 water concentrated to 10 molal. Thus as the normative assemblage of evaporatively precipitated salts dissolves with increasing relative humidity, the carbonate concentration is determined from the Na concentration.

Charge Balance–Because of the approximations used to derive the water composition for the LRH Salts Model, particularly the treatment of carbonate, the composition is not necessarily charge balanced. Adjustments are made where appropriate, by adjusting the speciation of carbon between bicarbonate and carbonate. This is equivalent to an artificial adjustment of pH, and is needed because the mineral assemblage (minus nitrates) is dissolved congruently between 50 percent and 85 percent relative humidity, rather than according to a mechanistic model that includes pH.

Assumptions on Pitzer Database Development for the HRH Model

Modeling the behavior of electrolytes in concentrated aqueous solutions (>>1 molal ionic strength) is performed using ion-interaction equations, implemented in the EQ3/6 code. These semi-empirical equations are used to estimate activity coefficients that correct for non-ideal electrolyte behavior in concentrated saline waters. The EQ3/6 code includes the option to use Pitzer equations, with either of two Pitzer-type chemical databases. The Pitzer option extends the working range of the model from 1 molal ionic strength (using the B-dot equation) to 6 molal, and possibly 10 molal or higher (CRWMS M&O 2000g)

The two Pitzer databases included with EQ3/6 are the HMW and PIT databases (CRWMS M&O 2000g). The HMW database is internally consistent, with 9 elements and 17 aqueous species. Many components important to potential repository modeling are not included in the HMW database, including Al, Fe, Si, F, and N. Also, the database is only applicable at 25°C.

The PIT database contains a larger set of components and aqueous species than the HMW database, and is applicable to temperatures spanning the range needed for potential repository modeling. However, the PIT database is not completely internally consistent, and does not include any carbon or silica species. The PIT database is unqualified and therefore designated as to-be-verified.

A new Pitzer database was developed to include data from the HMW or PIT databases, and to add species not present in these databases. Specifically, the new PT4 database includes Na, K,

Ca, Mg, Cl, F, CO$_3$, SO$_4$, NO$_3$, SiO$_2$, Fe(III), Al, H, and H$_2$O at low and high·ionic strength and temperatures ranging from 20°C to 95°C. Following published work on the extension of the Pitzer database (CRWMS M&O 2000g), coefficients for H$_3$SiO$_4^-$, Fe(OH)$_4^-$, and Al(OH)$_4^-$ are assumed to be identical to those for HSO$_4^-$, while the coefficients for H$_2$SiO$_4^{-2}$ are assumed to be identical to those for SO$_4^{-2}$. The Pitzer coefficients for aqueous SiO$_2$ (or H$_4$SiO$_4$) are assumed to be identical to those for aqueous CO$_2$ (or H$_2$CO$_3$). Further details of the construction of the PT4 database are provided in the Precipitates and Salts Analysis/Model Report (CRWMS M&O 2000g).

For the PT4 database to claim a temperature range up to 100°C, temperature derivatives of the cation-anion parameters are estimated. For the parameters not available in the PIT database, it is assumed that median values for all of the "known" species apply. Thirty values from the PIT database are used to determine the median values for this purpose. The same EQ3/6 basis species can be used in the COM, PIT, HMW, and PT4 databases, for the aqueous species and solids considered. Thus, the solubility data for minerals defined in the COM, PIT, and HMW databases can be imported to the PT4 database without recalculation.

The PT4 database contains all of the minerals and gases originally within the PIT database plus CO$_2$ (g) and a number of carbonates, silicates, and other minerals from the COM database. The additional gas and mineral phases were added because of their potential importance in potential repository modeling.

Although validation of the PT4 database is demonstrated for the intended use in Section 6.5, the database is currently designated as to-be-verified. The identifications of minerals to be suppressed in the calculations are also to-be-verified. These assumptions do not affect calculations in dilute solutions.

In addition to the foregoing discussion, the following assumptions and uncertainties are identified in development of the HRH Salts Model (Pitzer model):

Standard State of Water or Brine–For the HRH Salts Model, non-standard state water is not considered. Only dissolved salts are considered to affect liquid-vapor equilibrium, and not capillarity, adsorption, double-layer effects, etc. This is justified because the effects are small, or affect only a small volume of the water present.

Oxidizing Conditions–Redox conditions within the drift are assumed to be oxidizing. Reduced chemical species or oxidation-reduction reactions are not included in the model. This is justified because oxidizing conditions prevail in the host rock, both in the gas-phase and in the form of solid-phase precipitates such as hematite and MnO$_2$.

3.1.2.5.3.3   Model Uncertainties

The principal uncertainties associated with the LRH and HRH Salts Models are related to representing solution composition at high ionic strength. The LRH Salts Model includes an approximation for the carbonate content, so pH is approximated during the interval of thermal evolution when this model applies. The HRH Salts Model is based on extensions to the Pitzer database, particularly the inclusion of new species and extrapolation to elevated temperatures.

These are approximations, and there are corresponding limitations on model validity as discussed below.

Another uncertainty is related to application of the LRH and HRH Salts Models to in-drift conditions. This concerns the mobility of fluids with the calculated compositions. Treating the EBS as a flow-through system, whereby salts are redissolved and the brines are transported out of the EBS shortly thereafter, may underestimate residence times for salts and brines. This is because during this time interval:

- Small volumes of liquid will be present in the EBS, so liquid saturation will be limited

- Hydraulic conductivity of backfill and other EBS materials will be small, so flow velocities will be limited

- Different salts will tend to form in different locations in the EBS, and there may be spatial heterogeneity of hydrologic processes.

Accordingly, the drip shield could be exposed to concentrated solution conditions for longer than predicted using a flow-through model. Again, this uncertainty relates to the applicability of results from the LRH and HRH Salts Models, and not to the predicted chemical compositions.

3.1.2.5.3.4   Model Development

The LRH Salts Model is developed for relative humidity less than 85 percent, conditions for which the deliquescent behaviors of soluble salts control the aqueous chemistry. For such conditions, the seepage influx either evaporates completely, or concentrates to a stable brine. The LRH Salts Model consists of a set of algebraic calculations performed within a Mathcad file.

The HRH Salts Model is developed for relative humidity greater than 85 percent, conditions for which soluble salts are fully dissolved, and the relative rates of evaporation and seepage control the aqueous chemistry. A modified Pitzer modeling approach is used in conjunction with the EQ3/6 chemical modeling code.

The Condensed Water Model is developed for the relatively simple problem of water condensed on an inert surface, in the presence of gas-phase CO_2 at elevated temperature. The EQ3/6 code is used for this application, in conjunction with the COM database.

Each of these models is discussed in the following sections.

LRH Model Development

In the LRH Salts Model, seepage water enters the drift and is subject to evaporation. At early times, the relative humidity is sufficiently low to vaporize all influent water, so the dissolved solids in the seepage accumulate. As discussed above, accumulated nitrate salts dissolve when the relative humidity increases 50 percent. For precipitates produced from evaporated J-13 water, the nitrate brine is mostly from KNO_3 and a small amount of $NaNO_3$.

As the relative humidity rises from 50 to 85 percent, the LRH Salts Model simulates brine generation by gradually dissolving the chloride, carbonate, and sulfate salts that have accumulated (and may continue to accumulate from seepage inflow). This period is divided into equal-length time intervals during which all the brine generated flows out of the drift (or reaction cell). (However, as discussed later, the model allows for some mixing between time increments.) The model dissolves these salts according to the assumed interpolation function:

$$f = 10^{\frac{4(t - t_{85})}{t_{85} - t_{50}}} \qquad \text{(Eq. 3-15)}$$

where f is the dissolved fraction of the total moles of chloride, carbonate, and sulfate present, and t is the time. The constants t_{50} and t_{85} are the times when relative humidity reaches 50 percent and 85 percent. The value of f increases exponentially as t approaches t_{85}. The different salts that may be present at each time step are treated congruently. The fraction dissolved for NO_3 and K is unity at the time relative humidity reaches 50 percent.

The total amount of each component present at any given time is the sum of the dissolved and undissolved fractions. For each time interval, the total amount of each component is calculated by taking the amount from the previous interval, subtracting the dissolved fraction from the previous interval, and adding the contribution from seepage in the current time interval. The model thereby allows transport of the dissolved species out of the EBS. Mixing and dispersion are incorporated by subdividing each time increment into half-increments, and using a moving backward-average scheme.

The dissolved/undissolved fractions and total inventory of Na at each time step are calculated by charge balance after the values for the other components are determined. The procedure maintains any charge balance errors introduced with the composition of influent seepage, but ensures that the aqueous phase composition is physically realizable. Further details are documented in the Precipitates and Salts Analysis/Model Report (CRWMS M&O 2000g).

Condensed Water Model Development

This model calculates the composition of pH and ionic strength for water that may condense on inert surfaces, such as the underside of the drip shield. Water vapor condenses on such surfaces wherever the temperature and relative humidity permit. The model does not predict the timing, amount, or location of the condensation. Rather, it predicts the pH and ionic strength on equilibration with gas-phase CO_2 at temperature. The condensing surfaces are assumed to be free from traces of soluble solids. EQ3/6 is used with the COM database for CO_2 fugacity values of 10^{-1}, 10^{-3}, 10^{-4}, 10^{-5}, 10^{-6}, 10^{-7}, and 10^{-9} atm, and temperatures of 25, 45, 75, and 95°C. The results are provided as look-up data.

HRH (Pitzer) Salts Model Development

The HRH Salts Model incorporates a modified Pitzer database, to calculate liquid phase compositions for ionic strength to approximately 10 molal. This is done within the framework of the existing EQ3/6 chemical modeling code. However, EQ3/6 includes Pitzer constants for only some of the components and temperature conditions needed for the HRH Salts Model. A

modified Pitzer database (PT4) is used, which includes the species CO_3, Si, Al, and Fe(III), for temperatures to 100°C. Derivation of the PT4 database was discussed previously, and details are provided in the Precipitates and Salts Analysis/Model Report (CRWMS M&O 2000g).

The HRH Salts Model is used in two modes: a simple evaporation mode, and a solid-centered flow-through mode. The simple evaporation mode is used to predict the evolution of a given solution (e.g., J-13 water) as it evaporates up to 10 molal. The second mode is used to predict the evaporative evolution of influent seepage.

HRH Salts Model–Simple Evaporation

Evaporation may be accomplished by the titration feature in EQ3/6 in two ways in this analysis. The traditional way is to declare an evaporation reactant (e.g., "H_2O") and designate it as an "aqueous" reactant type with a rate constant ("rk1") value of -1. Reaction progress is allowed to proceed from zero to approximately 55.5, which is the number of moles of water in a kilogram of water. The reaction progress endpoint must be iteratively adjusted to achieve the final target ionic strength. Another method is to designate the evaporating water as a "special" reactant with appropriate molalities of H and O (approximately 111.0 molal and 55.5 molal, respectively). The rate constant ("rk1") value is set to -1 and the reaction progress is varied from 0 to almost 1 (depending the desired ionic strength). Either method can be used with the PT4 modified-Pitzer database to produce equivalent results.

HRH Salts Model–Solid-Centered Flow-Through Model with Evaporation

The EQ3/6 HRH Salts Model simulates evaporation within the drift using the solid-centered flow-through mode, addendum for EQ3/6. This software works with EQ3/6 and has the limitation that the liquid-phase water flux out of the cell is equal to the influent flux. For the HRH Salts Model, it would be more realistic for the liquid-phase water flux out of the cell to be equal to the difference between the influent seepage and evaporation mass fluxes.

The approach used for the HRH Salts Model is to approximate the evaporative evolution of influent seepage, for steady-state boundary conditions, during discrete time intervals. The time intervals should, therefore, be defined so that the reaction cells have large flow-through liquid volume compared with the resident liquid volume.

The steady-state solution composition calculated in this manner is controlled by the influent seepage composition and the relative evaporation rate defined previously. The evaporative concentration factor is calculated from

$$\frac{C_{out}}{C_{in}} = \frac{1}{1 - R_{rel}}$$

(Eq. 3-16)

which applies only for $R_{rel} < 1$. It should be noted that some components of the influent seepage will precipitate as evaporation occurs, so the concentration factor applies only to conservative species.

The solid-centered flow-through option of the EQ3/6 is implemented by defining two reactants and reactant types, a "displacer" and a "special" reactant. The influent seepage is the "displacer" and water evaporation is the "special" reactant. By setting the "displacer" reactant rate constant ("rk1") equal to unity for all simulations, the reaction progress is equivalent to the number of liters (or pore volumes) entering the reaction cell. The reactant rate constant ("rk1") for the "special" evaporation reactant is set equal to -R_{rel}, thus establishing the evaporation rate.

The solid-centered flow-through approach described above is used with the PT4 modified Pitzer database.

3.1.2.5.3.6   Model Validation for LRH Salts Model

The LRH Salts Model is a simple bounding model. Although there are no specific evaporation test data available to evaluate the accuracy of the LRH model, the model is valid because it produces reasonable trends and results for an evolving brine composition while negotiating the transition from dry conditions to 85 percent relative humidity where the HRH Salts Model takes over. Given accurate inputs (e.g. seepage composition) the LRH Salts Model provides results that are conservative and within an order of magnitude of independently developed data for chloride concentration and ionic strength. This degree of accuracy is acceptable because it greatly reduces the potential ranges of these variables, thereby reducing uncertainty.

Although simplifying assumptions are used to reduce complexity, especially where constraint data are lacking, these simplifications tend to be conservative. In particular, they tend to result in a shorter dry period, by not allowing dry conditions for relative humidity greater than 50 percent, in the presence of nitrate salts. The model also produces elevated chloride concentrations at low relative humidity, which is conservative and consistent with properties of pure salts (CRWMS M&O 2000ab).

The LRH Salts Model is constrained by the results of the HRH Salts Model at 85 percent relative humidity and by dry conditions below 50 percent relative humidity. At 50 percent relative humidity and above, the brine composition is constrained by handbook properties for a saturated aqueous solution of sodium and potassium nitrate, and the volume of brine is constrained by mass balance. From 50 to 85 percent relative humidity, the LRH Salts Model makes a smooth transition in aqueous concentrations, as would be expected because the activity of water increases from 0.5 to 0.85, proportional to the relative humidity, during this transition. During this transition, mass balance and charge balance are maintained. Any remaining sulfate, chloride, and carbonate salts are increasingly dissolved as the relative humidity rises, subject to common-ion effects on solubility (CRWMS M&O 2000g).

The LRH Salts Model results predict that as relative humidity increases above 50 percent, the chloride concentration quickly and conservatively approaches the high ionic strength end point of the EQ3/6 Pitzer model. High chloride concentrations are conservative because they can potentially increase corrosion rates.

The LRH Salts Model results that are important for TSPA are a decrease in ionic strength and an increase in chloride concentration as the relative humidity rises from 50 to 85 percent. These

performance measures constitute the intended use of the LRH Salts Model. From the foregoing discussion, the LRH Salts Model is bounding, and valid for its intended use.

3.1.2.5.3.7 Model Validation for the Condensed Water Model

The Condensed Water Model relies on well known and widely used chemical data which describe the solubility of CO_2 in pure water as a function of temperature, and its aqueous speciation. The Condensed Water Model is therefore valid, subject to the validity of inputs which include CO_2 fugacity vs. time in the potential repository environment, and the possible presence of rock dust on otherwise chemically inert surfaces.

3.1.2.5.3.8 Model Validation for the HRH Salts Model

This section describes model validation activities for the HRH Salts Model. The first approach taken involves modeling of laboratory tests described previously, in which synthetic J-13 water and synthetic porewater were evaporated. In the second approach, model calculations are compared with handbook solubility values for simple salts.

Two evaporation tests using synthetic J-13 water are simulated using the HRH Salts Model. The first test was conducted in an open beaker at 85°C (evap4). Detailed description of this test was provided previously in conjunction with the Normative Precipitates and Salts Model. The second test was conducted at 90°C and fixed 85 percent relative humidity, and the test results were summarized previously in the section on input data.

Open-Beaker Evaporation of Synthetic J-13 Water at 85°C

Figure 3-44 shows reasonable agreement between the measured and modeled values for pH, which increased to approximately 10, for the "evap4" test. Modeling was performed using the modified Pitzer formulation with the PT4 database. The modeled pH is controlled by the fugacity of carbon dioxide which is fixed at $10^{-3.4}$ atm to approximate the open-beaker condition. For the data set shown in the figure, the water was evaporatively concentrated to 157×. According to the HRH Salts Model calculations, the maximum ionic strength was approximately 0.34 molal compared with 0.25 molal calculated from the measured data.

Reported and modeled concentrations compare closely (within an order of magnitude) for Na, K, fluoride, bicarbonate, chloride, nitrate, and sulfate (CRWMS M&O 2000g). However, the model underestimates the reported concentrations of total dissolved Si and Ca by more than an order of magnitude, and underestimates the reported concentration of dissolved Mg by two orders of magnitude. These discrepancies may have been caused by kinetic limitations on precipitation, or by incorporation of particulate matter in the analytical samples, in the laboratory tests. Precipitates including chalcedony, calcite, and sepiolite are predicted by the model, but separation and analysis of precipitates were not performed at this stage of the test.

Evaporation of Synthetic 100× J-13 Water at 90°C and 85 percent Relative Humidity

A synthetic solution representing 100× concentrated J-13 water was contacted with crushed tuff at 90°C, then dripped into a Teflon™ beaker that was open to a controlled atmosphere at 90°C

and 85 percent relative humidity ("Batch 1" test). The solution was evaporated to approximately 5 percent of the original volume.

The composition of the final solution is calculated using the HRH Salts Model with the PT4 database. Figure 3-45 shows the predicted change in pH and ionic strength as a function of the concentration factor. There were no pH measurements reported from the test. The CO_2 fugacity was fixed at $10^{-3.4}$ atm, and the temperature at 85°C. The ionic strength approximation for the final solution (based on the reported chemical analysis) was approximately 3.7 molal, which is close to the value calculated by the model.

Model results agree with the observed concentrations for Na, K, fluoride, and sulfate (CRWMS M&O 2000g). For comparison of model results with the data, it is assumed that the reported nitrate concentration (relative to the original nitrate concentration) represents the bulk concentration factor for the solution.

The model overestimates the reported bicarbonate concentration, probably because of the way the model corrects for charge imbalance by adjusting dissolved in organic carbon. In addition, the model underestimates the reported concentration of dissolved Ca by a factor of 30, and underpredicts the reported concentration of dissolved Mg by 2 orders of magnitude. These discrepancies may have been caused by kinetic limitations on precipitation, or by incorporation of particulate matter in the analytical samples, in the laboratory tests. Precipitates including calcite, brucite, sellaite, fluorite, and villiaumite are predicted by the model, but separation and analysis of precipitates were not performed in the test.

Open-Beaker Evaporation of Synthetic Porewater at 75°C

Figure 3-46 shows reasonable agreement between the measured and modeled values for pH, which decreased to approximately 6.3 for the "evap3" test. Modeling was performed using the modified Pitzer formulation with the PT4 database. The modeled pH was controlled by the fugacity of carbon dioxide which is fixed at $10^{-3.4}$ atm to approximate the open-beaker condition. For the data set shown in the figure the water was evaporatively concentrated to 1243x. According to the HRH Salts Model calculations, the maximum ionic strength was approximately 5 molal compared with 2.8 molal calculated from the measured data.

Additional modeling results closely approximate the reported dissolved concentrations of Na, K, Mg, Ca, and chloride concentrations (CRWMS M&O 2000g). However, model results underestimate the reported concentrations of total dissolved Si, and dissolved sulfate, by at least an order of magnitude at a concentration factor of 1243. Concentrations of nitrate, bicarbonate, and fluoride were not reported. In the model, precipitation of chalcedony and anhydrite limited the total dissolved Si and dissolved sulfate concentrations predicted at a concentration factor of 1243. Gypsum, which is similar to anhydrite, was identified in solid-phase separates using XRD. Upon evaporation to dryness, tachyhydrite, which was predicted to precipitate, was identified by XRD. Other minerals predicted to precipitate include calcite, carnallite, fluorite, sellaite and halite. These minerals were not observed using XRD, which may be the result of kinetic factors inhibiting precipitation, or of minute quantities making identification difficult.

Evaporation of Pure Salt Solutions

The HRH Salts Model was also used to model the solubility of several Na and K salts that are potentially important products of evaporating J-13 water. The solubilities calculated are compared to handbook values in Table 3-24. Salts that are predicted by the model to have solubilities exceeding 10 molal are shown as "> 10 molal".

Table 3-24. Comparison of Handbook Aqueous Solubilities of Sodium and Potassium Salts at 100°C with Values Calculated Using the HRH Salts Model with the PT4 Database

Salt	Handbook Aqueous Solubility at 100°C (molal)	Pure Phase Solubility at 100°C Calculated by EQ3/6 Relative Humidity Model (molal)
NaCl	6.70	7.21
KCl	7.60	6.12
$Na_2CO_3 \cdot H_2O$	4.2	3.99
K_2CO_3	11.3	> 10 [a]
NaF	1.21	1.01
KF	26	> 10 [a]
Na_2SO_4	3.01	1.55
K_2SO_4	1.38	0.83
$NaNO_3$	21.2	3.60
KNO_3	24.4	3.60

[a] Exceeds range of model

Source: Precipitates and Salts Analysis/Model Report (CRWMS M&O 2000g)

The HRH Salts Model calculates solubilities for many salts that are within a factor of 2 of the handbook values (except for salts with solubilities exceeding 10 molal, the limit of the model). Among these, the largest differences are for the nitrates, which are underestimated by a factor of approximately 6. The consequence is that the model may predict the precipitation of nitrate salts from concentrating waters, when it should not. This discrepancy may be related to the procedure used to approximate Pitzer data for nitrate, in the PT4 database.

Summary

The HRH Salts Model provides valid approximations for pH and ionic strength in evaporated J-13 water and synthetic porewater, and for the solubilities of salts. These are key performance measures used in TSPA to model degradation of corrosion-resistant materials. For the test problems evaluated, pH was calculated to within 1 unit of observed values, and ionic strength was within a factor of 2.

Greater discrepancies are encountered when the predicted concentrations of individual species are compared with observed values, particularly species for which Pitzer data are estimated (PT4 database). If the initial solution composition is dominated by such species, less agreement could result between predictions and observations, for pH and ionic strength.

3.1.2.5.4 Model Results

The following sections summarize results reported in the Precipitates and Salts Analysis AMR (CRWMS M&O 2000g) and provide some example figures. These results represent modeling that directly supports TSPA, with the final products being look-up tables.

3.1.2.5.4.1 LRH Salts Model Results

Results discussed in this section are for influent seepage flux of 1 L/yr, with the composition of J-13 water, and using a fixed CO_2 fugacity of 10^{-3} atm. Reported results for the LRH Salts Models include the cumulative mass of each chemical component entering the drift (a reaction cell) over time, and the fraction of this mass for each component that is dissolved. The dissolved concentrations for several components are shown in Figure 3-47, plotted as functions of time according to the methods and assumptions for the LRH Salts Model. A constant rate of seepage inflow (1 L/yr) is assumed.

The results also include mass balance calculations, which show the partitioning of mass for each component between dissolved and precipitated phases. Figure 3-48 shows the sum of nitrate, chloride, sulfate, and carbonate salts (primarily Na-salts) dissolved as brine, and the mass of water in that brine, as functions of time according to the methods and assumptions for the LRH Salts Model.

The results are relatively insensitive to the CO_2 fugacity. The effects of varying the CO_2 fugacity have been calculated and are incorporated into the lookup tables discussed above. The temperature is fixed at 95°C for the LRH Salts Model because lower temperatures produce relative humidity values that are too high (>85 percent) for the model. The lookup table values tend to be insensitive to the influent seepage flux, within a range that is substantially less than percolation or seepage conditions that could impact the thermal-hydrologic conditions in the drifts. In other words, large values of the influent seepage flux would be associated with temperature perturbations, and would affect the duration of elevated temperature in the potential repository, so there is an upper limit of seepage for the application of LRH Salt Model results calculated using 1 L/yr.

3.1.2.5.4.2 HRH Salts Model Results

The HRH Salts Model is used to predict the composition of water subjected to simple evaporation, and to evaporation combined with addition of incoming seepage. The following discussion presents results for simple evaporation of J-13 water, and evaporation when a constant incoming seepage is allowed. The figures and text are taken from the Precipitates and Salts Analysis/Model Report (CRWMS M&O 2000g) which provides additional details.

3.1.2.5.4.3 Evaporation of J-13 Water

Evaporation of average J-13 water is simulated using the modified Pitzer model and the PT4 database. The temperature is 95°C and the CO_2 fugacity is fixed at 10^{-3} atm. Figure 3-49 shows the evolution of pH and ionic strength; the modeled pH approaches 10, then decreases to about 9 at a concentration factor of 10,000. Although the HRH Salts Model development is

limited to 10 molal ionic strength, results beyond this range are presented in this section to show the model response.

Calculations show that the elements C, Cl, K, Na, N, and S simply concentrate without precipitating except in small amounts. Fluoride concentrates until fluorite (CaF_2) precipitates. The elements Si, Al, Ca, Mg, and Fe precipitate in significant quantities relative to their aqueous concentrations.

Figure 3-50 shows the evolution of precipitates formed. Among the precipitates included in the model, calcite and chalcedony are produced in the greatest quantity. Sepiolite and fluorite (at later times) are the next most abundant. The model predicts precipitation of several smectite clays (Ca-montmorillonite, Na-nontronite, and Ca-nontronite) and a zeolite (Na-clinoptilolite), at abundances which are several orders of magnitude less than for chalcedony and calcite.

3.1.2.5.4.4 Results for Evaporation Combined with Constant Incoming Seepage

When evaporation flux exceeds influent seepage flux, water in the reaction cell will become increasingly concentrated so that the only possible steady-state conditions are complete vaporization (i.e., dry conditions with salt deposits) or a brine system that is controlled by the relative humidity. When the influent seepage flux is less than the evaporation flux, evaporative concentration and steady through-flow occur, and the steady-state aqueous-phase composition predicted by the HRH Salts Model applies after a sufficient number of through-flow pore volumes.

The evolution of water in the potential repository drifts, as temperature falls and relative humidity rises over time, can be generalized as evolution from brine to increasingly dilute water. This evolution is modeled as a succession of time intervals, during each of which the incoming seepage flux and composition are constant, the temperature and evaporation flux are constant, and the system composition reaches a steady state. At each time interval, the model converges to constant solution composition after approximately 10 pore volumes. The relative evaporation rate and the incoming seepage composition are the important factors in achieving steady conditions.

The calculated figures and tables (response surfaces) represent steady-state conditions after a sufficient number of pore volumes have flowed through the reaction cell. Evaporative concentration results are calculated for J-13 water, equilibrated with CO_2 fugacities of 10^{-1}, 10^{-3}, and 10^{-6} atm. Figure 3-51 and Figure 3-52 show the pH, calculated as a function of concentration factor, for two values of the CO_2 fugacity. These results show that pH is more sensitive to CO_2 than to the relative evaporation rate.

The results for ionic strength indicate slight sensitivity to CO_2 fugacity and temperature. For J-13 water, the ionic strength can reasonably approximated by direct application of the concentration factor. Deviations from this response are caused by precipitation.

3.1.2.5.4.5 Condensed Water Model Results

Calculations show that the pH and ionic strength of condensed water are sensitive to temperature and the CO_2 fugacity. Figure 3-53 shows that the pH decreases considerably as the CO_2 fugacity

increases above 10^{-5} atm. Increased temperature results in a higher pH, as CO_2 exhibits retrograde solubility. At low CO_2 fugacities, the pH is insensitive to the CO_2 fugacity and temperature. Ionic strength is small for all conditions modeled, indicating that temperature is more important to ionic strength predictions when the CO_2 fugacity is low. When the CO_2 fugacity is high, it determines ionic strength for condensed water.

3.1.2.6   EBS Colloids Model

This model bounds the impact of ferric-oxide and ferric-oxyhydroxide colloids on RN transport in the invert, specifically considering the impacts resulting from use of steel in the EBS. The results show that the effect of steel in the EBS is bounded, depending on the affinity of corrosion products for radionuclides of interest (e.g. Pu).

In this model the size distribution and maximum concentration of colloids are estimated from natural analogs, and assumed to be entirely hematite colloids. Other colloid types may be present including clays, silica, and waste form colloids (spent fuel or waste glass). Laboratory results discussed below indicate that ferric-oxide colloids have greater affinity for radionuclides of interest than silica or clays. However, waste form colloids have the potential to transport radionuclides and are not considered in this model, therefore the model may not bound the overall potential for colloidal transport.

Aqueous colloids are suspensions of solid particles in water. The diameters of the particles typically range from a few nanometers to a few thousand nanometers, which produces a very large surface area per unit mass of material. The behavior of colloids is, accordingly, controlled by surface forces and processes, including electrostatic repulsion or attraction and surface chemical reactions with species in solution. The stability and capacity of colloids to adsorb radionuclides are complex functions of solution chemistry, temperature, and other variables.

Radionuclide-bearing colloids can adversely affect potential repository performance because they can travel large distances in groundwater with little or no retardation. Radioactive colloids include intrinsic colloids (i.e., radionuclides provide the dominant metal species in the particles, as in hydrous actinide polymers or colloidal actinide silicate and phosphates) and pseudocolloids (formed by the sorption, entrainment, or other incorporation of radionuclides on or within colloidal particles of other materials).

Although they have been extensively studied in the laboratory, actinide polymers do not appear to be important for the potential Yucca Mountain potential repository. No actinide polymers have been reported in studies on the degradation by water contact of commercial spent nuclear fuel (CSNF) and defense high-level waste (DHLW) glass (CRWMS M&O 2000t). However, intrinsic colloids of actinide silicates and phosphates were generated along with pseudocolloids. In addition, recent laboratory studies (CRWMS M&O 2000t) demonstrate that Pu is as rapidly sorbed by pseudocolloids from hydrous Pu(IV) polymers as it is from solutions of Pu(V). Hence, the bounding analysis that follows will focus on the behavior of radioactive pseudocolloids, and the term "colloid" should be understood to mean pseudocolloids in the remainder of this discussion.

The most important colloid-forming materials for radionuclide sorption include clay minerals (particularly smectites) and colloidal iron oxides (such as hematite and goethite). Radionuclides can also be sorbed on colloidal silica, but with a generally smaller sorption coefficient than with clays and iron oxides. Clays are present as components of colloids naturally found in Yucca Mountain groundwater and are also generated when either waste form is corroded by water, as is documented extensively in (CRWMS M&O 2000t). Colloidal iron compounds may be generated from the large masses of ferrous alloys used in large quantities within the waste package as well as in the ex-container EBS. As shown in Table 3-4, even without including the iron content of the waste package and its internals, there is more than 10^6 g of Fe per meter of emplacement drift.

A conceptual model for colloid generation, mobility, and affinity for radionuclides within the EBS is combined with available data on colloidal transport and sorption capacity for radionuclides to produce a bounding analysis of the degree to which colloids may increase the aqueous concentrations of radionuclides above their respective solubility limits

3.1.2.6.1   Conceptual Framework for Colloids Model

Colloids are considered stable if they do not agglomerate and settle out of a static suspension over the time period of interest. The stability of colloids suspended or entrained in groundwater (i.e., their tendency to remain suspended) is a function of pH, oxygen potential (Eh), ionic strength, composition of the colloidal particles, temperature, flow velocity, and the composition and structure of the medium through which the groundwater is moving (CRWMS M&O 2000t). It is unlikely that the evolution of these variables after closure of the potential repository can be predicted accurately, however, the available information does permit a bounding analysis that comprises the following elements:

- Colloid particle size distributions have been measured in groundwater samples pumped from 18 wells in the vicinity of Yucca Mountain. The composition of these particles is being investigated, but this information is not yet available. The data represent the concentration of colloidal material that can be transported in groundwater along flow pathways between the potential repository and the accessible environment. The representation is conservative because colloid concentrations near a pumping well are probably increased by enhanced colloid detachment, caused by flow velocity that is greater than for undisturbed flow of natural groundwater.

- The abundance of iron in the EBS will provide a large source of oxides and oxyhydroxide corrosion products. There is no compelling argument to preclude formation of colloids from these corrosion products, so it is conservative to assume that all of the products are of colloidal size. Entrainment of colloids in the groundwater and release to the host rock will occur only after sufficient water reenters the drift to support advective flow.

- When transport of ferric-oxide begins, the size distribution will be similar, and is assumed to be identical, to the distribution of natural colloids discussed previously. The underlying concept is that colloids outside the observed size range will not be

transported over long distances, either because they are unstable or because they become attached to the porous media through which the water flows.

- For this model, the total concentration of each radionuclide is expressed as the sum of the concentration in solution and that adsorbed on colloidal particles. It can be expressed as an enhancement factor (a simple function of colloid mass concentration and sorption coefficient) multiplied by the solubility limit for the radioelement.

- Laboratory data shows that sorption of actinides on ferric-oxide colloids is essentially irreversible. In the model, sorption coefficients are bounded by laboratory data.

- Sorption on silica and clays is reversible and of smaller magnitude than sorption on ferric-oxide colloids. Accordingly, considering only the ferric-oxide colloids results in a conservative bound for long-distance colloidal transport of radionuclides.

3.1.2.6.2   Colloid Size Distribution and Concentration

Data for size distribution and colloid concentration are plotted in Figure 3-54 and Figure 3-55. Particle concentrations in counts per milliliter are given for sizes ranging from 50 to 200 nm at 10-nm increments. Analysis of the data shows that the normalized distribution (fraction of particles within each size range) is closely approximated by a log-normal distribution for each of the samples; it also shows that the parameters of these distributions are so similar that a single distribution can represent the colloid size distribution for all 18 wells. The distribution of measured data from each well, and two composite log-normal curves (one for nine Nye County well samples and one for nine Yucca Mountain well samples) are shown in Figure 3-54. The composite log-normal curves are nearly identical.

Mathematically, the normalized log-normal distributions are represented as follows:

$$F(D_c) = \Phi\left(\frac{\ln(D_c) - \mu_c}{\sigma_c}\right) \qquad \text{(Eq. 3-17)}$$

where

D_c = colloid particle diameter, nm

μ_c = mean of the natural log of the colloid particle diameter, nm

σ_c = standard deviation of the natural log of the colloid particle diameter, nm

$\Phi(x)$ = normal probability integral for any variable x

The final average parameters recommended for the normalized colloid size distribution are $\mu_c = 4.4258$ and $\sigma_c = 0.3509$. The total number of colloid particles per milliliter in the 18 groundwater samples is also closely approximated by a log-normal distribution, of the form

$$F(N) = \Phi\left(\frac{\ln(N) - \mu_N}{\sigma_N}\right) \qquad \text{(Eq. 3-18)}$$

where

N = total number of colloid particles, counts per milliliter

μ_N = mean of the natural log of the total number of colloid particles per milliliter

σ_N = standard deviation of the natural log of the total number of colloid particles per milliliter

$\Phi(x)$ = normal probability integral for any variable x

The parameters of the distribution are estimated by direct calculation of the natural-log mean and natural-log standard deviation from the data, resulting in $\mu = 19.4841$ and $\sigma = 1.9911$.

3.1.2.6.3 Sorption Coefficients

Iron compounds are of particular importance because the corrosion products can readily form colloids. Also, two corrosion products (hematite and goethite) summarized in Table 3-25 have high sorption coefficients, and sorption on these minerals may be irreversible. Corrosion products of other metals are expected to be less important sources of colloids than ferric-oxide, primarily because of the abundance of steel in the drift.

Table 3-25. Sorption Coefficient (K_d) Values in mL/g for Sorption of Pu(IV), Pu(V), and Americium-243 on Hematite, Goethite, Montmorillonite, and Silica Colloids

Radionuclide	Water	Sorption Coefficient Values			
		Hematite	Goethite	Montmorillonite	Silica PST-1
Pu(IV)	Natural	2×10^5 [a]	7×10^4	3×10^3	5×10^3
	Synthetic	7×10^5	2×10^5	2×10^5	3×10^4
Pu(V)	Natural	1×10^5	6×10^4	1×10^4	ND
	Synthetic	1×10^5	2×10^5	1×10^4	ND
^{243}Am	Natural	1×10^5	ND	1×10^4	1×10^4
	Synthetic	1×10^5	ND	1×10^4	5×10^3

Source: CRWMS M&O 2000t

NOTES: Colloid concentrations are at 1000 mg/L for Pu and at 200 mg/L for Am.
ND = no data

These experiments used both natural J-13 well water (NAT-J-13) and synthetic J-13 water (SYN-J-13). Suspensions of colloids in each of these dilute electrolytes were prepared for hematite, goethite, montmorillonite, and two different silica materials. Average particle sizes were 139 nm for both types of silica colloids, between 100 and 200 nm for goethite, 334 nm for montmorillonite, and 416 nm for hematite. Radionuclide solutions comprised Pu(V) at 2.74×10^{-7} M in both electrolytes, colloidal Pu(IV) at 2.40×10^{-7} M in NAT-J-13 and 2.35×10^{-7} M in SYN-J-13, and ^{243}Am at 1.26×10^{-8} M in both electrolytes. The particle size of the Pu(IV) colloid was less than 10 nm. All solutions had pH values between 8.0 and 8.4.

Three series of experiments were run:

- Sorption of Pu(IV) and Pu(V) on 1,000 mg/L suspensions of each colloid (hematite, goethite, montmorillonite, two types of silica)

- Sorption of [243]Am on 200 mg/L suspensions of each of the above colloids except goethite

- Sorption of Pu(V) and [243]Am on suspensions of each of the above colloids except goethite for concentrations of 10, 50, 100, 150, 200, 1,000, and 5,000 mg/L

Not all of the combinations listed were reported. The [243]Am experiments in Series 3 apparently were not complete at the time the report was prepared. Partition coeffiient (K_d) values obtained in Series 1 and 2 are shown in Table 3-25.

In addition to the sorption measurements, data were reported on the desorption of Pu(IV) and Pu(V) from Pu-loaded samples of hematite, goethite, montmorillonite, and silica colloids after 96 hr of sorption. After 150 days of agitation in natural or synthetic J-13 water, desorption was far from complete for any of the colloids, per the following:

- Essentially no Pu was desorbed from hematite.

- Less than 1 percent of Pu was desorbed from goethite.

- About 8 percent of Pu(IV) and less than 1 percent of Pu(V) was desorbed from montmorillonite.

- About 20 percent of Pu(IV) and 6 percent of Pu(V) was desorbed from silica colloids.

Based on this laboratory work, a bounding sorption coefficient value of $K_d = 7 \times 10^5$ mL/g is used in this model. These laboratory results show that sorption is irreversible for Pu. It is possible that sorption on montmorillonite (and possibly other clays) and silica could be reversible over a time of decades, but complete reversibility is not evident from the reported data. However, given the large amount of steel in the emplacement drifts, iron colloids are likely to be present in greater amounts. Also, they have greater affinity for Pu, so behavior of the siliceous colloids is less important to radionuclide transport.

3.1.2.6.4   Bounding Values of Radionuclide Solubility Enhancement Factor

The enhancement factor for colloidal transport represents the factor by which the total amount of a radionuclide in groundwater is increased over the amount in solution at the time the radionuclide was adsorbed. For irreversible adsorption, the amount in solution may be equal to, less than, or greater than the solubility limit at any point along the flow path after the colloid is "loaded" with radionuclide. Mathematically, the enhancement factor E is defined by

$$E = \frac{C_{Total}}{C_0} = 1 + K_d M_C \qquad \text{(Eq. 3-19)}$$

where:

C_{Total} = total radionuclide concentration in solution and suspension (units consistent with C_0)

C_0 = radionuclide solubility limit (units consistent with C_{Total})

K_d = sorption coefficient, mL/g colloid

M_C = mass concentration of colloids, g/mL of suspension.

Assuming spherical particles, the mass concentration of colloids is given by

$$M_C = \frac{\pi \rho D_C^3}{6} \cdot N \qquad \text{(Eq. 3-20)}$$

where ρ is the density of the colloid particles, assumed constant. In this equation, both D_C and N are log-normally distributed random variables, with parameters discussed previously. These random variables appear to be independent, exhibiting little or no correlation in the data. The distribution of particle diameter is rather narrow, which implies that most of the uncertainty or variability arises from the total particle count. For a bounding analysis, one can average the mass concentration over the particle diameter distribution, as follows:

$$\langle M_C \rangle_{D_c} = \frac{\pi \rho \langle D_C^3 \rangle}{6} \cdot N \qquad \text{(Eq. 3-21)}$$

where the left-hand side is a random variable representing the mass concentration averaged over the particle diameter distribution.

The notation $\langle X \rangle$ denotes the average of the random variable x over its distribution. For a log-normal distribution with parameters μ and σ, the average of x^3 is given by

$$\langle x^3 \rangle = \exp\left(3\mu + \frac{9\sigma^2}{2} \right) \qquad \text{(Eq. 3-22)}$$

Using the parameters for the size distribution results in

$$\langle D_C^3 \rangle = \exp\left(3 \cdot 4.4258 + \frac{9 \cdot 0.3509^2}{2} \right) = 1.0161 \times 10^6 \text{ nm}^3 \qquad \text{(Eq. 3-23)}$$

The density of anhydrous hematite (5.240 g/mL) (CRWMS M&O 2000t) is an upper bound on the density of hydrous hematite. This value is used to obtain an order of magnitude estimate for the mass of a spherical colloid particle with a diameter cubed equal to 1.0161×10^6 nm^3, using Equation 3-21. The result is 2.7878×10^{-9} µg per particle.

All that remains is to calculate the total mass of colloids per mL of suspension, which requires a value for the total number of particles per milliliter. As noted previously, N is also log-normally

distributed, with parameters $\mu = 19.4841$ and $\sigma = 1.9911$. Specific values for the enhancement factor require selecting a fractile on the cumulative distribution function (CDF) of N. Calculations for several fractiles are documented in Attachment XVI and are summarized in Table 3-26. At the 99th percentile, this analysis predicts an enhancement factor of less than 100.

Table 3-26. Summary of Calculations for the Colloid Mass at Different Fractiles of the Log-Normal Distribution for the Number of Particles per mL

CDF for Number of Particles per mL	Standardized Normal Variable	Colloid Particles per mL	Colloid Mass μg/mL	Enhancement Factor for K_d = 7.E+05 mL/g
0.99000	2.3263	3.0E+10	8.3E+01	59
0.97500	1.9600	1.3E+10	4.0E+01	29
0.95000	1.6449	7.7E+09	2.1E+01	16
0.90000	1.2816	3.7E+09	1.0E+01	8.3
0.84027	0.9956	2.1E+09	5.9E+00	5.1
0.75000	0.6745	1.1E+09	3.1E+00	3.2
0.50000	0.0000	2.9E+08	8.1E−01	1.6

Source: CRWMS M&O 2000t

NOTE: The enhancement factor estimate is also shown, based on the largest value of K_d reported in Table 3-25.

The value of the standardized normal variable reported here was carried to one additional significant figure in the calculation, and is reported here without modification.

The 84th percentile corresponds to the arithmetic mean number of particles predicted by this bounding analysis, resulting in an enhancement factor of approximately 1 percent.

At the 99th percentile, the estimated total mass of colloidal hematite is 82.9 mg/L. For comparison, the total dissolved solids (TDS) content of J-13 water averages about 250 mg/L. Evaporative concentration, and interaction of seepage water with cement grout, would further increase the TDS. Except for the extreme right tail (p > 0.95) of the colloid mass CDF, colloids will be less than 10 percent of the TDS content.

Calculation of the enhancement factor as a function of K_d, at the 99th percentile gives the following results:

- For $K_d = 10^6$, $E = 83.9$

- For $K_d = 10^5$, $E = 9.3$

- For $K_d = 10^4$, $E = 1.8$

Factors of 2 are not generally considered significant in radionuclide release and transport calculations for potential repository performance assessment, so this bounding analysis suggests that colloid-enhanced radionuclide transport will be important only if the colloid has a sorption coefficient equal to or greater than 10^5 mL/g.

3.1.2.6.5 Bounding Values for Colloid Diffusion Coefficient

One potential function of the invert ballast in the ex-container EBS is to provide, under the drip shield, a diffusion barrier between the waste package and the host rock. If water is successfully diverted by the backfill/drip shield system and effectively drained from the drift into the host rock, little or no water would flow beneath the waste package. Potentially, the water content in this region could be kept so low that diffusion rather than advection would dominate radionuclide transport. A model for diffusivity of dissolved radionuclides is documented in the Invert Diffusion Properties AMR (CRWMS M&O 2000h). For an invert material with 50 percent porosity and 5 percent water saturation, the diffusion coefficient of a dissolved ion will be about three orders of magnitude below its value in bulk solution (i.e., with no porous medium present).

It could be supposed that no colloidal transport would be possible without advective flow. However, diffusion along a surface film of water is possible, at least for the smaller size colloids. Figure 3-56 summarizes values for the diffusion coefficient in dilute suspensions as a function of particle diameter, over a range of colloids (CRWMS M&O 2000t). These values apply in bulk suspensions and are reduced from typical values for dissolved species by two to three orders of magnitude. Even with an enhancement factor of 10 or so, diffusion-controlled radionuclide mass release as particles would be from 10 to 100 times lower than the diffusion of dissolved species. Actual diffusivity in a water film may be even lower because the Stokes–Einstein equation assumes no interaction of the diffusing particle with any substance other than the solvent. Therefore, diffusion of colloids through the invert can be neglected entirely in performance assessment.

3.1.2.6.6 EBS Colloids Model Validation

This model is based on inferences relating the abundance and size of natural colloids in Yucca Mountain groundwaters, with the concentrations of ferric-oxide and ferric-oxyhydroxide colloids in the EBS. In addition, sorption coefficients and reversibility are inferred from laboratory tests on hematite colloids.

As stated previously, the intended use of this model is to bound the effect of steel in the EBS, on the potential for colloidal transport of radionuclides. The model is bounding because the entire mobile colloid load in EBS waters is assigned to hematite colloids, which have relatively high affinity for radionuclides such as Pu. Other colloids such as clays and silica will be present and tend to decrease the hematite colloid concentration. The model is also bounding because sampling of groundwater from wells is more dynamic than percolation in the EBS will be, so colloids tend to be mobilized at greater concentrations. Another important bounding aspect of this model is that sorption of Pu is considered irreversible, so that once sorbed, the enhanced mobility of pseudo-colloidal transport in the groundwater system persists for the lifetime of the radionuclide.

Whereas hematite is the most stable Fe-oxide likely to form in the potential repository, other solids such as goethite and ferrihydrite could also be present. These "lower" oxides can have greater surface area and sorption capacity for radionuclides. It is possible that these phases will mature to hematite with time in the repository, however, the endpoints and timing of such

evolution are not established. It is likely that the bounding approximations mentioned above, would encompass any differences in potential radionuclide transport that could be attributed to the lower oxides.

From this discussion it is concluded that the EBS Colloids Model is bounding, and valid for its intended use.

3.1.2.7 Chemical Reference Model

The Chemical Reference Model calculates the evolution of water composition in the EBS, and the precipitation and dissolution of minerals, for time periods to 10,000 years. The bounding TH model selected in Section 3.1.2.1 is combined with gas fugacity results from Section 3.1.2.2, and normative mineral assemblages produced using the method of Section 3.1.2.5. Other processes including microbial, colloidal, and introduced material effects, are evaluated in the context of the Chemical Reference Model.

The primary objective for the Chemical Reference Model is to support the design basis for the drip shield and waste package by identifying bounding environmental conditions. This is a detailed assessment of a single TH model, using the most comprehensive available, temperature-dependent, chemical system. By contrast, the chemical calculations that are incorporated directly into TSPA involve fewer species and more approximate methods of chemical modeling.

The Chemical Reference Model uses the evolution of maximum CO_2 and O_2 fugacities from Section 3.1.2.2, but also uses these results to evaluate CO_2 mass balance in the drifts and the surrounding host rock, as a function of time. The effects of carbon steel corrosion, and leaching from cementitious materials, are evaluated by comparing reference model results with scoping chemical calculations.

3.1.2.7.1 Conceptual Model Development and Alternative Models

The modeling approach relies on representing the in-drift environment and the host rock as a set of zones, or reaction cells. Temporal evolution is represented by a series of discrete time periods extending to 10,000 years. Within each time period the environmental conditions at each zone, and the fluxes between zones, are constant.

The host-rock processes that control the chemistry of water entering the drifts as seepage, are summarized in Figure 3-57. The composition of J-13 well water is used as a far-field reference composition because it is an analog for fracture waters in the host rock, and because it produces alkaline pH conditions when evaporatively concentrated. Unsaturated porewater samples from nonwelded tuff units above the potential repository horizon, and a small number of samples from the welded host rock (Tptpmn), have compositions that are enriched in chloride, sulfate, and calcium (CRWMS M&O 2000t). However, J-13 water is the composition predicted by chemical models based on host-rock mineralogy. Also, perched water samples from below the potential repository horizon, and natural-analog fracture water samples from Rainier Mesa, have compositions similar to J-13 water.

Reaction cells in the Chemical Reference Model have residence times of months to years, so kinetic hindrance of dissolution/ precipitation reactions is not critical. As concluded in Section 3.1.2.3.3.1, quartz exhibits kinetics that are relatively slow among the minerals modeled, but quartz equilibrium is a reasonable approximation for the reference model. Important equilibrium processes include interaction of formation waters with cristobalite and calcite in the host rock, and redissolution of evaporatively precipitated minerals in the drifts.

As pointed out in Section 3.1.2.2, reactive transport simulation that incorporates TH and chemical processes is a possible alternative to some parts of this system model. The fine spatial and temporal discretization that is possible with some numerical simulators, corrects some of the artifacts of granularity in the zones and time periods used in this model. For example, the mass accumulation of precipitates and salts in the invert, that is predicted by this model, is exaggerated because temporal granularity extends the time interval during which there is seepage inflow and no outflow, due to complete evaporation in the drift. Conversely, the peak temperatures, fluxes, and other environmental conditions in the drift can be underestimated when their evolution is represented by constant conditions within discrete time intervals. Reactive transport simulations also have limitations, particularly with respect to modeling the chemistry of concentrated solutions and evaporative precipitation, and the number of species and mineral phases that can be considered.

Modeling of Precipitates and Salts

A simplified treatment of precipitates and salts accumulation, and the consequent chemical environment on the surface of the drip shield, is used in this model. One result is that for bounding the environmental conditions at the drip shield, salts or brines are considered to be present from the onset of liquid flow into the drift, through the duration of the 10,000-yr performance period. Salts will accumulate from episodic seepage, or movement of condensate that can form within the drifts. Over the long-term, brines will form as relative humidity increases, according to the discussion of brine formation in the Precipitates and Salts Model (Section 3.1.2.5).

The predicted quantity of precipitates and salts, and the timing of their remobilization, are calculated but considered uncertain. This is justified because results presented in Section 3.1.2.1 show that there is wide variation in the timing and potential quantity of salt accumulation in the backfill and the invert, for a range of potential repository conditions. For some locations and flux conditions, the potential salt accumulation in the drift will be slight (at the edge of the layout, with low flux or minimal seepage). For other conditions (center of the potential repository, high seepage) the accumulation could be 10^6 times greater (Figure 3-25 through Figure 3-28). For low-flux conditions the duration of boiling conditions may be 3,000 years or more, whereas for high-flux conditions the duration may be 400 years or less (Figure 3-19). Seepage conditions in the drifts are controlled by fractures and likely to be strongly heterogeneous, so in the same section of emplacement drift there could be large local differences in the accumulation and duration of precipitates and salts.

3.1.2.7.2   Input Data, Assumptions, and Uncertainties for Chemical Modeling

Reference Chemical Composition of Fracture Water in the Host Rock

Naturally occurring percolating fracture waters have not been observed in the host rock, possibly because fracture flow is episodic. As discussed previously, J-13 water is a reasonable analogue for fracture water that percolates through the host rock and may seep into drifts. The major chemical constituents of J-13 water, and measured data representing the effects of evaporative concentration, are discussed in Section 3.1.2.5. That model shows how J-13 water, compared with matrix porewaters that contain relatively more chloride and sulfate than bicarbonate anions, produces more alkaline pH conditions during evaporative concentration.

Thermal-Hydrologic Conditions

Zone-averaged temperature, liquid fluxes, vapor fluxes, and liquid masses are calculated by the TH Model (Section 3.1.2.1). The composite zones representing the emplacement drifts, and the host rock, are defined in Figure 3-15 and Figure 3-16. Selection of the L4C4 potential repository location with the "upper" infiltration distribution, as a reference model for use in chemical modeling, is described in Section 3.1.2.1. The liquid water and water vapor fluxes between composite zones, and the liquid mass, average temperature, and evaporative concentration factor for each composite zone, are also calculated using the models discussed in that section.

CO_2 and O_2 Fugacities

For chemical modeling, the CO_2 and O_2 maximum fugacities for each time period are calculated in Section 3.1.2.2. These fugacities are considered uniform throughout the zones modeled. A mass-transfer relationship between flux and fugacity is also developed, and is used for comparison with consumption rate estimates in this section.

Thermodynamic Data

The thermodynamic data used for these calculations consists of the "data0.com" file supplied with EQ3/6. Only a subset of the data in this file are important to the chemical modeling presented in this section. The majority of the data used are also part of the "data0.sup" file.

A number of potential minerals removed from the calculations by artificially suppressing their formation. This is accomplished in part by using an input file-suppression option in EQ3/6. However, because the number of minerals to be suppressed exceeds the hard-coded array limits, a number of these minerals are eliminated from a special copy of the "data0.com" data file. This reduced data file ("data0.elh") and a list of the suppressed phases, are included in source documentation (CRWMS M&O 2000t).

The rationale for suppressing certain minerals is twofold. First, it is recognized that kinetics generally prevents the formation of certain phases under the conditions of temperature and pressure in the potential repository system, on the pertinent time scale. Second, it is recognized that the existing thermodynamic database overestimates the stability of a number of silicate minerals with respect to clay minerals. Both arguments are supported by observed mineral assemblages, including those at Yucca Mountain in both fractures and the tuff matrix. The

mineral assemblages in the calculations are thus partly controlled by judgment, and not just by the available thermodynamic data (CRWMS M&O 2000t).

Kinetics of Quartz Precipitation

The kinetics of quartz precipitation is potentially important because of the use of quartz sand backfill. In the rock surrounding the drift, quartz and cristobalite (a less stable, naturally occurring polymorph) coexist in chemical disequilibrium over geologic time. The concentration of dissolved silica corresponds to near-equilibrium with cristobalite and supersaturation with respect to quartz. This condition is maintained in the rock at Yucca Mountain because of the slow growth kinetics of quartz. That condition could be replaced in the sand backfill by one of near-equilibrium with quartz, resulting in a significant decrease in dissolved silica.

The precipitation and dissolution of silicate minerals is generally accepted to be a surface area-mediated process (i.e., the rate is proportional to the area of the mineral-water interface). A published rate law (Section 3.1.2.3.3.1) describing the kinetics for dissolution and precipitation of quartz and other SiO_2 minerals is used to examine the rate of quartz growth (via overgrowths) in the backfill (CRWMS M&O 2000t). The results show that water-quartz equilibrium is a reasonable and conservative approximation.

Model Uncertainties

The principal uncertainties associated with this model arise from heterogeneity of hydrologic processes, and from spatial and temporal discretization. This model represents the host rock, backfill, and invert as reaction cells, but flow focusing and nonuniform hydrologic properties could cause flow to bypass regions of the EBS. One possible consequence would be that brine conditions derived from precipitates and salts, could persist on the surface of the drip shield for longer than predicted. Spatial and temporal discretization increase the accumulation of precipitates and salts (Section 3.1.2.7.5).

3.1.2.7.3 Modeling Approach and Implementation

The Chemical Reference Model combines input from the Thermal Hydrology Model, Gas Flux and Fugacity Model, Precipitates and Salts Model (CRWMS M&O 2000t) to produce a description of chemical processes in the EBS. The model describes the EBS environment for a set of bounding conditions selected so that the results can be used as the basis for design.

3.1.2.7.3.1 Modeling Water Composition in the Host Rock Above the Drift (Zone 1/2)

The host rock above the drift is represented by a compositional boundary condition at Zone 0 and by a reaction cell at Zone 1/2. The calculated composition in Zone 1/2 represents the composition of seepage, modified by elevated temperature, CO_2 fugacity, partial evaporation, and chemical interaction with the host rock. The flux of water from Zone 0 to Zone 1/2 is calculated by the TH Model, and the composition of this flux is similar to that of J-13 water (CRWMS M&O 2000af).

Using EQ3/6 to represent the host rock (Zone 1/2), separate models for each time period are prepared. These are equilibrium models using EQ3NR, which is part of the EQ3/6 code package

(CRWMS M&O 2000t). The equilibrium approach is justified because the starting far-field (Zone 0) composition is already close to solubility equilibrium with host rock minerals. Estimates of reactive surface area for the host rock are not required.

The calculations for the far-field and near-field host rock waters (Zone 0 and Zone 1/2) are based on a conceptual model for J-13 water in which the bicarbonate, H^+, and Ca^{2+} components are mutually controlled by the fugacity of CO_2, equilibrium with calcite, and electrical charge balance. The model also assumes that the minor Al^{3+}, Fe^{2+}, and Mg^{2+} components are controlled by equilibrium with selected ideal clay minerals and that minor Mn^{2+} is controlled by equilibrium with pyrolusite (MnO_2). Other components are taken to follow specified concentrations based on previous work referenced in the EBS Physical and Chemical Environment Analysis/Model Report (CRWMS M&O 2000t), corrected for evaporative concentration.

When applied to the reference composition of J-13 well water, using a subsurface CO_2 fugacity of 10^{-3} atm, this modeling approach yields almost exactly the observed Ca^{2+} concentration and a pH of approximately 8.1. The model is also supported by the fact that because fracture water in the UZ very likely coexists with calcite, so that equilibrium with that mineral is highly likely. The calculated pH is higher than the average value of 7.41 reported for J-13 water (CRWMS M&O 2000t), and the likely reason is different CO_2 conditions in the aquifer compared with the UZ.

The expected thermodynamic controls on the solution composition can be extrapolated up to approximately the boiling point of the water. One additional constraint is required to represent the concentration of aqueous silica. This is set to be the greater of: 1) the concentration reported for J-13 water (CRWMS M&O 2000t), or 2) the concentration corresponding to solubility equilibrium with cristobalite. Values of the CO_2 fugacity from the Gas Flux and Fugacity Model (Section 3.1.2.2), and evaporative concentration factors calculated from the TH Model (Section 3.1.2.1) for Zone 1/2 waters, are also applied here.

3.1.2.7.3.2 Modeling Water Composition and Mineral Precipitation in the Backfill (Zone 3/4)

According to the TH Model results, water from the host rock (Zone 1/2) does not enter the backfill (Zone 3/4) until Time Period 2 (300 to 700 years). During this time period the liquid influx is balanced by vapor outflux, and the calculated liquid water mass in the backfill (Zone 3/4) is small. The cumulative liquid influx during the time period is approximately 10^4 times the resident mass. Accordingly, the formation of precipitates is calculated ignoring the liquid residue. This is justified because small amounts of water will be dispersed in the backfill as tightly held pore water, chemically bound water, and as brine (when humidity conditions permit).

3.1.2.7.3.3 Modeling the Normative Assemblage of Evaporative Minerals Formed in the Backfill (Zone 3/4)

Using the host rock (Zone 1/2) water composition for Time Period 2, an assemblage of minerals is calculated using the normative approach described in Section 3.1.2.5. All of the solutes in the

influent water are precipitated to form the assemblage, which is a simple approximation. The approximation is conservative in the sense that all the salts which can form, are considered to be in contact with the drip shield, and may form brines from interaction with gas-phase humidity, but are not remobilized during Time Period 2 regardless of the humidity.

The LRH Salts Model described in Section 3.1.2.5 (applicable to relative humidity < 85 percent) allows the most soluble salts (e.g. nitrates) to dissolve as the relative humidity increases. The brines that can form (e.g., nitrates, chlorides, carbonates) are potentially mobile in the relative humidity range from 50 percent to 85 percent or greater. For the reference model described here, the relative humidity is calculated to be in approximately this same range when evaporative precipitation occurs, so concentrated brine can exist, but it is regarded as immobile.

Note that trace species, particularly lithium and boron, are neglected in the normative assemblages identified in this model.

3.1.2.7.3.4 Modeling Redissolution of Precipitates When Liquid Flux Returns to the Backfill (Zone 3/4)

All calculations involving reactions between influent water and backfill or evaporative precipitates, are performed using the EQ6 code (this is also part of the EQ3/6 V7.2b package). The evaporative mineral assemblage comprises minerals many of which have solubilities greater than 1 molal (e.g., niter, halite, thermonatrite). It is possible for much of the accumulated mineral mass to be redissolved by a small amount of water. However, it is also possible that salt dissolution could be hindered by spatial heterogeneity of flow processes, relative to the accumulation of salts.

For this model, redissolution is assumed to occur congruently, with a resulting solution ionic strength of 1 molal (CRWMS M&O 2000t). Congruent dissolution means that the dissolution rate for each solid is proportional to its abundance, and that complete dissolution of all precipitates and salts occurs at the same time. Congruent dissolution is a simple concept that prolongs the residence time for the more soluble salts.

The 1 molal ionic strength limit corresponds to the upper limit for use of the B-dot activity coefficient model (CRWMS M&O 2000t). Using this limit (in conjunction with discrete time periods and stepwise constant flow conditions) may overestimate the residence time for the normative mineral assemblage. It nevertheless indicates relatively rapid removal (within a few years; see below). This shows that even if large quantities of precipitates and salts are deposited, they can be readily redissolved and removed by seepage fluxes which are comparable in magnitude to those which evaporated to produce the precipitates in the first place.

The use of 1 molal as the ionic strength limit is not bounding with respect to the most concentrated solution conditions that could exist on the drip shield. Instead, the bounding case is represented by the normative assemblage of salts, having equilibrated to the ambient relative humidity. The 1-molal calculation provides insight as to solution chemistry that will occur in the presence of seepage, whereby the salt accumulation is gradually remobilized, with less than full efficiency, by the dripping water. The solution ionic strength could be greater than or less than 1 molal when seepage occurs, and will vary locally.

Redissolution in the backfill is modeled by introducing the water composition from the host rock (Zone 1/2) into the backfill (Zone 3/4) at the start of Time Period 3 (700 to 1,500 years). In the EQ6 model, the normative evaporative mineral assemblage is titrated congruently into 1 kg of liquid water until the ionic strength is 1 molal (within 1 percent). Quartz is present as the major component of the sand backfill, and controls the concentration of dissolved silica in the resulting liquid phase, as discussed below.

A sensitivity calculation using EQ6, and a published rate law and kinetic data for quartz growth, is performed to assess the need to consider rate-limited reactivity for quartz. The calculation starts with a water composition whereby the other processes (e.g., precipitate dissolution) are completed to equilibrium. The quartz sand surface area discussed previously is used in the rate calculation. The calculation shows a marked decline in dissolved silica over a time of less than one year. Because the quartz sand surface area is a lower bound, a shorter time period could produce the same result. Also, the decline in dissolved silica follows an exponential decay function in which most of the decline takes place early in any time interval; thus, most of the effect could be achieved in even less time. Because of these factors, all other calculations involving the quartz sand backfill were made using instantaneous equilibration with quartz.

3.1.2.7.3.5 Modeling Water Composition and Mineral Precipitation in the Invert (Zone 5/6)

According to the TH results (produced using the model described in Section 3.1.2.1) water from the backfill (Zone 3/4) does not enter the invert (Zone 5/6; which includes the lower backfill plus the crushed-tuff invert) until Time Period 3 (700 to 1,500 years). During this time period the liquid influx is balanced by vapor outflux, and the calculated liquid water mass in the invert (Zone 5/6) is limited. The cumulative liquid influx during the time period is approximately 3600 times the resident mass of liquid water.

3.1.2.7.3.6 Modeling the Normative Assemblage of Evaporative Minerals Formed in the Invert (Zone 5/6)

Using the backfill (Zone 3/4) water composition for both Time Period 3A and Time Period 3B, an accumulation of evaporatively precipitated minerals is calculated using the approach described in Section 3.1.2.5. The general approach is the same as the normative model for precipitates in the backfill, discussed above. During Time Period 3A the precipitates in the backfill (Zone 3/4) are dissolved, producing a water with assumed ionic strength of 1 molal, that subsequently flows to the invert (Zone 5/6) and evaporates. During Time Period 3B the composition of water flowing from the backfill to the invert is more dilute, because the accumulated precipitates are completed redissolved. The duration of Time Period 3B is approximately 100 times longer than Time Period 3A, so potentially significant solute mass is transported to the invert during this period in the model. Note that trace species, particularly lithium and boron, are neglected in the normative assemblages identified in this model.

3.1.2.7.3.7 Modeling Redissolution of Precipitates When Liquid Flux Returns to the Invert (Zone 5/6)

Like the backfill, the evaporative mineral assemblage in the invert will comprise mineral which have solubilities greater than 1 molal (e.g., niter, halite, thermonatrite). As discussed for Zone 3/4, it is possible for much of the accumulated mineral mass to be redissolved by a small amount of water, but other factors may hinder salt dissolution. Redissolution is assumed to occur congruently, with resulting solution ionic strength limited to 1 molal.

Redissolution is modeled by introducing the water composition from the backfill (Zone 3/4) into the invert (Zone 5/6) at the start of Time Period 4 (1,500 to 2,500 years). In the EQ6 model, the evaporative mineral assemblage is titrated into 1 kg of liquid water until the ionic strength is 1 molal (within 1 percent). Equilibrium with quartz is again assumed because of the large surface area presented by the portion of the backfill that is present in Zone 5/6. Crushed tuff is present in the invert, and it is likely that the concentration of silica may increase once the water reaches this material. However, the surface area of the tuff is much less than for the sand, so such a potential increase in dissolved silica is neglected in the present calculations.

3.1.2.7.4 Chemical Reference Model Validation

The reference model is valid for its intended use, which is to improve understanding of changes in the EBS bulk chemical environment during thermal evolution of the potential repository, and to support post-closure aspects of the design basis for the drip shield and waste package. For the given inputs from the TH model (Section 3.1.2.1) and the Gas Flux and Fugacity Model (Section 3.1.2.2) the Chemical Reference Model provides valid predictions of solution composition and mineral precipitation and dissolution. These predictions are based on use of EQ3/6 software implemented in accordance with past practices. The thermodynamic and kinetic data used were taken from widely used sources. There are uncertainties associated with the reference model, particularly the discretization discussed previously. However, these are bounding, or are caused by calculating the average composition of the bulk environment, and are therefore consistent with the intended use of the model.

3.1.2.7.5 Results for the Reference Model

3.1.2.7.5.1 Water Composition in the Host Rock Above the Drift (Zone 1/2)

The water compositions calculated for the host rock (Zone 1/2), for each time period, are shown in Table 3-27.. Water compositions are affected principally by temperature-dependent solubility and P_{CO_2}. Prograde solubility of cristobalite increases the silica concentration with temperature.

Note that lower CO_2 fugacities result in higher pH values. This pH increase corresponds to loss of CO_2. Also, the pH values represent somewhat more alkaline conditions than would be calculated for ambient temperature (e.g., 31°C) owing to the contraction of the upper end of the practical pH range at elevated temperatures. The pH is effectively controlled by the $H_3SiO_4^-$/cristobalite buffer (noting that solubility of aqueous SiO_2 in these waters is controlled by cristobalite) and not by the HCO_3^-/CO_3^{2-} buffer. There is a loss of dissolved Ca^{2+} that is effectively due to precipitation of calcite. The dissolved components Al^{3+}, Fe^{2+}, Mg^{2+}, and Mn^{2+}

vary but remain minor. Small changes in the concentrations of relatively conservative species such as Cl⁻, F⁻, SO_4^{2-}, NO_3^-, Na^+, and K^+ are caused by evaporative concentration (or condensative dilution, represented by concentration factors less than unity).

Normative Assemblage of Precipitates and Salts Formed in the Backfill

Using the host rock (Zone 1/2) water composition for Time Period 2, an assemblage of minerals is calculated using the approach described in Section 3.1.2.5. The results are shown in Table 3-28 for a half-drift model. Approximately 20 kg (full-drift basis) of various precipitates, mostly amorphous silica, are predicted to accumulate in the backfill above the springline rises to about 10.8 in Time Period 3A (the maximum value encountered in the calculations presented here). This is mainly because of the strong evaporative concentration (90.6 percent), which concentrates the OH- component in solution to about 0.62 molal. In later time periods, the extent of evaporation is not so great, and the pH does not rise so high. Approximately 14.6 years are needed to redissolve the accumulated precipitates into a solution with 1 molal ionic strength, using the input data and assumptions adopted.

3.1.2.7.5.2   Redissolution of Precipitates Formed in the Backfill (Zone 3/4)

The results from EQ6 modeling of precipitate redissolution and other processes in Time Period 3A are shown in Table 3-29. In Time Period 3A, quartz and calcite are precipitated as the evaporative precipitates (apart from calcite) are redissolved. Both of these minerals are present at the start of this time period, and more of each is deposited. CO_2 is initially evolved during redissolution (including titration of calcite into solution) but is consumed in Time Period 3B (an "open-system" or constant-fugacity CO_2 boundary condition is used). The pH increases to approximately 10.8 in Time Period 3A (the maximum value encountered in the calculations presented here). This is mainly because of the strong evaporative concentration (90.6 percent), which concentrates the OH- component in solution to about 0.62 molal. In later time periods, the extent of evaporation is not so great, and the pH does not rise so high. Approximately 14.6 years are needed to redissolve the accumulated precipitates into a solution with 1 molal ionic strength, using the input data and assumptions adopted. ·

Table 3-27. Calculated Water Composition in the Host Rock (Zone 1/2) for Time Periods 1 through 5

	Nominal Time (years)				
	100	500	1000	2000	5000
Temperature (°C)	80.81	90.05	88.42	79.96	51.69
P_{CO2} (atm)	9.084E-07	1.805E-06	1.536E-06	5.405E-06	3.314E-05
P_{O2} (atm)	2.384E-04	4.736E-04	4.030E-04	1.416E-03	8.608E-03
Evaporation/ Condensation Factor	1.088	0.9778	0.8782	0.9895	0.9995
pH	9.318	9.139	9.162	9.140	9.243
I (molal)	4.273E-03	4.041E-03	3.961E-03	2.924E-03	2.486E-03
Al^{3+}	1.940E-06	2.407E-06	2.265E-06	1.417E-06	2.904E-07
$B(OH)_3$(aq)	1.365E-05	1.227E-05	1.101E-05	1.242E-05	1.255E-05
Ca^{2+}	6.365E-04	6.392E-04	6.866E-04	2.385E-04	4.316E-05
Cl^-	2.191E-04	1.969E-04	1.769E-04	1.993E-04	2.013E-04
F^-	1.249E-04	1.122E-04	1.007E-04	1.135E-04	1.147E-04
Fe^{2+}	8.812E-16	4.994E-16	5.449E-16	9.124E-16	5.698E-15
HCO_3^-	2.250E-05	2.305E-05	2.194E-05	6.406E-05	7.237E-04
K^+	1.403E-04	1.260E-04	1.132E-04	1.276E-04	1.288E-04
Li^+	7.492E-06	6.771E-06	6.051E-06	6.771E-06	6.915E-06
Mg^{2+}	3.148E-10	3.464E-10	3.460E-10	8.011E-10	7.715E-09
Mn^{2+}	1.363E-14	3.649E-14	2.911E-14	2.578E-14	3.708E-15
NO_3^-	1.541E-04	1.385E-04	1.244E-04	1.401E-04	1.415E-04
Na^+	2.167E-03	1.948E-03	1.750E-03	1.971E-03	1.991E-03
SO_4^{2-}	2.084E-04	1.873E-04	1.682E-04	1.895E-04	1.914E-04
SiO_2(aq)	3.584E-03	3.741E-03	3.665E-03	2.804E-03	1.275E-03
Sr^{2+}	5.022E-07	4.451E-07	3.995E-07	4.565E-07	4.565E-07

Source: CRWMS M&O 2000t

NOTE: All concentrations in mol/kg H_2O unless otherwise specified

[a] Calculated data from EQ3NR output files for Zone 1/2 (filenames "Z1w_0100.3o", "Z1w_0500.3o", "Z1w_1000.3o", "Z1w_2000.3o", and "Z1w_5000.3o")

Table 3-28. Normative Evaporative Mineral Assemblage Predicted to Accumulate in the Backfill (Zone 3/4; multiply by 2 to obtain full-drift basis) during Time Period 2 (300 to 700 years)

Mineral	Formula	Moles of Precipitates (mol/m)[a]	Molar Mass (kg/mol)[a]	Mass of Precipitates (kg/m)[a]
Niter	KNO_3	3.993E+00	1.011E-01	4.038E-01
Na-niter	$NaNO_3$	3.934E-01	8.500E-02	3.344E-02
Fluorite	CaF_2	1.778E+00	7.808E-02	1.388E-01
Villiaumite	NaF	0.000E+00	4.199E-02	0.000E+00
Sylvite	KCl	0.000E+00	7.455E-02	0.000E+00
Halite	$NaCl$	6.239E+00	5.844E-02	3.646E-01
Mg-smectite [b]	$Mg_{0.165}Al_{2.33}Si_{3.67}O_{10}(OH)_2$	6.652E-05	3.667E-01	2.439E-05
Ca-smectite [b]	$Ca_{0.165}Al_{2.33}Si_{3.67}O_{10}(OH)_2$	3.266E-02	3.676E-01	1.201E-02
Na-smectite [b]	$Na_{0.333}Al_{2.33}Si_{3.67}O_{10}(OH)_2$	0.000E+00	1.420E-01	0.000E+00
Thenardite	Na_2SO_4	5.934E+00	1.420E-01	8.429E-01
Anhydrite	$CaSO_4$	0.000E+00	1.361E-01	0.000E+00
Tachyhydrite	$CaMg_2Cl_6O_{10} \cdot 12H_2O$	0.000E+00	6.776E-01	0.000E+00
Calcite	$CaCO_3$	1.847E+01	1.001E-01	1.848E+00
Magnesite	$MgCO_3$	0.000E+00	8.431E-02	0.000E+00
Thermonatrite	$Na_2CO_3 \cdot H_2O$	2.161E+01	1.240E-01	2.679E+00
Amorphous Silica	SiO_2	1.184E+02	6.009E-02	7.116E+00
Total				1.344E+01

Source: CRWMS M&O 2000t

NOTES: [a] Values correspond to accumulation in a half-drift model. Multiply by two to obtain accumulation in the full drift cross-section.

Table 3-29. Composition of Water in the Backfill (Zone 3/4) after Return of Liquid Water, Starting with Redissolution of Evaporative Precipitates in Time Period 3A

	Time Period			
	3A	3B	4	5
Temperature (°C)	96.05	96.05	86.95	56.95
P_{CO2} (atm)	1.536E-06	1.536E-06	5.405E-06	3.314E-05
P_{O2} (atm)	4.030E-04	4.030E-04	1.416E-03	8.608E-03
Evaporation/Condensation Factor	10.635	10.635	1.0950	1.004
pH	11.081	9.920	9.276	9.319
I (molal)	1.001E+00	2.025E-02	2.812E-03	2.502E-03
Al^{3+}	1.815E-03	2.410E-05	1.551E-06	2.915E-07
$B(OH)_3(aq)$	1.170E-04	1.172E-04	1.360E-05	1.260E-05
Ca_2^+	7.280E-06	3.548E-05	1.194E-04	3.061E-05
Cl^-	1.485E-01	1.882E-03	2.182E-04	2.021E-04
F^-	6.836E-02	1.072E-03	1.243E-04	1.152E-04
Fe^{2+}	5.788E-15	5.372E-15	9.990E-16	5.721E-15
HCO_3	7.208E-02	1.549E-04	7.878E-05	8.148E-04
K^+	9.502E-02	1.205E-03	1.397E-04	1.293E-04
Li^+	6.427E-05	6.439E-05	7.414E-06	6.943E-06
Mg^{2+}	5.583E-13	4.525E-11	8.771E-10	7.746E-09
Mn^{2+}	5.583E-13	3.098E-13	2.823E-14	3.722E-15
NO_3^-	1.044E-01	1.323E-03	1.534E-04	1.421E-04
Na^+	1.469E+00	1.862E-02	2.158E-03	1.999E-03
SO_4^{2-}	1.412E-01	1.790E-03	2.075E-04	1.922E-04
$SiO_2(aq)$	7.139E-01	7.821E-03	1.481E-03	5.339E-04
Sr^{2+}	9.846E-08	8.840E-07	4.998E-07	3.648E-07
Moles Dissolved (<0 = Formed) per 1 kg Influent H2O				
Halite	1.380E-02			
Niter	8.833E-03			
$NaNO_3$	8.706E-04			
Mg-smectite	1.472E-07			
Thenardite	1.313E-02			
Thermonatrite	4.781E-02			
SiO_2 (amophous)	2.620E-01			
Fluorite [a]	3.170E-03			
Ca-smectite	7.227E-05			
Calcite	-3.900E-03	-6.832E-04	-1.295E-04	-1.267E-05
Quartz	-1.988E-01	-2.930E-03	-1.451E-03	-7.432E-04
Moles Evolved (<0 = Used) per 1 kg Influent H2O				
CO_2 (g)	3.720E-02	-6.800E-04	-1.400E-04	-1.000E-04

Source: CRWMS M&O 2000t

NOTES: All concentrations in mol/kg H_2O unless otherwise specified.

Normative species with zero predicted abundance are not reported in this table.

Fluorite is solubility-limited and slow to dissolve; the figure shown results in removal of ~80% of the accumulated fluorite.

3.1.2.7.5.3 Water Composition After Redissolution of Precipitates and Salts in the Backfill (Zone 3/4)

After Time Period 3, the water composition in Zone 3/4 returns to conditions that are similar to those in the host rock (Zone 1/2) except for the effects of evaporative concentration, and interaction with quartz. Calcite continues to precipitate as seepage flows from the host rock into the backfill, and CO_2 continues to be consumed (Table 3-29).

3.1.2.7.5.4 Normative Assemblage of Evaporative Minerals Formed in the Invert (Zone 5/6)

Two normative mineral assemblages are calculated, one for Time Period 3A (when precipitates from the backfill are remobilized to the invert) and one for Time Period 3B (solute derived mainly from the host rock, and transported through the backfill). The results are shown in Table 3-30 for a half-drift model. As much as 200 kg of various precipitates, mostly amorphous silica, is predicted to precipitate in the lower backfill and invert (full-drift basis).

3.1.2.7.5.5 Redissolution of Precipitates and Salts Formed in the Invert (Zone 5/6)

The evaporite minerals are redissolved in Time Period 4A (analogous to the backfill in Time Period 3A). The results from EQ6 modeling of precipitate redissolution are shown in Table 3-31. Quartz and calcite precipitate as the normative assemblage (apart from calcite) is redissolved. Approximately 7.1 years are required to redissolve the accumulated precipitates into a solution with 1 molal ionic strength.

3.1.2.7.5.6 Water Composition After Redissolution of Precipitates and Salts in the Invert (Zone 5/6)

After Time Period 4, the water composition in the invert (Zone 5/6) returns to conditions that are similar to those in the host rock (Zone 1/2); this can be verified by comparing water \compositions for Time Period 4B and Time Period 5 in Table 3-31. As the normative assemblage is dissolved during Time Period 4A, CO_2 is evolved, but during Time Period 4B there is little inter-phase transfer of CO_2 (note that an open-system, or constant-fugacity, CO_2 boundary condition is used). This is probably because the influent waters to the invert (Zone 5/6) have already reacted to elevated temperature, and contact with quartz and calcite, in the host rock and backfill.

3.1.2.7.5.7 CO₂ Consumption by Abiotic Chemical Processes in the EBS

In this model, CO_2 is consumed or produced by several types of chemical processes:

- Evaporation/condensation processes in which CO_2 is exchanged with the gas-phase

- Precipitation/dissolution reactions involving species such as calcite and thermonatrite

- Cement leaching in which alkaline fluids are discharged to the EBS environment and react with gas-phase CO_2

Table 3-30. Normative Evaporative Mineral Assemblage Predicted to Accumulate in the Invert (Zone 5/6; multiply by 2 to obtain full-drift basis) during Time Period 3 (700 to 1500 years)

Mineral	Formula	Moles Precipitates Time Period 3A (mol/m)[a]	Moles Precipitates Time Period 3B (mol/m)[a]	Total Moles Precipitates (mol/m)[a]	Molar Mass (kg/mol)[a]	Mass of Precipitates (kg/m)[a]
Niter	KNO_3	6.228E+01	3.081E+01	9.309E+01	1.011E-01	9.413E+00
Na-niter	$NaNO_3$	6.140E+00	3.037E+00	9.177E+00	8.500E-02	7.800E-01
Fluorite	CaF_2	4.772E-03	9.075E-01	9.123E-01	7.808E-02	7.123E-02
Villiaumite	NaF	4.480E+01	2.560E+01	7.040E+01	4.199E-02	2.956E+00
Sylvite	KCl	0.000E+00	0.000E+00	0.000E+00	7.455E-02	0.000E+00
Halite	$NaCl$	9.733E+01	4.813E+01	1.455E+02	5.844E-02	8.501E+00
Mg-smectite [b]	$Mg_{0.165}Al_{2.33}Si_{3.67}O_{10}(OH)_2$	2.218E-09	7.014E-06	7.016E-06	3.640E-01	2.554E-06
Ca-smectite [b]	$Ca_{0.165}Al_{2.33}Si_{3.67}O_{10}(OH)_2$	0.000E+00	0.000E+00	0.000E+00	3.667E-01	0.000E+00
Na-smectite [b]	$Na_{0.333}Al_{2.33}Si_{3.67}O_{10}(OH)_2$	5.106E-01	2.646E-01	7.752E-01	3.676E-01	2.850E-01
Thenardite	Na_2SO_4	9.259E+01	4.578E+01	1.384E+02	1.420E-01	1.965E+01
Anhydrite	$CaSO_4$	0.000E+00	0.000E+00	0.000E+00	1.361E-01	0.000E+00
Tachyhydrite	$CaMg_2Cl_6O_{10}{:}12H_2O$	0.000E+00	0.000E+00	0.000E+00	0.67764	0.000E+00
Calcite	$CaCO_3$	0.000E+00	0.000E+00	0.000E+00	1.001E-01	0.000E+00
Magnesite	$MgCO_3$	0.000E+00	0.000E+00	0.000E+00	8.431E-02	0.000E+00
Thermonatrite	$Na_2CO_3{:}H_2O$	3.146E+02	1.539E+02	4.685E+02	1.240E-01	5.810E+01
Amorphous Silica	SiO_2	4.660E+02	1.990E+02	6.651E+02	6.009E-02	3.996E+01
Total						1.397E+02

Source: CRWMS M&O 2000t

NOTE: [a] Values correspond to accumulation in a half-drift model. Multiply by two to obtain accumulation in the full drift cross-section.

These processes are summarized in Table 3-32 which combines results from EQ3 models of Zone 1/2 water composition, the CO_2 demand represented by precipitation of the normative mineral assemblage in Zone 3/4 and Zone 5/6, the EQ6 models for the redissolution of these precipitates and the subsequent flow of water through the EBS, and the CO_2 demand from cement leachate. In Table 3-32 the calculated CO_2 budget is shown for the host-rock/EBS system defined two ways:

- In-drift processes only, including solid-solution equilibrium, evaporation/condensation, and precipitation/dissolution reactions in the backfill (Zone 3/4) and the invert (Zone 5/6).

- In-drift processes, plus all reactions in the host rock referenced to the Zone 0 temperature.

Table 3-31. Composition of Water in the Invert (Zone 5/6) after Return of Liquid Water, Starting with Redissolution of Evaporative Precipitates in Time Period 4A

	Time Period		
	4A	**4B**	**5**
Temperature (°C)	88.46	88.46	58.90
P_{CO_2} (atm)	5.405E–06	5.405E–06	3.314E–05
P_{O_2} (atm)	1.416E–03	1.416E–03	8.608E–03
Evaporation/Condensation Factor	1.046	1.046	1.003
pH	10.952	9.268	9.320
I (molal)	9.999E–01	2.931E–03	2.504E–03
Al^{3+}	1.477E–03	1.622E–06	2.924E–07
$B(OH)_3(aq)$	1.419E–05	1.423E–05	1.264E–05
Ca^{2+}	7.209E–06	1.219E–04	2.987E–05
Cl^-	1.188E–01	2.282E–04	2.027E–04
F^-	5.949E–02	1.300E–04	1.155E–04
Fe^{2+}	1.042E–15	1.045E–15	5.738E–15
HCO_3^-	1.538E–01	7.555E–05	7.912E–04
K^+	7.605E–02	1.461E–04	1.297E–04
Li^+	7.734E–06	7.755E–06	6.964E–06
Mg^{2+}	2.381E–13	8.473E–10	7.769E–09
Mn^{2+}	2.945E–14	2.953E–14	3.733E–15
NO_3^-	8.355E–02	1.605E–04	1.425E–04
Na^+	1.176E+00	2.257E–03	2.005E–03
SO_4^{2-}	1.130E–01	2.170E–04	1.928E–04
$SiO_2(aq)$	4.039E–01	1.543E–03	5.355E–04
Sr^{2+}	8.039E–08	5.228E–07	3.659E–07
Moles Dissolved (<0 = formed) per 1 kg Influent H_2O			
SiO_2 (amophous)	5.171E–01		
Halite	1.137E–01		
Niter	7.277E–02		
$NaNO_3$	7.173E–03		
Fluorite	7.906E–04		
Villiaumite	5.533E–02		
Mg-smectite	6.084E–09		
Na-smectite	6.069E–04		
Thenardite	1.082E–01		
Thermonatrite	3.661E–01		
Calcite	–9.031E–04	-2.856E–06	-8.281E–07
Quartz	–1.336E–01	-5.682E–06	0.000E+00
Moles Evolved (<0 = Used) per 1 kg Influent H_2O			
CO_2 (g)	2.178E–01	0.000E+00	0.000E+00

Source: CRWMS M&O 2000t

NOTE: All concentrations in mol/kg H_2O unless otherwise specified
Normative species with zero predicted abundance are not reported in this table.

Table 3-32. CO_2 Produced in the EBS and Host Rock from Evaporation/Condensation, Dissolution/Precipitation, and Cement Leachate Equilibration Processes

Rate of CO_2 Production

Time Period	Nominal Time (yr)	Maximum 1-D CO_2 Flux to Potential Repository (kg/m-sec)	In-Drift (Full-Drift) Total CO_2 Budget Produced (kg/m-sec)	Incl. Host Rock (wrt Zone 0) CO_2 Budget Produced (kg/m-sec)	In-Drift with Cement CO_2 Budget Produced (kg/m-sec)	Percent Change in CO_2 Budget w/ Cement (%)
1	100	8.03E-10	0.000E+00	-1.839E-10	0.000E+00	0.00
2	500	8.03E-10	-1.726E-10	-1.053E-10	-1.741E-10	0.83
3A	1000	8.03E-10	-7.630E-09	-6.935E-09	-7.637E-09	0.09
3B	1000	8.03E-10	-8.243E-10	-1.291E-10	-8.310E-10	0.81
4A	2000	8.03E-10	4.451E-08	4.454E-08	4.451E-08	-0.01
4B	2000	8.03E-10	-4.472E-11	-1.294E-11	-5.028E-11	12.44
5	5000	8.03E-10	-2.293E-11	7.244E-13	-3.888E-11	69.60

Cumulative CO_2 Production

Time Period	Time Period Duration (yr)	Cumulative 1-D CO_2 Flux to Potential Repository (kg CO_2/m)	In-Drift (Full-Drift) Total Cumulative CO_2 Produced (kg CO_2/m)	Incl. Host Rock (wrt Zone 0) Cumulative CO_2 Produced (kg CO_2/m)	In-Drift with Cement Cumulative CO_2 Produced (kg CO_2/m)
1	250	6.34E+00	0.00E+00	-1.45E+00	0.00E+00
2	400	1.65E+01	-2.18E+00	-2.78E+00	-2.20E+00
3A	14	1.68E+01	-5.55E+00	-5.84E+00	-5.57E+00
3B	786	3.67E+01	-2.60E+01	-9.05E+00	-2.62E+01
4A	7	3.69E+01	-1.62E+01	7.94E-01	-1.64E+01
4B	993	6.21E+01	-1.76E+01	3.89E-01	-1.79E+01
5	5000	1.89E+02	-2.12E+01	5.03E-01	-2.41E+01

Source: CRWMS M&O 2000t

NOTES: Positive values for CO_2 production signify release of CO_2 to the gas phase; negative production signifies net consumption.

Half-drift (symmetry model) results are multiplied by two to obtain full-drift results.

In other words, the CO_2 produced and consumed as percolation moves within the host rock, at elevated temperature, outside the range of significant evaporation. The CO_2 consumption rates from Table 3-32 are also plotted in Figure 3-58. For the reference model, in-drift processes dominate the CO_2 budget in the system that includes the host rock. The maximum consumption of CO_2 occurs in Time Period 3 when precipitates and salts are accumulating in the drift.

A long-term, cumulative CO_2 deficit is calculated to occur (and would be replaced by transport of gas-phase CO_2 or dissolution of carbonate). In Time Period 4A when the precipitates are mobilized out of the drift, the cumulative CO_2 deficit decreases by approximately half. At the end of Time Period 5 the cumulative CO_2 deficit represents calcite that undergoes the following transitions:

- Calcite is precipitated in the drifts or in the host rock above the drifts

- Percolating waters dissolve calcite in similar amounts from pre-existing calcite in the host rock below the drifts

- The dissolved calcite is removed from the system by percolation.

This sequence represents a net loss of CO_2 from the system, because the drifts and the host rock above the drifts retain more calcite than initially.

The maximum 1-D CO_2 flux computed using the model developed in Section 3.1.2.2, multiplied by the drift spacing (81 m), is shown in Figure 3-58 for comparison to the consumption rates. For all time periods the available CO_2 flux is greater than the consumption. However, the consumption rate in the drifts exceeds that which can be supplied by direct, 1-D transport as discussed in Section 3.1.2.2.

In summary, most of the CO_2 consumption in the system is associated with carbonate precipitation in the drifts. Peak consumption is driven by evaporative precipitation of carbonates, and gas-phase CO_2 transport will probably be most important in meeting this demand. Calcite continues to precipitate in the drifts during cooldown, and to be dissolved in similar amounts from the host rock below the drifts. If the mass balance is expanded to include the host rock in the vicinity (defined by the Zone 0 temperature) some additional CO_2 consumption is included.

Table 3-33. CO_2 Consumption by Cement Degradation and Other Processes in the Engineered Barrier System

Time Period	Nominal Time (yr)	Leachate Flow per Rockbolt (m^3/yr)	Number of Rockbolts (m^{-1})	Leachate Total Flow Rate (kg/m-sec)	Effluent Aqueous Total CO_2 [b] (mg/L)	Calcite Ppt from Leachate Equilibration [b,c] (g/L)	Total CO_2 Produced [d] (kg/m-sec)
1	100	0	4	0.000E+00	0	0	0.000E+00
2	500	7.520E–05	4	9.532E–09	1.00	0.62	-1.708E–12
3A	1000	3.310E–04	4	4.196E–08	1.00	0.64	-7.888E–12
3B	1000	3.310E–04	4	4.196E–08	1.00	0.64	-7.888E–12
4A	2000	1.680E–04	4	2.129E–08	4.00	0.82	-5.753E–12
4B	2000	1.680E–04	4	2.129E–08	4.00	0.82	-5.753E–12
5	5000	2.540E–04	4	3.220E–08	21.4	1.29	-1.591E–11

Source: CRWMS M&O 2000t

NOTES: [a] Time Period 3A is 14.6 years, and Period 3B is 785.4 years; Period 4A is 7.1 years, and Period 4B is 992.9 years (nominal values).

[b] Use J-13 water as influent water composition, with bicarbonate 128.9 mg/L.

[c] After equilibration with CO_2 and quartz in the drift.

[d] Negative production signifies consumption

3.1.2.7.5.8   Potential Effects from Cementitious Materials

The in-drift CO_2 balance is expanded to include leachate from rockbolt cement. The leachate flow rate from 4 rockbolts per meter of drift, and the consumption of gas-phase CO_2 by leachate equilibration, are shown in Table 3-33. (The consumption rate calculated in that table is also incorporated in the CO_2 balance presented in Table 3-32.) The leachate flow rate and chemistry are described by the Cementitious Materials Model (Section 3.1.2.3).

These results show that the CO_2 demand from equilibration of the leachate with CO_2 and quartz sand in the EBS is small compared with consumption and production from other causes, during the thermal period. This result is primarily controlled by the small flow rate of leachate, which in turn is related to the permeability of the grout. During the thermal period, the leachate flow could increase by an order of magnitude without substantially affecting the CO_2 balance. This provides some margin for degradation of the rockbolt geometry and greater exposure of the grout.

Leachate composition is similar to the water in the backfill that results from evaporative concentration during the thermal period (compare Table 3-9 with Table 3-29). In the Cementitious Materials Model degradation is represented by ettringite and portlandite dissolution, so the only aqueous species that will be significantly affected by the cement are Ca, sulfate, and pH. The pH is readily buffered by CO_2 and quartz sand in the drifts, while the sulfate behaves as a conservative species for as long as water is present in the drifts. The principal difference between the composition of leachate and other water in the drifts is the concentration of Ca. Because the leachate flow rate will tend to be a small fraction of the total seepage flow rate, the excess Ca will be diluted, and the effect on the bulk chemical environment will be minor.

3.1.2.7.6   Summary of the Chemical Reference Model

Chemical reaction-cell modeling shows that mobile water in the backfill can approach pH 11 when evaporative salts and precipitates are present. As discussed in Section 3.1.2.5, higher pH may occur locally in waters that are saturated with respect to salts such as thermonatrite. As relative humidity increases during cooldown, the salt-saturated brines will eventually become diluted, and pH will decrease.

Calculations performed for the Chemical Reference Model show that precipitates can be readily redissolved and removed, by seepage fluxes which are comparable in magnitude to those which evaporated to produce the precipitates. There are no chemical constraints that would prevent rapid redissolution of precipitates and salts, however, there may be hydrologic factors such as flow heterogeneity that limit access of water to soluble salts.

The evolution of pH and ionic strength in reaction cells representing the host rock, backfill, and invert, using the reference model, is shown in Figure 3-59 and Figure 3-60. The reference model is chosen to maximize seepage influx, evaporative solution concentration, and formation of precipitates and salts. Some important comments on the reference model results are as follows:

- Temporal and spatial granularity causes overestimation of the total mass of precipitated salts, and the residence time of salts in the backfill and invert. Spatial granularity also produces averaging of the calculated chemical conditions in the host rock, backfill, and invert, thus the pH and other factors may be under-predicted.

- Redissolution of precipitates and salts may occur faster (with higher pH and dissolved solids) or slower (lower pH and dissolved solids) than predicted by the reference model.

- Saturated brines will form when precipitates and salts are present, and there is sufficient humidity. The reference model considers the chemical effects when precipitated salts are diluted to 1 molal ionic strength by seepage, however, because of hydrologic uncertainty the bounding chemical condition is the continued presence of salts which are in equilibrium with the humidity in the drift environment.

For application of the reference model to bounding conditions for corrosion of the drip shield, saturated brine would be present after the start of Time Period 2 (300 to 700 years), when relative humidity exceeds 50 percent (for nitrate salts) or 85 percent (for other salts). The different salts can occur separately, or in mixtures. Brine concentration will decrease as the relative humidity increases.

Based on the foregoing discussion, relative humidity can be used as a "master variable" in bounding models for water composition in contact with the drip shield or waste package. Evolution of relative humidity at the drip shield surface, for the four TH models calculated in Section 3.1.2.1, is shown in Figure 3-61. The implications of temperature and relative humidity threshold conditions on potential microbial growth and activity, is shown in Figure 3-62.

3.1.2.8 Analysis of the Effects of Drift Degradation on the Physical and Chemical Environment

This section describes the process and results of the *Drift Degradation Analysis* (CRWMS M&O 2000ad) and its effects on the physical and chemical environment. The deterioration of the rock mass surrounding the potential repository emplacement drifts is predicted based on the probabilistic key-block analysis. This model provides a boundary condition for analysis of the potential mechanical degradation of the drip shield from rockfall, which is ongoing and not presented in this report.

Key blocks are formed at the surrounding rock mass of an excavation by the intersection of three or more planes of structural discontinuities as shown in Figure 3-63. This analysis provides an assessment of the possible formation of key blocks within the repository horizon based on the orientations of discontinuities present in the ESF Main Loop and in the ECRB Cross Drift. Block failure due to seismic and thermal effects is also analyzed.

3.1.2.8.1 Conceptual Basis for the Probabilistic Key-Block Analysis

Key blocks are formed at the surrounding rock mass of an excavation by the intersection of three or more planes of structural discontinuities. The *Drift Degradation Analysis* provides an assessment of the possible formation of key blocks within the potential repository horizon, based on the orientations of discontinuities present in the Exploratory Studies Facility (ESF) main loop and in the enhanced characterization of the potential repository block (ECRB) cross drift. Block failure due to seismic and thermal effects has also been analyzed.

As part of initial planning, technical literature sources were reviewed to determine the most appropriate approach to be used in developing a key-block analysis for the Yucca Mountain Site Characterization Project. As a result, the Discrete Region Key Block Analysis (DRKBA) software was selected. The DRKBA probabilistic approach is unique and is distinguished from

traditional key-block analyses in that it not only assesses the maximum size of key blocks, but it also predicts the number of potential key blocks that will be formed within a referenced length of tunnel. The DRKBA approach also allows for a variety of tunnel and jointing configurations. DRKBA simulates structural discontinuities as circular discs placed in the rock mass according to probabilistic distributions determined from tunnel-mapping data. Joint planes are simulated by a Monte Carlo technique from probability distributions representing the orientation, spacing, and trace length of the corresponding joint set. DRKBA then analyzes these blocks to determine if they are geometrically feasible and mechanically stable.

The DRKBA software employs a bipolar Watson distribution for joint-orientation data. The principal axis orientation and a concentration factor k are the required inputs for the bipolar Watson distribution. The concentration factor k is an index of the concentration: the larger the value of k, the more the distribution is concentrated towards the principal axis orientation. Joint radii (see assumption 5.1), spacings, and positionings are simulated with Beta distributions. The Beta distribution is a four-parameter distribution with the following parameters:

- Parameter a—represents one end of the closed interval upon which the Beta distribution is defined

- Parameter b—represents the other end of the closed interval upon which the Beta distribution is defined

- Parameter p—determines the shape of the distribution curve; value is calculated from the mean deviation of the transformed data

- Parameter q—determines the shape of the distribution curve; value is calculated from the standard deviation of the transformed

The transformed data were obtained by normalizing the data with the maximum value. The cohesion and friction angle of the joints are simulated as a bivariate normal distribution. Inputs for the mean and standard deviation of the joint strength parameters are required.

3.1.2.8.2   Input Data and Assumptions

Input Data

Two sets of geometrical data for joints collected by field mapping or by laboratory testing were used in the drift-degradation analysis (CRWMS M&O 2000ad, Section 4.0). The first set, collected from the ESF main loop (i.e., the north ramp, main drift, and south ramp), is referred to as the ESF data. The second set, collected from the ECRB cross drift, is called the ECRB data. Qualified joint-mapping data for the Topopah Spring tuff crystal-poor upper lithophysal zone (Tptpul) and Topopah Spring tuff crystal-poor middle nonlithophysal zone (Tptpmn) lithologic units are available from the ESF data. Qualified joint-mapping data for the Tptpul, Tptpmn, Topopah Spring tuff crystal-poor lower lithophysal zone (Tptpll), and Topopah Spring tuff crystal-poor lower nonlithophysal zone (Tptpln) lithologic units are available from the ECRB data.

Mapping data from the ESF being used in the analysis includes U.S. Geological Survey/U.S. Bureau of Reclamation (USGS USBR) full-periphery geologic maps (FPGMs) and the detailed line survey (DLS). Developed fracture data include joint-set orientation, joint spacing, joint-trace length, and joint offset from the DLS (CRWMS M&O 2000ad, Section 4.0). Fracture strike and dip data contained in the electronic files of the FPGMs were used to determine fracture-set orientation; fracture-set spacing and trace-length data were obtained from the DLS. All fracture-spacing information for the primary joint sets has been converted to true spacing.

Joint-strength parameters, including cohesion and friction angle based on laboratory shear-strength test data from core specimens, were used in the analysis. Rock-density data and intact-rock elastic properties were obtained from laboratory tests performed on the rock cores from the north ramp geotechnical and the systematic drilling boreholes.

Design-basis seismic ground motion parameters are provided for both Category 1 and Category 2 design-basis events (CRWMS M&O 2000ad, Section 4.0). The peak ground accelerations for the horizontal motion in the frequency range of 5 to 10 Hz were selected for this analysis. Three levels of seismic events are included:

- **Level 1**—corresponds to a 1000-year event (Category 1)
- **Level 2**—corresponds to a 5000-year event
- **Level 3**—corresponds to a 10,000-year event (Category 2)

The Level 2 (5000-year event) value was estimated based on the Category 1 and Category 2 values.

Assumptions

The main assumptions used in the drift degradation analysis are as follows (CRWMS M&O 2000ad, Section 5.0):

- The key-block analysis simulated in the DRKBA software does not include a ground-support element. All key blocks predicted in this analysis are therefore the blocks that fail in an unsupported opening. This assumption is necessary because of the limitation of the DRKBA program. The assumption apparently will lead to a conservative prediction of key blocks for the preclosure period and is considered adequate for the postclosure period.

- This analysis uses an alternative method for joint-strength reduction to simulate the seismic effect on the occurrence key blocks. This method is verified based on the simulation using the distinct element code UDEC (CRWMS M&O 2000ad, Attachment V).

3.1.2.8.3 Approach for the Probabilistic Key-Block Analysis

The approach toward the drift-degradation analysis involves the following:

- Analyze blocks that have fallen in the field and their associated joints.

- Collect and assess joint-geometrical data and joint-frictional properties data from the ESF main loop and ECRB cross drift to develop the joint-modeling inputs for DRKBA.

- Analyze the joint data, including the maximum block size, to assess potential formation of key blocks using DRKBA.

- Analyze the seismic and thermal effects on joint and block movement.

- Analyze the DRKBA block-size distribution data for each lithologic unit within the potential repository host horizon.

- Determine the number and average volume of rockfall per unit length of drift for various levels of seismic hazard.

- Evaluate postclosure frequency of block failure for 10,000 years.

- Analyze the drift profile showing the progressive movement of joints and blocks with time.

Details on each step of the approach are provided in the *Drift Degradation Analysis* (CRWMS M&O 2000ad, Section 6.3).

3.1.2.8.4 Summary of Analysis Results

The following discussion is extracted from the Drift Degradation Analysis (CRWMS M&O 2000ad). For brevity, tables of results are presented only for the Tptpmn (middle non-lithophysal) host rock unit. Similar tables for the Tptpul (upper lithophysal) and the Tptpll (lower lithophysal) are available. The Tptpmn unit is selected because it contains the greatest abundance of fractures, and thus greater probability of consequential rockfall.

Prediction of Key-Block Size and Distribution for Static Conditions

A range of drift orientations with the drift azimuth varied in 15° increments is considered in the static analyses. Figure 3-64 presents the key-block analysis results in the format of cumulative frequency of occurrence for the Tptpmn unit. The cumulative frequencies of occurrence corresponding to 50, 75, 90, 95 and 98 percentile block volume for this unit are listed in Table 3-34.

The maximum block sizes predicted from the analyses are also presented, and the predicted block size is generally small. For example, the 95-percentile block ranges from 1.35 to 3.70 m³ for the Tptpmn unit. For a layout azimuth of 105°, the 98-percentile block 4.57 m³ for the Tptpmn unit.

The predicted numbers of key blocks per unit length of emplacement drift are listed in Table 3-35 for the three potential host rock units. The numbers of key blocks formed in the lithophysal rock (i.e., the Tptpul and Tptpll units) are predicted to be scarce. Key blocks are more predominant in the Tptpmn unit; the number of blocks ranges from 26 to 63 per 1 km of

Table 3-34.   Block Volume Corresponding to Various Levels of Predicted Cumulative Frequency of Occurrence, Emplacement Drift in Tptpmn Unit

Cumulative Frequency of Occurrence (percent)	Drift Orientation (Azimuth in degree)											
	0	15	30	45	60	75	90	105	120	135	150	165
50	0.04	0.04	0.10	0.04	0.04	0.04	0.04	0.04	0.04	0.10	0.07	0.04
75	0.24	0.38	0.50	0.27	0.21	0.16	0.21	0.33	0.35	0.44	0.33	0.24
90	1.18	1.20	1.68	1.15	0.92	0.47	0.92	1.18	1.03	1.63	1.23	1.20
95	3.04	2.93	3.70	2.85	1.71	1.35	1.60	2.45	2.17	3.04	2.11	2.79
98	7.12	5.68	5.76	5.90	3.30	1.80	2.25	4.57	4.86	5.65	5.71	4.86
maximum	19.86	9.84	17.34	11.34	12.64	5.00	8.20	9.19	10.89	19.33	21.39	9.47

NOTES: Values shown are cubic meters.
From CRWMS M&O 2000ad, Table 12

Table 3-35. Predicted Number of Key Blocks per Unit Length (km) along Emplacement Drift

Lithologic Unit	Drift Orientation (Azimuth in degree)											
	0	15	30	45	60	75	90	105	120	135	150	165
Tptpul	12	18	12	14	13	14	16	15	18	20	16	13
Tptpmn	47	42	53	33	35	26	40	37	53	63	57	48
Tptpll	4	5	5	4	3	2	1	3	5	3	6	5
Tptpln	12	6	7	8	5	5	2	3	5	8	8	7

Source: CRWMS M&O 2000ad, Table 15

drift. The orientations that are predicted to have a higher number of blocks are, in general, parallel to the major high-angle joint sets. This trend is consistent with that observed for the prediction of the maximum block size.

Quasi-Static (Seismic) Analysis Results

Figure 3-65 presents the key-block–size distribution for Tptpmn unit for the three levels of seismic events considered. The cumulative frequencies of occurrence corresponding to the 50th, 75th, 90th, 95th, and 98th percentile block volume for the Tptpmn unit are listed in Table 3-36. The maximum block sizes predicted from the analyses are included. The analysis results indicate that the seismic effect on the rockfall-size distribution is relatively minor.

Table 3-36. Block Volume Corresponding to Various Levels of Predicted Cumulative Frequency of Occurrence, Performance Confirmation Drift in Tptpmn Unit, with Seismic Consideration

Cumulative Frequency of Occurrence	Static	Static Plus Seismic		
		Level 1	Level 2	Level 3
50 percent	0.04	0.04	0.04	0.04
75 percent	0.33	0.41	0.47	0.47
90 percent	1.18	1.37	1.74	1.74
95 percent	2.45	2.90	3.44	3.44
98 percent	4.57	5.68	8.25	8.25
maximum	9.19	19.89	19.89	19.89

NOTES: Values shown are cubic meters.
From CRWMS M&O 2000ad, Table 17

Table 3-37. Predicted Number of Key Blocks per Unit Length (km) along Emplacement Drift, with Seismic Consideration

Lithologic Unit	Static	Static Plus Seismic		
		Level 1	Level 2	Level 3
Tptpul	15	15	17	17
Tptpmn	37	38	40	40
Tptpll	3	3	3	3
Tptpln	3	3	5	5

NOTE: From CRWMS M&O 2000ad, Table 20

Table 3-38. Predicted Average Volume of Key Blocks per Unit Length along Emplacement Drift, with Seismic Consideration

Lithologic Unit	Static (m³/km)	Static Plus Seismic (m³/km)		
		Level 1	Level 2	Level 3
Tptpul	4.9	5.0	9.5	12.1
Tptpmn	18.2	25.9	32.3	32.3
Tptpll	0.8	0.8	0.8	0.8
Tptpln	3.0	5.5	14.4	14.4

NOTE: From CRWMS M&O 2000ad, Table 21

The predicted numbers of key blocks per unit length of drift are listed for the different units in Table 3-37. Static results are also included for comparison. The comparison shows that there is an insignificant impact on the number of rockfalls for a 1,000-year event earthquake (Level 1) and only a minor impact on the number of rockfalls for a 5,000-year event earthquake (Level 2) or a 10,000-year event (Level 3).

The predicted average volume of rockfall per unit length of drift is listed in Table 3-38. The trend for the average volume of rock fall per kilometer is similar to that for the predicted number of key blocks per kilometer.

3.1.2.8.5 Rock Fall Related to Time-Dependent and Thermal Effects

The analysis uses an approach that accounts for the time-dependent and thermal effects with degradation of joint cohesion. The development and justification for this approach are described in the *Drift Degradation Analysis* (CRWMS M&O 2000ad, Section 6.3.5 and Attachment VI).

Four different times are selected for the analysis: 0 yr (static condition), 200 yr, 2,000 yr, and 10,000 yr. The corresponding degraded joint cohesion for each time is listed in Table 3-39. The reduction of joint-cohesion is predicted to be very small in the period between 2,000 and 10,000 yr.

Because backfill is part of the EBS during the postclosure period, backfill is included in the analysis for the consideration of time-dependent and thermal effects. It is apparent that the blocks that form around the springline area will no longer occur in the analysis with backfill.

The predicted number of key blocks per kilometer of drift for the drip shield orientation is listed in Table 3-40. Only minor increases in the number of key blocks are predicted between 200 and 2,000 yr; no change is predicted from 2,000 to 10,000 yr. The predicted average volume of rockfall per unit length of drift is listed in Table 3-41. Thee results indicate that time-dependent and thermal effects will have a minor impact on rockfall.

3.1.2.8.6 Effect of Drift Degradation on the Physical and Chemical Environment

The predicted number of rock blocks, average volume of blocks, and detailed size-distribution of blocks, as presented in general, suggest minor impact of rockfall on the in-drift physical and chemical environment. The degradation analysis, however, does not address the effect of rockfall to the displacement of the backfill material and the potential structural damage to drip shields due to rockfall.

Table 3-39. Reduced Joint Cohesion to Account for Time-Dependent and Thermal Effects

Period (year)	Joint Cohesion (Pa)
0 (Static)	99,873
200	21,674
2,000	10,998
10,000	10,776

NOTE: From CRWMS M&O 2000ad, Table 22

Table 3-40. Predicted Number of Key Blocks per Unit Length (km) along Emplacement Drift, with Time-Dependent and Thermal Consideration

Lithologic Unit	Static	Year 200	Year 2000	Year 10000
Tptpul	15	14	15	15
Tptpmn	37	37	39	39
Tptpll	3	4	4	4
Tptpln	3	4	5	5

NOTE: From CRWMS M&O 2000ad, Table 23

Table 3-41. Predicted Average Volume of Key Blocks per Unit Length (km) along Emplacement Drift, with Time-Dependent and Thermal Consideration

Lithologic Unit	Static	Year 200	Year 2000	Year 10,000
Tptpul	4.9	5.1	8.8	8.8
Tptpmn	18.0	15.8	19.0	19.0
Tptpll	0.8	0.8	0.9	0.9
Tptpln	3.0	3.4	8.4	8.4

NOTE: From CRWMS M&O 2000ad, Table 24

3.1.3   Engineered Barrier System Radionuclide Transport Model

The EBS radionuclide-transport model provides an analysis of the transport of radionuclides through the EBS, once they are released from breached waste packages. The model includes advective-dispersive-diffusive transport, and radionuclide sorption. Results generated by the *Water Distribution and Removal Model* (CRWMS M&O 2000q, pp. 68–69) provide input to the one-dimensional transport equation used in the analysis. The following sections describe the model input, assumptions, development, validation, and results.

3.1.3.1   Input Data

The following sections summarize model input data from the *Water Distribution and Removal Model* (CRWMS M&O 2000q, pp. 68–69) and other description of the drift environment as described by the *Engineered Barrier System Radionuclide Transport Model* (CRWMS M&O 2000b, pp. 23–24).

Input Data from the Water Distribution and Removal Model

Hydrologic input corresponds to the base case of steady-state, focused seepage inflow at constant, ambient temperature, from the *Water Distribution and Removal Model* (CRWMS M&O 2000q, pp. 49–55). This input shows that in the invert, liquid flux is decreased below the drip shield, and increased to the sides outside the protection of the drip shield.

The most important aspect of the drift environment, for radionuclide transport in the invert, is the volumetric water content, represented by liquid saturation in the invert. Liquid saturation is influenced by inflow rate, water evaporation rate, and temperature. Saturation is also controlled by the drainage capacity of fractures in the host rock directly below the invert. These effects are discussed in detail in the *Engineered Barrier System Radionuclide Transport Model* (CRWMS M&O 2000b, pp. 23–24). In thermal-hydrology simulations using the "lower" infiltration distribution, the dryout zone is relatively extensive and persists longer, and liquid flux in the invert is smaller. Conversely, for the "higher" infiltration distribution, water returns to the EBS environment sooner, and liquid flux in the invert is greater. These effects are acknowledged in this model, and addressed through selection of input data and interpretation of model results.

Properties and Hydrologic Conditions in the Crushed Tuff Invert

The physical properties of the crushed-tuff invert include the path length and distance, porosity, and grain density. These model inputs are discussed in more detail by the *Engineered Barrier System Radionuclide Transport Model* (CRWMS M&O 2000b, p. 15).

The hydrologic description of the invert includes the liquid flux rate, saturation, and pore-water velocity. The *Water Distribution and Removal Model* (CRWMS M&O 2000q, p. 68) presents these parameters for the glacial and present-day infiltration rates.

Volumetric moisture content is the fractional volume in the invert material occupied by water, and is always less than or equal to the porosity. In results reported by the *Water Distribution and Removal Model* (CRWMS M&O 2000q; Table 7 and Table 20) the volumetric moisture content in the invert is determined to be 0.071 for the glacial climate. For drier conditions which could result from less infiltration (i.e., 1 mm/year) the volumetric moisture content would approach the residual moisture content of 0.05 (CRWMS M&O 2000ae, p. 23).

Dispersivity is the degree of hydrodynamic dispersion in the porous medium, and produces effects on solute distribution that are analogous to molecular diffusion. A conservatively small estimate for dispersivity of crushed tuff, over a flowpath distance of 1 m, would be approximately 10 cm. This is similar to values cited in the literature for laboratory and field experiments (CRWMS M&O 2000b, p. 19). Dispersivity can be much greater for regional groundwater flow; however, because of the scale of the invert, smaller values apply. A reasonable range of values for dispersivity for the invert is from 0.4 to 10 cm (CRWMS M&O 2000b, p. 19).

The molecular diffusion coefficient (units of m^2/year) is a measure of the diffusion of a solute (CRWMS M&O 2000h, p. 18). The tortuosity relation based upon Archie's Law from the *Invert Diffusion Model* (CRWMS M&O 2000h, p. 20), is used to determine the soil/liquid diffusion coefficient. The soil/liquid diffusion coefficient can be determined by multiplying the binary diffusion coefficient for water (molecular diffusion coefficient of water) by the tortuosity factor. As bounding input for estimating diffusion coefficients for radionuclides derived from spent fueled and high-level waste, coefficients for tritiated water (CRWMS M&O 2000b, pp. 18–19) in normal and heavy water, measured over a temperature range of 1° to 45°C, are reported. The measurements show a temperature dependence from 1.1×10^{-5} cm^2/sec at 1°C to $3.6 \times$

10^{-5} cm^2/sec at 45°C. For this model a representative value of 2.30×10^{-5} cm^2/sec (0.073 m^2/yr) is used (CRWMS M&O 2000b, p. 19).

The partition coefficient is the ratio of the mass of dissolved material adsorbed by the invert material, to the mass in solution. Calculations of invert performance are performed for five ranges of partition coefficients (CRWMS M&O 2000b, p. 20), assuming a uniform parametric distribution for each. The selected ranges are 0 to 1, 1 to 5, 5 to 10, 10 to 50, and 50 to 100 cm^3/g.

A summary of the parameters used as input to the EBS Radionuclide Transport Model, including representative values and alternative values used for sensitivity testing, is presented in Table 3-42.

3.1.3.2 EBS Radionuclide Transport Model Assumptions

In addition to the 1-D modeling framework, and the property distributions discussed above, this model assumes that the solute concentration in the gas phase is negligible and that solutes do not react together. The invert is assumed to be compositionally homogeneous (CRWMS M&O 2000b, p. 19). Other assumptions, such as neglecting transverse dispersion, are also identified. These assumptions are consistent with the 1-D transport modeling approach.

3.1.3.3 EBS Radionuclide Transport Model Uncertainties

Ponding of water could occur in the emplacement drifts due to clogging of drainage capacity in the invert and the drift floor. The possible consequences include high fluxes of liquid water through breached waste packages. Being mobilized in a flow of water parallel to the drift axis, radionuclides would be transported to a major fault or fracture where drainage through the host rock could occur. Transport of radionuclides through the UZ would thus occur at higher velocity, and with less water-rock interaction, than if releases are better distributed. Clogging could occur because of fines migration, geochemical alteration of EBS materials, or precipitation of uranium compounds derived from the waste form. This alternative view requires clogging of the natural drainage capacity in the drift floor, which was addressed in Section 3.1.1.

The EBS flow models and radionuclide transport model, regard flow in the drifts to be steady-state. This is justified from a hydrologic perspective because the storage capacity for water in the drifts is small compared with the potential through-flow over time periods of interest (i.e. many years). However, there may be more storage capacity available for radionuclides, if they are retarded on substrates such as steel corrosion products. Stored radionuclides could be released as large pulses when flow conditions change. This uncertainty is probably not important because increased flow rates will cause increased dilution. For example, if the concentration of a given radionuclide is inversely proportional to the EBS flow rate, then the release rate is constant. Alternatively, if the concentration remains constant, there could be changes in the release rate but no change in storage. If the concentration is directly proportional to flow rate, changes in the release rate would be dampened by changes in storage. In any event, changes in storage would not change the peak concentration of any radionuclide that exhibits linear (or nearly so) sorption behavior. This discussion pertains to reversible sorption, because there can be no change in irreversibly stored species.

3.1.3.4 Development of the EBS Radionuclide Transport Model

The EBS is designed to divert water flow around the waste package, to the invert. Water that flows through any breaches in the drip shield may contact the waste package, and eventually cause advective release of radionuclides. Liquid flow bearing dissolved radionuclides will mix, in the invert, with water diverted by the drip shield. The release of radionuclides from the waste package will result in a time-dependent concentration of radionuclides that is considered a unit concentration in this model (Figure 3-66). Note that in a steady-state flow field where pore velocities and volumetric moisture content are constant, the contaminant-transport equation is linear, and the principle of superposition can be used to obtain a solution to the problem where inlet concentration varies with time.

If the transport of radionuclides through the invert is dominated by molecular diffusion, the time to breakthrough of radionuclides would increase compared to the breakthrough time for advection-dominated transport. The invert material (crushed tuff) is considered to be nonsorbing, so sorption is excluded from the base case.

The dispersion-diffusion coefficient (D) is calculated by dividing the effective dispersion–diffusion coefficient (D_e), which is the summation of the hydrodynamic dispersion coefficient (D_{lh}) and the molecular diffusion coefficient (D_{sl}), by the volumetric moisture content (CRWMS M&O 2000b, pp. 29–31).

To assess radionuclide breakthrough times, calculations are performed for various cases, varying the volumetric moisture content, flux, temperature, and drainage capacity of the host rock.

Table 3-42. Summary of Parameter Values and Ranges Used in Base Case of the Radionuclide-Transport Model

Parameter Name, Units	Representative Value	Alternative Values for Sensitivity
Flowpath length (m)	0.61	0.5–0.7
Volumetric water content	0.071	0.05–0.07
Porewater velocity (m/yr)	0.031	0.013–0.031
Liquid water flux (m/yr)	0.0022	0.001–0.0042
Porosity	0.55	0.28–0.55
Dispersivity (m²/yr)	0.1	0.004
Molecular diffusion coefficient (m²/yr)	0.073	0.034–0.11
Grain density (g/cm³)	2.53	2.49–2.72
Partition coefficient (cm³/g)	0	0–1, 1–5, 5–10, 10–50, & 50–100

NOTE: From CRWMS M&O 2000b, p. 33

Table 3-43. Summary of Sensitivity and Uncertainty Analysis for the One-Dimensional Solute-Transport Equation

Partition Coefficient (K_d) Range, ml/g (Mean)	Fifth Percentile Time (y) to $C/C_0 =$		Fiftieth Percentile Time (y) to $C/C_0 =$		Sensitivity Ranking
	0.01	0.5	0.01	0.5	
0–1 (0.5)	2	16	13	104	J_w, K_d, α_L, L, ϕ, θ, ρ_s, D_{wl}
1–5 (3)	17	166	74	590	J_w, α_L, K_d, L, ϕ, θ, ρ_s, D_{wl}
5–10 (7.5)	52	534	189	1487	J_w, α_L, L, ϕ, θ, K_d, ρ_s, D_{wl}
10–50 (30)	162	1618	730	5842	J_w, α_L, K_d, L, ϕ, θ, ρ_s, D_{wl}
50–100 (75)	520	5316	1883	14784	J_w, α_{L}, L, ϕ, θ, K_d, ρ_s, D_{wl}

NOTES: Parameters listed in the sensitivity ranking, including range and mean for the simulations:
Flowpath distance (0.5–0.7 m, 0.6 m)
J_w Darcy velocity (0–4.2 mm/y, 0.021 mm/y)
K_d Distribution coefficient (see column 1)
ϕ Porosity (0.28–0.55, 0.41)
ρ_s Grain density (2.49–2.72 g/cc, 2.61 g/cc)
θ Volumetric water content (0.05–0.07, 0.06)
α_L Dispersivity (0.004 - 0.1 m, 0.052)
D_{wl} Molecular diffusion coefficient (0.035 - 0.11 m²/yr, 0.074 m²/yr)

All distributions are assumed to be uniform, between the limits indicated. **Boldface** indicates the absolute value of the Monte Carlo correlation coefficient is $\geq$ 0.2. ***Boldface italic*** indicates the absolute value of the correlation coefficient is $\geq$ 0.5.
From CRWMS M&O 2000ad

The 1-D advection–dispersion–diffusion equation is given by (CRWMS M&O 2000b, p. 29):

$$\frac{d}{dt}C_1 = D \cdot \frac{d^2}{dz^2}C_1 - V \cdot \frac{d}{dz}C_1 \qquad \text{(Eq. 3-24)}$$

If flow conditions are steady, and solute is instantaneously introduced at the inlet (at t=0), the solution to Equation 3-24 for nonretarded transport with inlet concentration C_0 is (CRWMS M&O 2000b):

$$\frac{C_1}{C_0} = \frac{1}{2}\left(\text{erfc}\left(\frac{L - V \cdot t}{2 \cdot \sqrt{D \cdot t}} \right) + \exp\left(\frac{V \cdot L}{D} \right) \cdot \text{erfc}\left(\frac{L + V \cdot t}{2 \cdot \sqrt{D \cdot t}} \right) \right) \qquad \text{(Eq. 3-25)}$$

where C_1/C_0 is the ratio of outlet to inlet solute concentration, L is the flowpath distance, V is the porewater velocity, D is the dispersion-diffusion coefficient, and t is time. Retardation is incorporated by dividing the porewater velocity (V) and the dispersion-diffusion coefficient (D) by a retardation coefficient calculated from the partition coefficient in the usual manner (CRWMS M&O 2000b).

The dependence of the dispersion-diffusion coefficient for crushed tuff on tortuosity and molecular diffusion has been investigated (CRWMS M&O 2000h). Measured diffusion coefficients are compared with values derived using a Millington Quirk relation, and Archie's law, in Figure 3-67. This figure shows that at low volumetric moisture contents, the relation based upon Archie's Law (CRWMS M&O 2000h) is comparable to the Millington—Quirk relation (CRWMS M&O 2000b, p. 32) and both are in approximate agreement with measured data for crushed tuff.

3.1.3.5 EBS Radionuclide Transport Model Validation

This model provides perspective on the characteristics of invert materials, and EBS hydrologic performance, that most affect radionuclide transport through the invert. An important assumption is that of 1-D vertical flow. Model results show that there is significant dependence of breakthrough time on the flowpath, from spatial variations in liquid water flux in the invert.

The 1-D advective-dispersive-diffusive transport model represented by Equations 3-24 and 3-25 is an accepted and valid model for solute transport, subject to assumptions on dimensionality, flow conditions, sorption reversibility, and other characteristics of solute-solid interaction. Significant uncertainty is associated with quantifying the partition coefficient (shown to be the most sensitive parameter) and specifying the flow path for thousands of years. Accordingly, for TSPA the partition coefficient is assumed to be zero, which means no credit is taken for retardation in the EBS.

3.1.3.6 EBS Radionuclide Transport Model Results

Base Case

The liquid water flux in the invert directly below the waste package is approximately 4 mm/yr, reduced from 42 mm/yr in the host rock for glacial infiltration conditions. The volumetric moisture content is approximately 0.071 for this case (CRWMS M&O 2000b, p. 43). The radionuclide breakthrough curve calculated using Equation 3-25, is presented in Figure 3-68 (CRWMS M&O 2000b, p. 37). Similar results are obtained for the present-day climate (not shown). These results show that the breakthrough is substantial after 10 yr and complete after 100 yr. The analysis also shows that breakthrough occurs more rapidly for grid blocks off the drift centerline where the liquid water flux is greater. Porewater velocity in the vertical direction increases with distance from the centerline.

Effect of Engineered Drainage Features on EBS Transport

Several analyses addressed the effects of engineered drainage features, which are not incorporated in the conceptual design, but could be installed to mitigate insufficient drainage capacity in the host rock at the drift floor, caused by fracture plugging or initial conditions. Because the effective 1-D flowpath distance is much greater with the potential use of engineered drainage features, the calculated radionuclide transport response is improved. The radionuclide breakthrough curve is compared to the base case in Figure 3-69. Similar improvement is calculated for the present-day climate (not shown).

Sensitivity Analysis

The *Engineered Barrier System Radionuclide Transport Model* (CRWMS M&O 2000b, p. 40) includes a sensitivity analysis of breakthrough time, for radionuclide transport in the invert. The analysis applies the Monte-Carlo method, using the 1-D transport equation solution (Equation 3-25). The analysis determines the sensitivity of breakthrough time, to variation of each input parameter within the ranges shown in Table 3-42. The parameters are treated as statistically independent, uniformly distributed random variables.

The Monte Carlo simulation is reported for 1,000 iterations. The random seed for initialization is fixed (at unity) to allow reproducibility of the results. Latin hypercube sampling is used to increase sampling density near the limits of the input distributions.

Table 3-43 is a summary of the sensitivity analysis for 1-D solute transport. The results show that breakthrough time increases with increasing sorption, and that sorption is the most sensitive parameter. An invert comprised of a sorptive material would most effectively delay the release of radionuclides from the EBS. Further, the results show that liquid water flux is a sensitive parameter, while the molecular diffusion coefficient is least sensitive. Dispersivity, flowpath length, and volumetric moisture content are of intermediate sensitivity.

3.1.4 Multi-Scale Thermal-Hydrologic Model

The Multi-Scale Thermal-Hydrologic (MSTH) model and corresponding analysis (CRWMS M&O 2000i) describes the thermal-hydrologic (TH) evolution throughout the potential repository. (The terms thermohydrology and thermal-hydrology are used interchangeably in this discussion and the supporting documentation.) The MSTH Model describes the evolution of thermodynamic conditions in the near-field environment (NFE) and the EBS.

Figure 3-70 illustrates the potential repository footprint used in the model; this footprint closely approximates the actual plan view of the potential repository perimeter within which waste is to be emplaced. Thirty-one locations (or "chimneys") are shown, spanning the potential repository block. These locations sample the lateral variability in properties (such as the thickness of each stratum) and in surface boundary conditions. These are arranged in five "columns" spaced approximately 250 m apart from east to west and in seven "lines" spaced about 500 m apart from north to south. For example, L4C4 is located approximately 1500 m southerly and 750 m westerly from L1C1, which is near the NE corner of the footprint.

3.1.4.1 Input Data, Assumptions, and Model Uncertainties

Input Data

The calculations presented in this PMR are based on the following inputs or data:

- The potential repository footprint is modeled for a total of 70,000 MTU of waste, including 63,000 MTU of CSNF and 7000 MTU of DHLW.

- The TSPA-SR 1-D drift-scale base-case hydrologic property sets for the case of no perching are used. Three infiltration-flux scenarios are included: the "mean," "lower,"

and "upper" flux distributions. Future climate change is incorporated using a time-varying infiltration flux.

- Areal mass loading (AML) is nominally 60 MTU/acre.

- Waste packages are placed in the emplacement drifts in a line with approximately 10 cm between the ends of waste packages.

- Emplacement drifts are arranged with a uniform spacing of 81 m between centerlines of emplacement drifts.

- The distribution of hydrostratigraphic units used in the UZ Flow and Transport Model (UZ Model), is based on the Geologic Framework Model (GFM V3.1).

- The drift-scale models used in the MSTH Model incorporate numerical grid discretization that is comparable to or finer than that used in previous MSTH Model calculations (CRWMS M&O 2000i).

- Each drift segment in the potential repository is ventilated during the entire preclosure period; for base case analyses, this is assumed to be 50 years. During the preclosure period, at least 70 percent of the heat generated by waste packages, is removed by ventilation. Emplacement drifts are backfilled at the end of the preclosure period, and drip shields are emplaced at the same time as backfill.

The calculations presented in this PMR do not address the coupling of geochemical or geomechanical processes to TH behavior. Uncertainties associated with input data and calculations are documented in the *Multi-Scale Thermohydrologic Model* (CRWMS M&O 2000i).

Assumptions

The following assumptions are used in the MSTH Model and corresponding analysis:

- It is assumed that the 50 northernmost emplacement drifts are used for the emplacement of 70,000 MTU of waste.

- The assumed value for tortuosity of the backfill and invert materials is 0.7. This assumption is used in all NUFT input files.

- The assumed value for satiated saturation of the invert and backfill materials is 1.0, which is used in all NUFT input files. This is an upper bound for this parameter.

- The thermal conductivity data is provided for both dry and wet conditions. The conduction-only SDT, DDT, and SMT models cannot explicitly represent the influence of liquid saturation on thermal conductivity. Because the rock matrix is nearly fully saturated initially, and for much of the thermal period, the "wet" value of thermal conductivity is assumed for conduction-only models.

Model Uncertainties

The following discussion identifies two categories of model uncertainties for the MSTH Model: 1) related to the TH modeling approach using NUFT, and 2) related to the multi-scale estimation methodology. Uncertainties related to TH modeling are:

- Dependence of thermal conductivity for the host rock, on water content.

- Effects of episodic variation of percolation flux in the host rock, on water penetration into the drifts during the thermal period.

- Effects of spatially heterogeneous fracture properties in the host rock, on the evolution of thermodynamic conditions in the drift.

- Discrepancy between values of the water potential in the fracture continuum and the matrix continuum, at the same locations, for ambient, steady-state conditions.

- Dependence of drift seepage on numerical model gridding, and spatial heterogeneity of hydrologic properties.

These uncertainties can be addressed through further model development, and sensitivity studies, and do not necessarily require data collection. The MSTH Model presents a large number of TH models that describe temperature, humidity, and flux conditions throughout the potential repository. It should be noted that drift seepage is not calculated directly from these models, rather, the calculated liquid flux in the host rock is used as input to an abstracted seepage model (for TSPA-SR) that is not described in this report.

The key uncertainties related to multi-scale estimation methodology are:

- Mountain-scale gas-phase circulation effects.

- Representativeness of interpolation based on correlation of performance measures across different types of conduction-dominated and TH models.

- Movement of mass (e.g. water vapor) along the drift axis, from warmer to cooler regions.

These uncertainties can be addressed through comparison of MSTH Model results with other (more computationally intensive) numerical simulations in which the potential repository is represented at mountain-scale, but drift-scale processes are represented by embedded fine-scale grids.

3.1.4.2   Multi-Scale Thermal-Hydrologic Model Development

The MSTH Model efficiently estimates TH conditions in the NFE and EBS as functions of time, waste package type, and location in the potential repository. Such estimation could require a numerical model with millions of grid blocks if a brute-force, monolithic model were used. The

MSTH Model relates the results from different types of smaller models, to capture the key factors affecting NFE and EBS TH conditions:

- Potential repository-scale variability of percolation flux

- Temporal variability of percolation flux (as influenced by climate change)

- Uncertainty in percolation flux (as addressed by the mean, high, and low flux scenarios)

- Potential repository-scale variability in hydrologic properties (e.g., those governing matrix imbibition diffusivity and capillary wicking in fractures)

- Edge-cooling effect (which increases with proximity to the edge of the potential repository)

- Dimensions and properties of the EBS components such as the drip shield, engineered backfill, and the invert

- Waste package-to-waste package variability in heat-generation rate

- Potential Repository-scale variability in overburden thickness

- Potential Repository-scale variability in thermal conductivity (with an emphasis on the host-rock units).

The MSTH Model calculates 38 TH variables in the NFE and EBS for 610 subdomains in the potential repository and for 8 different WPs as a function of time for approximately 352 calculational timesteps. The total of 38 TH variables arises from a combination of ten thermodynamic variables (such as temperature and relative humidity) and 13 drift-scale locations (such as the WP, and the drip-shield surface). These TH variables are determined for three infiltration flux scenarios: the "mean," "upper," and "lower" infiltration flux distribution scenarios. For each calculational timestep, the MSTH Model calculates $38 \times 610 \times 8$ TH data values, resulting in 185,440 data values. Multiplying by 352 calculational timesteps results in approximately 65 million TH data points for a complete time evolution, for a given infiltration-flux scenario.

Table 3-44 lists specific thermal-hydrologic variables or parameters that can be predicted by use of the MSTH Model.

The need for a multi-scale modeling approach stems from the fact that the performance measures depend on TH behavior within a few meters of the emplacement drifts and also on thermal and TH behavior on a potential repository (or mountain) scale. A single numerical model (e.g., embedding a 3-D drift-scale model with a relatively fine mesh into a 3-D mountain-scale model with a coarse mesh) would require an infeasible number (millions) of grid blocks. The MSTH Model has been developed for estimating the results that would be obtained if such a single model were possible. In addition to coupling the drift scale and mountain scale, the MSTH

Model also allows for consideration of the effect of different waste package types (e.g., different CSNF waste packages, co-disposal of defense HLW) on the various performance measures.

The MSTH Model consists of four major models and includes multiple scales (mountain and drift), multiple dimensions (1-D, 2-D, and 3-D), and different assumptions regarding the coupling of heat transfer to fluid flow (conduction-only and fully coupled thermal-hydrologic). The four types of models are:

- LDTH (line-averaged-heat-source, drift-scale, thermal-hydrologic) model
- SMT (smeared-heat-source, mountain-scale, thermal-conduction) model
- SDT (smeared-heat-source, drift-scale thermal-conduction) model
- DDT (discrete-heat-source, drift-scale thermal-conduction) model

It is useful to think of the LDTH model as the "core" model. These 2-D drift-scale TH models are run for 31 locations spaced throughout the potential repository area, for several areal mass loading (AML) values (nominal value and lower) to represent the influence of edge-cooling effects. The LDTH model includes the hydrologic processes and parameters (e.g., surface infiltration rates, hydrologic properties). The potential repository-scale variability of the hydrostratigraphy within the potential repository footprint is represented by the 31 locations. These are regularly distributed over the potential repository footprint, and each has an associated hydrostratigraphic column. These 31 columns represent the mountain-scale lateral variability of hydrostratigraphy within the potential repository footprint (CRWMS M&O 2000i).

In the LDTH models, the relative humidity at the ground surface is fixed at 100 percent to control the egress of moisture as vapor. The drip shield and waste package are represented as impermeable for the entire duration of the MSTH Model simulations.

and follow the same average thermal decay function (as a percentage of initial heat output). The 70 percent heat-removal efficiency, and the 50-yr ventilation period, are applied uniformly throughout the potential repository footprint.

The remaining three models, which are conduction only, are required to account for the influence of 3-D mountain-scale heat flow and 3-D drift-scale heat flow on drift-scale TH behavior. The coupling of 3-D mountain-scale heat flow to 2-D drift-scale TH behavior is accomplished with the SMT and the SDT models. The SMT is 3-D and includes the influence of thermal-property variation in the mountain, lateral heat loss to conduction at the potential repository edges, and overburden-thickness variation with location, assuming a uniform, planar (i.e., smeared) heat source throughout the potential repository area. The SDT model is a 1-D (vertical) model, run at the same 31 locations and for the same AMLs as the LDTH models. To obtain the "line-averaged" drift-wall temperature (which is roughly equivalent to an average waste package location), the relationship between the drift-wall temperature in the LDTH model, and the "smeared" potential repository-plane temperature in the SDT model is used to modify the temperatures in the SMT model; this results in an MSTH-model drift-wall temperature that

Table 3-44. Thermal-Hydrologic Variables Predicted with the Multi-Scale Thermal-Hydrologic Model at 610 Potential Repository Locations

Thermal-Hydrologic Variable	Drift-Scale Location at Which Predicted
Temperature	NFE host rock (5 m above crown)
	NFE host rock (mid-pillar at potential repository horizon)
	Maximum lateral extent of boiling
	Upper drift wall (crown of the drift)
	Lower drift wall (below invert)
	Drift wall (perimeter average)
	Backfill (crown)
	drip shield (perimeter average)
	drip shield (upper surface)
	waste package (surface average)
	Invert (average)
Relative humidity	Drift-wall (perimeter average)
	Backfill (crown)
	drip shield (perimeter average)
	waste package
	Invert (average)
Liquid saturation (matrix)	Drift wall (perimeter average)
	drip shield (perimeter average)
	Invert
Liquid-phase flux	NFE host rock (5 m above crown)
	NFE host rock (3 m above crown)
	Drift wall (crown)
	drip shield (crown)
	drip shield (upper surface average)
	drip shield (lower side at the base)
	Invert (average)
Gas-phase air-mass fracture	drip shield (perimeter average)
Gas-phase pressure	drip shield (perimeter average)
Capillary pressure	drip shield (perimeter average)
	Invert (average)
	Drift wall (crown; in matrix)
	Drift wall (crown; in fractures)
Gas-phase (water vapor) flux	Drift wall (perimeter average)
Gas-phase (air) flux	Drift wall (perimeter average)
Evaporation rate	Backfill (crown)
	drip shield (crown)
	drip shield (perimeter total)
	Invert (total)

approximates the effects of the most important TH processes at the drift-scale and the geometry effects of the mountain scale. At this stage of the MSTH Model abstraction methodology, the influence of 3-D drift-scale heat flow has not yet been added.

Because the SMT and SDT models share the same smeared-heat-source approximation and thermal-conduction representation of heat transfer, the relation between the SDT model temperature and the LDTH model drift-wall temperature allows for the SMT model temperature to be "corrected" for the influence of TH processes on temperature and for the influence of 2-D drift-scale dimensionality (orthogonal to the axis of the drift). The SMT, SDT, and LDTH models all share a blended heat-generation history, which blends the heat-generation histories of the entire waste package potential repository; hence, the heat-generation history is effectively that of an "average" waste package. The DDT model is a 3-D drift-scale model, which includes individual waste packages (with distinctive heat-generation histories) and accounts for thermal radiation in addition to thermal conduction between the waste packages and drift surfaces. The drift-wall temperatures for an average waste package—calculated with the combined use of the LDTH, SMT, and SDT models—are then further modified to account for waste package-specific deviations using the DDT model. This is accomplished using relations between local temperatures at various "point" locations along the drift (such as on the drift wall, drip shield surface, and waste package surface) and the corresponding line-averaged temperature in the DDT model.

For the DDT models, the waste package sequence in one modeled drift segment is repeated throughout the potential repository footprint. All emplaced waste packages fall into one of four major categories: 1) 21-PWR (pressurized-water reactor) waste packages, 2) 44-BWR (boiling-water reactor) waste packages, 3) HLW, and 4) drip shield NF. With respect to waste package-to-waste package variability, 42.9 percent of the waste packages are 21-PWR waste packages, 28.6 percent are 44-BWR waste packages, 21.4 percent are HLW waste packages, and 7.1 percent are drip shield NF waste packages. All waste packages are emplaced at the same time.

The results of the MSTH Model are integrated with the use of the Multi-Scale TH Abstraction Code (MSTHAC). Details of MSTHAC and the four type of models (LDTH, SMT, SDT, and DDT) are documented in the *Multi-Scale Thermohydrologic Model* (CRWMS M&O 2000i).

3.1.4.4 Multi-scale Thermal-Hydrologic Model Validation

The MSTH Model is performed using a method based on industry-standard finite-difference software that includes both mass and energy balances. The results depend on the inputs, and all inputs to the MSTH Model are to-be-verified. Model documentation addresses input data, assumptions, initial and boundary conditions, software, uncertainties, and other information as required to replicate the model results.

Several different validation approaches are used for the MSTH Model, including the following:

- **Inspection of model inputs and outputs.** A comprehensive analysis has been performed (CRWMS M&O 2000i) to evaluate the relationships between model inputs and outputs. This analysis involved more than 150 plots covering a wide range of input and output conditions.

The analysis indicates that the MSTH Model produces results that are consistent with current understanding of the physical processes that are accounted for in the model.

- **Black-box testing of MSTHAC.** Certain computational modules of the MSTH Model abstraction code (CRWMS M&O 2000i) were evaluated using test problems that allowed for verification by independent hand calculations.

- **Comparison of NUFT TH model results against the Large Block Test.** The Multi-Scale Thermohydrologic Model (CRWMS M&O 2000i) discusses the comparison of NUFT TH model results with data from the Large Block Test and the Drift Scale Test, and references other documentation that describes these results in more detail. A brief summary of this comparison is provided below.

- **Comparison of MSTH Model results against alternative numerical models.** A direct comparison is reported between an earlier version the MSTH Model, and a 3-D mountain-scale TH model (CRWMS M&O 2000i). A brief summary of this comparison is provided below.

On the basis of these multiple validation approaches and the results, it is concluded that the MSTH Model is valid for its intended use.

3.1.4.4.1 Comparison of NUFT TH Models with the Large Block Test

The NUFT model is used to simulate the entire history of the Large Block Test (see CRWMS M&O 2000i for details and references). The NUFT TH model of the LBT used the same hydrologic property set as used in the MSTH Model presented in this report. As an example of model comparison, Figure 3-71 shows the simulated temperature profile along Borehole TT1 at six times from 30 to 400 days, compared to observed temperature. The results show some over-prediction of temperature at earlier times, but the difference between simulated and measured temperatures decreases at later time. At 300 days and 400 days (25 days after power shutdown), the model is in close agreement. Evaluation of goodness-of-fit to measured temperatures shows accuracy of a few degrees Celsius; for temperatures measured along Borehole TT1. The difference improves markedly after power shutdown.

Figure 3-72 shows the simulated and measured liquid-phase saturation profiles along Borehole TN3, which is a vertical borehole used for neutron probe measurements of water content in the LBT. The field measurement times, 103, 361, and 501 days are compared to simulation times of 100, 365, and 500 days (the saturation varies slowly, so small differences between measurement and simulation times are negligible). The simulated dryout zone develops more slowly than observed, but the difference decreases with time. At 365 and 500 days, the model is in close agreement.

3.1.4.4.2 Comparison of NUFT TH Models with the Drift Scale Test

The NUFT model is used to simulate the Drift Scale Test (DST) heating period from test startup to the present (see CRWMS M&O 2000i for details and references). As an example of model comparison, Figure 3-73 compares the simulated and measured temperatures along Borehole

ESF-HD-137 at 365 and 547 days. The model results are in close agreement with measured temperatures, only slightly overpredicting temperatures in the superheated (T>100°C) zone and slightly underpredicting temperatures in the sub-boiling zone.

In general, agreement between the 3-D model and measured temperatures is poor for all locations close to the heated drift, at times less than 100 days. This results from representing the heated drift cross-section in the 3-D model as square, rather than cylindrical. On the other hand, the 2-D LDTH submodels more closely represent the cylindrical geometry. At times greater than 1 yr, agreement between 3-D model simulations and measured temperatures improves. The regions for which there is close agreement between simulated and measured temperatures fall into two categories: (1) the sub-boiling zone and (2) the zone of boiling and super-boiling temperatures along the heated drift. Close agreement in the sub-boiling zone indicates that heat flow there is dominated by conduction and that the assumed value of thermal conductivity is reasonable. Because of the relatively high, matrix liquid saturation in the sub-boiling zone, the wet value of thermal conductivity applies. Close agreement in the region close to the heated drift indicates that: (1) thermal radiation is adequately represented inside the heated drift, (2) heat flow in the boiling and above-boiling zones is dominated by conduction, and (3) the value of dry thermal conductivity is reasonable.

These results show that the submodels used in the MSTH Model, together with the use of the drift-scale hydrologic property set, are valid for their intended use. The results also show that the DDT submodel (which represents how thermal radiation affects 3-D heat flow in the EBS and near field) is valid for its intended use.

3.1.4.4.3 Comparison of the MSTH Model with an Alternative Numerical Model

Figure 3-74 compares the drift-wall temperature predicted by the MSTH Model with those predicted by an east-west cross-sectional mountain-scale TH model (see CRWMS M&O 2000i for details of the property sets and other model inputs, and references). The mountain-scale TH model is coarsely gridded, so the RH in the drift, and liquid-phase saturation at the drift wall, were not calculated. Accordingly, the comparison is limited to drift-wall temperature from the MSTH Model, vs. drift temperature from the mountain-scale TH model.

Before comparing the two approaches (Figure 3-74) it is important to discuss other differences in the models:

- The temperature predicted by the MSTH Model is the perimeter-averaged drift-wall temperature adjacent to an average 21-PWR medium-output WP. The MSTH Model includes in-drift 3-D calculations of WP temperatures, therefore some drift-wall locations are hotter than shown in Figure 3-74, while some are cooler. The temperature prediction in the mountain-scale model is for a grid block that occupies the entire drift, so it produces a lumped representation of the drift temperature.

- The mountain-scale TH model uses a line-averaged heat source that axially smoothes the differences between hotter and cooler WP locations.

- The initial areal power density (at emplacement) in the MSTH Model is 92.3 kW/acre, compared to 99.4 kW/acre in the mountain-scale TH model.

- The mountain-scale TH model representation of the heated footprint of the potential repository extends slightly further to the west than in the MSTH Model.

At the center of the potential repository (L4C3) the approaches predict nearly the same duration of boiling (Figure 3-74a). At the edge location (L4C1) which is 100 m from the western edge of the repository in the MSTH Model, the mountain-scale TH model predicts a longer duration of boiling (Figure 3-74b). During the post-boiling period, the temperatures predicted by the approaches are in close agreement. During the early heating period, the coarse gridding of the mountain-scale TH model does not capture the rapid drift-wall temperature rise that the more finely detailed MSTH Model predicts. Because of the coarse gridding, the mountain-scale TH model tends to overpredict the temperature at the mid-pillar location and thereby prevents condensate from draining between drifts. This results in greater condensate accumulation in the host rock above the potential repository horizon, which leads to unrealistic heat-pipe behavior. This behavior is demonstrated by the fluctuation in drift temperature from approximately 300 yr to 600 yr (Figure 3-74a). Note that at approximately 400 yr when the heat pipe zone has dried out, the temperature agrees with that predicted by the MSTH Model. Given the obvious differences between the MSTH Model and the mountain-scale model approaches, they are in reasonable agreement throughout much of the thermal evolution of the potential repository.

3.1.4.5 Multi-Scale Thermal-Hydrologic Model Results

The major results of the MSTH Model calculations are summarized in this section. During the preclosure period, host-rock temperatures remain below the boiling point for the mean- and upper-infiltration flux cases, while boiling occurs in the host rock for the lower-flux case. During the preclosure period, peak waste package temperatures of 100°C (for the mean flux case) and 110°C (for the low flux case) occur at 10 to 15 years; peak drift-wall temperatures of 86°C (for the mean flux case) and of 96°C (for the low flux case) occur at 20 to 25 years. Edge-cooling effects do not strongly affect preclosure temperatures. After the initial heat-up stage, relative humidity on waste packages varies from 45 percent to 75 percent during the preclosure period.

During the postclosure period, peak waste package temperatures of 305°C (for the mean flux case) and 315°C (for the low flux case) occur at 60 years. With regard to the influence of WP-to-WP variability in heat-generation rate, the difference in peak WP temperature between the hottest and coldest WP is 42°C.

During the postclosure period, peak temperatures on the lower drift wall of 195°C (for the mean flux case) and 205°C (for the low flux case) occur at 65 years; peak temperatures on the upper drift wall of 125°C (for the mean flux case) and 134°C (for the low flux case) occur at 65 years. The large (70°C) temperature difference between the upper and lower drift wall arises from the waste package, drip shield, and backfill configuration in the emplacement drift. Because the Overton Sand backfill acts as an insulator (K_{th} = 0.33 W/m°C), and because there is more of this insulative backfill above the waste package and drip shield than below, much of the heat generation from waste packages is focused to the floor of the drift, causing the large disparity in

temperature between the lower and upper drift wall. To reduce this disparity, it would be necessary to balance the amount of insulation above and below the waste package and drip shield.

During the very early postclosure period, the edge-cooling effect has a small effect on temperatures. By 100 years, the influence of edge-cooling is considerable, with waste package temperatures varying by 120°C from the potential repository edge to the geographic center of the potential repository; the outer 100 to 200 m of the potential repository are influenced by edge-cooling at 100 years.

The large difference in temperature between center and edge locations indicates a promising thermal-management option for a potential repository with an extended ventilation period (e.g., 100 years). Because the influence of edge-cooling penetrates significantly (by 100 to 200 m) from the edge toward the center by 100 years, it would be possible to emplace the hottest waste packages in the edge region while limiting peak temperatures. Cooler waste packages would be emplaced in the center region which does not experience edge-cooling effects in this time frame. In other words, the center region of the potential repository (an inherently hotter region) could receive a disproportionately large share of cooler waste packages, thereby reducing peak waste package temperatures in the center region. This thermal–load-balancing would also serve to reduce the variability in relative humidity predicted for waste packages at the edge vs. center locations.

Liquid-phase flux in the host rock above the drift is influenced by dryout and the thermal reflux of moisture. One of the important objectives of the design concept analyzed in the MSTH Model (CRWMS M&O 2000i) is to eliminate condensate buildup above the potential repository horizon, and thereby reduce the magnitude of the heat-pipe effect, in which liquid flux is fed by condensation. In the LDTH models, heat-pipe behavior above the dryout zone still enhances liquid-phase flux to well above ambient percolation fluxes. However, the duration of time that decay heat significantly enhances liquid-phase flux above the dryout zone is greatly reduced relative to the 80-MTU/acre potential repository analyzed in Total System Performance Assessment–Viability Assessment (TSPA-VA). An increase in liquid-phase flux lasts for less than 600 years (the duration of the present-day climate period). The magnitude of the ambient percolation flux during the monsoonal-climate period (600 < t < 2000 years) and during the glacial-climate period (2000 years < t) is comparable to, or greater than, that generated by decay heat from waste packages during the early preclosure period.

An important process affecting TH behavior in the emplacement drifts concerns the influence, on seepage into drifts, of the hydrologic properties of the Overton Sand backfill. During the early part of the preclosure period, the backfill is dry. As the temperature at the drift wall declines below the boiling point, the TH models predict that water flows from the fractures into the Overton Sand backfill. This flow is facilitated by the van Genuchten α value for Overton Sand being smaller than that of the fracture continuum representing the host-rock. (It is likely that if a coarser material were used with a value of α larger than that of the fracture continuum, the flow would be decreased. In the limit, if no backfill were used, the flow would be zero unless seepage occurred.)

Another process influencing liquid-phase flux in the drift is the heat-pipe effect. During the gradual rewetting of the backfill, the magnitude of liquid-phase reflux in the backfill above the drip shield can exceed the ambient percolation flux. Just as the magnitude of thermally driven liquid-phase reflux in the host-rock above the drift can locally exceed the background percolation flux, the magnitude of liquid-phase flux in the backfill above the drip shield can also exceed the background percolation flux. The low thermal conductivity and corresponding temperature gradient in the backfill facilitates vapor flux away from the drip shield, whereas gravity and capillarity induce liquid flux toward the drip shield. This response can result in a large evaporative flux on the surface of the drip shield. Because moisture returns to the backfill when temperature on the drift wall decreases below the boiling point, the onset of evaporation on the drip shield occurs first at the potential repository edge and then proceeds inward toward the center of the potential repository.

Another factor influencing liquid-phase flux in the drift is the geometry of the drip shield backfill, and invert. The liquid flux in the backfill beside the drip shield, encounters a restricted region for flow. Depending on the geometry of flow in the backfill, the flux can be focused by a factor of four, which is comparable to the ratio observed between the liquid-phase flux next to the lower side of the drip shield and the host-rock percolation flux.

An important EBS performance measure is the length of time the RH on the waste packages remains low. Relative humidity reduction on waste packages results from the following:

- **Relative humidity reduction at the drift wall** (and in the host rock) decreases strongly with proximity to the edge of the potential repository; significant reduction in drift-wall RH persists for 100 to 1000 years (depending on proximity to the edge) for the mean and upper infiltration-flux cases and for about 200 to 2000 years for the low flux case.

- **Relative humidity reduction on the drip shield** is relatively insensitive to proximity to the edge of the potential repository. Eventually, RH on the drip shield approaches 100 percent, similar to the host rock. For the mean and upper flux cases, this takes about 1000 to 2000 years to occur; for the low flux case, this takes about 3000 to 6000 years to occur. The end of the period of RH reduction on the drip shield corresponds to the time that seepage in the backfill has reached a steady-state condition.

- **Relative humidity reduction on the waste package** persists long after RH reduction on the drip shield has ceased. The persistence of decreased RH at the waste package, arises because of the temperature difference between the waste package and the drip shield. Because the interval between the waste package and the drip shield is an open cavity, thermal radiation controls this temperature difference. Additional design measures to promote a greater temperature difference, could prolong the lower-RH conditions at the waste package.

The maximum lateral extent of boiling temperatures (away from the drift wall) is a good indication of spatial extent of rock dryout around the emplacement drifts. The lateral extent of boiling is considerably greater for the low infiltration-flux case than for the mean or upper flux cases. For the median waste package location, the maximum lateral extents of boiling are 8.4 m, 9.1 m, and 10.5 m for the upper, mean, and low flux cases, respectively. The hottest (and driest)

waste package location in the low flux case has a maximum lateral extent of boiling of 18 m; therefore, because the drifts are 81 m apart, a maximum of 44.4 percent of the potential repository horizon is driven to the boiling point. The hottest (and driest) waste package locations in both the mean and upper flux cases have a maximum lateral extent of boiling of 9.7 m; therefore, a maximum of 24 percent of the potential repository horizon is driven to the boiling point. For the range of infiltration flux considered, the maximum percentage of the potential repository horizon that can be driven to the boiling point lies between 24 percent and 44.4 percent.

There is much greater difference in dryout behavior (as evidenced by the maximum lateral extent of boiling and by RH reduction) between the mean and low infiltration-flux cases than between the mean and upper flux cases. Therefore, if one considers a percolation threshold above which rock dryout becomes substantially limited by percolation, the threshold would be near the mean infiltration-flux case. Larger values of the percolation flux greatly limit the extent of boiling temperatures and rock dryout.

3.2 INTEGRATED MODEL DEVELOPMENT

No single model can describe all aspects of the EBS and its interaction with the surrounding host rock, especially because the approach must remain flexible to accommodate an evolving engineering design. Rather, the focus is on the modeling and analysis of the basic processes of fluid flow, heat transfer, radionuclide transport, and chemical interaction, as controlled or influenced by design, operating practices, and characteristics of the disturbed natural system.

The *Engineered Barrier System Process Model Report* documents the development and application of a linked set of process models, and their abstractions, as input to TSPA for determining the contribution of the EBS total system performance. As described at the beginning of Chapter 3, this PMR contains four major process models, documented in Sections 3.1.1 through Section 3.1.4. These sections summarize the conceptual development, model implementation, input data, codes and routines, model results, and limitations on use, for each process model. The EBS PMR also contains a major analysis of FEPs relevant to the EBS, in Section 2.4.

Because the EBS is not associated with any Principal Factors in the Repository Safety Strategy (Rev 3), model development relies heavily on the use of defensible bounding calculations. This has been especially appropriate where data are limited, or the future evolution of the system is highly uncertain.

Process model uncertainties and validation are discussed in Sections 3.1.1 through 3.1.4. Section 3.2.1 summarizes the abstraction and preparation of process model results for input to the TSPA Model.

3.2.1 Abstraction of the Models

3.2.1.1 Abstraction of the Physical and Chemical Environment Model

In general, knowledge of the physical and chemical environment in the emplacement drifts is required to quantify EBS processes and to predict the quantitative transport of released

radionuclides. Description of the environment includes: (1) evolution of groundwater flow in the EBS and transport pathways into the host rock, and (2) composition of groundwater moving along those pathways. Information on physical environment characteristics is needed to quantify groundwater movement is in the drift that transports radionuclides by advection. Brine composition is needed to predict breaching of drip shields and waste packages by corrosion, and to quantify processes that release and transport radionuclides. The purpose of the *Physical and Chemical Environment Abstraction* (CRWMS M&O 2000j) is to summarize:

- The role of in-drift physical and chemical environments in the Total System Performance Assessment (TSPA)

- The configuration of engineered components (features) and critical locations in drifts

- Processes and critical locations of processes that can affect the P&CE

- Couplings and relationships among features and processes in the drifts

- Methods for using conceptual and parameter inputs to the TSPA

- Parameters calculated by process models transmitted to .

Note that the physical and chemical environment parameters ultimately used in the TSPA largely depend on the input requirements of the drip shield and waste package corrosion models, and the EBS transport model, as they are implemented in the TSPA. Physical and chemical environment parameters are used by the TSPA to simulate the following aspects of performance:

- Corrosion of drip shields and waste packages

- Salt precipitation, salt redissolution, and resulting groundwater compositions at one or more locations in the drifts and in released groundwater

- Mobilization and release of materials from the engineered barrier system both in dissolved and colloidal form

Specific parameters that are available for use in the TSPA are summarized in Table 3-45.

Table 3-45. Parameters available for TSPA

Applicable Process	Water Composition Input Parameters to TSPA-SR
Drip Shield Corrosion	pH Chloride concentration
Waste Package Corrosion	pH Chloride concentration Model to calculate mass of microbes per unit drift length
EBS Transport by Colloids in Invert	Ionic strength Concentration and composition of colloids
Radionuclide Mobilization and Release from Engineered Barrier System and Corresponding Groundwater Chemical Environment	PH Ionic strength Total dissolved carbonate Chloride concentration Oxygen fugacity Carbon dioxide fugacity Concentration and composition of colloids

The parameters listed in Table 3-45 specify groundwater compositions and microbial masses for potential application at the following three locations:

- At the outer surface of the drip shield
- At the outer surface of the waste package
- Within the invert

The following sections summarize the AMRs that provide abstracted physical and chemical environment parameters for use in the TSPA.

3.2.1.1.1   In-Drift Gas Flux and Composition

As summarized in this section, the *In-Drift Gas Flux and Composition Analysis/Model Report* (CRWMS M&O 2000e) provides a basis for abstracting the values of the gas flux and composition in the emplacement drifts for the following major geochemical constituents:

- Carbon dioxide (CO_2)
- Oxygen (O_2)
- Nitrogen (N_2)
- Steam or water vapor (H_2O)

This model includes the following important processes affecting gas composition in the drift:

- Ambient and thermally perturbed fluxes of gas into the drift from the geosphere

- Fluxes of aqueous solutions into the drift

- Possible source terms for gas constituents in water just outside the drift

- Boiling of the water in the emplacement drift

- Possible chemical reactions among the groundwater, gases, and engineered materials within the emplacement drift

- Radiolysis

The major introduced materials that may act as sources or sinks for oxygen and carbon dioxide in the gas phase are evaluated for their potential to alter the in-drift gas composition. That is, mass-balance calculations that consider the major potential sinks of both O_2 and CO_2 are assessed to track gas composition within the drift relative to the incoming gas composition.

This model predicts that gas composition everywhere within the drift is homogeneous because gas-transport rates are sufficiently high, even if only diffusive movement of gas constituents is considered, to mix gases in this unsaturated environment at the scale of a drift diameter. For consideration of local gas heterogeneity, more detailed process models of the in-drift environment would be needed.

For the effects of radiolysis, this model assumes that the production of gaseous radiolytic products in the drift is bounded by the in-package capacity to produce gaseous radiolytic products.

All metals and alloys in the disposal drifts are considered equivalent to iron (Fe) for the purpose of the mass-balance calculation for gas-phase constituents. This assumption is used only to simplify the calculation of the amount of oxygen consumed in corrosion of the metals and alloys. Other metals than Fe are present in the disposal drifts, particularly in the spent fuel wastes and associated packages and containers; this assumption, however, is expected to introduce an error of less than one order of magnitude in the calculated oxygen demand. This degree of uncertainty will have no effect on the scoping mass-balance approach used in this abstraction.

The carbon (C) contained in the mild steel in the disposal drifts is assumed to not act as a significant source of CO_2 to the in-drift gas mixture. Because the abstraction model has determined that more than ample CO_2 is available (from the gas flux through the drifts) to completely saturate available CO_2 sinks, this assumption can have no significant impact on the results of this analysis.

The conceptual model and mass-balance calculations presented here suggest that the in-drift gas flux and composition will not be strongly affected by interactions with in-drift and near-drift materials. However, in-drift gases will be displaced by steam during the thermal period, thus reducing the amounts of all gases (except water vapor) in the drifts during that period. The resulting decrease in oxygen O_2 fugacity, is not expected to be sufficient to affect redox reactions occurring in the repository.

The conclusion that more than ample fluxes of CO_2 and O_2 are available to meet the requirements for chemical reactions taking place in the drifts is based on results from thermal-hydrologic models such as those for the TSPA-Viability Assessment, discussed in Section 3.1.2.2. It is noted that the gas fluxes predicted by these models result from large-scale

circulation in the UZ throughout the volume of host rock occupied by the repository, thus knowledge of large-scale properties and processes is implicit in the use of these results.

Finally, if the boundary-condition composition of any gas-phase constituent entering the drift were to be decreased by more than an order of magnitude, consideration of the compositionally driven diffusion of that constituent from the water in the host rock just outside the drift may be included to improve the realism of the analysis. Such additional potential sources would be added to those represented by the gas flux and liquid seepage flux. A detailed discussion of uncertainties and limitations appears in the *In-Drift Gas Flux and Composition Analysis/Model Report* (CRWMS M&O 2000e).

The model is considered valid and appropriate for its intended use (bounding the gas fluxes and compositions within emplacement drifts), because this abstraction uses conservative approaches.

3.2.1.1.2   Introduced Materials

Introduced materials include cement grout, backfill, invert, and metallic materials or alloys. The following section addresses cement, backfill, and invert materials. These materials are also discussed in Section 3.1.2.3, along with metals, alloys, and other materials.

Seepage-Cement Interaction

The purpose of the seepage–cement interactions analysis (CRWMS M&O 2000l) is to predict the time required for carbonation through reaction with gas phase carbon dioxide of the calcium hydroxide [$Ca(OH)_2$] and other susceptible calcium-bearing phases present within the cementitious grout used to anchor the rockbolts in the drift ground-support system. The time required for complete carbonation is calculated for three different partial pressures of CO_2: 1 ppm, 100 ppm, and 1000 ppm.

For this analysis, Fick's First Law of Diffusion is used to make two estimates:

- Amount of CO_2 that can be provided by steady-state diffusion under for the stated conditions

- Relationship between the degree of depletion of the atmospheric CO2 in the gas phase, and the distance to a rockbolt undergoing carbonation with a third analysis estimated time required for carbonation through reaction with aqueous-phase CO_2

From current understanding of geochemical carbonation processes, stoichiometry determines the mass of CO_2 required to quantitatively transform portlandite or other reactive calcium phase into an equivalent amount of calcite. Because the transformation of portlandite into calcite is kinetically very fast, the transfer of atmospheric CO_2 (by diffusion through the rock matrix to the grouted rockbolt) controls the rate of portlandite carbonation. In summary, this analysis has derived the time required for diffusion-controlled carbonation of the grout surrounding a rockbolt. This analysis shows that the time required for carbonation is proportional to the product of CO_2 partial pressure and the gaseous diffusion coefficient of CO_2. This analysis also establishes the relationship between the depletion, under steady-state conditions, of the local gaseous CO_2 concentration and the distance from the rockbolt grout to the CO_2 source.

Seepage-Backfill Interaction

A summary of the analysis of seepage–backfill interactions is discussed next. This analysis (CRWMS M&O 2000k) addresses potential dissolution and precipitation interactions of seepage with quartz sand backfill, and is presented in Section 3.1.2.3. Incoming seepage is affected by evaporation, which is addressed in a separate analysis/model report (CRWMS M&O 2000g). Evaporation in the drift and surrounding host rock will affect the quantity and composition of seepage, especially during the first few thousand years. Seepage composition is potentially important in evaluating interaction with the backfill. The following processes are incorporated in the seepage–backfill interactions model:

- Evaporative concentration of incoming seepage
- Precipitation of dissolved solids resulting from evaporative concentration
- Dissolution of precipitates and backfill

This model is an application of the High Relative Humidity (HRH) Salts Model (Pitzer model) developed in the *In-Drift Precipitates/Salts Analysis* (CRWMS M&O 2000g) and described in Section 3.1.2.5. It evaluates the potential interaction of evaporated seepage with the backfill.

The seepage-backfill interaction model is conceptually identical to the HRH Salts Model described in Section 3.1.2.5, which calculates the composition of evaporatively concentrated seepage water, except that the solubility equilibrium of quartz is also monitored in the calculations. Solubility equilibrium for quartz-sand backfill is investigated by examining the quartz saturation indices for each of the cases simulated by the HRH Salts Model (Section 3.1.2.5). These cases include a set of simulations for solution composition corresponding to relative humidity (RH) of 85 percent and greater. Cases for RH less than 85 percent are ignored in this model because such concentrated conditions favor precipitation of silica and supersaturation of quartz (CRWMS M&O 2000g).

The results indicate that the interaction of the backfill with seepage derived from evaporated J-13 well water will likely be negligible. Dissolution of quartz sand is not predicted except for unlikely scenarios. Predictions of quartz saturation are reasonable because evaporating water tends to favor precipitation rather than dissolution of silica. The greatest potential sources of uncertainty in these analyses are the predicted inputs (e.g., the seepage rate and seepage composition) that feed the analyses.

Seepage-Invert Interaction

A conceptual model for seepage–invert interactions is developed and reported in *Seepage/Invert Interactions* (CRWMS M&O 2000m). The model identifies possible pathways for seepage into the invert, and material interactions with the seepage. It estimates the conditions that will prevail as the environment evolves. The purpose of the model is to qualitatively evaluate the physical and chemical conditions and processes in the invert.

The invert is composed of the same Topopah Spring welded tuff that makes up the host rock. During the thermal period, however, the invert is expected to experience thermal conditions not

reached in the host-rock. Porosity in the invert will provide locations where silica, silicates, and evaporite minerals, including soluble alkali salts, will precipitate.

The invert will contain steel and copper metal components, which will provide surfaces where transition-metal carbonates, hydroxides, sulfates, and chlorides may form by reaction with seepage. These phases are not likely to be sufficiently abundant to buffer conditions in the physical and chemical environment, or to alter the chemical composition of water passing through the invert.

For a finite period, liquid seepage passing through emplacement drifts will have elevated ionic strength. Seepage composition will evolve as the precipitated salts are dissolved. Depending on the mass of precipitates produced and the flux of seepage into the invert, the elevated ionic strength may be sufficient to destabilize colloids or to counteract sorption.

Interaction with seepage will produce mineralogical and physical changes in the crushed tuff invert material. Expansion of alteration products, and long-term physical confinement by the overlying backfill, could decrease porosity and thereby decrease permeability. In the current design, the portion of the invert under the DS is not physically confined, and may therefore undergo smaller decreases in porosity or permeability. Conceptually, invert–seepage reactions are therefore expected to create preferred flowpaths immediately beneath the WPs. However, the permeability in this portion of the invert will not increase, and the transmissivity of the invert overall, will tend to decrease with time.

3.2.1.1.3   Microbial Effects

The purpose of the *In-Drift Microbial Communities Model* (CRWMS M&O 2000f) is to bound the biomass that could be present within a given length of repository drift. The outputs from this model support the microbially influenced corrosion (MIC) aspects of WP corrosion modeling, and evaluation of colloidal transport of radionuclides. Refer to Section 3.1.2.4 for a discussion of potential microbial effects on the EBS and a description of the microbial communities model (MING).

The MING code is used in the *In-Drift Microbial Communities Model* (CRWMS M&O 2000f) to develop biomass and microbial abundance estimates for the potential repository. The code and the associated conceptual model do not attempt to quantify the effects of microbial colonies or biofilms on potential repository materials; instead, they attempt to bound the overall, bulk effect of microbes on the in-drift geochemical environment (IDGE).

- For TSPA, the MING code will provide scenario-dependent results for abundance of microbes per meter of drip shield or WP through time, for each WP type and potential repository configuration. The different scenarios will include WP types (e.g. 21-PWR vs. DHLW) and other conditions:

- Drift ground-support options (e.g. use of steel, and grouted rockbolts)

- Different material lifetimes, based on estimates of general corrosion rates

- Different drift boundary conditions, such as TH results for the center of the potential repository vs. the edge

- Aqueous transport concepts (e.g. dripping conditions on the WP, vs. no dripping on the WP until the DS is breached)

Each such scenario can be used by the WP-degradation model to represent the variability and distribution of microbes over the surface of the DS and the WP. Biomass will be applied to the WP surface by estimating the surface area that can be covered by a one-cell thick biofilm, thus the proportion of the WP surface that is subject to MIC will be estimated. The results of the WP-degradation model will be used directly in TSPA calculations.

Figure 3-42 (Section 3.1.2.4) shows a typical abstraction given as a plot of grams of biomass produced per lineal meter of emplacement drift per year versus time.

Three validation tests were conducted for the *In-Drift Microbial Communities Model* (Section 3.1.2.4). The first test replicated a model that was constructed for the Swiss low-level repository program. The result indicates that MING handles the types of calculations that are required where natural barrier components are combined with the engineered barrier components to calculate microbial growth. The second test demonstrates that the model can simulate ambient conditions within the Exploratory Studies Facility (ESF), and other analog measurements. The second test also confirms that water availability limits microbial growth in the potential repository host rock. Calculated results also show that the microbial community is limited by the availability of redox energy. The third test indicates that the numbers of organisms reported by MING are generally within an order of magnitude of values measured in controlled laboratory tests. The model results confirm the conclusions reported from lab experiments, namely, that the availability of water (growth media) is a primary factor limiting microbial growth, and that phosphorous is the primary limiting nutrient in the potential host rock. The results also show that in energy-limited systems, the impacts due to gas availability, variations in pH and water chemistry, and material lifetimes, are relatively small. However, in nutrient-limited systems, these influences produce greater impacts. Results from these tests indicate that model predictions are accurate to within an order of magnitude, and that the model is valid for its intended use in TSPA.

3.2.1.1.4   Precipitates and Salts

The *In-Drift Precipitates/Salts Analysis* (CRWMS M&O 2000g) evaluates the effects of evaporation on water composition at a given location in the EBS (e.g. the drip shield surface). Evaporation has a marked effect on water composition and, for the current design, will likely produce brines and salts in the EBS. See Section 3.1.2.5 for more detailed description of the precipitates and salts process models, defined here to include the Low Relative Humidity (LRH) Salts Model, and the High Relative Humidity (HRH) Salts Model.

Results from the precipitates and salts models will be implemented directly in TSPA calculations. For TSPA the evolution of the potential repository is divided into time periods, in each of which several environmental parameters are estimated (abstracted) as representative, constant values. Environmental parameters that are inputs to the In-Drift Precipitates/Salts

Analysis include temperature, relative humidity, seepage flux, seepage flux composition, and evaporation rate. For each combination of these inputs, a unique solution from the precipitates and salts models is developed.

Calculated results for a plausible subset of possible environmental conditions are used to develop a response surface, for use in TSPA to interpolate results for any combination of input conditions. Input variables are limited to a small number of values, including estimated minima and maxima. The response surfaces define the pH, chloride concentration, and ionic strength as dependent variables, and are implemented as lookup tables. The look-up tables include the following independent variables: temperature, relative humidity, and seepage flux composition, and relative evaporation rate (i.e., evaporation rate relative to seepage rate). At a particular time step, the pH, chloride concentration, and ionic strength are obtained or interpolated from these tables, from within the TSPA. Table 3-46. is an example of the lookup tables in *In-Drift Precipitates/Salts Analysis* (CRWMS M&O 2000g):

Table 3-46. Lookup Table for Average J-13 Well Water Seepage at $P_{CO_2} = 10^{-1}$ atm

Input Parameters			Precipitates/Salts Model Output		
RH (%)	T (°C)	R^{es}	pH	Chloride (molal)	Ionic Strength (molal)
< 50.3	na[a]	na	dry	dry	dry
50.3	na	na	8.65	3.77E-03	3.65E+01
51.0	na	na	8.65	4.52E-02	3.49E+01
53.1	na	na	8.65	1.87E-01	2.95E+01
55.2	na	na	8.65	3.06E-01	2.49E+01
60.5	na	na	8.65	6.03E-01	1.35E+01
65.7	na	na	8.65	7.26E-01	8.77E+00
71.0	na	na	8.65	7.56E-01	7.62E+00
76.2	na	na	8.65	7.62E-01	7.39E+00
81.5	na	na	8.65	7.58E-01	7.56E+00
85.0	na	na	8.65	7.52E-01	7.79E+00
> 85	95	0	6.58	2.01E-04	3.74E-03
> 85	95	0.1	6.62	2.23E-04	4.15E-03
> 85	95	0.5	6.83	4.02E-04	6.85E-03
> 85	95	0.9	7.31	2.01E-03	2.21E-02
> 85	95	0.99	8.14	1.98E-02	2.09E-01
> 85	95	0.999	8.67	1.73E-01	1.82E+00
> 85	95	> or = 1	8.65	7.52E-01	7.79E+00
> 85	75	0	6.42	2.01E-04	3.74E-03
> 85	75	0.1	6.47	2.23E-04	4.15E-03
> 85	75	0.5	6.71	4.02E-04	7.51E-03
> 85	75	0.9	7.21	2.01E-03	2.44E-02
> 85	75	0.99	8.03	1.98E-02	2.09E-01
> 85	75	0.999	8.59	1.73E-01	1.82E+00
> 85	75	> or = 1	8.65	7.52E-01	7.79E+00
> 85	45	0	6.21	2.01E-04	3.74E-03

Input Parameters			Precipitates/Salts Model Output		
RH (%)	T (°C)	R^{es}	pH	Chloride (molal)	Ionic Strength (molal)
> 85	45	0.1	6.25	2.23E-04	4.15E-03
> 85	45	0.5	6.50	4.02E-04	7.47E-03
> 85	45	0.9	7.03	2.01E-03	2.66E-02
> 85	45	0.99	7.85	1.98E-02	2.16E-01
> 85	45	0.999	8.47	1.73E-01	1.82E+00
> 85	45	> or = 1	8.65	7.52E-01	7.79E+00
> 85	25	0	6.08	2.01E-04	3.74E-03
> 85	25	0.1	6.12	2.23E-04	4.16E-03
> 85	25	0.5	6.37	4.02E-04	7.47E-03
> 85	25	0.9	6.95	2.01E-03	2.91E-02
> 85	25	0.99	7.74	1.98E-02	2.21E-01
> 85	25	0.999	8.40	1.73E-01	1.84E+00
> 85	25	≥ or = 1	8.65	7.52E-01	7.79E+00

^{a} not applicable

From CRWMS M&O 2000g

This set of results was obtained by implementing the precipitates and salts model for several values of each input parameter, spanning the possible combinations of values for the parameters. The input variables are limited to a small number of input parameter values, including approximate minima and maxima. The only input parameter that is not varied in this table is seepage composition, which is taken to be average J-13 well water. An additional lookup table was generated using the seepage composition developed in the THC model abstraction (CRWMS M&O 2000y).

Validation tests are reported for the precipitates and salts models in Section 3.1.2.5, which show that the models are valid for their intended uses. The abstraction of process model results into TSPA through the use of lookup tables is valid as long as chemical conditions do not depend on the local history of such conditions, which requires that input conditions vary slowly over time. The HRH Salts Model results (for RH greater than 85 percent) are steady-state values derived from constant input conditions. The LRH Salts Model results (for RH less than 85 percent) are also controlled by RH. These two models are discussed further below.

For the HRH model, it is shown in Section 6.6.1.2 of the *In-Drift Precipitates/Salts Analysis* (CRWMS M&O 2000g) that after as few as 10 pore volumes, the chloride concentration of the water within the reaction cell is not affected by the initial concentration. Instead, it depends primarily on the chloride concentration in the incoming seepage (C_i^s) and the relative evaporation rate (R^{es}). The derived equation relating these parameters is:

$$\frac{C_i^{rs}}{C_i^s} = \frac{1}{1 - R^{es}}$$

where c_i^{rs} is the steady state molal concentration of soluble component i in the reaction cell. For example, a R^{es} value of 0.9 (i.e., an effective evaporation rate equal to 90 percent of the incoming seepage rate) implies that the steady-state concentration of a highly soluble component (e.g., chloride) will be 10 times the concentration in incoming seepage. This equation can be used if components do not reach solubility limits, which may change with time in conjunction with changes in pH and CO_2 fugacity. If the chemical evolution of evaporated seepage in a flow-through cell is evaluated for constant input conditions, and sufficient through-flow (e.g., more than 100 reaction cell volumes following a sharp change of input conditions, fewer for more gradual changes) then the results will not be affected by history.

For the LRH model, RH controls the composition of the equilibrated solution because it fixes the activity of water. Thus, the importance of RH, combined with the presence of Na, Cl, NO_3, K, CO_3, and SO_4 which form hygroscopic brines, abates the effect of history on the brine composition. Although the abundance of accumulated salts may affect the quantity and characteristics of brine produced, the potential history effects on estimated chloride concentration and ionic strength are negligible (for the intended use of the model).

3.2.1.1.5 Colloids

Several types of colloids are expected to be generated within the potential Yucca Mountain repository system. Mineral colloids include clays, iron oxides and oxyhydroxides (ferrihydrite, goethite, and hematite), and silica; organic colloids include microbes and fragments as well as humic and fulvic acids.

Colloids will be present at the WF, in the drift, and in the unsaturated and saturated zones. At the WF, colloids will be produced during the degradation of the WF and WP. In the potential repository drifts, additional colloids may be produced from the degradation of steel and cementitious components of the EBS. Other types of colloids (mineral and organic) will be present in the UZ and SZ and may migrate into the potential repository, or along transport pathways. Colloids present in the WF and WP environments are discussed below, based on the conceptual models described in *In-Drift Colloids & Concentrations Analysis/Model Report* (CRWMS M&O 2000d).

Intrinsic, or "true" colloids are formed from polymerization of hydrolyzed radionuclide ions. For intrinsic colloids to form the fluid composition must be saturated with respect to a solid phase, so formation of intrinsic colloids is limited by solubility. Intrinsic colloids were not detected in experimental investigations of spent fuel at Argonne National Laboratory (ANL).

Pseudocolloids may be formed by the incorporation, adsorption, or ion-exchange of dissolved radionuclides onto existing colloids, which may be formed either from WF degradation, EBS material degradation, or introduced with groundwater. Radionuclides that might otherwise sorb to immobile substrates can instead attach to mobile, colloidal particles and thereby increase the "source term" which describes the total inventory of (dissolved plus colloidal) radionuclides. Colloids may facilitate radionuclide migration both within the potential repository and in the far field.

Waste form colloids, or primary colloids, may provide the most significant contribution to colloid-facilitated radionuclide transport. These colloids form from nucleation of colloids from waste-form dissolution and spallation of colloid-sized waste-form alteration products that contain radionuclides; they have the potential for increasing mobile concentrations higher than achievable with real colloids or pseudocolloids.

Three types of groundwater colloids may be present at Yucca Mountain:

- **Mineral fragments** tend to be hydrophilic (i.e., hard particles that are kinetically stabilized or destabilized by electrostatic forces) and may consist of crystalline or amorphous solids. Steric coatings may enhance the stability of mineral fragments as colloids, by preventing close contact. Mineral fragments may act as substrates for sorption of radionuclides (they may also consist of precipitated or coprecipitated actinide solids).

- **Humic substances** are hydrophobic particles that are stabilized by solvation forces. They can be powerful substrates for uptake of metal cations and are relatively small (less than 100,000 atomic mass units).

- **Microbes** are relatively large colloidal particles that are stabilized by hydrophilic coatings on their surfaces. Microbes may act as substrates for extracellular actinide sorption, or they may actively bioaccumulate radionuclides intracellularly.

Because of the relatively large sizes of microbes, they are very susceptible to filtration in geologic media. Consequently, microbe-facilitated contaminant transport is not considered in the abstraction. Further, considering the limited complexation capacity of humic substances in the system, humic substances are not considered as groundwater colloids.

Clays, silica, hematite, and goethite colloids occur as mineral colloids in groundwater in the vicinity of Yucca Mountain, with clays and silica the most abundant. It is assumed for simplicity and conservatism that groundwater colloids are clays and that (1) iron oxide or oxyhydroxide colloids are present in very small amounts, and (2) plutonium (Pu) and (AM) sorb more strongly to, and generally desorb more slowly from, clays than silica colloids. Accordingly, silica colloids are neglected in this conservative approach.

It is assumed that small quantities of these colloids will enter a failed WP and be available to interact with released radionuclides. Further, it is assumed that groundwater entering the drift and invert from the surrounding unsaturated zone will mix, under certain circumstances, with releases from a failed WP and that the groundwater colloids will likewise be available to interact with released radionuclides. The groundwater is assumed to contain smectite colloids whose stability and concentration are determined by the ionic strength and pH of the groundwater.

There are three types of colloids in the release: (1) WF colloids, assumed to be smectite, (2) WP corrosion colloids, assumed to be iron oxide or oxyhydroxide, and (3) groundwater colloids, assumed to be smectite. Some of these colloids are associated with radionuclides as they exit the WP. The WF colloids may have irreversibly attached (embedded) or reversibly attached

(sorbed) radionuclides. Sorption of radionuclides on groundwater colloids, or colloids derived from corrosion products, is assumed to be reversible.

The mass of radionuclides irreversibly attached to WF colloids is determined from reaction within the WP. The mass of radionuclides reversibly attached to all three types of colloids is determined from the product of three parameters: (1) the mass concentration of dissolved (aqueous) radionuclide in the fluid, (2) the mass concentration of colloid material in the fluid, and (3) the radionuclide distribution coefficient (K_d) for each specific radioelement on each colloid type.

The mass concentration of radionuclides leaving the WP is calculated at each time step, in the TSPA. The mass concentration of colloids is affected by the ionic strength and pH of the fluid, and is also determined at each time step. The K_ds for the various radionuclides on the two mineralogical colloid types have been measured in the laboratory.

Once the groundwater and WP releases mix within the invert, a fluid of combined chemistry is produced, and new mass concentrations of dissolved radionuclides and colloids, as well as masses of radionuclides sorbed onto colloids, are calculated in the TSPA. The total mass of radionuclides sorbed onto colloids, comprises mass concentrations for radionuclides irreversibly and reversibly attached to WF (smectite) colloids, reversibly attached to corrosion product (iron oxide or oxyhydroxide) colloids, and reversibly attached to groundwater (smectite) colloids.

3.2.1.2   Abstraction of the Engineered Barrier System Radionuclide Transport Model

Radionuclide transport out of the WF and WP, through the invert system, and into the unsaturated zone (UZ) is dependent on several events. The WP must degrade, providing a path out of the WP, and the WF must also degrade to allow radionuclide release. The primary transport medium is water: either a water film or moving water is necessary for radionuclide transport out of the WP and through the remainder of the EBS. Following are the key factors affecting transport of radionuclides through the EBS:

- Performance of the DSs
- Performance of the WPs
- Protection provided by cladding
- WF degradation rate
- Entry and movement of water through WPs
- Solubilities of radionuclides
- Transport of radionuclides through and out of the WPs
- Transport of radionuclides through the invert below the WPs
- Colloidal transport of radionuclides

After the WPs are emplaced, radioactive decay of the waste will heat the drifts and locally perturb the normal percolation of water. As the drifts cool, some of the water percolating through the mountain may drip into the drifts and subsequently contact some of the DSs. Over time, the DS, WP, and other components of the EBS are expected to degrade.

Once a DS is breached, water may contact the WP. Once a WP is breached, water may enter the package as water vapor or as drips. If the cladding is also breached, radionuclides may start to dissolve in the water. The dissolved concentration of each radionuclide mobilized from the WF cannot exceed the radionuclide solubility limit, unless suspended colloids are included. Colloids may be important for two reasons: they may increase the release of radionuclides from the WP, and they may increase the transport velocity of radionuclides. Radionuclides mobilized in water as dissolved or colloidal species may then be transported by advective and diffusive transport from the WF, through the WP, and out of breaches in the WPs. Once outside the package, the radionuclides will be transported through the invert predominantly by diffusion, if water is not flowing through the invert, or by advection, if an appreciable amount of water is flowing through the invert.

The emphasis in the *Engineered Barrier System Radionuclide Transport Abstraction* (CRWMS M&O 2000a) is on a conservative approach that bounds the response of the EBS. These conservatisms are appropriate because of the uncertainty in the response of a very complex engineered system over long periods of time. This model is valid and appropriate for its intended use because this abstraction is designed to be a bounding, conservative model. Following are noteworthy features and conservatisms in this abstraction:

- **Seepage through the DS always falls on a WP**–DS placement in the current potential repository design is such that any separations between shields should be above the small axial gap between adjacent packages. This feature is ignored because the quartz-sand backfill that falls through the DS separation will probably fill the axial gap and provide a flow path onto the WP.

- **Seepage is assumed to uniformly wet the DS and WP**–Because seepage will vary spatially and temporally over the approximately 10,000 WPs in the potential repository, it seems reasonable to represent the response of groups of WPs as averages for performance assessment. In this average, the DS or WP is assumed to be uniformly wet so that each patch or pit, independent of its exact position on the surface of the WP, will always experience a small advective flux. Note that WP degradation modeling for the TSPA-SR only predicts the location of patches and pits in terms of the upper or lower surfaces of the WP; thus, the independence of position is consistent with WP degradation calculations.

- **There is no advective flow or transport through a stress-corrosion crack (SCC) in the WP**–Current analyses show that a thin film will bridge the crack with a fluid-filled meniscus that prevents advective flow into the crack. In addition, such cracks will only occur in the shadow of the skirt around the welded end cap, making it unlikely that large volumes of water will reach the crack through vertical drips and seepage

- **The WF is assumed to be covered with a thin liquid film that supports radionuclide diffusion at all times**–Radionuclides will be released by diffusion through a stress-corrosion crack, even when the DS is intact and there is no advective flux into the WP. Note that this transport pathway also functions in the TSPA model when the package is hot and in-package evaporation may be sufficient to maintain the WF in dry conditions.

- **Release of radionuclides through advective transport is independent of the number of patches or pits through the WP**–Advective transport out of the WP is based on a flow-through model that is independent of the number of penetrations through the WP. For example, a WP with one or more penetrations on its upper surface and none on its lower surface will still have advective transport into the invert.

- **Cracks and pits are assumed to be filled with corrosion products and to be fully saturated**–These assumptions enhance diffusion.

The use of a bounding diffusion coefficient for all radionuclides may overestimate the diffusivity of actinide complexes by an order of magnitude. The assumption to ignore the effect of saturation on diffusivity has the effect of overestimating diffusivity by two to three orders of magnitude. These assumptions enhance diffusion.

The following sections provide a summary of the EBS transport abstraction model (CRWMS M&O 2000a).

3.2.1.2.1   Flow and Transport Pathways

The conceptual model for flow through the EBS identifies eight key flow pathways.:

- **Seepage Flux**–This is the input flux or boundary condition.

- **Through the Drip Shield to the Waste Package**–Flux through the DS is based on the ratio of patch and pit areas to the total surface area of the DS. Patch and pit areas of the DS and WP are calculated by the Waste Package Degradation software (WAPDEG).

- **Drip Shield to Unsaturated Zone (Diversion around DS)**–Any seepage flux that doesn't go through the DS is assumed to bypass the EBS and flow straight into the UZ.

- **Through the WP to WF**–Flux into the WP is proportional to the product of the flux through the DS and the ratio of patch/pit areas to total surface area of the WP.

- **Waste Package to Invert (Diversion around WP)**–Flow that doesn't go through the WP is diverted to the invert.

- **Invert to WP (Evaporation)**–If the DS is cooler than the invert, all the evaporative flux from the invert is assumed to drip on the WP. If the DS is hotter than the invert, there is no dripping on the WP from the evaporative flux.

- **Waste Form to Invert**–All the flux from the WP flows to the invert, independent of patch/pit location on the WP.

- **Invert to UZ**–All the flux into the invert is released into the UZ.

The waste form is the source of all radionuclides in the potential repository system. Radionuclides can be transported downward, through the invert and into the UZ. Transport can occur through advection when there is a fluid flux through the waste package, and by diffusion

through thin films in the waste package when there are stress corrosion cracks in the lids of the package. Diffusion through SCCs will probably be the only transport mechanism during the first few thousand years because SCCs are the only viable failure mechanism in this time frame.

There will be no transport through the quartz sand backfill under any conditions. Upward diffusion through the backfill is impossible before the drip shield fails because a continuous flow path does not exist between the waste package and the backfill. After the drip shield fails upward diffusion will be negligible in comparison to the downward advective flux through the drip shield.

The diffusion coefficient in the invert is based on the self-diffusivity of water at 25°C as a bounding value for all radionuclides. The effects of temperature are incorporated, based on the Nernst-Einstein formulation (CRWMS M&O 2000h). The effects of porosity and saturation are conservatively ignored.

Partition coefficients for all radionuclides are conservatively set to zero in the waste package and invert.

The drip shield is a potentially important component of the EBS. The thermal and mechanical response of the drip shield has been evaluated for five mechanisms: (1) thermal expansion, (2) floor heave, (3) rock fall, (4) seismic response, and (5) waste package support failure.

Thermal expansion, floor heave and rock fall will produce minor structural response in relation to the potential slippage or overlap between adjacent drip shields. These mechanisms have therefore been screened out from the TSPA-SR.

Seismic response is the key mechanism that may lead to separation of adjacent drip shields. The seismic analysis in this AMR is based on the 1-in-10,000 year earthquake. It is a conservative (bounding) analysis in the sense that it assumes that all the inelastic strain from the earthquake can be concentrated at one or a few locations and that the sand backfill is not represented in the analysis. The sand backfill is important because of its large mass relative to that of the drip shield. Future analyses will consider less probable earthquakes, such as a 1-in-100,000 year event, and the response of the other components (i.e., the backfill) of the EBS.

Pedestal failure has the potential to shift the drip shield if the waste package falls to the invert and rolls into contact with the shield. This scenario is more likely during an earthquake, when the ground motions may increase the load on the pedestal and impart additional momentum to the waste package. Given this association and the bounding nature of the analysis for seismic response, the response to pedestal failure is assumed to be included in the seismic response for TSPA-SR.

3.2.1.2.2 Colloid-Facilitated Transport

It is anticipated that colloids will occur in the EBS from three sources: (1) waste package (WP), (2) groundwater, and (3) degradation of introduced materials.

It is assumed that small quantities of groundwater colloids, and possibly colloids from degradation of introduced materials, will enter a failed WP, interact with released radionuclides,

and then leave the failed WP. Further, it is assumed that groundwater entering the drift and invert from the surrounding UZ will, under certain circumstances, mix with releases from a failed WP, and the groundwater colloids will likewise be available to interact with released radionuclides.

- If the DS and WP have failed, incoming groundwater from above flows downward through the breach in the DS, into and through the WP, and downward into the invert. Releases from a breached WP migrate downward through the invert and may mix with the groundwater in the invert. The mixed fluid migrates downward through the invert into the UZ.

The groundwater is assumed to contain smectite colloids whose stability and concentration are determined by the ionic strength and pH of the groundwater. The WP release is assumed to be a fluid containing colloids and dissolved radionuclides resulting from the reaction of waste with groundwater that has entered the WP.

There are three types of colloids in the release:

- Waste-form colloids, assumed to be smectite
- Waste-package–corrosion colloids, assumed to be iron (hydr)oxide
- Groundwater colloids, assumed to be smectite

Some of these colloids have associated radionuclides as they leave the WP. The WF colloids may have irreversibly attached (embedded) or reversibly attached (sorbed) radionuclides. The corrosion and groundwater colloids may have reversibly attached radionuclides.

The mass of radionuclides irreversibly attached to the WF colloids is determined from reaction within the WP. The mass of radionuclides reversibly attached to all three types of colloids is determined by the product of three parameters:

- Mass concentration of dissolved (aqueous) radionuclide in the fluid

- Mass concentration of colloid material in the fluid

- Radionuclide distribution coefficient (k_d) of a specific radionuclide on a specific colloid mineralogical type

3.2.2.3   Abstraction of the Multi-Scale Thermohydrologic Thermal-Hydrologic Model

The purpose of the analysis and model report, *Abstraction of Near-Field Environment Drift Thermodynamic Environment and Percolation Flux* (CRWMS M&O 2000w), is to abstract the multi-scale, process-level thermal hydrology (TH) model results (CRWMS M&O 2000c) so that they can be implemented in the TSPA model.

The multi-scale TH process model describes how potential repository decay heat affects the EBS and the near-field environment (NFE) host rock. That is, it provides a description of how the temperature, relative humidity (RH), and both the liquid- and gas-phase flows change with time in the EBS and the host rock.

The purpose of the abstraction described in this section is to provide a simplified view of the process-level TH description, and to provide a direct feed to TSPA consisting of the following:

- Temperature
- Liquid saturation
- Relative humidity
- Evaporation rate
- Percolation flux as a function of time.

An averaging process ("binning") is used to compute these quantities, based on a subdivision of the repository footprint that preserves a wide range of TH variability. This process also transforms certain physical quantities: for example, the liquid water velocity in the invert (in mm/yr) to a volumetric flow rate (m³/yr) in the invert (multiplying by the appropriate flow area). Further, the maximum and minimum peak WP temperatures are identified in the abstraction. Finally, the process-level model "raw" output is written in a format that is readily input to TSPA.

Process model results which are used directly in TSPA include: WP temperature, RH at the WP surface, and the percolation flux in the host rock 5 meters above the crown of the emplacement drift. The temperature and RH are used for the corrosion model, and the percolation flux is input to the seepage model. The abstraction of TH data must represent the potential variability and uncertainty in TH conditions. Therefore, this abstraction provides a qualitative and quantitative description of TH variability (e.g. from variability in the host rock unit, edge proximity, waste type, infiltration rate, and climate state), and also provides a description of the uncertainty of TH results associated with different infiltration-rate characterizations (lower, mean, and upper) and the associated hydrologic property sets.

All abstracted TH results provided to TSPA are based on a subdivision of the potential repository into five bins according to the local infiltration rates (1,246 total combinations for each infiltration flux case). The five infiltration "bins" are: 0 to 3 mm/yr, 3 to 10 mm/yr, 10 to 20 mm/yr, 20 to 60 mm/yr, and ≥60 mm/yr. The infiltration-rate characterization specified for this subdivision is the glacial-transition climate state. This climate state begins 2,000 years after waste emplacement and persists for approximately 10^6 years. Pre-defined infiltration rate ranges are specified to cover the entire range of possible glacial climate state infiltration rates. Location dependent data from the process model are then used to populate the five pre-defined infiltration bins. As an example, 21 WP location dependent data files (as described by the results of the Multi-Scale TH Model) populate the infiltration rate bin of 0 to 3 mm/yr for the low infiltration rate case. Therefore, the TH abstractions for this bin will be based on those 21 WP location dependent results from the process model. To assemble all the relevant TH data belonging in each particular infiltration bin, a procedure is used to sort the process-level TH results according to infiltration rate.

All of the abstraction quantities previously described are computed (or reformatted) by a simple software routine developed for this abstraction model. The routine has the ability to accept input commands, based on infiltration-rate binning requirements, and compute (or reformat) the abstracted data necessary for input into the TSPA model on a per-bin basis. This means that the averaged quantities (e.g., WP RH), maximum/minimum WP peak surface temperature, and

reformatted raw data will be computed (or abstracted) by the routine for each of the infiltration bins, as defined by TSPA (CRWMS M&O 2000w, Sections 5.1.1, 6.1, and 6.2).

Finally, the abstracted TH data used by the TSPA model are analyzed (CRWMS M&O 2000w; Section 6.3) for resulting trends and indicators of potential repository performance. In particular, time-histories of temperature, liquid saturation, percolation flux, evaporation rates, and maximum and minimum WP surface temperatures are analyzed for each infiltration bin for locations in both the EBS and the NFE host rock.

The use of infiltration bin-averaged TH values obtained from the multi-scale TH abstraction is considered valid for a number of reasons:

- The infiltration bin-averaged values preserve and emphasize the overall variability and uncertainty in the TH results used for TSPA.

- For instances where an average value would not represent uncertainty or variability associated with a TH variable (e.g. the average WP temperature vs. the maximum WP temperature) a range of process model results is also input directly to TSPA. For example, in addition to the average curve, the abstraction routine provides temperature curves for the maximum and minimum WP temperatures in each of the predefined infiltration bins. The waste package temperature variability, and uncertainty with respect to infiltration rate, are thereby reported for each of the infiltration bins.

- The percolation flux at 5 m above the crown of the drift is input to TSPA as repository footprint location-dependent data. An average value is not used for the percolation flux, so that more complete representation of variability (i.e. with respect to location, host rock unit, and edge proximity) and uncertainty (i.e. infiltration-rate cases: lower, mean, and upper) is be input to the TSPA seepage model.

The TSPA corrosion model uses Multi-Scale TH Model results directly as input, thus capturing in the abstraction the potential variability and uncertainty included in the process model.

3.3 KEY ISSUES FOR THE EBS DEGRADATION, FLOW, AND TRANSPORT PMR

The Nuclear Regulatory Commission (NRC) has identified 10 key technical issues (KTIs) as a means of evaluating the technical adequacy of YMP technical work in support of a license application.

Issue resolution status reports (IRSRs) are issued periodically by the NRC, providing a summary of the issue and its subissues, what is and is not known about them, and indicating where additional information may be required. Chapter 4 and the Appendix provide a detailed discussion of these issues and the degree to which acceptance criteria for their resolution are met by the current revision of the EBS PMR.

Other issues concerning the EBS have been identified by peer reviews of Project documents and by the NWTRB. These issues are summarized in Table 3-47, along with a discussion of the current Project understanding for each issue.

Table 3-47. Issues Germane to the EBS Process Model Report

ISSUE (as stated in source)	SOURCE	DISCUSSION
Additional supporting research is needed in a number of areas, including water compositions in contact with the waste package, critical crevice corrosion temperatures, neptunium solubility and technetium sorption on degraded waste package materials.	VA, Volume 3, Section 6.5.2.7, page 6-34 (DOE 1998c)	Both detailed process models and bounding models for the evolution of water chemistry over this time period are developed in supporting AMRs and summarized in Section 3.1.2. Other issues are covered in other PMRs.
Modeling assumptions should be consistent across different process models, unless there is a defensible technical rationale.	VA, Volume 3, Section 6.5.3.3, page 6-35 (DOE 1998c)	The Analysis/Model Reports (AMR) are thoroughly reviewed to help ensure consistency among assumptions made in more than one document about a given parameter. In addition, the Process Model Reports (PMR) that summarize and integrate the results of the AMRs have been subjected to a review by a single review team, one of whose main objectives is to identify inconsistencies among the PMRs. Finally, assumptions used in the AMRs that feed TSPA are documented in the TSPA document. These measures provide confidence that consistent assumptions are used as appropriate among the various models that support the TSPA.
Detailed documentation of the assumptions used in performance assessments is of fundamental importance to the transparency (and credibility) of the TSPA.	VA, Volume 3, Section 6.5.3.4, page 6-35 (DOE 1998c)	The transparency and traceability of TSPA analyses is required to ensure the calculations supporting the TSPAs are clear and consistent. As described in AP 3.10Q, the purpose of Section 5 of the AMRs is to document the assumptions made to perform the analysis or to develop the model, along with a rationale for those assumptions. In support of meeting this goal, detailed documentation of assumptions is presented in section 5 of the AMRs supporting the PMRs.
Rockfall effects need to be considered in the design and performance of the Yucca Mountain repository system.	VA, Volume 3, Section 6.5.3.7, page 6-36 (DOE 1998c)	Rockfall calculations based on key-block analyses are documented in the *Drift Degradation Analysis* AMR (CRWMS M&O 2000ad), and summarized in Section 3.1.2. Only a small percentage of the total length of emplacement drifts is expected to experience rockfall within 10,000 years of closure, even without ground support, taking into account both seismic and thermal effects. The use of backfill in EDA II prevents significant mechanical damage from rockfall. In January 2000, a design change, prompted by thermal

Table 3-47. Issues Germane to the EBS Process Model Report (Continued)

ISSUE (as stated in source)	SOURCE	DISCUSSION
		considerations, was initiated to remove backfill and change the drift orientation to minimize the size of key blocks. Revision or ICN of the AMR and the EBS PMR will assess consequences of this change.
The effects of the drip shield and backfill on the thermal and moisture regime between the drip shield and the waste package and evaluating the corrosion behavior of titanium when it is in contact with backfill or rockfall. The vulnerability of the drip-shield connections to vibratory earthquake motion also needs to be addressed.	NWTRB Letter to DOE (8-3-99) (Cohen 1999)	The thermal and moisture conditions between the DS and WP are the subject of ongoing experimental investigations, and are addressed in the *Water Distribution and Removal AMR* (CRWMS M&O 2000q), and Section 3.1.1. The remaining parts of this issue are addressed in the WP PMR and its supporting AMRs.
Experimental data are lacking throughout the treatment of the waste package and EBS. In particular, the effect of realistic and extreme environments to come in contact with Alloy 22 and critical temperature for crevice corrosion of Alloy 22.	Final Report Total System Performance Assessment Peer Review Panel February 11, 1999 Section II.C (Budnitz et al. 1999)	The bulk chemical environment within emplacement drifts is bounded by analyses summarized in section 3.1.2.7 of the EBS PMR. The effects of the bulk chemical environment and local environments on corrosion of WP alloys is within the scope of the WP PMR
Proper account has not been taken of the TH interactions between adjacent drifts and the effects of natural convection. The possibility of heat pipe instability in some locations, with resulting condensate seepage (as observed in the Large Block Test) cannot be predicted. The method also overpredicts the performance of drifts at the repository edge. Coarse scale factors, such as a reduction of the actual heat load to an effective value, are introduced to handle such problems. Although the methodology is a creative approach, it needs to be tested against real data (perhaps in conjunction with the Drift Scale Test) to validate the results of the analyses.	Final Report Total System Performance Assessment Peer Review Panel February 11, 1999 Section IV.B, Page 55 (Budnitz et al. 1999)	Heat pipe instability has not been observed in the field for any test except the Large Block Test (LBT). The LBT was specifically designed to produce conditions favorable to such instability. The design analyzed in this report was selected to maintain sub-boiling conditions in the central region of the pillars. This will provide drainage pathways for condensate and tend to eliminate heat pipe instabilities. Similar thermal modeling approaches with the NUFT code have been used to compare with the Drift Scale Test as part of model validation
The project staff should initiate a detailed, on-going review of the EBS models and should include the actual use and comparison of modeled results from the RIP code to modeled results from other geochemical codes and databases. The present EBS analysis uses only limited experimental data and, more	Final Report Total System Performance Assessment Peer Review Panel February 11, 1999 Section IV.B, Page 98 (Budnitz et al. 1999)	EBS models and other key process models are documented in a series of process model reports (PMRs), subject to extensive review within the M&O and by DOE before final acceptance. Experimental data for specific processes and functions of the EBS are being obtained in ongoing work at the Atlas Test Facility. These data provide input for

Table 3-47. Issues Germane to the EBS Process Model Report (Continued)

ISSUE (as stated in source)	SOURCE	DISCUSSION
importantly, there has been no effort to demonstrate that such an approach produces reasonable results. This situation can be significantly improved by designing experiments to confirm the modeled results of the EBS...		both development and confirmation of EBS process models.
As has been properly noted by the project, the effects of colloid-facilitated transport remain one of the major sources of uncertainty. At present there is no convincing way to estimate the type, amounts or stability of colloids.	Final Report Total System Performance Assessment Peer Review Panel February 11, 1999 (Budnitz et al. 1999)	A bounding model for colloid concentrations and associated sorbed radionuclides is summarized in Section 3.1.2.6. According to this bounding calculation, iron oxyhydroxides, with high sorption capacity for actinides, are the most important. The total aqueous concentration of these radionuclides is expected to be less than 100 times the amount in solution.
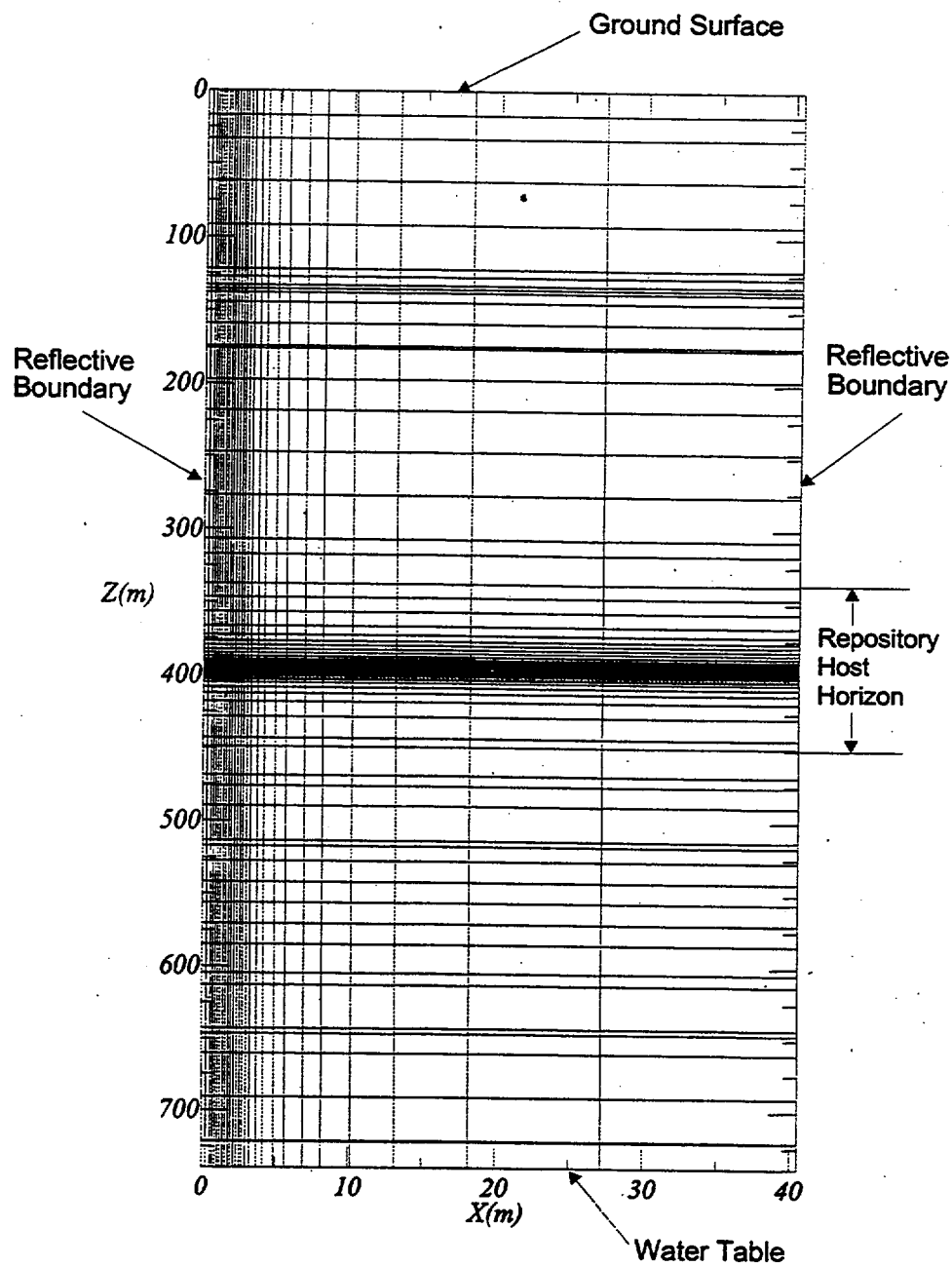
Figure 3-1. Model Domain and Boundary Conditions
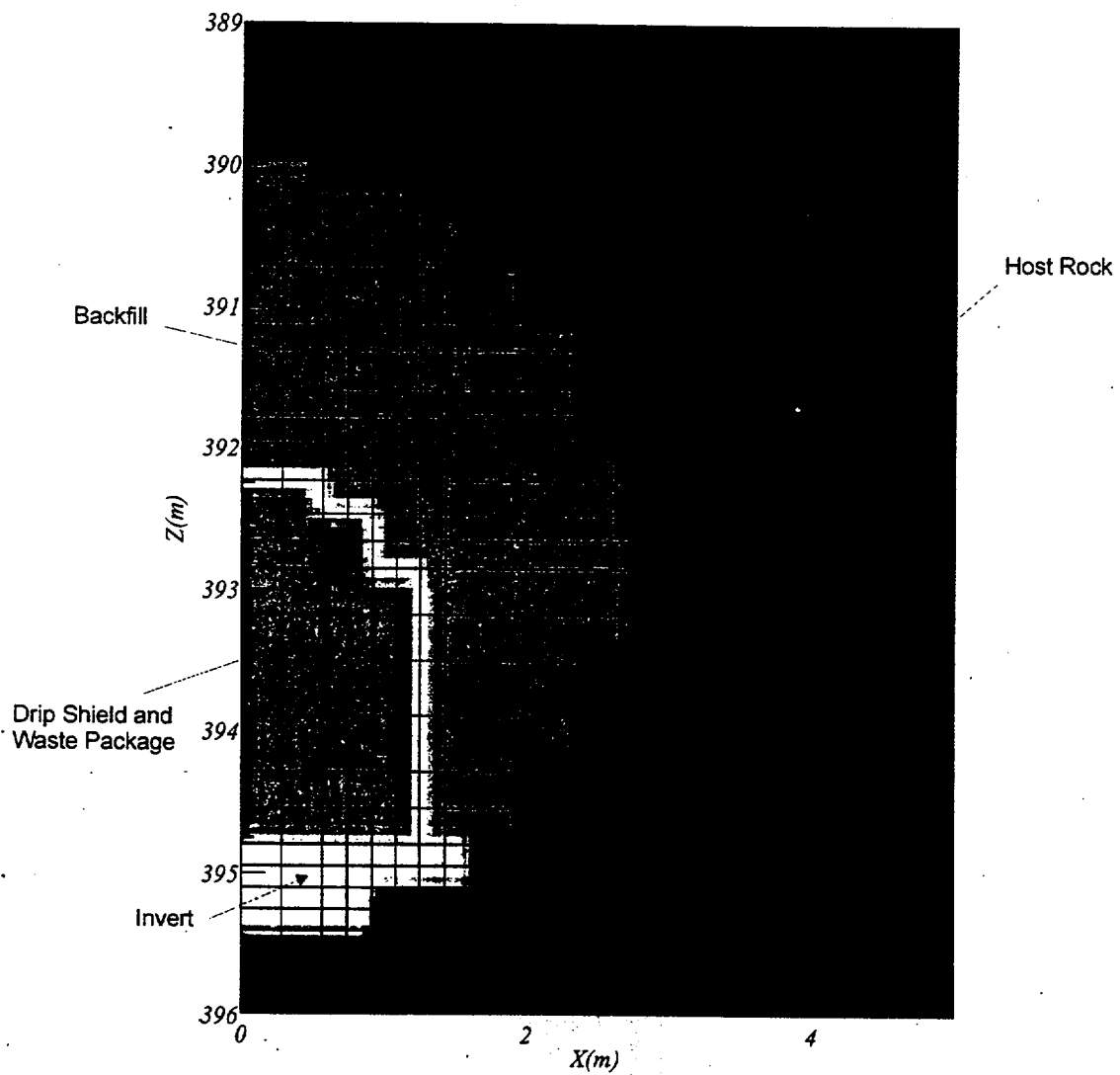
Note: Colors are for presentation only.

Figure 3-2. Engineered Barrier Segment Block Model
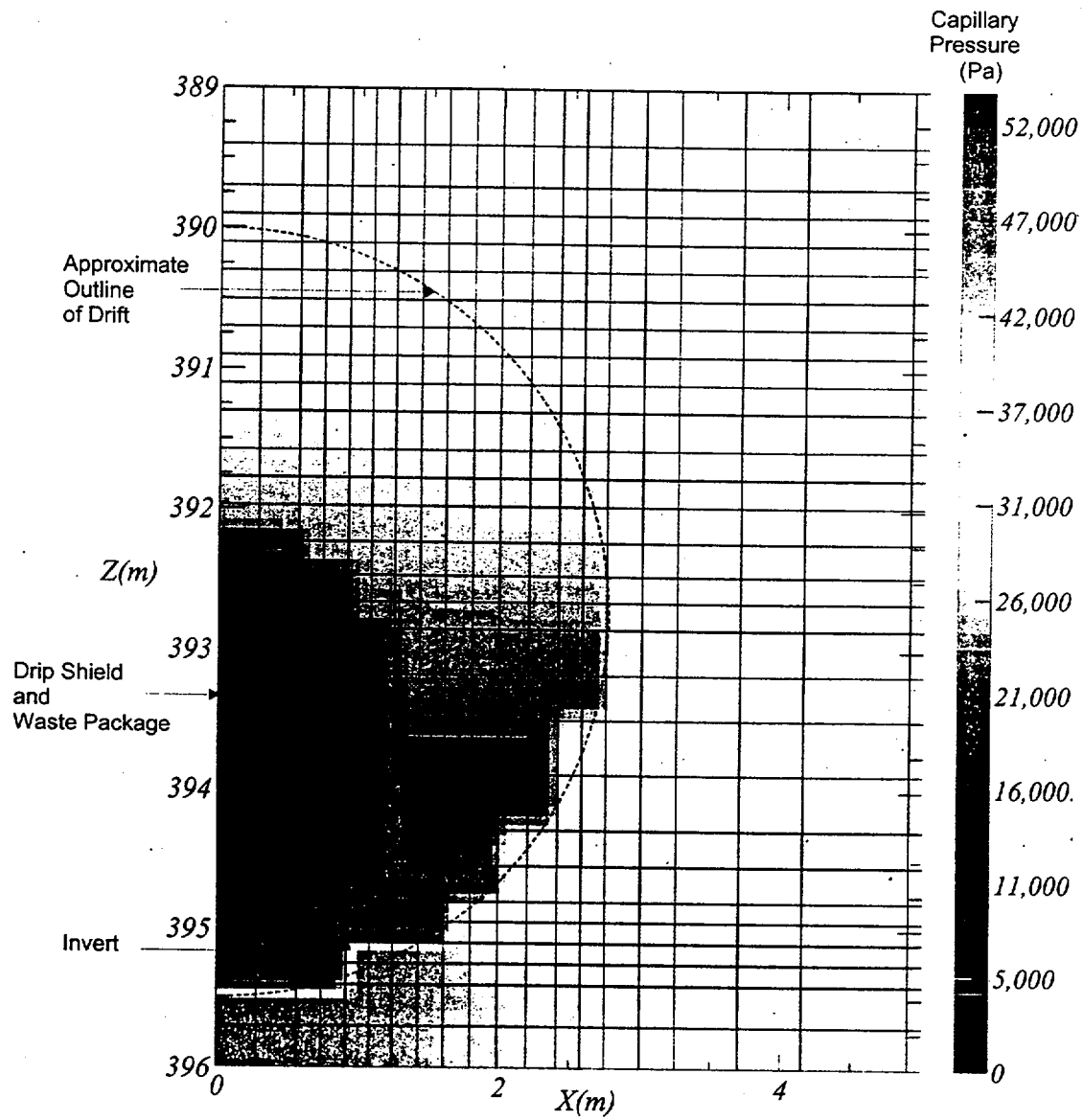
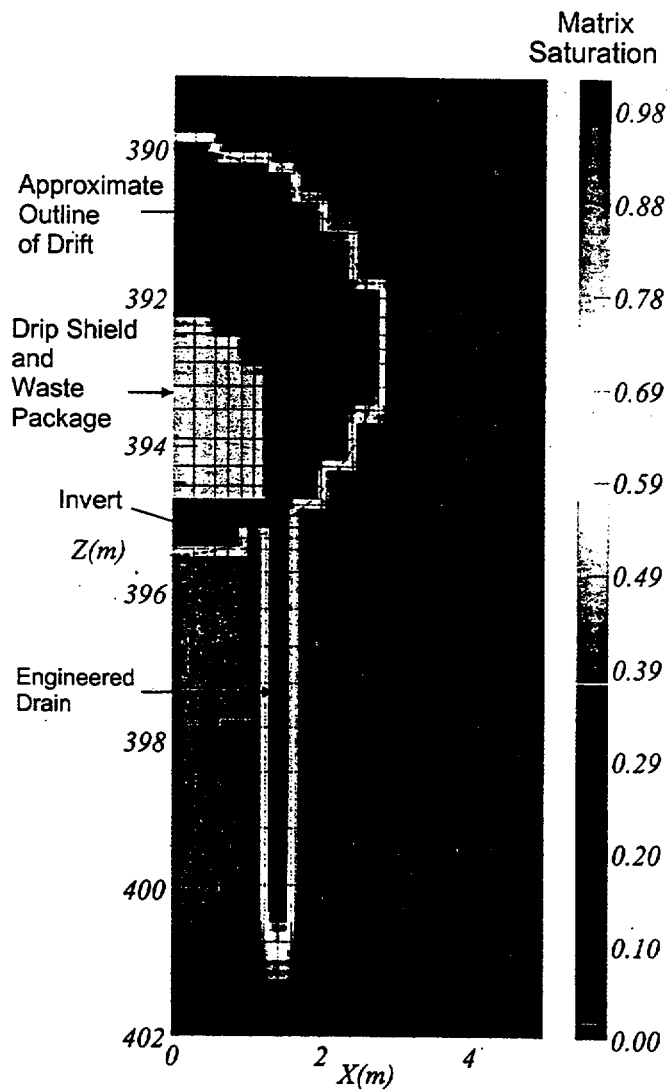Figure 3-3. Matrix Capillary Pressure for Focused Flow At Steady State at Isothermal Temperature Near the Repository Horizon (Case 1)
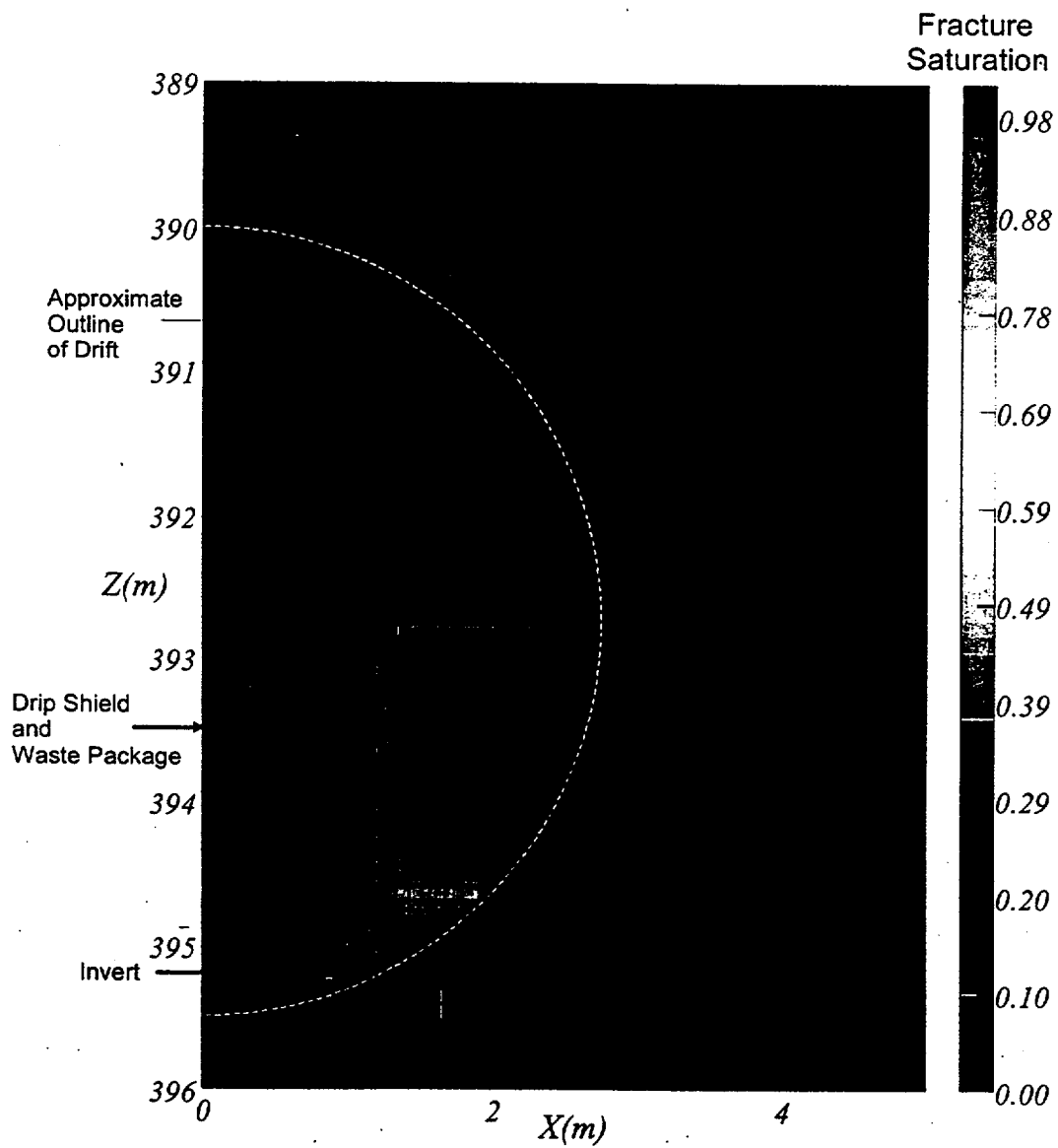
Figure 3-4. Fracture Saturation Levels for Focused Flow at Steady State at Isothermal Temperature Near the Repository Horizon (Case 1)
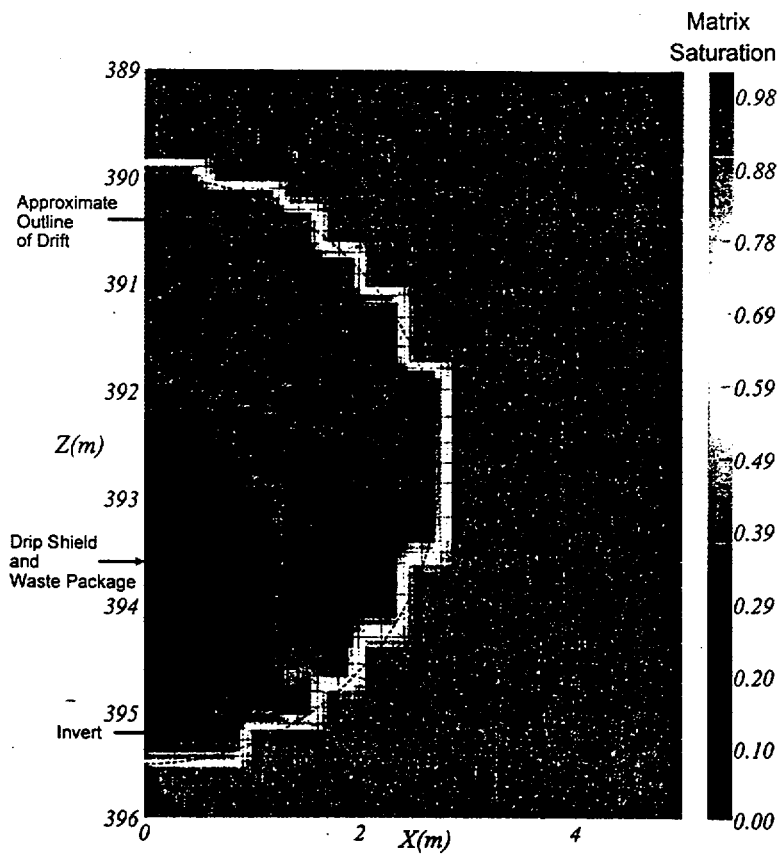
Figure 3-5. Matrix Saturation Levels for Focused Flow at Steady State at Isothermal Temperature Near the Repository Horizon (Case 1)
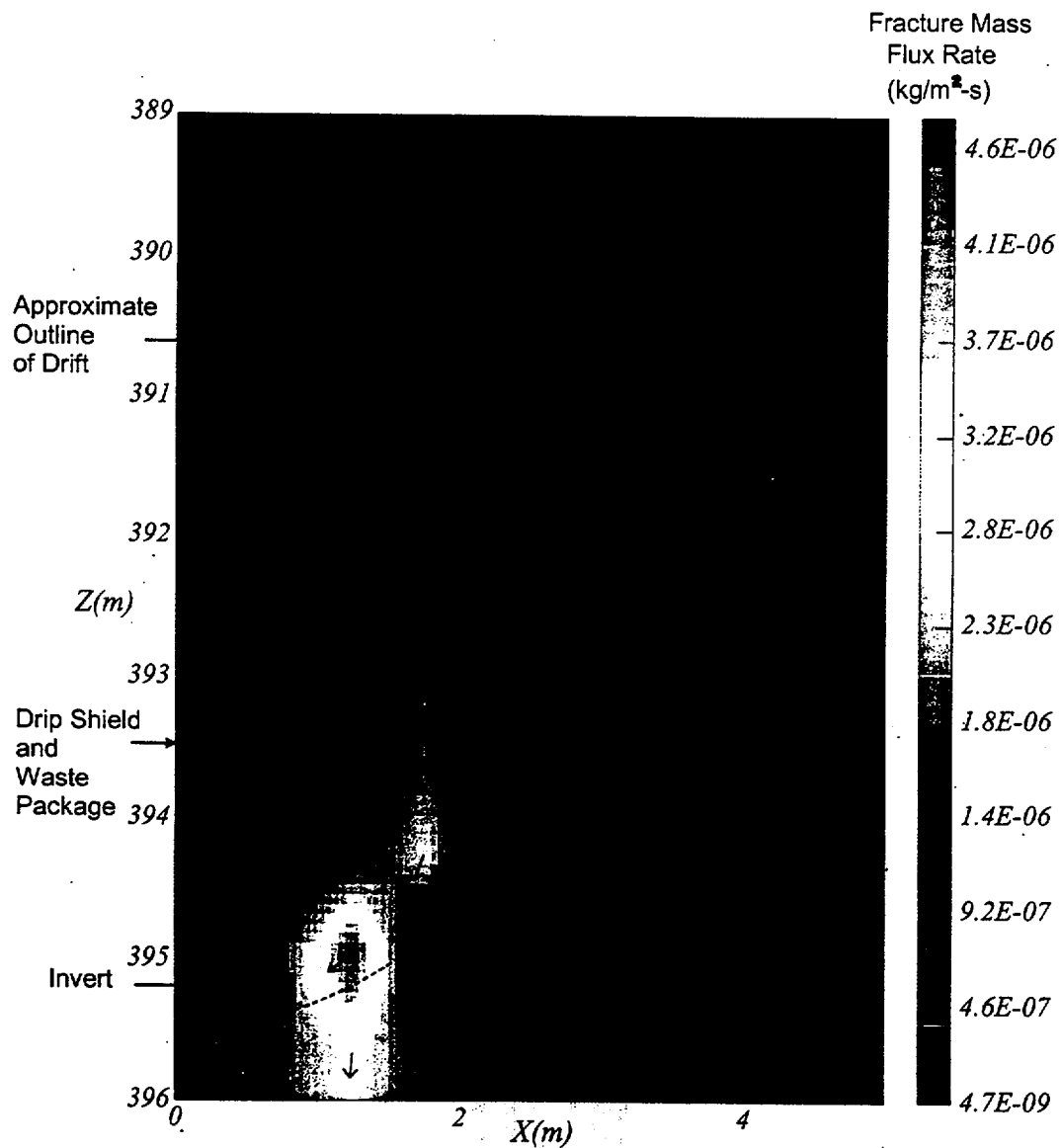
Figure 3-6. Fracture Mass Flux Rates (kg/m²-s) and Direction of Flow for Focused Flow at Steady State at Isothermal Temperature Near the Repository Horizon (Case 1)
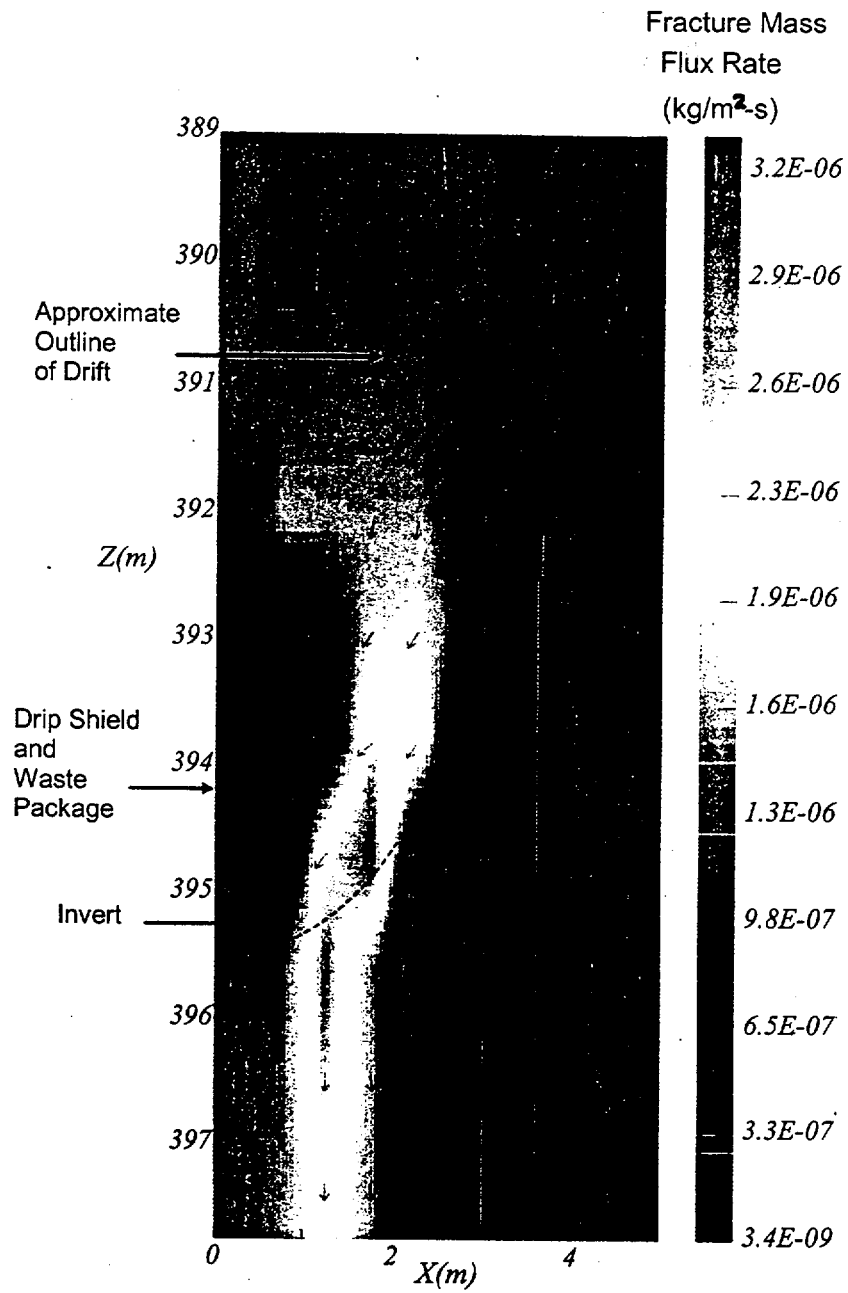
Figure 3-7. Fracture Mass Flux Rates (kg/m²-s) and Direction of Flow for Focused Flow for Repository Heating Near the Repository Horizon After 1,000 Years (Case 3)
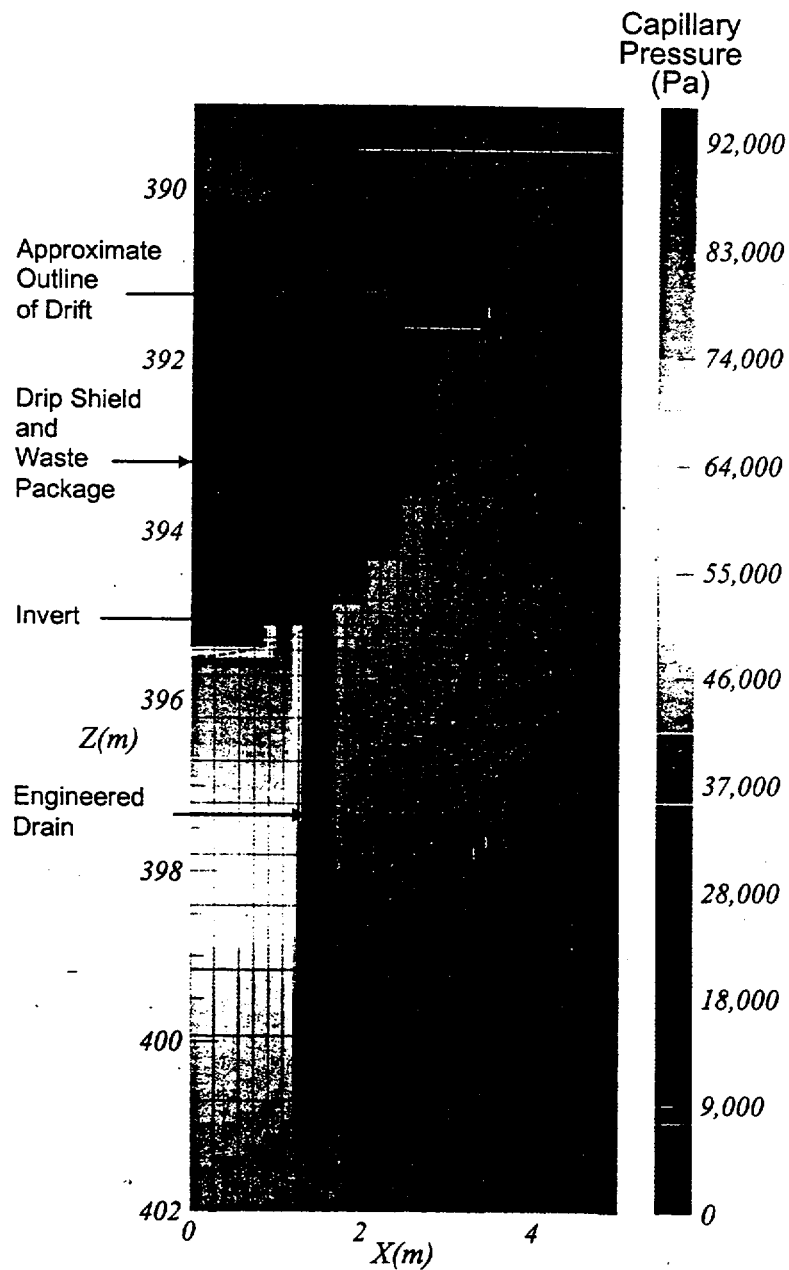
Figure 3-8. Matrix Capillary Pressure for Focused Flow at Steady State at Isothermal Temperature Near the Repository Horizon for Plugged Fractures with an Engineered Drain (Case 9)
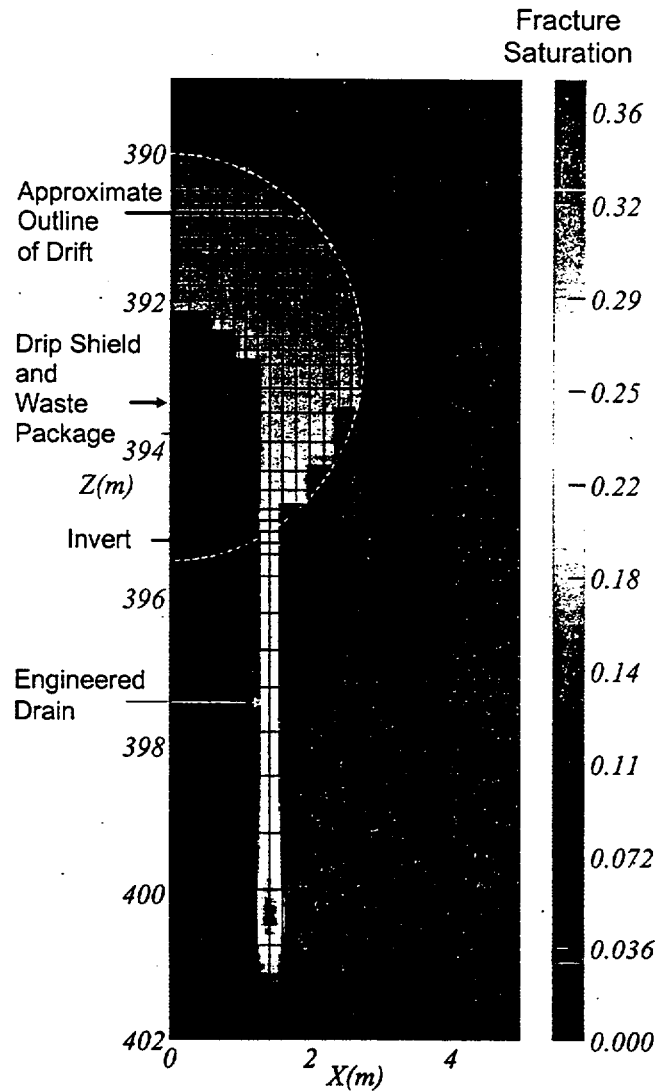
Figure 3-9 Fracture Saturation Levels for Focused Flow at Steady State at Isothermal Temperature Near the Repository Horizon for Plugged Fractures with an Engineered Drain (Case 9)

Figure 3-10. Matrix Saturation Levels for Focused Flow at Steady State at Isothermal Temperature Near the Repository Horizon for Plugged Fractures with an Engineered Drain (Case 9)
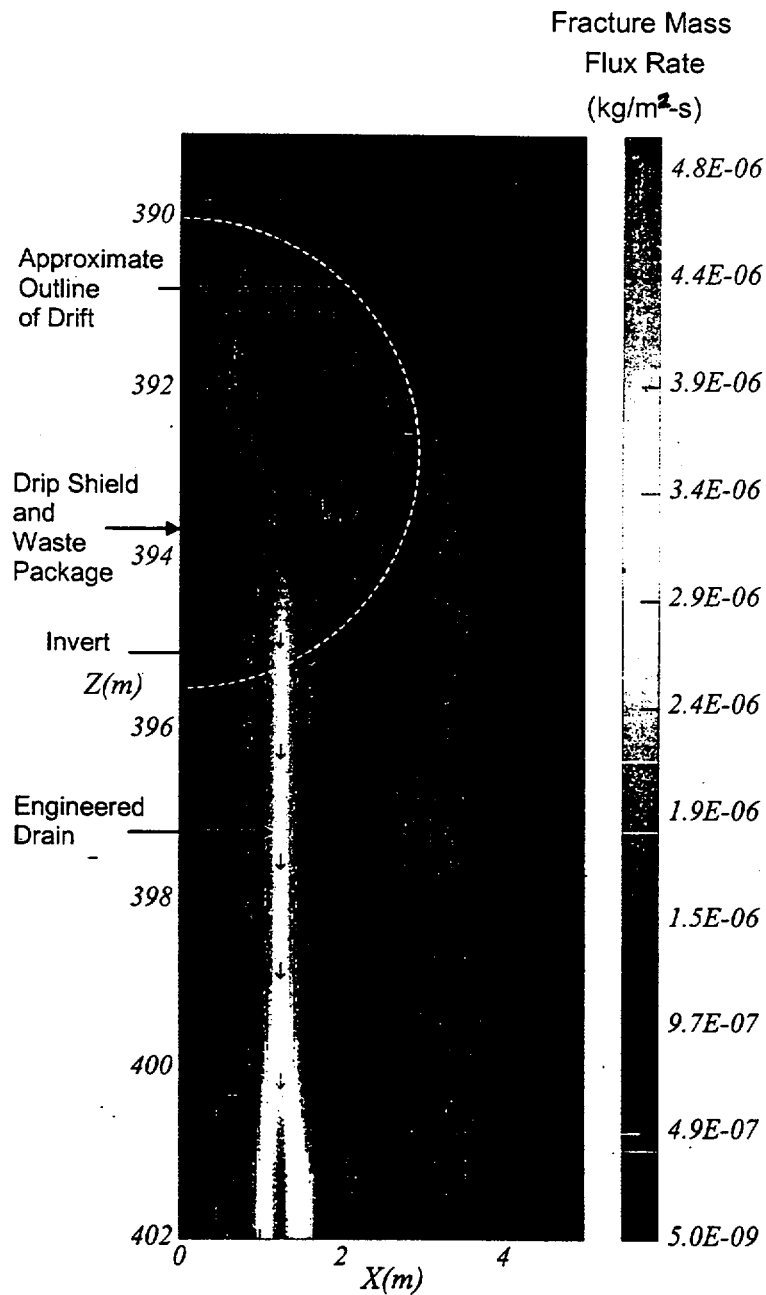
Figure 3-11. Fracture Mass Flux Rates (kg/m²-s) and Direction of Flow for Focused Flow at Steady State at Isothermal Temperature Near the Repository Horizon for Plugged Fractures with an Engineered Drain (Case 9)
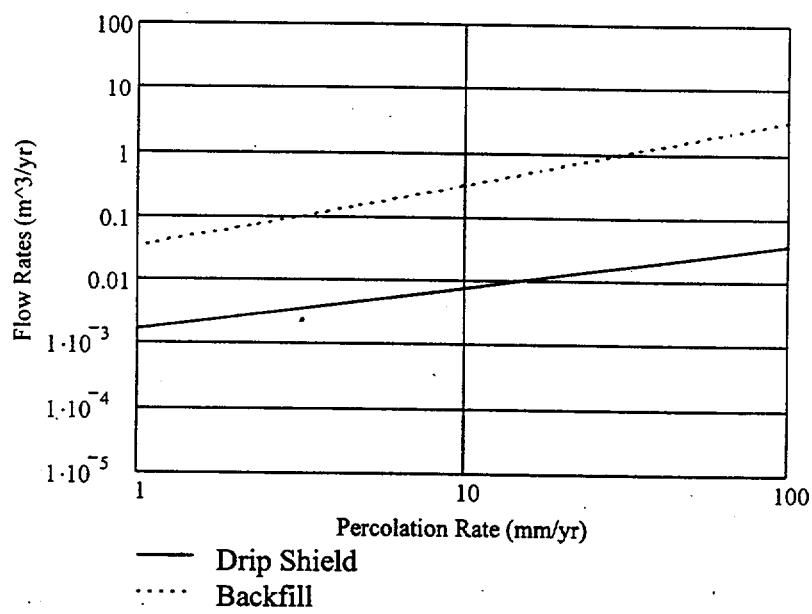
Figure 3-12. Drip Shield and Backfill Flow Rates as a Function of Backfill Percolation.

EBS Physical & Chemical Environment Process Model Structure
(Section numbers shown in parentheses.)

Figure 3-13. Relations Between Submodels Used for the EBS Physical and Chemical Environment

**Drip Shield
and Backfill**

Water Vapor Moving
Outward from Drift Area

Dryout Zone

water flow

heat transfer,
convection + conduction

00018DC_EBS_PMR-11.ai
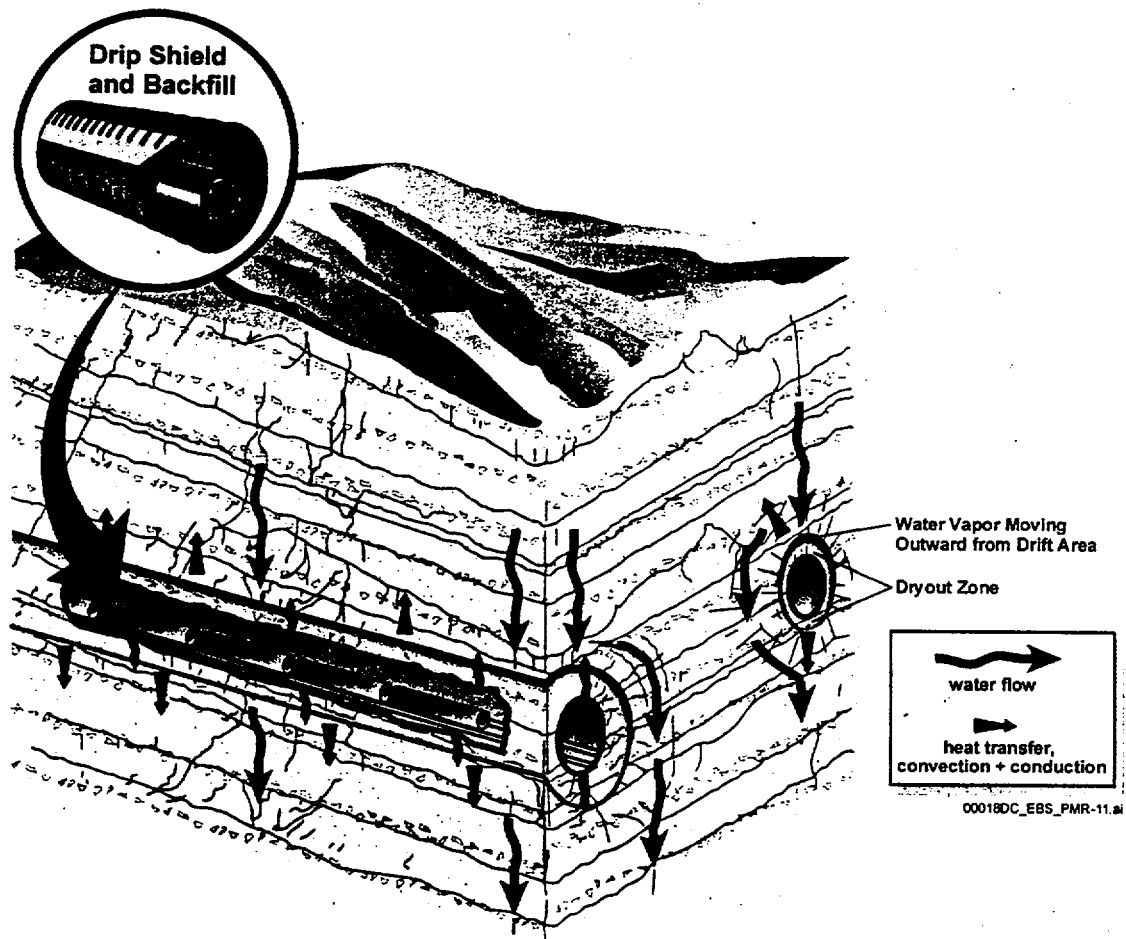
Figure 3-14. Schematic of thermal-hydrology processes affecting the flux of water as liquid and vapor.
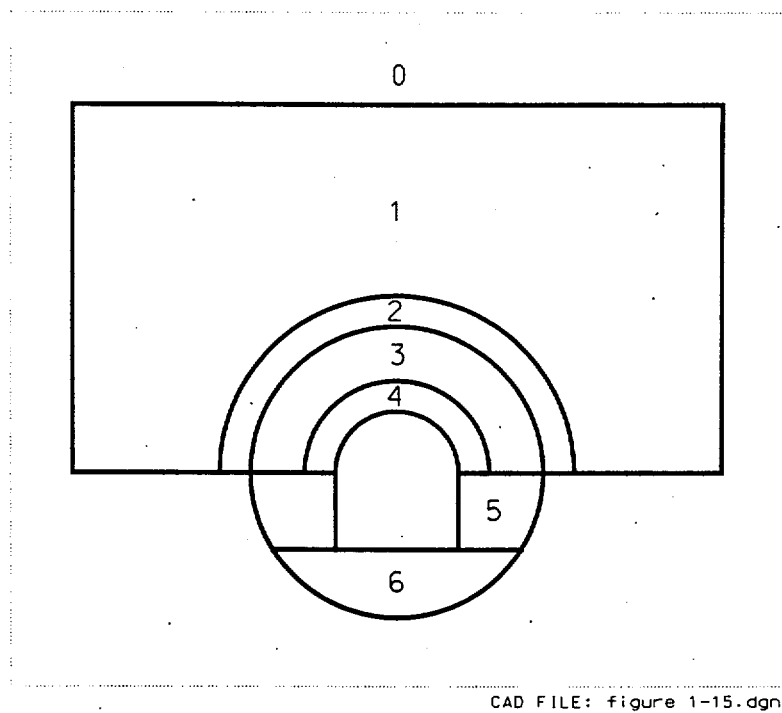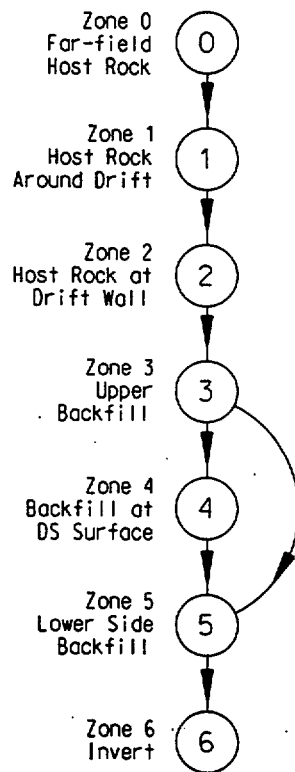
Figure 3-15. Schematic Drawing Showing the Zones Defined for Chemical Modeling and the Connectivity of the Zones
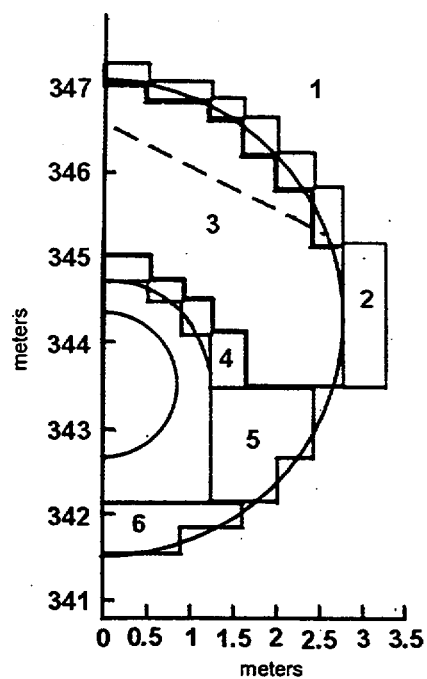
Figure 3-16. Representation of Zone Boundaries in the Model Grid, Showing Boundaries Between Zones 1 through 6

Liquid Flux Between Zones - I4c4 "upper"

Legend:
- Calc. Flux (Zone 1 to 2)
- Calc. Flux (Zone 2 to 3)
- Calc. Flux (Zone 3 to 4)
- Calc. Flux (Zone 3 to 5)
- Calc. Flux (Zone 4 to 5)
- Calc. Flux (Zone 5 to 6)
- Abstr. Flux (Zone 1 to 2)
- Abstr. Flux (Zone 2 to 3)
- Abstr. Flux (Zone 3 to 4)
- Abstr. Flux (Zone 3 to 5)
- Abstr. Flux (Zone 4 to 5)
- Abstr. Flux (Zone 5 to 6)

Y-axis: Zone-to-Zone Flow per Unit Length of Drift — 0.0E+00, 5.0E-06, 1.0E-05, 1.5E-05

X-axis: Time (yr) — 100, 1000, 10000

NOTE: The flux values assigned to uniform time intervals, used for stepwise representation of the thermal evolution in chemical reaction cell modeling, are also plotted.

Figure 3-17. Liquid Fluxes Between Zones for the I4c4 Location and the "Upper" Infiltration Distribution

Simulation time of 1000 yr
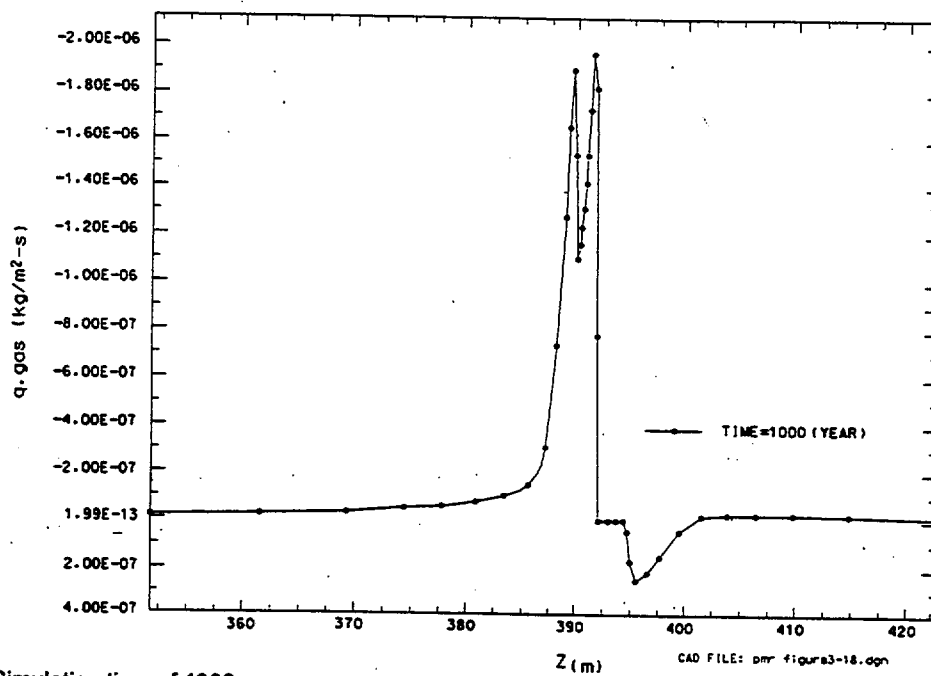
Figure 3-18. Vertical Component of the Gas-Phase Total Mass Flux (Air and Water Vapor)
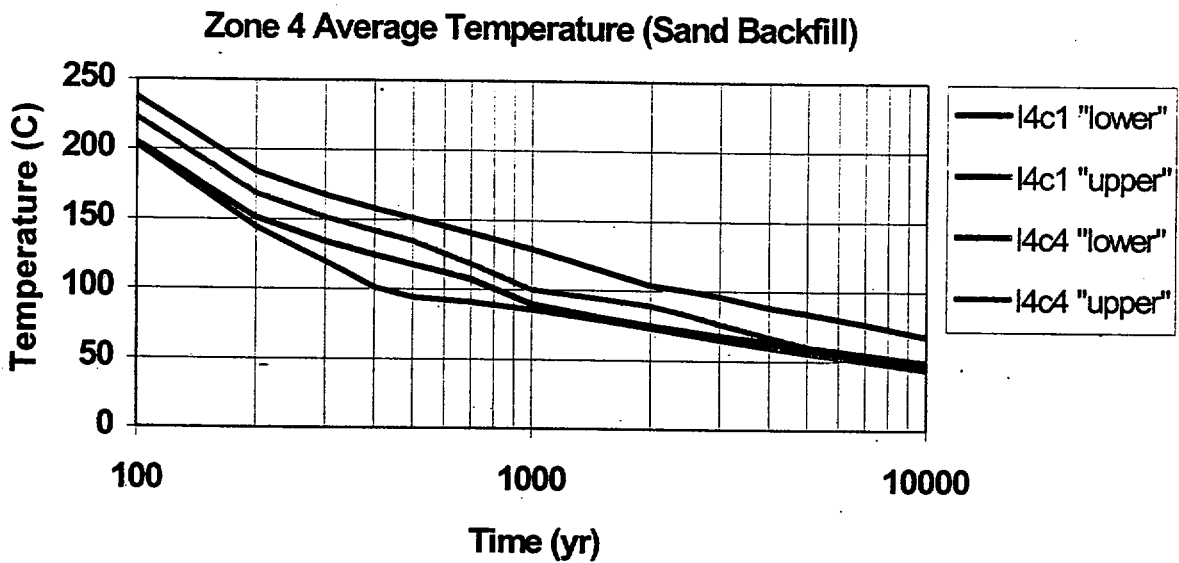
Zone 4 Average Temperature (Sand Backfill)

Legend:
- I4c1 "lower"
- I4c1 "upper"
- I4c4 "lower"
- I4c4 "upper"

NOTES: Backfill at the drip-shield surface

Calculated for the I4c1 and I4c4 locations, using the "upper" and "lower" infiltration distributions
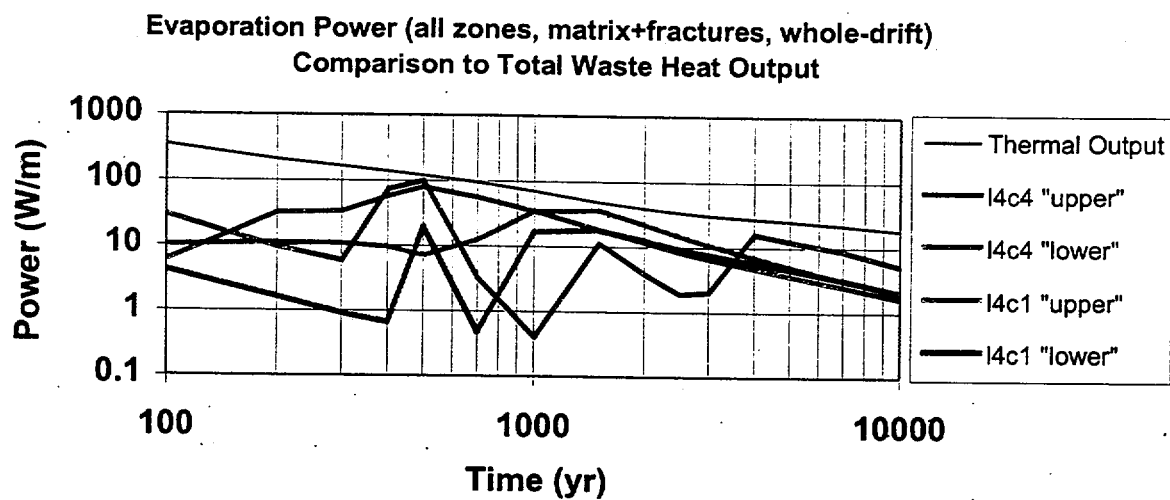
Figure 3-19. Average Temperature for Zone 4
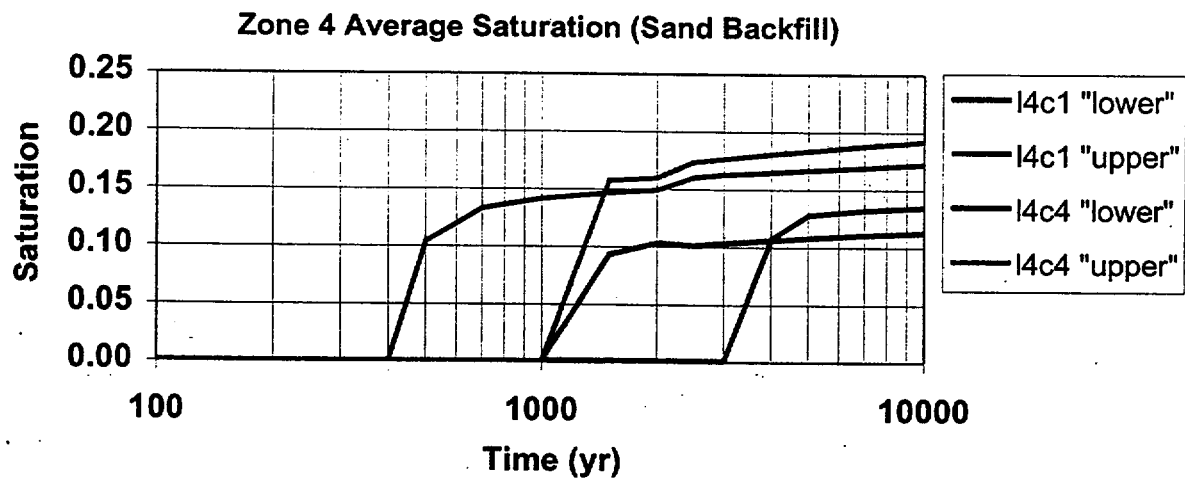
Zone 4 Average Saturation (Sand Backfill)

Figure 3-20. Average Saturation for Zone 4

NOTES: Backfill at the drip-shield surface

Calculated for the I4c1 and I4c4 locations, using the "upper" and "lower" infiltration distributions

Zone 4 Average Air Mass-Fraction (Sand Backfill)

Legend:
- I4c1 "lower"
- I4c1 "upper"
- I4c4 "lower"
- I4c4 "upper"
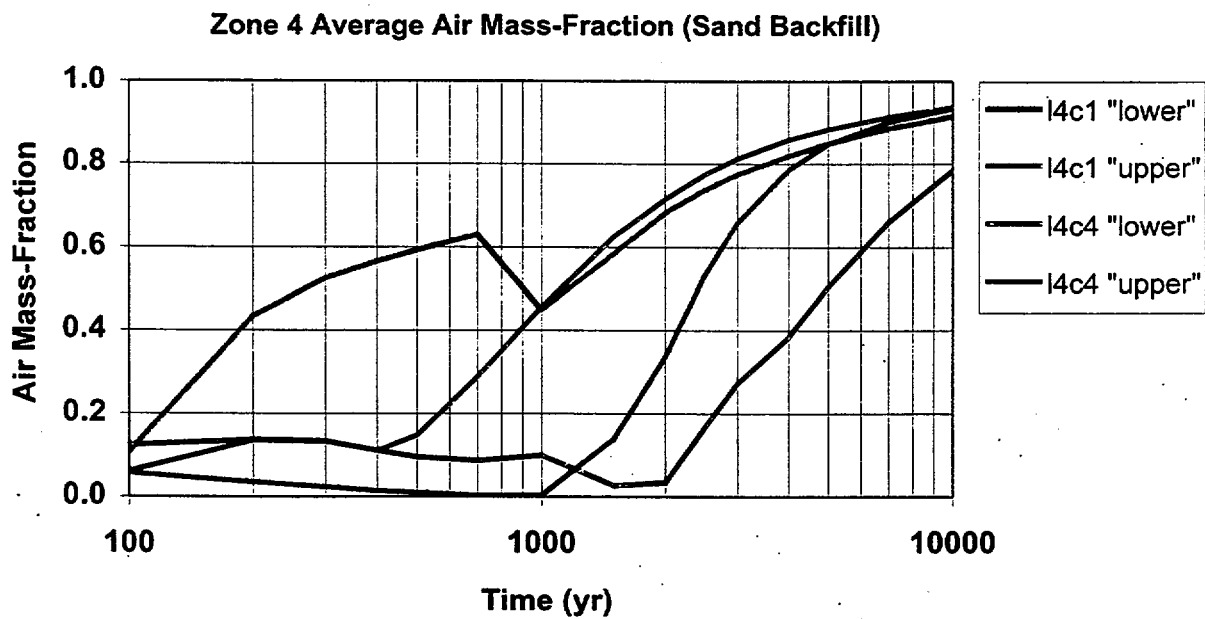
NOTES: Backfill at the drip-shield surface

This plot compares NUFT output for the I4c1 and I4c4 locations and the "upper" and "lower" infiltration distributions.

Figure 3-21. Average Air Mass-Fraction for Zone 4 as a Function of Time
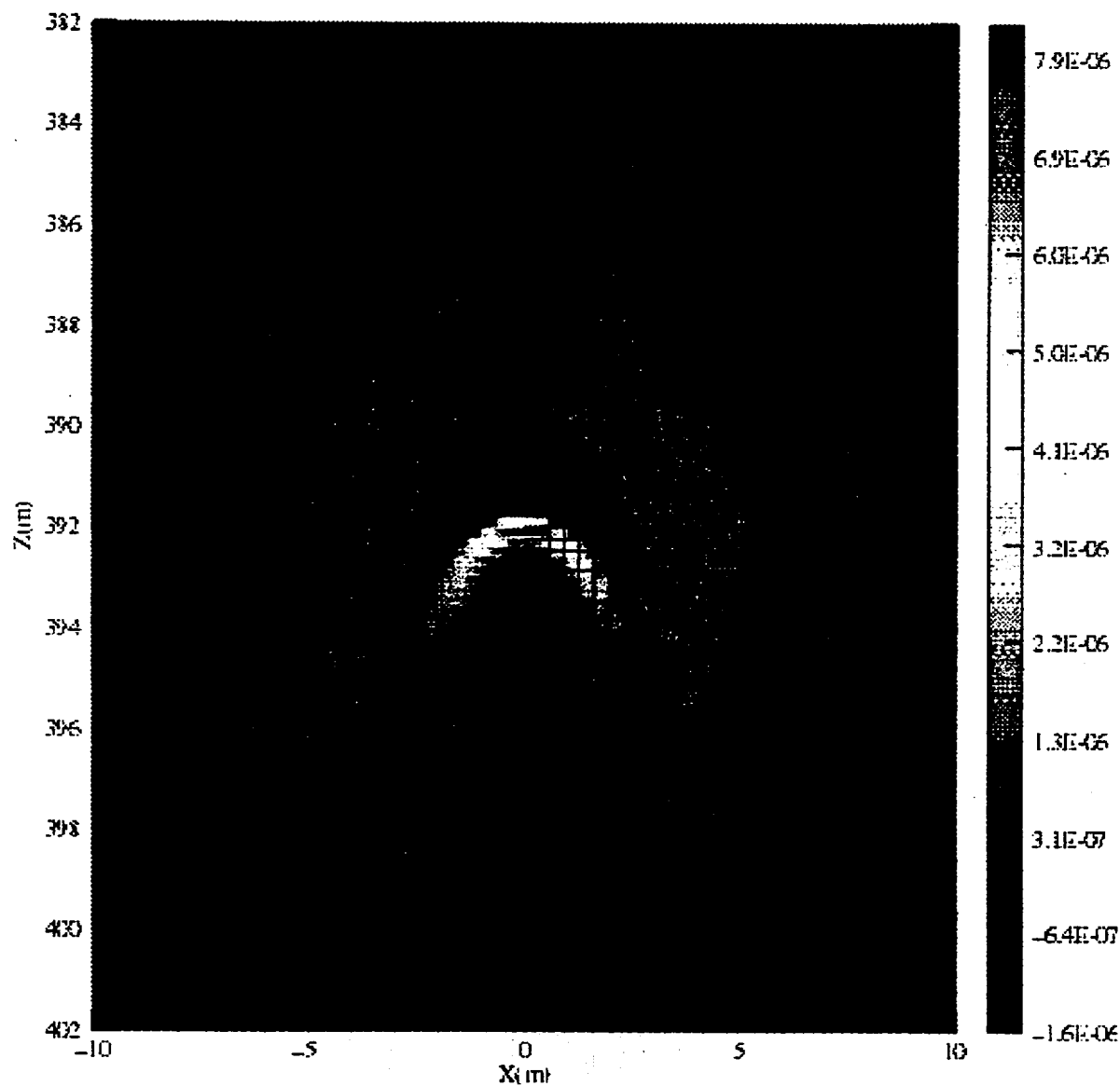
NOTES: The plotted variable is the evaporation rate from the fracture continuum. The color bar gives values for the mass rate of evaporation per unit volume (kg/m³-sec). Positive values indicate evaporation; negative values indicate condensation. The model grid is plotted for reference.

Figure 3-22. Fracture Evaporation Rate Field for the I4c4 Location with the "Upper" Infiltration Distribution at Simulation Time of 1000 yr

Evaporation Power (all zones, matrix+fractures, whole-drift)
Comparison to Total Waste Heat Output

Legend:
- Thermal Output
- I4c4 "upper"
- I4c4 "lower"
- I4c1 "upper"
- I4c1 "lower"

X-axis: Time (yr)
Y-axis: Power (W/m)

NOTES: Compares the I4c1 and I4c4 locations and the "upper" and "lower" infiltration distributions
The average thermal output (lineal power loading) is plotted for comparison.

Figure 3-23. Plot of Total Evaporation vs. Time for All Zones, Including Fractures + Matrix

Figure 3-24. Vertical Component of the Gas-Phase Total Mass Flux (Air + Water Vapor) Along a Horizontal Profile Passing through the Drift Centerline
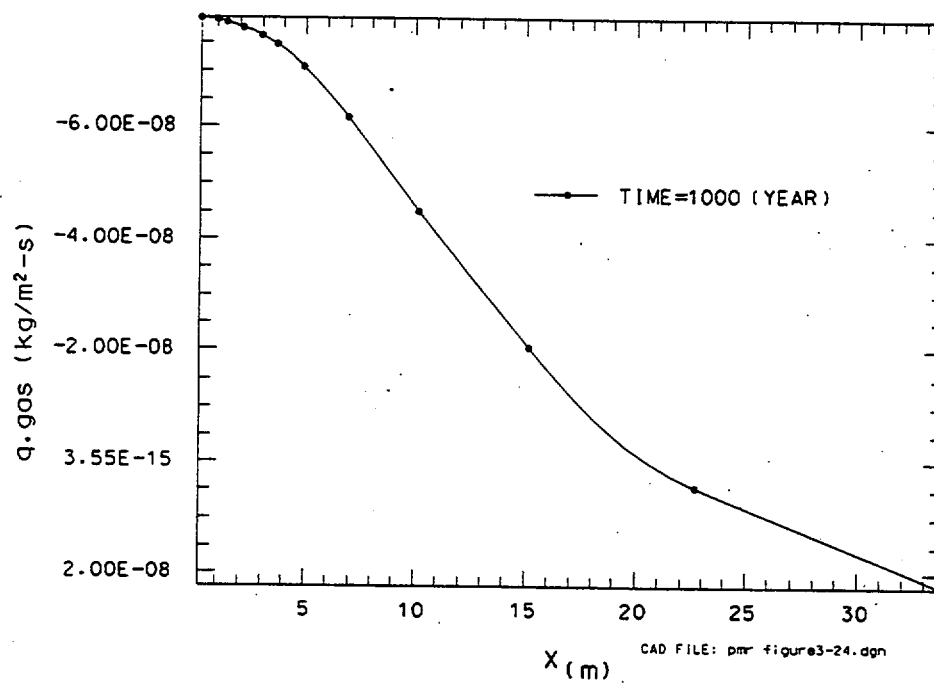
NOTES: For the l4c4 location and "upper" infiltration distribution
Upward mass flux is negative in this figure.
Simulation time of 1000 yr

Conservative Solute Accumulation in Zones
I4c4 location, "upper" infiltration
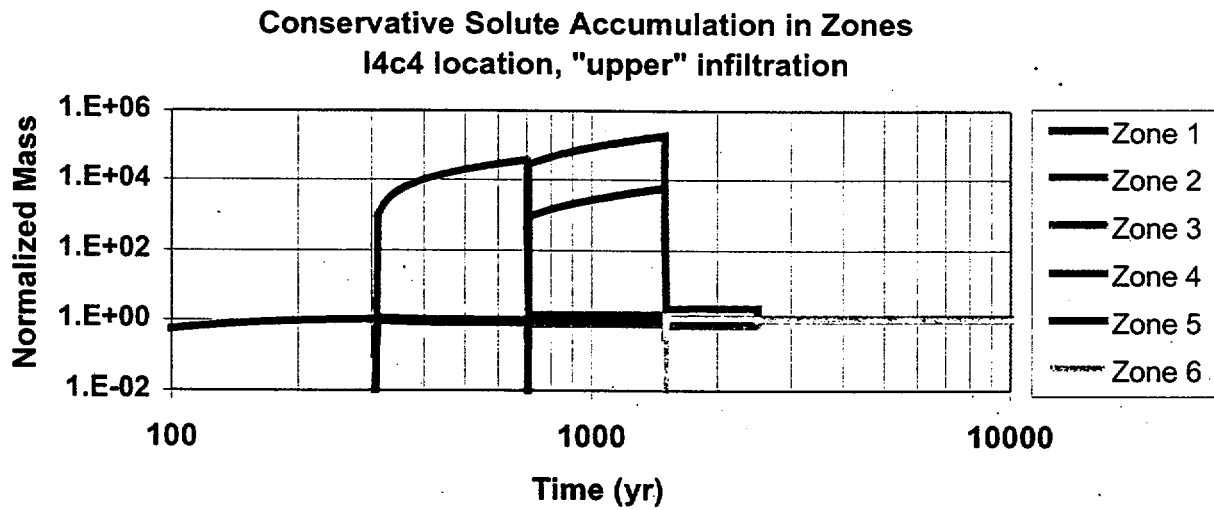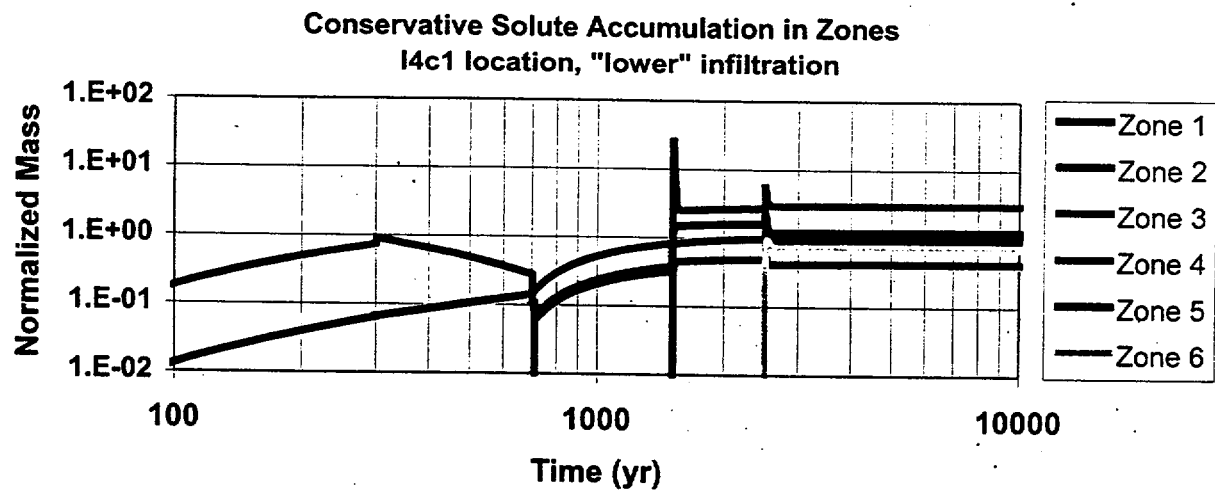

Figure 3-25. Normalized Mass of an Ideal Conservative Solute in Each Zone for Each of Five Time Intervals for the I4c4 Location (Repository Center) with the Upper Infiltration Distribution

Conservative Solute Accumulation in Zones
I4c4 location, "lower" infiltration
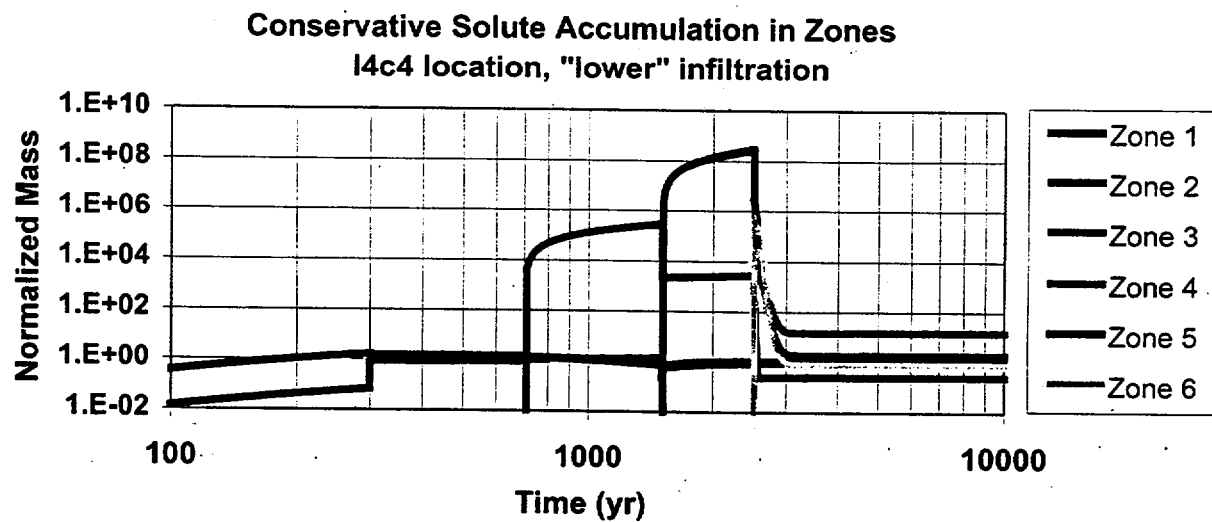
Figure 3-26. Normalized Mass of an Ideal Conservative Solute in Each Zone for Each of Five Time Intervals for the I4c4 Location with the Lower Infiltration Distribution
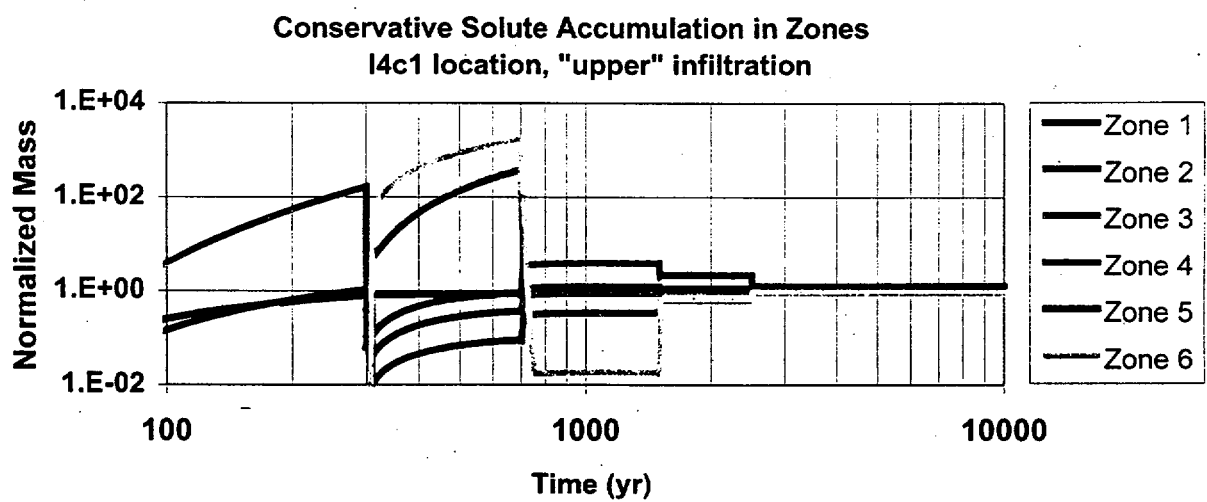
Figure 3-27. Normalized Mass of an Ideal Conservative Solute in Each Zone for Each of Five Time Intervals for the I4c1 Location with the Upper Infiltration Distribution
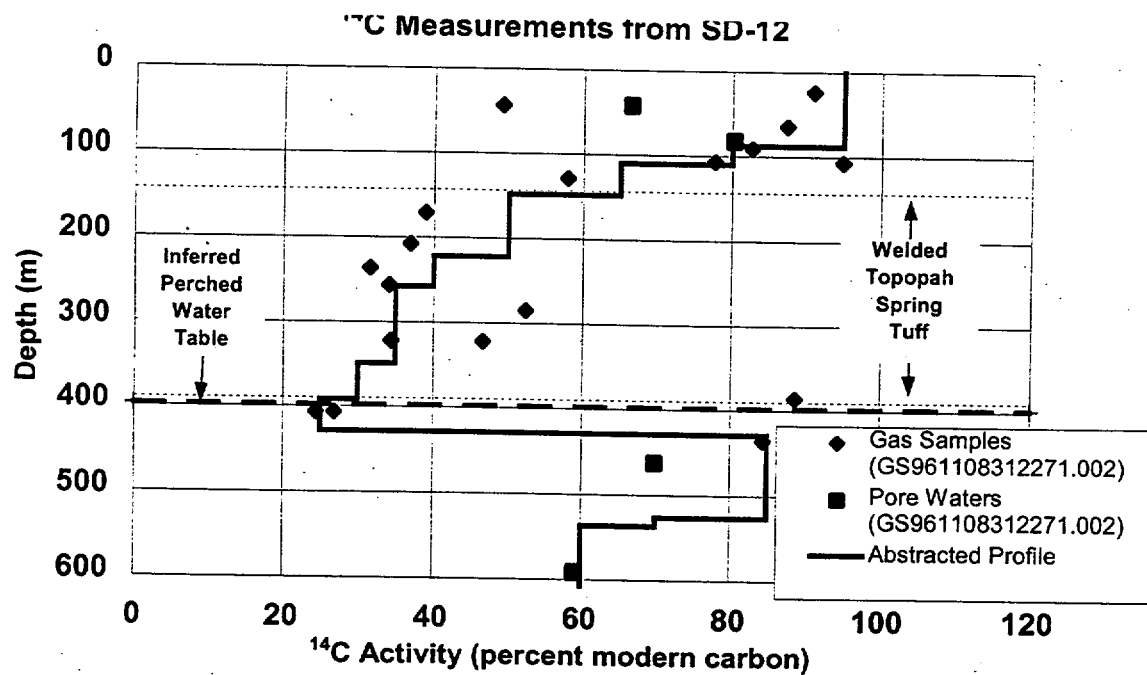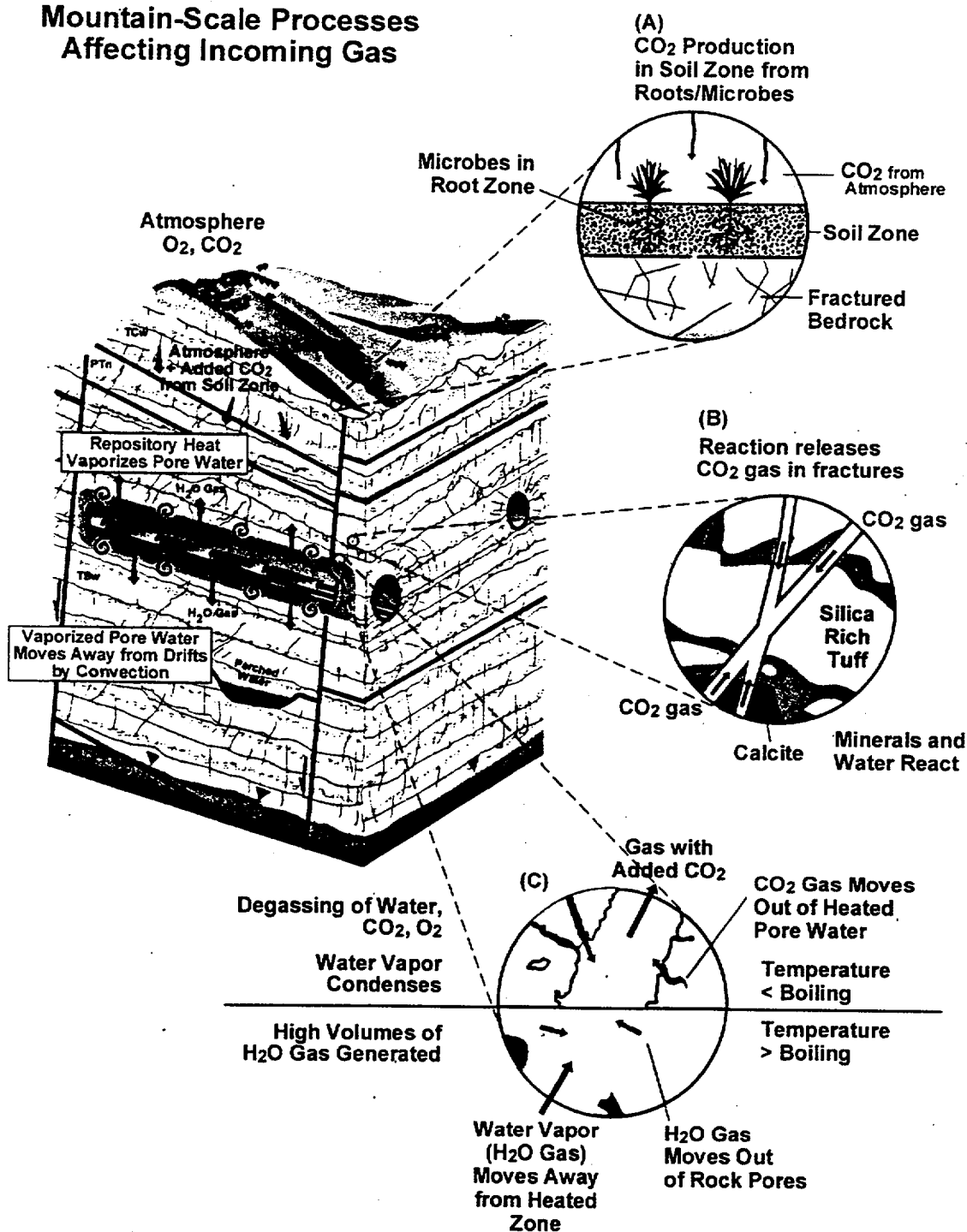
Figure 3-28. Normalized Mass of an Ideal Conservative Solute in Each Zone for Each of Five Time Intervals for the I4c1 Location with the Lower Infiltration Distribution

¹⁴C Measurements from SD-12

Figure 3-29. Observed Distribution of ^{14}C Activity with Depth in Borehole SD-12

Mountain-Scale Processes Affecting Incoming Gas

(A)
CO_2 Production in Soil Zone from Roots/Microbes

Microbes in Root Zone

CO_2 from Atmosphere

Atmosphere O_2, CO_2

Soil Zone

Fractured Bedrock

Atmosphere + Added CO_2 from Soil Zone

Repository Heat Vaporizes Pore Water

H_2O Gas

TCw

PTn

TSw

H_2O Gas

Vaporized Pore Water Moves Away from Drifts by Convection

Perched Water

(B)
Reaction releases CO_2 gas in fractures

CO_2 gas

Silica Rich Tuff

CO_2 gas

Calcite

Minerals and Water React

Gas with Added CO_2

(C)

Degassing of Water, CO_2, O_2

Water Vapor Condenses

High Volumes of H_2O Gas Generated

CO_2 Gas Moves Out of Heated Pore Water

Temperature < Boiling

Temperature > Boiling

Water Vapor (H_2O Gas) Moves Away from Heated Zone

H_2O Gas Moves Out of Rock Pores

00018DC_EBS_PMR-02.ai

Figure 3-30. Schematic of processes affecting the availability of CO2 and other gases during the thermal period.
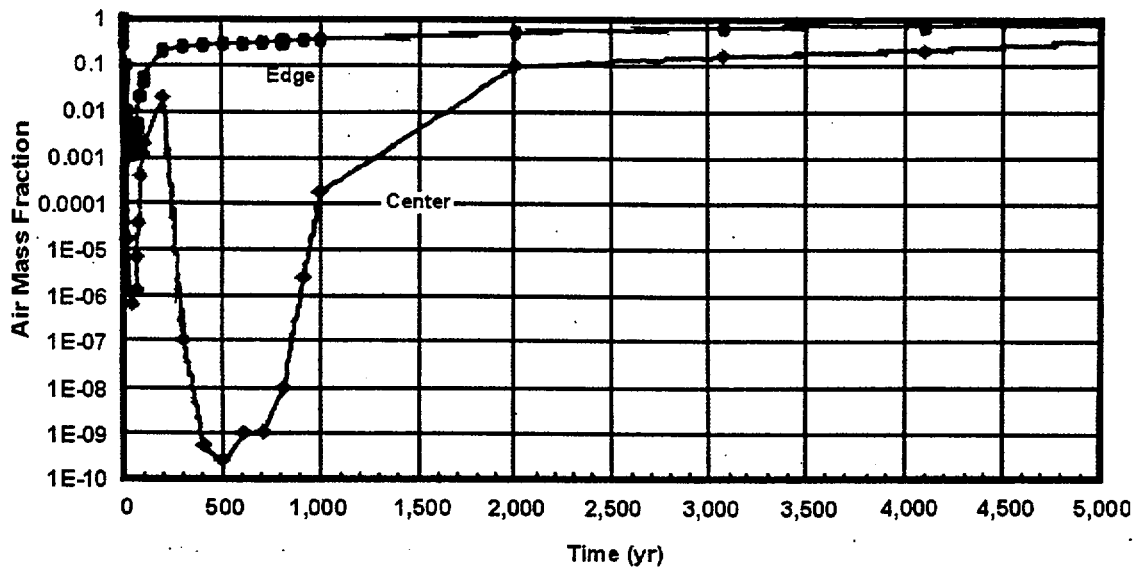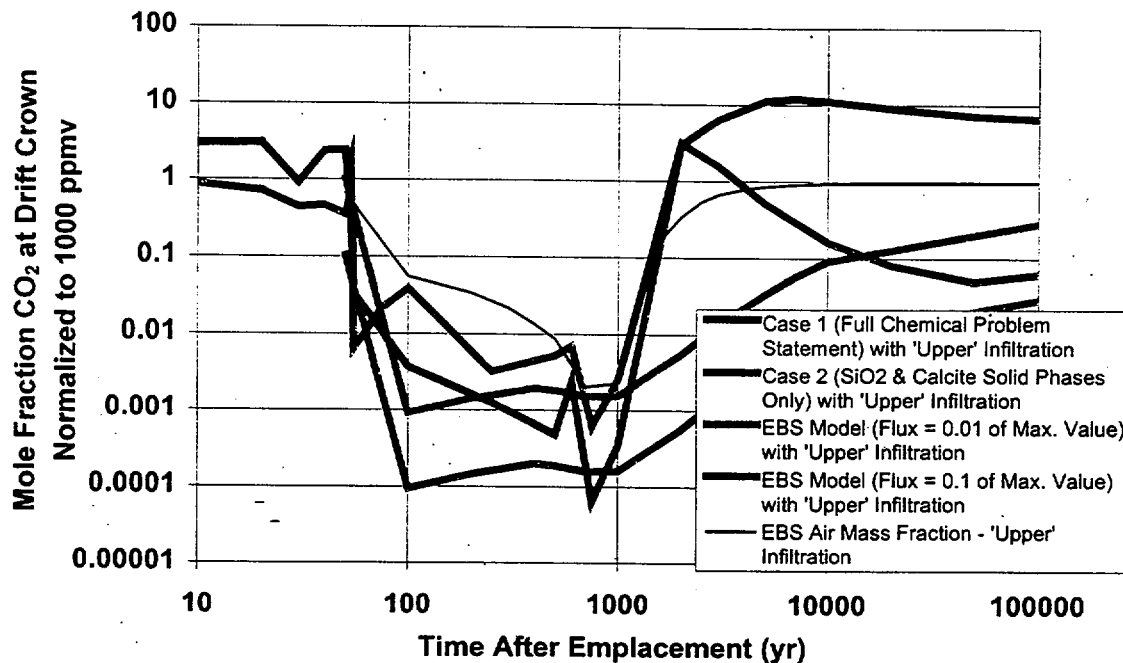
00018DC EBS-PMR-2D.cdr

Figure 3-31. Evolution of Air Mass-Fraction Calculated for Repository Center and Edge Locations, for the
Viability Assessment Repository Design
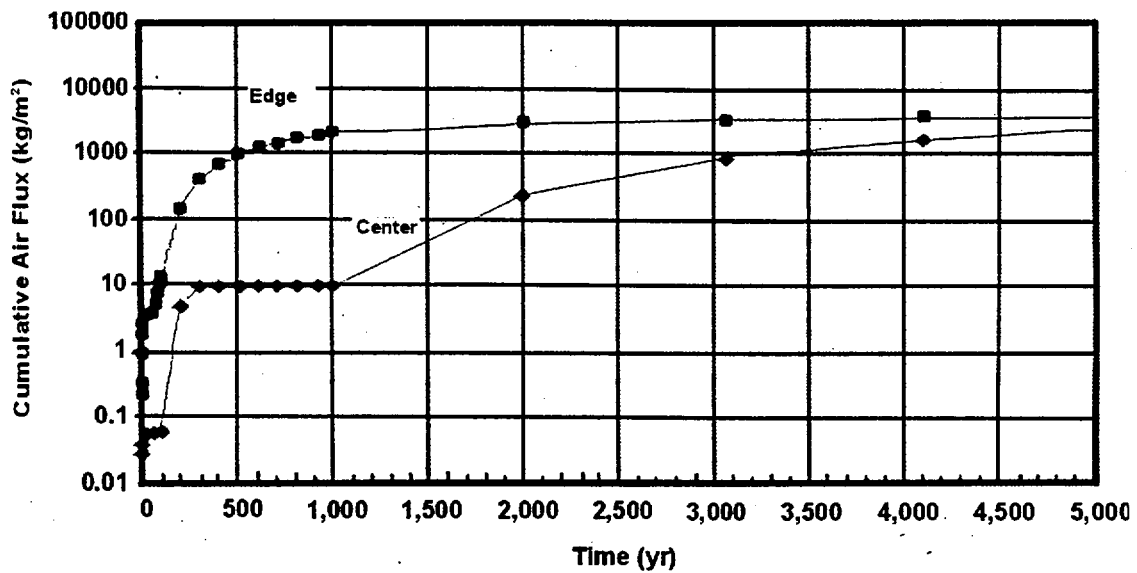
Figure 3-32. Cumulative Air Flux Flowing Through the Repository Horizon, Calculated for Repository Center and Edge Locations for the Viability Assessment Repository Design
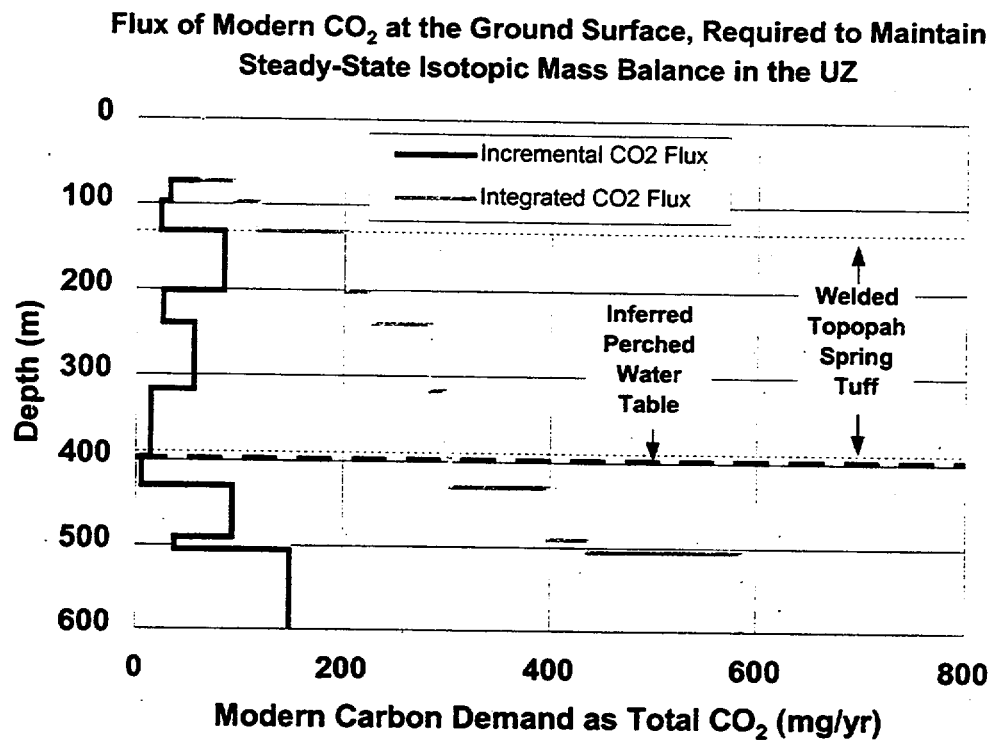
Figure 3-33. Comparison of Reactive Transport Simulation of CO2 Fugacity, with Results from the Gas Flux and Fugacity Model

Notes: Reactive transport calculations are taken from files: "case1_15.xls" and "case2_15.xls."
Results from the Gas Flux and Fugacity Model are described in this report.
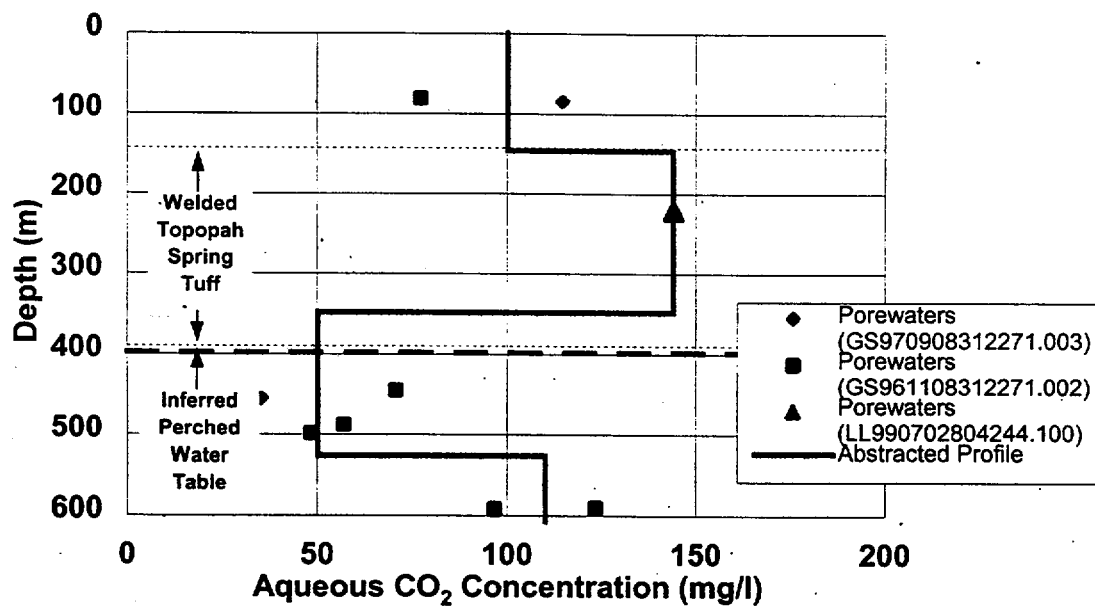
NOTE: From borehole SD-12 and in core samples from the Drift-Scale Test heated drift

Figure 3-34. Observed Distribution of Porewater CO_2 Concentration in Core Samples

Flux of Modern CO₂ at the Ground Surface, Required to Maintain Steady-State Isotopic Mass Balance in the UZ

Figure 3-35. Calculated Flux of $^{14}CO_2$ Required to Maintain Steady-State Isotopic Conditions in the Unsaturated Zone

NOTE: From borehole SD-12 and in core samples from the Drift-Scale Test heated drift
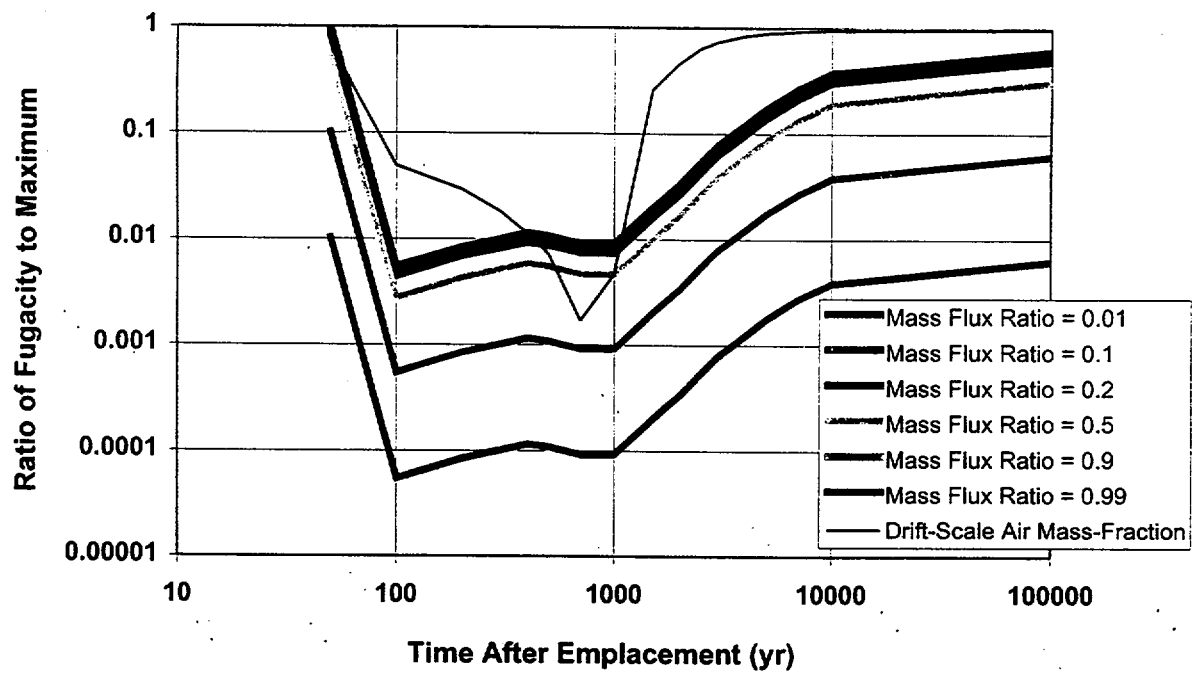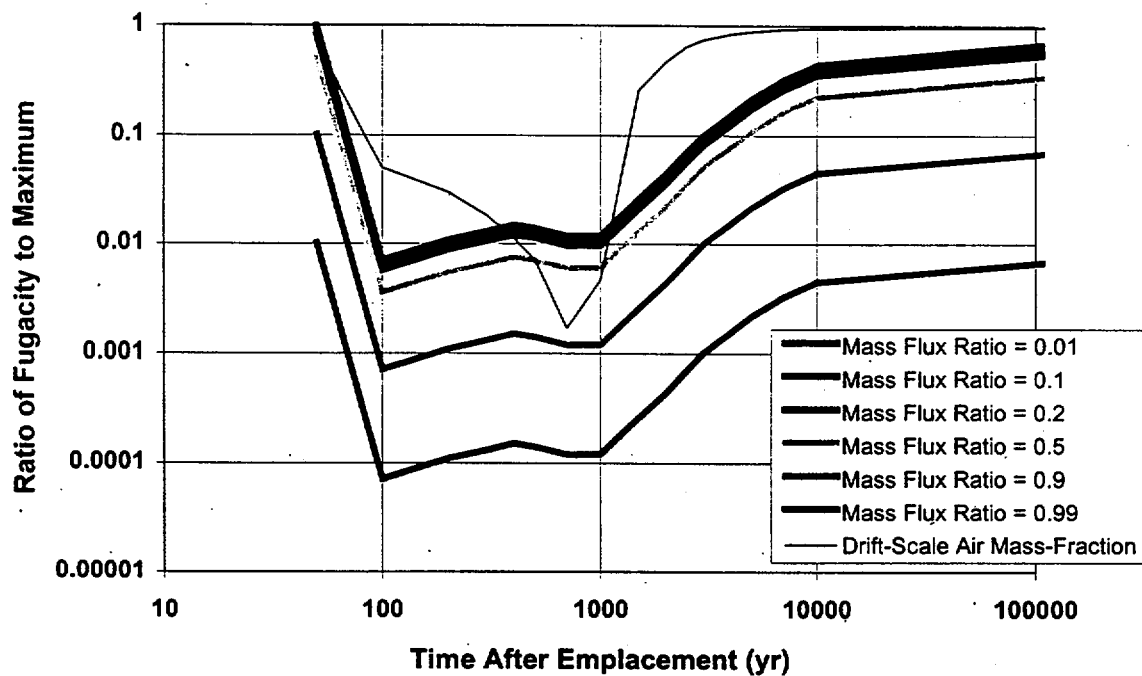Expressed as the flux of aqueous total CO_2 containing modern carbon
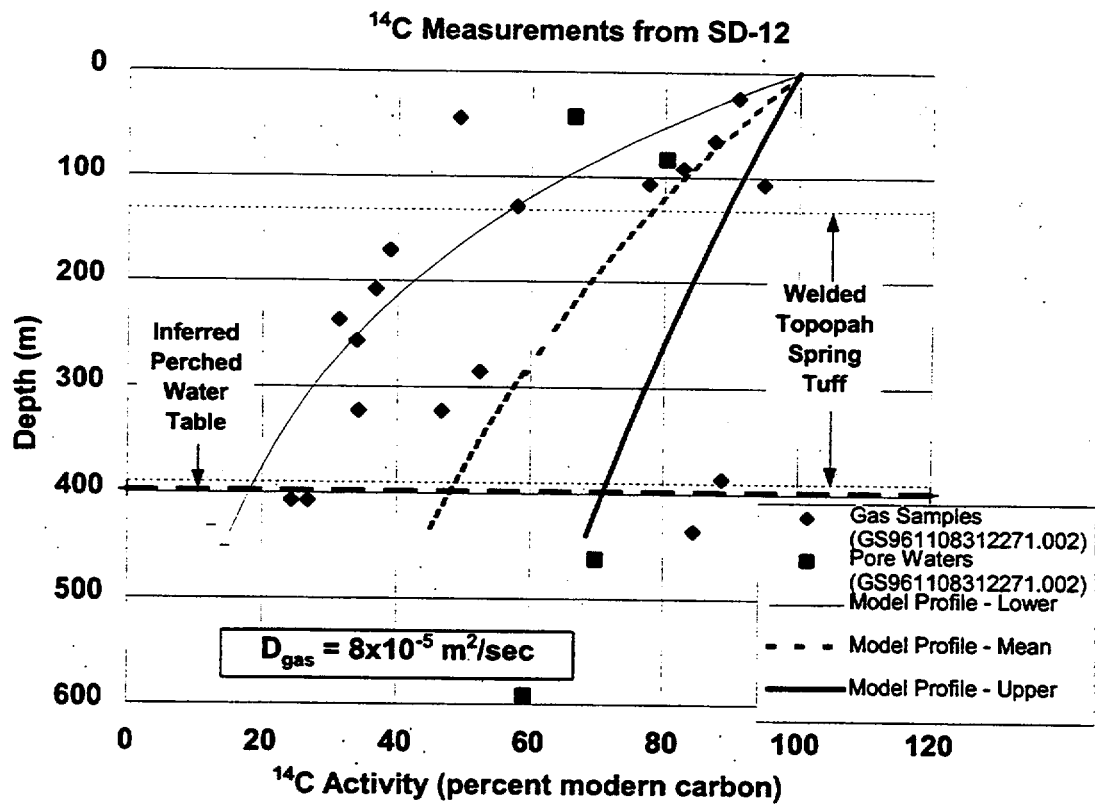
Figure 3-36. Exponential Model Fit to ^{14}C Activity vs. Depth in Borehole SD-12

NOTE: Ratios shown to the maximum value at the ground surface, vs. time, for different values of the CO_2 mass flux

Figure 3-37. Lower-Bound Ratios of the CO_2 Concentration (Fugacity) at Repository Depth

NOTE: Ratios shown to the maximum value at the ground surface, vs. time, for different values of the CO_2 mass flux

Figure 3-38. Lower-Bound Ratios of the O_2 Concentration (Fugacity) at Repository Depth
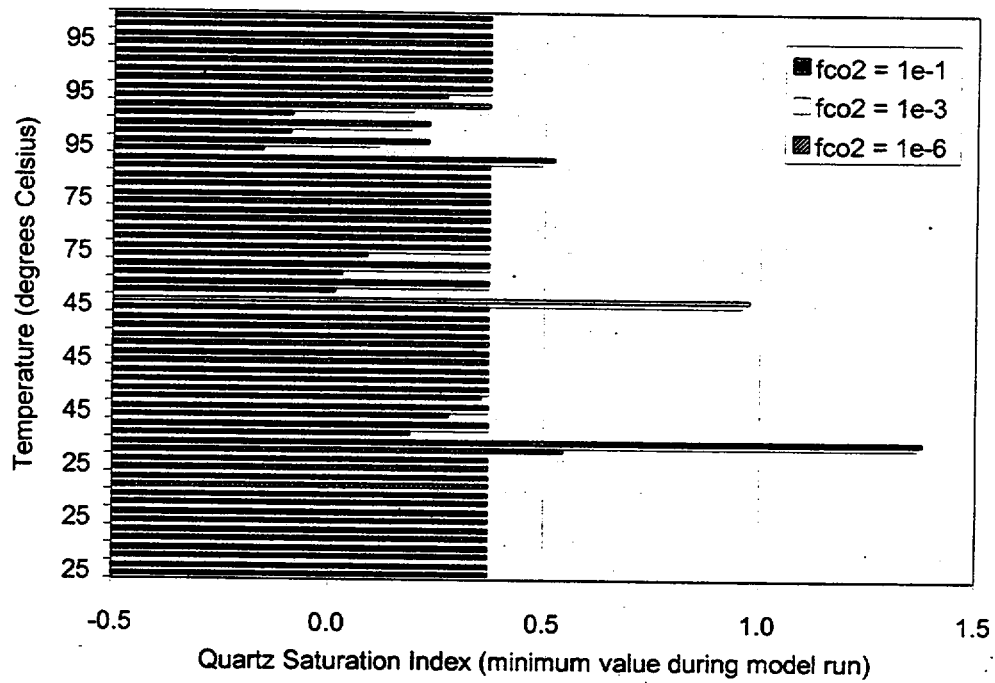
Figure 3-39. Plot of Quartz Saturation Indices for All Cases Evaluated for Seepage/Backfill Interaction (from Seepage/Backfill Interaction Analysis/Model Report; CRWMS M&O 2000k)
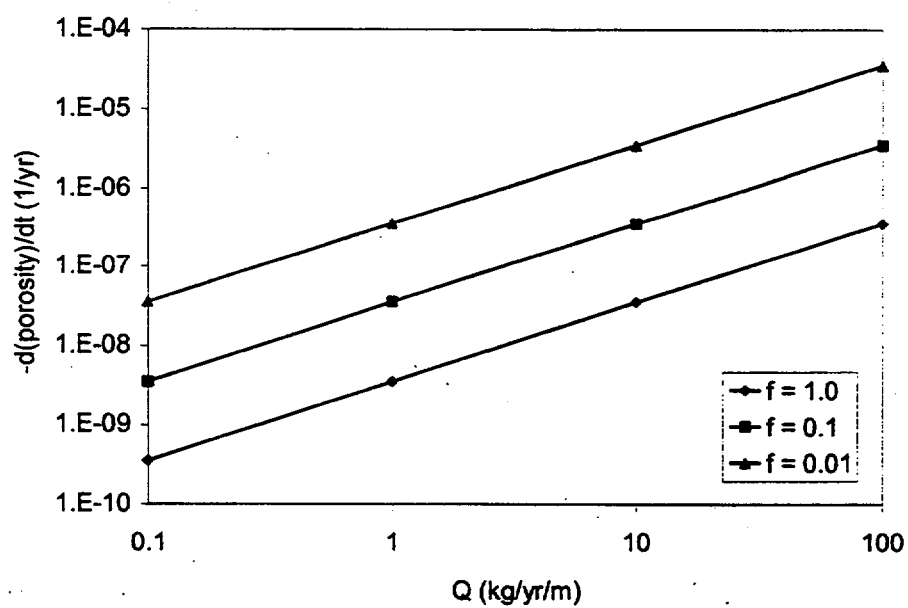
Figure 3-40. Porosity Reduction Rate vs. Seepage Rate of J-13 and the Focus Factor (from Seepage/Backfill Interaction Analysis/Model Report; CRWMS M&O 2000k)
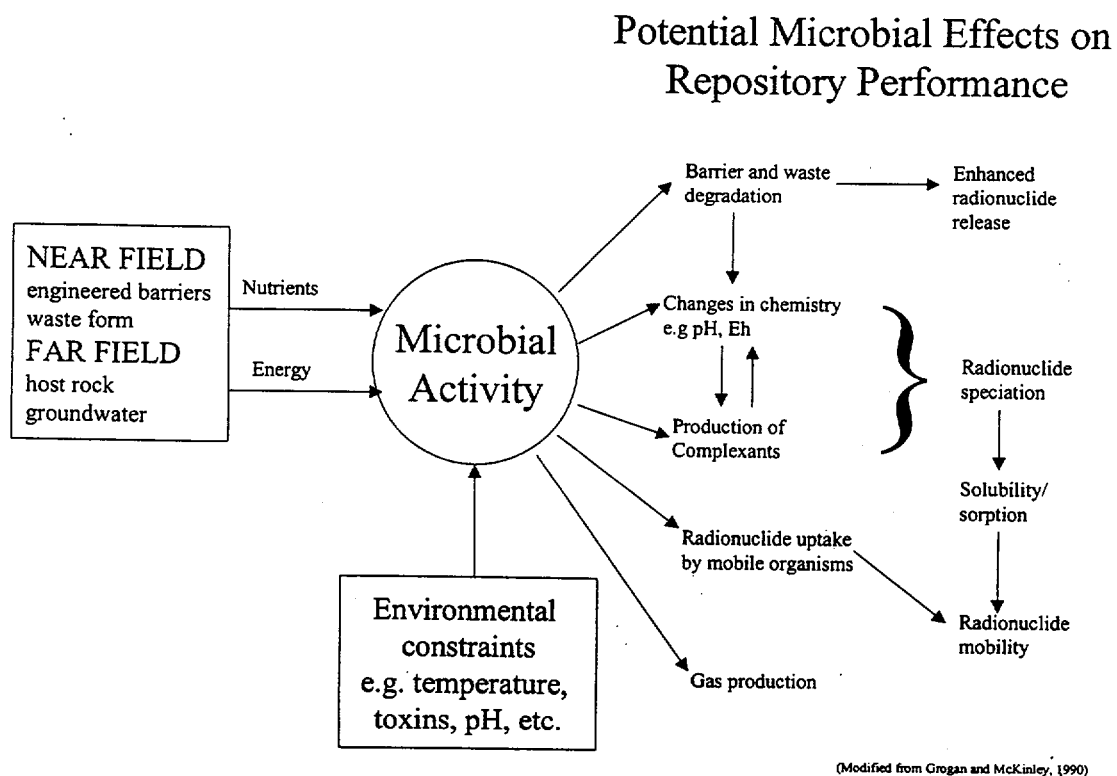
Potential Microbial Effects on Repository Performance

Figure 3-41. Simplified Flow Diagram of the Potential Effects of Microbial Activity on Repository Performance

TSPA-VA Results

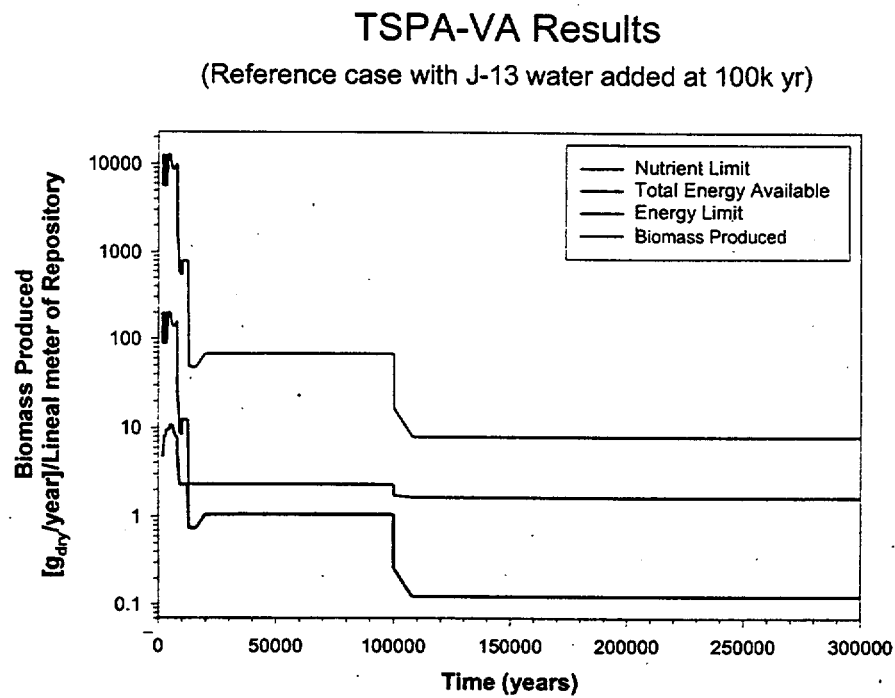### (Reference case with J-13 water added at 100k yr)

Figure 3-42. Results of TSPA-VA Model for Microbial Communities in the Repository Emplacement Drifts
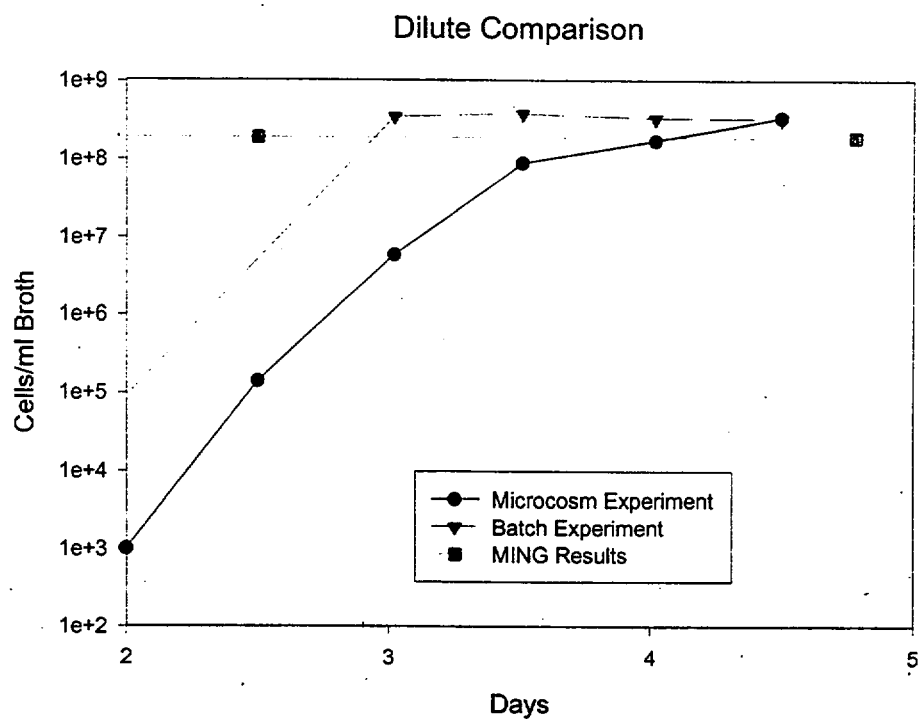
Figure 3-43. Comparison of Growth Rate Experiments in DC Growth
Media with Calculated Values in MING

Figure 3-44. pH and Ionic Strength vs. Evaporative Concentration for Synthetic J-13 Water, Comparing Data and Model Calculations ("evap4" test)
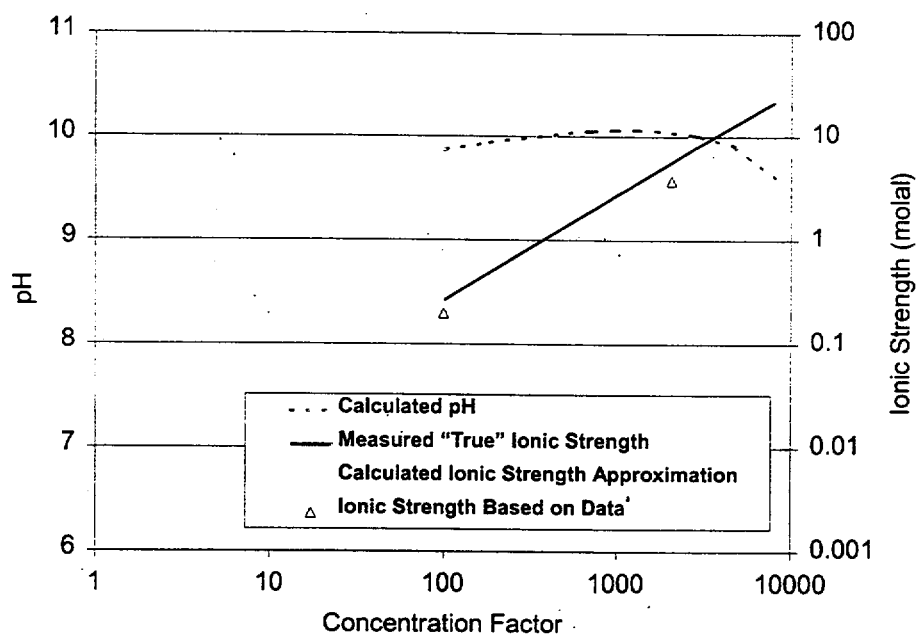
Figure 3-45. pH and Ionic Strength for Synthetic 100x J-13 Water, Comparing Data and Model Calculations ("Batch 1" test).
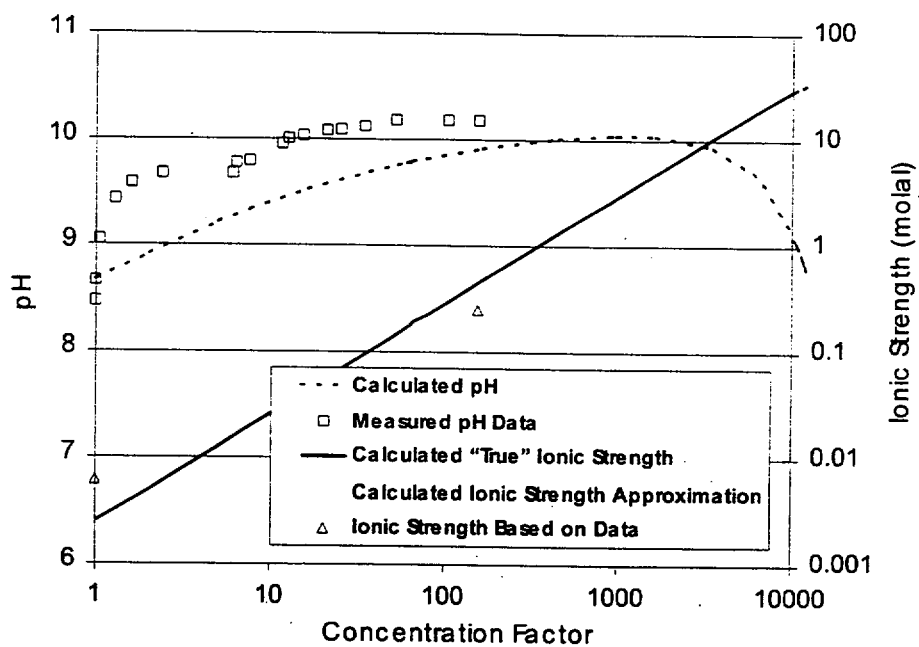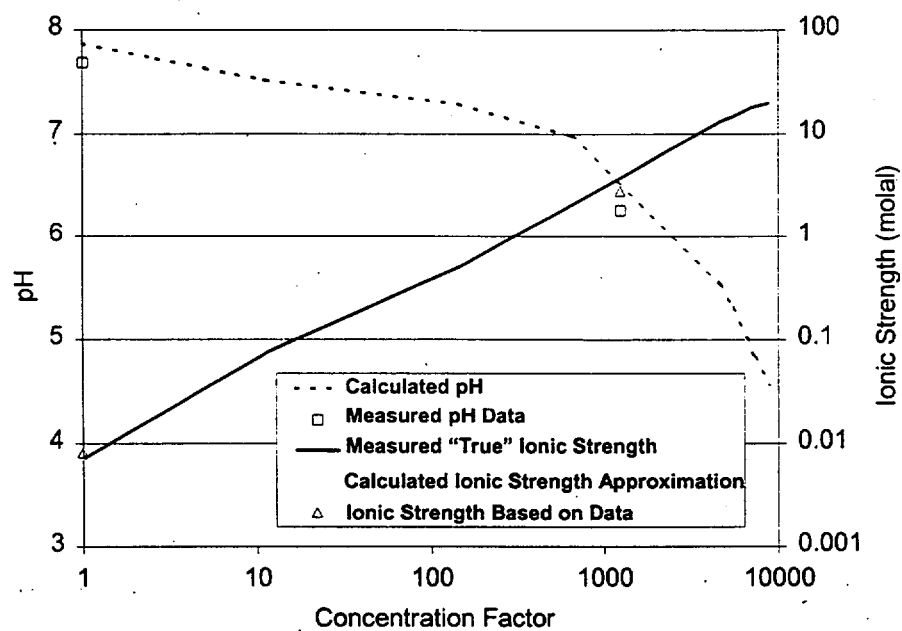
Figure 3-46. pH and Ionic Strength vs. Evaporative Concentration for Synthetic J-13 Water, Comparing Data and Model Calculations ("evap3" test).
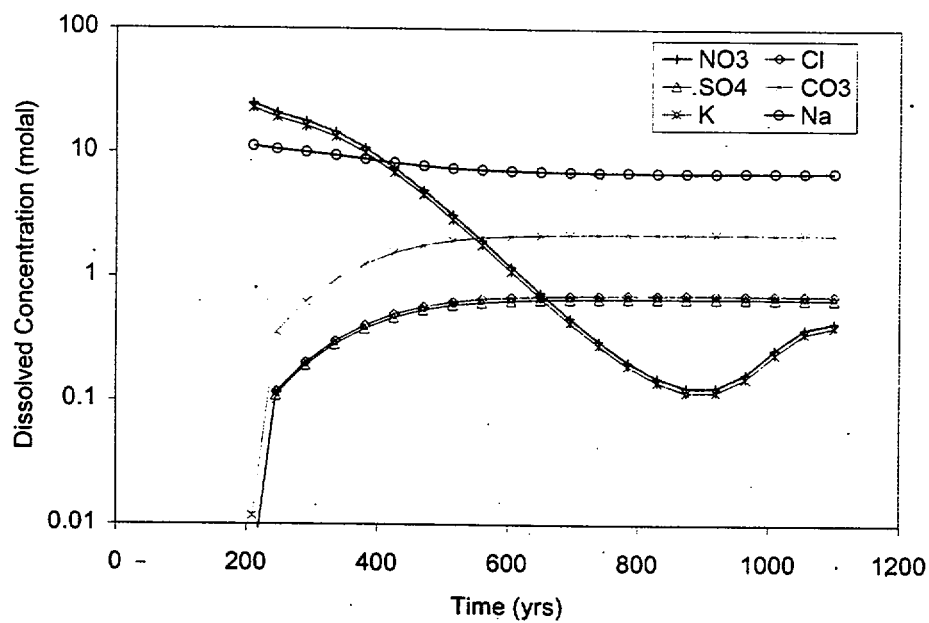
Figure 3-47. Dissolved Concentration vs. Time (J-13 water, Q_{seep} = 1 L/yr, P_{CO2} = 10^{-3} atm).
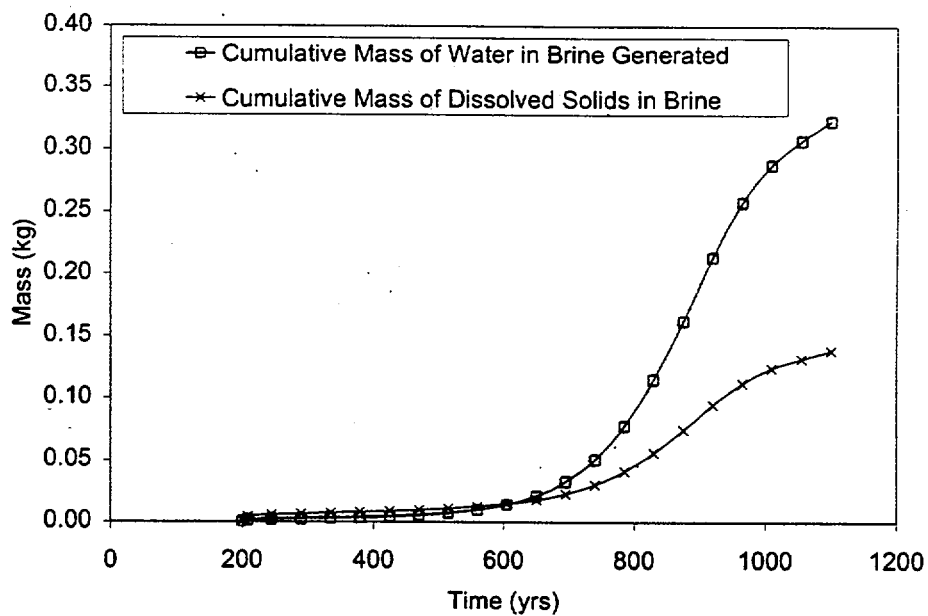
Figure 3-48. Cumulative Mass of Water and Dissolved Ions in Generated Brine vs. Time (J-13 water, Q_{seep} = 1 L/yr, P_{CO2} = 10^{-3} atm).
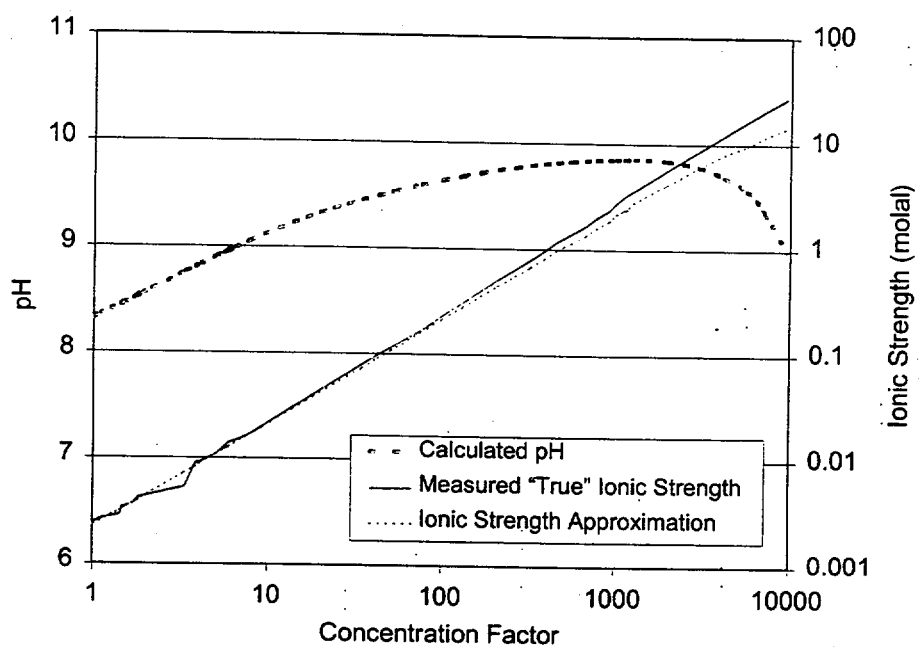
Figure 3-49. pH and Ionic Strength Predictions from Simple Evaporation of Average J-13 Well Water at 95°C and f_{CO2} of 10^{-3}.
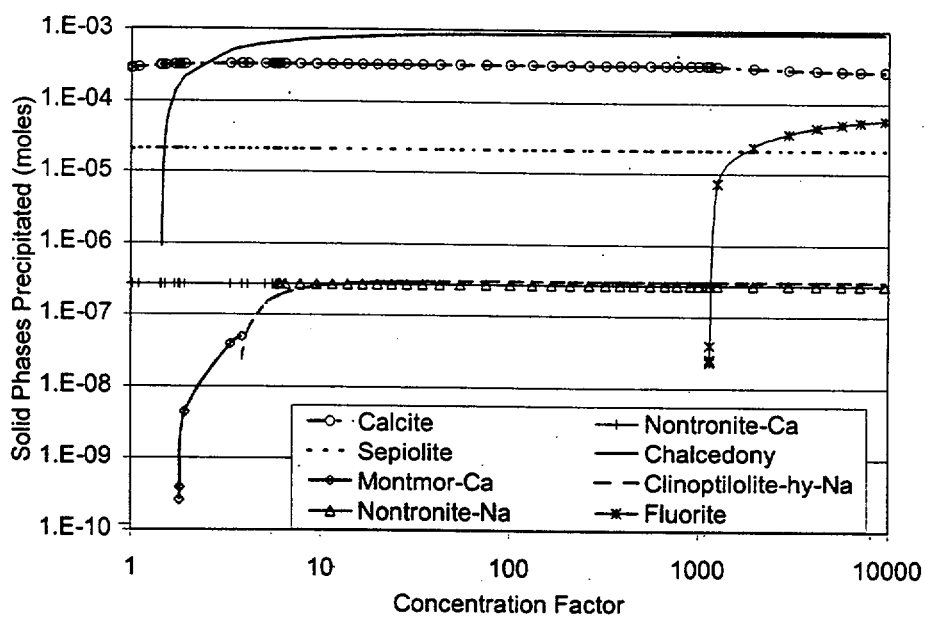
Figure 3-50. Mineral Precipitation Predictions from Simple Evaporation of Average J-13 Well Water at 95°C and f_{CO2} of 10^{-3}.
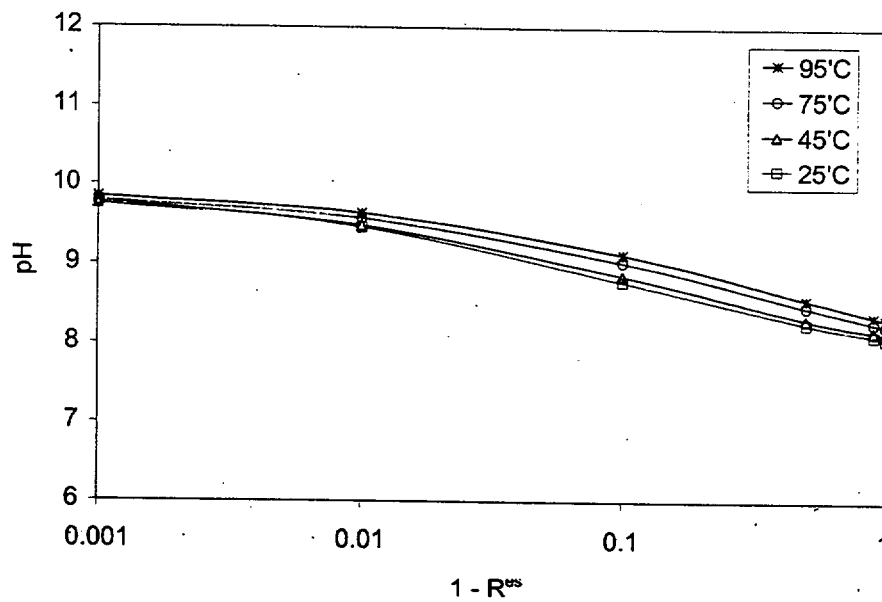
Figure 3-51. J-13 Steady State pH vs. (1-R^{es}) and Temperature ($f_{CO2} = 10^{-3}$).
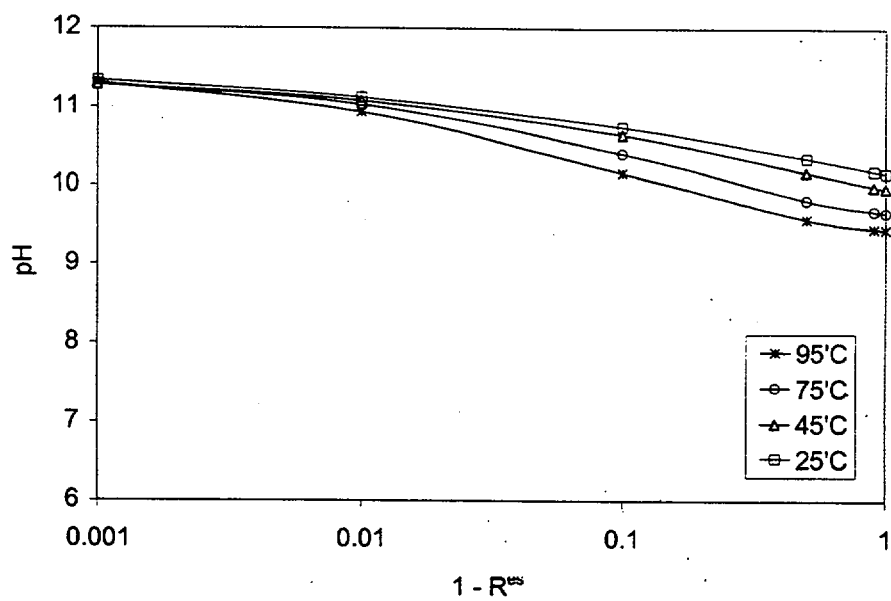
Figure 3-52. J-13 Steady State pH vs. $(1-R^{es})$ and Temperature $(f_{CO2} = 10^{-6})$.
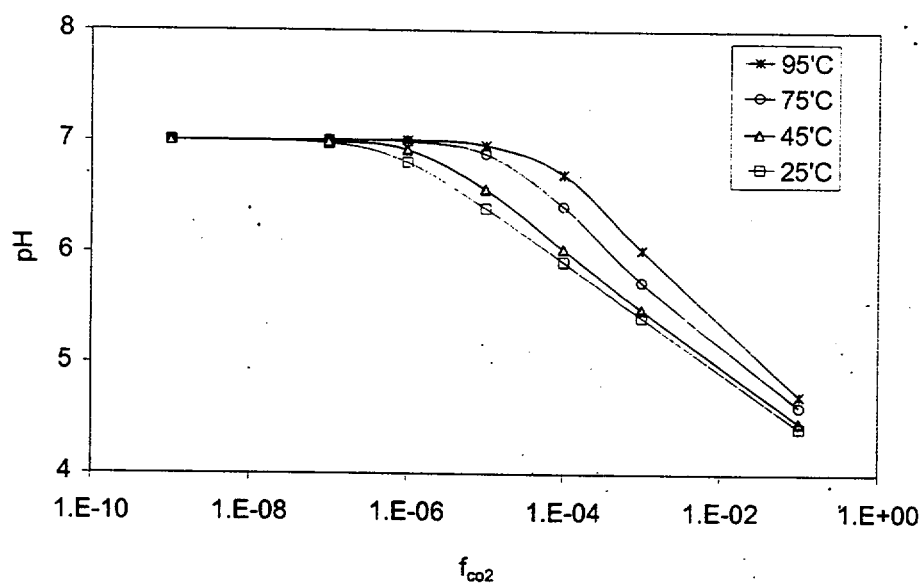
Figure 3-53. Predicted pH of Condensed Water for a Range of Temperatures and CO_2 Fugacities (f_{CO2}).

(A) Colloid Size Distribution, Yucca Mountain Wells

(B) Colloid Size Distribution, Nye County Wells
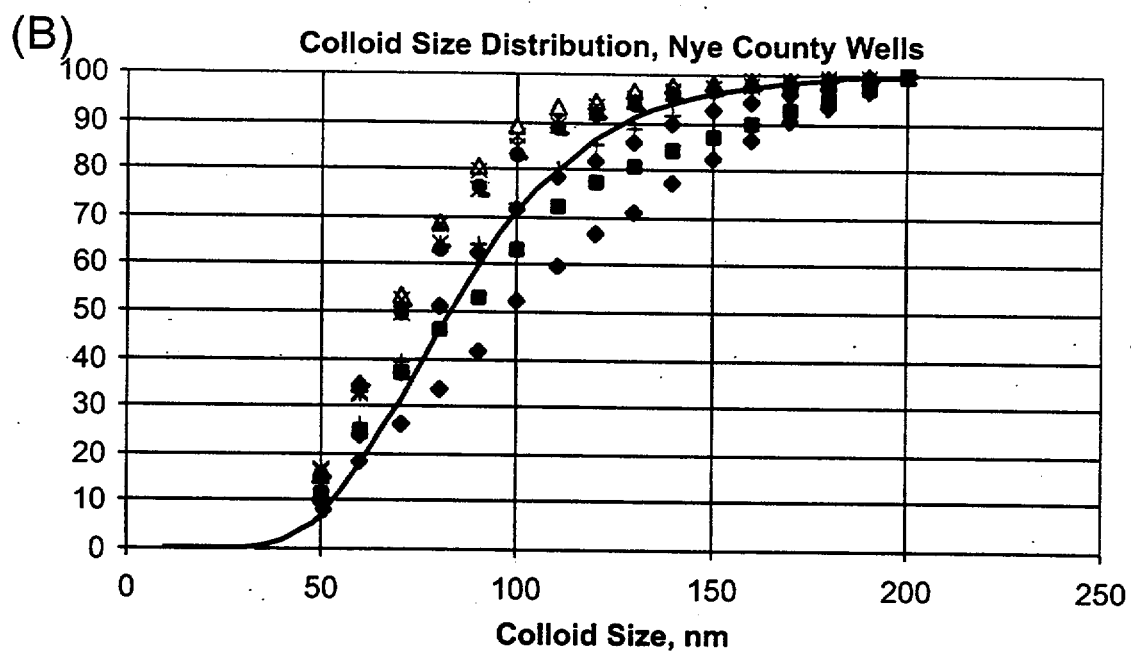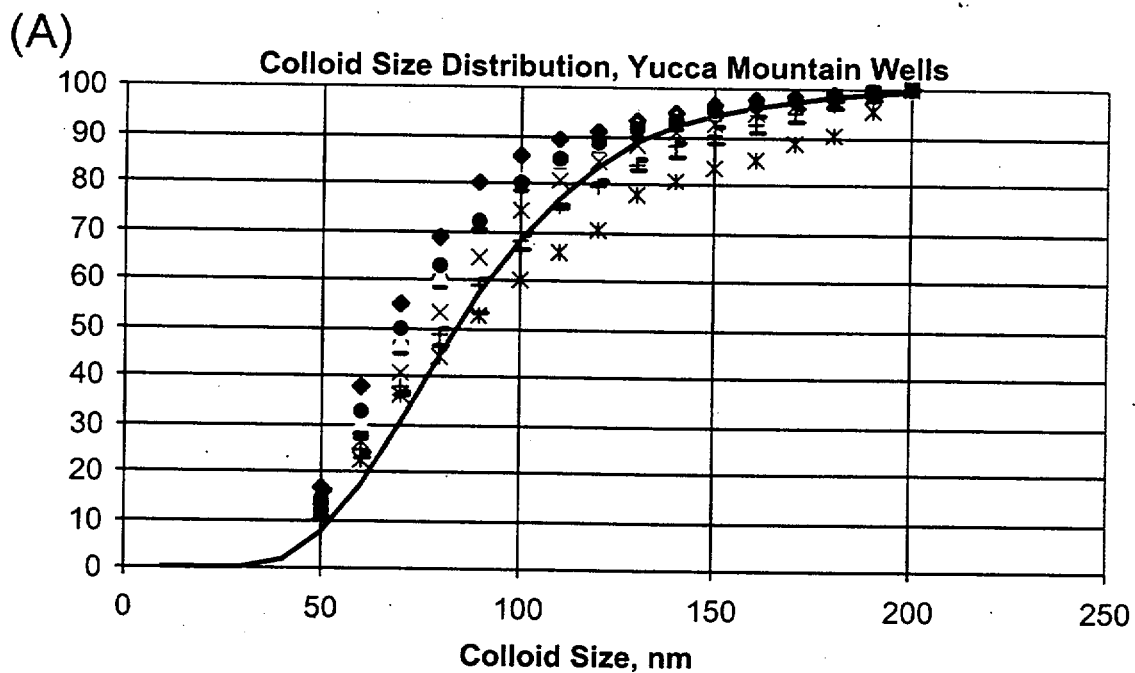
NOTES: A Data from Yucca Mountain wells.
B Data from Nye County wells.
The upper solid curve is for a log-normal distribution with $\mu = 19.2688$ and $\sigma = 2.0441$, based on regression. The lower solid curve is for a log-normal distribution with $\mu = 19.4841$ and $\sigma = 1.9911$, calculated directly from the data. Both curves agree well with the data points

Figure 3-54. Particle Size Distribution for Colloids in Groundwater Samples near Yucca Mountain

Colloid Particle Count
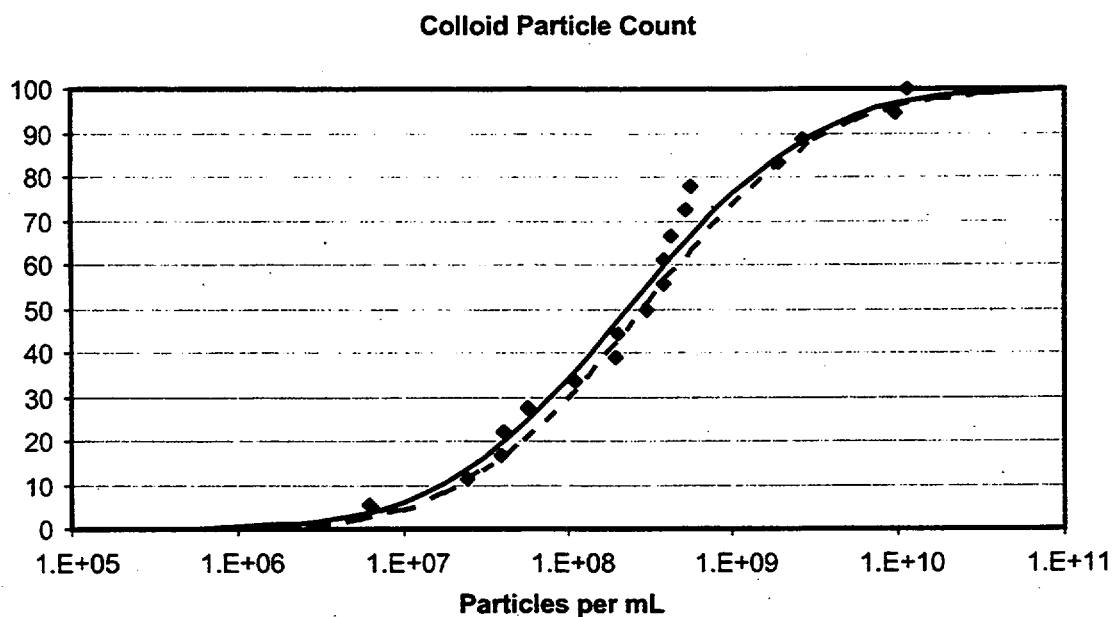
NOTES: Data points are shown for all 18 wells sampled. Two log-normal distributions are shown: The solid curve is based on Nye County data, and the dashed curve is based Yucca Mountain data. The distributions are almost indistinguishable in the plots, and the parameters are not significantly different at the 95% confidence level.

Figure 3-55. Distribution of Total Number of Colloid Particles per Milliliter in Groundwater Samples Near Yucca Mountain

Diffusivity vs. Particle Diameter

$$y = 0.4217x^{-1.1625}$$
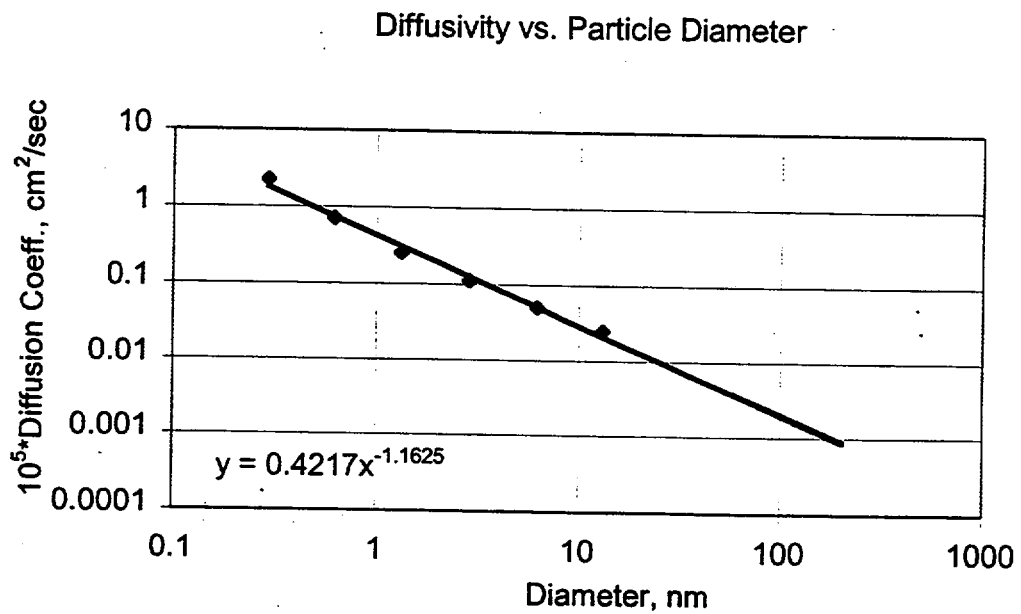
NOTES: Estimate appears conservative.
Values shown with points are handbook values (CRWMS M&O 2000t)
Values shown with line are from Stokes-Einstein equation (CRWMS M&O 2000t)

Figure 3-56. Estimated Diffusion Coefficient as a Function of Particle Size Using the Stokes-Einstein Equation, Compared with Handbook Values

Mountain-Scale Processes Affecting Incoming Water

(A)
Unsaturated Zone Pore Water (Nonwelded Units) Higher in Chloride and Sulfate than J-13 Water

(C)
Water Moving in Fractures is Similar to J-13 Water and Water at Ranier Mesa

Water

CO_2

CO_2 Gas

Calcite

(B)
Perched and Tuff Aquifer Water (J-13) Dilute Sodium Carbonate Calcite Close to Saturation

(D)

Temperature < Boiling

Temperature > Boiling

H_2O Gas

CO_2

Condensed Water Reacts with Minerals

Calcite

Tuff Minerals + Alteration Products

Water Condenses on Pore Walls

Precipitates form on Pore Walls (Salts,Carbonates, Silicates)

Boiling Water Minerals Concentrate and Precipitate

00018OC_EBS_PMR-03.ai

Figure 3-57. Schematic of processes affecting the composition of seepage.

CO$_2$ Budget from Chemical Reference Model
(L4C4 location; "upper" infiltration)
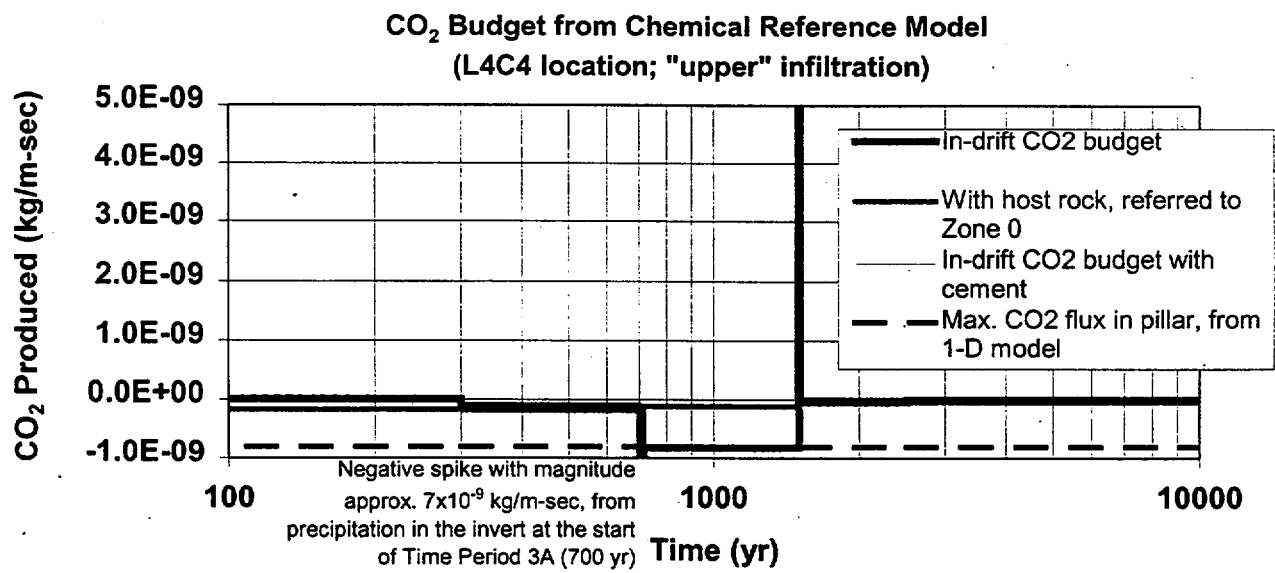
Figure 3-58. CO2 Budget for Reference Model (L4C4 location; "upper" infiltration)

pH Evolution for Reference Model

The backfill and invert are dry until Time Period 3 (700 to 1500 yr) and Time Period 4 (1500 to 2500 yr), respectively.

Host Rock (Zone 1/2)

Backfill (Zone 3/4)

Invert (Zone 5/6)
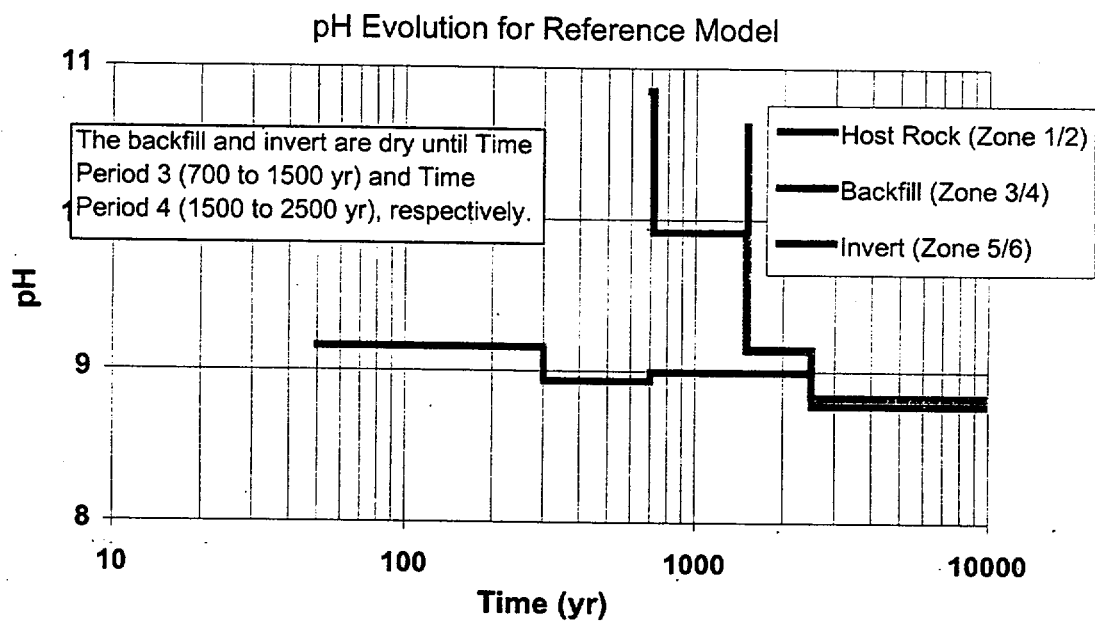
Figure 3-59. pH vs. Time for the Chemical Reference Model

Ionic Strength Evolution for Reference Model

The backfill and invert are dry until Time
Period 3 (700 to 1500 yr) and Time
Period 4 (1500 to 2500 yr), respectively.

Host Rock (Zone 1/2)

Backfill (Zone 3/4)

Invert (Zone 5/6)
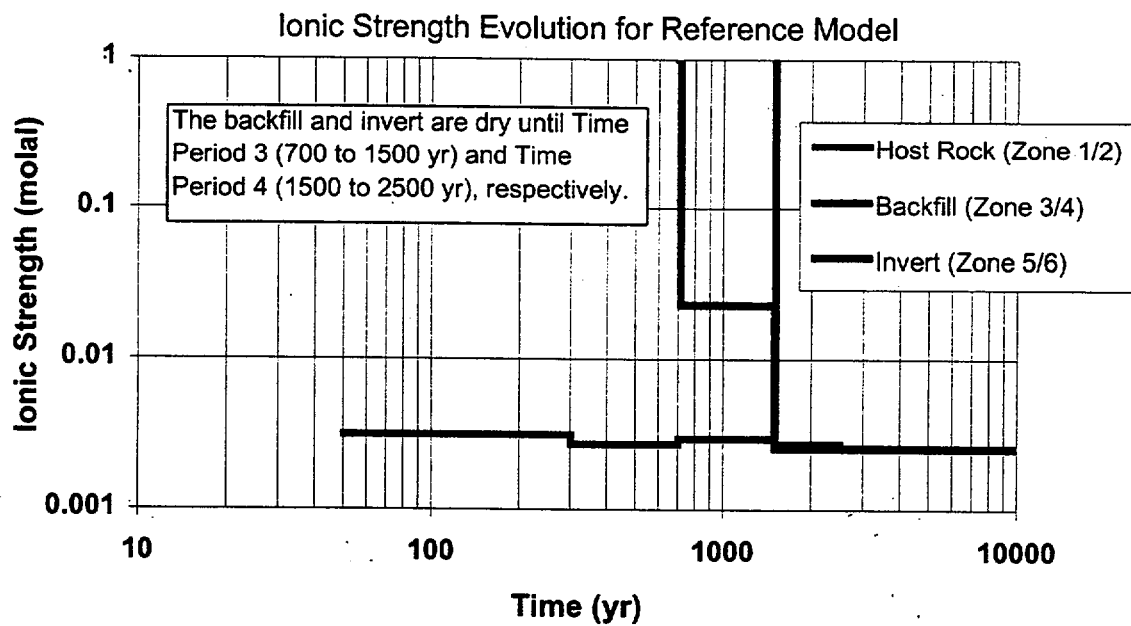
Figure 3-60. Ionic Strength vs. Time, for the Chemical Reference Model

RH vs. Time at the Drip Shield Surface (Zone 4)(CRWMS M&O 2000t)

Water enters zone

Brine dilution by humidity,
and deliquescence points of various salts.

Nitrate, chloride, sulfate brines;
most deliquescent are nitrates, divalent chloride salts.

L4C4 center location; "upper" infiltration
L4C4 center location; "lower" infiltration
L4C1 edge location; "upper" infiltration
L4C1 edge location; "lower" infiltration

Time (yr)

Figure 3-61. Relative Humidity vs. Time at the Drip Shield Surface

Conditions for MIC at the Drip Shield Surface (Zone 4) (CRWMS M&O 2000t)
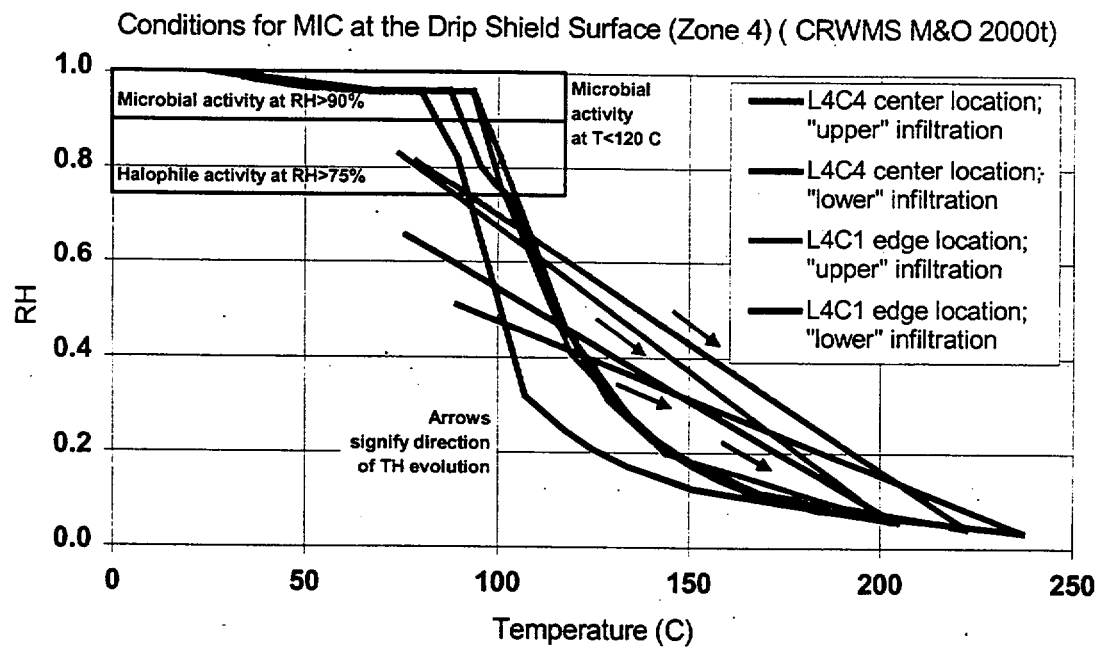
Figure 3-62. Conditions for MIC at the Drip Shield Surface

Key Block Formed by the Intersection of an
Excavation with
Three Fracture Planes

Stereographic Projection of
Key-Block-Forming Fracture Planes

N

133/83

338/12

W

E

235/87

S

Tunnel
Excavation
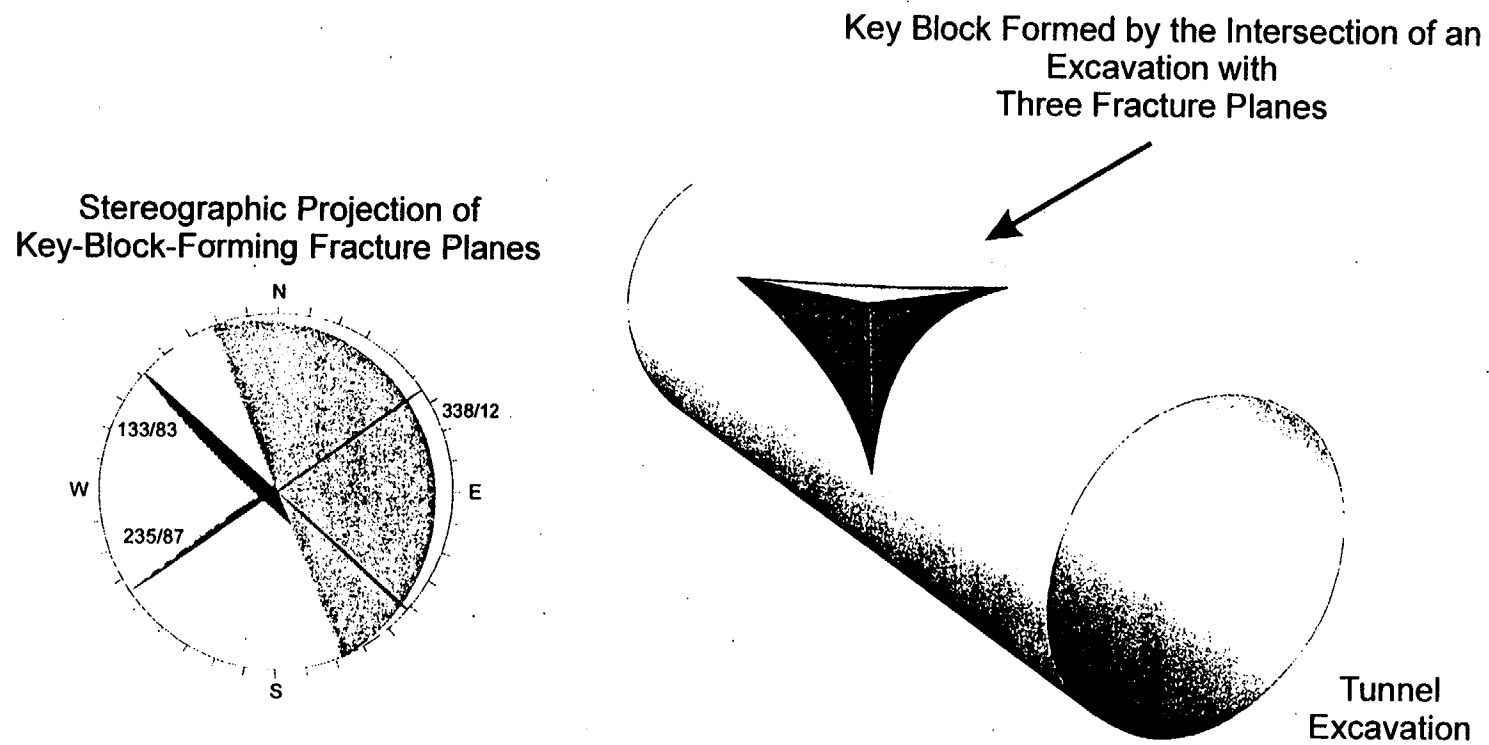
Figure 3-63. Illustration of a Typical Key Block and Associated Fracture Planes
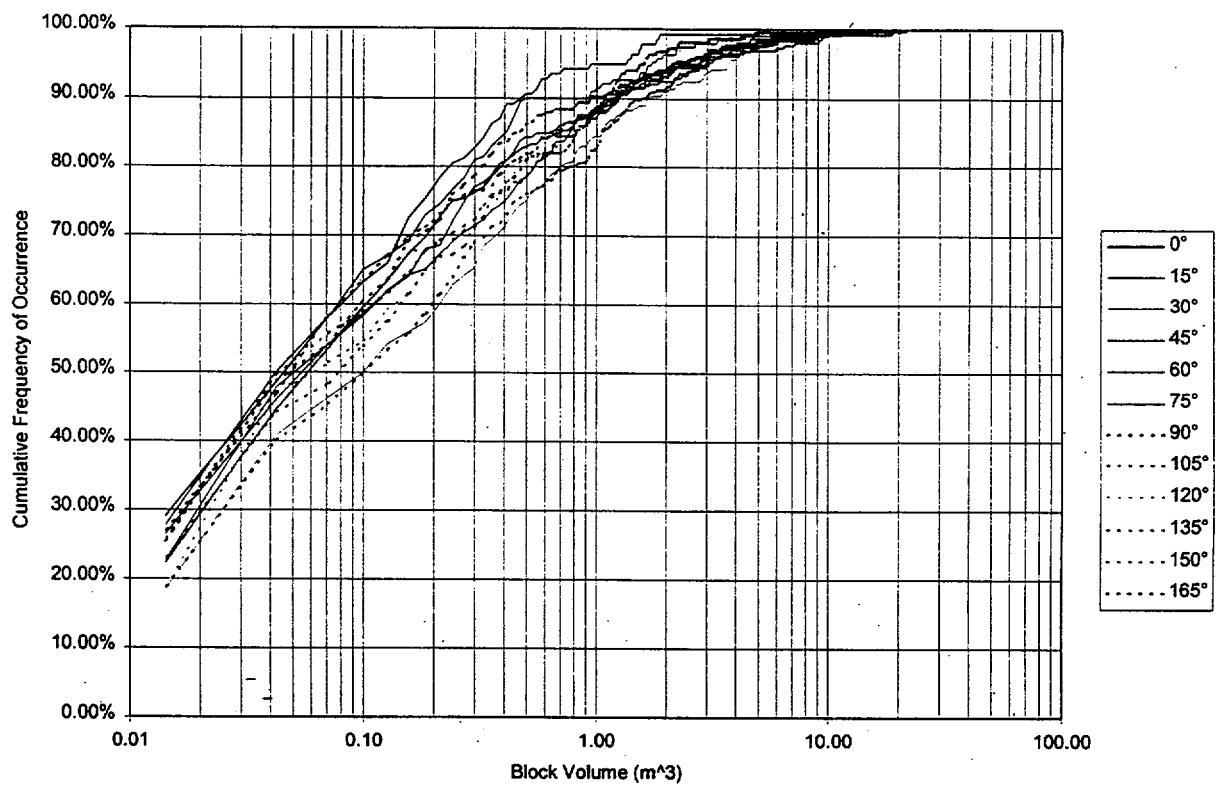
Figure 3-64. Cumulative Block Size Distribution for Various Drift Orientations in the Tptpmn Unit, Static Condition
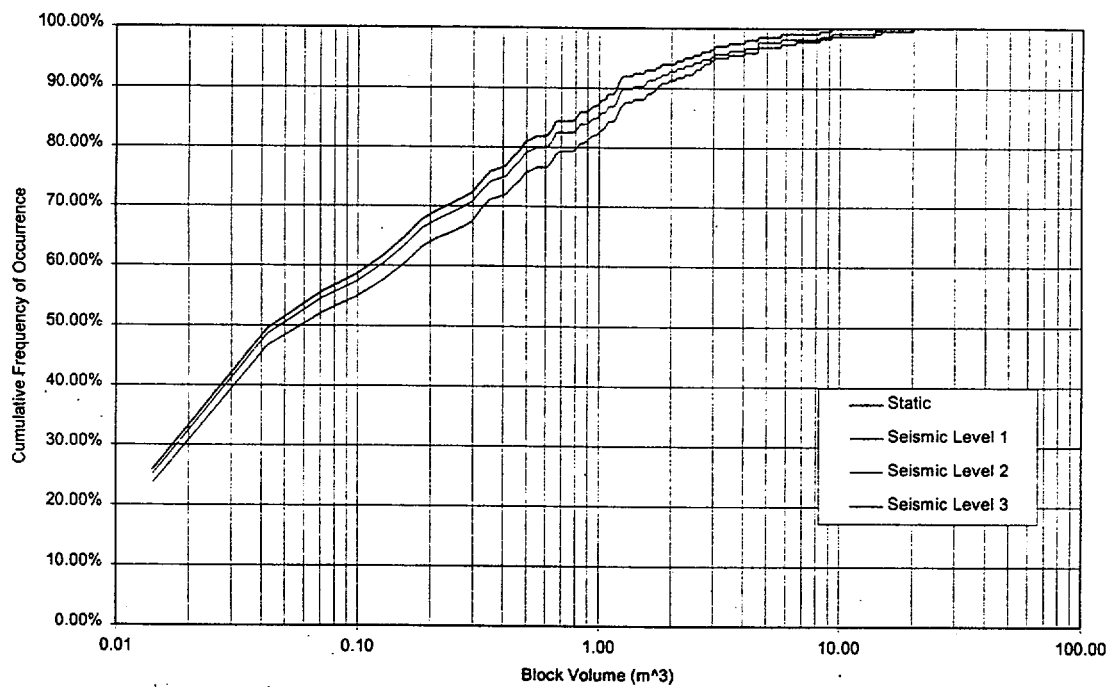
NOTE: The seismic level 2 and seismic level 3 distribution curves are identical.

Figure 3-65. Cumulative Key Block Size Distribution for Seismic Consideration in the Tptpmn Unit
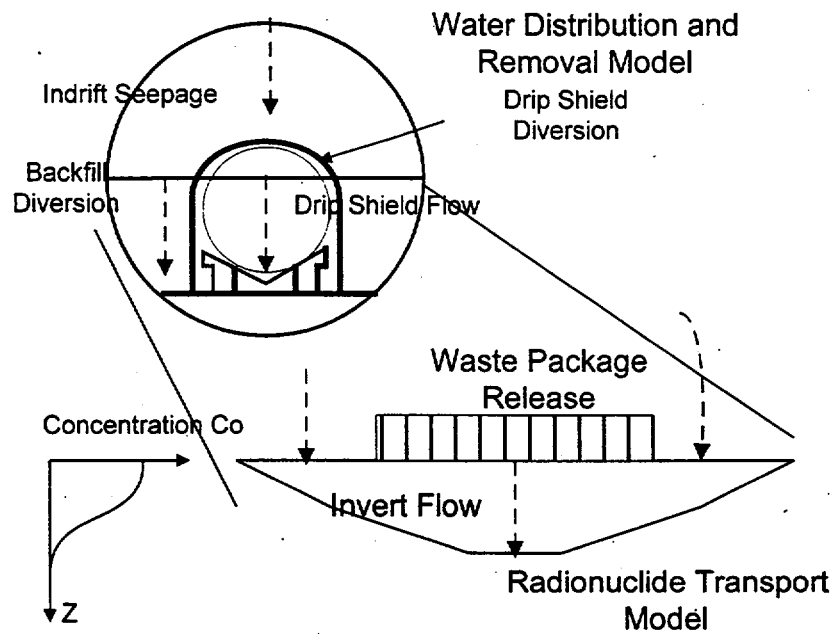
Figure 3-66. Conceptual Model for Radionuclide Transport Model
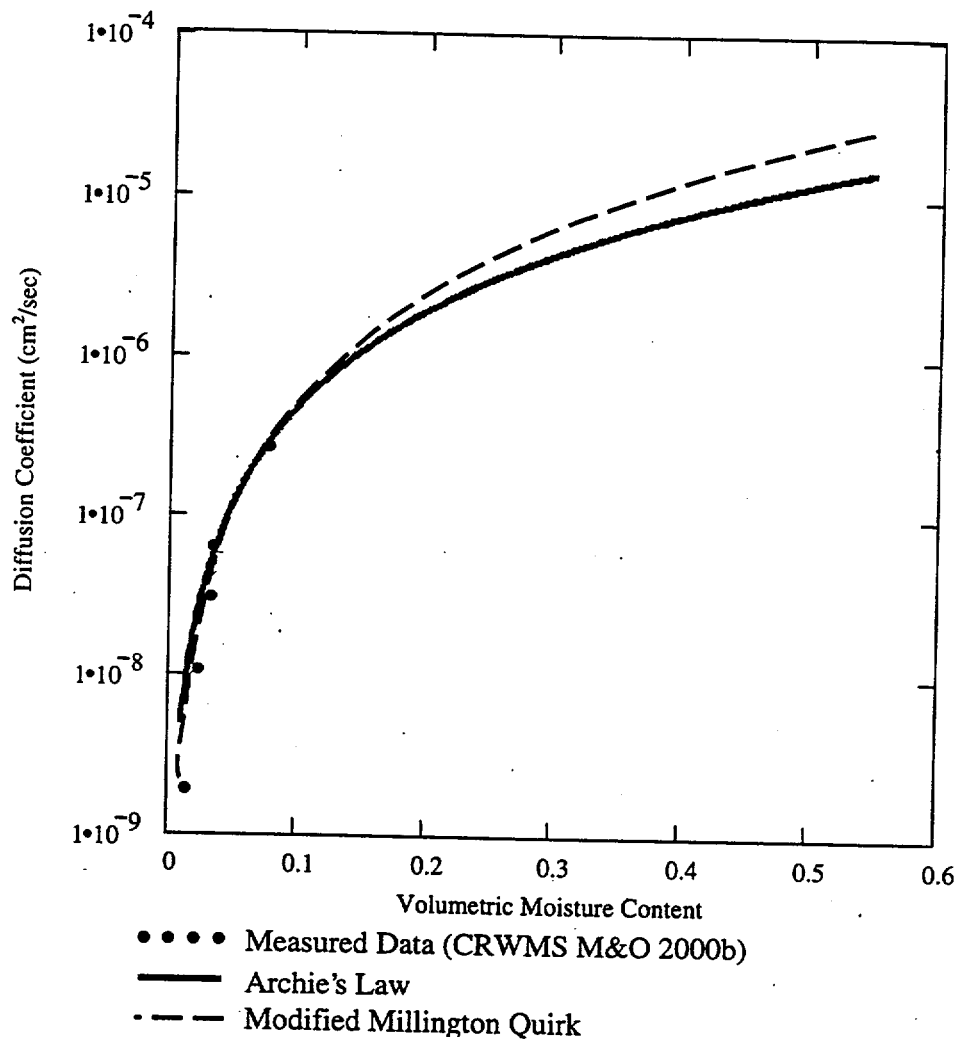
Figure 3-67. Comparison of Measured Data for Crushed Tuff with Archie's Law, and the Modified Millington Quirk Relation.
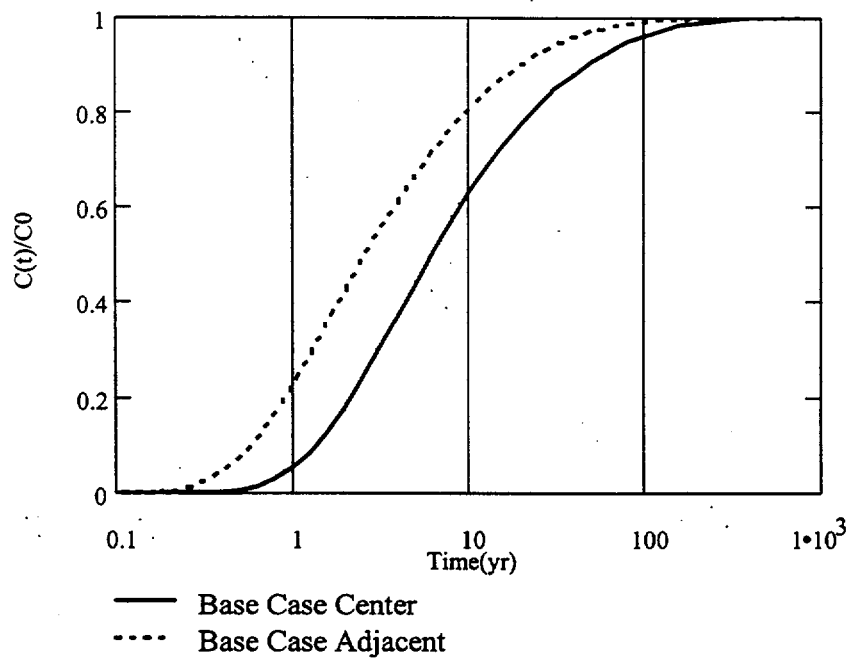
Figure 3-68. Breakthrough for One Dimensional Advection/Dispersion/Diffusion for the Base Case
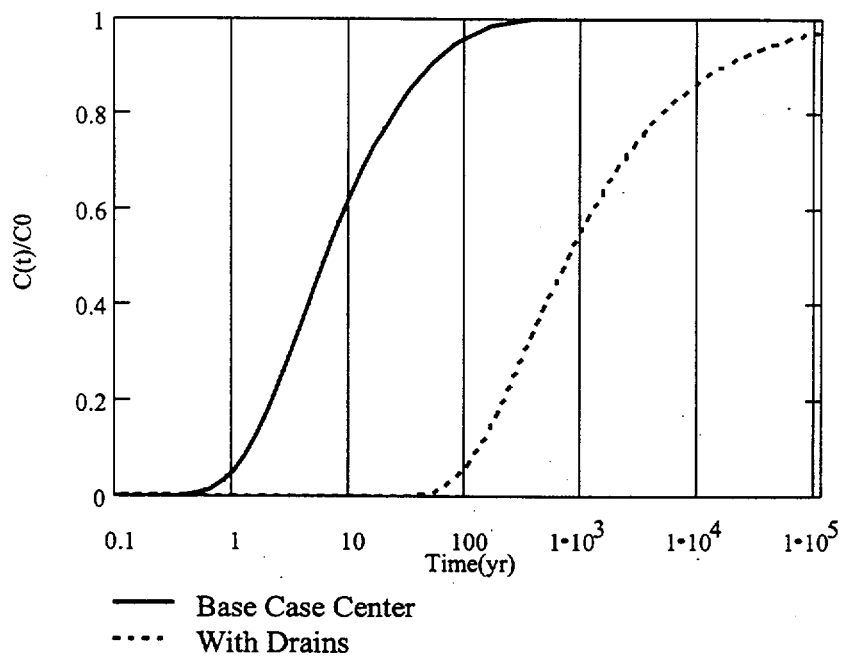
Figure 3-69. Effect of Sand Drains on Breakthrough for the Glacial Climate
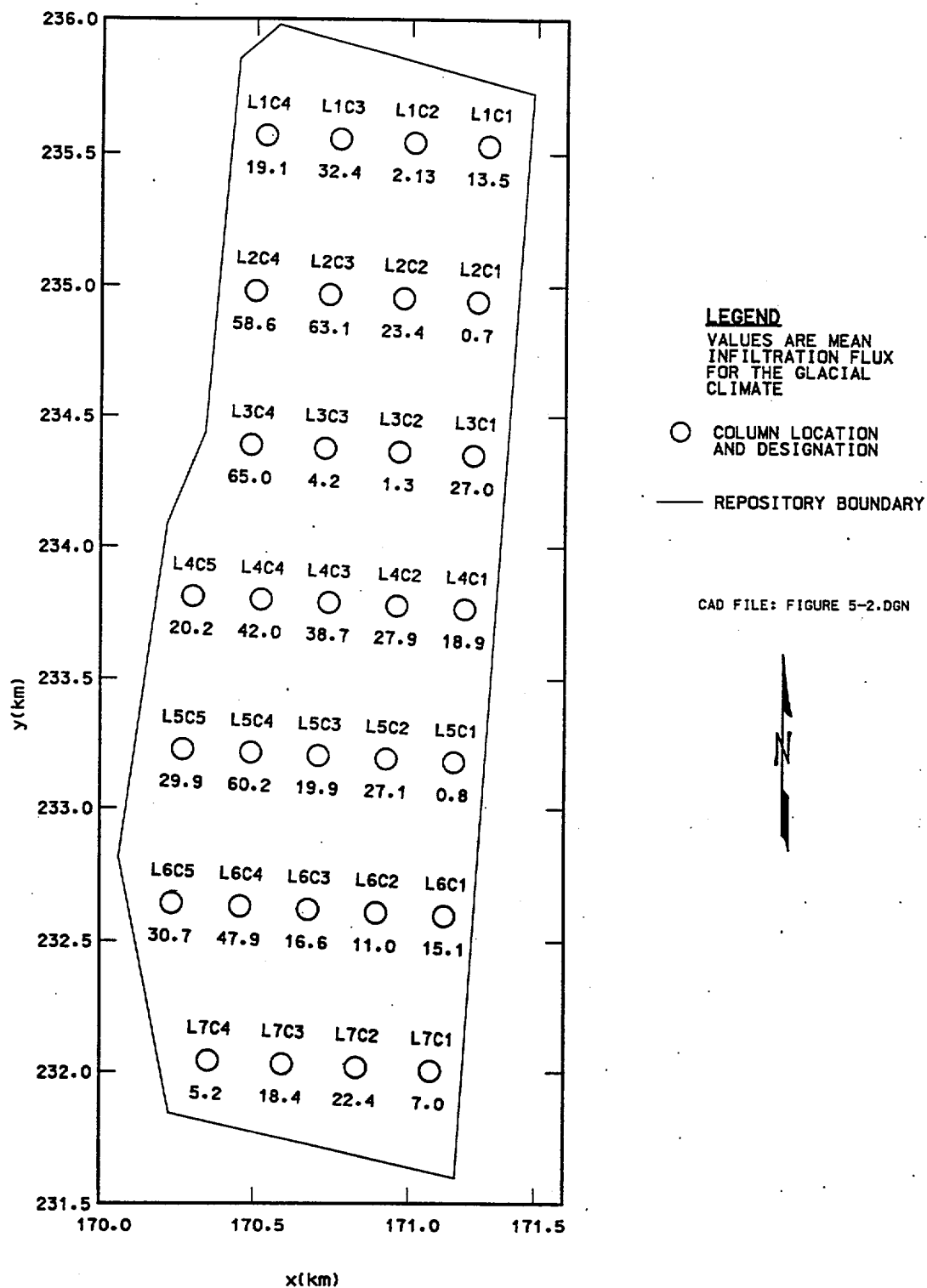
Figure 3-70. Repository Perimeter, Model Repository Footprint, Chimney Locations and Upper Bound values of Infiltration Flux
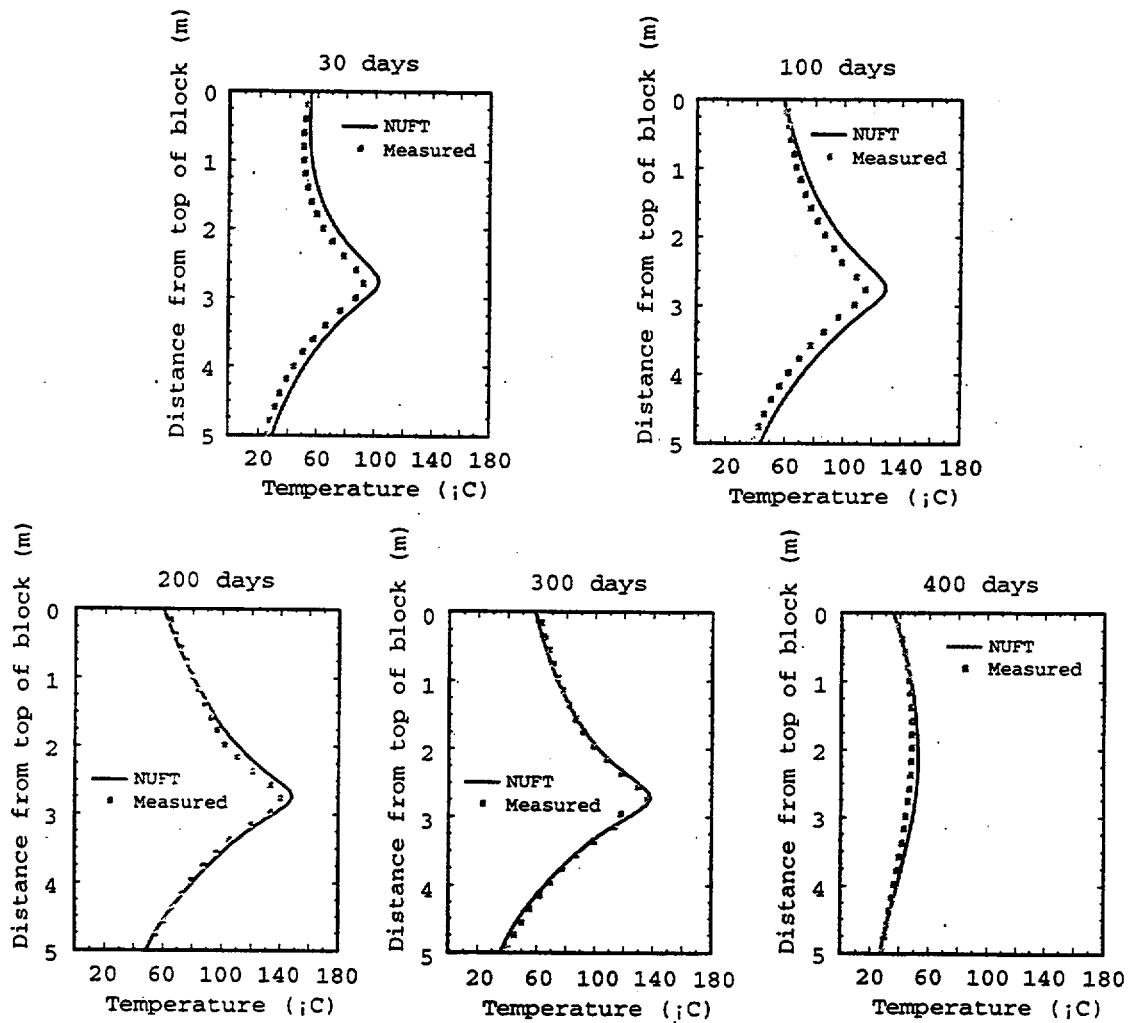
Figure 3-71. Comparison of NUFT-simulated and measured temperatures from the LBT, along Borehole TT1, at six times from 30 days to 400 days.
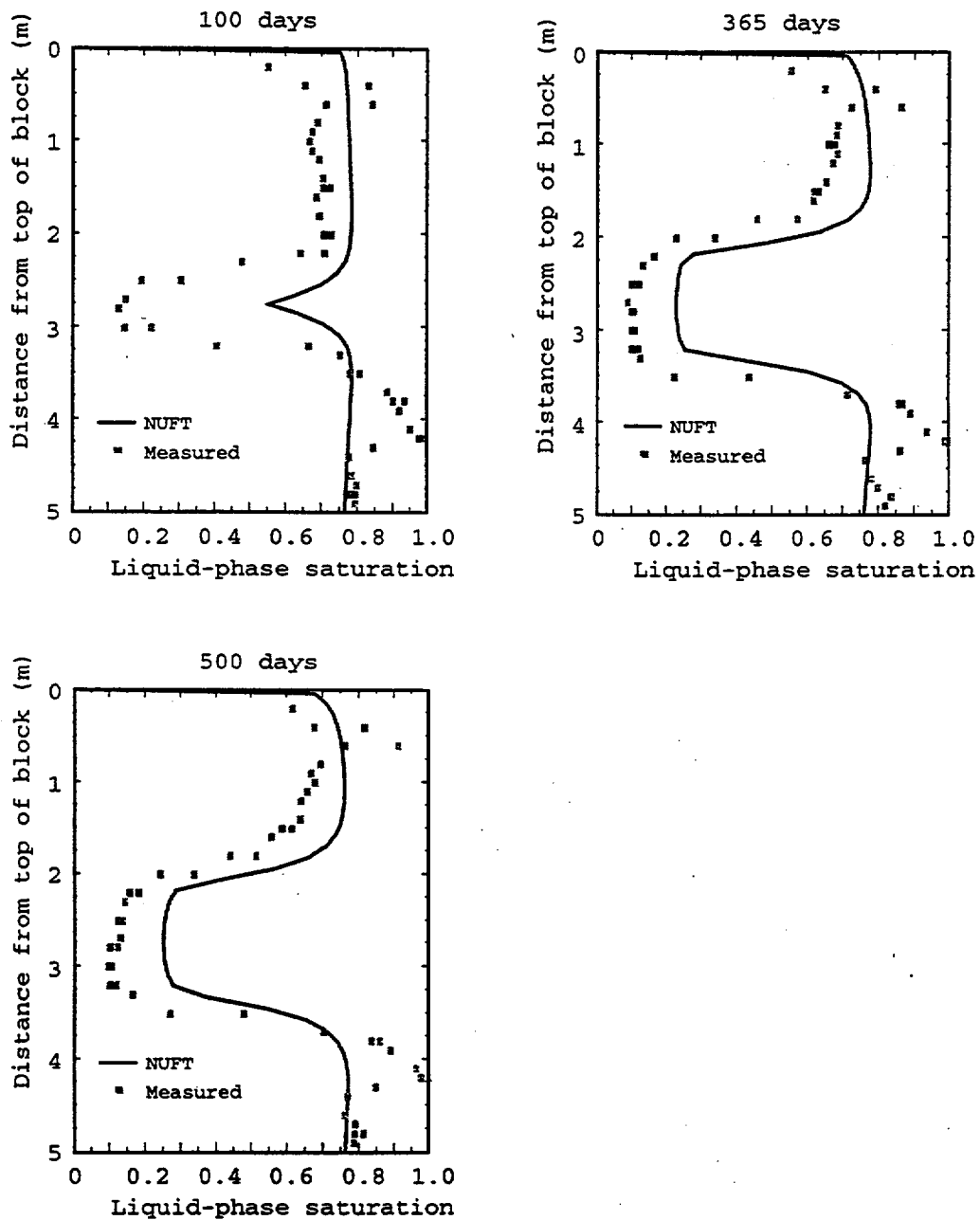
Figure 3-72.   Comparison of NUFT-simulated vs. measured liquid saturation from the LBT, along Borehole TN3, at three times from 100 days to 500 days.
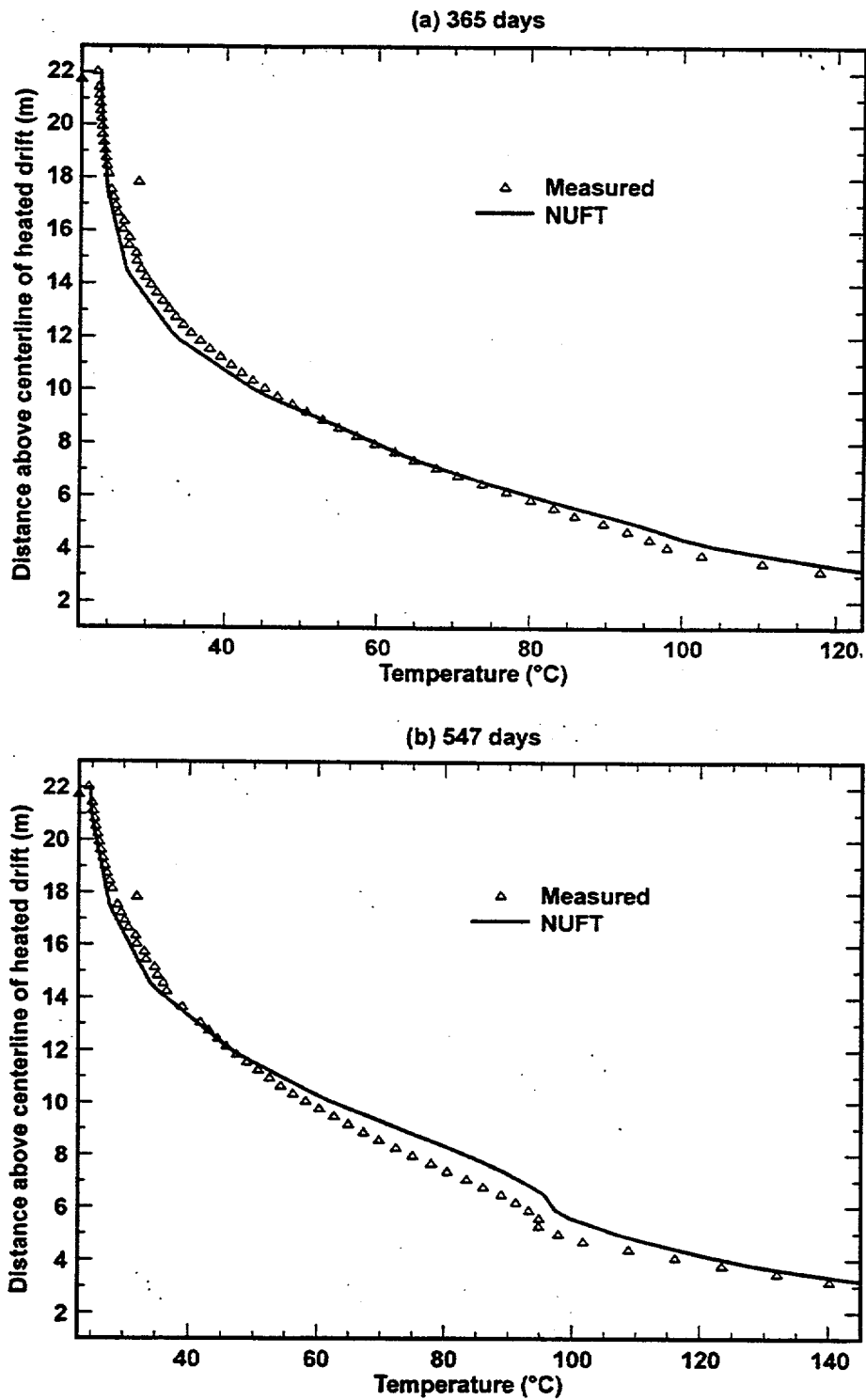
Figure 3-73.   Comparison of NUFT LDTH submodel calculations, and measured temperatures from the DST, along Borehole ESF-HD-137 at: (a) 365 days and (b) 547 days.
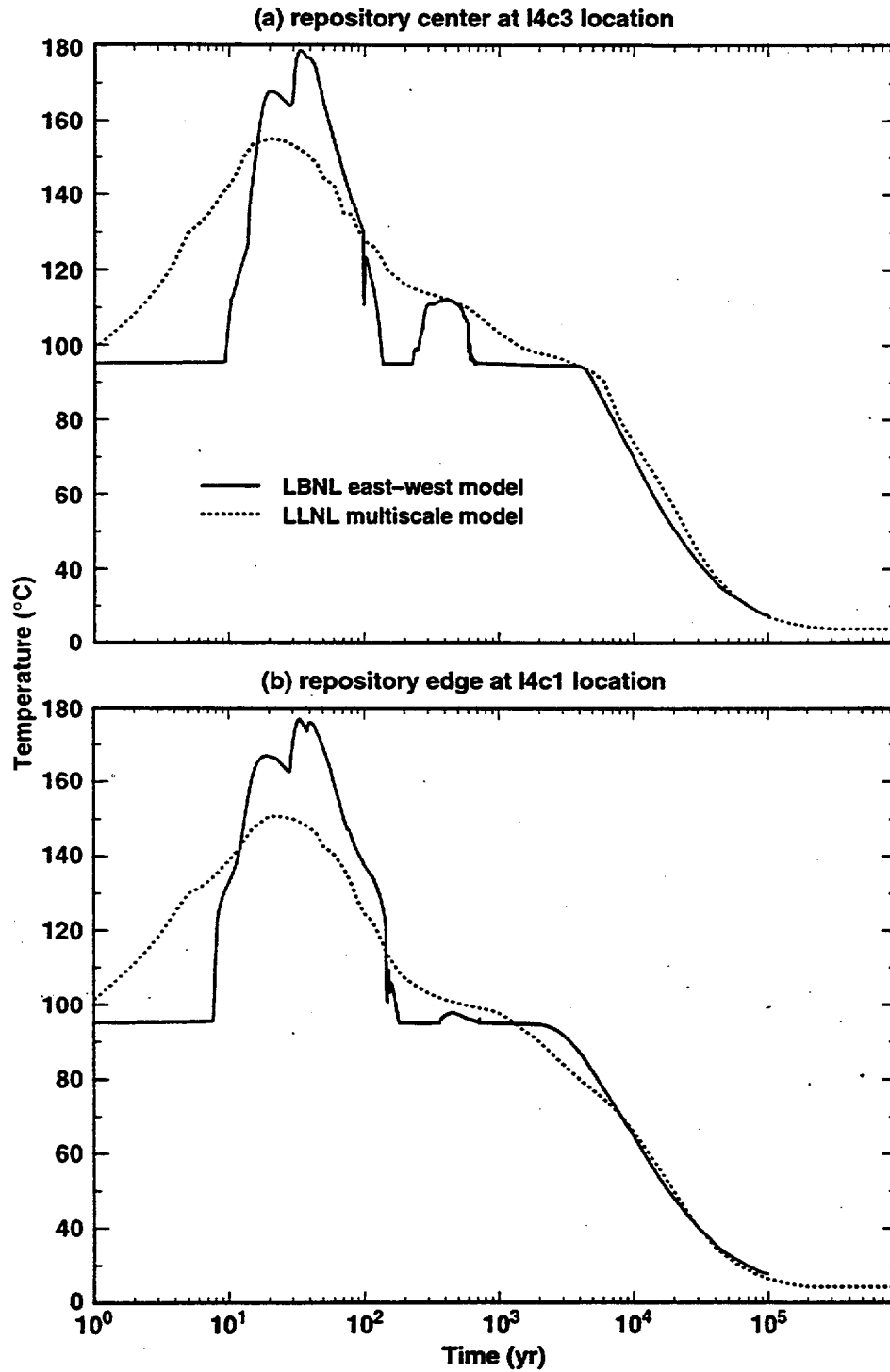
Figure 3-74. Comparison of temperatures by the MSTH Model and the mountain-scale TH model, at (a) center of the repository (L4C3 location) and (b) 100 m from the edge of the repository (L4C1 location).

4. RELATION WITH THE NUCLEAR REGULATORY COMMISSION ISSUE-RESOLUTION STATUS REPORTS

4.1 SUMMARY OF THE KEY TECHNICAL ISSUES

As part of the review of site characterization activities specified in the Nuclear Regulatory Commission's (NRC) geologic repository regulations, the NRC has undertaken an ongoing review of information on Yucca Mountain site characterization activities so as to allow early identification and resolution of potential licensing issues. The principal means for achieving this goal is through informal, pre-licensing consultation with the DOE. This approach attempts to reduce the number of, and to better define, issues that may be in dispute during the NRC licensing review, by obtaining input and striving for consensus from the technical community, interested parties, and other groups on such issues.

The NRC has focused pre-licensing issue resolution on those topics most critical to the postclosure performance of the proposed geologic repository. These topics are called Key Technical Issues (KTIs). Each KTI is subdivided into a number of sub-issues. The KTIs are:

- Activities Related to Development of the EPA Standard
- Container Lifetime and Source Term
- Evolution of the Near-Field Environment
- Igneous Activity
- Radionuclide Transport
- Repository Design and Thermal Mechanical Effects
- Structural Deformation and Seismicity
- Thermal Effects on Flow (TEF)
- Total System Performance Assessment (TSPA) and Integration
- Unsaturated Zone (UZ) and Saturated Zone (SZ) Flow under Isothermal Conditions.

Identifying KTIs, integrating their activities into a risk informed approach, and evaluating their significance for post-closure performance helps ensure that NRC's attention is focused where technical uncertainties will have the greatest affect on the assessment of repository safety.

Early feedback among all parties is essential to define what is known, what is not known and where additional information is likely to make a significant difference in the understanding of future repository safety. Issue Resolution Status Reports (IRSRs) are the primary mechanism that the NRC staff uses to provide DOE with feedback on KTI sub-issues. IRSRs focus on NRCs acceptance criteria for issue resolution and the status of issue resolution, including areas of agreement or when the staff currently has comments or questions. Open meetings and technical exchanges between NRC and the DOE provide additional opportunities to discuss issue resolution, identify areas of agreement and disagreement and develop plans to resolve such disagreements.

4.2   RELATIONSHIP OF THE ENGINEERED BARRIER SYSTEM PROCESS MODEL REPORT TO THE KEY TECHNICAL ISSUES

The EBS PMR provides technical analyses that relate to five of the key technical issues (KTIs) and their associated issue resolution status reports (IRSRs). Table 4-1 shows these KTIs and their subissues that relate directly to this PMR. These are discussed in the subsequent subsections.

Table 4-1.   Issue-Resolution Status Report and Key Technical Issues Related to the Engineered Barrier System Process Model Report

Key Technical Issues	Subissues Applicable to EBS PMR
Container Life and Source Term	Subissue 1
	The Effects of Corrosion Processes on the Lifetime of the Containers
	Subissue 3
	The Rate at Which Radionuclides in Spent Nuclear Fuel are Released from the Engineered Barrier Subsystem Through the Oxidation and Dissolution of Spent Fuel
	Subissue 4
	The Rate at which Radionuclides in High-Level Waste Glass are Released from the Engineered Barrier Subsystem
	Subissue 6
	The Effects of Alternative Engineered Barrier Subsystem Design Features on Container Lifetime and Radionuclide Release From the Engineered Barrier Subsystem
Evolution of the Near-Field Environment	Subissue 1
	Effects of Coupled Thermal-Hydrologic-Chemical (THC) Processes on Seepage and Flow
	Subissue 2
	Effects of Coupled THC Processes on the Waste Package Chemical Environment
	Subissue 3
	Effects of Coupled THC Processes on the Chemical Environment for Radionuclide Release
	Subissue 4
	Effects of Coupled THC Processes on Radionuclide Transport Through Engineered and Natural Barriers
Repository Design and Thermal-Mechanical Effects (TEF)	Subissue 1
	Implementation of an Effective Design-Control Process Within the Overall Quality Assurance Program
	Subissue 2
	Design of the Geologic Repository Operations Area for the Effects of Seismic Events and Direct Fault Disruption
	Subissue 3
	Thermomechanical Effects on Underground Facility Design and Performance
Thermal Effects on Flow	Subissue 1
	Is the U.S. Department of Energy Thermohydrologic Testing Program,

Table 4-1. Issue-Resolution Status Report and Key Technical Issues Related to the Engineered Barrier System Process Model Report (Continued)

Key Technical Issues	Subissues Applicable to EBS PMR
	Including Performance Confirmation Testing, Sufficient to Evaluate the Potential for Thermal Reflux to Occur in the Near Field?
	Subissue 2
	Is the U.S. Department of Energy Thermohydrologic Modeling Approach Sufficient to Predict the Nature and Bounds of Thermal Effects on Flow in the Near Field?
	Subissue 3
	Does the U.S. Department of Energy Total System Performance Assessment Adequately Account for Thermal Effects on Flow?
Total System Performance Assessment and Integration (TSPA)	Subissue 4
	Scenario Analysis

4.2.1 Container Life and Source Term IRSR

The primary issue of this KTI on container life and source term (CLST) is adequacy of the EBS design and provision of reasonable assurance that containers will be adequately long-lived and that radionuclide releases from the EBS will be sufficiently controlled so that container design and packaging of spent nuclear fuel (SNF) and high-level waste (HLW) glass will make a significant contribution to overall potential repository performance. This IRSR is focused on the containers and waste forms as the primary engineered barriers, but it also considers other engineered subsystem enhancements (i.e., ceramic coatings, drip shields, backfill) incorporated as options in the EBS design (NRC 1999a, Section 2.0).

There are six subissues associated with this KTI, as discussed in the CLST IRSR (NRC 1999a). Four of the six subissues are directly related to the EBS PMR and are described below:

Subissue 1:   The Effects Of Corrosion Processes On The Lifetime Of The Containers

This subissue relates to the adequacy of DOE's consideration of the effects of corrosion processes on the lifetime of the containers. The applicable criteria relates to environmental conditions within the WP emplacement drifts that may promote the corrosion processes, taking into account the possibility of irregular wet and dry cycles that may enhance the rate of container degradation. The models presented in Sections 3.1.1 through 3.1.4 consider the effects of waste package heat generation in increasing temperature and evaporation within the EBS. For example, the EBS Physical and Chemical Model (Section 3.1.2) initially develops a TH model calculation for estimating water fluxes during the thermal period. This information is used to evaluate gas flux during the thermal period, CO_2 and O_2 fugacity which in turn are used to estimate the evolution of leachate composition, and the formation of salts and precipitates in the backfill and on the drip shield.

Subissue 3:   The Rate at Which Radionuclides in Spent Nuclear Fuel are Released from the Engineered Barrier Subsystem Through the Oxidation and Dissolution of Spent Fuel

This subissue relates to the adequacy of the effect of the rate of degradation of SNF on the subsequent release of radionuclides and the rate of release from the EBS. The first acceptance

criteria relates to whether the DOE has considered all categories of SNF planned for disposal at the proposed YM repository. It should be recognized that the issue relates primarily to the performance of the waste package and waste form for all categories of SNF. For a given waste form/waste package releases, the EBS radionuclide transport model is based upon a unit release of radionuclides due to a breached WP that can be applied to the SNF. The EBS radionuclide model is a general release model that can be applied to all categories of SNF for a given waste package release.

The DOE has identified and considered the likely processes for SNF degradation and the release of radionuclides from the EBS, and requires adequacy for numerical models by incorporating uncertainties, and utilizing spent fuel test results. Note that most of the criteria apply to the waste package and waste form. The EBS PMR provides information (Sections 3.1.3, 3.2.3.1.3, 3.2.3.2.3, and 3.2.3.1.5) on the drip shield corrosion environment and flow through the drip shield that affects radionuclide transport from the waste package.

Subissue 4: The Rate at which Radionuclides in High-Level Waste Glass are Released from the Engineered Barrier Subsystem

This subissue relates to the adequacy of DOE's consideration of the effects of degradation of HLW glass, taking into account the rate of degradation and its effect on the rate of radionuclide releases from the EBS. The EBS Water Distribution and Removal Model provides a bounding analysis of the amount of water that would flow through backfill and drip shield and potentially contact waste packages that is the primary influence on degradation of HLW. Discussions are presented (Section 3.2.3.1.3., 3.2.3.1.5 and 3.2.3.2.3) on colloids and microbial effects based upon available data relevant to the degradation of HLW glass.

Subissue 6: The Effects of Alternative Engineered Barrier Subsystem Design Features on Container Lifetime and Radionuclide Release From the Engineered Barrier Subsystem

This subissue addresses the effects of alternate EBS design features, such as backfill, drip shields, and ceramic coatings, on container lifetime and radionuclide release from the EBS. The subissue requires that the DOE consider likely processes for the degradation of HLW glass and the release of radionuclides from the EBS due to dissolution of the primary phase; formation of secondary minerals and colloids; microbial action; and radionuclide releases and transport from the WP emplacement drifts. Section 3.1.3 presents a discussion of radionuclide release through the EBS for a unit release that can be applied.

The subissue involves identification and consideration of the effects of backfill, and the timing of its emplacement, on the thermal loading of the repository, WP lifetime (including container corrosion and mechanical failure), and the release of radionuclides from the EBS. Further the subissues involves specialized issues such as the humid-air corrosion regime, and the potential for condensate to form below the drip shield. The EBS WD&R (Section 3.1.1), the EBS P&CE (Section 3.1.2), and the EBS Multiscale Models (Section 3.1.4) provide analyses incorporating the placement of backfill at the time of repository closure. The Multiscale model provides an analysis of the relative humidity surrounding the waste package that when coupled with corrosion data from the Waste Package model allows a determination of humid air corrosion.

The interaction of flowing water with introduced materials including the grout, steel, and backfill is considered in the Physical and Chemical Environment Model (Section 3.1.2).

The subissue involves the geochemistry of the groundwater. The P&CE Model (Section 3.1.2) provides a Chemical Summary Model that integrates several submodels and describes the evolution of water composition and solid precipitates in the backfill above the drip shield, the invert, and the lower part of the backfill. Further, it evaluates CO_2 mass balance in the drifts and the surrounding host rock as it evolves with time. The assessment includes the effects of carbon steel corrosion, leaching from cementitious materials, microbial processes, and colloidal processes on the bulk chemical environment.

4.2.2 Evolution of the Near-Field Environment IRSR

The primary focus of the near-field environment (NFE) KTI is the coupling of thermal hydrologic, and chemical processes that could effect the drift environment. The near field is considered to be the part of the site for which changes in the physical and chemical properties that result from construction of the underground facility or from heat generated by the emplaced radioactive waste will affect performance of the potential repository. Evolution of the near field is expected to include coupling of thermal, hydrologic, and chemical processes that could affect parts of the mountain. These coupled processes could affect components of the NBS and the EBS and thereby affect potential repository system performance. The introduction of potential repository construction materials and WP materials may also perturb the NFE (NRC 1999b, Section 2.0).

There are five subissues associated with this KTI, as discussed in the ENFE IRSR (NRC 1999b). Four subissues are directly related to the EBS PMR and are described below:

Subissue 1:   Effects of Coupled THC Processes on Seepage and Flow

As stated in the IRSR this subissue focuses on explaining the importance of the THC coupled processes to seepage and flow (NRC 1999b). Note that the subissue applies to seepage which is covered in the UZ Flow and Transport Model, and flow through backfill, drip shields, and invert which is the subject of the EBS PMR.

The subissue involves the criterion that mathematical models for coupled THC effects on seepage and flow be consistent with conceptual models, based on inferences about the near field environment, field data and natural alteration observed at the site, and the expected engineered materials. The Water Distribution and Removal Model, the P&CE Model, and the Multiscale Model provide predictions of seepage and flow that are based upon the selection of a consistent set thermal properties, and hydrologic properties for the active fracture model. The active fracture model, and the drift scale properties sets for these models are consistent with properties sets used in the UZ model which were determined by inverse modeling methods.

Subissue 2   Effects of Coupled THC Processes on the Waste Package Chemical Environment

The P&CE Model is based upon a two dimensional thermal hydrologic analysis that accounts for temporal waste heat loading, and variations in percolation rates. The P&CE Model analyzes evolution of leachate composition from the grout and backfill for the EBS is provided when

contacted with J13 groundwater. The P&CE Model considers initially the composition of J13 groundwater that is used for developing a precipitates and salts normative submodel which is in turn used in the chemical system model. Where appropriate, bounding calculations have been performed to estimate physical effects such as flow through drip shields (Section 3.1.1), the potential for condensation below the drip shield (Section 3.1.1) and chemical effects such as the alteration of groundwater chemistry (Section 3.1.2).

Subissue 3   Effects of Coupled THC Processes on the Chemical Environment for Radionuclide Release

The EBS radionuclide transport model (EBS PMR Section 3.1.3) provides an analysis of release based upon the thermal hydrological calculations in the WD&R model. The EBS radionuclide transport model (EBS PMR Section 3.1.3) is an advection/dispersion/diffusion model based upon TH coupled modeled in the WD&R model. The EBS radionuclide transport model (EBS PMR Section 3.1.3) provides an analysis of release based upon the thermal hydrological calculations in the WD&R model.

The WD&R model considers the temporal variations in conditions affecting the TH effects, and provides a bounding calculation for chemical effects due fracture plugging that would alter saturation levels and porewater velocities. The EBS radionuclide transport (Section 3.1.3) model provides a sensitivity analysis for the chemical retardation that bounds temporal and spatial variations in the chemical retardation factor that reflects the chemical environment. For the base case, the EBS radionuclide transport takes no credit for chemical retardation which is a bounding assumption for radionuclide transport.

The EBS Colloids submodel is based upon relevant data for the size and concentration of colloids that account for variability through probability distributions. Based upon these data bounding values for radionuclide solubility, and colloid diffusion coefficient were calculated.

Subissue 4:   Effects of Coupled Thermal-Hydrologic-Chemical Processes on Radionuclide Transport Through Engineered and Natural Barriers

This subissue primarily focuses on explaining the importance of the results of different coupled processes to radionuclide transport(NRC 1999b). The EBS Radionuclide Transport model is based upon a two dimensional thermal hydrologic analysis that considers initial temperature and pressure boundary conditions. The EBS Radionuclide Transport Model provides bounding analysis for a conservative range of parameters. The base case analysis neglects the effects of chemical retardation on radionuclide transport and therefore conservatively neglects chemical sorption.

4.2.3   Repository Design and Thermal-Mechanical Effects IRSR

The primary focus of the repository design and thermal mechanical effects (RDTME) KTI is the review of design, construction, and operation of the geologic repository operations area (GROA) with respect to the preclosure and postclosure performance objectives, taking into consideration long-term thermomechanical (TM) processes. Consideration of the time-dependent TM coupled response of a jointed rock mass is central to potential repository design and necessary for

performance assessment (PA) at the Yucca Mountain (YM) site. Consequently, that is the focus of the preclosure and postclosure elements of this KTI (NRC 1999c, Section 2.1).

Three of the four subissues for the RDTME KTI are directly related to this PMR, as described below.

Subissue 1: Implementation of an Effective Design-Control Process Within the Overall Quality Assurance Program

This subissue focuses on the NRC staff's evaluation of DOE's implementation of design control process for design, construction, and operation of the ESF (NRC 1999c). Note that in general design considerations as they relate to such criteria as design bases, appropriate quality standards, design interfaces, and the preparation of design calculations are not considered directly in this PMR. The acceptance criterion will be applied appropriately in the design process.

Subissue 2: Design of the Geologic Repository Operations Area for the Effects of Seismic Events and Direct Fault Disruption

As stated in the IRSR this subissue focuses on the design of the GROA for the effects of seismic events and direct fault disruption as identified in the seismic topical reports (NRC 1999c). Design considerations related to seismic issues are not included in this PMR. The acceptance criterion will be applied appropriately in the seismic design process.

Subissue 3: Thermomechanical Effects on Underground Facility Design and Performance

This subissue consists of three major components; (i) TM effects on underground facility design; (ii) effect of seismically induced rockfall on WP performance; and (iii) postclosure TM effects on flow into the emplacement drifts (NRC 1999c). 8. Both drift- and repository-scale models of the underground facility are used in TM analyses to establish the intensity and distribution of ground movement (rock deformations, collapse, and other changes that may affect the integrity or geometrical configuration of openings within the underground facility). The number and variety of models permit the examination of conditions along drift-parallel and drift-normal directions. The drift degradation analysis is based upon a drift scale model that considers changes in rock mass properties throughout the repository. Other issues regarding drift degradation are presented in Appendix A.

Rockfall analysis considers the possibility of multiple blocks failing onto a WP, and the extent of the potential rockfall area around in individual emplacement drifts as well as over the entire repository as functions of time and seismic activity.

4.2.4 Thermal Effects on Flow IRSR

The IRSR states that the primary technical aspects of the thermal effects on flow (TEF) KTI is the estimation of temperature, moisture content, and humidity at the WP surface and estimation of temperature and thermally driven water flux with respect to the transport of radionuclides from failed WPs.

As explained in the IRSR, it is necessary to understand the spatial and temporal effects of the thermal load on liquid-phase and gas-phase fluxes and the resulting effects on temperature and relative humidity of the WP environment at the potential repository. This will provide confidence in predictions of containment and long-term waste isolation. Because the focus of the staff review of DOE's program is on the adequacy of DOE's treatment of thermally perturbed liquid-phase and gas-phase fluxes (particularly thermal reflux) in testing, modeling, and PA program areas, this KTI is divided into the following three subissues (NRC 1999d, Section 2.0).

All three of the subissues for the TEF KTI are directly related to this PMR and are described in the following subsections.

Subissue 1:   Is the U.S. Department of Energy Thermohydrologic Testing Program, Including Performance Confirmation Testing, Sufficient to Evaluate the Potential for Thermal Reflux to Occur in the Near Field?

This subissue focuses on information needed to verify conceptual models used to predict thermally driven flow in the near field. The most important technical element relates to designing and conducting tests to evaluate potential repository conditions that could lead to refluxing of water into the underground facility. (NRC 1999d, Section 4.1.2). Thermohydrologic tests are designed and conducted with the explicit objective of testing conceptual and numerical models so that critical thermohydrologic processes can be observed and measured.

Tests are currently being planned and conducted for testing of the process models. Tests are being conducted at quarter scale to simulate thermal and hydrological effects within the drift. The tests record temperature, relative humidity, and saturation levels within the EBS components that can be directly compared with results from the Water Distribution and Removal Model or other TH models. The quarter-scale tests are being conducted with J13 groundwater. The tests simulate the interaction of the J13 groundwater with EBS components that would result in the formation of precipitates on EBS components.

Subissue 2:   Is the U.S. Department of Energy Thermohydrologic Modeling Approach Sufficient to Predict the Nature and Bounds of Thermal Effects on Flow in the Near Field?

This subissue focuses on the sufficiency of DOE's thermohydrologic modeling approach (process-level models) to predict thermally driven flow in the near field. The NRC staff review of the DOE's thermohydrologic analyses will place particular emphasis on technical elements of the acceptance criteria that are related to incorporating the physics of refluxing of water into conceptual and numerical models (NRC 1999d, Section 4.2.2). Sufficient data on EBS processes are not available at the current time for the Water Distribution and Removal Model (Section 3.1.1), and the Physical and Chemical Environment Model. Where appropriate, bounding calculations have been performed to estimate physical effects such as flow through drip shields (Section 3.1.1), and chemical effects such as the alteration of groundwater chemistry (Section 3.1.4).

The degree of multidrift dry-out zone coalescence will be a function of the thermal load specified in the final design of the repository. Recent, proposed design modifications by DOE to reduce the repository thermal load to approximately 60 MTU/acre will minimize, if not eliminate, dry-out zone coalescence. Recent DOE models that include the active fracture model adequately predict the extent of dryout surrounding the emplacement drifts.

The EBS process models for thermal hydrological effects are based upon initial conditions, boundary conditions, and computational domains consistent with site characteristics. The thermal hydrology models used in Sections 3.1.1 through 3.1.4 are based upon the selection of NBS hydrologic and thermal properties used in the UZ process model. The initial conditions, and boundary conditions for the models for specific locations use the same infiltration rates, and temperature and pressure boundary conditions are consistent with the UZ process Model (Section 3.1.4).

The potential repository-scale heterogeneity is represented by the drift scale active fracture properties set which captures the properties for various strata. Lateral variability within the potential repository footprint is represented by the 31 drift-scale-model locations used in the MSTH model. These locations are regularly distributed over the potential repository footprint. This reduces the general three dimensional problem to a series of two dimensional problems.

Subissue 3:   Does the U.S. Department of Energy Total System Performance Assessment Adequately Account for Thermal Effects on Flow?

This subissue focuses on DOE adequately accounting for TEF in the TSPA. The NRC staff review will particularly emphasize on the potential adverse effects on repository performance resulting from the influx of liquid water or water vapor into an emplacement drift (NRC 1999d, Section 4.3.2). At the present time, data needs have been identified, and quarter scale testing is being performed to evaluate the performance of the EBS components for influxes of liquid water. Where appropriate, bounding calculations have been performed to estimate physical effects such as flow through drip shields (Section 3.1.1).

4.2.5   Total System Performance Assessment (TSPA) and Integration IRSR

The objective of this KTI is to describe an acceptable methodology for conducting performance assessments of repository. As stated in this IRSR the focus is to describe an acceptable methodology for conducting assessments of repository performance and using these assessments to demonstrate compliance with the overall performance objectives and requirements for multiple barriers (NRC 1998).

The acceptance criteria for each subissue address five fundamental elements of the DOE's TSPA model for the Yucca Mountain Site (NRC 1998 p. 10):

- Data and model justification
- Data uncertainty and verification
- Model Uncertainty
- Model verification
- Integration.

The subissue for scenario analysis for this KTI relates to the EBS PMR.

This scenario-analysis subissue focuses on the attributes of an acceptable methodology for identifying, screening, and selecting Features, Events, and Processes (FEPs) for inclusion in the TSPA (NRC 1998, p. 4). FEPs that could affect future system performance are used to formulate scenarios. This includes construction of scenario classes, assignment of probabilities to scenario classes, and their incorporation in the TSPA to assure completeness.

A systematic method was applied to identify and screen FEPs for the EBS process models. The FEPs have been identified and grouped into two broad categories of primary and secondary FEPs. The primary FEPs capture the issues associated with the secondary FEPs. The FEPs are further divided into "included" and "excluded" FEPs. Included FEPs are those directly represented in TSPA models and process models that support the TSPA. Analyses have focused on the identification and screening of FEPs; this work partially addresses this subissue.

5. SUMMARY AND CONCLUSIONS

5.1 INTEGRATED EFFECTS OF THE ENGINEERED BARRIER SYSTEM

The post-closure evolution of environmental conditions within the emplacement drift is the result of complex interactions of the engineered system with the surrounding host rock, including its contained fluids. In this context, "engineered system" includes the potential repository layout, the thermal management strategy, the design of physical components (waste packages, drip shields, supports, etc.) and the choice of materials and fabrication methods.

Waste package surface temperature is one example of post-closure environmental conditions. Within a few years of closure, WP surface temperatures reach peak values and then begin to decline. The magnitude of this peak and its timing depend upon the WP location within the repository, the thermal-hydrologic properties of the host rock and the engineered materials, the duration and intensity of ventilation, the spacing between WPs and between drifts, and the WP thermal power decay curve. The MSTH Model accounts approximately for the effects of all these on WP temperature, and also incorporates the effect of changes in infiltration flux estimated to occur as the climate changes over the next 10,000 years. The parameters subject to engineering and operating control are the drift and WP spacing, thermal management strategy (such as blending or aging the waste and ventilating the drifts after emplacement), and the thermal-hydrologic properties of the materials within the drift (particularly the presence or absence of backfill).

This emphasizes the fact that the integrated effects of the EBS depend strongly on design details, and the results documented in this PMR are strictly valid only for the EDA II conceptual design. However, the collection of analyses and models presented here is flexible enough to assess the effects of different designs and operating practices on the performance of a potential repository. As this report entered its final draft stage, the design was modified to eliminate backfill. Change requests were initiated in January 2000 to remove backfill from the reference design and to change the emplacement drift orientation to minimize the effects of rockfall. Many of the quantitative results developed in the supporting AMRs will change as a result. However, it is expected that detailed analyses of the impact of removing backfill, coupled with detailed design of the EBS, will produce a system with performance equal to or better than the EDA II conceptual design.

The potential for galvanic coupling and, consequently, accelerated corrosion rates of some of the metallic components of the EBS are under consideration. As documented in Section 3.1.2.3, a wide variety of alloys will be used in the system, all thermodynamically unstable, and spanning a wide range of reactivity. Galvanic effects are to be evaluated before final material selections are made.

5.2 NATURAL AND ENGINEERED ANALOGS

Analogs have limited application for the EBS. Many of the engineered materials have been manufactured for only a few decades or less, and there are no directly relevant observations on the longevity of, say, titanium drip shields exposed to conditions anticipated to occur in the potential repository over the next 10,000 years.

Consequently, direct measurement of material properties and the integrated behavior of EBS components provide the principal means of developing and testing these process models. Specific examples of such tests and experiments are:

- Field-scale thermal tests are instrumental in building confidence in the TH models, which are used in Sections 3.1.1, 3.1.2.1, and 3.1.4. Laboratory-measured properties (heat capacitance, rock density, thermal conductivity, porosity, permeability, van Genuchten parameters of imbibition behavior) are used in all of these models. Water samples from the SHT and DST have been analyzed and are found to be similar to J-13 water.

- The cement mineral assemblage adopted in Section 3.1.2.3 is based on observations documented in the engineering literature.

- Direct laboratory testing is relied on to establish limiting conditions for microbial growth and activity in the host rock, as discussed in Section 3.1.2.4.

- Direct laboratory testing of precipitates formed on evaporation of simulated J-13 water and matrix porewater, is used to establish normative mineral assemblages, and as validation for the extended Pitzer model.

However, analogs have been used when available. As noted in a number of places in Section 3.1.2, the use of J-13 water as an analog for water percolating through the fractures is commonplace in most of the chemical modeling. Another use of analogs is in the application of the microbial communities model to Rainier Mesa, which is in many ways an analog to Yucca Mountain under the wetter climatic conditions expected to commence in another few hundred years. Specific examples of the use of analogs in the EBS PMR are given below:

- Section 3.1.2.2 uses the behavior of radiocarbon at ambient conditions, as an analog for the transport of CO_2 and other gases during the thermal period and after cooldown. This model corroborates other approaches for predicting gas-phase composition, including the air mass-fraction approach and reactive transport simulations of the host rock.

- Section 3.1.2.4 relies on analogs to specify the behavior of microbes--the potential for growth and activity--at extreme environmental conditions. Specifically, the requirements that T<120C and RH>0.9, or RH>0.75 for halophiles, or RH>0.55 for fungi, are derived from the microbiology literature. Also, field samples from the ESF and Rainier Mesa have been evaluated to determine microbial abundance.

- Section 3.1.2.3 cites the Corrosion Products AMR, which heavily relies on the inorganic chemistry literature to describe the behavior of metals under conditions representative of the repository.

- Section 3.1.2.5 supports the use of J-13 water as an analog for fracture waters in the host rock. Notwithstanding occurrence of matrix porewater that differs in composition from J-13 water, the fact that EQ3/6 correctly predicts the composition of J-13 water based on a straightforward conceptual model, supports the use of J-13 composition to represent

mobile water in fractures of the UZ. Perched waters from the site resemble J-13 water, and are also analogs for mobile fracture waters.

- Section 3.1.2.6 uses observations of colloid size and abundance in natural groundwaters near Yucca Mountain, as analogs for use in the EBS Colloids Model. Steel in the EBS is identified as a potentially prolific source of colloids, analogous to observations of colloidal iron in nature (the corresponding possibility of acidification is not addressed in any of the EBS models, but is addressed in crevice corrosion models).

5.3 SUMMARY OF RESULTS AND CONCLUSIONS FROM THE MAJOR ANALYSIS/MODEL REPORTS

All of the following conclusions are based on the EDA II design, which includes engineered backfill. As noted above, a design change initiated in January 2000 requires the removal of backfill, and the selection of an emplacement drift orientation that minimizes the size of the largest key blocks that could fall on the drip shields. The change in drift orientation, coupled with a sufficiently robust drip shield system, is expected to adequately protect the WPs from mechanical degradation.

Analyses and calculations performed for six of the AMRs supporting the EBS PMR are currently being revised. Since the EBS is not a principal factor in the Repository Safety Strategy, the ultimate impact on total system performance is not expected to be significant.

5.3.1 Water Distribution and Removal

The following points summarize the important results and conclusions from the Water Distribution and Removal AMR and its supporting AMRs:

- Flow modeling of the EBS and the surrounding host rock, using capillary properties of the backfill combined with fracture parameters from the UZ model, predicts that the backfill tends toward capillary equilibrium with the fractures as the host rock temperature and water content return to pre-emplacement values. The water saturation in the backfill ultimately reaches 30 to 40 percent with the estimated glacial infiltration flux of 42 mm/year at the location modeled.

- Thermal effects on the flow distribution and capillary pressure levels are almost completely dissipated by 1000 years after closure.

- Potential impact of plugging fractures beneath the emplacement drift was investigated by a bounding analysis. As might be expected, if fractures plug, the saturation in the invert would increase to nearly 100 percent for glacial infiltration flux values.

- Although not part of the baseline design, the model results show that drain holes packed with sand would maintain low moisture content in the invert if the fractures were to plug. Also, the drain holes could reduce liquid water flux through the invert by about 4 orders of magnitude, relative to natural drainage, even if there were no fracture

plugging. Both of these conclusions depend on engineering the drain holes to assure their intersection with high-permeability connected fractures.

- A bounding analysis of the diversion capacity of the drip shield covered by capillary backfill shows that leakage flux at the drip shield joints should not exceed 10 percent of the total flux through the backfill.

- No combination of model parameters led to a prediction of condensation beneath the drip shield. This is consistent with limited experimental data from quarter-scale experiments in progress.

- The drift-degradation analysis indicates that the combination of time-dependent reduction in joint cohesion, thermal stresses, and seismic events will produce rockfall in less than 2.5 percent of the total length of emplacement drifts. This analysis assumes that the ground system is not effective after closure.

- The calculated percentage (from the ventilation analysis) of decay heat removed at 10 cms is 68 percent after 50 yr, 73 percent after 100 yr, and 77 percent after 200 yr. At 15 cms, the corresponding percentages were 74, 78, and 82 percent, respectively.

5.3.2 Physical and Chemical Environment

The following points summarize the important results and conclusions from the Physical and Chemical Environment AMR, arranged by its models:

5.3.2.1 Thermal-Hydrology

- Location (center vs. edge) and the local infiltration flux (and its variation with time from the climate model) are the primary factors that determine peak temperatures, temperature history, humidity, and the potential for seepage and evaporation in the drifts.

- The minimum air mass-fraction is approximately 10^{-3} under conditions of maximum thermal output and maximum infiltration flux. This is based on 2-D modeling which is inherently conservative; the minimum air mass-fraction may be greater.

- Evaporation tends to be localized to a thin zone that encompasses the dryout zone, and that recedes toward the drip shield surface with time, as the thermal source-strength decays. Thus there is the potential for accumulation and refluxing of solutes from the host rock in to the drifts.

- Substantial accumulation of soluble salts may occur from evaporation, and the zones need not be dry for this to occur. A bounding analysis has shown that the mass of soluble salts that could accumulate at the drip shield surface, is on the order of 10^5 times that which is present in 1 kg of water at the reference composition. This translates to the potential for maximum accumulation of several kilograms of nitrate, chloride, sulfate, and carbonate salts per meter of drip shield, during the thermal period. This result

depends closely on the seepage flow rate. Because of the timing of salt accumulation, there is the potential for aqueous corrosion conditions to occur at temperatures up to approximately 120°C, because saturated brines can begin to form when the relative humidity increases to 50 percent.

- There is less potential for the accumulation of soluble salts at repository-edge locations than at central locations because there is less heat available for evaporation.

- There is greater potential for solute accumulation in the invert than elsewhere in the EBS, because the invert temperature is always higher during cooldown.

5.3.2.2   Gas Flux and Fugacity

- The broader pillars in the low-thermal design permit a slight circulation, whereby the gas-phase mass flux near the centers of the pillars is directed downward. The magnitude of the downward flux is much smaller than the upward flux near the drifts, but it probably results in mixing of air, which increases the minimum air mass-fraction significantly. The result is that calculated fugacities for CO_2 and O_2 are increased, compared to calculated values for previous repository design concepts (e.g. VA design).

- Evaluation of ambient radiocarbon distribution in the UZ has shown that there is a substantial flux of CO_2 (e.g., 586 mg CO_2/yr/m^2 at borehole SD-12) into the UZ from the near-surface soil zone. The flux is carried by recharge water percolation, and by gas-phase dispersive transport in response to barometric fluctuations at the surface. Using estimates for liquid recharge flux and dissolved inorganic carbon concentration, gas-phase mass transfer is inferred to provide 299 mg CO_2/yr/m^2 to the UZ above the Calico Hills unit. This transfer is much greater than could be provided by molecular diffusion, which implies that advective-dispersive processes are active.

5.3.2.3   Introduced Materials

- Chemical modeling shows that the composition of evaporated seepage water is completely or nearly saturated with respect to quartz when it contacts the backfill. Conditions for which quartz dissolution is predicted to be possible are unlikely, involving high temperature, low CO_2 fugacity, and high seepage flow rates through the drifts.

- The calculations also show that significant porosity reduction in quartz-sand backfill is unlikely unless a high rate of seepage is sustained, and evaporated in a small fraction of the backfill volume (less than 10 percent).

- Steel present in the drifts will begin to corrode when humidity increases during cooldown. Corrosion test data show that the structural steel used for ground support, invert structural support, and rails will corrode much faster than the drip shield or waste package. No credit was taken for the contribution of the ground support system to drift stability after closure.

- Oxidation of carbon steel will be complete in hundreds to a few thousand years. The most important effects will be to consume oxygen in the environment, and produce iron corrosion products. Some of the corrosion product material will be in the form of colloidal particles with the potential to increase the transport of radionuclides.

- The invert contains crushed tuff ballast material as well as carbon steel. The effects of this material on the chemistry of water will depend on the seepage flow rate. Low flow rates will increase the effects of chemical interaction with the tuff, and diminish the mobility of chemical species including radionuclides. Larger flow rates will cause chemical interactions with the water to be dominated by the host rock.

5.3.2.4   Microbial Effects

- Laboratory tests and modeling results show that microbial activity in the host rock is limited primarily by lack of moisture, and that phosphate is an important limiting nutrient. The waste package may not be subjected to MIC for as long as the drip shield prevents contact with seepage water, backfill, steel, and crushed tuff.

- Laboratory tests show that MIC can accelerate the corrosion rate for carbon steel similar to that intended for use in the EBS, by a factor of 6 or more. This will tend to enhance the effects of steel corrosion on the bulk chemical environment.

- Modeling of microbial growth and activity using nutrient mass and free energy balance, and estimated degradation rates for introduced materials, shows that the total production of biomass is on the order of 10 g per meter of drift per year during the first 10,000 years. Based on such a small generation rate, effects on the bulk chemical environment are probably negligible, but localized microbial activity could accelerate corrosion.

5.3.2.5   Precipitates and Salts

- Seepage into the drifts during the thermal period will tend to evaporate, and if the rate of evaporation is great enough, precipitates and salts will form. The nature of these solids is predicted using a normative model based on laboratory test data. At the final stages of evaporation, the gas-phase CO_2 composition will determine whether carbonates or hydroxides are formed (e.g., thermonatrite or sodium hydroxide). However, the formation of either sodium or calcium hydroxide is considered unlikely because these precipitates would occur only at an improbably low value of CO_2 fugacity.

- For J-13 water, highly alkaline conditions occur at late stages of evaporation. For waters containing more sulfate or chloride compared with bicarbonate, the pH remains near neutral during evaporation, but the salts produced (e.g., sodium chloride, calcite) are qualitatively similar. Alkaline conditions are assumed to be most corrosive for the drip shield and the waste package, so J-13 water is used as a reference composition.

- Salts formed by evaporation of J-13 water tend to be deliquescent, i.e. they absorb water from the air and dissolve, at relative humidity (RH) less than 100 percent. Therefore,

the bounding condition for performance of the drip shield is the presence of saturated brines, which will contain nitrates for RH greater than 50 percent, and chlorides, sulfates, and carbonates as humidity increases. The duration of contact with brines will vary across the potential repository, depending on local thermal-hydrologic conditions. Approximate chemical models have been developed to describe the evolution of water composition in the EBS as the deliquescent salts dissolve, and liquid water reenters the drifts during the thermal period.

5.3.2.6   Colloids

- The presence of structural steel in the EBS environment ensures that ferric-oxide and -hydroxide colloids will be present, in addition to colloids from the host rock contributed by seepage flow. The best available analogs for colloids that can be transported through the UZ at Yucca Mountain are provided by the distributions groundwater colloids sampled in saturated-zone boreholes.

- The affinity of ferric colloids for radionuclides has been tested in the laboratory, and is probably most important for radioelements such as Pu and Am. These elements have limited solubility, but high affinity, so sorption to colloids can produce a relatively large increase in mobility. Sorption of Pu to hematite colloids is essentially irreversible, i.e., significant desorption is not observed in laboratory tests.

- Based on analog data for colloid concentration, and laboratory data for radionuclide affinity, the total concentration for Pu in EBS waters could increase by an order of magnitude or more, depending on the sorptive distribution coefficient.

5.3.2.7   Chemical System

- The evolution of water composition is calculated for a reference model, which was selected for thermal-hydrologic conditions that maximize evaporation and precipitation of salts in the drifts. The model represents the bulk environment with some dilution; ionic strength is limited to 1 molal. It does not apply to the transition period between the bounding condition of saturated brines in contact with the drip shield surface, and dilution of the brines to 1 molal.

- The calculations show that the bulk chemical environment approaches pH 11 during the thermal period, which occurs as the seepage encounters evaporated precipitates and salts, and is diluted. After the precipitates and salts are completely redissolved, the pH remains at approximately pH 10 or lower because of decreased CO_2 in solution. As cooldown progresses the pH decreases to values in the range 8 to 9.

- With elevated pH and ionic strength, there are commensurate increases in the concentrations of Na, K, Ca, Mg, chloride, sulfate, and carbonate. These results are sensitive to the CO_2 fugacity. Evaluation of CO_2 mass balance in the drifts plus the host rock and cement used in grouted rockbolts, shows that the CO_2 demand can probably be met by the predicted available supply. The CO_2 is stored in precipitates such as calcite and thermonatrite, released on dissolution of those precipitates. Calcite will precipitate

in the host rock above the potential repository, and pre-existing calcite in fractures will dissolve at cooler temperatures below the potential repository. This is equivalent to a shift in calcite abundance that favors the host rock above the drifts.

- Quartz sand is relatively inert and thus tends to provide minimal chemical input to biotic and abiotic corrosion processes that could impact the drip shields, however, it does provide readily available sites for quartz precipitation from high-pH silica-bearing solutions. Quartz can act as a pH buffer, lowering pH when it dissolves, but the pH tends to further increase when quartz is precipitated.

- The effects of cement grout that may be used for rockbolts in a portion of the potential repository are small, primarily because the grout has very low permeability. The amount of water that interacts with the grout will be limited, even if the grout degrades structurally. The composition of cement leachate will be similar to evaporatively concentrated waters that are predicted to result from heating. Mixing of the cement leachate with other seepage, and interaction with backfill and CO_2, will neutralize the impact of leachate on the bulk chemical environment.

5.3.3 Radionuclide Transport

- A bounding model for aqueous diffusion coefficients in partially saturated backfill indicates that diffusivity may be reduced by two orders of magnitude below the corresponding value in free water, provided the water content can be maintained low enough.

- Retardation by the invert will not significantly reduce long-term radionuclide release rates.

- The steady-state diffusive flux through the invert, in the absence of significant advective flow, could result in very low release rates.

5.3.4 Thermohydrology

- The Multiscale Thermohydrologic (MSTH) Model calculates the key TH variables (liquid flux, temperature, relative humidity, gas flux, air-mass fraction, and evaporation rate) as functions of time.

- Parameters significantly affecting TH behavior include site-scale variability of percolation flux, temporal variability of percolation flux, uncertainty in percolation flux, edge-cooling effects, dimensions and properties of the EBS components, variability of WP heat output, site-scale variability in thermal conductivity, and overburden thickness.

- During the pre-closure period, predicted host-rock temperatures remain below the boiling point for the mean and high infiltration flux cases, while boiling is predicted for the low flux case.

- Before closure, the maximum predicted waste package surface temperature is 110°C.

- Heat loss at the edges of the potential repository does not significantly affect pre-closure temperatures.

- After the initial heat-up stage, *RH* on WPs varies from 45 to 75 percent during the pre-closure period.

- Peak post-closure WP temperatures of 305°C (for the mean flux case) and 315°C (for the low flux case) occur at 60 yr. The difference in peak temperature between the hottest and coldest WP is 42°C.

- Peak post-closure temperatures on the lower drift wall of 195°C (for the mean flux case) and 205°C (for the low flux case) occur at 65 yr.

- Peak post-closure temperatures on the upper drift wall of 125°C (for the mean flux case) and 134°C (for the low flux case) occur at 65 yr.

- The model predicts that the duration of RH reduction at the drift wall grows shorter with proximity to the edge of the potential repository. The reduction lasts for 100 to 1000 years, depending on proximity to the edge, for the mean and high infiltration-flux cases, and for about 200 to 2000 years for the low flux case.

- The predicted duration of RH reduction on the drip shield is relatively insensitive to edge effects. Eventually, *RH* on the drip shield approaches 100 percent as it equilibrates with the host rock. For the mean and high flux cases, this occurs between about 1000 and 2000 years. For the low flux case, it occurs in about 3000 to 6000 years. The time to reach RH near 100 percent corresponds to the time at which seepage into the drift reaches steady state.

- The predicted duration of RH reduction on the WP is much longer than the duration for the DS, because the WP remains hotter than the DS long after seepage returns to the drift

- For the range of infiltration flux considered, between 24 and 44 percent of the host rock in the pillars is predicted to reach or exceed the boiling point.

5.4 GENERAL CONCLUSIONS OF THE EBS DEGRADATION, FLOW, AND TRANSPORT PROCESS MODEL REPORT

This report demonstrates that EBS performance is sufficiently well understood to support reasonable predictions of the environmental conditions at the drip shields and waste packages, and of conditions that will affect radionuclide transport in the emplacement drifts. Confidence has been increased through the use of available field and laboratory test data, and bounding models, to address predictive uncertainty.

Process model uncertainties are identified in this report, and alternative models are discussed. Validation is addressed throughout the discussion of process model, with emphasis on comparison of model results to test data, and to analogs where such information is available. Where appropriate, collection of data that could result in further model improvement, is

discussed in the text. Process model uncertainties are appropriately represented in the approaches to abstraction of model results for TSPA.

This document may be affected by technical product input information that requires confirmation. Any changes to the document that may occur as a result of completing the confirmation activities will be reflected in subsequent revisions. The status of the input information quality may be confirmed by review of the Document Input Reference System database.

6. REFERENCES

6.1 DOCUMENTS CITED

Barnard, R.W.; Wilson, M.L.; Dockery, H.A.; Gauthier, J.H.; Kaplan, P.G.; Eaton, R.R.; Bingham, F.W.; and Robey, T.H. 1992. *TSPA 1991: An Initial Total-System Performance Assessment for Yucca Mountain.* SAND91-2795. Albuquerque, New Mexico: Sandia National Laboratories. ACC: NNA.19920630.0033.

Budnitz, B.; Ewing, R.C.; Moeller, D.W.; Payer, J.; Whipple, C.; and Witherspoon, P.A. 1999. *Peer Review of the Total System Performance Assessment-Viability Assessment Final Report.* Las Vegas, Nevada: Total System Performance Assessment Peer Review Panel. ACC: MOL.19990317.0328.

Cohen, J.L. 1999. Comments on the Scientific Program, June 1999 Nuclear Waste Technical Review Board Meeting. "Letter from J.L. Cohen (NWTRB) to L.H. Barrett (OCRWM), August 3, 1999." ACC: MOL.20000317.0405.

CRWMS M&O 1994. *Total System Performance Assessment - 1993: An Evaluation of the Potential Yucca Mountain Repository.* B00000000-01717-2200-00099 REV 01. Las Vegas, Nevada: CRWMS M&O. ACC: NNA.19940406.0158.

CRWMS M&O 1995. *Total System Performance Assessment - 1995: An Evaluation of the Potential Yucca Mountain Repository.* B00000000-01717-2200-00136 REV 01. Las Vegas, Nevada: CRWMS M&O. ACC: MOL.19960724.0188.

CRWMS M&O 1996. *Probabilistic Volcanic Hazard Analysis for Yucca Mountain, Nevada.* BA0000000-01717-2200-00082 REV 0. Las Vegas, Nevada: CRWMS M&O. ACC: MOL.19971201.0221.

CRWMS M&O 1997. *Near-Field Geochemical Environment Abstraction/Testing Workshop Results.* B00000000-01717-2200-00188. Las Vegas, Nevada: CRWMS M&O. ACC: MOL.19980612.0027.

CRWMS M&O 1998a. Not used.

CRWMS M&O 1998b. Not used.

CRWMS M&O 1998c. "Waste Package Degradation Modeling and Abstraction." Chapter 5 of *Total System Performance Assessment-Viability Assessment (TSPA-VA) Analyses Technical Basis Document.* B00000000-01717-4301-00005 REV 01. Las Vegas, Nevada: CRWMS M&O. ACC: MOL.19981008.0005.

CRWMS M&O 1998d. "Near-Field Geochemical Environment." Chapter 4 of *Total System Performance Assessment-Viability Assessment (TSPA-VA) Analyses Technical Basis Document.* B00000000-01717-4301-00004 REV 01. Las Vegas, Nevada: CRWMS M&O. ACC: MOL.19981008.0004.

CRWMS M&O 1998e. "Waste Form Degradation, Radionuclide Mobilization, and Transport Through the Engineered Barrier System." Chapter 6 of *Total System Performance Assessment-Viability Assessment (TSPA-VA) Analyses Technical Basis Document.* B00000000-01717-4301-00006 REV 01. Las Vegas, Nevada: CRWMS M&O. ACC: MOL.19981008.0006.

. CRWMS M&O 1998f. Not used.

CRWMS M&O 1998g. "Thermal Hydrology." Chapter 3 of *Total System Performance Assessment-Viability Assessment (TSPA-VA) Analyses Technical Basis Document.* B00000000-01717-4301-00003 REV 01. Las Vegas, Nevada: CRWMS M&O. ACC: MOL.19981008.0003.

CRWMS M&O 1999a. *Engineered Barrier System Performance Modeling (WP#12012383MX).* Activity Evaluation, July 12, 1999. Las Vegas, Nevada: CRWMS M&O. ACC: MOL.19990719.0317.

CRWMS M&O 1999b. Not used.

CRWMS M&O 1999c. *Development Plan for the Engineered Barrier System Degradation, Flow, and Transport Process Model Report.* TDP-EBS-MD-000029 REV 00. Las Vegas, Nevada: CRWMS M&O. ACC: MOL.19991025.0033.

CRWMS M&O 1999d. Not used.

CRWMS M&O 1999e. Not used.

CRWMS M&O 1999f. Not used.

CRWMS M&O 1999g. *In Drift Corrosion Products.* ANL-EBS-MD-000041 REV 00. Las Vegas, Nevada: CRWMS M&O. ACC: MOL.20000106.0438.

CRWMS M&O 1999h. Not used.

CRWMS M&O 1999i. Not used.

CRWMS M&O 1999j. *Ventilation Model.* ANL-EBS-MD-000030 REV 00. Las Vegas, Nevada: CRWMS M&O. ACC: MOL.20000107.0330.

CRWMS M&O 1999k. Not used.

CRWMS M&O 1999l. Not used.

CRWMS M&O 1999m. Not used.

CRWMS M&O 2000a. *EBS Radionuclide Transport Abstraction Model for TSPA-LA AMR.* Input Transmittal 00110.T. Las Vegas, Nevada: CRWMS M&O. ACC: MOL.20000313.0401.

CRWMS M&O 2000b. *Engineered Barrier System Radionuclide Transport Model.* Input Transmittal 00088.T. Las Vegas, Nevada: CRWMS M&O. ACC: MOL.20000313.0416.

CRWMS M&O 2000c. *Engineered Barrier System Features, Events, and Processes and Degradation Modes Analysis.* ANL-EBS-MD-000035 REV 00. Las Vegas, Nevada: CRWMS M&O. ACC: MOL.20000217.0216.

CRWMS M&O 2000d. *Colloidal Concentration AMR.* Input Transmittal 00115.T. Las Vegas, Nevada: CRWMS M&O. ACC: MOL.20000313.0398.

CRWMS M&O 2000e. *In Drift Gas Flux Composition AMR.* Input Transmittal 00095.T. Las Vegas, Nevada: CRWMS M&O. ACC: MOL.20000309.0495.

CRWMS M&O 2000f. *Microbial Communities AMR.* Input Transmittal 00109.T. Las Vegas, Nevada: CRWMS M&O. ACC: MOL.20000313.0400.

CRWMS M&O 2000g. *Precipitates Salts Analysis AMR.* Input Transmittal 00097.T. Las Vegas, Nevada: CRWMS M&O. ACC: MOL.20000309.0497.

CRWMS M&O 2000h. *Invert Diffusion Properties Model.* ANL-EBS-MD-000031 REV 00. Las Vegas, Nevada: CRWMS M&O. ACC: MOL.20000203.0694.

CRWMS M&O 2000i. *Multiscale Thermohydrologic Model.* Input Transmittal 00124.T. Las Vegas, Nevada: CRWMS M&O. ACC: MOL.20000313.0784.

CRWMS M&O 2000j. *Physical and Chemical Environment Abstraction Model AMR.* Input Transmittal 00099.T. Las Vegas, Nevada: CRWMS M&O. ACC: MOL.20000309.0499.

CRWMS M&O 2000k. *Seepage/Backfill Interactions AMR.* Input Transmittal 00096.T. Las Vegas, Nevada: CRWMS M&O. ACC: MOL.20000309.0496.

CRWMS M&O 2000l. *Seepage/Cement Interactions.* ANL-EBS-MD-000043 REV 00. Las Vegas, Nevada: CRWMS M&O URN-0123. Submit to RPC

CRWMS M&O 2000m. *Seepage/Invert Interactions AMR.* Input Transmittal 00100.T. Las Vegas, Nevada: CRWMS M&O. ACC: MOL.20000309.0500.

CRWMS M&O 2000n. Not used.

CRWMS M&O 2000o. Not used.

CRWMS M&O 2000p. Not used.

CRWMS M&O 2000q. *Water Distribution and Removal Model.* Input Transmittal 00083.T. Las Vegas, Nevada: CRWMS M&O. ACC: MOL.2000310.0060.

CRWMS M&O 2000r. *EBS FEPS/Degradation Modes Abstration.* Input Transmittal 00121.T. Las Vegas, Nevada: CRWMS M&O. ACC: MOL.20000315.0370.

CRWMS M&O 2000s. *Summary of In-Package Chemistry for Waste Forms.* ANL-EBS-MD-000050 REV 00. Las Vegas, Nevada: CRWMS M&O. ACC: MOL.20000217.0217.

CRWMS M&O 2000t. *Physical/Chemical Environment Model AMR.* Input Transmittal 00119.T. Las Vegas, Nevada: CRWMS M&O. ACC: MOL.20000313.0419.

CRWMS M&O 2000u. Not used.

CRWMS M&O 2000v. Not used.

CRWMS M&O 2000w. *Abstraction of Near Field Environment Drift Thermodynamic Environment and Percolation Flux.* Input Transmittal 00108.T. Las Vegas, Nevada: CRWMS M&O. ACC: MOL.20000313.0399.

CRWMS M&O 2000x. *Drift Scale Coupled Processes (DST, THC Seepage) Models.* MDL-NBS-HS-000001. Las Vegas, Nevada: CRWMS M&O URN-0042. Submit to RPC

CRWMS M&O 2000y. *In-Drift Thermal-Hydrological-Chemical Model.* ANL-EBS-MD-000026 REV 00. Las Vegas, Nevada: CRWMS M&O. ACC: MOL.20000113.0488.

CRWMS M&O 2000z. Not used.

CRWMS M&O 2000aa. *Unsaturated Zone Flow and Transport Model and Abstractions for TSPA-SR Process Model Report.* TDR-NBS-HS-000002 REV 00. Las Vegas, Nevada: CRWMS M&O URN-0101. Submit to RPC

CRWMS M&O 2000ab. Not used.

CRWMS M&O 2000ac. Not used.

CRWMS M&O 2000ad. *Drift Degradation Analysis.* ANL-EBS-MD-000027 REV 00. Las Vegas, Nevada: CRWMS M&O. ACC: MOL.20000107.0328.

CRWMS M&O 2000ae. *Water Diversion Model.* ANL-EBS-MD-000028 REV00. Las Vegas, Nevada: CRWMS M&O. ACC: MOL.20000107.0329.

CRWMS M&O 2000af. *Water Drainage Model.* ANL-EBS-MD-000029 REV 00. Las Vegas, Nevada: CRWMS M&O. ACC: MOL.20000117.0216.

DOE (U.S. Department of Energy) 1998a. Not used.

DOE 1998b. Not used.

DOE 1998c. *Total System Performance Assessment.* Volume 3 of *Viability Assessment of a Repository at Yucca Mountain.* DOE/RW-0508. Washington, D.C.: U.S. Department of Energy, Office of Civilian Radioactive Waste Management. ACC: MOL.19981007.0030.

DOE (U.S. Department of Energy) 2000. *Quality Assurance Requirements and Description.* DOE/RW-0333P, Rev. 9. Washington, D.C.: U.S. Department of Energy, Office of Civilian Radioactive Waste Management. ACC: MOL.19991028.0012.

Hardin, E.L. 1998. *Near-Field/Altered-Zone Models Report.* UCRL-ID-129179. Livermore, California: Lawrence Livermore National Laboratory. ACC: MOL.19980630.0560.

Liu, H.H.; Doughty, C.; and Bodvarsson, G.S. 1998. "An Active Fracture Model for Unsaturated Flow and Transport in Fractured Rocks." *Water Resources Research, 34,* (10), 2633-2646. Washington, D.C.: American Geophysical Union. TIC: 243012.

Murphy, W.M. 1995. "Contributions of thermodynamic and mass transport modeling to evaluation of groundwater flow and groundwater travel time at Yucca Mountain, Nevada." *Scientific Basis for Nuclear Waste Management XVIII, Symposium held October 23-27, 1994, Kyoto, Japan.* Murakami, T. and Ewing, R.C., eds. *353,* 419-426. Pittsburgh, Pennsylvania: Materials Research Society. TIC: 216341.

NRC (U.S. Nuclear Regulatory Commission) 1998. *Issue Resolution Status Report Key Technical Issue: Total System Performance Assessment and Integration.* Rev. 1. Washington, D.C.: U.S. Nuclear Regulatory Commission. ACC: MOL.19990105.0083.

NRC (U.S. Nuclear Regulatory Commission) 1999a. *Issue Resolution Status Report Key Technical Issue: Container Life and Source Term.* Rev. 2. Washington, D.C.: U.S. Nuclear Regulatory Commission. TIC: 245538.

NRC (U.S. Nuclear Regulatory Commission) 1999b. *Issue Resolution Status Report Key Technical Issue: Evolution of the Near-Field Environment.* Rev. 2. Washington, D.C.: U.S. Nuclear Regulatory Commission. ACC: MOL.19990810.0640.

NRC (U.S. Nuclear Regulatory Commission) 1999c. *Issue Resolution Status Report Key Technical Issue: Repository Design and Thermal-Mechanical Effects.* Rev. 02. Washington, D.C.: U.S. Nuclear Regulatory Commission. ACC: MOL.20000306.0670.

NRC (U.S. Nuclear Regulatory Commission) 1999d. *Issue Resolution Status Report Key Technical Issue: Thermal Effects on Flow.* Rev. 2. Washington, D.C.: U.S. Nuclear Regulatory Commission. ACC: MOL.19991021.0156.

Triay, I.; Degueldre, C.; Wistrom, A.; Cotter, C.; and Lemons, W. 1996. *Progress Report on Colloid-Facilitated Transport at Yucca Mountain.* Milestone No. 3383. Los Alamos, New Mexico: Los Alamos National Laboratory. ACC: MOL.19970616.0061.

Wilder, D.G., ed. 1996. *Near-Field and Altered-Zone Environment Report.* UCRL-LR-124998. Volume II. Livermore, California: Lawrence Livermore National Laboratory. ACC: MOL.19961212.0121; MOL.19961212.0122.

Wilkins, D.R. and Heath, C.A. 1999. "Direction to Transition to Enhanced Design Alternative II." Letter from Dr. D.R. Wilkins (CRWMS M&O) and Dr. C.A. Heath (CRWMS M&O) to Distribution, June 15, 1999, LV.NS.JLY.06/99-026, with enclosures, "Strategy for Baselining EDA II Requirements" and "Guidelines for Implementation of EDA II." ACC: MOL.19990622.0126; MOL.19990622.0127; MOL.19990622.0128.

Wilson, M.L.; Gauthier, J.H.; Barnard, R.W.; Barr, G.E.; Dockery, H.A.; Dunn, E.; Eaton, R.R.; Guerin, D.C.; Lu, N.; Martinez, M.J.; Nilson, R.; Rautman, C.A.; Robey, T.H.; Ross, B.; Ryder, E.E.; Schenker, A.R.; Shannon, S.A.; Skinner, L.H.; Halsey, W.G.; Gansemer, J.D.; Lewis, L.C.; Lamont, A.D.; Triay, I.R.; Meijer, A.; and Morris, D.E. 1994. *Total-System Performance Assessment for Yucca Mountain – SNL Second Iteration (TSPA-1993).* SAND93-2675. Executive Summary and two volumes. Albuquerque, New Mexico: Sandia National Laboratories. ACC: NNA.19940112.0123.

YMP (Yucca Mountain Site Characterization Project) 1998. *Q-List.* YMP/90-55Q, Rev. 5. Las Vegas, Nevada: Yucca Mountain Site Characterization Office. ACC: MOL.19980513.0132.

6.2 CODES, STANDARDS, REGULATIONS, AND PROCEDURES

AP-2.13Q, Rev. 0, ICN 0. *Technical Product Development Planning.* Washington, D.C.: U.S. Department of Energy, Office of Civilian Radioactive Waste Management. ACC: MOL.19990701.0617.

AP-3.4Q, Rev. 1, ICN 2. *Level 3 Change Control.* Washington, D.C.: U.S. Department of Energy, Office of Civilian Radioactive Waste Management. ACC: MOL.20000207.0711.

AP-3.10Q, Rev. 2, ICN 0. *Analyses and Models.* Washington, D.C.: U.S. Department of Energy, Office of Civilian Radioactive Waste Management. ACC: MOL.20000217.0246.

AP-3.11Q, Rev. 0, ICN 1. *Technical Reports.* Washington, D.C.: U.S. Department of Energy, Office of Civilian Radioactive Waste Management. ACC: MOL.19991130.0149.

AP-3.15Q, Rev. 1, ICN 1. *Managing Technical Product Inputs.* Washington, D.C.: U.S. Department of Energy, Office of Civilian Radioactive Waste Management. ACC: MOL.20000218.0069.

AP-SI.1Q, Rev. 2, ICN 4. *Software Management.* Washington, D.C.: U.S. Department of Energy, Office of Civilian Radioactive Waste Management. ACC: MOL.20000223.0508.

QAP-2-0, Rev. 5. *Conduct of Activities.* Las Vegas, Nevada: CRWMS M&O. ACC: MOL.19980826.0209.

Appendix A

EBS PMR/IRSR Acceptance Criteria Matrix (includes only those that apply)

IRSR   *Container Life and Source Term (Revision 2)*

Subissue   *CLST All Subissues*

Acceptance Criteria Applicable to All Six Subissues

Acceptance Criterion	PMR Approach and Section Reference
Acceptance Criteria 1 The collection and documentation of data, as well as development and documentation of analyses, methods, models, and codes, were accomplished under approved quality assurance and control procedures and standards.	Activities associated with development of this Process Model Report and its related Analysis/Model Reports were determined to be subject to the quality assurance program as described in the Quality Assurance Requirements and Description (DOE 1999) document. As such, collection of related data, development of analyses and models, and use and validation of software is subject to the requirements of procedures developed to implement quality assurance program requirements.
Acceptance Criteria 2 Expert elicitations, when used, were conducted and documented in accordance with the guidance provided in NUREG-1563 or other acceptable approaches.	No expert elicitation was conducted for this PMR.
Acceptance Criteria 3 Sufficient data (field, laboratory, and natural analog) are available to adequately define relevant parameters for the models used to evaluate performance aspects of the subissues.	The EBS PMR uses a combination of field, laboratory, and natural analog data that can be broadly categorized into the geological, thermal, mechanical, hydrological, chemical and biological data of the NBS, and the geological, thermal, mechanical, hydrological, chemical and biological data of the EBS which consists of introduced materials such as grout, steel support, backfill and invert materials. For each of the supporting models presented, different data are used as input as documented in the respective AMRs (Table 1-1). In general the geological, thermal and hydrological data of the NBS and EBS support analysis of the flux of liquid water or water vapor to and from the drift such as in the Water Distribution and Removal Model or the Multiscale Model. Thermal and mechanical data of the NBS support the analysis of drift degradation. Biological data support analysis of microbial activity (Section 3.1.2). The chemical data of the groundwater, and its initial alteration due to evaporation leading to chemical precipitation and subsequent redissolution support the analysis of the formation of salts within the EBS, and the Chemical Summary Submodel (Section 3.1.2). Data on EBS processes are being collected at the current time for the Water Distribution and Removal Model (Section 3.1.1), and the Physical and Chemical Environment Model. Where appropriate, bounding calculations have been performed to estimate physical effects such as flow through drip shields (Section 3.1.1), and

Acceptance Criteria Applicable to All Six Subissues	
Acceptance Criterion	**PMR Approach and Section Reference**
	chemical effects on the alteration of groundwater.
Acceptance Criteria 4 Sensitivity and uncertainty analyses (including consideration of alternative conceptual models) were used to determine whether additional data would be needed to better define ranges of input parameters.	In general where assumptions have been used and documented in individual AMRs (Table 1-1) in the absence of data, sensitivity and uncertainty analyses have been performed to assess their impact and the need to collect additional data. Where parameters for stated assumptions are uncertain, and performance is sensitive to the parameter, laboratory scale and quarter scale testing has been identified to provide confirmation of stated assumptions. As an example, the analysis methods that have been developed by the YMP for evaluating thermal-hydrological effects for a porous media apply in a limited way to predicting heat and mass transfer through the EBS. Sensitivity analyses have been used (Section 3.1.1) to assess flow through the drip shield, and quarter scale and column tests are being performed to evaluate flow through the drip shield. As another example, the thermal-hydrological models were used to conduct sensitivity analyses for the potential for condensation under the drip shield for the repository environment which is also being tested at quarter scale.
Acceptance Criteria 5 Parameter values, assumed ranges, test data, probability distributions, and bounding assumptions used in the models are technically defensible and can reasonably account for known uncertainties.	In the preparation of the respective AMRs (Table 1-1) for the EBS PMR, assumptions for parameter values, assumed ranges, test data, probability distributions, and bounding assumptions are documented through applicable QA procedures. The basis for each assumption is stated, and the need for confirmation is identified. For example, in evaluating the performance of the drip shield, an assumption was made as to the occurrence based upon the parallel plate theory.
Acceptance Criteria 6 Mathematical model limitations and uncertainties in modeling were defined and documented.	Section 3.2.1 documents model uncertainties as they relate to the performance of the NBS and the EBS. While data have been developed for the NBS, model uncertainties of a conceptual nature as they relate to episodic flow through the PTn are documented. Model uncertainties associated with the EBS are also stated. In addition, model uncertainties are documented in each of the respective AMRs (Table 1-1). The Multi-Scale Thermohydrologic Model (Section 3.1.4) presents a large number of TH models that describe variable temperature, humidity, and flux conditions throughout the potential repository. It should be noted that EBS process models provide the basis for selecting robust designs for EBS performance and waste isolation in the face of model uncertainty.
Acceptance Criteria 7 Primary and alternative modeling approaches consistent with available data and current scientific understanding were investigated and their results and limitations considered in evaluating the subissue.	Section 3.1.2 addresses alternative models involving fully coupled THC. Such simulation methods can be applied as they become available, and as the required data, including numerical settings used to operate the simulation codes are qualified. The approach used in this PMR is applied to address conceptual issues and to evaluate bounding conditions for the performance of engineered barriers.
Acceptance Criteria 8 Model outputs were validated through comparisons with outputs of detailed process models, empirical observations, or both.	The validation of thermal-hydrological effects in the EBS is being evaluated through laboratory and quarter scale testing. Where information is currently available, experimental data and observations have been used for model validation. For example, the HRH salts model which is based upon an EQ3/E6 chemical equilibrium analysis was validated against evaporation tests with reasonable agreement between modeled and measured values.

Subissue   **CLST All Subissues**

Acceptance Criteria Applicable to All Six Subissues	
Acceptance Criterion	**PMR Approach and Section Reference**
Acceptance Criteria 9 The structure and organization of process and abstracted models were found to adequately incorporate important design features, physical phenomena, and coupled processes.	The EBS process and abstracted models incorporate the important design features such as drip shield, backfill, grout and steel support. The EBS process models (Sections 3.1.1 through 3.1.4) account for the important physical phenomena and coupled processes. For example, the analysis of CO2 and O2 fugacity is based upon flux of recharge from TH modeling and analysis.

Subissue   **CLST Subissue 1: The Effects of Corrosion Processes on the Lifetime of the Containers**

Acceptance Criterion	PMR Approach and Section Reference
Acceptance Criterion	**PMR Approach and Section Reference**
Acceptance Criteria 2 DOE has identified the broad range of environmental conditions within the WP emplacement drifts that may promote the corrosion processes listed previously, taking into account the possibility of irregular wet and dry cycles that may enhance the rate of container degradation.	The models presented in Sections 3.1.1 through 3.1.4 consider the effects waste package heat generation in increasing temperature and evaporation within the EBS. For example, the EBS Physical and Chemical Model Section 3.1.4) initially develops a TH model calculation for estimating water fluxes during the thermal period. This information is used to evaluate gas flux during the thermal period, CO2 and O2 fugacity which in turn are used to estimate the evolution of leachate composition, and the formation of salts and precipitates in the backfill and on the drip shield. The models analyze for a wide variety of environmental conditions that can develop due to irregular wetting and drying.

Subissue   **CLST Subissue 3: The Rate at Which Radionuclides in Spent Nuclear Fuel are Released from the Engineered Barrier Subsystem Through the Oxidation and Dissolution of Spent Fuel**

Acceptance Criterion	PMR Approach and Section Reference
Acceptance Criterion	**PMR Approach and Section Reference**
Acceptance Criteria 1 DOE has considered all categories of SNF planned for disposal at the proposed YM repository.	The EBS radionuclide transport model provides an analysis for a unit release of radionuclides due to a breached WP that can be applied to the radionuclide release from SNF. EBS PMR Section 3.1.3
Acceptance Criteria 4 DOE has identified and considered likely processes for SNF degradation and the release of radionuclides from the EBS, as follows: dissolution of the irradiated	Note that most of the criteria apply to the waste package and waste form. The EBS Water Distribution and Removal, and Physical and Chemical Environment Models provide information on drip shield corrosion environment, and flow through the drip shield.

Subissue   *CLST Subissue 3: The Rate at Which Radionuclides in Spent Nuclear Fuel are Released from the Engineered Barrier Subsystem Through the Oxidation and Dissolution of Spent Fuel*

Acceptance Criterion	PMR Approach and Section Reference
UO2 matrix, with the consequent formation of secondary minerals and colloids; prompt release of radionuclides; degradation in the dry air environment; degradation and failure of fuel cladding; preferential dissolution of intermetallics in DOE SNF; and release of radionuclides from the WP emplacement drifts.	EBS PMR Sections 3.1.3, 3.2.3.1.3, 3.2.3.2.3, and 3.2.3.1.5
Acceptance Criteria 5 DOE has demonstrated that the numerical models used for SNF degradation and radionuclide release from the EBS are adequate representations, including consideration of uncertainties, of the expected SNF performance and are not likely to overestimate the actual performance in the repository environment.	The WP PMR provide special studies that evaluate that evaluate for given WP environment the release of radionuclides from the waste form that allows an evaluation of SNF performance.
Acceptance Criteria 7 DOE has justified the use of SNF test results not specifically collected for the YM site for the environmental conditions expected to prevail after breaching of the containers at the YM site.	A bounding analysis for colloid transport is based upon colloid size distributions measured and reported in groundwater samples pumped from 18 wells in the vicinity of Yucca Mountain.

Subissue   *CLST Subissue 4: The Rate at Which Radionuclides in High-Level Waste Glass are Released From the Engineered Barrier Subsystem*

Acceptance Criterion	PMR Approach and Section Reference
Acceptance Criteria 1 DOE has taken into account all types of HLW glass planned for YM disposal.	The EBS Water Distribution and Removal Model provides a bounding analysis of the amount of water that would flow through backfill and drip shield and potentially contact waste packages.
Acceptance Criteria 4 DOE has identified and considered likely processes for the degradation of HLW glass and the release of radionuclides from the EBS, i.e., dissolution of the primary phase; formation of secondary minerals and	Section 3.1.3 presents a general discussion of radionuclide release through the EBS. Microbial effects on are presented in EBS PMR Section 3.2.3.1.3. EBS PMR Sections 3.2.3.1.5 and 3.2.3.2.3 identify and consider the likely processes for the transport of colloids.

Subissue   *CLST Subissue 4: The Rate at Which Radionuclides in High-Level Waste Glass are Released From the Engineered Barrier Subsystem*

Acceptance Criterion	PMR Approach and Section Reference
colloids; microbial action; and radionuclide releases and transport from the WP emplacement drifts.	

Subissue   *CLST Subissue 6: The Effects of Alternate Engineered Barrier Subsystem Design Features on Container Lifetime and Radionuclide Release From the Engineered Barrier Subsystem.*

Acceptance Criterion	PMR Approach and Section Reference
Acceptance Criteria 1 DOE has identified and considered the effects of backfill, and the timing of its emplacement, on the thermal loading of the repository, WP lifetime (including container corrosion and mechanical failure), and the release of radionuclides from the EBS.	The EBS WD&R, the EBS P&CE, and the EBS Multiscale Models provide analyses incorporating the placement of backfill at the time of repository closure. Further, the models consider the efficiency of initial heat removal due to preclosure ventilation. EBS PMR Sections 3.1.1 and 3.1.3.
Acceptance Criteria 4 DOE has identified and considered the effects of drip shields (with backfill) on WP lifetime, including extension of the humid-air corrosion regime, environmental effects, breakdown of drip shields and resulting mechanical impacts on WP, the potential for crevice corrosion at the junction between the WP and the drip shield, and the potential for condensate formation and dripping on the underside of the shield.	Studies are ongoing. The Water Distribution and Removal Model considers the flow performance of drip shield connectors. The WD&R (Section 3.1.1) considers the potential for condensation to form below the drip shield. The Multiscale model provides an analysis of the relative humidity surrounding the waste package that when coupled with corrosion data from the Waste Package model allows a determination of humid air corrosion. The interaction of flowing water with introduced materials including the grout, steel, and backfill is considered in the Physical and Chemical Environment Model. The Physical and Chemical Environment identifies the quantities of materials and their potential environmental effects on the EBS (Section 3.1.2). Note that crevice corrosion is addressed in the Waste Package PMR EBS PMR Sections 3.1.1, 3.1.2, and 3.1.4
Acceptance Criteria 6 DOE has identified the chemical composition of the water in the environment surrounding the WPs and its evolution with time.	Section 3.1.2 provides a Chemical Summary Submodel that integrates several submodels and describes the evolution of water composition and solid precipitates in the backfill above the drip shield, the invert, and the lower part of the backfill. Further, it evaluates CO_2 mass balance in the drifts and the surrounding host rock as it evolves with time. The assessment includes the effects of carbon steel corrosion, leaching from cementitious materials, microbial processes, and colloidal processes on the bulk chemical environment. EBS PMR Section 3.1.2

CLST Subissue 6: The Effects of Alternate Engineered Barrier Subsystem Design Features on Container Lifetime and Radionuclide Release From the Engineered Barrier Subsystem.

Acceptance Criterion	PMR Approach and Section Reference
Acceptance Criteria 7 DOE has justified the use of test results for drip shields, ceramic coatings, and backfill materials not specifically collected for the YM site for the environmental conditions expected to prevail at the proposed YM repository.	The EBS process models that have been developed are based upon assumptions that require test results for model validation. The quarter and laboratory scale test results are justified for model validation for the performance of the drips shield and backfill system.
Acceptance Criteria 8 DOE has conducted a consistent, sufficient, and suitable corrosion testing program at the time of LA submittal. In addition, DOE has identified specific plans for further testing to reduce any significant area(s) of uncertainty as part of the performance confirmation program.	Performance confirmation is not addressed in this PMR. The acceptance criterion will be applied appropriately to the Performance Confirmation Program.

Data and Model Justification for Subissue 1

Acceptance Criterion	PMR Approach and Section Reference
Criterion 3 Sufficient data were collected on the characteristics of the natural system and engineered materials, such as the type, quantity, and reactivity of material, to establish initial and boundary conditions for conceptual models and simulations of THC coupled processes that affect seepage and flow.	The Physical and Chemical Environment identifies the quantities of materials and data needs for the degradation of cementitious materials such as grout, steel and backfill materials and their potential for alteration of the backfill and the near field environment (Section 3.1.2). The effects of the coupled THC processes on EBS flow is considered in the Water Distribution and Removal Model and Multiscale Model. The Water Distribution and Removal Model uses bounding assumptions in regards to the reduction in permeability of fractures in the floor and evaluates the effects of such alteration on seepage through the EBS.(Section 3.1.1) due to such degradation.

EBS PMR Sections 3.1.1 and 3.1.2 |

Integration for Subissue 1

Acceptance Criterion	PMR Approach and Section Reference
Criterion 1 DOE considered all the relevant features, events, and processes. The abstracted models adequately incorporated important design features, physical phenomena, and couplings, and used consistent and appropriate assumptions throughout.	The FEPs for the EBS are identified in Table 2-2. Specifically, the relevant FEPs that relate to flow through the EBS components relate to the FEP categories for the drip shield, the invert, sand drains, condensation below the drip shield, refluxing of flow, flow along the DS wall, movement of backfill through gaps and separations in the DS, and fluid flow into gaps and separations in the DS. The major features, events and processes involving flow through the backfill, DS, and invert are presented in each of the respective AMRs as summarized in Sections 3.1.1 through 3.1.4. In addition, for FEPs involving probabilistic events associated with the degradation of design features such as separation of drip shield, and backfill in contact with WP, additional analyses are provided in EBS PMR abstractions.
Criterion 2 Models reasonably accounted for known temporal and spatial variations in conditions affecting coupled THC effects on seepage and flow.	The EBS Multiscale Model accounts for temporal variations due to changes in waste package heat loading, and spatial variations in infiltration flux, and stratigraphy for various chimney locations in the repository. These variations are incorporated into the Multiscale model and results in variations in predicted seepage into the EBS.

EBS Section 3.1.4 |
| Criterion 3 Not all THC couplings may be determined to be important to performance, and DOE may adopt assumptions to simplify PA analyses. If potentially important couplings are neglected, DOE should provide a technical basis for doing so. The technical | In each of the respective AMRs (Table 1-1), the assumptions supporting the AMR are documented. In those models where assumptions are made neglecting important couplings, the technical basis for each assumption is stated. For example, the effects of chemical precipitation of salts within the floor fractures was evaluated through sensitivity studies in the Water Distribution and Removal model by assuming the fractures are plugged as a bounding assumption instead of a detailed THC analysis involving chemical precipitation for fracture |

Integration for Subissue 1

Acceptance Criterion	PMR Approach and Section Reference
basis can include activities such as independent modeling, laboratory or field data, or sensitivity studies.	plugging. EBS Section 3.1.1 through 3.1.4
Criterion 4 Where simplifications for modeling coupled THC effects on seepage and flow were used for PA analyses instead of detailed process models, the bases used for modeling assumptions and approximations were documented and justified.	As discussed above, for each of the respective AMRs (Table 1-1) involving PA analyses and abstraction, the bases for modeling assumptions are stated. See EBS Section 3.1.1 through 3.1.4

ENFE Subissue 1: Effects of Coupled Thermal-Hydrologic-Chemical Processes on Seepage and Flow

Model Uncertainty for Subissue I	
Acceptance Criterion	**PMR Approach and Section Reference**
Criterion 1 Appropriate models, tests, and analyses were used that are sensitive to the THC couplings under consideration for both natural and engineering systems, as described in the following examples. The natural-setting data indicate processes that should be evaluated include: (i) zeolitization of volcanic glass, which could affect flow pathways; (ii) precipitation of calcite and opal on the footwall of fracture surfaces and the bottoms of lithophysal cavities, which indicates gravity-driven flow in open fractures that could affect permeability and porosity; and (iii) potential dehydration of zeolites and vitrophyre glass, which could release water affecting heat and fluid flow. The effects of THC coupled processes that may occur due to interactions with engineered materials or their alteration products include: (i) changes in water chemistry that may result from interactions between cementitious materials and groundwater, which, in turn, may affect seepage and flow; (ii) dissolution of the geologic barrier (e.g., tuff) by a hyperalkaline fluid that could lead to changes in the hydraulic properties of the geologic barrier; and (iii) precipitation of calcite or calcium-silica-hydrate phases along fracture surfaces as a result of migration of a hyperalkaline fluid that could affect hydraulic properties.	The effects of THC coupled processes for EBS cementitious materials are analyzed by the cementitious materials submodel. This model (Section 3.1.2) develops reasonable bound estimates for the chemistry of the grout leachate. The altered groundwater chemistry is considered in the Chemical Summary Submodel (Section 3.1.2.3.7) that considers the evolution of water composition and solid precipitates in the backfill above the drip shield, and the invert and lower part of the backfill for the reference EBS Physical and Chemical Environment Model. While a detailed evaluation has not been made for the precipitation of calcite or calcium-silica-hydrate phases along fractures in the invert as a result of the hyperalkaline fluid, a bounding analysis appropriate for THC effects assuming the fractures were plugged was made in the Water Distribution and Removal Model (Section 3.1.1) with the resulting hydraulic conductivity of the fractures equal to the permeability of the matrix. Sections 3.1.1, 3.1.2 and Section 3.1.2.3.7
Criterion 2 Given the current design of the repository, it will be acceptable to ignore the potential effects of microbial processes on seepage and flow.	The growth of microbes is limited by water, and nutrients. Water is not available in the unsaturated zone to sustain growth that would alter porosity. EBS PMR 3.1.2.4
Criterion 3 Alternative modeling approaches consistent with available data and current scientific understanding were investigated, and their results and limitations were appropriately considered.	Sections 3.1.1 through 3.1.2 present alternative models for Water Distribution and Removal, Bulk Physical and Chemical Environment in the EBS, and Radionuclide Transport respectively.
Criterion 4 DOE provided a reasonable description of	In each of the respective AMRs in Table 1-1, the DOE provided descriptions of conceptual, and detailed

Model Uncertainty for Subissue 1

Acceptance Criterion	PMR Approach and Section Reference
the mathematical models included in its analyses of coupled THC effects on seepage and flow. The description included a discussion of alternative modeling approaches not considered in its final analysis and the limitations and uncertainties of the chosen model.	models as required by AP-3.10Q that provide a reasonable description of modeling thermal-hydrologic phenomena for predicting seepage and flow in the EBS. With regards to the Water Distribution and Removal Model, the P&CE model, and the multiscale models that use NUFT.

Model Verification for Subissue 1

Acceptance Criterion	PMR Approach and Section Reference
Criterion 1 The mathematical models for coupled THC effects on seepage and flow were consistent with conceptual models based on inferences about the near-field environment, field data and natural alteration observed at the site, and expected engineered materials.	The Water Distribution and Removal Model, the P&CE Model, and the Multiscale Model provide predictions of seepage and flow that are based upon the selection of a consistent set thermal properties, and hydrologic properties for the active fracture model. The active fracture model, and the drift scale properties sets for these models are consistent with properties sets used in the UZ model which were determined by inverse modeling methods. All EBS models use a consistent set of thermal and hydrologic properties for the backfill, invert, and drip shield.
Criterion 2 DOE appropriately adopted accepted and well-documented procedures to construct and test the numerical models used to simulate coupled THC effects on seepage and flow.	The DOE used appropriate procedures to construct and test numerical models for predicting seepage and flow. For the case of the Water Distribution and Removal Model, the results of the NUFT calculations were compared to a closed form analytical solution for the prediction of fluxes in and near the EBS (CRWMS M&O 2000q). The software codes and routines used for the models are subject to verification and testing under the procedure AP-SI.1Q.
Criterion 3 Abstracted models for coupled THC effects on seepage and flow were based on the same assumptions and approximations shown to be appropriate for closely analogous natural or experimental systems. Abstracted model results were verified through comparison to outputs of detailed process models and empirical observations. Abstracted model results were compared with different mathematical models to judge robustness of results.	The following discussion considers EBS flow. The current abstracted EBS flow model for the Physical and Chemical Model Abstraction relating to the WP environment is conceptual in nature. The model abstractions are based upon similar assumptions in that similar flow path components such as flow in and around the drip shield is identified in the process model abstraction (CRWMS M&O 2000j). In certain cases, the process model abstractions develop probabilistic analysis approaches that are more appropriately handled in TSPA studies. For example, a probabilistic analysis is developed for drip shield separation, and the potential contact of water with the waste package in the model abstraction. Since the abstracted flow model for the EBS Physical and Chemical Model Abstraction is conceptual (CRWMS M&O 2000j), no comparisons have been made between outputs, and the empirical observations such as are currently being made in the quarter scale tests. Since the abstracted flow model for the Physical and Chemical Model Abstraction is conceptual, abstracted model results have not been compared with different mathematical models to address the robustness of the

Subissue   *ENFE Subissue 1: Effects of Coupled Thermal-Hydrologic-Chemical Processes on Seepage and Flow*

Model Verification for Subissue 1	
Acceptance Criterion	**PMR Approach and Section Reference**
	,results.

Programmatic for Subissue 1	
Acceptance Criterion	**PMR Approach and Section Reference**
Criterion 1 Data and models were collected, developed, and documented under acceptable quality assurance (QA) procedures.	Activities associated with development of this Process Model Report and its related Analysis/Model Reports were determined to be subject to the quality assurance program as described in the Quality Assurance Requirements and Description (DOE 1999) document. As such, collection of related data, development of analyses and models (Table 1-1), and use and validation of software is subject to the requirements of procedures developed to implement quality assurance program requirements.
Criterion 2 Deficiency reports concerning data quality on issues related to coupled THC effects on seepage and flow were closed.	The PMRs are prepared according to the procedure Analyses and Models, AP-3.10Q which was developed to address data deficiency and quality issues. At the current time, the data used for the analyses and models (Table 1-1) are obtained from controlled sources that are undergoing qualification, and will be closed after completion of data qualification activities.
Criterion 3 If used, expert elicitations were conducted and documented in accordance with the guidance in NUREG-1563 (Kotra, et al., 1996) or other acceptable approaches.	No expert elicitation was conducted for this PMR.

Subissue   *ENFE Subissue 2: Effects of Coupled Thermal-Hydrologic-Chemical Processes on the Waste Package Chemical Environment*

Data and Model Justification for Subissue 2	
Acceptance Criterion	**PMR Approach and Section Reference**
Criterion 1 Available data relevant to both temporal and spatial variations in conditions affecting coupled THC effects on WP chemical environment were considered.	The P&CE Model is based upon a two dimensional thermal hydrologic analysis that accounts for temporal waste heat loading, and variations in percolation rates. The P&CE Model analyzes evolution of leachate composition from the grout and backfill for the EBS when contacted with J-13 groundwater. EBS PMR Section 3.1.2 and Section 3.2.3.1.3
Criterion 2 DOE's evaluation of coupled THC processes properly considered site characteristics in	The P&CE Model is based upon a two dimensional thermal hydrologic analysis that considers initial temperature and pressure boundary conditions. The P&CE Model considers initially the composition of J-13

Data and Model Justification for Subissue 2

Acceptance Criterion	PMR Approach and Section Reference
establishing initial and boundary conditions for conceptual models and simulations of coupled processes that may affect the WP chemical environment.	groundwater that is used for developing a precipitates and salts normative submodel which is in turn used in the Chemical Summary submodel. EBS PMR Section 3.1.2
Criterion 3 Sufficient data were collected on the characteristics of the natural system and engineered materials, such as the type, quantity, and reactivity of material, to establish initial and boundary conditions for conceptual models and simulations of THC coupled processes that affect the WP chemical environment.	Data on EBS processes are being collected at the current time for the Water Distribution and Removal Model (Section 3.1.1), and the Physical and Chemical Environment Model. Where appropriate, bounding calculations have been performed to estimate physical effects such as flow through drip shields (Section 3.1.1), the potential for condensation below the drip shield (Section 3.1.1) and chemical effects such as the alteration of groundwater chemistry (Section 3.1.2). EBS PMR Sections 3.1.1 and 3.1.2
Criterion 4 A nutrient and energy inventory calculation (e.g., McKinley, West, and Grogan, 1985; Grogan and McKinley, 1990; Noy, et al., 1996) was used to determine the potential for microbial activity that could impact the WP chemical environment.	The EBS Physical and Chemical Model Environments consider these effects on the growth of microbial communities. The Microbial communities model considers steel alloys, and organic substances on the microbial growth rate. Further, the model is implemented with the MING V1.0 modeling code that combines the nutrient and thermodynamic approaches. The model assumes that all usable energy for microorganisms is derived from oxidation reduction (redox) reactions. EBS PMR Sections 3.1.2 and 3.2.3.1.3
Criterion 5 Should microbial activity be sufficient to allow microbial influenced corrosion (MIC) of the WP, then the time-history of temperature, humidity, and dripping should be used to constrain the probability for MIC.	The EBS P&CE Environment Model provides an analysis of the effects of temperature, humidity, and dripping on the growth of microbial communities. The Microbial Communities Model considers the relative humidity which in turn depends on the temperature and dripping environment. The model considers how temperature, humidity, and dripping constrain microbial growth such as dryout of the EBS and high temperatures during the thermal period. Section 3.1.2 and 3.2.3.1.3
Criterion 6 Sensitivity and uncertainty analyses (including consideration of alternative conceptual models) were used to determine whether additional new data are needed to better define ranges of input parameters.	In general where assumptions have been used and documented in individual AMRs (Table 1-1) in the absence of data, sensitivity and uncertainty analyses have been performed to assess their impact and the need to collect additional data. Where parameters for stated assumptions are uncertain, and performance is sensitive to the parameter, laboratory scale testing has been identified to provide confirmation of stated assumptions. As an example, EBS PMR Section 3.1.2
Criterion 7 If the testing program for coupled THC processes on WP chemical environment is not complete at the time of license application, or if	Performance confirmation is not addressed in this PMR. The acceptance criterion will be applied appropriately to the Performance Confirmation Program.

Data and Model Justification for Subissue 2	
Acceptance Criterion	**PMR Approach and Section Reference.**
sensitivity and uncertainty analyses indicate additional data are needed, DOE has identified specific plans to acquire the necessary information as part of the performance confirmation program.	

Data Uncertainty and Verification for Subissue 2	
Acceptance Criterion	**PMR Approach and Section Reference**
Criterion 1 Reasonable or conservative ranges of parameters or functional relations were used to determine effects of coupled THC processes on the WP chemical environment. Parameter values, assumed ranges, probability distributions, and bounding assumptions were technically defensible and reasonably accounted for uncertainties.	In the preparation of the respective AMRs (Table 1-1) for the EBS PMR, assumptions for parameter values, assumed ranges, test data, probability distributions, and bounding assumptions are documented through the AP-3.10Q procedure. The basis for each assumption is stated, and the need for confirmation is identified.
Criterion 2 Uncertainty in data due to both temporal and spatial variations in conditions affecting coupled THC effects on WP chemical environment were considered.	Section 3.2.1 documents model uncertainties as they relate to the performance of the NBS and the EBS. While data have been developed for the NBS, model uncertainties of a conceptual nature as they relate to episodic flow through the PTn nonwelded tuff are documented. Model uncertainties associated with the EBS are also stated. In addition, model uncertainties are documented in each of the respective AMRs (Table 1-1). For example as discussed in Section 3.1.4, the Multi-Scale Thermal-Hydrologic Model presents a large number of TH models that describe variable temperature, humidity, and flux conditions throughout the potential repository. It should be noted that EBS process models provide the basis for selecting robust designs for EBS performance and waste isolation in the face of model uncertainty.
Criterion 3 DOE's evaluation of coupled THC processes properly considered the uncertainties in the characteristics of the natural system and engineered materials, such as the type, quantity, and reactivity of, material, in establishing initial and boundary conditions for conceptual models and simulations of THC coupled processes that affect the WP chemical environment.	Data on EBS processes are being collected at the current time for the Water Distribution and Removal Model (Section 3.1.1), and the Physical and Chemical Environment Model. Where appropriate, bounding calculations have been performed to estimate physical effects such as flow through drip shields (Section 3.1.1), and chemical effects such as the alteration of groundwater chemistry (Section 3.1.4). EBS PMR Section 3.1.2
Criterion 4 The initial conditions, boundary conditions, and computational domain used in sensitivity analyses involving coupled THC effects on	The EBS TH submodel used in the P&CE model are based upon initial conditions boundary conditions, and computational domains consistent with site characteristics. The thermal hydrology models used in Sections 3.1.1 through 3.1.4 are based upon the selection of NBS hydrologic and thermal properties used in the UZ

Data Uncertainty and Verification for Subissue 2	
Acceptance Criterion	**PMR Approach and Section Reference**
WP chemical environment were consistent with available data.	Process Model. The initial conditions, and boundary conditions for the models for specific locations use the same infiltration rates, and temperature and pressure boundary conditions consistent with the UZ Process Model (Section 3.1.4)

Further, the submodels used for evaluating CO2 and O2 gas fugacity is consistent with available data from borehole SD 12 (Section 3.1.2). The submodels used for evaluating precipitates, and salts, and alteration of groundwater consistently use the J-13 groundwater chemistry as input.

EBS PMR Sections 3.1.1 through 3.1.4 |
| Criterion 5 DOE's performance confirmation program will assess whether the natural system and engineered materials are functioning as intended and anticipated with regard to coupled THC effects on WP chemical environment. | Performance confirmation is not addressed in this PMR. The acceptance criterion will be applied appropriately to the Performance Confirmation Program. |

Integration for Subissue 2	
Acceptance Criterion	**PMR Approach and Section Reference**
Criterion 1 DOE has considered all the relevant features, events, and processes. The abstracted models adequately incorporated important design features, physical phenomena, and couplings, and used consistent and appropriate assumptions throughout.	Important features, events, and processes are identified in EBS PMR Section 2.4.1.

The FEPs for the EBS are identified in Table 2-2. Specifically, the relevant FEPs that relate to Thermal-Hydrologic-Chemical Processes on the Waste Package Chemical Environment Release are addressed in the microbial activity Energy /Nutrient Balance Microbial Model (Section 3.1.2) The Cementitious Materials Submodel addresses the alteration of infiltrate chemistry due to physical and chemical properties of the EBS. as summarized in Sections 3.1.1 through 3.1.4.

See EBS PMR Section 2.4.1 |
| Criterion 2 Models reasonably accounted for known temporal and spatial variations in conditions affecting coupled THC effects on WP chemical environment. | The EBS P&CE Model is based upon the thermal hydrology that accounts for thermal refluxing.

EBS PMR Section 3.1.2 |
| Criterion 3 Not all THC couplings may be determined to be important to performance, and DOE may adopt assumptions to simplify performance assessment analyses. If potentially important couplings are | In each of the respective AMRs (Table 1-1), the assumptions supporting the AMR are documented. In those models where assumptions are made neglecting important couplings, the technical basis for each assumption is stated. For example in the Chemical Reference Submodel that is part of the P&CE Model, it is assumed that a normative assemblage of salts, having equilibrated to the ambient relative humidity (Section 3.1.2.7). The |

Integration for Subissue 2

Acceptance Criterion	PMR Approach and Section Reference
neglected, DOE should provide a technical basis for doing so. The technical basis can include activities such as independent modeling, laboratory or field data, or sensitivity studies.	technical basis for this assumption is provided. EBS Section 3.1.1 through 3.1.4
Criterion 4 Where simplifications for modeling coupled THC effects on WP chemical environment were used for performance assessment analyses instead of detailed process models, the bases used for modeling assumptions and approximations were documented and justified.	The EBS P&CE Model states bases for process model development. EBS PMR Section 3.1.2

Model Uncertainty for Subissue 2

Acceptance Criterion	PMR Approach and Section Reference
Criterion 1 Appropriate models, tests, and analyses were used that are sensitive to the THC couplings under consideration for both natural and engineering systems as described in the following examples. The effects of THC coupled processes that may occur in the natural setting or due to interactions with engineered materials or their alteration products include: (i) TH effects on gas and water chemistry; (ii) hydrothermally driven geochemical reactions such as zeolitization of volcanic glass, which could affect water chemistry and WP environmental conditions; (iii) dehydration of hydrous phases liberating moisture that may affect the WP environment; (iv) effects of microbial process on the WP environment; and (v) changes in water chemistry that may result from the release of corrosion products from the WP and interactions between cementitious materials and groundwater, which, in turn, may affect the WP chemical environment.	The EBS P&CE model analyzes these effects. The Gas Flux and Fugacity Submodel analyzes TH effects for CO_2 and O_2 gas fugacity (Section 3.1.2.5). These results are then used in the Chemical Summary Submodel (Section 3.1.2.7) to estimate changes in groundwater chemistry during various stages of the thermal cycle. The Chemical Summary Submodel inputs information from the TH 2D submodel, and evaluates water composition in the surround rock such as in the drift above the repository. The Chemical Summary Submodel uses the composition for Time Period 2, and calculates an assemblage of evaporative minerals using the normative approach. The microbial growth submodel evaluates the potential for microbial growth, and concludes that no microbial growth will occur for temperatures greater than 120 degrees C. The cementitious materials submodel evaluates interactions between the cementitious grout, and groundwater. · EBS PMR Section 3.1.2
Criterion 2 Alternative modeling approaches consistent with available data and current scientific	The EBS P&CE Model considers alternative modeling approaches.

Model Uncertainty for Subissue 2

Acceptance Criterion	PMR Approach and Section Reference
understanding were investigated, and their results and limitations were appropriately considered.	The P&CE model is consistent with the available data regarding introduced materials, CO_2 fugacity, TH effects, and groundwater chemistry. Alternative models for cementitious materials, steel corrosion, and gas phase mass fluxes of O_2 and CO_2 were investigated as summarized in Section 3.1.2. The alternative approach for modeling the EBS physical and chemical environment involves fully coupled, reactive transport simulations. These were investigated, but found to be restricted to a chemical species and precipitates with limited flexibility to handle ionic strength limitations. EBS PMR Section 3.1.2
Criterion 3 DOE provided a reasonable description of the mathematical models included in its analyses of coupled THC effects on WP chemical environment. The description included a discussion of alternative modeling approaches not considered in its final analysis and the limitations and uncertainties of the chosen model.	For the WP environment, the DOE provides a reasonable description of the mathematical models. The thermal hydrological model based upon NUFT is described in Section 3.1.2.1. Certain specialized models were developed as part of the EBS PMR. For example, these include the conservative solute analysis in Section 3.1.2.1. The system of differential equations is described. Further, in Section 3.1.2.2, steady state methods for 14CO2 transport in the UZ and through the EBS were described. Modeling limitations and uncertainties as they relate to the PC&E environment are described throughout Section 3.1.2. Note that the EBS PMR is a summary document. As part of the AP-3.10Q process for documentation, each of the respective AMRs presented in Table 1-1 is documented in detail. For example, the description of the EQ3/6 analysis for the Chemical Summary Submodel is presented in CRWMS M&O 2000t. As described above, and discussed in EBS PMR Section 3.1.2, alternative models are presented for fully coupled THC modeling.

Model Verification for Subissue 2

Acceptance Criterion	PMR Approach and Section Reference
Criterion 1 The mathematical models for WP chemical environment were consistent with conceptual models based on inferences about the near-field environment, field data and natural alteration observed at the site, and expected engineered materials.	The P&CE Model thermal hydrology provides a prediction of seepage and flow that are based upon the same conceptual active fracture model. The active fracture model, for the NBS is consistent with the active fracture model for the UZ.
Criterion 2 DOE appropriately adopted accepted and well-documented procedures to construct and test the numerical models used to simulate the WP chemical environment.	Each respective AMR (Table 1-1) which were prepared according to AP-3.10Q with discussion of quality assurance, computer software, model inputs, and model assumptions. For analyses involving the use of software routines, the routines were verified by separate hand calculations. In other cases, the more complex models are compared with experimental test data. For example, as discussed in Section 3.1.2.5, two evaporation tests using synthetic J-13 water were simulated using the HRH Salts Model. The comparison of

Model Verification for Subissue 2	
Acceptance Criterion	**PMR Approach and Section Reference**
	the model predictions for measured pH and ionic strength compare with measured data. EBS PMR Section 3.1.2
Criterion 3 Abstracted models for coupled THC effects on WP chemical environment were based on the same assumptions and approximations shown to be appropriate for closely analogous natural or experimental systems. Abstracted model results were verified through comparison to outputs of detailed process models and empirical observations. Abstracted model results were compared with different mathematical models to judge robustness of results.	The EBS PMR provides a discussion for the validation of the EBS P&CE Model. The current abstracted model for the Physical and Chemical Model Abstraction relating to the WP environment is conceptual in nature. The model abstractions are based upon similar assumptions in that similar flow path components such as flow in and around the drip shield and major chemical interactions such as the formation of precipitates and salts during repository heating, and the dilution of brines during repository cooling are identified in the process model abstraction (CRWMS M&O 2000j) In certain cases, the process model abstractions develop probabilistic analysis approaches that are more appropriately handled in TSPA. For example, a probabilistic analysis is developed for drip shield separation, and the potential contact of water with the waste package in the model abstraction. Since the Physical and Chemical Model Abstraction is conceptual (CRWMS M&O 2000j), no comparisons have been made between outputs, and the empirical observations such as are currently being made in the quarter scale tests. Moreover, abstracted model results have not been compared with different mathematical models to address the robustness of the results. EBS PMR Section 3.2.2

Programmatic for Subissue 2	
Acceptance Criterion	**PMR Approach and Section Reference**
Criterion 1 Data and models were collected, developed, and documented under acceptable quality assurance (QA) procedures.	Activities associated with development of this Process Model Report and its related Analysis/Model Reports were determined to be subject to the quality assurance program as described in the Quality Assurance Requirements and Description (DOE 1999) document. As such, collection of related data, development of analyses and models, and use and validation of software is subject to the requirements of procedures developed to implement quality assurance program requirements.
Criterion 2 Deficiency reports concerning data quality on issues related to coupled THC effects on waste package chemical environment were closed.	The EBS P&CE model has been prepared according to AP-3.10Q and AP-3.15Q to address quality assurance deficiency issues. The AP-3.10Q procedure addresses previous deficiencies in obtaining input data from controlled sources of information, and in the documentation of software. AP-3.15Q provides the process for managing inputs to each AMR. Existing deficiencies are in the process of being closed with the preparation of the P&CE AMR

Subissue

ENFE Subissue 2: Effects of Coupled Thermal-Hydrologic-Chemical Processes on the Waste Package Chemical Environment

Programmatic for Subissue 2

Acceptance Criterion	PMR Approach and Section Reference
	according to AP-3.10Q.
	EBS PMR Section 1.3
Criterion 3 If used, expert elicitations were conducted and documented in accordance with the guidance in NUREG-1563 (Kotra, et al., 1996) or other acceptable approaches.	No expert elicitation was conducted for this PMR.

Subissue

ENFE Subissue 3: Effects of Coupled Thermal-Hydrologic-Chemical Processes on the Chemical Environment of Radionuclide Release

Data and Model Justification for Subissue 3

Acceptance Criterion	PMR Approach and Section Reference
Criterion 1 Available data relevant to both temporal and spatial variations in conditions affecting coupled THC effects on the chemical environment for radionuclide release were considered.	The EBS radionuclide transport model (EBS PMR Section 3.1.3) provides an analysis of release based upon the thermal hydrological calculations in the WD&R model. The EBS radionuclide transport model (EBS PMR Section 3.1.3) is an advection/dispersion/diffusion model. The WD&R model considers the temporal variations in conditions affecting the TH effects, and provides a bounding calculation for chemical effects due fracture plugging that would alter saturation levels and porewater velocities. The EBS radionuclide transport (Section 3.1.3) model provides a sensitivity analysis for the chemical retardation that bounds temporal and spatial variations in the chemical retardation factor that reflects the chemical environment. For the base case, the EBS radionuclide transport takes no credit for chemical retardation which is a bounding assumption for radionuclide transport.
	The EBS Colloids submodel is based upon relevant data for the size and concentration of colloids that account for variability through probability distributions. Based upon these data bounding values for radionuclide solubility, and colloid diffusion coefficient were calculated.
	EBS Sections 3.1.2.6 and 3.1.3
Criterion 2 DOE's evaluation of coupled THC processes properly considered site characteristics in establishing initial and boundary conditions for conceptual models and simulations of coupled processes that may affect the chemical environment	The EBS radionuclide transport model (EBS PMR Section 3.1.3) provides an analysis of release based upon the thermal hydrological calculations in the WD&R model. The physical processes in the EBS radionuclide transport model include advection, dispersion and diffusion. The advection through the EBS, and in particular in the invert is based upon initial and boundary conditions for the NBS and EBS in the Water Distribution Model (Section 3.1.1).

Subissue

ENFE Subissue 3: Effects of Coupled Thermal-Hydrologic-Chemical Processes on the Chemical Environment of Radionuclide Release

Data and Model Justification for Subissue 3

Acceptance Criterion	PMR Approach and Section Reference
for radionuclide release.	The EBS Radionuclide Transport Model (Section 3.1.1) provides analysis that can be scaled to the release of radionuclides from the WP. EBS PMR Sections 3.1.1 through 3.1.3
Criterion 3 Sufficient data were collected on the characteristics of the natural system and engineered materials, such as the type, quantity, and reactivity of material, in establishing initial and boundary conditions for conceptual models and simulations of THC coupled processes that affect the chemical environment for radionuclide release.	Data on EBS processes are being collected at the current time for the Water Distribution and Removal Model (Section 3.1.1), and the Physical and Chemical Environment Model. Where appropriate, bounding calculations have been performed to estimate physical effects such as flow through drip shields (Section 3.1.1), and chemical effects such as the alteration of groundwater chemistry (Section 3.1.4). EBS PMR Sections 3.1.1 through 3.1.3
Criterion 4 A nutrient and energy inventory calculation was used to determine the potential for microbial activity that could impact radionuclide release.	The EBS P&CE Model provides a bounding analysis for a nutrient and energy inventory. EBS PMR Sections 3.1.2 EBS PMR Section 3.1.2 and Section 3.2.3.1.3.
Criterion 5 Should microbial activity be sufficient to potentially affect the chemical environment for radionuclide release, then the time-history of temperature, humidity, and dripping should be used to constrain the probability for microbial effects, such as production of organic by-products that act as complexing ligands for actinides and microbial-enhanced dissolution of the HLW glass form.	See discussion presented above. See EBS PMR Section 3.1.2 and 3.2.3.1.3
Criterion 6 Sensitivity and uncertainty analyses (including consideration of alternative conceptual models) were used to determine whether additional new data are needed to better define ranges of input parameters.	The EBS PMR provides a discussion of alternative conceptual models for the EBS P&CE and Radionuclide Transport Models. The EBS radionuclide transport model (EBS PMR Section 3.1.3) provides an analysis of release based upon the thermal hydrological calculations in the WD&R model. The EBS radionuclide transport model (EBS PMR Section 3.1.3) is an advection/dispersion/diffusion model. The WD&R model considers the temporal variations in conditions affecting the TH effects, and provides a bounding calculation for chemical effects due fracture plugging that would alter saturation levels and porewater velocities. The EBS radionuclide transport (Section 3.1.3) model provides a sensitivity or uncertainty analysis for the chemical retardation that bounds temporal and spatial variations in the chemical retardation factor that reflects the chemical environment. For

Data and Model Justification for Subissue 3

Acceptance Criterion	PMR Approach and Section Reference
	the base case, the EBS radionuclide transport takes no credit for chemical retardation which is a bounding assumption for radionuclide transport. The EBS Colloids submodel is based upon relevant data for the size and concentration of colloids that account for variability through probability distributions. Based upon these data bounding values for radionuclide solubility, and colloid diffusion coefficient were calculated. EBS PMR Section 3.1.2
Criterion 7 If the testing program for coupled THC processes on the chemical environment for radionuclide release from the engineered barrier system is not complete at the time of license application, or if sensitivity and uncertainty analyses indicate additional data are needed, DOE has identified specific plans to acquire the necessary information as part of the performance confirmation program.	Performance confirmation is not addressed in this PMR. The acceptance criterion will be applied appropriately to the Performance Confirmation Program.

Data Uncertainty and Verification for Subissue 3

Acceptance Criterion	PMR Approach and Section Reference
Criterion 1 Reasonable or conservative ranges of parameters or functional relations were used to determine effects of coupled THC processes on the chemical environment for radionuclide release. Parameter values, assumed ranges, probability distributions, and bounding assumptions were technically defensible and reasonably accounted for uncertainties.	The EBS Radionuclide and Transport Model provides a bounding analysis based upon the thermal hydrology from the WD&R Model. The physical processes in the EBS radionuclide transport model include advection, dispersion and diffusion. The advection through the EBS, and in particular in the invert is based upon reasonable parameters for the NBS and EBS in the Water Distribution Model (Section 3.1.1). The EBS Radionuclide Transport Model (Section 3.1.1) provides reasonable estimates for dispersion and diffusion. The EBS Radionuclide Transport Model neglects chemical retardation for the base case analysis which is a conservative assumption. Further, it considers a reasonable range of parameters in defining the probability distribution functions for all parameters including chemical retardation in the sensitivity analysis. EBS PMR Section 3.1.1 through 3.1.3
Criterion 2 Uncertainty in data due to both temporal and spatial variations in conditions affecting coupled THC effects on the chemical environment for	The EBS Radionuclide Transport Model is based upon thermal hydrology that accounts for the temporal and spatial variations.

Data Uncertainty and Verification for Subissue 3	
Acceptance Criterion	**PMR Approach and Section Reference**
radionuclide release were considered.	Section 3.2.1 documents model uncertainties as they relate to the performance of the NBS and the EBS. These uncertainties in data due to temporal and spatial variations are addressed in the thermal hydrology submodel in which changes in the waste package heating are considered. Spatial variations are addressed by considering the L4C4 column in the center of the repository, and the L4C1 column at the edge of the repository. It should be noted that EBS process models provide the basis for selecting robust designs for EBS performance and waste isolation in the face of model uncertainty.

The EBS Radionuclide Transport Model (Section 3.1.1) provides reasonable estimates for dispersion and diffusion. It compares the relationships for diffusion coefficients using two differe3nt methods, and measured data. The EBS Radionuclide Transport Model neglects chemical retardation for the base case analysis which is a conservative assumption. Further, it considers a reasonable range of parameters in defining the probability distribution functions for all parameters including chemical retardation in the sensitivity analysis.

EBS PMR Section 3.1.2 |
| Criterion 3 DOE's evaluation of coupled THC processes properly considered the uncertainties in the characteristics of the natural system and engineered materials, such as the type, quantity, and reactivity of material, in establishing initial and boundary conditions for conceptual models and simulations of THC coupled processes that affect the chemical environment for radionuclide release. | Data on EBS processes are being collected at the current time for the Water Distribution and Removal Model (Section 3.1.1), and the Physical and Chemical Environment Model. Where appropriate, bounding calculations have been performed to estimate physical effects such as flow through drip shields (Section 3.1.1), and chemical effects such as the alteration of groundwater chemistry (Section 3.1.4).EBS PMR Sections 3.1.2 through 3.1.3 |
| Criterion 4 The initial conditions, boundary conditions, and computational domain used in sensitivity analyses involving coupled THC effects on the chemical environment for radionuclide release were consistent with available data. | The EBS Radionuclide Transport Model (Section 3.1.1) provides reasonable estimates for dispersion and diffusion. The EBS Radionuclide Transport Model neglects chemical retardation for the base case analysis which is a conservative assumption. Further, it considers a reasonable range of parameters that address initial conditions, boundary conditions and computational domain for all parameters including chemical retardation in the sensitivity analysis.

EBS PMR Sections 3.1.2 through 3.1.3 |
| Criterion 5 DOE's performance confirmation program will assess whether the natural system and engineered materials are functioning as intended and anticipated with regard to coupled THC effects on the chemical environment for radionuclide release from the EBS. | Performance confirmation is not addressed in this PMR. The acceptance criterion will be applied appropriately to the Performance Confirmation Program. |

ENFE Subissue 3: Effects of Coupled Thermal-Hydrologic-Chemical Processes on the Chemical Environment of Radionuclide Release

Integration for Subissue 3

Acceptance Criterion	PMR Approach and Section Reference
Criterion 1 DOE considered the relevant features, events, and processes. The abstracted models adequately incorporated important design features; physical phenomena and couplings; and used consistent and appropriate assumptions throughout.	Important features, events, and processes are identified in EBS PMR Section 2.4.1. The FEPs for the EBS are identified in Table 2-2. Specifically, the relevant FEPs that relate to chemical processes on the chemical environment of radionuclide Release are addressed in the microbial activity Energy /Nutrient Balance Microbial Model (Section 3.1.2) The Cementitious Materials Submodel addresses the alteration of infiltrate chemistry due to physical and chemical properties of the EBS as summarized in Sections 3.1.1 through 3.1.4. EBS PMR Sections 2.4.1 and 3.1.3
Criterion 2 Models reasonably accounted for known temporal and spatial variations in conditions affecting coupled THC effects on the chemical environment for radionuclide release.	The EBS Radionuclide Transport Model (EBS PMR Section 3.1.3) does not take credit for chemical retardation. The EBS radionuclide transport (Section 3.1.3) model provides a sensitivity analysis for the chemical retardation that bounds temporal and spatial variations in the chemical retardation factor that reflects the chemical environment. For the base case, the EBS radionuclide transport takes no credit for chemical retardation which is a bounding assumption for radionuclide transport. The EBS Colloids submodel is based upon relevant data for the size and concentration of colloids that account for variability through probability distributions. Based upon these data bounding values for radionuclide solubility, and colloid diffusion coefficient were calculated. EBS PMR Sections 3.1.2 through 3.1.3
Criterion 3 Not all THC couplings may be determined to be important to performance, and DOE may adopt assumptions to simplify PA analyses. If potentially important couplings are neglected, DOE should provide a technical basis for doing so. The technical basis can include activities, such as independent modeling, laboratory or field data, or sensitivity studies.	In each of the respective AMRs (Table 1-1), the assumptions supporting the AMR are documented. In those models where assumptions are made neglecting important couplings, the technical basis for each assumption is stated. In the EBS radionuclide transport model, the base case neglects chemical retardation as determined from the chemical environment. This is a conservative assumption since the effects of chemical retardation would increase the breakthrough time. EBS Section 3.1.3
Criterion 4 Where simplifications for modeling coupled THC effects on the chemical environment for radionuclide release were used for PA analyses instead of detailed process models, the bases used for modeling assumptions and approximations were	The EBS Radionuclide Transport Model provides a bounding calculation. As stated in the previous comment, it is conservative to neglect chemical retardation due to sorption in the invert. EBS PMR Sections 3.1.2 through 3.1.3

Integration for Subissue 3

Acceptance Criterion	PMR Approach and Section Reference
documented and justified.	

Model Uncertainty for Subissue 3

Acceptance Criterion	PMR Approach and Section Reference
Criterion 1 Appropriate models, tests, and analyses were used that are sensitive to the THC couplings under consideration for both natural and engineering systems as described in the following examples. The effects of THC coupled processes that may occur in the natural setting or due to interactions with engineered materials or their alteration products include: (i) TH effects on gas and water chemistry; (ii) hydrothermally driven geochemical reactions, such as zeolitization of volcanic glass; (iii) dehydration of hydrous phases liberating moisture; (iv) effects of microbial processes; and (v) changes in water chemistry that may result from interactions between cementitious, or WP, materials and groundwater, which, in turn, may affect the chemical environment for radionuclide release.	The EBS Radionuclide Transport Model provides a bounding calculation. For the base case, the effects of chemical retardation are neglected (Section 3.1.3) which is a conservative assumption. The effects of Ca, Si, and Mg precipitation that would result in possible reduction in porosity are investigated in Section 3.1.2.5, and are found to be negligible. It is unlikely that pore water velocities would be altered by a reduction in porosity. EBS PMR Sections 3.1.2 through 3.1.3
Criterion 2 Alternative modeling approaches consistent with available data and current scientific understanding were investigated, and their results and limitations were appropriately considered.	The EBS Radionuclide Transport Model considers alternative modeling approaches. Section 3.1.3 considers two alternative modeling approaches for radionuclide transport through the EBS. These include the potential for ponding of water which would result in the release of radionuclides through flow parallel to the drift and down a fault or fracture system. The second alternative involves steady state flow through the invert.
Criterion 3 DOE provided a reasonable description of the mathematical models included in its analyses of coupled THC effects on the chemical environment for radionuclide release. The description included a discussion of alternative modeling approaches not considered in its final analysis and the limitations and uncertainties of the chosen model.	In the Water Distribution and Removal AMR, the Physical and Chemical Environment Model and the EBS Radionuclide Transport AMR, the DOE provided descriptions of conceptual, and detailed models as required by AP-3.10Q that provide a reasonable description of modeling thermal-hydrologic phenomena for predicting seepage and flow in the EBS. EBS PMR Sections 3.1.1 through 3.1.3

Model Verification for Subissue 3	
Acceptance Criterion	**PMR Approach and Section Reference**
Criterion 1 The mathematical models for coupled THC effects on the chemical environment for radionuclide release were consistent with conceptual models based on inferences about the near-field environment, field data and natural alteration observed at the site, and expected engineered materials.	The Water Distribution and Removal Model, the P&CE Model, and the Multiscale Model provide predictions of seepage and flow that are based upon the active fracture model. The conceptual model for the prediction of advection or pore water velocities, and radionuclide transport due to advection/dispersion/diffusion through the EBS is consistent with conceptual models for the UZ.
Criterion 2 DOE appropriately adopted accepted and well-documented procedures to construct and test the numerical models used to simulate coupled THC effects on the chemical environment for radionuclide release.	The DOE used appropriate procedures to construct and test numerical models for predicting seepage and flow. The Radionuclide Transport Model was developed using a closed-form analytical solution for one-dimensional contaminant transport implemented in software routines. The Radionuclide Transport Model represents an industry standard approach for contaminant transport based upon the TH analysis in the Water Distribution and Removal Model (CRWMS M&O 2000q). The results of the model from the software routines based upon the closed form solution were compared to hand calculations for verification. The software codes used for the models are subject to verification and testing under the procedure AP-SI.1Q.
Criterion 3 Abstracted models for coupled THC effects on the chemical environment for radionuclide release were based on the same assumptions and approximations shown to be appropriate for closely analogous natural or experimental systems. Abstracted model results were verified through comparison to outputs of detailed process models and empirical observations. Abstracted model results were compared with different mathematical models to judge robustness of results.	The current abstracted model for the Radionuclide Nuclide Transport Abstraction is conceptual in nature. The model abstractions are based upon similar assumptions in that similar flow path components such as flow in and around the drip shield to the invert and major chemical interactions such as neglecting chemical retardation in the invert are identified in the process model abstraction (CRWMS M&O 2000a) In certain cases, the process model abstractions develop a probabilistic analysis approaches that are more appropriately handled in TSPA studies. Since the Radionuclide Transport Abstraction is conceptual (CRWMS M&O 2000a), no comparisons have been made between outputs, and the empirical observations such as are currently being made in the quarter scale tests. Since the Radionuclide Transport Abstraction is conceptual, abstracted model results have not been compared with different mathematical models to address the robustness of the results.

Subissue   *ENFE Subissue 3: Effects of Coupled Thermal-Hydrologic-Chemical Processes on the Chemical Environment of Radionuclide Release*

Programmatic for Subissue 3	
Acceptance Criterion	**PMR Approach and Section Reference**
Criterion 1 Data and models were collected, developed, and documented under acceptable quality assurance (QA) procedures.	Activities associated with development of this Process Model Report and its related Analysis/Model Reports were determined to be subject to the quality assurance program as described in the Quality Assurance Requirements and Description (DOE 1999) document. As such, collection of related data, development of analyses and models, and use and validation of software is subject to the requirements of procedures developed to implement quality assurance program requirements.
Criterion 2 Deficiency reports concerning data quality on issues related to coupled THC effects on radionuclide release were closed.	The EBS Radionuclide Transport Model is being prepared according to AP-3.10Q to address quality assurance deficiency issues. The EBS Radionuclide Transport PMRs is prepared according the procedure Analyses and Models, AP-3.10Q which was developed to address data deficiency and quality issues. At the current time, the data used for this model are obtained from controlled sources that are undergoing qualification, and will be closed after completion of data qualification activities. EBS PMR Section 3.1.3
Criterion 3 If used, expert elicitations were conducted and documented in accordance with the guidance in NUREG-1563 or other acceptable approaches.	No expert elicitation was conducted for this PMR.

Subissue   *ENFE Subissue 4: The Effects of Coupled Thermal-Hydrologic-Chemical Processes on the Radionuclide Transport Through Engineered and Natural Barriers*

Data and Model Justification for Subissue 4	
Acceptance Criterion	**PMR Approach and Section Reference**
Criterion 1 Available data relevant to both temporal and spatial variations in conditions affecting coupled THC effects on transport of radionuclides in the near field were considered.	The EBS Radionuclide Transport Model is based upon a two dimensional thermal hydrologic analysis that accounts for temporal waste heat loading, and variations in percolation rates. Further, it considers a reasonable range of parameters that address spatial variations in conditions for all parameters including chemical retardation in the sensitivity analysis. EBS PMR Sections 3.1.2 through 3.1.3
Criterion 2 DOE's evaluation of coupled THC processes properly considered site characteristics in establishing initial and boundary conditions for conceptual models and simulations of coupled processes that may affect radionuclide transport in the	The EBS Radionuclide Transport model is based upon a two dimensional thermal hydrologic analysis that considers initial temperature and pressure boundary conditions. The EBS Radionuclide Transport Model provides bounding analysis for a conservative range of parameters. The base case analysis neglects the effects of chemical retardation on radionuclide transport and therefore conservatively neglects chemical initial and boundary conditions.

Data and Model Justification for Subissue 4	
Acceptance Criterion	**PMR Approach and Section Reference**
near field.	EBS PMR Sections 3.1.2 through 3.1.3
Criterion 3 Sufficient data were collected on the characteristics of the natural system and engineered materials, such as the type, quantity, and reactivity of material, in establishing initial and boundary conditions for conceptual models and simulations of THC coupled processes that affect transport of radionuclides in the near field.	Data on EBS processes are being collected at the current time for the Water Distribution and Removal Model (Section 3.1.1), and the Physical and Chemical Environment Model. Where appropriate, bounding calculations have been performed to not take credit for chemical retardation in the invert (Section 3.1.3) . EBS PMR Sections 3.1.2 through 3.1.3
Criterion 4 A nutrient and energy inventory calculation was used to determine the potential for microbial activity that could adversely affect radionuclide transport through engineered and natural barriers.	The EBS P&CE Model provides a bounding analysis for a nutrient and energy inventory. EBS PMR Section 3.1.2
Criterion 5 Should microbial activity be sufficient to potentially cause adverse microbial effects on transport of radionuclides through engineered and natural barriers, then the time-history of temperature, humidity, and water saturation in engineered and natural materials should be used to constrain the probability for these effects.	See the discussion presented above. See EBS PMR Section 3.1.2.
Criterion 6 Sensitivity and uncertainty analyses (including consideration of alternative conceptual models) were used to determine if additional new data are needed to better define ranges of input parameters.	The EBS PMR provides a discussion of alternative conceptual models for the EBS Radionuclide Transport Model. In the EBS Radionuclide Transport model, assumptions have been used and documented. In the absence of data, sensitivity and uncertainty analyses have been performed to assess their impact and the need to collect additional data. EBS PMR Section 3.1.3
Criterion 7 If the testing program for the effects of coupled THC processes on radionuclide transport is not complete at the time of license application, or if sensitivity and uncertainty analyses indicate additional data are needed, DOE has identified specific plans to acquire the necessary information as	Performance confirmation is not addressed in this PMR. The acceptance criterion will be applied appropriately to the Performance Confirmation Program.

Data and Model Justification for Subissue 4	
Acceptance Criterion	**PMR Approach and Section Reference**
part of the performance confirmation program.	

Data Uncertainty and Verification for Subissue 4	
Acceptance Criterion	**PMR Approach and Section Reference**
Criterion 2 Uncertainty in data due to both temporal and spatial variations in conditions affecting coupled THC effects on radionuclide transport in the near field were considered.	The EBS radionuclide transport model (EBS PMR Section 3.1.3) provides an analysis of release based upon the thermal hydrological calculations in the WD&R model. The EBS radionuclide transport model (EBS PMR Section 3.1.3) is an advection/dispersion/diffusion model. The WD&R model considers the temporal variations in conditions affecting the TH effects, and provides a bounding calculation for chemical effects due to fracture plugging that would alter saturation levels and porewater velocities. The EBS radionuclide transport (Section 3.1.3) model provides a sensitivity analysis for the chemical retardation that bounds temporal and spatial variations in the chemical retardation factor that reflects the chemical environment. For the base case, the EBS radionuclide transport takes no credit for chemical retardation which is a bounding assumption for radionuclide transport. EBS PMR Sections 3.1.1 through 3.1.3
Criterion 1 Reasonable or conservative ranges of parameters or functional relations were used to determine effects of coupled THC processes on transport of radionuclides in the near field. Parameter values, assumed ranges, probability distributions, and bounding assumptions were technically defensible and reasonably accounted for uncertainties.	The EBS Radionuclide Transport Model (EBS PMR Section 3.1.3) provides a bounding analysis (EBS PMR Section 3.1.3) based upon the thermal hydrology from the WD&R Model (EBS PMR Sections 3.1.1 through 3.1.2). For the base case analysis, the conservative assumption to neglect chemical retardation effects is made. A sensitivity analysis is presented in Section 3.1.3 for the assumed range of parameters that is technically defensible, and that reasonably accounts for uncertainties.
Criterion 3 DOE's evaluation of coupled THC processes properly considered the uncertainties in the characteristics of the natural system and engineered materials, such as the type, quantity, and reactivity of material, in establishing initial and boundary conditions for conceptual models and simulations of THC coupled processes that affect transport of radionuclides in the near field.	The EBS Radionuclide Transport Model provides a bounding calculation. For the base case, the effects of chemical retardation are neglected (Section 3.1.3) which is a conservative assumption. The effects of Ca, Si, and Mg precipitation that would result in possible reduction in porosity are investigated in Section 3.1.2.5, and are found to be negligible. It is unlikely that pore water velocities would be altered by a reduction in porosity. EBS PMR Sections 3.1.1 through 3.1.3
Criterion 4 The initial conditions, boundary conditions, and computational domain used in	The WD&R TH Model used to provide pore water velocities and saturation levels in the Radionuclide Transport model is based upon initial conditions boundary conditions, and computational domains consistent

Data Uncertainty and Verification for Subissue 4

Acceptance Criterion	PMR Approach and Section Reference
sensitivity analyses involving coupled THC effects on radionuclide transport in the near field were consistent with available data.	with site characteristics. In general, the thermal hydrology models used in Sections 3.1.1 through 3.1.4 are based upon the selection of NBS hydrologic and thermal properties used in the UZ process model. The initial conditions, and boundary conditions for the models for specific locations use the same infiltration rates, and temperature and pressure boundary conditions consistent with the UZ process Model (Section 3.1.4) EBS PMR Sections 3.1.2 through 3.1.3
Criterion 5 DOE's performance confirmation program will assess whether the natural system and engineered materials are functioning as intended and anticipated with regard to coupled THC effects on transport of radionuclides in the near field.	Performance confirmation is not addressed in this PMR. The acceptance criterion will be applied appropriately to the Performance Confirmation Program.

Integration for Subissue 4

Acceptance Criterion	PMR Approach and Section Reference
Criterion 1 DOE considered all the relevant features, events, and processes. The abstracted models adequately incorporated important design features, physical phenomena, and couplings, and used consistent and appropriate assumptions throughout.	Important features events, and processes are identified in EBS PMR Section 2.4.1. The FEPs for the EBS are identified in Table 2-2. Specifically, the relevant FEPs include drainage inhibited by fracture plugging, drainage through drains, and the influence of drift environment. Note that the effect of drift environment on the transport of colloidal species was adequately incorporated in Section 3.1.2.6. EBS PMR Sections 2.4.1, 3.1.1 and 3.1.2
Criterion 2 Models reasonably accounted for known temporal and spatial variations in conditions affecting coupled THC effects on transport of radionuclides in the near field.	The EBS Radionuclide Transport Model (EBS PMR Section 3.1.3) is based upon the thermal hydrology from the WD&R Model. The EBS radionuclide transport model (EBS PMR Section 3.1.3) provides an analysis of release based upon the thermal hydrological calculations in the WD&R model. The EBS radionuclide transport model (EBS PMR Section 3.1.3) is an advection/dispersion/diffusion model. The WD&R model considers the temporal variations in conditions affecting the TH effects, and provides a bounding calculation for chemical effects due to fracture plugging that would alter saturation levels and porewater velocities. The EBS radionuclide transport (Section 3.1.3) model provides a sensitivity analysis for the chemical retardation that bounds temporal and spatial variations in the chemical retardation factor that reflects the chemical environment. For the base case, the EBS radionuclide transport takes no credit for chemical retardation which is a bounding assumption for radionuclide transport.

Integration for Subissue 4	
Acceptance Criterion	**PMR Approach and Section Reference**
	The EBS Colloids submodel is based upon relevant data for the size and concentration of colloids that account for variability through probability distributions. Based upon these data bounding values for radionuclide solubility, and colloid diffusion coefficient were calculated. EBS PMR Sections 3.1.1 through 3.1.3
Criterion 3 Not all THC couplings may be determined to be important to performance, and DOE may adopt assumptions to simplify performance assessment analyses. If potentially important couplings are neglected, DOE should provide a technical basis for doing so. The technical basis could include activities, such as independent modeling, laboratory or field data, or sensitivity studies.	The EBS Radionuclide Transport Model provides a bounding analysis. In each of the respective AMRs (Table 1-1), the assumptions supporting the AMR are documented. In those models where assumptions are made neglecting important couplings, the technical basis for each assumption is stated. In the EBS radionuclide transport model, the base case neglects chemical retardation as determined from the chemical environment. This is a conservative assumption since the effects of chemical retardation would increase the breakthrough time. EBS PMR Sections 3.1.2 through 3.1.3
Criterion 4 Where simplifications for modeling coupled THC effects on radionuclide transport in the near field were used for performance assessment analyses instead of detailed process models, the bases used for modeling assumptions and approximations were documented and justified.	The EBS Radionuclide Transport Model provides a bounding calculation. As stated in the previous comment, it is conservative to neglect chemical retardation due to sorption in the invert. EBS PMR Sections 3.1.2 through 3.1.3

Model Uncertainty for Subissue 4

Acceptance Criterion	PMR Approach and Section Reference.
Criterion 1 Appropriate models, tests, and analyses were used that are sensitive to the THC couplings under consideration for both natural and engineering systems as described in the following examples. The effects of THC coupled processes that may occur in the natural setting or due to interactions with engineered materials or their alteration products include: (i) TH effects on gas and water chemistry in the unsaturated zone and saturated zone; (ii) precipitation of calcite and opal on the footwall of fracture surfaces and the bottoms of lithophysal cavities, which indicates gravity-driven flow in open fractures, and isolation of transport pathways from sorption sites in the rock matrix; (iii) zeolitization of volcanic glass, that could affect transport pathways; (iv) precipitation and dissolution of oxides and hydroxides on fracture surfaces, illitization of smectite, and recrystallization of zeolites to analcime, which could affect sorption characteristics; (v) effects of microbial processes; (vi) effects of corrosion products of container materials and waste forms on transport of radionuclides in the near field; and (vii) changes in hydraulic and sorptive properties of the natural system resulting from interactions between cementitious materials and groundwater.	The EBS Radionuclide Transport Model provides a bounding analysis. As stated above the effects of chemical retardation in the EBS are not taken credit for in increasing breakthrough time in the invert. The EBS Colloids Submodel is based upon relevant data for the size, and concentration of colloids that account for variability through probability distributions. Based upon these data, bounding values for radionuclide solubility and colloid diffusion coefficients were calculated. EBS PMR Sections 3.1.2 through 3.1.3
Criterion 2 Alternative modeling approaches consistent with available data and current scientific understanding were investigated, and their results and limitations were appropriately considered.	The EBS PMR provides a discussion of alternative conceptual models for the EBS Radionuclide Transport Model (Section 3.1.3). The EBS Radionuclide Transport Model is consistent with available data regarding the properties of the invert. An alternative view regarding the effects of storage capacity was presented. It was found that this alternative view is not likely to be important because increased EBS flow rates will cause increased dilution. EBS PMR Section 3.1.3
Criterion 3 DOE provided a reasonable description of the mathematical models included in its analyses of coupled THC effects on radionculide transport in the	For the Radionuclide Transport Model, the DOE provides a reasonable description of the mathematical models. The thermal hydrological model based upon NUFT is described in Section 3.1.1. The basic contaminant transport equation is presented in Section 3.1.3. Alternative models were discussed in Section

Model Uncertainty for Subissue 4

Acceptance Criterion	PMR Approach and Section Reference
near field. The description included a discussion of alternative modeling approaches not considered in its final analysis and the limitations and uncertainties of the chosen model.	3.1.3 with regards to reduction in drainage capacity, and storage capacity in the invert. (EBS PMR Sections 3.1.1 through 3.1.3).

Model Verification for Subissue 4

Acceptance Criterion	PMR Approach and Section Reference
Criterion 1 The mathematical models for coupled THC effects on radionuclide transport in the near field were consistent with conceptual models based on inferences about the near-field environment, field data and natural alteration observed at the site, and expected engineered materials.	The Water Distribution Model which was used for the Radionuclide Transport Model provides predictions of seepage and flow that are based on the active fracture model. The conceptual model for the prediction of advection or pore water velocities and radionuclide transport due to advection/dispersion/diffusion through the EBS is consistent with conceptual models for the UZ.
Criterion 2 DOE appropriately adopted accepted and well-documented procedures to construct and test the numerical models used to simulate coupled THC effects on transport of radionuclides in the near field.	The EBS Radionuclide Transport Model is based upon a well documented and accepted procedure for evaluating contaminant transport as stated in the previous comment. The radionuclide transport model was prepared according to AP-3.10Q with discussion of quality assurance, computer software, model inputs, and model assumptions. For analyses involving the use of software routines, the routines were verified by separate hand calculations. EBS PMR Sections 3.1.3, and 3.2.2.3.
Criterion 3 Abstracted models for coupled THC effects on radionuclide transport were based on the same assumptions and approximations shown to be appropriate for closely analogous natural or experimental systems. Abstracted model results were verified through comparison to outputs of detailed process models and empirical observations. Abstracted model results were compared with different mathematical models to judge robustness of results.	The current abstracted model for the Radionuclide Nuclide Transport Abstraction is conceptual in nature. The model abstractions are based upon similar assumptions in that similar flow path components such as flow in and around the drip shield to the invert and major chemical interactions such as conservatively neglecting sorption in the process model abstraction (CRWMS M&O 2000a) In certain cases, the process model abstractions develop a probabilistic analysis approaches that are more appropriately handled in TSPA studies. Since the Radionuclide Transport Abstraction is conceptual (CRWMS M&O 2000a), no comparisons have been made between outputs, and the empirical observations such as are currently being made in the quarter scale tests. Since the Radionuclide Transport Abstraction is conceptual, abstracted model results have not been compared with different mathematical models to address the robustness of the results.

Model Verification for Subissue 4

Acceptance Criterion	PMR Approach and Section Reference
	EBS PMR Section 3.1.2,3.1.3, 3.2.3 and 3.3.

Programmatic for Subissue 4

Acceptance Criterion	PMR Approach and Section Reference
Criterion 1 Data and models were collected, developed, and documented under acceptable quality assurance (QA) procedures.	Activities associated with development of this Process Model Report and its related Analysis/Model Reports were determined to be subject to the quality assurance program as described in the Quality Assurance Requirements and Description (DOE 1999) document. As such, collection of related data, development of analyses and models, and use and validation of software is subject to the requirements of procedures developed to implement quality assurance program requirements.
Criterion 2 Deficiency reports concerning data quality on issues related to coupled THC effects on waste package chemical environment were closed.	The EBS P&CE Model, and the Radionuclide Transport Model are prepared according to AP-3.10Q to address quality assurance deficiency issues.
	The AP-3.10Q procedure addresses previous deficiencies in obtaining input data from controlled sources of information, and in the documentation of software. AP-3.15Q provides the process for managing inputs to each AMR. Existing deficiencies are in the process of being closed with the preparation of the P&CE AMR according to AP-3.10Q.
	EBS PMR Section 3.1.2
Criterion 3 If used, expert elicitations were conducted and documented in accordance with the guidance in NUREG-1563 or other acceptable approaches.	No expert elicitation was conducted for this PMR.

IRSR **Repository Design and Thermal-Mechanical Effects (Revision 2)**

Subissue RDTME Subissue 1: Implementation of an Effective Design Control Process within the Overall Quality Assurance Program

Acceptance Criterion	PMR Approach and Section Reference
1. The applicable regulatory requirements are identified.	Design considerations are not included in this PMR. The acceptance criterion will be applied appropriately in the design process.
2. The design bases associated with the regulatory requirements are defined.	Design considerations are not included in this PMR. The acceptance criterion will be applied appropriately in the design process.
3. The regulatory requirements of Acceptance Criterion 1 and the design bases of Acceptance Criterion 2 are appropriately translated into specifications, drawings, procedures, and instructions.	Design considerations are not included in this PMR. The acceptance criterion will be applied appropriately in the design process.
4. Appropriate quality standards are specified in the design documents.	Design considerations are not included in this PMR. The acceptance criterion will be applied appropriately in the design process.
5. Any deviations from the standards specified under Acceptance Criterion 4 are properly controlled, documented, and justified.	Design considerations are not included in this PMR. The acceptance criterion will be applied appropriately in the design process.
6. Measures are established for selection of materials, parts, equipment, and processes that are essential to functions of structures, systems, and components that are important to safety and waste containment and isolation.	Design considerations are not included in this PMR. The acceptance criterion will be applied appropriately in the design process.
7. Design interfaces are identified, controlled, and appropriately coordinated among participating design organizations.	Design considerations are not included in this PMR. The acceptance criterion will be applied appropriately in the design process.
8. Procedures are established for review, approval, release, distribution, and revision of documents involving design interfaces.	Design considerations are not included in this PMR. The acceptance criterion will be applied appropriately in the design process.
9. Measures are established for verifying or checking the accuracy of design calculations (e.g., performing design reviews using alternate or simplified calculational methods).	Design considerations are not included in this PMR. The acceptance criterion will be applied appropriately in the design process.

Subissue   *RDTME Subissue 1: Implementation of an Effective Design Control Process within the Overall Quality Assurance Program*

Acceptance Criterion	PMR Approach and Section Reference
10. If testing is employed for verification of design adequacy for its intended service life, the testing is conducted under the most adverse conditions.	Design considerations are not included in this PMR. The acceptance criterion will be applied appropriately in the design process.
11. The design verification is conducted by independent and qualified professionals who did not participate in the original design efforts.	Design considerations are not included in this PMR. The acceptance criterion will be applied appropriately in the design process.
12. In addition to being applied to the original design, the design control process is also applied to design changes and to field changes, and these changes are properly documented.	Design considerations are not included in this PMR. The acceptance criterion will be applied appropriately in the design process.

Subissue   *RDTME Subissue 2: Design of the Geologic Repository Operations Area for the Effects of Seismic Events and Direct Fault Disruption*

Methodology proposed in the TR is adequate if the following criteria are satisfied:

Acceptance Criterion	PMR Approach and Section Reference
4. Uncertainties associated with the proposed methodology that would significantly affect or impede the repository design process and development of inputs to performance assessments have been considered adequately.	Design considerations related to seismic issues are not included in this PMR. The acceptance criterion will be applied appropriately in the seismic design process.
6. To the extent that the proposed design methodology depends on site-specific test data, such data are available now, are being gathered now, or there are plans for gathering such data during site characterization and before submittal of the license application.	Design considerations related to seismic issues are not included in this PMR. The acceptance criterion will be applied appropriately in the seismic design process.
5. The various steps involved in the proposed methodology are transparent.	Design considerations related to seismic issues are not included in this PMR. The acceptance criterion will be applied appropriately in the seismic design process.
2. If available, documented case histories of the	Design considerations related to seismic issues are not included in this PMR. The acceptance criterion will be

RDTME Subissue 2: Design of the Geologic Repository Operations Area for the
Effects of Seismic Events and Direct Fault Disruption

Methodology proposed in the TR is adequate if the following criteria are satisfied:

Acceptance Criterion	PMR Approach and Section Reference
performance of structures, systems, and components important to safety designed using the proposed methodology are presented in the topical report. In the absence of documented case histories, no serious problems have been identified that would impede applying the methodology.	applied appropriately in the seismic design process.
1. Sufficient technical reasoning is provided for the proposed methodology.	Design considerations related to seismic issues are not included in this PMR. The acceptance criterion will be applied appropriately in the seismic design process.
3. The proposed methodology does not contradict established methodologies and principles tested and documented in the license applications for nuclear power plants and independent spent fuel storage installations.	Design considerations related to seismic issues are not included in this PMR. The acceptance criterion will be applied appropriately in the seismic design process.
8. Any major assumptions or limitations to the proposed methodology are identified, and the implications regarding design and performance are discussed in the topical report.	Design considerations related to seismic issues are not included in this PMR. The acceptance criterion will be applied appropriately in the seismic design process.
7. To the extent that the proposed methodology depends on analytical/computer models, such models have been verified, calibrated, and validated to the extent practical, or there are plans for such activities prior to license application submittal or during the performance confirmation period, as appropriate.	Design considerations related to seismic issues are not included in this PMR. The acceptance criterion will be applied appropriately in the seismic design process. Performance confirmation is not addressed in this PMR. The acceptance criterion will be applied appropriately to the Performance Confirmation Program.
9. The contents of TR-2 are consistent with the contents of TR-1 and, taken together, the two topicals reports support the development of inputs for design and performance assessments, as described in TR-3.	Design considerations related to seismic issues are not included in this PMR. The acceptance criterion will be applied appropriately in the seismic design process.

Subissue **RDTME Subissue 2: Design of the Geologic Repository Operations Area for the Effects of Seismic Events and Direct Fault Disruption**

TR adequacy depends on initial acceptance review of TR-2 meeting these criteria:

Acceptance Criterion	PMR Approach and Section Reference
2. The subject of the topical report is currently undergoing pre-licensing evaluation.	Design considerations related to seismic issues are not included in this PMR. The acceptance criterion will be applied appropriately in the seismic design process.
1. The topical report addresses all important-to-safety (or important-to-waste-isolation) topics pertaining to the scope of the topical report.	Design considerations related to seismic issues are not included in this PMR. The acceptance criterion will be applied appropriately in the seismic design process.
3. NRC's acceptance of the topical report would result in increased efficiencies in the staff review of DOE's license application.	Design considerations related to seismic issues are not included in this PMR. The acceptance criterion will be applied appropriately in the seismic design process.
4. The topical report contains complete and detailed information on each element of the scope of the report.	Design considerations related to seismic issues are not included in this PMR. The acceptance criterion will be applied appropriately in the seismic design process.

Subissue **RDTME Subissue 3: Thermal-Mechanical Effects on Underground Facility Design and Performance**

Component 1 - Thermal-Mechanical Effects on Design of Underground Facility

Acceptance Criterion	PMR Approach and Section Reference
1. Approved QA control procedures and standards were applied to collection and documentation of data, methods, models, and codes.	Activities associated with development of this Process Model Report and its related Analysis/Model Reports were determined to be subject to the quality assurance program as described in the Quality Assurance Requirements and Description (DOE 1999) document. As such, collection of related data, development of analyses and models, and use and validation of software is subject to the requirements of procedures developed to implement quality assurance program requirements.
2. If used, expert elicitations are conducted and documented in accordance with the guidance in NUREG-1563 or other acceptable guidelines.	No expert elicitation was conducted for this PMR.
3. TM analyses of the repository design are based on site-specific thermal and mechanical properties, the spatial variation of such properties, and temporal variations caused by post-emplacement TMHC processes, as appropriate, including the consideration of seismic effects relevant to the YM site within the	Design considerations are not included in this PMR. The acceptance criterion will be applied appropriately in the design process.

Component 1 - Thermal-Mechanical Effects on Design of Underground Facility	
Acceptance Criterion	**PMR Approach and Section Reference**

rock mass.

4. The process to develop inputs to TM design includes consideration of associated uncertainties and documents the potential impacts on design.	Design considerations are not included in this PMR. The acceptance criterion will be applied appropriately in the design process.
5. The seismic and fault-displacement data inputs for design are consistent with those established in seismic design TR-3.	Design considerations related to seismic issues are not included in this PMR. The acceptance criterion will be applied appropriately in the seismic design process.
6. The methodologies used for the TM design and analyses are consistent with that established in DOE Seismic TR-2.	Design considerations related to seismic issues are not included in this PMR. The acceptance criterion will be applied appropriately in the seismic design process.
7. The TM design and analyses make use of appropriate constitutive models that represent jointed rock mass behavior under prolonged heated conditions. The models are tested as appropriate (verified, validated, and calibrated) before the submittal of the LA. (For those aspects of the models for which long-term experimental data are needed, continued verification and validation during performance confirmation are considered acceptable as long as detailed plans and procedures for such continued activities are found in the LA.)	Design considerations are not included in this PMR. The acceptance criterion will be applied appropriately in the design process. Performance confirmation is not addressed in this PMR. The acceptance criterion will be applied appropriately to the Performance Confirmation Program.
8. Both drift- and repository-scale models of the underground facility are used in TM analyses to establish the intensity and distribution of ground movement (rock deformations, collapse, and other changes that may affect the integrity or geometrical configuration of openings within the underground facility). The number and variety of models permit the examination of conditions along drift-parallel and drift-normal directions.	The drift degradation analysis is based upon a drift scale model that considers changes in rock mass properties throughout the repository. The drift degradation analysis presented in Section 3.1.2.8 analyzes data at the drift scale based upon data from the ESF main loop and the ECRB cross drift. Maximum block sizes within the several units of the repository horizon are analyzed. The distribution of block sizes due to variations in strength, deformational and geometrical properties of the rock matrix and the fractures in underground conditions is analyzed. The DRKBA is a three dimensional analysis that takes into account the orientation of the joints relative to the drift orientation. EBS PMR Section 3.1.2.8
9. The principles formulating the TM analytical methodology, underlying assumptions, resulting	Design considerations are not included in this PMR. The acceptance criterion will be applied appropriately in the design process.

Component 1 - Thermal-Mechanical Effects on Design of Underground Facility

Acceptance Criterion	PMR Approach and Section Reference
limitations, and various steps involved in the design procedures are clearly explained and justified.	
10. Time sequences of thermal loading used in TM design and analyses are clearly defined.	Design considerations are not included in this PMR. The acceptance criterion will be applied appropriately in the design process.
11. The TM design and analyses consider the presence of roof supports (bolts, shotcrete, concrete, and steel liners, as applicable), consider the interaction between rock and supports, and address the degradation of supports with time under high temperature moisture conditions as they affect the maintainability of stable openings during the extended preclosure period.	Design considerations are not included in this PMR. The acceptance criterion will be applied appropriately in the design process.
12. Results of the TM analyses, including the consideration of ground support (e.g., liners), are accounted in the determination of maintenance requirements for the underground facility.	Design considerations are not included in this PMR. The acceptance criterion will be applied appropriately in the design process.
13. The design discusses maintenance plans for keeping the underground openings stable, with particular attention to maintaining the option for retrieval. (If the details of retrieval operations/plans are found in other sections of the LA, a reference to such sections would be acceptable.)	Design considerations are not included in this PMR. The acceptance criterion will be applied appropriately in the design process.

Component 2 - Effects of Seismically Induced Rockfall on Waste Package Performance

Acceptance Criterion	PMR Approach and Section Reference
1. Approved QA and control procedures and standards were applied to collection, development and documentation of data, methods, models, and codes.	Activities associated with development of this Process Model Report and its related Analysis/Model Reports were determined to be subject to the quality assurance program as described in the Quality Assurance Requirements and Description (DOE 1999) document. As such, collection of related data, development of analyses and models, and use and validation of software is subject to the requirements of procedures developed to implement quality assurance program requirements.
2. It used, expert elicitation is conducted and documented in accordance with the guidance in NUREG-1563 or other acceptable approaches.	No expert elicitation was conducted for this PMR.

RDTME Subissue 3: Thermal-Mechanical Effects on Underground Facility Design and Performance

Component 2 - Effects of Seismically Induced Rockfall on Waste Package Performance	
Acceptance Criterion	**PMR Approach and Section Reference**
3. The seismic hazard inputs used to estimate rockfall potential are consistent with the inputs used in the design and PAs as established in DOE's TR-3 reviewed and accepted by NRC.	The drift degradation analysis is based upon design basis seismic ground motion. The seismic hazard inputs used to estimate rockfall potential are consistent with the inputs used in the design and PAs as established in DOE's TR-3 reviewed and accepted by NRC. Both Frequency-Category-1 and Frequency-Category-2 design basis ground motion as defined in DOE's TR-3 have been considered in the Drift Degradation AMR to estimate rockfall potential. The peak ground accelerations associated with each Frequency-Category were provided by NEPO and used as inputs in the Drift Degradation AMR. EBS PMR 3.1.2.8
4. Size distribution of rocks that may potentially fall on the WPs is estimated from site-specific data (e.g., distribution of joint patterns, spacing, and orientation in three dimensions) with adequate consideration of associated uncertainties.	The drift degradation analysis is based upon a probabilistic key block analysis. The key block analysis presented in Section 3.1.2.8 is based upon the collection of data for joint patterns, spacing, and orientation from underground detailed line surveys conducted in the ESF main loop and the ECRB cross drift. The joint data is analyzed statistically to account for uncertainties in joint properties. EBS PMR Section 3.1.2.8
6. The TM analyses that provide the background conditions on which seismic loads are superimposed consider time-dependent jointed rock behavior.	The drift degradation analysis considers the change in rock mass properties due to thermal loading. As discussed in Section 3.1.2.8, the analysis accounts for time-dependent and thermal effects with joint cohesion degradation as discussed in CRWMS M&O 1999d. EBS PMR Section 3.1.2.8
7. Rockfall analyses consider, in a rational and realistic way through dynamic analyses, the possibility of multiple blocks failing onto a WP simultaneously, and the extent of the potential rockfall area around an individual emplacement drift as well as over the entire repository as functions of ground motions.	The drift degradation analysis is a probabilistic model that considers the probability of multiple blocks falling. Rockfall analyses consider, in a rational and realistic way through dynamic analyses, the possibility of multiple blocks failing onto a WP simultaneously, and the extent of the potential rockfall area around an individual emplacement drift as well as over the entire repository as functions of. ground motions. EBS PMR Section 3.1.2.8

Component 3 - Thermal-Mechanical Effects on Flow into Emplacement Drifts	
Acceptance Criterion	**PMR Approach and Section Reference**
1. Approved QA, control procedures, and standards were applied to collection, development and documentation of data, methods, models, and codes.	Activities associated with development of this Process Model Report and its related Analysis/Model Reports were determined to be subject to the quality assurance program as described in the Quality Assurance Requirements and Description (DOE 1999) document. As such, collection of related data, development of analyses and models, and use and validation of software is subject to the requirements of procedures developed to implement quality assurance program requirements.
2. If used, expert elicitation is conducted and documented in accordance with the guidance in NUREG-1563 or other acceptable approaches.	No expert elicitation was conducted for this PMR.
3. Time-dependent changes in size and shape of the emplacement drifts due to thermally induced ground movements (rock deformations, collapse, and other changes that may affect the integrity and geometrical configuration of underground openings) are estimated taking into account the uncertainties in the context of their impacts an performance.	The drift degradation analysis estimate the changes in size and shape of emplacement drifts. Time-dependent changes in size and shape of the emplacement drifts due to thermally induced ground movements are estimated in the Drift Degradation AMR. The full range of joint geometry variability based on tunnel mapping data has been used in the Drift Degradation AMR to account for uncertainty in rock mass behavior. Furthermore, a conservative approach to estimate the time-dependent effects on opening size and shape has been used in the Drift Degradation AMR to account for uncertainty. EBS PMR Section 3.1.2.8.

IRSR

Thermal Effects on Flow (Revision 2)

Subissue
TEF Subissue 1: Is The U.S Department Of Energy Thermohydrologic Testing Program, Including Performance Confirmation Testing, Sufficient To Evaluate The Potential For Thermal Reflux To Occur In The Near Field?

Programmatic Acceptance Criterion

Acceptance Criterion	PMR Approach and Section Reference
1. DOE's thermohydrologic testing program was developed under acceptable quality assurance procedures (QAP). Data were collected and documented under purview of these procedures.	Activities associated with development of this Process Model Report and its related Analysis/Model Reports were determined to be subject to the quality assurance program as described in the Quality Assurance Requirements and Description (DOE 1999) document. As such, collection of related data, development of analyses and models, and use and validation of software is subject to the requirements of procedures developed to implement quality assurance program requirements.
2. Expert elicitation may be used for, but not necessarily limited to, assessing if conceptual models bound the range of thermally driven refluxing expected at YM, in addition to thermohydrologic testing to provide conservative bounds to estimates. All expert elicitation are conducted and documented in accordance with NUREG - 1563 or other acceptable approaches.	No expert elicitation was conducted for this PMR.

Technical Acceptance Criteria

Acceptance Criterion	PMR Approach and Section Reference
1.1 Thermohydrologic tests are designed and conducted with the explicit objective of testing conceptual and numerical models so that critical thermohydrologic processes can be observed and measured.	Tests are being conducted at quarter scale to simulate thermal and hydrological effects within the drift. The tests record temperature, relative humidity, and saturation levels within the EBS components that can be directly compared with results from the Water Distribution and Removal Model or other TH models.
1.4 Thermohydrologic tests are designed and conducted for temperature ranges expected for repository operating conditions.	The tests being conducted simulate waste package heating with a waste package heater, and repository heating through peripheral heaters. These heaters develop a temperature environment within the EBS that is identical to the EBS repository environment.
1.3 Thermohydrologic tests are designed and conducted at different scales to discern scale effects on observed phenomena.	The quarter scale test simulate repository conditions at an increased scale relative to bench scale experiments to discern scale effects on observed effects.
1.2 Thermohydrologic tests are designed and	The quarter-scale tests are being conducted with J-13 groundwater. The tests simulate the interaction of the J-

Subissue

TEF Subissue 1: Is The U.S Department Of Energy Thermohydrologic Testing Program, Including Performance Confirmation Testing, Sufficient To Evaluate The Potential For Thermal Reflux To Occur In The Near Field?

Technical Acceptance Criteria

Acceptance Criterion	PMR Approach and Section Reference
conducted with explicit consideration of TH, thermal-chemical, and hydrologic-chemical couplings.	13 groundwater with EBS components that would result in the formation of precipitates and salts due to evaporation of water, and the resulting concentration of solutes.
1.8 Thermohydrologic tests are designed and conducted such that the thermal test environment is sufficiently characterized so that uncertainty in property values does not result in unacceptable uncertainty in thermal test results interpretation	The Quarter Scale Tests provide information on temperature, relative humidity and saturation levels at representative sampling locations to account for uncertainty in property values.
1.7 Thermohydrologic tests are designed and conducted to account for all mass and energy losses/gains in the thermal test system.	The Quarter Scale Tests measure the amount of water injected into the test cell, the amount of water stored in EBS components, and the amount of water ejected by weighing of the test cell.
1.6 Thermohydrologic tests are designed and conducted to evaluate the possibility for occurrence of cyclic wetting/drying on WP surfaces.	The quarter scale tests simulate repository conditions by setting central heater and peripheral heater power that results in the drying effects due to temperature increase, and wetting effects due to temperature decrease within EBS components.
1.5 Thermohydrologic tests are designed and conducted to determine if water refluxes back to the heaters during the heating or cool-down phases of the tests.	The quarter scale tests simulate the thermal-hydrologic environment during the cooldown phase, and at high percolation rates that bounds water seepage due to refluxing.
3. If the thermohydrologic testing program is not complete at the time of LA submittal, DOE has explained why the testing program does not need to be completed for the LA and identified specific plans for completion of the testing program as part of the performance confirmation program.	See M&O Status response presented above. The EBS PMR provides bounding calculations in the absence of complete data, and model uncertainties. For example, for the base case analysis for radionuclide transport, the calculations do not consider chemical retardation which is a conservative assumption. EBS PMR Section 3.1.3 Performance confirmation is not addressed in this PMR. The acceptance criterion will be applied appropriately to the Performance Confirmation Program.
1.9 Thermohydrologic tests are designed and conducted such that the accuracy in the measurement of the test environment saturation is sufficient to discern the relative ability of different conceptual models to represent TH processes in heated partially	Heat Dissipation Probes are used to assess saturation levels in the EBS backfill and invert components. The probes have sufficient resolution to discern changes in saturation levels, and to provide a comparison to the predictions of TH models.

Subissue

TEF Subissue 1: Is The U.S Department Of Energy Thermohydrologic Testing Program, Including Performance Confirmation Testing, Sufficient To Evaluate The Potential For Thermal Reflux To Occur In The Near Field?

Technical Acceptance Criteria	
Acceptance Criterion	**PMR Approach and Section Reference**
saturated fractured porous media.	

Subissue

TEF Subissue 2: Is the U.S. Department of Energy Thermohydrologic Modeling Approach Sufficient to Predict the Nature and Bounds of Thermal Effects on Flow in the Near Field?

Programmatic Acceptance Criterion	
Acceptance Criterion	**PMR Approach and Section Reference**
1. DOE's thermohydrologic modeling analyses were developed and documented under acceptable quality assurance procedures (QAP).	Activities associated with development of this Process Model Report and its related Analysis/Model Reports were determined to be subject to the quality assurance program as described in the Quality Assurance Requirements and Description (DOE 1999) document. As such, collection of related data, development of analyses and models, and use and validation of software is subject to the requirements of procedures developed to implement quality assurance program requirements.
2. Expert elicitation may be used for, but not necessarily limited to, selecting a conceptual model and its parameters.. All expert elicitation are conducted and documented in accordance with NUREG - 1563 or other acceptable approaches.	No expert elicitation was conducted for this PMR.

| Subissue | TEF Subissue 2: Is the U.S. Department of Energy Thermohydrologic Modeling Approach Sufficient to Predict the Nature and Bounds of Thermal Effects on Flow in the Near Field? |

Technical Acceptance Criterion

Acceptance Criterion	PMR Approach and Section Reference
1.1 Sufficient data are available to adequately define relevant parameters, parameter values, and conceptual models. Specifically, DOE should demonstrate that uncertainties and variabilities in parameter values are accounted for using defensible methods. The technical bases for parameter ranges, probability distributions or bounding values used are provided. Parameter values (single values, ranges, probability distributions, or bounding values) are derived from site-specific data or an analysis is included to show the assumed parameter values lead to a conservative effect on performance.	Data on EBS processes are being collected at the current time for the Water Distribution and Removal Model (Section 3.1.1), and the Physical and Chemical Environment Model. Where appropriate, bounding calculations have been performed to estimate physical effects such as flow through drip shields (Section 3.1.1), and chemical effects such as the alteration of groundwater chemistry (Section 3.1.4). The technical bases for the parameter ranges for the process models are presented in the PMR. EBS PMR Sections 3.1.1 through 3.1.4
1.2 Sufficient data are available to adequately define relevant parameters, parameter values, and conceptual models. Specifically, DOE should demonstrate that analyses are consistent with site characteristics in establishing initial conditions, boundary conditions, and computational domains for conceptual models evaluated.	Data on EBS processes are being collected at the current time for the Water Distribution and Removal Model (Section 3.1.1), and the Physical and Chemical Environment Model. Where appropriate, bounding calculations have been performed to estimate physical effects such as flow through drip shields (Section 3.1.1), and chemical effects such as the alteration of groundwater chemistry (Section 3.1.4). The EBS Process models are consistent with the site characteristics for the models developed. EBS PMR Sections 3.1.1 through 3.1.4.
2.1 Models are based on well-accepted principles of heat and mass transfer applicable to unsaturated geologic media.	The EBS Process Models are based upon well accepted principles for heat and mass transfer. The NUFT and TOUGH2 codes are used by DOE to simulate heat and mass transfer through partially saturated, fractured porous media. These codes are based on well-accepted principles of heat and mass transfer applicable to unsaturated geologic media. EBS PMR Sections 3.1.1 through 3.1.4.
2.2 Models include, at a minimum, the processes of evaporation and condensation and the effects of discrete geologic features	The EBS Process Models are based upon NUFT calculations incorporating phase changes for the fracture model. Currently, they do not simulate evaporation and condensation for an open void space. Data on open void space EBS processes being collected at the current time for the Water Distribution and Removal Model (Section 3.1.1), and the Physical and Chemical Environment Model. Where appropriate, bounding calculations have been performed for seepage flow to the drift. EBS PMR Sections 3.1.1 and 3.1.2

TEF Subissue 2: Is the U.S. Department of Energy Thermohydrologic Modeling Approach Sufficient to Predict the Nature and Bounds of Thermal Effects on Flow in the Near Field?

Technical Acceptance Criterion

Acceptance Criterion	PMR Approach and Section Reference
2.3 Models include, at a minimum, an evaluation of important thermohydrological phenomena, such as: (i) multidrift dry-out zone coalescence, (ii) lateral movement of condensate, (iii) cold-trap effect, (iv) repository edge effects, and (v) condensate drainage through fractures.	The EBS Multiscale Thermal Hydrologic Model provides analysis of repository of thermohydrological phenomena at various locations within the repository. The degree of multi-drift dry-out zone coalescence will be a function of the thermal load specified in the final design of the repository. Recent, proposed design modifications by DOE to reduce the repository thermal load to 60 MTU/acre will minimize, if not eliminate, dry-out zone coalescence. Recent DOE models that include the active fracture model appear to adequately predict the extent of dryout surrounding the emplacement drifts.

EBS PMR Sections 3.1.1, 3.1.2, and 3.1.4 |
| 2.4 Models include all significant repository design features. | The models are based upon the current significant EDA-II repository design features as stated in the PMR.

All EBS-PMR sections apply. |
| 2.5 Models are capable of accommodating variation in infiltration. | The models have analyzed thermal-hydrological phenomena for the present day, monsoon, and glacial climates.

See EBS PMR Sections 3.1.1 through 3.1. |
| 2.6 Conceptual model uncertainties have been defined and documented and effects on conclusions regarding performance assessed. | Each of the supporting EBS Process Models address specific issues of model uncertainty. For uncertain conditions, bounding assumptions are used throughout where appropriate.

See EBS PMR Sections 3.1.1 through 3.1. |
| 2.7 Mathematical models are consistent with conceptual models, based on consideration of site characteristics. | In each EBS process model, the mathematical models are consistent with conceptual models. Note the AP-3.10Q process requires that detailed process models are consistent with conceptual models.

The EBS process models for thermal hydrological effects are based upon initial conditions boundary conditions, and computational domains consistent with site characteristics. The thermal hydrology models used in Sections 3.1.1 through 3.1.4 are based upon the selection of NBS hydrologic and thermal properties used in the UZ process model. The initial conditions, and boundary conditions for the models for specific locations use the same infiltration rates, and temperature and pressure boundary conditions consistent with the UZ process Model (Section 3.1.4)

EBS PMR Sections 3.1.1 through 3.1.4 |
| 2.8 Alternative models and modeling approaches, which are consistent with available data and current | Section 3.1.2 addresses alternative models involving fully coupled THC. Such simulation methods can be applied as they become available, and as the required data, including numerical settings used to operate the |

TEF Subissue 2: Is the U.S. Department of Energy Thermohydrologic Modeling Approach Sufficient to Predict the Nature and Bounds of Thermal Effects on Flow in the Near Field?

Technical Acceptance Criterion

Acceptance Criterion	PMR Approach and Section Reference
scientific understanding, have been investigated, limitations defined, and results appropriately considered.	simulation codes are qualified. The approach used in this PMR is applied to address conceptual issues and to evaluate bounding conditions for the performance of engineered barriers.
2.9 Results from different mathematical models have been compared to judge robustness of models.	Different mathematical models are used for comparison between closed form and numerical solutions. The DOE used appropriate procedures to construct and test numerical models for predicting seepage and flow. For the case of the Water Distribution and Removal Model, the results of the NUFT calculations were compared to a closed form analytical solution for the prediction of fluxes in and near the EBS (CRWMS M&O 2000q). The software codes used for the models are subject to verification and testing under the procedure AP-SI.1Q. EBS PMR Sections 3.1 See also CRWMS 2000b, CRWMS 2000i CRWMS 2000q and CRWMS 2000t.
2.10 Models used to predict shedding around emplacement drifts are shown to contain an adequate level of heterogeneity in media properties.	The EBS Multiscale TH Model considers 31 chimney locations within the repository that captures an adequate level of heterogeneity in percolation rates at the repository horizon. EBS Section 3.1.4
2.11 TH models have been demonstrated to be appropriate for the temperature regime expected at the repository.	The thermal hydrological calculations are appropriate for the expected regime. The current EDA-II design is based upon an 80 m emplacment drift spacing with waste canisters placed together to develop a line thermal loading. The repository is a subboiling repository. The models are based upon the NUFT thermal hydrological code that is appropriate for this temperature regime. EBS PMR Sections 3.1.1 through 3.1.4
2.12 Models include radiative heat transport unless it is shown that radiative heat loss by a WP is not significant.	The EBS multiscale thermal hydrological model includes radiative heat transfer. For thermal effects within the drift, the NUFT calculations consider radiative heat transport. The RADPRO software routine calculates view factors using a standard approach in heat transfer analysis. EBS PMR Section 3.1.4
2.13 Models include the effect of ventilation particularly if ventilation could result in deposition or	Ventilation effects are included in the EBS multiscale thermal hydrological model. Data on EBS processes for evaporation and condensation are being collected at the current time for the Water Distribution and Removal

TEF Subissue 2: Is the U.S. Department of Energy Thermohydrologic Modeling Approach Sufficient to Predict the Nature and Bounds of Thermal Effects on Flow in the Near Field?

Technical Acceptance Criterion	
Acceptance Criterion	**PMR Approach and Section Reference**
condensation of moisture on a WP surface.	Model (Section 3.1.1), and the Physical and Chemical Environment Model. Where appropriate, bounding calculations have been performed to estimate physical effects such as the formation of condensation. EBS PMR Section 3.1.4
3. Coupling of processes has been evaluated using a methodology in accordance with NUREG-1466 or other acceptable methodology. Coupled processes may be uncoupled, if it is shown that the uncoupled model results bound the predictions of the fully-coupled model results.	The EBS Process models provide bounding calculations in the absence of data or uncertainty in data. Section 3.1.2 addresses alternative models. Such simulation methods can be applied as they become available, and as the required data, including numerical settings used to operate the simulation codes are qualified. The approach used in this PMR is applied to address conceptual issues and to evaluate bounding conditions for the performance of engineered barriers. See EBS PMR Sections 3.1.1 through 3.1.4
4. The dimensionality of models, which include heterogeneity at appropriate scales and significant process couplings, may be reduced, if shown that the reduced dimension model bounds the predictions of the full dimension model.	The EBS multiscale thermal hydrologic model considers the appropriate dimensions for specific problems. The potential repository-scale heterogeneity is represented by the drift scale active properties set which captures the properties for various strata. Lateral variability within the potential repository footprint is represented by the 31 drift-scale-model locations used in the MSTH model. These locations are regularly distributed over the potential repository footprint. This reduces the general three dimensional problem to a series of two dimensional problems. EBS PMR Section 3.1.4
5. Equivalent continuum models are acceptable for the rock matrix and small discrete features, if it can be demonstrated that water in small discrete features is in continuous hydraulic equilibrium with matrix water. Significant discrete features, such as fault zones, should be represented separately unless it can be shown that inclusion in the equivalent continuum model (ECM) produces a conservative effect on calculated overall performance.	Equivalent continuum models are used as appropriate where conservative bounding assumptions are made. In the Water Distribution and Removal Model, an active fracture concept for a dual continuum model is used for the NBS with properties selected from inverse modeling. This modeling approach simulates matrix-fracture interaction. For evaluating the condensation below the drip shield, the ECM approach was used, and is considered a bounding calculation since the treatment of the fractured rock as an equivalent continuum tends to retain water within the EBS. EBS PMR Section 3.1.1
6. Accepted and well-documented procedures have been adopted to construct and calibrate numerical models used.	Inverse modeling is used to calibrate properties for the natural barrier system in the EBS Process Models. See EBS PMR Section 3.1.3

Subissue	TEF Subissue 2: Is the U.S. Department of Energy Thermohydrologic Modeling Approach Sufficient to Predict the Nature and Bounds of Thermal Effects on Flow in the Near Field?

Technical Acceptance Criterion

Acceptance Criterion	PMR Approach and Section Reference
7. Results of process-level models have been verified by demonstrating consistency with results/observations from field-scale, thermohydrologic tests. In particular, sufficient physical evidence should exist to support the conceptual models used to predict thermally driven flow in the near field.	Comparison of the EBS Process Models to field scale tests is in progress.

Subissue	TEF Subissue 3: Does The U.S. Department Of Energy Total System Performance Assessment Adequately Account For Thermal Effects On Flow?

Programmatic Acceptance Criterion

Acceptance Criterion	PMR Approach and Section Reference
1. DOE's analyses were developed and documented under acceptable quality assurance procedures (QAP).	Activities associated with development of this Process Model Report and its related Analysis/Model Reports were determined to be subject to the quality assurance program as described in the Quality Assurance Requirements and Description (DOE 1999) document. As such, collection of related data, development of analyses and models, and use and validation of software is subject to the requirements of procedures developed to implement quality assurance program requirements.
2. Expert elicitation may be used for, but not necessarily limited to, justifying the use of abstracted models in DOE's TSPA. All expert elicitation are conducted and documented in accordance with NUREG - 1563 or other acceptable approaches.	No expert elicitation was conducted for this PMR.

Subissue **TEF Subissue 3: Does The U.S. Department Of Energy Total System Performance Assessment Adequately Account For Thermal Effects On Flow?**

Technical Acceptance Criterion

Acceptance Criterion	PMR Approach and Section Reference
2.1 Sufficient data are available to adequately define relevant parameters, parameter values and conceptual models. Specifically, DOE should demonstrate that uncertainties and variabilities in parameter values are accounted for using defensible methods. The technical bases for parameter ranges, probability distributions or bounding values used are provided. Parameter values (single values, -ranges, probability distributions, or bounding values) are derived from site-specific data or an analysis is included to show the assumed parameter values lead to a conservative effect on performance.	The technical bases for the parameter ranges for process models are stated throughout. Data on EBS processes are being collected at the current time for the Water Distribution and Removal Model (Section 3.1.1), and the Physical and Chemical Environment Model. Where appropriate, bounding calculations have been performed to estimate physical effects such as flow through drip shields (Section 3.1.1), and chemical effects such as the alteration of groundwater chemistry (Section 3.1.4).

EBS PMR Section 3.1 |
| 2.2 Analyses are consistent with site characteristics in establishing initial conditions, boundary conditions, and computational domains for conceptual models evaluated. | The EBS process models for thermal hydrological effects are based upon initial conditions boundary conditions, and computational domains consistent with site characteristics. The thermal hydrology models used in Sections 3.1.1 through 3.1.4 are based upon the selection of NBS hydrologic and thermal properties used in the UZ process model. The initial conditions, and boundary conditions for the models for specific locations use the same infiltration rates, and temperature and pressure boundary conditions consistent with the UZ process Model (Section 3.1.4)

EBS PMR Sections 3.1.1 through 3.1.4 |
| 3.1 Performance affecting heat and mass transfer mechanism, including processes observed in available thermohydrologic tests and experiments, have been identified and incorporated into the TSPA. Specifically, it is necessary to either demonstrate that liquid water will not reflux into the underground facility or incorporate refluxing water into the TSPA and bound the potential adverse effects of: (i) corrosion of the WP; (ii) accelerated transport of radionuclides; and (iii) alteration of hydraulic and transport pathways that result from refluxing water. | The EBS process models incorporate thermal refluxing in the thermal hydrological calculations. The Water Distribution Model, and the Multiscale Thermal-Hydrologic Model consider the waste package heat loading for the EDA-II design. The TH calculations consider the effects of this heat loading on the reduction of liquid moisture content, and the reduction in capillary pressure due to initial heating in EBS components, and the surrounding media. After waste package heat decays, the models simulate the increase in liquid moisture content, and increase in capillary pressure due to the refluxing of water.

EBS PMR Sections 3.1.1 through 3.1.4 |
| 3.2 Significant Geologic Repository Operations Area (GROA) underground facility design features, such as the addition of backfill or drip shields, that can result in changes in TSP have been identified and incorporated into the TSPA. | The EBS Process Models incorporate significant design features of the underground facility.

The process models incorporate underground design features with the inclusion of backfill and drip shields. The hydrologic performance of components as governed by their flow properties are incorporated into the models. |

TEF Subissue 3: Does The U.S. Department Of Energy Total System Performance Assessment Adequately Account For Thermal Effects On Flow?

Technical Acceptance Criterion	
Acceptance Criterion	**PMR Approach and Section Reference**

EBS PMR Sections 3.1.1 through 3.1.4

3.3 Conceptual model uncertainties have been defined and documented, and their effects on conclusions regarding TSP have been assessed.

Each of the major EBS process models is documented in a referenced report that includes a discussion of the model uncertainties.

EBS PMR Section 3.1.1 through 3.1.4

3.4 Mathematical models are consistent with conceptual models, based on consideration of site characteristics.

The EBS process models for thermal hydrological effects are based upon initial conditions boundary conditions, and computational domains consistent with site characteristics. The thermal hydrology models used in Sections 3.1.1 through 3.1.4 are based upon the selection of NBS hydrologic and thermal properties used in the UZ Process Model. The initial conditions, and boundary conditions for the models for specific locations use the same infiltration rates, and temperature and pressure boundary conditions consistent with the UZ Process Model (Section 3.1.4)

EBS PMR Sections 3.1.1 through 3.1.4

3.5 Alternative models and modeling approaches, consistent with available data and current scientific understanding, are investigated; limitations defined; and results appropriately considered.

Alternative models are presented.

Section 3.1.1 through 3.1.3 present alternative models for Water Distribution and Removal, Bulk Physical and Chemical Environment in the EBS, and Radionuclide Transport respectively. Section 3.1.2 addresses alternative models. Such simulation methods can be applied as they become available, and as the required data, including numerical settings used to operate the simulation codes are qualified. The approach used in this PMR is applied to address conceptual issues and to evaluate bounding conditions for the performance of engineered barriers.

3.6 Results from different mathematical models have been compared to judge robustness of results.

The results of the numerical calculations have been compared to hand calculations where appropriate.

The DOE used appropriate procedures to construct and test numerical models for predicting seepage and flow. For the case of the Water Distribution and Removal Model, the results of the NUFT calculations were compared to a closed form analytical solution for the prediction of fluxes in and near the EBS (CRWMS M&O 2000q). The software codes used for the models are subject to verification and testing under the procedure AP-SI.1Q.

EBS PMR Sections 3.1.1 through 3.1.4

4. Coupling of thermal processes has been evaluated using a methodology in accordance with NUREG-

The EBS Process Model use bounding calculations where appropriate. Section 3.1.2 addresses alternative models. Such simulation methods can be applied as they become available, and as the required data, including

Subissue

TEF Subissue 3: Does The U.S. Department Of Energy Total System Performance Assessment Adequately Account For Thermal Effects On Flow?

Technical Acceptance Criterion

Acceptance Criterion	PMR Approach and Section Reference
1466 (Nataraja and Brandshaug, 1992) or other acceptable methodology. Coupled processes may be uncoupled, if it is shown that the uncoupled model results bound the predictions of the fully-coupled model results.	numerical settings used to operate the simulation codes are qualified. The approach used in this PMR is applied to address conceptual issues and to evaluate bounding conditions for the performance of engineered barriers. EBS PMR Sections 3.1.1 through 3.1.4
5. The dimensionality of models used to assess the importance of refluxing water on repository performance may be reduced if it is shown that the reduced dimension model bounds the prediction of the full dimension model in performance.	The EBS Process Model use boundary calculations where appropriate. The potential repository-scale heterogeneity is represented by the drift scale active properties set which captures the properties for various strata. Lateral variability within the potential repository footprint is represented by the 31 drift-scale-model locations used in the MSTH model. These locations are regularly distributed over the potential repository footprint. This reduces the general three dimensional problem to a series of two dimensional problems. EBS PMR Sections 3.1.1 through 3.1.4
6. Results of the TSPA related to TEF have been verified by demonstrating consistency with results of process-level models.	The EBS Process Model use bounding calculations where appropriate. See EBS PMR Sections 3.1.1 through 3.1.4.
7. Sensitivity and importance analyses were conducted to assess the need for additional data or information with respect to TEF.	Sensitivity analyses are conducted where appropriate in the EBS Process Models. Data on EBS processes are being collected at the current time for the Water Distribution and Removal Model (Section 3.1.1), and the Physical and Chemical Environment Model. Where appropriate, sensitivity and importance analyses have been performed as described by the parametric studies in Sections. 3.1.1 through 3.1.4. EBS PMR Sections 3.1.1 through 3.1.4.

Element 1	
Acceptance Criterion	**PMR Approach and Section Reference**
T1 - DOE has identified a comprehensive list of processes and events that: (1) are present or might occur in the Yucca Mountain region and (2) includes those processes and events that have the potential to influence repository performance	Sections 1.5.1 and 2.4 of this PMR describes the features, events, and processes in this PMR. The AMR supporting this section, EBS Features, Events, and Processes/Degradation Modes Analysis, provides a list of the processes and events applicable to this PMR. The AMR provides a description of the screening arguments and dispositions for the FEPs and has been thoroughly reviewed by subject mater experts. Also, in parallel with the release of Revision 0 of the FEPs database, documentation will be produced to describe the development of the FEPs database. It is planned to include a description of the FEPs process in sufficient detail to demonstrate the comprehensiveness of the database. It will describe how FEPs were identified by a variety of methods, including expert judgment, informal elicitation, event tree analysis, stakeholder review, and regulatory stipulation.

Element 2	
Acceptance Criterion	**PMR Approach and Section Reference**
T1 - DOE has provided adequate documentation identifying how its initial list of processes and events has been grouped into categories.	Sections 1.5.1 and 2.4 of this PMR describes the features, events, and processes in this PMR. The AMR supporting this section, EBS Features, Events, and Processes/Degradation Modes Analysis, provides documentation and justification for screening arguments and TSPA dispositions. Documentation is maintained of all mapping of FEPs into primary and secondary categories. For comprehensiveness, traceability is maintained from the secondary to the related primary FEPs. In addition, in parallel with the release of Revision 0 of the FEPs database, documentation will be produced to describe the development of the FEPs database. It is planned to include a description of the categorization scheme with justification on why it is sufficient.
T2 - Categorization of processes and events is compatible with the use of categories during the screening of processes and events.	In parallel with the release of Revision 0 of the FEPs database, documentation will be produced to describe the development of the FEPs database. It is planned to include a description of the categorization scheme with justification on why it is sufficient. In addition, documentation is maintained of all mapping of FEPs into primary and secondary categories. For comprehensiveness, traceability is maintained from the secondary to the related primary FEPs.

Element 3

Acceptance Criterion	PMR Approach and Section Reference
T1 - Categories of processes and events that are not credible for the Yucca Mountain repository because of waste characteristics, repository design, or site characteristics are sufficient justification is provided for DOE's conclusions	Sections 1.5.1 and 2.4 of this PMR describes the features, events, and processes in this PMR. The AMR supporting this section, EBS Features, Events, and Processes/Degradation Modes Analysis, provides documentation and justification for screening arguments and TSPA dispositions. Documentation includes a statement of the screening decision for each FEP. Justification is provided for each excluded FEP including the criterion on which it was excluded and the technical basis for the screening argument.
T2 - The probability assigned to each category of processes and events is consistent with site information, well documented, and appropriately considers uncertainty.	Sections 1.5.1 and 2.4 of this PMR describes the features, events, and processes in this PMR. The AMR supporting this section, EBS Features, Events, and Processes/Degradation Modes Analysis, provides documentation and justification for screening arguments and TSPA dispositions. Probability estimates for FEPs are based on technical analysis of the past frequency of similar events consistent with site information, well documented, and appropriately considers uncertainty.
T3 - Processes and events may be screened from the performance assessment on the basis of their probability of occurrence, provided DOE has demonstrated that they have a probability of less than one chance in 10,000 of occurring over 10,000 years.	Sections 1.5.1 and 2.4 of this PMR describes the features, events, and processes in this PMR. The AMR supporting this section, EBS Features, Events, and Processes/Degradation Modes Analysis, provides documentation and justification for screening arguments and TSPA dispositions. Justification is provided for each excluded FEP including the criterion on which it was excluded and the technical basis for the screening argument. For excluded FEPs, documentation includes the criterion on which it was excluded and the technical basis for the screening argument. The probability assigned to FEPs may be one of the screening criteria. FEPs may be excluded from the TSPA only if they can be shown to have a probability of occurrence of less than .0000001/year.
T4 - Categories of processes and events may be omitted from the performance assessment on the basis that their omission would not significantly change the calculated expected annual dose, provided DOE has demonstrated that excluded categories of processes and events would not significantly change the calculated expected annual dose.	Sections 1.5.1 and 2.4 of this PMR describes the features, events, and processes in this PMR. The AMR supporting this section, EBS Features, Events, and Processes/Degradation Modes Analysis, provides documentation and justification for screening arguments and TSPA dispositions. For omitted categories, documentation includes the criterion on which it was excluded and the technical basis for the screening argument.

Element 4

Acceptance Criterion	PMR Approach and Section Reference
T1 - DOE has provided adequate documentation identifying: (1) whether processes and events have been address through consequence model abstraction or scenario analysis and (2) how the remaining categories of processes and events have been combined into scenario classes.	Sections 1.5.1 and 2.4 of this PMR describes the features, events, and processes in this PMR. The AMR supporting this section, EBS Features, Events, and Processes/Degradation Modes Analysis, provides documentation and justification for screening arguments and TSPA dispositions. FEPs that have not been excluded are identified as either expected FEPs or disruptive FEPs. Expected FEPs will be included in the TSPA-SR nominal scenario, which is simulated by the base case model described in the TSPA-SR documentation.

Element 4	
Acceptance Criterion	**PMR Approach and Section Reference**
T2 - The set of scenario classes is mutually exclusive and complete.	Sections 1.5.1 and 2.4 of this PMR describes the features, events, and processes in this PMR. The AMR supporting this section, EBS Features, Events, and Processes/Degradation Modes Analysis, provides documentation and justification for screening arguments and TSPA dispositions. Also, in parallel with the release of Revision 0 of the FEPs database, documentation will be produced to describe the development of the FEPs database. It is planned to include in the documentation, a description of the FEPs process in sufficient detail to demonstrate the set of scenario classes is mutually exclusive and complete.

Element 5	
Acceptance Criterion	**PMR Approach and Section Reference**
T1 - Scenario classes that are not credible for the Yucca Mountain repository because of waste characteristics, repository design, or site characteristics, individually or in combination, are identified and sufficient justification is provided for DOE's conclusions.	Sections 1.5.1 and 2.4 of this PMR describes the features, events, and processes in this PMR. The AMR supporting this section, EBS Features, Events, and Processes/Degradation Modes Analysis, provides justification for screening arguments and TSPA dispositions. Scenarios are screened using the same regulatory, probability, and consequence criteria used for screening individual FEPs. Documentation of this process includes identification of any scenarios that have been screened from the analysis and the technical basis for that screening decision.
T2 - The probability assigned to each scenario class is consistent with site information, well documented, and appropriately considers uncertainty.	Sections 1.5.1 and 2.4 of this PMR describes the features, events, and processes in this PMR. The AMR supporting this section, EBS Features, Events, and Processes/Degradation Modes Analysis, provides justification for screening arguments and TSPA dispositions. Probability estimates for scenario classes are based on analyses similar to probabilities assigned for individual FEPs.
T3 - Scenario classes may be omitted from the performance assessment on the basis of their probability of occurrence, provided: (1) the probability used for screening the scenario class is defined from combinations of initiating processes and events and (2) DOE has demonstrated that they have a probability of less than one chance in 10,000 of occurring over 10,000 years.	Sections 1.5.1 and 2.4 of this PMR describes the features, events, and processes in this PMR. The AMR supporting this section, EBS Features, Events, and Processes/Degradation Modes Analysis, provides justification for excluding scenario classes. The probability assigned to scenario classes is one of the screening criteria. Scenario classes may be excluded from the TSPA only if they can be shown to have a probability of occurrence of less than $10-8$/year. Justification is provided for each excluded scenario class, including the criterion on which it was excluded and the technical basis for the screening argument. In addition, in parallel with the release of Revision 0 of the FEPs database, documentation will be produced to describe the development of the FEPs database including a description of screening and specifying scenarios for TSPA analysis.
T4 - Scenario classes may be omitted from the performance assessment on the basis that their omission would not significantly change the calculated expected annual dose, provided DOE has demonstrated that excluded categories of processes and events would not significantly change the calculated expected annual dose.	Sections 1.5.1 and 2.4 of this PMR describes the features, events, and processes in this PMR. The AMR supporting this section, EBS Features, Events, and Processes/Degradation Modes Analysis, provides justification for excluding scenario classes. For excluded scenario classes, documentation includes the criterion on which it was excluded and the technical basis for the screening argument. In addition, in parallel with the release of Revision 0 of the FEPs database, documentation will be produced to describe the development of the FEPs database including a description of screening and specifying scenarios for TSPA analysis.